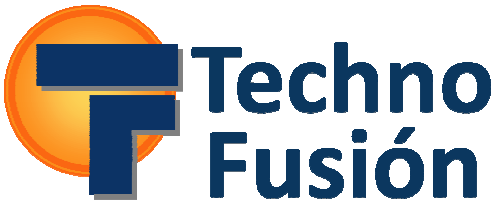

National Centre for Fusion Technologies

Scientific-Technical Report

September 2009

Property:

EDITORIAL CIEMAT
Avda. Complutense, 22
28040 – MADRID
2009

General Catalog of Official Publications
http://www.060.es

Legal deposit: M-45720-2009
ISBN: 978-84-7834-628-8
NIPO: 471-09-056-6

Authors and Contributions

This document has been elaborated with the enthusiastic contribution of a large group of researchers from seven Universities and Research Centres. We are enormously grateful to them for their help and support during these past two years.

Centro de Investigaciones Energéticas, Medioambientales y Tecnológicas de Madrid (CIEMAT): J. M. Arroyo, F. Carbajo, N. Casal, P. Fernández, J. Ferreira, A. García, I. García-Cortés, M. González, M. Hernández, M. T. Hernández, A. Ibarra, D. Jiménez, J.A. Jiménez, J.L. Martínez-Albertos, A. Moroño, F. Mota, C. Ortíz, E. Oyarzabal, V. M. Queral, L. Ríos, A. Ramos, R. Román, F. Tabarés, V. Tribaldos, J. P. de Vicente, R. Vila. *Universidad Politécnica de Madrid (UPM):* A. Abánades, R. Aracil, O. Cabellos, D. Díaz, S. Domingo, M. Ferré, L. Gámez, R. González, N. García, Y. Herreras, A. Lafuente, P. Martel, E. Martínez, J. M. Martínez-Val, E. Mínguez, J. Y. Pastor, M. Perlado, E. Río, J. Sanz, F. Sordo, M. Velarde, M. Victoria. *Universidad Nacional de Educación a Distancia (UNED):* M. García, D. López, A. Mayoral, F. Ogando, J. Sanz, P. Sauvan. *Universidad Carlos III de Madrid (UC3M):* D. Blanco, L. Moreno, M. A. Monge, R. Pareja. *Consejo Superior de Investigaciones Científicas (CSIC):* P. González, J. de No. *Universidad Autónoma de Madrid (UAM):* A. Climent, A. Muñoz. *Universidad de Alicante (UA):* M. J. Caturla. *Universidad de Sevilla (US)*: C. Arévalo.

General coordination: A. Ibarra (CIEMAT) & M. Perlado (UPM)
Material Production and Processing group coordination: R. Pareja (UC3M)
Material Irradiation group coordination: R. Vila (CIEMAT)
Plasma-Wall Interaction group coordination: F. Tabarés (CIEMAT)
Liquid Metal Technologies group coordination: A. Abánades (UPM)
Characterization Techniques group coordination: M. González (CIEMAT)
Remote Handling Technologies group coordination: R. Aracil (UPM)
Computer Simulation group coordination: J. Sanz (UNED, UPM)
English revision: K. McCarthy and B. Ph. Van Milligen (CIEMAT)
Project management and edition: D. Jiménez-Rey, R. Román & I. García-Cortés (CIEMAT)

Summary

The development of nuclear fusion is rapidly becoming a vital necessity in view of the continuing rise of the world's energy demand. Nuclear fusion offers a virtually endless source of energy that is both environmentally friendly and capable of meeting any foreseeable energy demand.

The progress of fusion constitutes one of the greatest technological challenges for humanity. Indeed, this field is one of the main areas of research of the European Union (EU), as was evident in June 2005, when the final agreement to construct ITER[1] (the *International Thermonuclear Experimental Reactor*) was signed, together with the USA, Russia, China, South Korea, Japan and India. ITER is an experimental reactor intended to demonstrate the scientific viability of fusion.

As the design of ITER is already defined, over the next 20 to 30 years the main focus will be on the development of technological components for future commercial reactors, rather than on basic plasma physics. The most important challenges for fusion research are the selection, development and testing of materials and the various elements for reactors, together with the design of energy extraction systems and tritium production methods.

At present, Spain has a unique opportunity to be at the forefront of this new technological field in Europe. However, there is a need for new facilities to simulate the extreme conditions to which materials and components will be exposed inside a fusion reactor.

The project outlined in this report describes the construction of a singular scientific and technological facility (the National Centre for Fusion Technologies -*TechnoFusión*) in the Madrid region, to create the infrastructure required to develop the technologies needed in future commercial fusion reactors, and to assure the participation of Spanish research groups and companies.

The Spanish scientific community has achieved an international recognition in the science and technology areas needed for the success of this ambitious project, as is evident from the results obtained by Spanish researchers in the fusion field over the past few decades. *TechnoFusión* intends to take advantage of the existing expertise of university research groups, public research institutions (*Organismo Público de Investigación, OPI*) and private companies. The performance of materials and components under the extreme conditions of a fusion reactor is largely unknown, and this is precisely what *TechnoFusión* intends to explore. For this purpose, facilities are required for the manufacture, testing and analysis of critical materials. Additional resources are planned to develop and exploit numerical codes for the simulation of materials in special environments, to develop remote handling technologies and other areas related to the management of liquid metals.

[1] ITER (originally the International Thermonuclear Experimental Reactor) is an international tokamak (magnetic confinement fusion) research/engineering project being built in Cadarache, France.

In summary, *TechnoFusión* focus is the creation of infrastructures for the following research areas: 1) material production and processing, 2) material irradiation, 3) plasma-wall interaction (thermal loads and the mechanism of atomic damage), 4) liquid metal technologies, 5) material characterization techniques, 6) remote handling technologies and 7) computer simulation.

Therefore, *TechnoFusión* Scientific-Technical Facility will thus consist of a complex of seven large research areas, many of which are unique in the World, with the following main technical objectives:

1) *Material production and processing*. There are still some uncertainties about the materials that will be used to construct future fusion reactors, partly because it has not yet been possible to reproduce the extreme conditions to which such materials will be subjected. Therefore, it is of utmost importance to dispose of facilities capable of manufacturing new materials on a semi-industrial scale and fabricating prototypes. Top priority materials include metals such as reinforced low activation ODS type steels (*Oxide Dispersion Strengthened steels*) and tungsten alloys. To manufacture such materials, equipment is required that currently is scarce or inexistent in Spain, such as a *Vacuum Induction Melting furnace* (VIM), a *Hot Isostatic Pressing furnace* (HIP), a furnace for sintering assisted by a Pulsed Plasma Current (*Spark Plasma Sintering*, SPS), or a *Vacuum Plasma Spraying* equipment (VPS).

2) *Material irradiation*. Even though the exact reactor conditions are only reproduced inside a fusion reactor, it is possible to simulate the effects of neutrons and gamma radiation on materials by irradiating with ion and electron accelerators.

The effect of neutronic radiation will be characterized by combining three ion accelerators: one tandem ion accelerator for irradiating with He, with an energy of 6 MV, another tandem ion accelerator for irradiating with H (or D), with an energy of 5 MV, and a cyclotron heavy ion accelerator, with k around 110, to implant heavy ions (Fe, W, Si, C) or high energy protons.

Additionally, a high magnetic field magnet, between 5 and 10 T, must be incorporated into this facility in order to study the simultaneous effect of radiation and magnetic fields on materials.

The effects of ionizing gamma radiation will be studied using a *Rhodotron®* electron accelerator with a fixed energy of 10 MeV that will be shared with other *TechnoFusión* facilities.

3) *Plasma-wall interaction*. Inside a fusion reactor, some materials will not be subjected only to radiation, but also to enormous heat loads in the case of plasma disruptions. In view of this, both: i) stationary conditions due to the intrinsic reactor properties: high density, low temperature and high power and ii) violent transient events (called ELMs in plasma physics literature) must be reproduced. Therefore, it is essential to dispose of a device (which it will be called “plasma gun”) to study plasma-material interactions simultaneously in steady state and transient regimes, thereby allowing an analysis of the modification of the materials and their properties in fusion reactors.

The mentioned plasma gun would consist of two main elements: (1) a linear plasma device capable of generating hydrogen plasmas with steady state particle fluxes of up to 10^{24} $m^{-2}s^{-1}$ (i.e., of the order of the expected ITER fluxes) and impact energies in the range of 1-10 eV, and (2) a device of the quasi-stationary plasma accelerators (*QSPA*) type, providing pulses lasting 0.1-1.0 ms and energy fluxes in the 0.1-20 MJm^{-2} range, in a longitudinal magnetic field of the order of 1 T or greater.

These devices are connected by a common vacuum chamber, allowing the exchange of samples, and their simultaneous or consecutive exposure to the steady state and transient plasma flows under controlled conditions. Both devices will operate with hydrogen, deuterium, helium, and argon.

4) *Liquid metal technologies*. A number of, ITER, DEMO (*DEMOstration Fusion Power Reactor*)[2], and IFMIF (*International Fusion Materials Irradiation Facility*)[3] components will use liquid metals as refrigerants, tritium generators, neutron reproducers, moderators, etc., all of them under extreme conditions. Therefore, these applications need further research to be finally implemented in such facilities.

The basic working scheme for liquid metal Facility in *TechnoFusión* is an arrangement of two liquid lithium loops, one of them coupled to the *Rhodotron®* electron accelerator to investigate the effects of gamma radiation on different conditions of the liquid lithium.

The main goals of this Facility are the studies of i) the free surface of liquid metals under conditions of internal energy deposition, and ii) the compatibility of structural materials and liquid metals in the presence of radiation. In addition, it will be possible to study the influence of magnetic fields on the cited phenomena as well as the development of methods for i) purification of liquid metals, ii) enrichment of lithium, iii) extraction of tritium, and iv) development of safety protocols for liquid metal handling.

5) *Characterization techniques*. Ambitious and well-understood research requires an accurate knowledge of the materials under study. Therefore, a range of techniques to characterize them under different situations is a key element in the global scheme of *TechnoFusión*. These techniques include mechanical testing (creep, nanoindentation, fatigue, etc.), compositional analysis (Secondary Ion Mass Spectrometry and Atomic Probe Tomography), and structural characterization (Energy Filtered Transmission Electron Microscopy, X-Ray Diffraction), as well as a number of material processing techniques (Focused Ion Beam Systems coupled to a Scanning Electron Microscope). Additional systems will be used to characterize physical properties (electrical, dielectric, optical, etc.).

Some of the above-mentioned techniques will be implemented to test the materials either in-beam –while being irradiating— or *in-situ*, inside the lithium loop. Needless to say, these techniques can also be performed before and after irradiation or before and after experiencing any other physical or chemical processes.

---

[2] DEMO (DEMOnstration Power Plant) is a proposed nuclear fusion power plant that is intended to build upon the expected success of the ITER experimental nuclear fusion reactor.

[3] IFMIF is a planned high-intensity neutron reactor whose spectrum should be equivalent to that of a fusion reactor. The final design comprises two deuteron accelerators impinging on a liquid lithium target to generate nuclear stripping reactions to provide the desired neutron spectrum

6) ***Remote handling technologies***. The conditions inside a fusion reactor are incompatible with a manual repair or replacement of parts. Therefore remote handling is indispensable. New robotic techniques, compatible with such hostile conditions, need to be developed; while existing techniques need certification in order to be applied at installations such as ITER or IFMIF.

Remote Handling Facility of *TechnoFusión* will contribute to this knowledge with: i) a large installation for the prototypes manipulation such as: *Diagnostic Port Plug* of ITER, *Test Blanket Modules* of ITER and Modules of irradiation of IFMIF, and ii) an Irradiated Room coupled to the electron accelerator –*Rhodotron*®— in order to carry out validation, certification and characterization of remote handling tools and machines in an uniform ionizing field equivalent to ITER-DEMO trying to simulate the fusion reactor environment.

7) ***Computer simulation***. To study conditions that cannot be reproduced experimentally and to accelerate the development of novel systems for a future commercial fusion power plant, *TechnoFusión* will stimulate an ambitious programme of computer simulations, combining existing experience in the fusion field with resources from the National Supercomputation Network[4]. The goals include the implementation of the global simulation of a commercial fusion reactor, the interpretation of results, the validation of numerical tools, and the development of new tools. Another indispensable goal is the creation of a data acquisition system and the visualisation of results.

Based on the existing experience of research groups at Universities, Public Research Organisations and company research departments, *TechnoFusión* proposes the development of a large scientific infrastructure in order to make a significant contribution to the development of new technologies needed for the construction of commercial fusion reactors. The project described here will permit the generation of highly relevant technological knowledge for all types of fusion reactors, irrespective of the underlying concept (magnetic or inertial confinement).

The goal of TechnoFusión is to bring together sufficient human and material resources to contribute significantly to the development of a safe, clean, and inexhaustible source of energy for future generations.

[4] http://www.bsc.es/index.php. September 2009.

CONTENTS

1. Introduction

1.1. Nuclear Fusion and the European Fusion Programme: strategies

Progress towards the achievement of fusion as an inexhaustible energy source that is respectful with the environment has received a strong impulse with the agreement between Europe, USA, Japan, Russia, China, South Korea, and India, on the construction of the experimental device *International Thermonuclear Experimental Reactor* (ITER, meaning *The Way* in Latin) at the french site of Cadarache.

These governments, representing more than half the world population, will contribute a total of 10.000 M€ over a period of 20 years to the construction and exploitation of ITER, whose main goal is to demonstrate that controlled fusion can be achieved scientifically. ITER is a device of the tokamak type, in which intense magnetic fields confine a toroidally shaped plasma. A mix of deuterium (D) and tritium (T) at a temperature of two hundred million degrees centigrade will produce fusion reactions that generate 10 to 50 times more energy than the power needed to maintain the reaction. Figure 1.1 shows a drawing of such a fusion reaction. One of the main reactions that will occur is:

$$D + T \rightarrow {}^{4}He\ (3.5\ MeV) + n\ (14.1\ MeV)$$

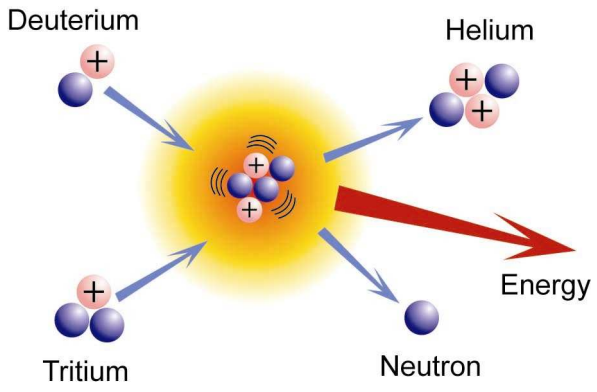

Figure 1.1. Sketch of the D-T fusion reaction. A deuterium nucleus and a tritium nucleus combine to produce a helium nucleus and a neutron, liberating an energy of 17.58 MeV.

In view of the fact that tritium is not available in nature in sufficient quantities, it must be regenerated inside the thermonuclear reactor. This is achieved by letting neutrons, originating from the fusion reactions, collide with lithium (Li) nuclei, thus inducing the following nuclear reactions:

$$n + {}^{6}Li \longrightarrow {}^{3}H + {}^{4}He$$

$$n + {}^{7}Li \longrightarrow {}^{3}H + {}^{4}He + n$$

ITER will demonstrate the scientific viability of controlled fusion, but the commercial generation of electricity based on thermonuclear fusion will require the prior solution of a number of technological problems. The main issues are related to materials, which must be capable of withstanding radiation and large thermal loads, remotely controlled maintenance systems needed to guarantee the availability of the plant, and tritium regeneration systems to guarantee self-sufficiency. The solution of these critical issues is required to demonstrate the technological viability of fusion.

Some of these issues require implementing large-scale projects. The most important of these are:

i) IFMIF (*International Fusion Materials Irradiation Facility*), an installation for testing the materials that will be used in a fusion reactor,

ii) JT60-SA, a superconducting tokamak that will allow experimenting with alternative concepts for the operation of ITER,

iii) CTF (*Compact Tokamak Facility*), a plasma-based massive neutron source for testing the radiation response of large-scale components.

If all these projects materialise over the next 20 years, a prototype fusion reactor will be built, called DEMO (*DEMOnstration Fusion Power Reactor*), around the year 2035. This timeline is known as the *Fast Track to Fusion Power* and it constitutes the official policy of the European Union (EU)[5].

The above indicates that the coming decades will experience large advances in thermonuclear fusion research and associated technologies, while shifting the main focus from basic research in plasma physics to the technological development of all the constituent systems of a fusion reactor, which will require planning and implementing large multinational projects.

Within Europe, an integrated approach to fusion research is adopted, coordinated by the European Commission via EURATOM[6] (*EURopean ATOMic Energy Community*). The main fusion research centres have signed "association agreements" with EURATOM, giving them direct and simplified access to the research funds of the Framework Programme[7]. With the exception of Germany, which has three large associated laboratories, all other member states have a single associated laboratory. In the case of Spain, CIEMAT (*Centro de Investigaciones*

[5] C. Llewelyn-Smith, *The need for fusion*, Fusion Engineering and Design 74 (2005) 3-8

[6] The founding treaty of the European Atomic Energy Community (EURATOM) was signed in 1957 with the goal of coordinating nuclear research and training in the European Community.

[7] The Framework Programme for research and Technological Development is the European Union's main tool for the funding of research. It contains a specific sub-programme for Nuclear Research (EURATOM) encompassing the community's activities on research, technological development, international cooperation, the dissemination of technical information, and training.

Energéticas, Medioambientales y Tecnológicas – Centre for Research on Energy, the Environment and Technology - in Madrid) coordinates the national efforts on fusion research.

The association agreement facilitates access to the community funds subject to economic audits and periodic revisions of the scientific and technical programme. These control mechanisms provide additional transparency (which is guaranteed anyway due to the national control mechanisms) and, above all, assure the coherence of the research programmes, avoiding the duplication of efforts and deviations from the main research lines.

Therefore, the integration of the *National Centre for Fusion Technologies (TechnoFusión)* in the European Programme is subject to some limitations, in view of the fact that the general rule is to avoid creating infrastructures whose functions are already adequately covered by other European centres. On the other hand, these same norms also oblige to undertake competitive programmes that address present fusion research and development needs. In any case, the cited norms are not incompatible with the creation of infrastructures that already exist in Centres of other countries, when they constitute strategic elements of the lines of research to be developed.

The long-term European Fusion programme

Part of the European Union Framework Programme for Technological Development and Research is financed through EURATOM, in particular european fusion research. The European Fusion Programme functions via two main mechanisms:

- Association Agreements between EURATOM and the European Union Member States (or organisations of these states), or non-member states associated with EURATOM. All Member States participate via this mechanism, as does Switzerland (from 1979) and, more recently, the Czech Republic, Hungary, Latvia, and Rumania.

- The *European Fusion Development Agreement* (EFDA) coordinates the technological activities and the scientific exploitation of the *Joint European Torus* programme (JET) and the european contributions to international collaborations. This agreement constitutes the top priority in the framework of the european contribution to the international project for demonstrating the scientific viability of fusion energy, ITER.

The Long-Term European Programme includes activities that are not directly related to ITER yet considered indispensable for the development of future fusion reactors. In order to define the scope of these activities, an evaluation was made of the specifications of the future fusion reactor DEMO[8]. This study, known as the *European Power Plant Conceptual Study* (PPCS), described four different types of fusion reactors with varying degrees of technological complexity and efficiency. The Long-Term European Programme was defined on the basis of the research and development needs identified in this work. Its main points are: 1) the development and experimental validation of the various conceptual designs of the *breeding blanket*, 2) the development and characterization of functional and structural materials

[8] D. Maissonier et al, DEMO and Fusion Power Plant Conceptual Studies in Europe, presented at the ISFNT-7 (2005)

required for the various fusion reactor concepts, and their validation at the IFMIF high intensity neutron source, having a spectrum similar to that expected in a fusion reactor, 3) the validation of the fuel cycle, with special emphasis on tritium control, and 4) the development and validation of remote handling components, indispensable for any future fusion power plant. Below, the main specifications of these activities are described in more detail[9].

The breeding blanket

The breeding blanket (Figure 1.2) consists of a set of modules covering the interior of the fusion reactor vessel, capable of supporting a high heat load and an intense neutron flux. Its main purpose is threefold: i) to assure self-sufficiency of the fusion reactor with regard to tritium (by producing, from lithium, at least the same amount of tritium as that which is consumed in the plasma), ii) to maximise the net efficiency of the power plant (by assuring the highest possible temperature of the coolant), and iii) to act as a radiation barrier (such that the components behind the breeding blanket receive the lowest amount of radiation possible).

Currently, Europe is developing two alternative concepts for the breeding blanket of DEMO, both based on helium cooling, which must be tested in experiments to be performed at ITER[10]. One is based on liquid metal, and the other on the use of Li and Be ceramics (acting as neutron multipliers) in the shape of small spheres. Both breeding blanket concepts require the optimisation of a set of parameters with mutually contradictory effects. The main issues subject to study can be summarised as follows:

- The design of a He cooled structure that allows a sufficient production of tritium while being capable of surviving any possible accidents.
- The study of the physical and mechanical properties of the Be spheres and Li ceramics under high irradiation doses.
- The *Magneto-Hydrodynamic* (MHD) properties of the liquid metal breeding blanket when it is subjected to intense magnetic fields.
- The control, extraction and handling of tritium in the breeding blanket.
- The response to neutrons and radiation from the plasma and the activation of the materials.
- The He cooling capacity of the breeding blanket, considering the large quantity of deposited heat.
- Breeding blanket control and diagnostic systems, for monitoring the system during irradiation.

[9] R. Andreani et al, Overview of the European Union fusion nuclear technologies development and essential elements on the way to DEMO, Fusion Engineering and Design 81 (2006) 25-32

[10] J.F. Salavy et al, Overview of the last progresses for the European Test Blanket Modules Projects, presented at the 21th SOFT, 2006 (http://soft2006.materials.pl/Presentations.php)

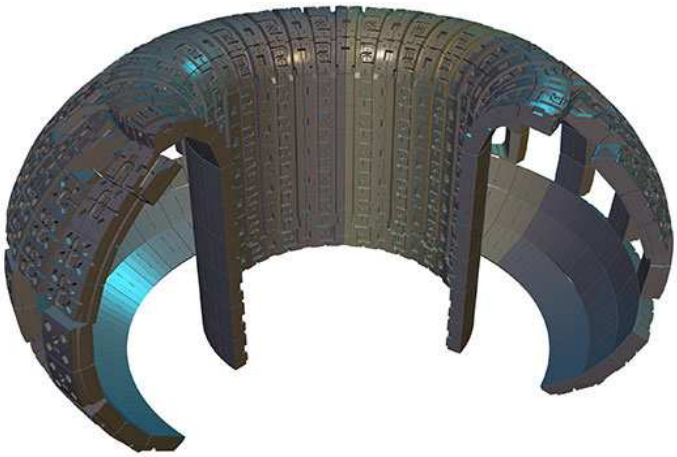

Figure 1.2. Virtual representation of ITER blanket modules.

Fusion materials

In the Long-Term European Programme, materials activities[11] are mainly concentrated on the study and characterization of EUROFER, ferritic-martensitic low-activation steel that will constitute the main structural material of DEMO and the breeding blankets, according to current designs. Presently, its characterization is virtually complete, with the exception of irradiation tests, which are being carried out by applying varying degrees of irradiation inside fission reactors, some of which are quite elevated (of the order of 80 dpa[12]). It is important to emphasise that the exposure to radiation inside fission reactors only provides qualitative information on radiation damage, as the radiation in a fusion reactor will generate H and He inside the material, so that the damage needs to be verified using a neutron source with a spectrum similar to the spectrum corresponding to the future reactors.

Less studied but equally interesting are the reinforced low activation steels obtained by oxide dispersion (*Oxide Dispersion Strengthened steels,* ODS). This type of steel would allow a slightly higher operating temperature (about 100 ºC higher) than the maximum temperature of EUROFER. Currently, the first irradiation studies are being prepared, the reproducibility of properties across manufacturers is being studied, and the possibility to improve the fracture tension is being evaluated.

Other interesting materials are silicon carbide composites, SiC_f/SiC with two possible applications: firstly, they are being proposed as high-temperature insulating materials in advanced designs of the breeding blanket based on liquid metal, with the purpose of reducing

[11] R. Laesser et al, Development, simulation and testing of structural materials for DEMO, presented at the 21th SOFT, 2006 (http://soft2006.materials.pl/Presentations.php)
[12] dpa = number of ion displacements per atom.

the magneto-hydrodynamic forces and, secondly and in the long term, as structural materials for advanced fusion reactor concepts, in view of the fact that they allow operation at very elevated temperatures. Currently, Europe is developing perfectly stoichiometric composites with a high degree of purity.

Finally, another family of materials included in the Long-Term European Programme, although with a lower priority, consists of tungsten (W) and its alloys[13]. Recently, these materials have received more attention due to their possible application in high-temperature He cooled divertors. In such divertors, a heat flux of the order of 10 MW/m^2 must be extracted, requiring highly pressurised He at a high temperature. The only material able to withstand such conditions is tungsten, in spite of its low ductility, its high ductile-fragile transition temperature, and the complications it presents for mechanisation purposes.

Another activity that has gained prominence in the materials area of the Long-Term European Programme is the first-principles based modelling of irradiation effects[14]. Over the last 15 years, the availability of increasing computing power in supercomputer centres, and the development of new algorithms, has given rise to a new branch of science that studies the behaviour of materials on the basis of the simultaneous simulation of millions of particles. The activities in the framework of the European Programme have concentrated mainly on simulating radiation effects in Fe and, more recently, in Fe and Cr. It is to be expected that the scope of these studies will be broadened to include the various components of the EUROFER steel and other materials, such as ODS and SiC_f/SiC, in the near future. It should be emphasised that this activity is essential for the interpretation and the comparison of the results that are currently being obtained from radiation exposure experiments in fission reactors, and future results that will be obtained at IFMIF.

IFMIF facility

This installation is a high-intensity neutron source with a broad energy spectrum, meant to reproduce the irradiation conditions of future fusion reactors. Its goal is to study and validate candidate materials for reactors in conditions similar to the actual expected environment. This objective imposes a set of conditions on the design of the source, which can be summarised as follows:

1) The neutron spectrum must be similar to that of a fusion reactor, as the effect of neutron radiation on materials depends critically on the neutron energy. More specifically, the parameter commonly used to express radiation effects is the ratio between the number of He atoms generated via nuclear reactions and the number of ions displaced from their position in the matrix (known as dpa).

2) The nature of the interaction with the material ions is of fundamental importance. Due to their interaction with the incident particles, the material ions receive an

[13] M. Kaufmann, Tungsten as First Wall Material in Fusion Devices, presented at the 21th SOFT, 2006 (http://soft2006.materials.pl/Presentations.php)
[14] J.L. Boutard et al, Modelling irradiation effects of EUROFER under Fusion Power Plant-relevant conditions, presented at the 21th SOFT, 2006 (http://soft2006.materials.pl/Presentations.php)

amount of energy that displaces them from their initial position (*recoil atoms*). The energy spectrum of such recoil atoms determines the type of defects that are produced in the material.

3) The radiation source must be continuous, since it is not evident that a pulsed radiation source produces equivalent effects.

4) The source must be capable of generating a dose equivalent to 150 dpa in a significant irradiation volume over a few years. This means that high neutron fluxes are required (of the order of 5 10^{17} n/m^2s) and that the device must operate with a high degree of availability (of the order of 70%). In addition, it must allow access to the irradiation zone, as it may be necessary to control the temperature and the atmosphere, or to perform *in-situ* experiments and measurements.

These requirements exclude neutron sources based on spallation reactions, while other sources, such as those based on plasma, have been rejected because of their high technological risk.

The broad range of materials to be studied and the complexity of the operational conditions further complicate the design of the neutron source. The first wall materials and the breeding blanket are the reactor elements that will be exposed to the highest neutron fluxes and the highest temperatures. Nevertheless, it is also necessary to understand the behaviour of materials located in other zones of the reactor, where they will be exposed to lower neutron fluxes.

Recent years have seen an increase of the international effort to design a neutron source meeting the cited requirements, under the auspices of the *International Energy Agency* (IEA). Figure 1.3 shows a three-dimensional view of the resulting design[15].

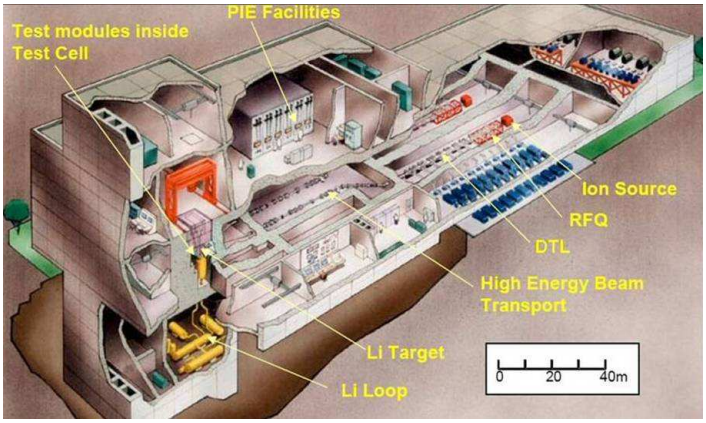

Figure 1.3. 3D view of the IFMIF facility for materials irradiation.

[15] IFMIF Comprehensive Design Report, January 2004.

This design incorporates two high intensity deuteron accelerators –about 125 mA each- with an energy of 40 MeV, impinging on a liquid Li target. Via nuclear *stripping* reactions a neutron spectrum is obtained with parameters suitable for the majority of the cited materials studies.

The installation will consist of three main areas and two secondary areas. The main areas are: the set of two accelerators, the target zone, and the irradiation zone. The secondary areas are: hot cells to analyse the samples after irradiation, and conventional installations.

Remote Handling

Europe is developing a program to identify and meet the remote handling needs of ITER (and DEMO, in the long term). In this context, a platform is being built to test divertor maintenance (*Divertor Test Platform*, DTP-2), involving a robot retriever capable of operating in the interior of the vacuum vessel, and containers for transporting the activated components from the reactor ports to the hot cell (where they can be treated). Nevertheless, many other remote handling needs may exist and it is important that they be identified. This activity also requires the development of new tools and procedures, which is part of the objective of the European Programme in this area. A diagram of some of the indispensable remote handling operations at ITER is shown in Figure 1.4.

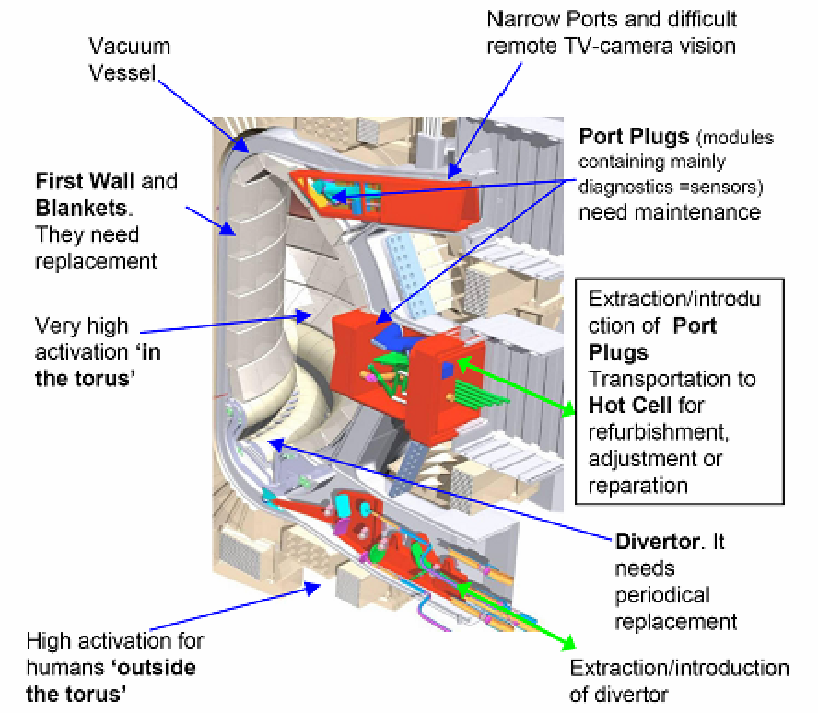

Figure 1.4. Examples of remote handling in a poloidal section of ITER.

1.2. ITER and DEMO: main technological and engineering solutions

ITER (Figure 1.5) is an experimental reactor of the tokamak type, capable of generating up to 500 MW of fusion energy, in cycles lasting up to 10 minutes. It will be 30 times more powerful than JET, and its size will be very similar to DEMO, the predecessor of future commercial power plants. The construction and operation of ITER is an international challenge of huge proportions for science, engineering and technology, requiring the expansion of the limits of current human knowledge. Its design is based on the main existing fusion experiments, such as EURATOM's JET in the UK, JT-60 (*Japan Torus*) in Japan, and TFTR (*Tokamak Fusion Test Reactor*) in the USA, apart from other fusion experiments of the EURATOM programme. In ITER, the knowledge and experience originating from all these experiments is combined (see Table 1.1).

ITER will generate ten times more energy than the energy needed to produce and heat the hydrogen plasma, allowing the scientists to study the physics of ignited plasma for the first time (i.e., a plasma that is heated by the fusion reactions in its interior, instead of the externally applied heating). It will also serve to demonstrate the heating, control, diagnostic, and remote handling systems that are indispensable in a true electrical power plant. ITER will also validate the plasma fuelling and impurity removal systems. The scientific challenge is enormous, but the growing worldwide demand for a clean and sustainable energy source is even larger.

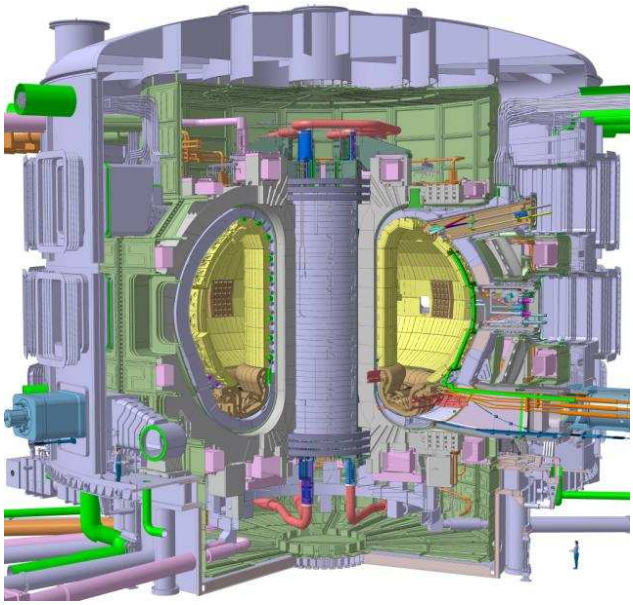

Figure 1.5. Virtual representation of ITER tokamak.

Table 1.1. Recent and operative magnetic fusion experiments with relevance for the development of fusion on the basis of a tokamak.

Machine	Country	a (m)	κ	R (m)	Ip (MA)	B_T(T)	P(MW)	Start of operation
ITER	*	2.00	1.75	6.20	15	5.3	73	
JET	EU	1.00	1.80	2.96	7.0	3.5	42	1983
JT-60	Japan	0.85	1.60	3.20	4.5	4.4	40	1991
TFTR	USA	0.85	1.00	2.50	2.7	5.6	40	1982 (closed)
TORE-SUPRA	France	0.80	1.00	2.40	2.0	4.2	22	1988
T-15	Russia	0.70	1.00	2.40	2.0	4.0	-	1989
DIII-D	USA	0.67	2.50	1.67	3.0	2.1	22	1986
ASDEX-U	Germany	0.50	1.70	1.67	1.4	3.5	16	1991
TEXTOR-94	Germany	0.46	1.00	1.75	0.8	2.6	8	1994
FT-U	Italy	0.31	1.00	0.92	1.2	7.5	-	1988
TCV	Switzerland	0.24	3.00	0.87	1.2	1.4	4.5	1982
C-MOD	USA	0.22	1.80	0.67	1.5	8.1	4.5	1982
MAST	UK.	0.50	3.00	0.70	2	0.6	6.5	1999
NSTX	USA	0.67	1.90	0.85	1.0	0.6	11.5	1999

a = minor radius
κ = elongation
R = major radius
Ip = plasma current
B_T = toroidal field
P = heating power

One of the major obstacles to the progress of ITER and DEMO is the development of materials capable of supporting the hostile environment inside a fusion reactor, including high magnetic fields and high energy and particle fluxes. At present, it is not decided what materials will be used in these extreme conditions. Therefore, it is necessary to undertake exhaustive studies to characterise materials in conditions that should be as similar as possible to the conditions expected in a fusion reactor. In this framework, *TechnoFusión* will offer an ideal test bed for analysing and testing candidate materials for fusion reactors, while at the same time allowing to perfect new technologies, indispensable for the progress of ITER and DEMO.

After the achievement of the first experimental fusion reactor ITER, around the year 2.035, the scientific community will be prepared to undertake the next step towards developing commercial fusion reactors. DEMO (Figure 1.6) will be the first prototype of a commercial nuclear fusion power plant, and will use many of the components that have been tested in ITER. Advanced materials research for fusion will progress in parallel to the implementation of ITER, and will help to find new technological solutions for the challenges posed by DEMO and by the first commercial fusion energy power plants.

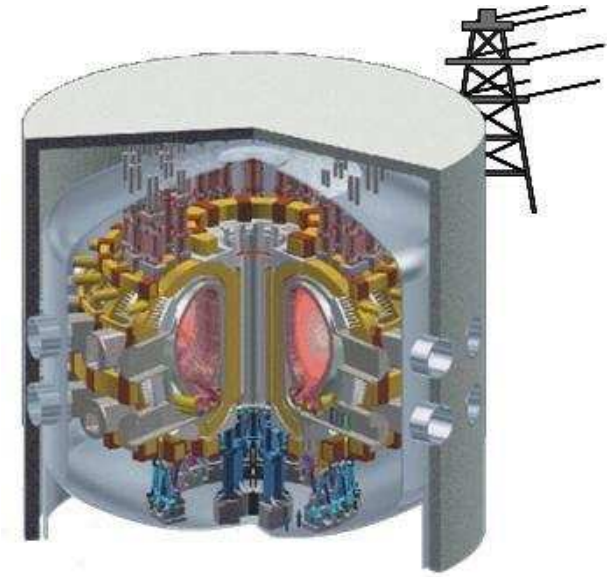

Figure 1.6. Design of DEMO, the first prototype of electrical power plant based on nuclear fusion.

2. Goals of the National Centre for Fusion Technologies

In recent years, Spain has gained a prominent position in the European fusion community as a consequence of Spain's candidature to host ITER at the Vandellós site. This prominence has materialised in the selection of Barcelona to host the European Fusion Agency, an entity that will manage the 2.000 M€ the EU will contribute to the construction of ITER. More importantly, fusion has received much public attention, resulting in a significant increase in the interest of companies and university groups to participate in the European Programme. Nevertheless, it will be difficult to maintain this situation and to benefit from the present positive mood in the absence of installations that allow participating in many of the areas of interest in the fusion field. In this framework, the construction of the Singular Installation of ***TechnoFusión*** is proposed, with the main objective to create a privileged platform to allow Spanish Research Centres, Universities, and companies to participate in the technological developments in the field of nuclear fusion. This Centre will place Spain at the forefront of research into the technological viability of fusion, while favouring its participation in the European Fusion Programme.

The ITER construction schedule covers 10 years, but due to the long manufacturing process of some components, the first contracts should be launched in 2009. This means that the technology required for the construction of those components must be available, so that only Spanish companies that already dispose of the required technology can hope to participate in their construction. In view of the long time needed for the development of new technology, *TechnoFusión* should focus on those areas that still require research and technological advances. Therefore, projects related to the European Long-Term activities were selected, along with IFMIF (in which Spain will have a certain prominence due to its contribution in the framework of the *Broader Approach*[16] *Agreement*, BA), and aspects of the ITER project that will be developed in the last phases of construction.

Furthermore, the "phase of engineering, validation, and prototypes" of the IFMIF project has been launched, and within about 4 to 5 years the international discussion concerning the site definition should begin. In view of this, it will be an additional objective of *TechnoFusión* to generate an infrastructure that will allow Spain to present a credible site candidature for IFMIF in due time, noting that this project has a value close to 1.000 M€. Nevertheless, this goal should be compatible with the continued activity in research and technological development of the Centre, even when the site candidature should not be successful. In any case, and apart from the site issue, the opportunities for Spanish industry and R+D Centres to participate in IFMIF will be significantly enhanced when Spain can build on the experience gained at this Large Installation and on its technical capacities.

[16] In February 2007, the EU and the Japanese Government signed the *Broader Approach* Agreement. The purpose of this collaboration is to complement the ITER project and to accelerate the implementation of fusion energy by performing R+D and developing some advanced technologies for the future demonstration fusion reactor (DEMO).

2.1. *Definition of prototype experiments*

Based on the above and on the various activities proposed for the *TechnoFusión* Installation, several types of experiments have been proposed that will contribute significantly to the objectives of the Centre.

2.1.1. Semi-industrial scale production of structural and functional materials for fusion

Presently, one of the main obstacles for the progress towards fusion lies in the production of reactor materials on an industrial scale. With few exceptions, candidate materials for application in fusion reactors are only produced on a laboratory scale. This is due, on the one hand, to the fact that the industry needs concrete norms and specifications before initiating the production of materials, and on the other, to the fact that the manufacturers are unwilling to invest in research and development when the market does not yet produce any demand and production costs are elevated. Results obtained using materials that are produced on a laboratory scale normally show large dispersions due to limitations of the amount of material, differences in composition, in production and processing techniques, etc., related to the fact that the materials are produced at different laboratories.

In view of the former, the European Fusion Programme has signalled the urgent need for some European laboratories to dispose of the capacity to manufacture single batches of material comprising several kilos (at least 50 kg/batch for steels or Fe-Cr alloys). In consequence, *TechnoFusión* will dispose of an installation for the production of structural and functional materials on a semi-industrial scale by means of a variety of techniques, some of which are quite scarce in Spain at this time. The *TechnoFusión's* Facility of materials production and processing will produce steels, Fe-Cr and V-Ti alloys, and oxide strengthened steels and alloys, in quantities from 2 to 50 kg, using techniques such as Inductive Melting in Vacuum, Mechanical Alloy production and Consolidation by applying an Isostatic Hot Press, or Sintering Assisted by a Continuous Pulsed Current. Also, structural and functional materials with nanostructure or ultra-fine grain size will be produced using an Isostatic Hot Press, or Sintering Assisted by a Continuous Pulsed Current, and W and B_4C coatings by the technique of Atmospheric Plasma Atomisation. In addition, certain materials will be processed by the application of thermo-mechanical treatments or Constant Angular Section Extrusion, in order to improve their mechanical properties.

2.1.2. Study of the effect on neutron radiation on nuclear reactor materials

The modification of materials by neutron radiation inside the fusion reactor is mainly due to two physical phenomena: 1) the displacement of the ions from their location in the crystalline network, leading to point defects, and 2) nuclear transmutation reactions, giving rise to the apparition of impurities (particularly H and He) in the interior of the materials.

Work with neutrons, like those produced at IFMIF, involves numerous technological difficulties, mainly due to the rigidity and the tremendous complexity of an installation of this type. In view of the former, these experiments will not be carried out using a neutron source, but the effect of neutron radiation will be simulated using ion implantation. In particular, H and He ions will be implanted simultaneously, along with heavy ions (Fe, Si, C, etc.), leading to similar point defects as those produced by a neutron flux. For this purpose, *TechnoFusión* will dispose of two light ion accelerators (H y He), and one heavy ion accelerator. These experiments will need to show that the damage produced in the material is equivalent, in terms of microstructure and impurities, to that produced in a fusion device.

These studies will provide support to the IFMIF and DEMO projects, both in the construction phase and in the operating phase of IFMIF.

2.1.3. Study of the joint effect of radiation and magnetic field on nuclear reactor materials

The materials composing the future reactors are not only subjected to large radiation doses, but also to intense magnetic fields. Up to now, only very few studies analyse the impact of radiation on the microscopic and/or macroscopic properties of the materials in the presence of magnetic fields. *TechnoFusión* will dispose of a high-field magnet (between 5 and 10 T) that will enable such studies. The execution of these experiments will require a neutraliser, in order to ensure that the particles used to irradiate the material are not deflected by the magnetic field.

2.1.4. Evaluation of radiological risks

Apart from analysing the radiation damage in nuclear reactor materials, *TechnoFusión* will perform a detailed evaluation of radiological risks associated with the operation of the accelerators (the generation of ionising gamma radiation, and, occasionally, high-energy neutrons).

Furthermore, the isotope content (both radioactive and stable) of some irradiated materials will be determined. Such studies provide information on the activation of materials and decay times (relevant for radiological safety), and on the degree of impurity, which is important from the point of view of eventual compositional changes and the generation of light gases (H and He) that should not exceed those expected in fusion conditions.

2.1.5. Studies concerning the interaction between the nuclear plasma and the surrounding reactor elements

Among the important technological challenges posed by the operation of ITER, the phenomena related to the interaction of the plasma with surrounding material elements (the

first wall, the divertor, limiters) are certainly among the few that can affect the success of the project directly.

Up to now, numerous experiments have been performed, both in the laboratory and in fusion devices, to determine the behaviour of the materials that have been selected for the divertor (carbon in the form of carbon fibre composites, and tungsten) and the first wall (Beryllium) of ITER, when these are subjected to high heat loads or high particle fluxes, and how these results depend on the prior irradiation by energetic particles. Some evidence exists to suggest that the simultaneous action of these mechanisms (high heat, particle, and radiation fluxes) can produce synergetic effects with as yet unknown consequences. In general, it is found to be very hard to extrapolate laboratory results to fusion devices, mainly because of the complexity of the conditions of the latter.

Presently, no single installation has the capacity to study the synergies mentioned above directly. The proposed installation for the study of the plasma-wall interaction at *TechnoFusión* pretends to fill this gap, thus becoming the first installation of its kind worldwide. To perform these studies, *TechnoFusión* will dispose of an installation (denominated "plasma gun") in which the interaction between plasmas and materials can be studied, both in steady state and during transients, simultaneously and in fusion reactor relevant conditions. These experiments will allow studying the behaviour, and the modifications, of the materials that are closest to the plasma inside the reactor.

2.1.6. Studies of liquid metal phenomena

Liquid metals are of utmost importance for fusion technology, in view of their role in system cooling components, tritium breeding blankets, and many elements exposed to the plasma: the first wall, divertors and limiters. *TechnoFusión* will dispose of a liquid lithium installation (denominated "lithium loop") that will allow validating the design tools for IFMIF; and a neutron source based on the interaction between deuterons and the free surface of a liquid lithium flow.

The proposed liquid metal installation can be used to perform the following experiments:

- *Studies on the stability of lithium for IFMIF and limiters*: the lithium loop will have a liquid metal free surface zone in vacuum conditions, which allows studying the stability of the free surface.

- *Studies of the interaction between liquid lithium and fusion materials*: the liquid metal loop will have a zone where the liquid lithium can be brought into contact with various candidate materials for fusion (EUROFER steels, ceramics, helium, beryllium, carbon fibre composites, etc.). Corrosion can be studied as a function of velocity and temperature, as well as the modification of the structural properties of alloys, etc.

- *Studies of the impact of radiation on the properties of the liquid lithium:* the free surface zone of the liquid lithium can be irradiated with gamma radiation (using

the electron accelerator) in order to determine the effect of internal heat deposition and to study the compatibility of structural materials with liquid metal and radiation.

- *Studies of lithium enrichment techniques*: currently, some conventional techniques exist for lithium enrichment, as well as some techniques that have not been tried. The installation will dispose of a lithium sub-loop where a proper technique for lithium enrichment will be developed.

- *Study of liquid metal purification system*: in view of the need to eliminate impurities and gases from the lithium after it has circulated through the experimentation zone, a purification system is needed that will itself be the object of further study, in order to improve the purification and recovery of lithium, of vital importance for IFMIF and ITER.

- *Tritium extraction system*: in another liquid lithium sub-loop, the retention, permeability, solubility and diffusivity of tritium will be studied. There, scaled-down versions of permeation barriers and tritium extraction systems will be developed, for future application in a nuclear reactor.

- *Safety studies*: various sub-loops will be implemented to study critical safety factors related to the handling of liquid lithium, such as its reaction with water, residues, impurity control, etc.

2.1.7. Characterization of manufactured and/or modified materials

The understanding of the mechanisms by which structural defects are formed in fusion reactor materials is essential to predict the behaviour of the devices and components and to be able to propose new alloys that are more resistant to the operational conditions of future reactors. To address this issue, the *TechnoFusión* installations will dispose of an important set of equipment and techniques for testing materials and components and to characterise the damage suffered by structural and functional materials, as well as components or elements with a certain complexity, in conditions similar to those occurring in a device like DEMO. Some of the cited techniques are: techniques for the analysis of the mechanical behaviour (machines for mechanical tests, thermal fluency, nano-indenting, etc.), techniques for compositional analysis (Secondary Ion Mass Spectrometry and Atom Probe Tomography), structural and micro-structural techniques (X-Ray Diffraction, Scanning and Transmission Electron Microscopy, etc.), materials processing techniques (Focused Ion Beam Systems), and techniques for the analysis of physical properties (electrical conductivity, dielectric properties, optical properties, etc.).

The main experiments that will be performed are:

- The optical, electrical and dielectric characterization of radiation damage.

- Compositional and structural characterization.

- Mechanical tests of irradiated material.
- Mechanical tests of materials during irradiation.
- Tests of new materials and components.

These experiments will allow determining the operational adequacy of the materials when irradiated with ions and neutrons or when in contact with fusion plasmas or liquid metal, etc.

2.1.8. Experiments in robotic and remote handling

The operation of future fusion reactors will require an extraordinary development of robotic systems for remote handling, whether autonomous or remotely controlled by an operator. In this respect, *TechnoFusión* will dispose of special installations where the various robotic devices and procedures for the maintenance and repair of nuclear fusion installations can be tested and optimised, such as ITER and IFMIF. These tasks will be centred on the following general work areas:

- *The development of specific robotic systems:* e.g., high performance robots for the handling of large or heavy objects.
- *Remote operation and control of robotic systems (remote robotics)*: e.g., remote handling tests of the ITER diagnostic ports or IFMIF prototype modules.
- *The validation and certification of elements and equipments exposed to radiation*: studies will be made regarding the radiation resistance of the components of robotic systems. Experiments will be performed using the electron beam to irradiate robots arms and other robotic elements, in a hall prepared for this purpose.

3. Scientific and technical structure of the Centre

TechnoFusión will be founded as a singular installation, structured around seven major facilities of research and experimentation for the development of various fusion-related technologies. A detailed description of each of these facilities will be provided in chapter 4 and following of this report. Below, a brief description of these facilities is given:

a) **Material Production and Processing**. The goal of this facility is the development of new experimental installations for the manufacture of components on a semi-industrial scale and of materials for the experiments of *TechnoFusión*. For this purpose, it will dispose of the required equipment to produce prototype materials with relevance for fusion, such as metals or oxide strengthened low activation steels, of the ODS type. The equipment used will include the following items, currently scarce in Spain: a Vacuum Induction Furnace, an Isostatic Hot Press Furnace, a Sintering Furnace Assisted by a Continuous Pulsed Current, and a Vacuum Plasma Projection System.

b) **Material Irradiation**. In this experimental facility, the effect of neutrons and gamma radiation on materials will be evaluated by simulating their effect using ions and electrons. This will allow testing components in a hostile environment similar to the situation in ITER. In order to simulate the neutron radiation, three ion accelerators will be used simultaneously: one light ion accelerator of the tandem type for irradiating with He, with an energy of 6 MV, one light ion accelerator of the tandem type for irradiating with H (or D), with an energy of 5-6 MV, and a heavy ion accelerator of the cyclotron type, with k = 110, to implant heavy ions (Fe, W, Si, C) or high energy protons. In addition, a high field magnet will be used to study the simultaneous effect of irradiation and magnetic fields on materials. The effect of ionizing gamma radiation will be simulated by an electron accelerator of the *Rhodotron* type with a fixed energy of 10 MeV.

c) **Plasma-Wall Interaction**. In order to reproduce the expected plasma-wall phenomena, two plasma generation devices will be used: a linear plasma device and a linear Quasi-Stationary Plasma Accelerator (QSPA). These devices will be capable of producing linear H, D, He, and Ar plasmas, both continuous and pulsed, that will be used to study the interaction of high density and low temperature plasmas with the structural materials of the first wall of the fusion reactor. In addition, these machines will be able to produce thermal heat loads to simulate transitory turbulent and perturbative events in the exterior of the plasma.

d) **Liquid Metal Technologies**. This experimental facility will dispose of various liquid lithium loops, connected to the electron accelerator with the purpose of characterising the lithium free surface and its compatibility with the structural material in combination with high radiation levels. In addition, the modification of the mentioned phenomena due to the presence of magnetic field will be studied. Finally, technologies associated with the purification of the liquid metal and material corrosion mechanisms will be developed.

e) **Characterization Techniques**. A wide range of techniques will be implemented for the exhaustive characterization of the materials prepared for and/or modified in the various experimental facilities of *TechnoFusión* (Material Production and Processing, Material Irradiation, Plasma-Wall Interaction, Liquid Metal Technologies, and Remote Handling Technologies). These techniques include mechanical techniques (electromechanical devices, miniature mechanical testing devices, thermal fluency testing devices, nano-indenting techniques, etc.), compositional techniques (Secondary Ion Mass Spectrometry and Atomic Probe Tomography), structural and microstructural techniques (High Resolution Transmission Electron Microscopy and X-Ray Diffraction), and material processing techniques (Focused Ion Beam Systems coupled to a Scanning Electron Microscope). Various systems will be used to characterise physical properties (electrical, dielectric, optical, etc.). Some of the mentioned techniques, such as the Secondary Ion Mass Spectrometry or the Atomic Probe Tomography, are not currently available in Spain, so that their incorporation in *TechnoFusión* has an important national significance.

f) **Remote Handling Technologies**. In order to perform robotics studies, an installation will be provided where large scale components can be manipulated in order to validate remote maintenance operations. Some of the prototypes under consideration are: an installation for the demonstration of the manipulation of the *Port Plugs* of ITER, an installation to study the remote manipulation of the *Test Blanket Modules,* which include the reactor first wall, the coolant, the tritium regeneration device, etc., and an installation to demonstrate the remote manipulation of the IFMIF irradiation modules. One of the installations will be connected to the electron accelerator, where the prototypes can be subjected to gamma radiation in order to simulate the operating conditions during maintenance operations in a reactor.

g) **Computer Simulation**. The goal of this facility is to develop a complete computer simulation of the components of the *TechnoFusión* installations and their dynamical behaviour in a future fusion reactor. Furthermore, solutions will be sought for various pending physics issues with a decisive impact on future technological advances in the fusion field. For this purpose, use will be made of the latest computational techniques and codes, such as ACAB, FISPACT, ORIGEN, CHEMCON, MELCOR, MACCS (for radioactive safety, waste management, etc.), MCNPX, PHITS, SRIM, TMAP, EMPIRE-II (for radiological protection, the analysis of nuclear data), etc.

An installation like *TechnoFusión* implies an important technological effort, even in the design and construction phases of the project. Thus, through this Centre, our country will become a scientific and technological country of reference, with the capacity to opt for large contracts for the development of fusion technology.

It should be emphasised that some of the proposed Areas of Research, like Material Irradiation, Plasma-Wall Interaction, and Remote Handling Technologies, as well as some equipment of the Facility for Material Production and Processing (VIM, SPS) or Characterization Techniques (SIMS, APT) constitute, by themselves, installations and techniques of significance, both nationally and internationally. Thus, although the main objective of *TechnoFusión* is the development of fusion technology, it will also provide services

to the international scientific community, providing a test bench for experiments in other fields of physics, chemistry, biology or other scientific disciplines.

4. Material Production and Processing

4.1. Introduction

The main critical materials in fusion reactor are those used in the structure of the plasma facing wall, (i.e. the blanket and the divertor, which are the devices for primary heat removal), plasma purification and tritium breeding, as well as others used in the vacuum vessel, cryostat, superconductor coils, magnet shield, containment structure and auxiliary systems for plasma heating and fuelling.The interaction of the plasma and radiation with *Plasma Facing Materials* (PFMs) and other component materials of the reactor vessel will be a severe problem because these materials will be subjected to very high fluxes of energetic particles and heat. The first wall of the plasma chamber will be irradiated by energetic charged particles, a very intense flux of electromagnetic radiation and neutrons with energy up to 14 MeV. This will modify the material properties at a rate, and to an extent, that will depend on proximity to the plasma. Perhaps, this is the more urgent issue to be resolved in order to make nuclear fusion an economical and safe energy resource. Plasma facing parts and other components next to the plasma will have to perform under extreme conditions so that the plasma can achieve the operating parameters that will make the fusion reactors into profitable devices for energy production. Therefore, the structural materials for fusion applications must possess a much broader combination of properties that those so far demanded for materials used in current power generation systems or other demanding devices.

There are three groups of key materials to be developed for nuclear fusion technology:

a) PFMs used for fabricating blanket and divertor system parts.

b) Structural materials for holding the first wall components, the plasma chamber and the magnetic shield, and for building the refrigeration system and other ancillary systems.

c) Materials termed as “functional materials” because they have the capability to work as tritium breeder, refrigerant or neutron multiplier, simultaneously. The ceramic materials used in plasma diagnostic systems also fall within this material type.

The PFMs are required to possess high thermal conductivity, good mechanical strength and toughness, low hydrogen retention, reduced activation induced by irradiation, as well as being radiation hard, plasma erosion resistant and non magnetic. At present, materials complying with all the design requirements established for the plasma facing components (PFCs) are not available. However, *Carbon Fiber Composites* (CFC), Be and W, and its alloys, are being considered as potential PFMs. However the properties of these materials, and their interactions with plasmas, are very different. Therefore, a full understanding of plasma and irradiation effects on these materials is imperative for developing the PFMs required for future fusion reactors.

W, and some of its alloys, appears to be the most promising PFMs for the divertor system due to their capability to withstand high heat fluxes and to resist plasma erosion. In addition, *Oxide Dispersion Strengthened steels* (ODS), coated by a protective W layer, are considered potential materials for building PFCs. In any case, the use of W and its alloys

demands improvements in their mechanical properties, and the behaviour and stability of their microstructure at high temperatures and under irradiation.

The above mentioned concerns for PFMs also arise for other structural materials that may be exposed to extreme conditions of irradiation, temperature and heat load, as well as thermal stresses, and fluids at high temperatures and pressures. These materials, as well as possessing low induced activation and very good mechanical properties, have to remain stable in an appropriate temperature range, and be radiation resistant. Some austenitic steels such as 316LN-IG (ITER Grade), specifically modified for application in ITER, *Reduced Activation Ferritic-Martensitic* (RAFM) steels, advanced ferritic steels with Cr content as high as 14 wt %, V-Ti alloys as well as SiC composites are candidate materials for such structural applications. Current research activities on these materials are focused on expanding their operating temperature window by means of improving their mechanical strength, toughness and radiation damage resistance, lowering the *Ductile-Brittle Transition Temperature* (DBTT), and stabilizing the microstructure via oxide dispersion.

Among other potential functional materials Be, Pb as well as $Be_{12}Ti$ and $Be_{12}V$ are considered for neutron multipliers, Li_2O based ceramics for tritium breeding and Li, Li-Pb and Li-Sn alloys as breeding coolants. In the case of ceramic materials for fusion applications, research program are focused on the effect of irradiation on electrical and thermal conductivity, optical properties, tritium retention and structural integrity.

At present, research and development of fusion materials are limited because effects on materials exposure to 14 MeV neutrons, as well as plasma from a power fusion reactor, are unknown due to the lack of facilities for accomplishing experiments under such conditions. A solution to this would be the build and start up of IFMIF. Another significant obstacle for fusion material development is their fabrication on an industrial scale. Currently, with some particular exceptions, materials with properties satisfying the design conditions required in fusion reactors are only produced on a laboratory scale. This occurs because industry demands precise specifications and standards before beginning their industrial production, as the costs are very high and companies are reluctant to undertake research on these materials as the current commercial demand is inexistent.

As outline above, current research and development of fusion materials falls on laboratories supported by public funds and associated with organizations responsible for the coordination of international fusion research programs. Under such circumstances, the research results obtained from materials that are produced in different laboratories usually yield discrepancies due to differences in the composition, fabrication techniques and processing conditions, as well as to a shortage of material for undertaking a rigorous and complete characterization.

The advisers and coordinators of the European Fusion Material Program bemoan the lack of interest of European industries to produce materials for fusion research laboratories. They have also highlighted the lack of research laboratories with capacity to manufacture in a single batch, a quantity of material sufficient for full characterization by the groups in charged of the investigation of the relevant material. In the European Program have been suggested the urgent need of having some European laboratories with the capability to manufacture a single batch so much material. These should be at least 50 kg per batch in the case of steels or

Fe-Cr alloys. In this sense, the **Material Production and Processing Facility (MPP)** of *TechnoFusión* will try to contribute to this part of the European Fusion Material Program.

4.2. Objectives

The present European Materials Fusion Program, in its middle- and long-term research activities, gives priority to research and development of the following materials:

1) Low activation steels for the blanket system, such as the EUROFER steel for the blanket module to be tested in ITER, and other nano-structured steels to be used in DEMO. The mid-term aim is to optimize the low activation steel for use in future reactors. The development of ODS steels is a long-term proposal. It is expected that such low-activation and radiation-hard steels can achieve a more stable microstructure with better mechanical behaviour at high temperatures than conventional steels to be used in the divertor and breeding blanket systems. Another research activity in this area is dedicated to nano-structured ferritic steel based on the Fe-14 wt% Cr alloy.

2) W and its ODS alloys for use in a divertor system cooled by He, where the operating temperature window may be 700 – 1350 ºC. The aim is to increase the microstructure stability at high temperatures, lower the DBTT and improve ductility at low temperatures.

3) SiC_f/SiC composites for advanced blanket systems cooled by Li-Pb. The aim is to develop new fibre coating manufacturing methods and techniques for optimizing the mechanical properties and thermal conductivity.

4) Functional graded materials, ceramics and coatings.

Although the guidelines of the present European Materials Fusion Program are mainly focused on the above mentioned types of materials, the corresponding programs in Japan, Russia and USA also maintain an intense long-term activity on Ti-V alloys and on an ample variety of functional materials.

Considering the guidelines of the European Materials Fusion Program, the main objectives of the MPP Facility are:

- To achieve facilities for producing batches of fusion materials within the framework of the European Program.

- To fabricate and process materials requested by users of *TechnoFusión*.

- To fabricate batches of structural materials of up to ~50 kg by means of the *Vacuum Induction Melting* (VIM) technique for fusion applications. These materials would be steels, Fe-Cr, V-Ti, and other alloys with precise control of impurities.

- To produce ODS steels, ODS Fe-Cr alloys, and ODS and non ODS W alloys by mechanical alloying and consolidation by *Hot Isostatic Pressing* (HIP) or *Spark Plasma Sintering* (SPS) techniques. It is intended to fabricate, by HIP, up to10 kg of material per batch.

- To produce nano-structured steels and alloys, or ultrafine grained, via HIP or SPS techniques.

- To achieve facilities for processing materials by thermo-mechanical treatments and severe plastic deformation techniques, such us *Equal Channel Angular Pressing* (ECAP), in order to improve their mechanical behaviour.

- To develop coating techniques with W and multifunctional ceramics layers using the *Vacuum Plasma Spraying* (VPS) technique.

The MPP Facility is planned for providing materials following the guidelines of the European Fusion Material Program and would direct its activities to develop the following materials and techniques:

1) Low activation and irradiation resistant materials for structural applications, specifically ODS and non-ODS steels and Fe-Cr model alloys.

2) ODS and non-ODS W alloys for the first wall and the divertor system.

3) Fabrication of nano-structured materials, metal-ceramic joining via the HIP and SPS techniques.

4) ECAP processing of steel and Fe-Cr alloys.

5) W and ceramic coatings produced by the VPS technique.

4.3. International status of the proposed technologies

4.3.1. Techniques of production and processing of fusion materials

(I) Vacuum Induction Melting furnace

VIM is the fabrication technique of metal alloys via melting and refining of metal components under high vacuum in an induction furnace. The metal components are melted in a crucible inside a vacuum chamber and the melt is then poured into moulds. This technique produces alloy ingots with a homogenous composition and extremely low content of interstitial impurities: e.g. O, N, H and P. VIM is the most successful technique for the fabrication of high purity steels and alloys that have metals such as Zr, Ti and V with a very high oxygen affinity. Compared with traditional steelmaking furnaces, modern VIM furnaces have several advantages:

1) Extremely pure steels and super alloys, as well as alloys containing reactive metals, can be produced.

2) Very precise control of temperature, composition and residual atmosphere.

3) Extraction from the melt of gasses and other impurities in solution.

4) Electromagnetic stirring for melt homogenization.

5) Very easy and safe operation.

Figure 4.1 shows some VIM applications in the production and processing of materials.

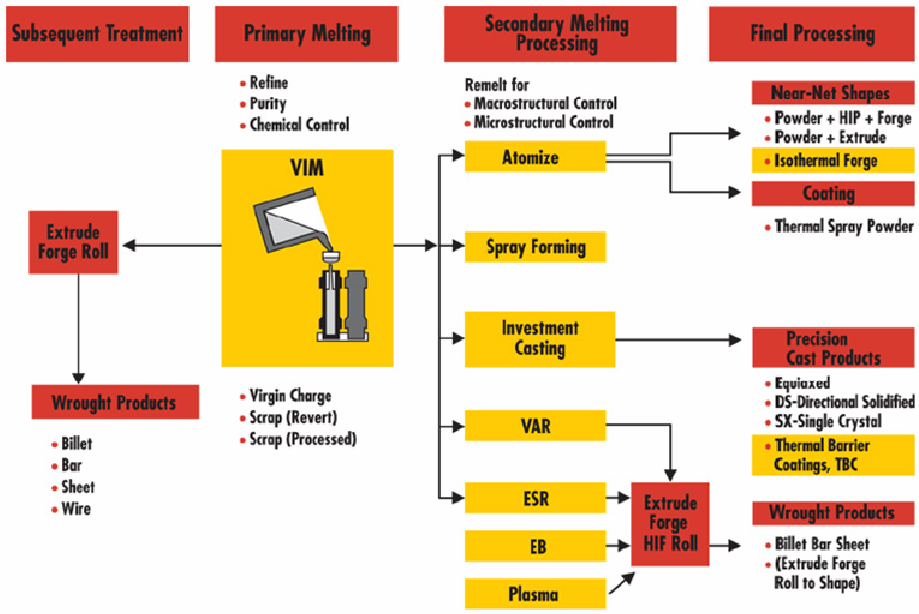

Figure 4.1. Applications of the VIM technique to fabrication and processing of materials.

(II) Hot Isostatic Pressing Furnace

The HIP technique consists of the simultaneous application of high pressure and heat to a material in order to achieve consolidation, sintering, shrink, densification and removal of internal porosity. Typically, temperatures and pressures above 1000 ºC and 90 MPa are employed. The pressure fluid is usually argon or nitrogen, and heating is by electric current. HIP can be used for processing any material: metals, ceramics, polymers, composites and polymers. This technique is successful for producing advanced alloys having a specific composition or microstructure, as well transparent ceramics, which cannot be developed by

other techniques. Moreover, it is used to diffusion bond similar and dissimilar materials that cannot be bonded otherwise.

The HIP technique is of great interest for fusion material development. It was originally developed for nuclear technology to join materials difficult to bond by diffusion, but its use has been extended to all fields of material production and processing. In the case of a starting material such as a mechanical alloyed powder, or a simple powder blend, it is encapsulated into steel cans or glass ampoules. After the process of HIP consolidation, the material should be fully dense, isotropic and porosity free, these being significant advantages compared to traditional sintering techniques or others such as consolidation by extrusion. The technique permits the fabrication of ingots of materials whose composition and microstructure is unattainable by casting from melt and subsequent forging or extrusion, as well as components with a complex geometry and precise dimensions.

At present, large furnaces with capabilities for operating at temperatures and pressures as high as 2200 ºC and 400 MPa, respectively, can be built. This has enabled HIP to be successfully applied in research and development of materials and processing techniques of interest for fusion technology, e.g. ODS steel and alloys, nano-structured materials, advanced composites and ceramics, as well as techniques of joining and coating.

(III) Spark Plasma Sintering Furnace

The SPS technique has appeared as an alternative consolidation and sintering technique to HIP and traditional sintering. Recent improvements in the SPS systems have converted this technique into the most suitable, among current techniques, for fabricating nano-structured and functionally graded materials, metallic and ceramics. During the SPS process material is consolidated very quickly by means of Joule heating produced by Direct Current (DC) pulses of very high current density that are applied maintaining an applied uniaxial pressure. The DC current pulses stimulate sintering of the material by virtue of plasma generation and electromigration induced by the high current density developed at the contact points between powder particles.

A SPS system equipped for the fabrication of advanced ceramics, functionally graded materials, and refractory alloys is proposed for the MPP Facility. This system will also have the capability to perform coating and diffusion bonding experiments.

(IV) Vacuum Plasma Spraying System

Protective coatings on PFCs or on other parts of the plasma chamber of a fusion reactor could be developed by projecting droplets of molten material at high velocity onto the substrate. The molten droplets form injecting powder of the protective metal or ceramic into a jet of hot plasma. An electric arc between a finger-like W cathode and a cylindrical Cu inner anode contour, or more simply a cone-shaped nozzle anode, creates the plasma, i.e. the VPS torch. The high droplet impact velocities and low oxidation associated with VPS permit the fabrication of ~100% dense coatings with thickness ranging between 20 µm and 2 mm or

more. During spraying the system chamber is maintained at a low pressure of inert residual gas, typically 50 – 200 mbar, in order to avoid oxidation of the coating. An additional advantage of VPS for protective coating is the possibility of performing surface treatments of the substrate, while inside the chamber, immediately before the coating process for improving adhesion of the coating to the substrate. Vacuum plasma spraying is preferred to atmospheric plasma spraying for oxidation sensitive materials such as W alloys, and/or where improved adhesion and density is required.

The general features of the SPS process are:

- Produces extremely clean coatings that are nearly fully dense
- Rapid processing times
- Spraying of refractory metals is possible
- Very thick coatings are possible
- Creation of near-net shapes is possible
- Superior control of coating thickness and surface characteristics. High deposition rate
- High bond of a coating to the substrate
- In-chamber final cleaning using *Reverse Transferred Arc* (RTA) process
- Coating of complex geometries
- Fully automated processes
- Flexible system configurations such as:
    - High volume, continuous-operation system configurations using one or more load lock systems and transfer chambers
    - Batch processing system configurations using robotics and other dedicated manipulation methods

The above characteristics allow development of functionally graded W coatings onto ODS steels for PFCs, thereby reducing concerns about thermal expansion coefficient mismatches between W and steel substrates.

4.3.2. Laboratories of reference in production and processing of fusion materials

As mentioned above, a laboratory for the production and processing of fusion materials with the herein proposed features is an urgent requirement for the European Program for Fusion Materials Development. At present, there exists a very limited number of fusion materials research centres with facilities to produce and process, using the proposed

techniques, the quantities of material required for planned characterization programs and irradiation experiments within existing international collaborations. These are:

- *Oak Ridge National Laboratory (Materials Science and Technology Division)*, Oak Ridge (USA).
- *Forschungszentrum Karlsruhe FZK (Institute for Materials Research I, II and III)*, Karlsruhe (Germany).
- *Commissariat à l´Energie Atomique (CEA)/ Direction des Sciences de la Matière*, en Grenoble, (France)

4.4. Projected devices and equipment

It is envisaged that the MPP Facility of *TechnoFusión* would have three separate areas, each of which with different facilities. These are listed below together with their proposed facilities.

- *Metal casting and processing*
  - A VIM furnace
  - Machines for material processing and for thermo-mechanical treatments: swaging, ECAP, rolling and forging.
- *Powder metallurgy and ceramic materials*
  - A HIP furnace
  - A SPS furnace
  - A VPS furnace
  - A cold isostatic press
  - Atmosphere controlled and vacuum furnaces
- *Control and analysis*
  - Equipment for control and analysis of raw and processed materials.

4.4.1. Vacuum Induction Melting furnace

This facility will be dedicated to the production of special steels, Fe-Cr alloys and super-alloys.

VIM and casting is the usual method for fabricating high purity steels and alloys having an accurate composition as well as an effective reduction of interstitial impurities and oxide formation that are detrimental to their mechanical properties. The basic required features for such a furnace are:

- Crucible volume: ~ 3 - 8 l
- Maximum steel capacity: ~ 50 kg
- Power supply for melting: ~ 100 kW
- Base vacuum: $1x10^{-5}$ mbar
- Pumping rate: 6 m^3/min

Accessories:

- Vacuum chamber for pre-heating mould and for casting in vacuum.
- Electromagnetic stir for melt homogenization.
- Automatic loading system.
- Systems for temperature and pressure measurements..

VIM systems with the above features will be built to order by specialized companies that will design and assemble these systems. For instance, ADL (Germany) design VIM systems that might fulfil our requirements. To date, two VIM designs from ADL have been considered for the MPP Facility:

a) A two chamber design VIM-VMC with a vertical mould chamber (Figure 4.2).

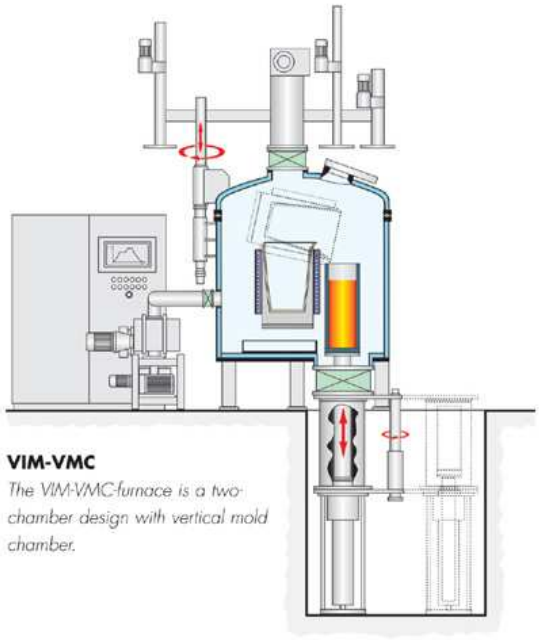

Figure 4.2. Two-chamber VIM-VMC design with vertical mould chamber.

b) A two chamber design VIM-HMC with a horizontal chamber for mould pre-heating and casting in vacuum (see Figure 4.3)

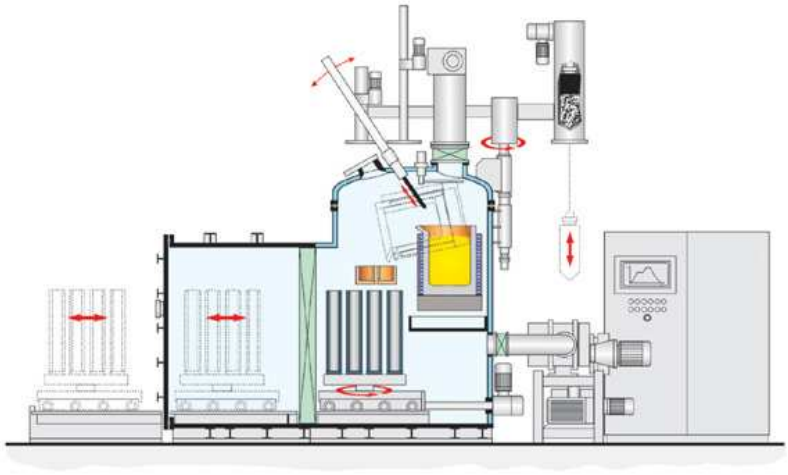

VIM-HMC

Typical charge wheights: 0.5 to 20 tons; two-chamber system with horizontal mold chamber.

Figure 4.3. Two-chamber VIM-HMC design with horizontal chamber for mould pre-heating and casting in vacuum.

4.4.2. Hot Isostatic Pressing furnace

This facility will be use for compacting metallurgy processed powdered alloys as well as structural and functional ceramics, and for joining and improvement of cast alloys. The required basic features are:

- Maximum working pressure: 400 MPa
- Maximum working temperature: 2000 ºC – 2200 ºC
- Hot zone dimensions: ~200 mm Ø×800 mm; minimum 140 mm Ø ×250 mm

There are two companies that offer HIP designs that incorporate these features with the required standards:

a) The model AIP10-60H furnace by American Isostatic Presses[17] (Figure. 4.4.) This furnace features a 140 mm Ø x 254 mm hot zone, a maximum working temperature and pressure of 2200 ºC and 414 MPa, respectively.

Figure 4.4. The AIP10-60H HIP furnace from American Isostatic Presses.

b) The model QIH21 furnace by Avure Technologies[18] for research and pilot production manufacture (Figure 4.5). It is a high capability furnace with a ~250 mm Ø x 900 mm hot zone, which allows processing of steel ingots of up to 12 kg. A layout of the system configuration is shown in Figure 4.6.

Figure 4.5. Avure Technology HIP furnace QIH21 for research and pilot production.

[17] http://www.aiphip.com/WebPages/hip.htm.
[18] http://www.hasmak.com.tr/tozpdf/Avure-HIP-Brochure.pdf.

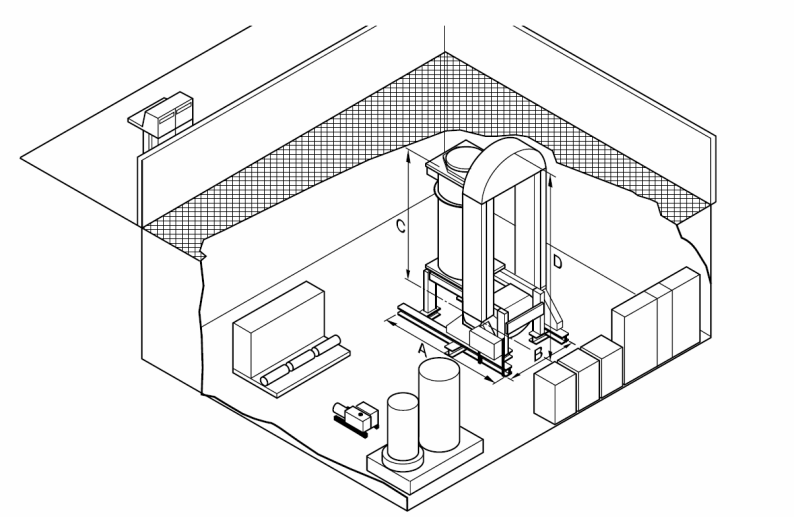

Figure 4.6. Dimensions of the HIP furnace QIH21. A = 1.9 m; B = 1.4 m; C = 2.7 m; D = 3.5 m.

4.4.3. Spark Plasma Sintering furnace

Such a facility would be used for fast sintering, joining, fabrication of nano-structured materials such as ODS alloys and functional ceramics, as well as coatings of functionally graded materials. The required basic features are:

- Maximum working temperature: ~ 2200 ºC
- Maximum pressing force: ~ 1.250 kN
- Maximum current: 30 kA DC
- Power supply: 350 kVA
- Pulse duration: 1 – 255 ms
- Double wall chamber for sintering in vacuum and controlled atmospheres
- System for working in hydrogen
- System for working in vacuum

The model FCT-HPD 125 furnace by FCT System GmbH[19] (Germany) satisfies these requirements. It can mount moulds as large as 350 ∅ mm x 300 mm and can achieve a maximum working temperature of 2400 ºC. The furnace is shown in Figure 4.7.

Figure 4.7. SPS model FCT-HPD furnace by FCT System GMBH.

4.4.4. Vacuum Plasma Spraying facility

This facility will be dedicated to developing protective surface coatings for PFMs, thereby permitting the desired operation of PFCs in the plasma chamber of a fusion reactor. The VPS system recommended for the Facility of MPP should have the following capabilities:

- A revolving stage for handling components for coating.
- A chamber for large work pieces.
- Manipulators for work pieces and plasma gun.
- Reverse transferred-arc for substrate cleaning.
- Plasma guns that give rise to minimum heating of the substrate under coating conditions.

[19] http://www.fct-keramik.de

- Variable operation conditions.
- Growing rates as fast as 10 μm/min.
- Power up to 180 kW.
- Coating thickness in the range 20 microns – 2 mm.

Sulzer Metco[20], the leading company in the development and construction of VPS systems, has recently improved the VPS technique by the development of a new *Low Pressure Plasma Spray* (LPPS) system, whose advantages and chamber configuration are shown in Figure 4.8. Such a system fulfils the above requirements for PFM protective coatings, in particular for the reliable coating of large surface areas with complex surfaces such as those of PFCs. The characteristics of a Sulzer Metco LPPS system are:

1) A large (4 m^3 volume) vertically oriented chamber that permits protective coating of large surfaces.
2) The use of a tungsten insert in the copper anode that allows torch operation with electrical currents exceeding 2.5 kA thereby achieving input powers well above 100 kW.
3) Adjustable positioning of the axial and radial positions of the plasma jet by means of linear movements of the gun along the torch (z-position) and/or perpendicular axis (x- and y-positions).
4) Fast charge and discharged without alterations in the chamber pressure.
5) Variable projection distance, between 15 and 135 cm, to allow different coating conditions.
6) Capability for coating surfaces, with complex geometries, as large as 70 cm x 70cm.
7) Advanced control of the chamber and plasma jet.
8) Plasma gun operation at spay pressures as low as 1 mbar.
9) Possibility for developing multi-coatings.

A schematic arrangement of the gun inside the LPPS chamber is shown in Figure 4.8, along with the installed plasma jet and particle diagnostics.

Figure 4.9 shows a Sulzer Metco VPS system with the above characteristics that would be successful for coating of large PFCs.

[20] www.sulzermetco.com

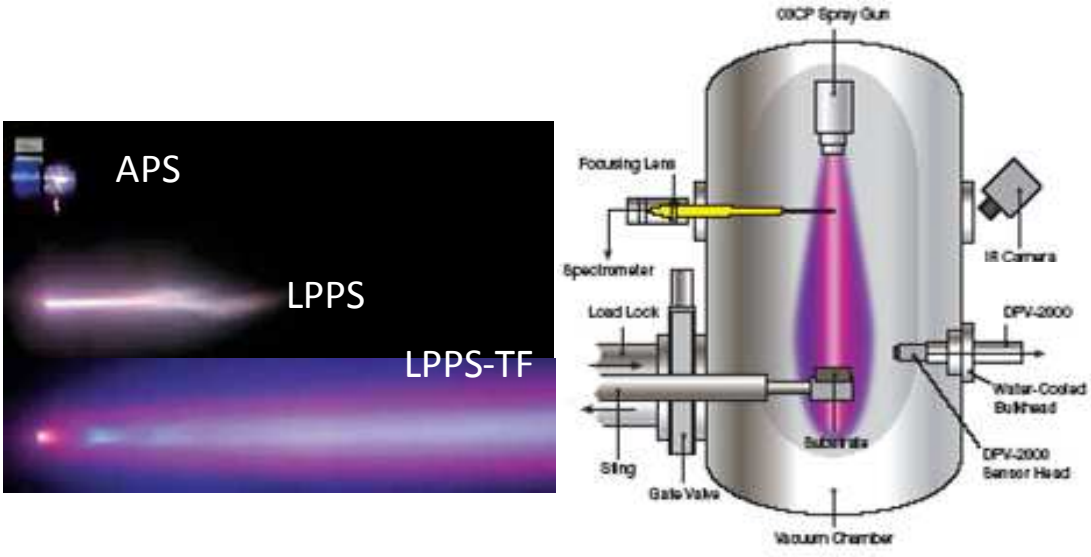

Figure 4.8. (Left) Comparative images of a plasma beam in (APS) an air plasma spray system at 1 bar and in a LPPS system operating (LLPS) at 50 mbar and (LPPS-TF) 1 mbar. (Right) Schematic layout of the Sulzer Metco LPPS-TF system for fast growing of extremely dense and thin coatings.

Figure 4.9. Sulzer Metco VPS system suitable for protective coating of large PFCs.

4.4.5. Attritor and planetary mills

It is also considered that the MPP Facility should be equipped with a high capacity attritor for powder processing in controlled atmospheres, at least, and several types of high-energy planetary mills for mechanical alloying as well as their corresponding sets of jars for proper powder processing. The characteristics of such equipment are detailed in: *Union Process*[21] y *Retsch*[22] .

The attritors and planetary mills will be installed in an area with the following services utilities:

- Temperature and humidity control in the range 5 – 25 ºC with maximum humidity below 60% at 25 ºC.
- Soundproof capability for a sound level of about 90 dB.
- Electric power supply and closed circuit water cooling.
- Supply of gasses (Ar, He, H, etc.).
- A cabinet for safe powder handling.
- Two glove boxes with controllable atmospheres.
- A system for air displacement detection.

4.4.6. Cold Isostatic Press

The MPP Facility should have a CIP system for compacting powders before sintering. The required specifications for this system are:

- Compacting vessel dimensions, (minimum): ~75 mm x 300 mm.
- Maximum pressure: ~ 400 MPa.
- Automatic control of pressurization and depressurization.
- A quick-fill reservoir and electrohydraulic pumping.
- A two-stage letdown system.

[21] www.unionprocess.com/pdf/lab_attritors.pdf
[22] www.retsch.com/dltmp/www/36276-acdd0376481f/brochure_ball_mills_en.pdf

The model AIP3-12-60C CIP system by American Isostatic Presses[23], shown in Figure 4.10 could fulfil the requirements.

Figure 4.10. The model AIP3-12-60C CIP system for American Isostatic Presses.

4.4.7. Vacuum and controllable atmosphere furnaces

Several furnaces for thermal treatment under high-vacuum and controllable atmosphere conditions will be needed in the MPP Facility. In addition, tubular furnaces suitable for degassing cans containing processed powders will be required.

4.4.8. Rotary swaging machine

Rotary swaging is a process for the precision formation of metal bars. The finished shape of a formed workpiece is obtained without, or with only a minimum amount, of additional final processing by machining. Swaging dies, usually formed by four die segments, perform high frequency radial movements simultaneously with short strokes. To prevent the formation of longitudinal burrs at the gaps between the dies, a relative rotational movement is applied between dies and the workpiece. The swaging dies rotate around the workpiece, or alternatively the workpiece rotates between the dies. The major advantages of rotary swaging processing as compared to other techniques are:

[23] www.aiphip.com

- It is an incremental forming process where the oscillating forming takes place in many small processing steps.
- It allows the development of fully homogenous material formation compared to a continuous process.
- It allows very high forming ratios in only one processing step as the deformability of the material is uniformly distributed over the cross-section.

The MPP Facility would have a rotary swaging machine for processing steel and alloy bars with improved mechanical properties. The technical characteristics of the swaging machine would be:

- A stroke frequency variable in the range 1.500 – 10.000 strokes per minute.
- Total stroke lengths ranging from 0.2 to 5 mm.
- A heating system for hot swag processing.
- Operation via the infeed method.

Figure 4.11 shows the rotary swaging machine model FELLS FR 25V[24] that fits the MPP Facility requirements

Figure 4.11. Rotary swaging machine model FELLS FR 25V.

[24] www.felss.de

4.4.9. Severe Plastic Deformation facility

Grain refinement down to submicron sizes, or even below 0.1 micron, can be attained by means of *Severe Plastic Deformation* (SPD) techniques. It has been demonstrated that the ultrafine grained microstructures induced by SPD processing can induce a remarkable improvement in the mechanical and tribological properties of metals. Among SPD methods the ECAP technique appears to be the most promising for fusion materials since: 1) it can yield an effective pure shear strain as high as ~1 per processing pass without significant changes in the dimensions of workpieces; 2) after several ECAP passes, extremely high cumulative strains and an ultrafine microstructure can be achieved in workpieces suitable for preparing bulk samples for mechanical testing.

The MPP Facility should be provided with an ECAP machine for processing fusion alloys. It would be an optimised prototype whose design would be based on results from ECAP experiments on low activation steels that researchers from this project are presently undertaking.

4.4.10. Equipments for analyses, control and mechanical testing of materials

The chemical composition and microstructure of materials processed in the MPP Facility, as well as of the starting raw materials, need to be accurately determined in order to know the effectiveness of the methods applied. As a minimum requirement, this Facility would be equipped with analysis systems for interstitial impurities: e.g. O, N, C, and S, in addition to facilities for performing structural characterization by X-ray diffraction, metalography and micro-hardness:

The MPP Facility should be provided with the following equipments:

- A model LECO THC600 analyser for simultaneous determination of O/N/H by IR and thermal conductivity.
- A model LECO CS230 analyser for simultaneous determination of C/S.
- A model LECO GDS-850A glow discharge atomic emission spectrometer for bulk analysis of metal alloys.
- An X-ray diffractometer.
- A Scanning Electron Microscope (SEM).
- Mechanical test machines.
- Micro-hardness.
- A metallographic microscope.

- A helium ultrapycnometer.
- A grindosonic instrument for the non-destructive measurement of elastic properties of materials.

The above listed facilities will be integrated into an auxiliary laboratory associated with the laboratories for casting and processing of materials.

In addition, the MPP Facility will have auxiliary equipment and tools for material cutting and preparation, e.g. precision balances, fast and precision cutting machines, various types of polishing machines, a sand blaster, oxyacetylene and arc welding sets, plus work benches equipped with a wide range of tools. These latter equipment and tools would be integrated in a sample preparation laboratory attached to the above mentioned auxiliary laboratory.

4.5. Experimental capacity

As mentioned previously in section 4.2, the main activity of the MPP Facility will be the pilot production and processing of promising fusion materials required by the research programs. Specifically, these materials will be:

- Steels, Fe-Cr and W alloys, ODS and non-ODS, via mechanical alloying and consolidation by HIP or SPS.
- Low-activation and radiation-resistant steels and alloys produced by the VIM technique.
- Functional materials and ceramics produced by SPS and HIP.
- Protective coatings created by means of the VPS technique.
- The joining of dissimilar materials by HIP or SPS.

The facilities proposed will allow producing and processing:

- Sufficient material for proper characterization by the different research groups involved in the material development.
- Materials specifically requested by *TechnoFusión* users for irradiation experiments.
- Up to 40 - 50 kg of cast materials.
- Bulk materials severely deformed by ECAP.
- A wide variety of functional materials and protective coatings.

4.6. Layout, supplies and safety requirements

(I) Rooms and utilities

The estimated space requirement for the MPP Facility is as follows:

- One plant of 400 m^2 for the following facilities: VIM, SPS, HIP, VPS, ECAP and rotary swaging. This plant would also contain a soundproof room for the attritors and mills used in powder processing, and separately, an enclosure with two glove boxes, a safety cabinet for powder handling plus containers for storing treated powders. The floor of this plant would be required to support weights up to about 500 kg/m^2 at the locations of the SPS and VIM. In addition, an overhead crane would be installed to service the area where the VIM, SPS and HIP are to be installed.
- One 40 m^2 laboratory for housing the mechanical testing machines.
- One 30 m^2 laboratory for housing material analysis and control equipment.
- One 30 m^2 laboratory for installing auxiliary equipment and machines.
- One 30 m^2 room to house a scanning electron microscope and X-ray diffractometer.
- One 20 m^2 room for workshop and tools.
- One 30 m^2 storeroom divided into two sections.
- 200 m^2 dedicated to offices and common areas.
- One 30 m^2 meeting room.

Related to the required supplies:

(a) Power supply:

- At least, 2 independent 3x400 V±10% lines for ~300 kVA plus 2 additional lines for 3x400 V ±10% to provide ~200 kVA in the plant.
- 4 three-phase lines with 15 kVA capacity for the plant.
- 2 three-phase lines with 10 kVA capacity for the SEM/x-ray laboratory.
- 2 three-phase lines with 15 kVA capacity for the mechanical testing laboratory.
- 1 three-phase line with 19 kVA capacity for the analysis and control laboratory.
- Conventional installation of 20 kW in the plant, laboratories and workshop.

(b) Water supply:

- A refrigeration system with closed circuit circulation and outdoor cooling tower.
- Required flow: At least 300 litres/min at 4 bar of pressure, for when the VIM and SPS furnaces operate simultaneously.

(c) Gas and compressed air supplies:

- A refrigeration system with closed circuit circulation and outdoor cooling tower.
- Required flow: At least 300 litres/min at 4 bar of pressure, for when the VIM and SPS furnaces operate simultaneously H_2.

(II) Safety

The room and enclosure for powder processing will be properly prepared for the safe manipulation of powders. This will include: a system for air displacement detection; a fireproof cabinet for chemical storage and a radioactive materials will not be processed or stored in the laboratories.

The installation of an oxygen displacement detection system will be required. In addition, in locations where equipment using H_2 gas is located, leak detection systems for this gas will be installed. In addition, a safety cabinet with an alarmed H2 detection and air extraction system will be needed for conducting mechanical alloying experiments with an attritor mill.

For certain equipment, such as attritor and planetary mills, additional safety measures will be required, e.g. soundproofing the room (noise level ~85 dB per system), installation of anti-vibration mounts given the high speeds that can reach (up to 500 rpm, etc.), etc.

Finally, there are no plans to work with radioactive materials or radiation sources, thus radiological safety measures will not need to be implemented.

5. Material Irradiation

5.1. Introduction

As mentioned above, materials for future fusion reactors will be exposed to a particular hostile environment as a consequence of the intense radiation built during the nuclear reaction. The hot plasma within the reactor will generate a massive flux of high-energy neutrons, gamma photons, and particles. All of which will affect not only the first wall of the reactor, but also other distant equipments such as plasma heating or diagnostic systems. Radiations, via atomic displacement phenomena and ionizing processes will generate a number of defects in the structure of the materials, affecting their physical properties. Moreover, neutron-induced nuclear reactions will generate transmutation products (impurities) that will contaminate the materials, modifying their physical behaviour, and therefore, their reliability as functional materials. The high temperatures and the intense magnetic fields arising during the operation of the reactor will also contribute to the modification of the structural properties.

Considering this scenario, the study of the effect on the confining materials of the neutron radiation generated in fusion reactors is one of the most important research topics to be carried out during the next years.

The effects of neutrons on materials involve, from a fundamental point of view, two physical phenomena: i) the displacement of ions from their equilibrium positions in the lattice creating point defects, and ii) the generation of nuclear transmutating reactions that contribute to the formation of impurities inside the material, with He and H as the most important ones. The ratio between the levels of He and H, and the amount of point defects is one of the main parameters to understand the effect of the radiation on materials.

The straight-forward approach to perform this type of studies is the use of neutron sources as IFMIF. However, these sources have a number of problems and very strict operating conditions, making new approaches for simulating their effects very interesting as well as necessary to decrease the radiological risks.

Computer simulations have concluded that the effect of neutrons can be represented, in a very accurate way, by the simultaneous irradiation with He, H and heavy ions capable of creating point defects (for example, Fe irradiated on steel). This triple irradiation will be a unique and singular tool for the experimental simulation of the effect of the neutron radiation on materials of interest for fusion reactors.

To study the effects of ionizing radiation on the physical characteristics of materials, a source capable of providing a uniform field of gamma radiation is needed. And to obtain reliable results, the dose rate must to be equivalent to the expected one in ITER (radiation levels between 100 and 500 Gy/h[25]). The most suitable gamma radiation source for the simulation of this effect is an electron accelerator with a flexible beam line, i.e., able to vary the beam position in a fast way to obtain a uniform radiation field. When the electron beam

[25] Private communication: J. Palmer (Remote Handling Field Coordinator en EFDA-CSU Garching)

collides with a thin film of the right material (usually a heavy metal), a gamma radiation field is generated in the surrounding zones.

The use of an electron accelerator has several advantages when compared to conventional gamma radiation sources (such as ^{60}Co): The disappearance of the radiation risk when the accelerator is switched off and the regulation of the gamma radiation flux by changing the beam current and energy. As a drawback, the emitted gamma radiation spectrum (mainly through *bremsstrahlung*) is different to the one expected in ITER[26], [27]. However, this difference is not significant since the relevant parameter in the interaction of ionizing radiation with matter is the level of electronic excitation, measured by the dose rate.

As it was mentioned before, the materials used in the future fusion reactors will work under intense magnetic fields (probably in a steady state or with small variations in time). Up to now, most of the studies of characterization of the effects of radiation on the macroscopic and microscopic properties of materials have not taken the presence of magnetic fields into account. The availability of magnets with a high magnetic fields (between 5 and 10 Tesla), together with the above-mentioned set of ion accelerators will enable a number of experiments to analyze the combined effects of radiation and magnetic fields on materials with interest for fusion reactors.

The **Material Irradiation Facility (MI)** is a key element for the *TechnoFusión* project due to the primary importance of the effects of neutronic and ionizing radiations on a number of materials and processes. Therefore, this Facility must be in close contact with the rest of *TechnoFusión´*s facilities. To name just a few, the Remote Handling and the Metal Liquid facilities involve an extensive use of high energy radiation sources, not to mention the relevance of the radiation in the selection of functional materials.

In conclusion, the MI Facility will be composed by three ion accelerators: one for implanting heavy ions (Fe, Si, C, etc.), and two for light ions (H and He). This combination will enable the study of the effects of neutron radiation on materials similar to those arising in reactors such as ITER and DEMO[28, 29, 30]. The MI Facility will also include an electron accelerator that will be shared by the Remote Handling and Liquid Metals facilities, and a high field magnet to study the combined effects of ionizing radiation and magnetic field in metallic alloys.

---

[26] V. Khripunov. "The ITER first wall as a source of photo-neutrons**".** Fusion Engineering and Design 56-57, (2001), p. 899-903.

[27] W. V. Prestwich and R. E. Coté, "Gamma-Ray Spectra of Co^{60} and Mn^{56} Following Resonance-Neutron Capture in Co^{59} and Mn^{55}", Phys. Rev. 155, p. 1223-1229 (1967).

[28] S. Hamada, Y. Miwa, D. Yamaki, Y. Katano, T. Nakazawa and K. Noda "Development of a triple beam irradiation facility". Journal of Nuclear Materials, 258-263 (1), p. 383-387 (1998).

[29] Y. Serruys, P. Trocellier, S. Miro, E. Bordas, M. O. Ruault, O. Kaitasov, O.Leseigneur, Th. Bonnaillie, S. Pellegrino, S. Vaubaillon and D. Uriot, "JANNUS: A multi-irradiation platform for experimental validation at the scale of the atomic modelling", Journal of Nuclear Materials 386-388, p. 967-970 (2009).

[30] D. Jiménez-Rey, R. Vila, A. Ibarra, F. Mota, Christophe J. Ortíz, J. L. Martínez-Albertos, R. Román, M. González, I. García-Cortés, and J. M. Perlado, "The multi-ion-irradiation Laboratory of *TechnoFusión* Facility and its relevance for fusion applications". To be published in Journal of Nuclear Materials.

5.2. Objectives

A primary goal of MI Facility is to understand the mechanisms generating the damage produced on the materials by the combination of heavy and light ions in terms of microstructure and impurities, and to increase in the knowledge of the damage produced by neutrons in a fusion reactor. Therefore, the initial effort will aim to establish the operating conditions of the ion accelerators to best simulate the effects of the neutron radiation without the use of a neutron source; that includes the choice of the most suitable accelerators/implanters.

Other goals of the facility include, as a first step, the demonstration of the capability of the facility to generate damage in a certain volume within the sample, and the production of such damage in a uniform and homogeneous way within the material. Two different approaches will be used for this task:

I. The triple irradiation technique. The irradiation of the target material with ions of the same species (i. e. Fe^{+} on Fe) while, simultaneously, implanting light ions (H and He). This triple irradiation will generate the same amount of lattice displacements (via the heavy ions) and the same amount of light ions (via H and He implantation) than the expected in fusion facilities.

II. The irradiation with high energy protons (in a range to be evaluated, but roughly between 20 and 40 MeV. The effects of this beam are two fold: First, according to some generally accepted calculations, this beam will create damage similar to that generated by neutrons from fusion reactors in very thicker areas (in the millimetre range) of the target material. Second, it will generate –at the same time as the damage— H and He via transmutation.

The computer simulations to justify the above-mentioned irradiation methods are described in Appendix IA as the radioprotection studies for the preliminary design of the *TechnoFusión* Facilities are paramount importance, the main obtained results are included in Appendix IB. On them, the following elements were taken into account in order to simulate accurately the effects of a neutron beam: i) the minimum energy of ions necessary to achieve the desired penetration; ii) the homogeneity of the irradiation profile along the whole irradiated volume; iii) the appropriate ratio of light elements to displacements per atom (see Figure 5.1); and iv) *Primary Knock-on Atom* (PKA) energy spectra. The PKA is the recoil atom being displaced by the direct collision --atomic or nuclear— of the incident particle.

The effects of activation and transmutation of the targets elements by means of light element implantation and by irradiation with protons were also studied. These simulations enabled further advances in the design of ion accelerators for both light and heavy ions. Figure 5.1 shows the correlation between generated He and atomic displacements for a Fe target after being irradiated for a week at two different groups of facilities: On the first place, some already existing nuclear fission reactors and particle accelerators. Secondly, the estimation of the results at future facilities as the neutron reactor IFMIF, ITER and DEMO. In the same graphic, the region where *TechnoFusión* facility is expected to operate is highlighted, and shows that the values of generated He vs. damage covered by the new nuclear fusion facilities fit in the operative range of *TechnoFusión*.

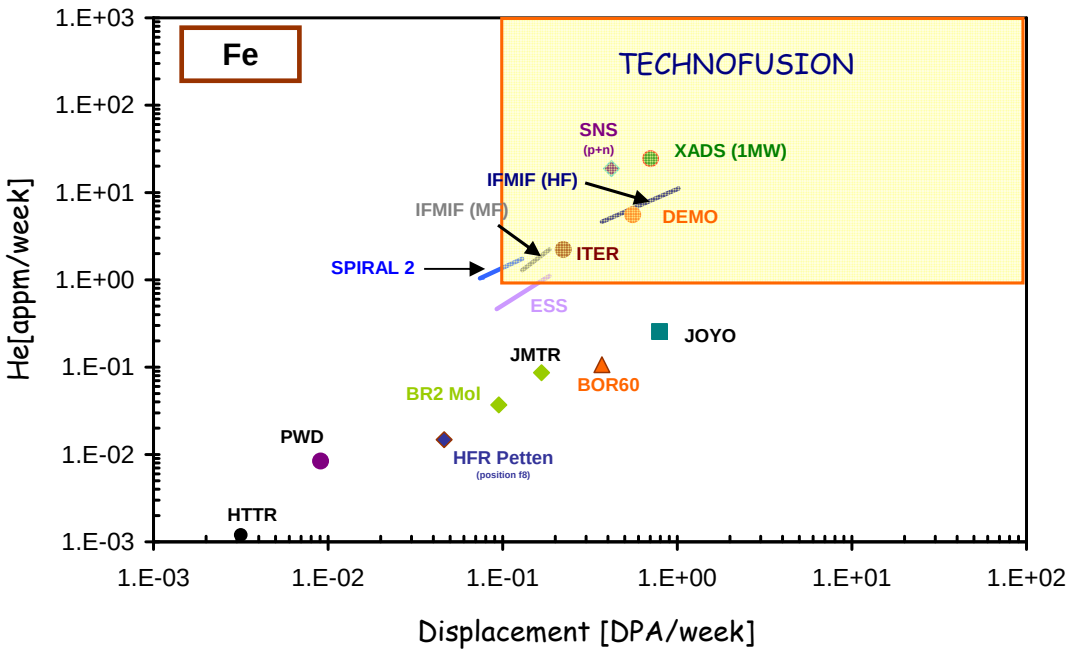

Figure 5.1. Comparison of the levels of damage and of impurities created at different facilities —particle accelerators, fission reactors, some planned fusion experiments, etc. The operative range of *TechnoFusión* covers the operating range of these planned nuclear fusion facilities.

Figure 5.2 shows a comparison between the damage function —*W(T)*— generated by protons (Figure 5.2a) and by Fe ions (Figure 5.2b) in iron, and the *W(T)* function generated by neutrons, as expected for future DEMO reactor. The damage function is the spectrum of kinetic energies of the PKAs $-\sigma_{PKA}(T)-$ generated by heavy ions or protons normalized to the damage each PKA creates, as a function of its initial kinetic energy[31]:

$$W(T) = \frac{1}{D/t}\int^{T} \sigma_{PKA}(T)\, N_d(T)\, dT\,, \qquad \text{eq. 5.1}$$

where *D/t* is the rate of damage created by atomic displacements, and $N_d(T)$ is the number of Frenkel pairs by PKA of energy *T*.

Figure 5.2 shows the calculated damage function irradiating with Fe ions and protons on an iron target. This allows us to compare both irradiation types with DEMO-HCLL (at two positions; first wall [FW] and breeder zone [BZ]). As we can see, both methods could be used to duplicate the neutron damage, but high energy Fe ions give the best approximation. The

[31] D. Leichtle, U. Fischer. "Qualification of irradiation effects on ceramic breeder materials in fusion and fission systems" Fusion Engineering and Design *51-52* (2000) 1-10.

damage curves of Fe ions of energies 300 to 500 MeV being included into the expected damage function covering from FW to BZ regions. The sharper curve observed in protons is related to the fact that they pass all the way through the sample, losing energy mainly by electronic stopping with fewer knock-on processes and in a narrower energy range.

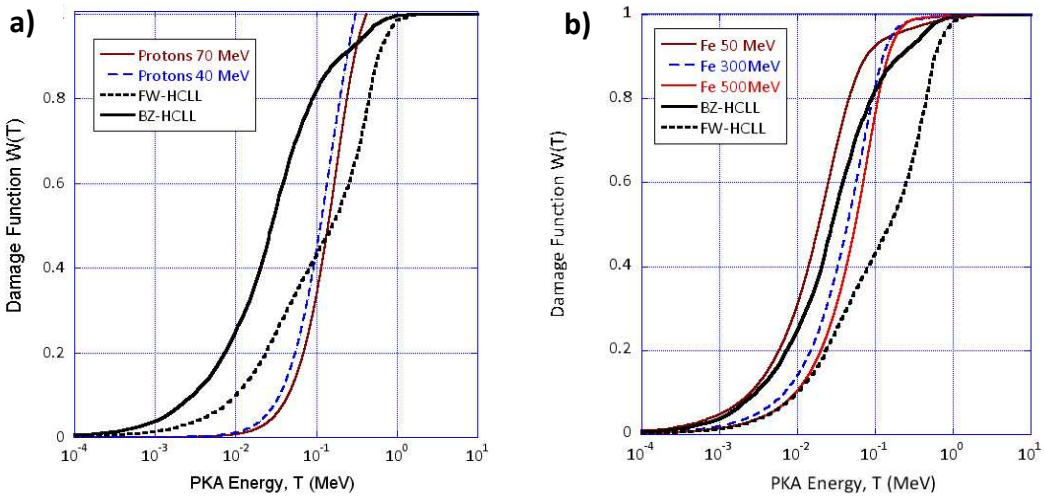

Figure 5.2. Damage functions generated for a Fe material with a) 40 and 70 MeV protons b) 50, 300 and 500 MeV Fe ions, compared with the damage function in DEMO HCLL (first wall [FW] and breeder zone [BZ]). T is the PKA kinetic energy upon which the Damage Function depends.

The disadvantage of this 40 to 70 MeV proton approach (see Appendix I) is that the appmHe/dpa ratio is generally higher than that expected for DEMO-FW-HCLL (in iron is three times higher for 40 MeV H^+). To reduce this rate, irradiations with lower energy protons (around 20 MeV) can be used. At this energy, the damage function does not change considerably whereas the production of He atoms is much lower.The He/dpa ratios calculated for different materials and positions are shown in Table I.A2 of Appendix I.A. This allows us to tailor the irradiation conditions to each material and DEMO position.

These procedures to modify materials allow significant studies in a large amount of problems associated to materials, some of them already identified, in the process of developing fusion facilities such as ITER, IFMIF and DEMO. The following are just a sample of these studies:

- Structural properties of materials such as ODS steels, vanadium alloys, tungsten and silicon carbides.

- Physical properties (permeability, corrosion, electric conductivity, etc.) of structural materials.
- Development and characterization of junctions and welding techniques.
- Characterization and modelling of the effect of the radiation on structural materials, coatings, junctions, welding joints, etc.
- Design and implementation of controlled experiments (controlling the level of generated point defects, concentration of impurities such as H and He, electronic excitement, presence of magnetic field, etc.) to model the effects of the radiation on materials.
- Characterization and modelling of the effect of the radiation on insulating materials for diagnostics.

Simultaneously, the set of techniques in the MI Facility at *TechnoFusión* will allow the study of more generic effects, not necessarily related to nuclear fusion phenomena:

• Evaluation of the effect of neutron radiation on materials candidates for use in next generation fision reactors.

• Evaluation of the combined effects of radiation and magnetic field on the above-mentioned materials.

• Study of radiological risks.

5.3. International status of the proposed technologies

5.3.1. Major international facilities for ion and electron irradiation

In Europe, JANNUS (*Joint Accelerators for Nanosciences and NUclear Simulation*) facility is currently been developed in Saclay, France, by the *Centre de Spectrométrie de Masse et de Spectrométrie Nucléaire* (CSNSM[32]). This facility has a similar strategy to that of the Material Irradiation Facility of *TechnoFusión*: both aim at using a triple beam for implantation. JANNUS will have one 3 MV heavy ion implanter, named *Epimèthèe* (a *Pelletron*), and two light ion implanters: a 2.5 MV *Van de Graaff* accelerator (*Yvette*), and a 2 MV *tandem accelerator* (*Japet*). Figure 5.3 shows a layout of the accelerators in JANNUS and their main characteristics. The ion species and the maximum estimated energies for the different accelerators in JANNUS are displayed on Table 5.1.

[32] http://www-csnsm.in2p3.fr

Table 5.1. Values for the maximum energy and the ion species on each of the three accelerators of the JANNUS facility.

Accelerator	Ion	Maximum energy
Epiméthée (Pelletron)	H, D, ^{3}He, C, N, O, Fe, Ni N_2	3 MeV
Yvette (Van de Graaff)	H, D, ^{3}He, ^{4}He	2.5 MeV
Japet (tandem)	H, halogen ions, P, S, metallic ions	2 MeV

The main drawback[33] of the accelerators in JANNUS is the low value of the maximum energy they can reach, in the order of 3 MeV, which means a penetration range of just a few hundreds of nanometres. Moreover, JANNUS will only have a Transmission Electronic Microscope (TEM) of 200 keV available for *in situ* analysis of the materials during the irradiation.

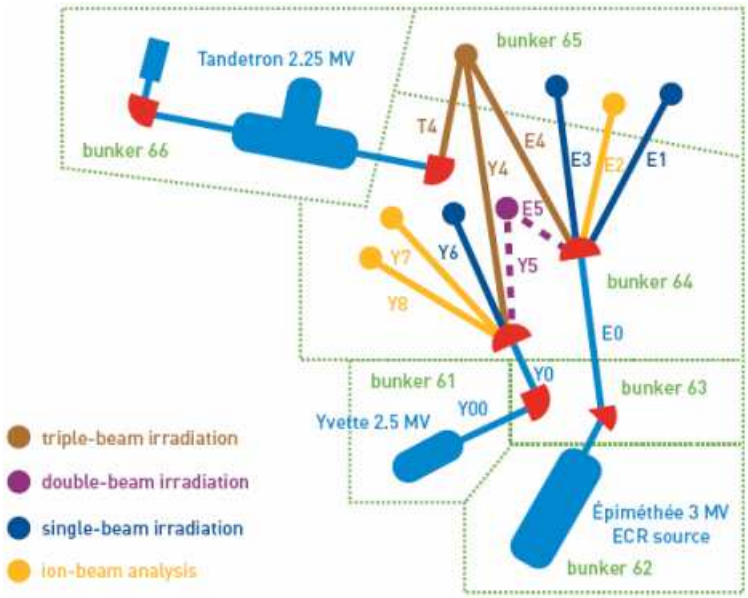

Figure 5.3. Diagram of the different irradiation points for the future JANNUS facility in Saclay. The maximum energies for each accelerator are also shown.

[33] Y. Serruys, P. Trocellier, S. Miro, E. Bordas, A. Barbu, L. Boulanger, O. Leseigneur, S. Cabessut, M.-O. Ruault, O. Kaïtasov, S. Henry, Ph. Trouslard, S. Pellegrino, S. Vaubaillon, and D. Uriot, CFRM-13 13th International Conference on Fusion Reactor Materials 2007, December 10 – 14, Nice (France).

Worldwide there is only one facility similar to *TechnoFusión*'s MI Facility: Japan's *Takasaki Ion Accelerators for Advanced Radiation Application*[34] (TIARA) (Figure 5.4):

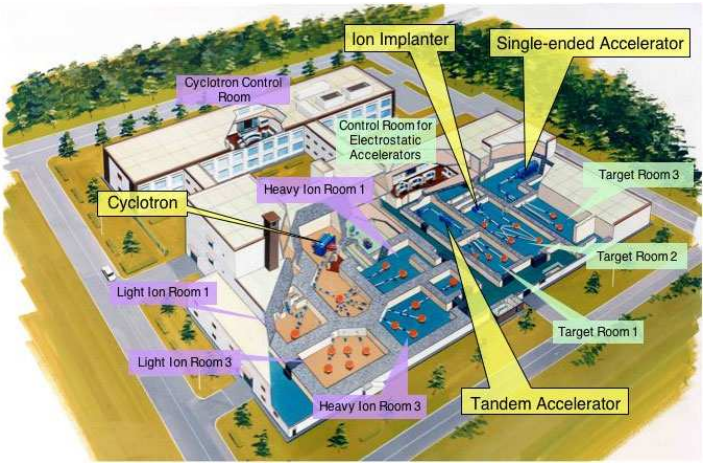

Figure 5.4. TIARA facility, in Takasaki, Gunma (Japan).

This facility has four ion accelerators: A heavy ion AVF cyclotron (*Azimutally Varying Field*) with[35] k =110, a 3 MV *tandem* accelerator, a 3 MV *single-ended* accelerator, and a 400 kV ion implanter. The TIARA complex offers a large variety of ion species, from light ions as H to heavy ions as Au, and covers a large range of energies –from keV to MeV (see Table 5.2 and Figure 5.5). The main studies carried out at TIARA facility are related to irradiation of materials and to biotechnology. However, TIARA accelerators also have their limitations, the main one being the impossibility to combine the cyclotron beam with those from the linear accelerators.

Other than JANNUS and TIARA, there are other facilities and research groups dedicated to the irradiation technologies all over the world. Table 5.3 shows a list of them together with the available accelerators. This list shows that the set of facilities linked to the technology of accelerators is limited due to the maximum energies they can achieve. For a complete analysis of the damage in materials by radiation it is necessary to irradiate at deeper penetration ranges and, therefore, with higher energies. Consequently, a new group of facilities is still required.

[34] S. Hamada, Y. Miwa, D. Yamaki, Y. Katano, T. Nakazawa and K. Noda. "Development of a triple beam irradiation facility". Journal of Nuclear Materials, 258-263 (1998), p. 383-387.
http://www.taka.jaea.go.jp/tiara/index.html. Checked on August 2009.

[35] K, the proton kinetic energy, is a constant that depends on the magnetic rigidity of the external orbit of the cyclotron (see Appendix II, "Dimensions and cost estimations of the heavy ion cyclotron accelerator", for more information).

In this context, the *TechnoFusión*'s MI Facility has the potential to become an international facility of reference, as it will have ion accelerators with the capacity to achieve up to 400 MeV for heavy ions.

Table 5.2. List of available ions and their energies for the different accelerators in TIARA facility.

Accelerator	Ion	Energy (MeV)
AVF cyclotron (K110)	H	5~90
	He	10~110
	Ar	94~990
	Kr	200~1030
	Xe	300~930
	Au	440~460
Tandem accelerator (3 MV)	H	0.8~6
	C	0.8~18
	Ni	0.8~18
	Au	0.8~21
Single-ended accelerator (3 MV)	H	0.4~3
	D	0.4~3
	He	0.4~3
	E	0.4~3
Ion implanter (400 kV)	H	0.02~0.4
	Ar	0.02~1.2
	Ag	0.02~1.2

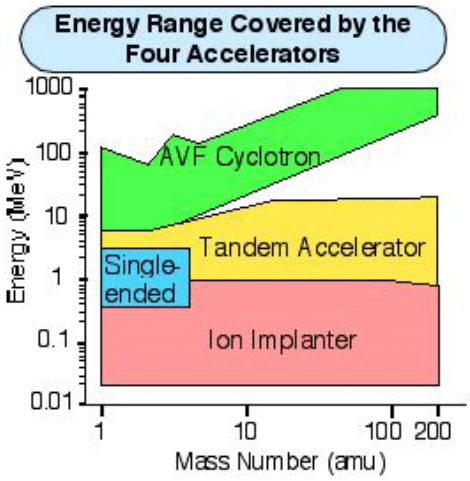

Figure 5.5. Graphic of the different ion energies versus atomic mass for the accelerators in TIARA.

Table 5.3. Research centres in the world dedicated to irradiation technologies.

Research Centre	Accelerators
IAE Kyoto[36] (Japan)	Van de Graaff (1 MV) accelerator Tandetron (1.7 MV) accelerator Singletron (1 MV) accelerator
HIT Tokyo[37] (Japan)	Van de Graaff (3.75 MV) accelerator Tandetron (1 MV) accelerator
CIRSE Nagoya University[38] (Japan)	Ion implanter (200 kV) Van de Graaff (2 MV) accelerator
Hokkaido University[39], Sapporo (Japan)	Ion implanter (300 kV) TEM (1MV)
MSD, IGCAR Kalpakkam[40] (India)	Ion implanter (400 kV) Tandetron (1.7 MV) implanter
FZ Rossendorf [41] (Germany)	Ion implanter (500 kV) Tandetron (3 MV) accelerator
FSU Iena[42] (Germany)	Ion implanter (400 kV) Tandem (3 MV) implanter
Salford University[43] (United Kingdom)	Ion implanter (100 kV) TEM (200 kV)
TIARA facility (Japan), managed by JAERI Takasaki[44]	Cyclotron accelerator AVF K110 Tandem (3 MV) accelerator Single-ended (3MV) accelerator Ion implanter (400 kV)
JANNUS Saclay, (France)[45]	Epimèthèe [Pelletron] (3 MeV) accelerator Van de Graaff [Yvette] (2.5 MeV) accelerator Tandem [Japet] (2MeV) accelerator

5.4. Projected devices

5.4.1. Ion accelerators

The main requirement for *TechnoFusión* MI´s accelerators is the capability to irradiate materials with penetration ranges of, at least, some tens of microns. Other than that, they also need to ensure the possibility of enabling a triple beam irradiation.

[36] A. Kohyama, Y. Katoh, M. Ando and K. Jimbo, Fusion Engin. Design 51-52 (2000), p. 789-795.
[37] Y. Kohno, K. Asano, A. Kohyama, K. Hasegawa and N. Igata, J. Nucl. Mater. 141-143 (1986), p. 794-798.
[38] M. Iseki, Y. Kikuza, S. Mori, K. Kohmura and M. Kiritani, J. Nucl. Mater. 233-237 (1996), p. 492-496.
[39] H. Tsuchida and H. Takahashi, J. Nucl. Mater. 239 (1996), p. 112-117.
[40] B. K. Panigrahi, The ion beam facilities at MSD, IGCAR Kalpakkam, Acts of the French-Indian Workshop, November 28 – 30, 2005, Saclay (France), http://www.igcar.ernet.in/igc2004/igcanr2006.pdf.
[41] J. R. Kaschny, R. Kögler, H. Tyrrof, W. Bürger, F. Eichhorn, A. Mücklich, C. Serre and W. Skorupa, Nucl. Instrum. Meth. Phys. Res. A551 (2005), p. 200-207.
[42] B. Breeger, E. Wendler, W. Trippensee, Ch. Schubert and W. Wesch, Nucl. Instrum. Meth. Phys; Res. B174 (2001), p. 199-204.
[43] S.E. Donnelly, Comportement des matériaux sous irradiation : un thème de l'Université de Salford, Communication to GDR PAMIR starting meeting, November 25 – 27, 2006, Caen (France), http://www.ganil.fr/ciril/gdr/pleniere.html.
[44] S. Hamada, Y. Miwa, D. Yamaki, Y. Katano, T. Nazakawa and K. Noda, J. Nucl. Mater. 258-263 (1998), p. 383-387.
[45] Y. Serruys, P. Trocellier, S. Miro, E. Bordas, A. Barbu, L. Boulanger, O. Leseigneur, S. Cabessut, M.-O. Ruault, O. Kaïtasov, S. Henry, Ph. Trouslard, S. Pellegrino, S. Vaubaillon, and D. Uriot, CFRM-13 13th International Conference on Fusion Reactor Materials 2007, December 10 – 14, Nice (France).

Electrostatic ion accelerators (Pelletron or Van der Graaf) are the most commonly used for light ions. Spain has already some experience in the operation of this type of accelerators, since there are several of them working at CIEMAT (Madrid), CMAM (Madrid) and CNA (Sevilla). These accelerators can be single-ended, with the ion sources at high voltage terminal, or *tandem*, with the high voltage terminal in the middle of the tank. For *tandem* accelerators, it is possible to obtain higher beam energies as ions are accelerated in two stages. Moreover, *tandem* accelerators allow the ion source not to be at the terminal voltage, as is the case for single-ended, enabling the use of different kinds of sources and increasing its versatility. The use of, at least, two ion sources is considered: one radiofrequency source for ions in a gas state, and one sputtering source for ions in a solid target.

Regarding the heavy ion accelerator, its main goal is the production of defects inside the material similar to those caused by neutron radiation, but without the inclusion of impurities. This means that the irradiation has to be carried out with the same atomic species as those present in the target sample or, in the case of more complex targets, with one its components. Taking into account the materials considered in the European Fusion Project for structural purposes; i. e. steel, W, and SiC; the heavy ion accelerator in MI Facility needs to accelerate Fe, W and Si. In order to ensure a large penetration range (between 5 and 90 µm, see Table 5.4) the ion energy has to be high enough —some hundreds of MeV— and therefore, cyclotron accelerators are more suitable than electrostatic ones.

For light ions, the results from the simulations carried out previously to this report[46] (see Appendix I) have shown that, in principle, no high beam currents are needed. In fact, for normal dose rates, currents in the order of nA are enough to reproduce the formation rate of H and He induced by neutrons, but for accelerated damage aging (up to total dpas expected in DEMO life), currents increase up to a few microamps. In addition, the desired penetration range is achieved with few MeV of energy. Table 5.4 shows the summary of energy values for different ions implanted in different target materials to achieve the same penetration range in the material, according to the above-mentioned simulations[46]. In every case, it is one of the three accelerators that limit the maximum penetration depth. The Table 5.4 shows the energy values assuming a He charge state of +2 at the second stage in a *tandem* accelerator, giving a total energy of 18 MeV. As it can be seen, although the case for He^+ is often the most restrictive, working at 18 MeV makes it possible to take advantage of the cyclotron potential to reach larger depths in the irradiated material. It is also worth to note that the H beam does not exceed the 5 MeV energy in any case, which could reduce the requirements for the terminal voltage in such tandem accelerator[46]. A margin can be added to this energy in order to use deuterium ions (up to 6 MeV) or for some other experiments (like direct irradiation with 10 MeV H^+).

[46] D. Jiménez-Rey, R. Vila, A. Ibarra, F. Mota, Christophe J. Ortiz, J. L. Martínez-Albertos, R. Román, M. González, I. García-Cortés, and J. M. Perlado, "The multi-ion-irradiation Laboratory of *TECHNOFUSIÓN* Facility and its relevance for fusion applications", to be published in Journal of Nuclear Materials.

Table 5.4. Ion energies to be used in the MI Facility assuming a He energy equal to or lower than 18 MeV (*tandem* at 6MV terminal voltage and charge states of -1 and +2). Underlined values on the tables indicate the ion/accelerator combination that limits the penetration range in the material.

		Heavy ion accelerator k =110 cyclotron		4 MV light ion accelerator		6 MV light ion accelerator	
Irradiated material	**Range (μm)**	**Ion**	**Energy (MeV)**	**Ion**	**Energy (MeV)**	**Ion**	**Energy (MeV)**
Fe ($7.8\ g/cm^3$)	26.6	Fe	<u>385</u>	H	2.5	He	10
W ($19.3\ g/cm^3$)	10.1	W	<u>373</u>	H	1.6	He	6
C ($2.3\ g/cm^3$)	148	C	96	H	4.5	He	<u>18</u>
SiO_2 ($2.2\ g/cm^3$)	175	Si	337	H	4.6	He	<u>18</u>
SiC ($3.2\ g/cm^3$)	122.4	Si	337	H	4.6	He	<u>18</u>
SiC ($3.2\ g/cm^3$)	122.4	Si	337	D	6.0	He	<u>18</u>

Results from these previous calculations have been considered to conclude that, for the *TechnoFusión* MI Facility, the following accelerators and characteristics will be required:

- *1 tandem accelerator for light ions with 6 MV terminal voltage to be used with He^+ ions.*
- *1 tandem accelerator for light ions with 4 to 5 MV terminal voltage to be used with protons (H^+).*
- *1 accelerator for heavy ions, cyclotron, with k = 110 to be used with heavy ions or high energy protons (E_{H+} ~20 - 40 MeV; see maximum energies in Table 5.4 for k=110).*

The exact requirements for the set of accelerators (beam energy, beam current, emittances, etc.) are in the process of evaluation. Following, the main requisites of *TechnoFusión´*s MI Facility are presented:

I) <u>Beam energy:</u> table 5.5 shows the expected maximum energies for the different ions to be implanted.

II) <u>Currents:</u> table 5.6 summarizes the minimum desirable beam currents for the different ion species in both types of accelerators together with the equivalent figures in TIARA facility.

Final currents currents depend on the combination of material choice, position in DEMO to reproduce, total dose and time available to irradiate. As an example Table 5.6 shows the He current needed to implant around 1000 appm He in a week.

Table 5.5. Fundamental ions and their maximum energies.

	Tandem accelerators			Cyclotron k=110				
	H	**D**	**He**	**C**	**Si**	**Fe**	**W**	**H**
A	1	1	1	12	28	56	184	1
Z	1	2		4	9	14	25	1
E (MeV)	8 to 10	2 - 6[47]	10 - 18	96	337	385	373	< 40

Table 5.6. Target currents for different ions in the tandem and in the cyclotron accelerators at MI Facility. TIARA current values are showed for comparison. Data in ion/s units. q = charge state. pnA, particle-nanoAmpere, is a current unit: nanoAmpere of single-charged particles

Light ions in a tandem accelerator	
Ion	**Target current (pnA)**
H	50-100
D	~10
He	50-100

Heavy ions in a k = 100 cyclotron		
Ion	**Target current (pnA)**	**TIARA**
C	500 – 1000	660 (q=3) 80 (q=5)
Si	200	15 (q=10)
O	200	750 (q=4) 250 (q=6)
Fe	25	120 (q=11) 35 (q=15)
W	3	60 (q=9)

III) Emittances: the emittance of a particle beam is the volume they occupied in the phase space (space and momentum) as they move. A beam of low emittance is a beam in which the particles are well confined and all of them have very similar momenta. A transport system allows only particles with a momentum close to the designed momentum. In actual terms, a small emittance favours the control of the beam, and increases the brightness.

For tandem accelerators, literature shows working values of 3.5 π mm mrad for a 1 MeV proton beam.

Companies DREEBIT[48] and Elytt Energy[49] have issued a viability study showing emittance values in the target below 20 π mm mrad, which is considered correct at this first stage of development, until the ion and the charge state were specified.

[47] Possibly limited by the activation of the material.
[48] DREEBIT GmbH. Zur Wetterwarte 50, Haus 301. 01109, Dresden, Germany. http://www.dreebit.com/
[49] Elytt Energy. Paseo de la Castellana 114, 3º, puerta 7. 28.046 Madrid. Spain. http://www.elytt.com

IV) Beam homogeneity: to achieve homogeneous irradiations in relatively large areas MI's accelerators should contain beam sweeping systems to scan large areas on the samples. At the present moment, several studies are being carried out to select the most suitable beam sweeping systems, and to consider the possibility of using a beam degrader, including its radiological consequences.

V) Angles of incidence on the sample: simultaneous irradiation with three parallel ion beams is not physically possible. Therefore, an important factor to take into account is the maximum angular separation between the ion beams. In TIARA, the irradiation with a triple beam takes place on the same plane, being the angles between beams of 15 degrees. On the contrary, *TechnoFusión´*s plans consider the possibility of locating the beams in a non-coplanar arrangement to reduce the angle between them.

The heavy ion beam, however, will be placed normal to the surface of the sample to avoid any kind of sputtering effect in the material.

VI) Beam lines: the triple irradiation is the key element in the facility and therefore it determines the design of the accelerators, and subsequently, the additional lines to develop. All these systems will establish the characteristics of the MI Facility building.

The study of the different optical elements to steer the beams into the different lines is also necessary. Parameters such as the beam energy and the deflection angles will determine the dimensions of the dipoles, bending magnets, and so on.

VII) Supplies: both the accelerators and the beam lines will need a set of supplies such as cooling systems, liquid nitrogen, compressed air, etc. The evaluation of the vacuum conditions, the dissipated heat or the working temperatures can be done, in a first approximation, taking as a reference other similar accelerators such as those in CMAM[50].

A technical area under the accelerator hall is planned to allow the location of the different lines to drive power, vacuum, gases, cryogenic liquids, etc, to the points where they were needed in the main hall.

VIII) Radiological safety aspects: the computer simulations will determine the radiation doses are being carried out for the different operation steps, and will specify the radiation shields required for the accelerator halls, supply rooms, beam lines, etc.

Considering all the above-mentioned requirements, the acquisition of two 5-6 MV tandem accelerators for light ions, one for H and another one for He, is proposed. It is important to note that the acquisition of these two accelerators is absolutely necessary because the implantation of H and He has to be performed simultaneously. For the third beam, the acquisition of a Cyclotron accelerator for heavy ions (and for high energy protons) with a k constant close to 110 is proposed.

The following sections cover a brief description of the proposed accelerators for the MI Facility:

[50] Internal document of CMAM HVEEA-4-35-174-0049. Installation Requirements and Recommendations. (2002)

5.4.1.1. Light ion accelerator with neutralizer

There are several companies (NEC[51] (USA), TOSHIBA (Japan), HVEE[52] (Netherlands)) able to provide electrostatic tandem accelerators with 5-6 MV in a period of about 1 year. Although not strictly necessary, it is desirable that both accelerators were equals to gain flexibility and to have easier maintenance. Figure 5.6 shows an example of a NEC accelerator.

Figure 5.6. Tandem electrostatic accelerator 4 MV made by NEC.

The neutralization of the ions, necessary for the irradiation of materials under magnetic fields, is obtained by making the beam to pass through a chamber filled with a weakly bonded electrons gas. In there, the charge exchange will take place at low energies.

This type of technology is used frequently in machines for plasma physics, because the heating system of neutral particle injectors must be very efficient. These charge exchange devices are expected to be efficient enough for the purpose of the linear accelerators planned for this facility. Nevertheless, this question remains open and needs further considerations and studies.

These proposed accelerators may also be used in several other applications such as material science (e. g. analysis with Ion Beam Analysis (IBA) techniques), nuclear and atomic physics, biology or even in studies on the historical and cultural heritage. In principle, these other applications have not been considered in the design of the MI Facility or in this report, although evidently, could be included in the moment of making a detailed design.

[51] National Electrostatics Corporation, 7540 Graber Road, P.O. Box 620310 Middleton, Wisconsin 53562. http://www.pelletron.com/

[52] High Voltage Engineering Europa B.V. P.O. Box 99. 3800 AB Amersfoort. The Netherlands. http://www.highvolteng.com/

5.4.1.2. Heavy ion accelerator

According to the computational evaluations performed by the Spanish engineering company Ellyt Energy[53] a k=110 cyclotron should be able to accelerate heavy ions to high energies at low cost. There are several options for the design and construction of this cyclotron:

a) Some contacts with the company IBA[54] have been started. At the present moment, this company produces cyclotrons only up to k=70 (Figure 5.7), but they have shown a great interest on the development of a cyclotron with the required characteristics by *TechnoFusión*.

b) There have been also contacts with the Massachusetts Institute of Technology group led by Prof. Timothy A. Antaya. This group has become specialized in superconductor coils, generating a significant decreasing in the size of the magnet, which allows for important savings in the iron for the magnet core.

c) Finally, the cyclotron design could be carried out by the *Elytt Energy* company.

The MI Facility cyclotron could also be used in other applications, such as radiotherapy (accelerating carbon ions, also of interest for fusion) or for isotope production. These other applications have not been considered in this report, but evidently, could also be included at the moment of making a detailed design.

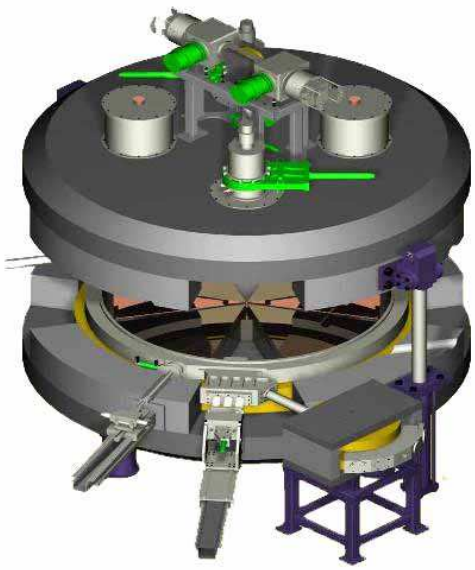

Figure 5.7. Scheme of Cyclone 70 heavy ion accelerator by IBA.

[53] ELYTT ENERGY. Paseo de la Castellana 114. 28046 Madrid. Spain. http://www.elytt.com. September 2009.
[54] IBA. Chemin du Cyclotron, 3 – 1348 Louvain-la-Neuve, Belgium. http://www.iba-worldwide.com. September 2009.

5.4.2. Electron accelerator

According to the calculations described on Appendix II, a 10 MeV electron beam with a current of 70 mA impinging upon a 1 cm thick Al film generates a gamma radiation field of 700 Sv/h at a distance of 3 m. These results were obtained assuming a point source. However, using an extended source (irradiating with the electron beam over a large area, or dividing the beam into several smaller sources) under the mentioned conditions (10 MeV and 70 mA), a dose rate of 100 - 500 Sv/h could be achieved for a volume of few cubic meters.

A constant-wave electron accelerator *Rhodotron®*[55] (Figure 5.8) is considered for the MI Facility as the most suitable device to generate the right dose of gamma rays in the irradiated samples. Currently, only the Belgian company *Ion Beam Applications* S. A. (IBA) manufactures them after an agreement CEA, home institution to J. Pottier, designer of this type of accelerator.

The main drawback of *Rhodotron®* accelerators is their fixed energies, with a maximum of 10 MeV, and therefore, they are not suitable for scans in energy or to tune this parameter. However, these systems can be built with different beam lines[56] at different energies (3, 5 and 10 MeV, for example), all of them fixed. Its current, though, is tuneable between 3 mA (IBA model TT-100) and 100 mA (IBA model TT-1000), and is extremely stable.

The electron beam from *Rhodotron®* systems can be extracted just at the exit of the magnets. Fractional values of the energy (i. e., 0.5 MeV) are not accessible and only integer values can be employed, starting from 1 MeV because the beam gains 1 MeV per cycle. The beam size at the accelerator exit ranges between 2 and 4 mm. However, using additional collimators these dimensions could be reduced.

IBA´s *Rhodotron®* offers the option of a system to spread the electron beam and turn it into a gamma radiation field. This system, called scanning horn, is combined with a target of water-cooled tantalum-iron. The radiation map obtained with it is shown in Figure 5.9. It can be opened up to distances of 1 m or more. To use the accelerator by the Remote Handling Technologies Facility, the system should be able to extend the beam in perpendicular direction to the previous one to obtain a square profile and, therefore, a more uniform gamma field to test the different devices. Estimations about the maximum irradiation volume for the Remote Handling Technologies Facility are shown in Appendix II.

The *Rhodotron´s®* radiation will also be shared by the Facility of Liquid Metal Technologies in the *TechnoFusión* Centre. The electron beam is an essential element to investigate the effects of an internal heat deposition on a lithium jet. A second application is the generation of tritium by the irradiation of lithium with gamma rays. These processes are more extensively described on the chapter 7 dedicated to the Facility of Liquid Metal Technologies.

---

[55] J. POTTIE. Nuclear Instruments and Methods in Physics Research B 40/41, (1989), p. 943.
Marc Van LANCKER et al. Nuclear Instruments and Methods in Physics Research B 151, (1999), p. 242.
http://www.iba-worldwide.com/industrial/products/rhodo.php, Sept 2009

[56] S. KORENEV. The Concept of Beam Lines from Rhodotron for Radiation Technologies. Proceedings of the 2003 Particle Accelerator Conference. IEEE

Figure 5.8. An IBA *Rhodotron*® electron accelerator with a maximum energy of 10 MeV.

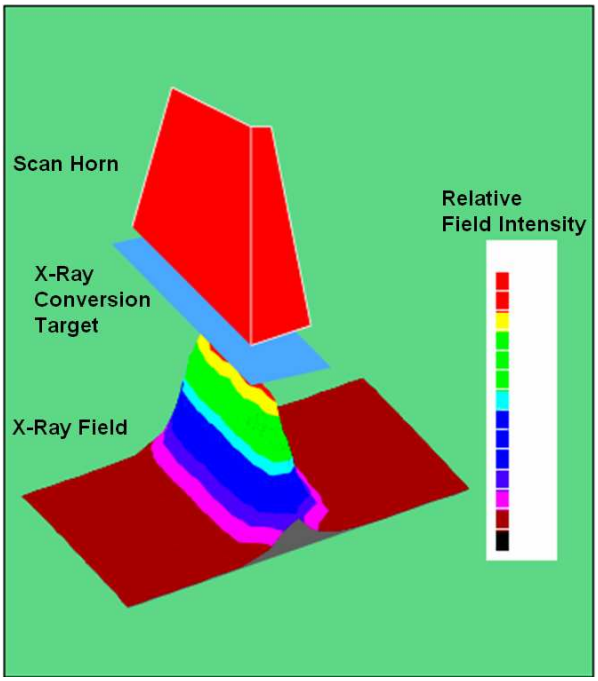

Figure 5.9. Spatial distribution of the intensity of gamma radiation at the exit of the converter with electron scanning system. Image courtesy of IBA.

5.4.3. High field magnet

The goal of having a high magnetic field is to test the performance of materials under similar conditions to those appearing in ITER: between 5 and 10 T of steady magnetic field, and heavy irradiation. The only technical requirement (other than the field intensity) is the necessity of an empty volume to place the sample holder with a temperature control, allowing some characterization measurements during the irradiation. In principle, an inner diameter of 20 - 30 cm should be enough for this purpose. The area where the magnetic field must be constant should be around 10 cm in length, and that implies a coil length of around 30 cm. Such a coil has to be made out of a superconductor material. There are companies (for instance, Oxford Instruments) manufacturing superconductive coils of up to 20 T, satisfying the above mentioned conditions.

5.4.4. Hot Cell

A hot cell is necessary at *TechnoFusión* to provide a secure environment for the processing, repair or refurbishment, and disposal of components that have become activated by exposure to ion irradiation. Special care must be taken to manipulate these activated materials and remote handling systems might become instrumental for this purpose.

5.5. Layout, supplies and safety requirements

(I) Space and facilities

The building for the MI Facility mainly depends on the dimensions and properties of the accelerators and of the characterization techniques. The performance of triple beam irradiation experiments is the figure of merit of the facility and therefore, the building must ensure its operability.

Figure 5.10 shows a proposal for the set of ion accelerators (tandem accelerators for light ions, and cyclotron) and their places in the MI installation, including a doble and a triple beam irradiation experimental areas. The special shielding required by its radioactive character was taken into account in the dimensions of the facility. Figure 5.11 shows a typical example of a cyclotron facility with 3-meter thick walls required to avoid radiation leakages.

Tables 5.7 and 5.8 summarize some of the main characteristics of the cyclotron hall and the additional support rooms for the operation of this accelerator. The proposed cyclotron for *TechnoFusión* Laboratories must have an infrastructure similar to the above-mentioned Cyclone 70 as well as those specified on these tables.

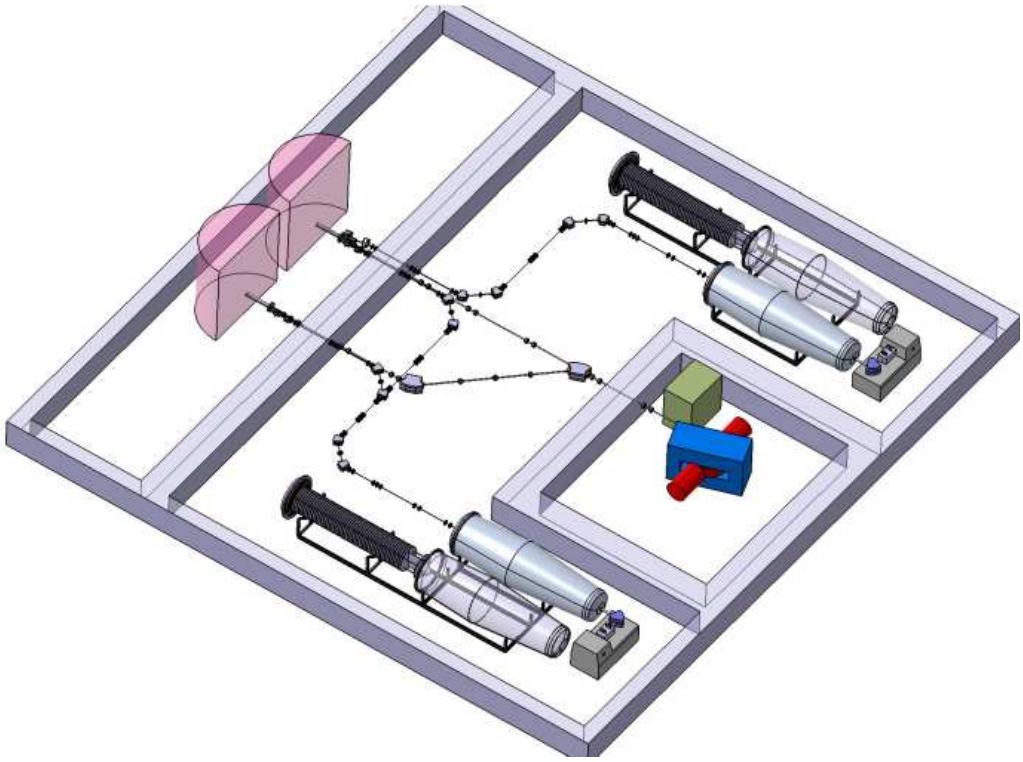

Figure 5.10. Conceptual design of the set of ion accelerators for the MI Facility. The building, include the shielding needed in any radioactive facility.

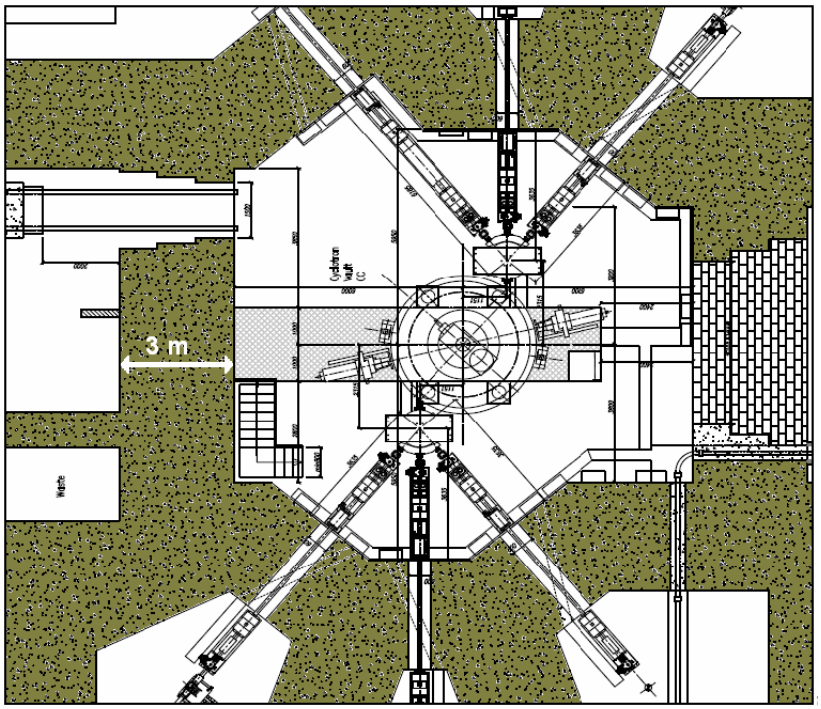

Figure 5.11. Sketch of the cyclotron vault and the irradiation rooms for cyclotron Cyclone 70 by IBA.

Table 5.7. Main characteristics of the cyclotron hall at MI Facility.

Recommended configuration of the cyclotron hall.	
Cyclotron hall	Interior dimensions (minimum): 8 m x 12 m x 5.4 m Main door: 1.5 m (height) x 2 m (width) Dimensions of the cyclotron hall and the irradiation rooms will also depend on the configuration system. Recommended shield for the vault: External walls of the irradiation room 3.7 m thick Walls between irradiation rooms: 3 m thick External walls of the Cyclotron vault: 3 m thick (ordinary concrete, density: 2.35 t/m^3) Load supported on the floor: 140 tons on 4 pillars (cyclotron) 2*10 tons on 4 pillars (magnet) Floor drains: fitted to the local health code and security rules. Pit dimensions: 2.1 m depth x 2 m width x 10 m minimum length. The pit must contain an entrance and be connected by cables to the power supply room. Temperature range: +17 to +25 °C. Humidity range: 35% to 65%, free of condensation. Dissipated power in air: less than 15 kW
Irradiation rooms	Dimensions: (about 60 m^2) * 2.5 m (height) Entrance door: 1.2 m (width) x 2 m (height) Temperature range: +17 to +25 °C Humidity range: 35% to 65%, free of condensation. Dissipated power in air: 2 kW
Power supply room	Interior dimensions: area: 70 m^2, free height: 3 m. Temperature range: +17 to +25 °C Humidity range: 35% to 65%, free of condensation. Dissipated power in air: 23 kW (in operation), 5 kW (stopped) The power supply room, the control rooms and the cyclotron room will be in very close range to avoid the use of long cables. No more than 30 m between them is proposed. Power supply room will be equipped with an elevated floor (40 cm height) with a load capacity of 2T / m.
Room for the cyclotron cooling system.	The cooling system has to be placed as close as possible to the cyclotron room, with access to a water supply. An area of 10m^2 is large enough to include the heat exchanger and the pump (1,6 m x 1,4 m, minimum dimensions). This area must have an easy access for the technical support. The cooling system should be placed at a different level compared to that of the cyclotron: maximum height gap of 7 m from the cyclotron plane. A possibility is to place the cooling system on the vault ceiling.
Cryopump and compressor	The compressor unit, with a weight of 90 kg (width: 445 mm, depth: 630 mm, height: 475 mm), will be placed either in a platform outside the cyclotron room or either inside the room. The length between compressor and cryopumps connections should not exceed 30 m.

Table 5.8. Main support facilities for the cyclotron of the MI Facility.

Specifications for the support facilities	
Power supply	400 V ±5% (between phases), 50-60 ±2 Hz, three AC phases + neuter + ground. Supplied power will depend on the energy expense, and regulated by local laws. For 70 MeV, two beam lines (500 μA): Required power: 500 kVA Required power: 600 kVA Power distributed by: IBA distribution rack [330 kVA], final anode amplifier [74 kVA], power supply source of the main coil, power supply room. The user will supply, install and cut the AC power cables at the entrance of the IBA in agreement with the local electrical rules.
Water for cooling system	Normal water supply in the cooling system room. Drain requirements based on the building regulations. Water pressure: between 2 and 5 bar. Flow: 370 l/min. Temperature: between 7 °C and 20 °C. Cooling power: < 262 kW (double beam, 500μA 70 MeV). Heat exchanger connection: DN 50 stainless steel. Power will be adapted to the cyclotron parameters.
Compressed air for valves	Pressure: between 500 kPa and 700 kPa. Quality: filtered, dry, oil free. Medium flow: < 2 l/min. Maximum flow: < 200 l/min. Dew point: > 10 °C at 25% humidity. Additional tank of compressed air, or compressed nitrogen, with at least 0.5 m^3 capacity, to allow the automatic closing of the valves in case of power failure. Installation of different connection points in the building, in agreement with IBA suggestions.
Dry nitrogen for the cyclotron and ion source ventilation	Pressure: between 50 and 100 kPa. Volume: For cyclotron ventilation: 8 m^3 (STP). For ion source ventilation: 0,3 m^3 (STP). Quality: filtered, dry, room temperature.
Gases for ion sources (hydrogen, deuterium, and helium)	Pressure: between 100 and 200 kPa. Quality: 99.9997%. Oxygen with industrial quality for the electrostatic deflector. Gases will be sent to the cyclotron through an electropolished stainless steel pipeline, in order to avoid gas contamination. The cleaning of the pipelines will be carried out before the installation of IBA systems.

Regarding the *Rhodotron®* electron accelerator, a building with a minimum volume of 6 x 6 x 5 m^3 is necessary. A good cooling system, a ~300 kW electric power, and an adequate suitable shield and control system for radiological risks are required. The building should be large and flexible enough to allow all the proposed procedures. In principle, two working areas are selected in the building: one of 30 x 20 x 10 m^3, where the remote control manipulation tests will be carried out without the presence of radiation, and a second one of 10 x 10 x 5 m^3, where the different qualifying procedures will be performed under radiation. This laboratory

(comprising both the accelerator and the testing building) will be considered as a radioactive facility and it will contain the required monitor and control systems.

One of the main added values of the MI Facility is the access, in the same laboratory, to a significant group of characterization techniques and simulation methods for reproducing the working conditions in fusion reactors (high heat fluxes, irradiation, etc.). This facility is unique and singular in Europe and in the world. Therefore, this laboratory has to be organized to allow the performance of different experiments with little changes and simple adaptation processes. These characteristics will require a special attention during the design period of the facility.

(II) Safety

A facility like *TechnoFusión´*s MI Facility precises of a careful evaluation of the radiological risks derived from it regular operation.

A primary set of risks are associated to the operation of the accelerators, which implies photon and high-energy neutron generation).

Other risks are connected to the generation of isotopes, both radioactive and stable. Information of the final activation of the samples (i. e., gamma and neutron radiation after the implantation), and of the time decay of they are of fundamental importance to determine the shielding of the building, and the safety procedures to access the experimental rooms.

Additional hazards in the facility will be I) electrical, II) magnetic, and III) chemical:

I. During operation, the facility will require high voltage supply units. These must be electrically isolated by means of Faraday cages and any other appropriate protection systems.

II. The presence in the facility of high magnetic fields, either from the cyclotron (about 6 or 7 T) or from the high magnetic field electromagnet (between 5 and 10 T) will restrict the access to the experimental room. Although there are no known effects on health caused by exposure to high magnetic fields, the *World Health Organization* (WHO) recommendations[57] are a time-weighted average of 200 mT during the working day for occupational exposure, with a ceiling value of 2 T.

Therefore, there must be signs indicating the presence of strong magnetic fields and the safety warnings for people with special needs—pacemaker users, people with ferromagnetic implants and devices, etc. This information must be located in areas with magnetic fields below 0.5 mT.

[57] World Health Organization. Electromagnetic Fields and Public Health. Retrieved from the Internet on August 2009. http://www.who.int/mediacentre/factsheets/fs299/en/index.html

There will also be clear signs prohibiting the access to areas where the field could exceed 3 mT with any ferromagnetic element. These objects could be projected by the field, damaging equipment and personnel.

III. The use of different hazardous gases –flammable, oxidizing, toxic— will require the separation of the testing area and the area for gas storage. Gases should also be separated according to the specific danger each of them posed.

Proper ventilation, protection from heat, and protection from direct sunlight are also needed. In the storage area for flammable gasses, wiring –if any— should be made according to regulations. The gases should be transported from the storage area to the plant by hermetic pipeline allowing a wide versatility in the use of these gases while maintaining an acceptable level of security. Finally, inside the facility there will be gas detectors for hydrogen, helium, sulphur hexafluoride, etc; gauges to measure oxygen levels; as well as fire prevention measures.

There are also risks associated to the presence of cryogenic liquids at the facility, mainly extreme cold and suffocation.

Finally, as a test facility, the risks may vary during its lifetime. Therefore there will be protective measures for the equipment and people related to the use and status of the facility. In this sense, MI Facility must comply with the Law on Prevention of Occupational Risks (BOE n º 269, 10/11/1995, RD 31/1995).

6. Plasma-Wall Interaction

6.1. Introduction

The operation of experimental fusion reactors in the coming decades and beyond (i.e., commercial reactors) will require expanding our knowledge concerning the behaviour of thermonuclear plasmas in magnetic confinement devices. Such knowledge involves understanding the relationships between operational parameters in present and future devices. For example, the integrated plasma flux impacting on the divertor tiles in a single ITER pulse typically corresponds to the integrated flux experienced over a whole year in present devices like JET. Similarly, the energy fluxes impacting the inner wall components of ITER during transitory events will exceed current values by one order of magnitude. Indeed, the energy content of ITER plasmas will be more than one order of magnitude (more precisely, a factor of 30) greater than that of present devices (such as JET), while the effective area of the inner wall components is only larger by a factor of 2. In addition, the corresponding fluxes in DEMO will typically be 5-10 times those of ITER. Consequently, significant advances are required in our current knowledge of plasma-material interaction, for which experiments are required.

Some of the main technological challenges for the operation of ITER are related to plasma-material interaction (related to first wall materials, limiters, or divertors) and the study of these issues is surely among the key measures of success of the project. Moreover, their impact on the design of DEMO is considerable, and in recent years the fusion community has therefore joined forces to study these phenomena. As a result, in 2002 the “EFDA Task Force”, centred on the topic of Plasma-Wall Interaction, was created as the first Task Force of its kind in the EU. This Task Force has helped to channel the efforts of different EURATOM associations towards the study of topics such as the erosion of plasma facing materials, fuel (deuterium-tritium) retention in materials, the response to high thermal loads, the generation of dust and pollutants, material mixing effects in the first wall, etc. From the beginning, the Plasma-Wall Interaction Group at CIEMAT (whose members will constitute the *TechnoFusión* Plasma-Wall Interaction group) has participated in several of the above-mentioned studies. Here, it is mentioned a particularly relevant contribution on the subject of the removal of trapped tritium from reactor walls, and on mechanisms for carbon transport and co-deposition in ITER.

Many experiments have already been carried out in laboratories and fusion devices to study the behaviour of selected materials for the divertor (CFC and tungsten), and the first wall (beryllium) when the latter are exposed to high thermal loads or high particle fluxes, and how this behaviour is affected when they are previously irradiated by energetic particles (though not by 13 MeV neutrons, as would be the case in a fusion reactor). In general, it is found to be extremely difficult to extrapolate laboratory results to fusion devices, which is caused mainly by the complexity of the reactor conditions, where processes occur such as the formation of mixtures of the initial constituents, possessing very different chemical and physical properties from those of the original pure constituents. Even though evidence exists that the simultaneous action of these conditions (high thermal load, high particle flux, and radiation) can produce a synergy with unknown results, at this time no facilities exist capable of directly studying such possible synergies. Therefore, the main goal of the proposed Plasma-Wall Interaction Facility of *TechnoFusión* is to become the first facility in the world having the capacity of studying all these phenomena simultaneously.

Present research in this field indicates that the interaction of the proposed materials and expected plasmas in devices such as ITER and DEMO can significantly modify the material properties due to: i) the retention of hydrogen isotopes in the surface layer and the formation of chemical compounds as a result of reactions between materials used in the inner components of the reactor vessel, ii) changes in the structure due to the high temperatures occurring during operation, iii) high neutron fluxes damaging the surrounding materials, and iv) (in transitory events) structural modifications due to the very large power fluxes, leading to surface damage of the material (i.e., the melting of metals, sublimation of ceramics, sputtering of aggregates, etc.), and surface fractures that affect both the material properties and its resistance. These damages result in diminished thermal conductivity, reduced mechanical resistance, permeability, retention of hydrogen isotopes, etc.

Obviously, the study of these processes can be carried out in the present and future nuclear fusion devices, but often, these devices do not allow a proper study of the interactions, requiring the characterization of the plasma and the materials with sufficient accuracy. Furthermore, setting up the necessary test components to perform these experiments in fusion devices is often difficult or complex, requiring much time. These considerations, along with the impossibility of replacing test components in reactors, have spawned the development of experimental facilities, specifically dedicated to the study of the interaction of materials with the peripheral plasma in thermonuclear fusion devices, by simulating the properties of these plasmas in steady state and during transitory events.

At the moment, several laboratories have experimental facilities capable of reproducing the characteristics of fusion reactor plasmas to different degrees and using different approaches, and their interaction with materials, in either steady state or transient regimes, although no facility is capable of simulating both. The reason for this is that devices designed to study steady state phenomena, like PSI-2 (Humboldt University, Berlin), PISCES-B (California University, San Diego), and Magnum-PSI (under construction at the FOM-EURATOM association), are intrinsically limited regarding the generation of energy pulses similar to transitory events in fusion reactors (usually ~ MJm^{-2} on a sub-ms time scale). On the other hand, devices capable of generating transient energy pulses, such as the Quasi-Stationary Plasma Accelerator (QSPA) at the TRINITI laboratory of the Russian Federation (QSPA-T), or the device at the Institute of Plasma Physics in Ukraine (QSPA-Kh50), lack the possibility to generate plasmas that last more than 1 ms, due to the physical principles on which they are based.

The transitory events may occur at certain typical repetition frequencies. For example, edge localized modes (ELM) will have a frequency of about 1 Hz in fusion reactors, and can have a significant effect on materials, modifying their behaviour as compared to with steady-state plasmas. Thus, it is essential to dispose of a device (which it will be called “plasma gun”) to study plasma-material interactions simultaneously in steady state and transient regimes, under conditions relevant to a fusion reactor, thereby allowing an analysis of the modification of the materials and their properties in fusion reactors. This is the objective of the **Plasma-Wall Interaction Facility (PWI)** of *TechnoFusión* Centre. The mentioned plasma gun would consist of two main elements:

a) A linear plasma device, similar to the existing PILOT-PSI device, capable of generating hydrogen plasmas with steady state particle fluxes of up to 10^{24} $m^{-2}s^{-1}$ (i.e., of the order of the expected ITER fluxes) and impact energies in

the range of 1-10 eV (although higher energies can be reached by polarizing the plasma with respect to the target).

b) A device of the QSPA type, providing pulses lasting 0.1-1.0 ms and energy fluxes in the 0.1-20 MJm^{-2} range, in a longitudinal magnetic field of the order of 1 T or greater.

These devices are connected by a common vacuum chamber, allowing the exchange of samples, and their simultaneous or consecutive exposure to the steady state and transient plasma flows under controlled conditions.

It is not yet decided what kind of materials will exposed to the plasma in ITER and DEMO, due to the incomplete knowledge of material behaviour under the extreme conditions of high particle flux, thermal loads, and neutron irradiation. The following issues are critical:

- The lifetime of the plasma facing materials
- Dust generation due to material erosion
- The in-vessel tritium inventory.

In spite of these uncertainties, and due to the time constraints of the project, a compromise has been reached for the initial phase of ITER, so that the divertor will be made of tungsten (in regions of moderate thermal load) and carbon (as a CFC). Due to the high degree of tritium retention in carbon scenarios, the substitution of CFC by tungsten in the reactor phase (D+T operation) is foreseen. However, the final decision depends on future results from the ASDEX-UG tokamak, now operating in a pure tungsten scenario, and from JET, fitted with an ITER-like wall. Such a wall includes a pure tungsten divertor, and uses beryllium as a vacuum vessel coating, in accordance with the ITER first wall proposal. Nevertheless, there exists a great difference between ITER (pulsed plasma) and DEMO (continuous plasma) regarding the total neutron dose, which will create uncertainties when extrapolating the results obtained in ITER to a continuous reactor. For these reasons, the research of materials under the cited extreme conditions constitutes one of the crucial issues of fusion research.

In recent years, research in laboratories possessing devices similar to those proposed for the *TechnoFusión* Plasma-Wall Interaction project has led to the discovery of new phenomena related to the first wall, with great potential for future application.

Mixed materials effects (in linear plasmas). These effects include the drastic reduction of the chemical erosion of carbon in the presence of beryllium, the formation of eutectic mixtures in the Be/W system with a melting point below that of pure W, the increase of tritium retention in beryllium when it forms part of carbides and oxides, the formation of W and Be carbides at the temperatures expected in the high thermal load region of the divertor, etc.

Thermal load effects (in plasma accelerators). The realistic simulation of material degradation in the divertor requires considering ELM's, with energy pulses greater than 1 MJm^{-2} lasting less than 1 ms, and with a repetition frequency of the order of 1 Hz. Although there are no experimental devices that can reproduce these conditions, it has been shown, in devices like QSPA, that material fatigue limits the maximum tolerable power in steady state

after a specific number of ELM-like pulses. In the case of C (as a CFC) and W, the former experiences erosion of the PAN component (glue of the individual fibres) with loads exceeding 0.5 MJm^{-2}. For the latter (W), the erosion process leads to the ejection of liquid metal, whose subsequent behaviour depends on the presence of magnetic fields and the plasma pressure at the surface. The formation of liquid metal can also give rise to shortcuts between the rods included in the design of the high heat flux components of the divertor (macro-brush structures). For a series of pulses with thermal loads below those needed for material melting (again of the order of 0.5 MJm^{-2}), the micro-fissures have been observed to grow into macroscopic cracks that can lead to material fracture. This can also give rise to the formation of activated dust.

Synergetic effects between plasma species. The simultaneous irradiation of materials by the various main particle species emitted by the plasma (deuterium, tritium, helium, and neutrons) sometimes produces synergetic effects. A representative example is the formation of defects in a material and the consequent tritium retention caused by the combined effect of neutron damage and irradiation by a tritium containing plasma. With respect to neutron damage, in ITER, with an estimated irradiation dose of 0.6 dpa (displacement per atom), it is known that the amount of retention due to neutron irradiation on tungsten would not be very different from the non-irradiated case. However, the situation in DEMO could be radically different, so that this material and similar refractory metals should be avoided in the final design. Additionally, the simultaneous implantation of several species at high fluxes can enhance tritium retention: for example, a species with low solubility such as helium originates aggregates (bubbles) that act as trapping sites for the main species (D, T). Furthermore, the pressures occurring in these cavities can damage the material and eject it towards the plasma (blistering). The probability of diffusion and surface and volume recombination is strongly dependent on the temperature (which depends on the plasma impact), and therefore some divertor areas always have the right conditions for these phenomena to occur. For example, recently it has been found that helium irradiation of tungsten leads to the development of nanometric structures with a high capacity for tritium retention. Again, these studies were carried out in a linear plasma device similar to that proposed in this report.

Another synergetic effect is produced by the combination of temperature and metal implantation. In this case, the implantation of hydrogen isotopes at relatively low temperatures (below the embrittlement point of the material) entails a severe mechanical degradation of the material. The periodic exposure of this material to ELM-like thermal pulses can severely degrade its power handling capacity.

At present, no experimental device exists capable of simultaneously reproducing the above-described phenomena. Making the correct choice of plasma facing materials, and developing strategies for a long device lifetime, will be only possible if extreme conditions can be reproduced in the laboratory, similar to those expected in ITER and DEMO. Therefore, the construction of the Plasma-Wall Interaction Facility is essential for performing such important experiments for the fusion program.

Finally, the characterization of low temperature and high density plasmas, typical of the divertor of a future reactor, has its own intrinsic value, due to its complex atomic and molecular physics. Consequently, an additional benefit of the proposed linear plasma device is the development of diagnostic methods based on atomic and molecular physics (spectroscopy, mass spectrometry, probes, etc.), suitable for ITER and other future devices. This task requires

producing continuous plasmas in a high magnetic field and with a high gas flux, and involves the management of superconductor coils and cascaded arc plasma sources capable of providing suitable high fluxes.

6.2. Objectives

A large number of important material related issues, identified in the course of the European Fusion Program, can be studied using known experimental techniques and methods for material modification. Some of these are:

- A study of the behaviour of materials relevant to ITER and DEMO at high particle fluxes of different species (H, D, He).
- A study of the behaviour of materials relevant to ITER and DEMO at high energy fluxes and at different temperatures.
- A study of the behaviour of materials relevant to ITER and DEMO at high particle fluxes from the plasma, with simultaneous high thermal loads.
- The effect of local magnetic fields and plasma pressure on the movement of liquid layers or gas clouds created by the plasma.
- The effect of sample orientation with respect to the plasma for the cited phenomena.
- A study of material mixing and its effect on the plasma-material interaction.
- The characterization and modelling of the effect of plasma irradiation of structural materials, shields, joints, welds, etc.
- The characterization and modelling of plasma-wall interactions for different kinds of materials.
- The characterization and modelling of plasma irradiation on insulating materials and diagnostic components.

The first and second of the above points require plasmas that are large enough to achieve saturation in the exposed material. It is also desirable that the particle flux directed towards the sample is sufficiently intense to facilitate the extrapolation of the results to the experimental conditions of ITER (see Table 6.1).

Table 6.1. Thermal and particle loads in ITER (1998 design).

Component **Material** **Area**	**Power flux** ($MW \cdot m^{-2}$)	**Particle flux** ($DT \cdot m^{-2} \cdot s^{-1}$)	**Energy** (eV)	**Neutron flux** ($n \cdot m^{-2} \cdot s^{-1}$)
First wall Be ~1000 m^2 Charge exchange neutrals (E_{mean}<100 eV)	0.5	10^{19}-10^{20}	100-500	<2.3x10^{18}
Limiter start-up Be ~10 m^2 Direct interaction with plasma and high power flux during the starting-up and switching off of the plasma	~8	10^{21}-10^{22}	100-500	<2.3x10^{18}
Divertor target (*strike-points*) C 75 m^2 High power and particle fluxes; energy deposition during disruptions and ELM's; electromagnetic loads during disruptions	<10-20 <40 (ELM's) <100(disrupt)	<10^{24}	1-30 (plasma temp.)	4-6x10^{17}
Divertor sides (*baffle*) W ~200 m^2 Charge exchange neutrals (M_{edia}<100 eV); direct interaction with SOL; power radiated from X point (i.e. MARFE's); possible power deposition during ELM's; electromagnetic loads during disruptions	3	10^{20}-10^{22}	> 3 (plasma temp.)	<2x10^{18}
Divertor Dome W 85 m^2 Charge exchange neutrals(E_{mean}<100 eV); power radiated from X point (i.e. MARFE's); energy deposition during VDE; electromagnetic loads during disruptions	3	10^{21}-10^{22}	>30 (plasma temp.)	<1.1x10^{18}
Divertor private flux region (liner) W 90 m^2 Radiated power dissipated on the divertor; re-irradiated energy during disruptions; electromagnetic loads during disruptions	<1	<10^{23}	<1	~4x10^{17}

Similarly, the study of transient high thermal loads requires a pulsed high power plasma with pulses of a short duration, so that ELM[58] effects can be simulated.

[58] Edge Localized Mode: A transitory relaxation event of the edge plasma that produces a high energy flux to the wall.

In order to achieve the objectives related to steady state plasmas, a cascade arc plasma source is proposed, designed to reach conditions similar to those of ITER in steady state. The main shortcoming of such a device is that it requires a high magnetic field. Alternatively, a LaB_6 source may be used. The latter produces particle fluxes that are one order of magnitude lower, while requiring a weaker field and providing a larger plasma diameter. However, to simulate the integrated fluxes expected at ITER, it would be necessary to increase exposure times. As mentioned above, high flux plasmas in a device with superconductor coils would open the possibility of studying divertor-like plasmas.

On the other hand, the best way to produce short pulse and high power plasmas is to use Quasi-Stationary Plasma Accelerators (QSPA).

The goal of the proposed steady-state (or continuous) plasma device would be to produce a homogeneous plasma with a radius ≥ 4 cm, a particle flux of up to 10^{24} $m^{-2}s^{-1}$, an ion impact energy in the range 1-10 eV (enhanced by means of polarization), and a total length of 1 to 2 m. Such a plasma would interact with a material sample under controlled temperature conditions in the 200 to 1500 ºC range. For this purpose, the sample is to be integrated in a heating-cooling system that can handle the mentioned temperature range.

The main working conditions for the linear plasma are:

- Particle flux > 10^{24} m^{-2} s^{-1}
- Electron density > 10^{20} m^{-3}
- Electron temperature < 10 eV
- Neutral pressure < 10 Pa
- Working gases: H_2, D_2, He, Ar

And for the QSPA:

- Energy density per pulse < 40 MJm^{-2}
- Pulse duration < 0,5 ms
- Peak intensity < 100 GWm^{-2}

6.3. International status of the proposed technologies

6.3.1. Major international facilities for Plasma-Wall Interaction research

The international research groups currently working on Plasma-Wall Interaction are:

- TRINITI, Troistk, Russia
- Institute of Plasma Physics, NSC KIPT, Kharkov, Ukraine
- Universidad de Nuevo Mexico, Albuquerque, USA
- Efremov Institute, San Petersburgo, Russia
- Japan Atomic Energy Research Institute, Naka, Japan
- Forschungszentrum, Jülich, Germany
- Budker Institute, Novosibirsk, Russia

6.3.2. State of the art of Plasma-Wall Interaction technologies

Below, there is a list of the designs of the main linear and pulsed plasma devices operating in the foremost international laboratories:

a) Stationary linear plasma devices (steady state)

Numerous linear plasma facilities are operating across the world. The following devices are especially relevant for Plasma-Wall studies in view of their parameters:

a) [i]*Nagoya University*, Japan
b) [ii]*Humboldt-Universität,* Department of Experimental Plasma Physics, Berlin, Germany.
c) [iii]University of California San Diego, USA.
d) [iv]*Kurchatov Institute*, Moscow, Russia.
e) [v]*FOM-Institute for Plasma Physics Rijnhuizen, Nieuwegein*, The Netherlands.
f) [vi]*Idaho National Laboratory*, Idaho, USA.

The main characteristics of these facilities are shown in Table 6.2. In addition, the operating schemes and brief descriptions are given below.

Table 6.2. Facilities of Linear Plasma / Divertor Simulator.

	NAGDIS-II[i] [6]	PSI-2[ii] [7]	PISCES-A[iii] [8]	PISCES-B[iii] [9]	LENTA[iv] [10]	Pilot-PSI[v] [11]	Magnum-PSI[v]* [12]	TPE[vi] [13]
Source	TP-D	PIG	PIG	PIG	e-Beam	CA	CA	PIG
Power [kW]	10.5	6.5	<10	-	7.5	45	270	-
Pressure at source [Pa]	10	0.1-1	0.1-1	0.1-1		104	104	0.1-1
Pressure at target [Pa]	0.1	0.01-0.1	10-3-1	10-3-1	0.2-7	1-10	<10	0.01
Ti target [eV]	50	<15	10-500	10-500	5	0.1-5	0.1-10	10-130
Te target [eV]	10	<30	<20	3-50	0.5-20	0.1-5	0.1-10	10-15
ni target [m^{-3}]	$6\cdot10^{19}$	10^{19}	10^{19}	10^{19}	10^{19}	10^{21}	10^{20}	10^{19}
Ionic flux to target [$m^{-2}s^{-1}$]	10^{22}	10^{22}	10^{21}-10^{22}	10^{21}-10^{23}	$5\cdot10^{21}$	$2\cdot10^{25}$	10^{24}	10^{23}
Energy flux to target [MW/m^2]	0.01	0.1	-	-	-	30	10	-
B [T]	0.25	0.1	-	0.04	0.2	1.6	3	0.2
Beam diameter at target [cm]	2	6-15	-	3-20	2.5	1.5	10	0.5

* Currently under construction. Expected parameters.

- **TPE (*Tritium Plasma Experiment*)**. This is a small size device whose main advantage is its capability to work with beryllium and tritium. Its configuration is similar to that of PISCES-B[59]. A picture of this device is shown in Figure 6.1.

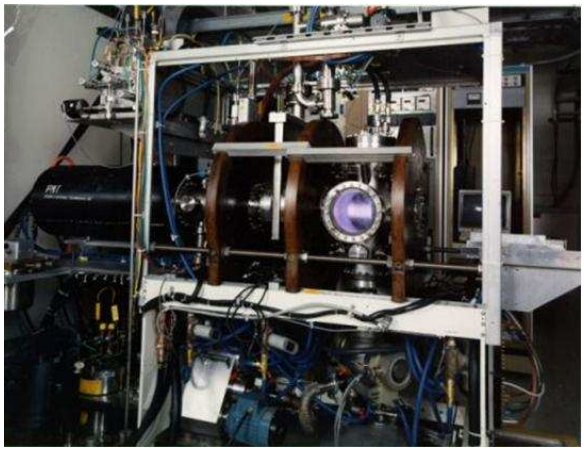

Figure 6.1. Picture of TPE linear plasma device installed at the Idaho National Laboratory, Idaho (USA).

- **PSI-2**. A diagram and a picture of this device[60] are shown in Figure 6.2.

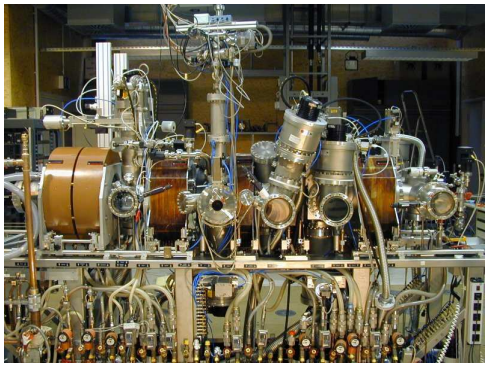

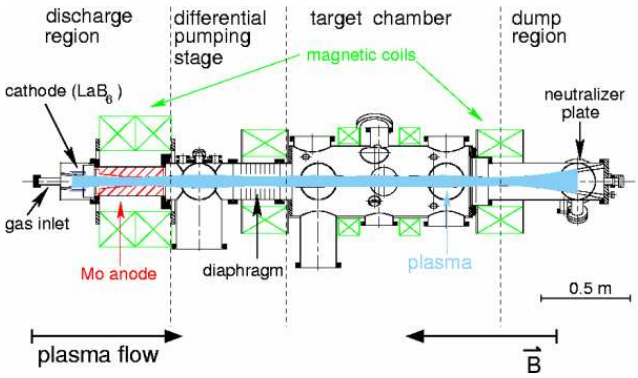

Figure 6.2. Linear plasma device at the Humboldt University, Berlin, (Germany).

[59] http://nuclear.inl.gov/fusionsafety/experiments/star.shtml
[60] http://plasma.physik.hu-berlin.de

- **PISCES-B**. This is a device with a LaB_6 cathode, like TPE, PISCES-A, and PSI-2, that allows working with Be[61]. A diagram is shown in Figure 6.3.

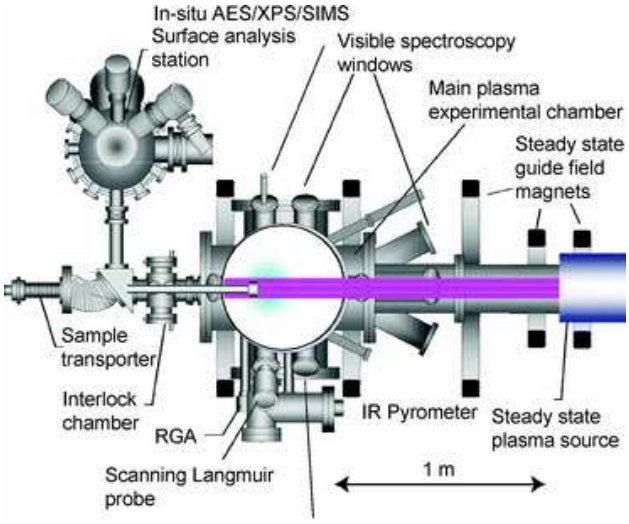

Figure 6.3. PISCES-B (a linear plasma device), University of California, San Diego, (USA).

- **LENTA**. This device[62] employs an electron beam to start the discharge. Figure 6.4 shows a sketch of the device.

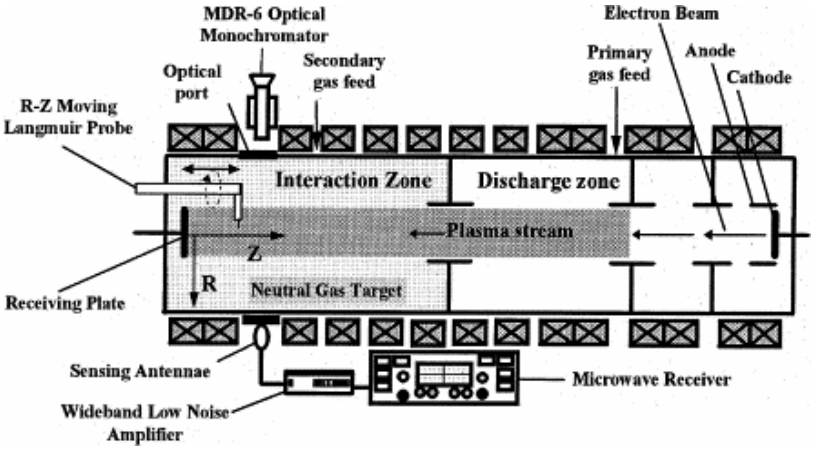

Figure 6.4. LENTA (linear plasma device), Kurchatov Institute, Moscow, (Russia).

[61] http://www.pisces.ucsd.edu/pisces/Research/DivertorPlasmaSimulators/tabid/66/Default.aspx.
[62] http://www.kiae.ru/nsi/usnsi.htm#lenta

- **NAGDIS-II**. It uses a LaB_6 cathode combined with an intermediate electrode and an appropriate magnetic field that provides good plasma confinement. This allows improved insulation between the discharge and the sample chamber. Figure 6.5[63] shows a picture of this device.

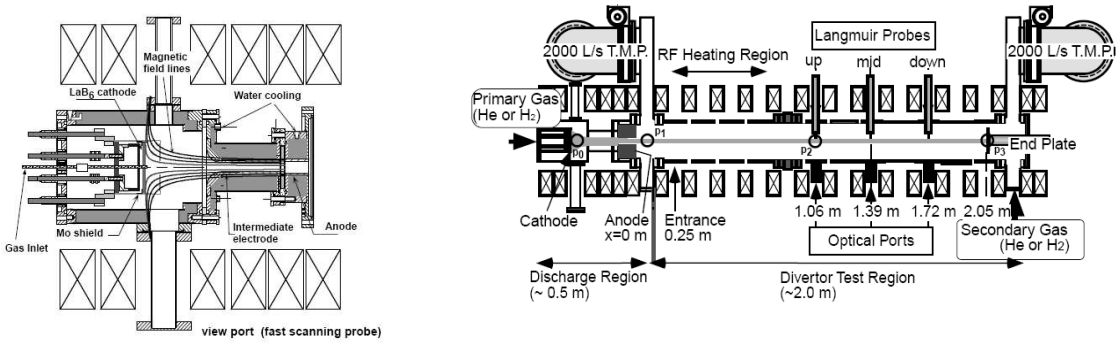

Figure 6.5. NAGDIS-II (a linear plasma device), Nagoya University, (Japan).

- **Pilot-PSI**. The main characteristic of this device is that the plasma is generated by a cascade arc. This kind of system allows operating the arc at higher pressures and particle fluxes than Penning-like discharge devices. Figure 6.6 shows a picture and a sketch of this facility.

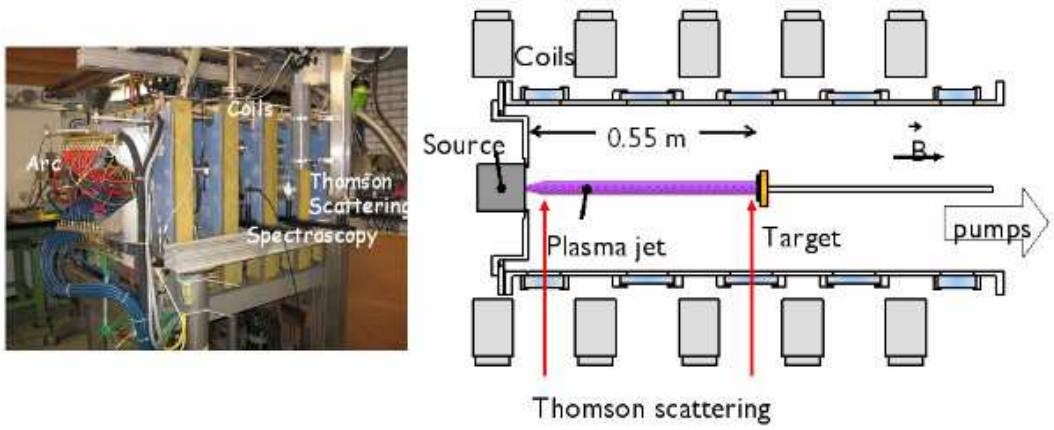

Figure 6.6. Pilot-PSI linear plasma device, FOM-Institute for Plasma Physics Rijnhuizen, Nieuwegein, (Netherlands).

[63] www.ees.nagoya-u.ac.jp/~web_dai5/english/NAGDIS_II.html

b) Quasi-stationary plasma accelerator devices (QSPA and QHPA)

The main high thermal flux or QSPA facilities currently in operation are:

a) [i]TRINITI, Troistk, Russia.
b) [ii]Institute of Plasma Physics, NSC KIPT, Kharkov, Ukraine.
c) [iii]University of Nuevo Mexico, Albuquerque, USA.
d) [iv]Efremov Institute, St. Petersburg, Russia.
e) [v]Japan Atomic Energy Research Institute, Naka, Japan.
f) [vi]Forschungszentrum, Jülich, Germany.
g) [vii]Budker Institute, Novosibirsk, Russia.

Table 6.3 summarizes the main characteristics of these facilities. Sketches and a review of their operational parameters are given below.

Table 6.3. High thermal flux devices at present.

D	E (MJ/m^2)	Pl (ms)	P (GW/m^2)	MJ·m^{-2}·s$^{-1/2}$	Ep (keV)	Dp (m^{-3})	B (T)	S (m)	A
MK-200UG[i] Pulsed plasma gun pulsed with drift tube[14]	15	0.04-0.05	300-400	~70	1.5 (ion)[1] 0.15[3]	$2\cdot10^{21}$ ($5\cdot10^{21}$)2	2	0.065	a, b, c, d, e
MK-200CUSP[i] CUSP trap [14]	2	0.015-0.020	150-200	~15	0.8 (ion) 0.15[3]	$(1.5-2)\cdot10^{22}$	2-3	0.005	a, b, c
MKT-U[i] Pulsed plasma gun pulsed with drift tube [15]	1-2	0.03	30-60	>6	1.2 (ion)[1]	$6\cdot10^{20}$	2	~0.07	d, e
QSPA[i] **Kh50**[ii] Quasi-stationary plasma accelerator[16]	5-10	0.25-0.6	10-50	6-20	0.1	$<1\cdot10^{22}$	0-1	0.05	d, e
QSPA-Kh50[ii] Quasi-stationary plasma accelerator[17]	10-40	0.2	37-80	22-90	0,3 (ion)	$(2-8)\cdot10^{21}$	0-2	~0.04	d, e
PLADIS[iii] Plasma gun [18]	0.5-20	0.08-0.5	-	~15	0.1 (ion)	n/a	-	0.02	d, e
VIKA[iv] Quasi-stationary plasma accelerator [19]	2-30	0.09-0.36	20-84	<20	0.2	$>1\cdot10^{22}$	0-3	0.06	c, d, e
ELDIS[iv] Electron beam[15]	<50	0,05-0,06	2	>100	120[4]	$(2-4)\cdot10^{22}$	0-4	-	e
JEBIS[v] Electron beam [20]	2.5	1.5-2	2	~2	70[4]	n/a	0	>0.005	e
JUDITH[vi] Electron beam [21]	5-10	1-5	2-6	2-10	120[4]	-	0	~0.004	e
GOL-3[vii] Long mirror trap [15]	8-10	0.01-0.02	1000-1300	>50	1-3[3,5] (thermal) 20-10^3 (fast)	10^{21}	2-5	0.06	b, d, e

D = Device; E = Energy Density; Pl = Pulse Length; P = Power Density; Ep = Particle Energy; Dp = Plasma Density; B = Magnetic Field; S = beam Size, D = Beam Diameter; A = Applications
[1]Decreases to 300 eV at the end of the pulse; [2]Increases at the end of the discharge; [3]Electron temperature; [4]Electrons; [5]Non-Maxwellian distribution function with a large contribution of 800 keV electrons.
[a]Vapour dynamics in strong magnetic field at inclined target ("shielding") [b]Production of secondary radiation and its interaction with nearby surfaces, [c]Net radiation power to target surface, [d]Erosion (vaporization and/or ablation), [e]Ablation.

- **QHPA P-50M**. Laboratory of Plasma Accelerator Physics. IMAPh NAS Belarus[64] . Figure 6.7 shows a diagram of this QHPA (Quasi-stationary High-current Plasma Accelerator) plasma gun. Its main characteristics are:

  - Discharge time 500 μs
  - Peak current 200 – 450 kA
  - Plasma velocity $(7 – 20)\cdot10^6$ cm/s
  - Electronic density $10^{16} – 10^{18}$ cm^{-3}
  - Electronic temperature 10 – 15 eV
  - Total energy 215 kJ
  - Vacuum chamber dimensions 0.8 x 0.8 x 4 m

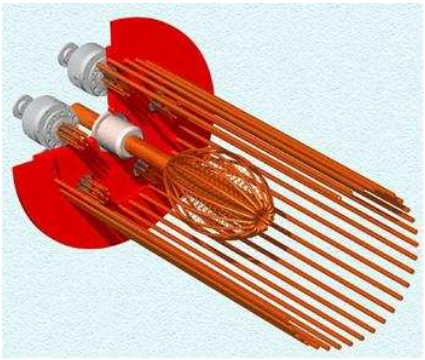

Figure 6.7. High thermal flux device QHPA P-50M. Laboratory of Plasma Accelerator Physics. IMAPh NAS, (Belarus).

- **QSPA Kh-50**. Institute of Plasma Physics. National Science Centre. Kharkov Institute of Physics and Technology. Ukraine[65]. Figure 6.8 shows a description of this plasma gun design.

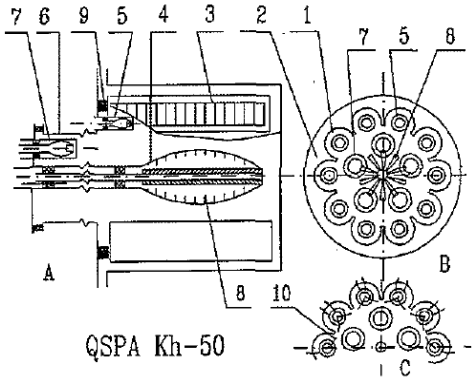

Figure 6.8. QSPA Kh-50. Institute of Plasma Physics. National Science Centre. Kharkov Institute of Physics and Technology, (Ukraine).

[64] http://imaph.bas-net.by/imaph/lpap/QHPA1.html
[65] http://www.kipt.kharkov.ua/en/ipp.html.

Several characteristics of these two QSPA devices are listed in Table 6.4.

Table 6.4. Characteristics of QSPA Kh-50 and QHPA P-50M.

DEVICE		P-50M	Kh-50
First stage	Number of input ionization chambers	4	5
	Length of the drift chamber (cm)	~20	80
Anode		Passive	Active
	Diameter (cm)	50	50
	Length (cm)	80	80
	Number of rods	36	(10)
	Number of anode ionization chambers	-	10
Cathode		Passive	Semi active
	Diameter (cm)	32	36
	Length (cm)	60	60
	Number of rods	16	20
Power supply	Capacitor bank (C(μF)xU(kV); Wc (kJ))	5600 x 10 (22400 x 5); 280	7200 x 25; 2250
	Voltage achieved, Uc (kV)	8.5 (4.5)	15
	Discharge achieved, Id (kA)	≤ 600	≤ 800
	Pulse length, (τ, ms)	0.26 (0.55)	0.3
Vacuum chamber	Length (m) x Diameter (m)	4.0x1.0	10.0x1.5

- **MK-200 (UG y CUSP)**. Troitsk Institute for Innovation & Fusion Research. Russia[66]. Figures 6.9 and 6.10 show a picture and a diagram of this device, respectively.

Figure 6.9. Photograph of the quasi-stationary plasma accelerator MK-200 (UG y CUSP), at the Troitsk Institute for Innovation & Fusion Research, (Russia)..

[66] http://www.triniti.ru/Triniti_eng/Base2.html#3

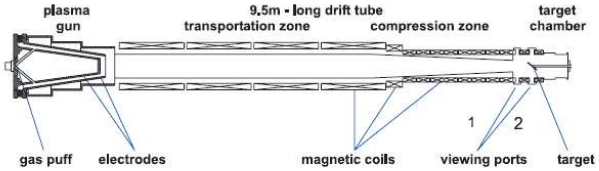

Fig. 1. Basic scheme of the MK-200 UG facility.

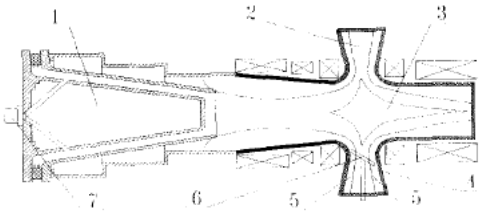

Fig. 1. Experimental facility MK-200 CUSP. (1) Plasma gun, (2) plasma escaping CUSP, (3) CUSP's plasma, (4) CUSP, (5) magnetic field lines, (6) target, (7) gas valve

.

Figure 6.10. Diagrams of the device MK-200 (UG y CUSP), at the Troitsk Institute for Innovation & Fusion Research, (Russia)..

- **QSPA-T (TIN-1)**. Troitsk Institute for Innovation & Fusion Research. Russia[67]. A picture of this machine is shown in Figure 6.11.

Figura 6.11. Photography of QSPA-T (TIN-1), *Troitsk Institute for Innovation & Fusion Research*, (Rusia).

6.4. Projected devices

6.4.1. Steady state linear plasma device

Currently, two types of systems are used to generate plasmas in the continuous regime. There are devices that employ penning-like discharges and those that employ cascade arc discharges.

[67] www.triniti.ru/Triniti_eng/Base2.html#3

Penning-like discharge devices. In this case, the plasma stream is achieved by means of a hot cathode of LaB_6[68] and a hollow anode (molybdenum or another refractory material), creating a cylindrical quasi-neutral plasma that is confined by an axial magnetic field (~ 0.1 – 0.2 T). The plasma ends on a target sample at about 1-2 m from the source (see Figure 6.12). The plasma properties depend on the current between the anode and the cathode (typically in the range of 50-500 A), on the applied magnetic field, and on the gas pressure, controlled by the differential pumping of the different regions of the device by means of turbo-molecular pumps (common pressures are 0.1-1 Pa in the discharge region, and 0-1 Pa in the plasma-material interaction region). The impact energy of the ions can be adjusted by applying an electric potential to the irradiated sample (polarization).

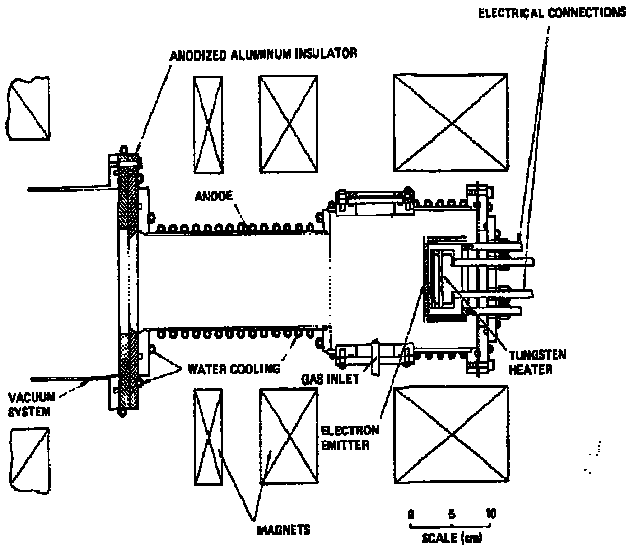

Figure 6.12. Description of a LaB_6 plasma source.

The maximum flux achieved in this type of devices is around 10^{23} $m^{-2}s^{-1}$ for electron temperatures below 10 eV (without polarization). The energy flux to the target is less than $1MW/m^2$.

Cascade-arc discharge devices[69,70] consist of a chamber with needle-like tungsten cathodes, a series of copper elements (insulated by boron nitride plates), and a final anode element with a long channel (see Figure 6.13). All these components are water-cooled. The

[68] D.M. Goebel, Y. Hirooka, and T.A. Sketchley, "Large-area lanthanum hexaboride electron emitter," Review of Scientific Instruments, Vol. 56, 1985, pp. 1717-1722

[69] G. Van Rooij, "Laboratory experiments and devices to study plasma surface interaction," Fusion Science and Technology, Vol. 53, 2008, pp. 298-304.

[70] G.M.W. Kroesen, D.C. Schram, and J.C.M. de Haas, "Description of a flowing cascade arc plasma," Plasma Chemistry and Plasma Processing, Vol. 10, 1990, pp. 531-551.

hydrogen flux into the source is 0.5-3.5 slm (standard litres per minute), providing a constant pressure of ~100 Pa. The arc operates in the 60-300 A range and the applied voltage can reach 200 V. Each arc element receives a power of 2.5-3 kW (reaching up to 45 kW in a one-channel source, and up to 135 kW in a three-channel source), resulting in a total power at the source of ~40 MW/m^2.

These devices generate plasmas with a diameter of about 5 mm that are driven through a chamber with a background pressure of 1-5 Pa. It is possible to achieve fluxes above 10^{24} H^+ $m^{-2}s^{-1}$, and electron temperatures of the order of 1 eV. To maintain the high densities (10^{21} m^{-3}) corresponding to these fluxes, it is necessary to apply strong magnetic fields (~1 T) [8].

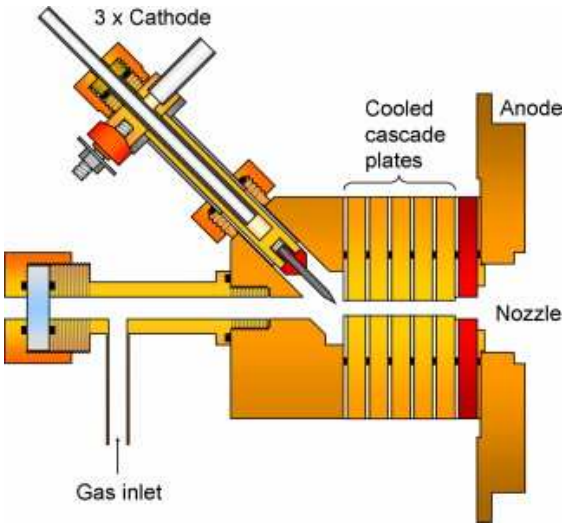

Figure 6.13. Drawing of a cascade arc plasma source.

In addition to the plasma source, a linear plasma device should have a series of diagnostic systems to allow the characterization of the plasma and the plasma-material interaction processes, such as:

- Several reciprocating Langmuir probes to determine the plasma temperature and density.
- Infrared thermography and calorimetry to determine the surface temperature at which the interaction occurs.
- Visible, infrared, and ultraviolet spectroscopy to determine the species that are formed due to the interaction in the plasma and in the target.
- Diagnostics of the background gas to determine the volatile species produced in the interaction, etc.

As a first step, the installation of a cascade arc source is planned, similar to the one employed at PILOT-PSI, generating a plasma jet with a diameter of 1.5 cm. This beam could be expanded by a suitable magnetic configuration to achieve irradiation of a greater sample area. This has the disadvantage of reducing the energy and particle flux at the target. In order to achieve a plasma beam diameter of around 5 cm in combination with high particle and energy fluxes, the implementation of a set of superconductor coils is also foreseen as the project unfolds. This will drive the plasma jet towards the sample.

At the moment, a collaboration exists between CIEMAT and FOM (The Netherlands) in the framework of EURATOM, for the development of cascade arc sources to generate plasma beams with larger diameters, namely in the 5-10 cm range. This work will be helpful for achieving the objectives proposed here, and for the development of new sources like MAGNUM-PSI (now under construction in FOM).

6.4.2. Quasi-Stationary Plasma Accelerator (QSPA)

The pulsed plasma device is based on a QSPA. In this device, a current is established between co-axial electrodes, ionizing the gas that is fed in and generating a plasma that is accelerated by the Ampere force induced by the current and an azimuthal magnetic field. This process can either be carried out in one stage (plasma generation and acceleration), or in two stages (plasma generation by a system of electrodes and subsequent acceleration). The QSPA is the magneto-hydrodynamic analogue of the Laval nozzle. Plasmas generated by this device can achieve energy fluxes of 0.1-20 MJm^{-2} in pulses of 0.1-1.0 ms, matching the expected values of transient events in fusion reactors (ELMs and disruptions).

A detailed diagram of one-stage QSPA coaxial electrodes is shown in Figure 6.14. The design of this plasma source is simpler than that of QSPA Kh-50, but more complex than QSPA-T (see Table 6.4). The outer electrode (the anode, consisting of a set of rods) has a diameter of 23-25 cm, while the inner electrode (the cathode, shaped like an ellipsoid) has a maximum diameter of 15-16 cm. The total length of the plasma source is approximately 60 cm. The whole system is contained in a vacuum chamber of 1.5-2 m length and 40 cm diameter.

The magnetic field, parallel to the vacuum chamber and of the order of 1 T, is generated by a set of coils. Its magnitude has to increase gradually from the plasma source (where ideally it has a value of around 0.1 T) to the sample, in order to avoid plasma loss due to strong field gradients.

Several compact valves will be operated simultaneously to feed in the gas, in order to achieve sufficient flexibility with regard to the plasma parameters and to reduce electrode erosion during long pulse operation. This flexibility is important when deuterium, helium, or other gases are used, apart from hydrogen.

Apart from systems that are common to every plasma generator, such as turbo-molecular pumps (with a pumping capacity of up to 1 litre of hydrogen per QSPA pulse), the operation of a QSPA device requires a specific power supply capable of handling short high power pulses. This type of power supply is typically based on a capacitor battery distributed into several sections, allowing the delivery of pulses of different lengths (0.25-0.5 ms). The

capacitance should exceed 10 mF in order to achieve pulses of around 0.5 ms. The power supply should provide a current of 0.5-0.7 MA in different regimes, with a voltage of about 25 kV, in order to raise the ion temperature of the plasma, and as a means to increase the electronic temperature during the thermalization that occurs as the plasma is driven through an increasing magnetic field. These requirements imply an accumulated energy of 2.5-3 MJ.

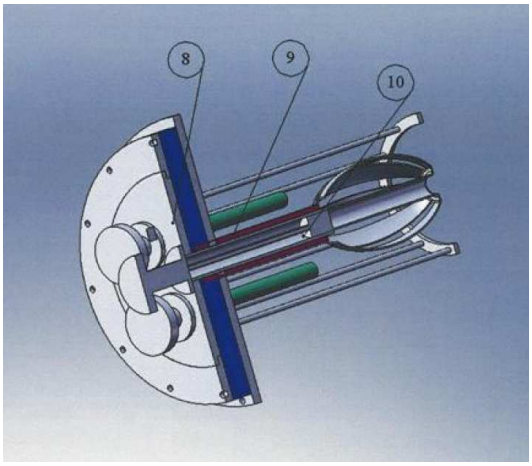

Figure 6.14. Diagram of one-stage QSPA coaxial electrodes proposed for *TechnoFusión*.

The sample exposed to the plasma has to be held in place by a setup capable of tilting it with respect to the plasma flow, varying the impact angle between 5º and 90º. Furthermore, the temperature of the sample needs to be controlled in the 200-1500 ºC range, prior to its interaction with the plasma.

Other systems essential for the correct operation of the QSPA device are:

- A synchronization unit (pulse generator), for which standard industrial solutions are available.
- A control system.
- Helmholtz coils, to produce the magnetic field of the discharge channel (these coils are not considered in the paragraph dedicated to the integration of both plasma generators).
- A commutator for discharge ignition (an ignitron, for example).

As with the linear device, the QSPA device requires appropriate diagnostic systems to characterise the plasma and corresponding data acquisition systems, such as sample thermography, high temporal resolution spectroscopy, calorimetry, probes, etc. A report written by the Institute of Plasma Physics QSPA group at Kharkov is included as an Appendix III.

6.4.3. Integration of the linear plasma device and the QSPA

The biggest challenge in the design of the *TechnoFusión* plasma wall interaction facility is the integration of both systems (the Linear Plasma Device and the QSPA) into a single device for the consecutive irradiation of samples. The linear plasma device will operate in steady state, while the QSPA will be pulsed. Their plasmas will be generated in their respective chambers, disposed in a collinear arrangement, to be transported by means of a magnetic field to the irradiation sample, which will be located between both devices.

The novel part of this proposal is the operation of both systems in a single machine, facilitating studies of plasma-wall interaction under fusion reactor conditions, including both steady state operation and transient events.

The proposed configuration which integrates both devices is a collinear one, where the sample chamber is located in the middle. This configuration takes advantage of a simple coil set-up, and moreover of the possibility of a low plasma angle of incidence irradiation over the sample. This low angle is relevant for the simulation of narrow incidence irradiation as in ITER divertor. The whole device will be composed of three independent chambers, which will be pumped independently and can be isolated one from each other by means of suitable valves. A movable sample holder would allow grazing incidence of plasmas on the target, alternating fastly between the steady and the pulsed plasmas. This configuration also allows other plasma-material interaction geometries, like normal incidence, without further re-arrangement.

Figure 6.15 shows the magnetic field generated by a coil set-up with the proposed configuration, where the QSPA device would be placed at the origin and the linear device (steady state) at the opposite end. The actual dimensions of the coils are under study, comparing diferent radius and their final cost, jointly with the geometric constraints they imposed. The following asumptions have been taken to carry out this analysis: coils are separated each other a distance equal to their radius and the magnetic field strength in the axis will be at least of 1.5 T. Furthermore, the QSPA's coils have to accomplish the KIPP design specifications detailed in AppendixIII , i.e., to generate a field of around 0.1 T at the source followed by a smoothly increasing field of aproximately 1 T/m up to reach its final value. As a preliminar result, the coil radius used to obtain Figures 6.15 to 6.17 is 20 cm.

The variation of the absolute value of the magnetic field along the axis of the device chamber is shown in Figure 6.17. It is seen that the magnetic field strength in the central part of the chamber, where the sample chamber will be placed, is quite constant, with a variation of around 1.3% in the axial field line without significant changes in a field line parallel to the axis at r = 2.5 cm. A uniform magnetic field is crucial to obtain homogeneous plasma on the target.

Strong magnetic fields[71] are required in order to achieve high flux plasma operation (10^{24} $m^{-2}s^{-1}$) with ITER-relevant parameters. This imposes severe constraints on the final design of the whole device. Economically, superconductor coils can be competitive in view of the savings they produce in terms of power supplies and machine operation. This type of magnets

[71] B. de Groot et al., "Extreme hydrogen plasma fluxes at Pilot-PSI enter the ITER divertor regime," Fusion Eng. Design 82 (2007): 1861-1865

can be employed in places where a strong and continuous magnetic field is required. If copper coils are used (combined with superconducting coils for the high field side), a water-cooling system is needed, although in pulsed systems (with long pulses) liquid nitrogen can also be used as a coolant, which has the advantage of reducing the power requirements for operation.

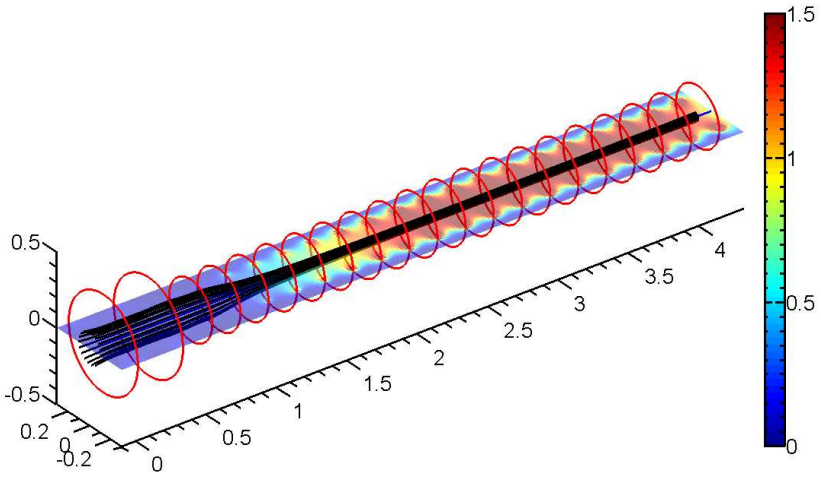

Figure 6.15. Proposed magnetic configuration for the integration of the linear plasma device and the QSPA. Red circles indicate the coil positions.

Due to the strong magnetic fields used in this facility a special care will be taken with the magnetic strength in the surroundings of the device (see Safety section). Concerning to this point, a map of the magnetic field around the device is shown in Figure 6.16, superimposed over a plane of a possible laboratory building. The level of 0.5 mT, which is a safety limit, appears as a red line in Figure 6.16, and is totally enclosed by the laboratory room.

The vacuum chambers will be designed using Monte Carlo codes like DS2V 4.5, developed by G. A. Bird (Figure 6.18).

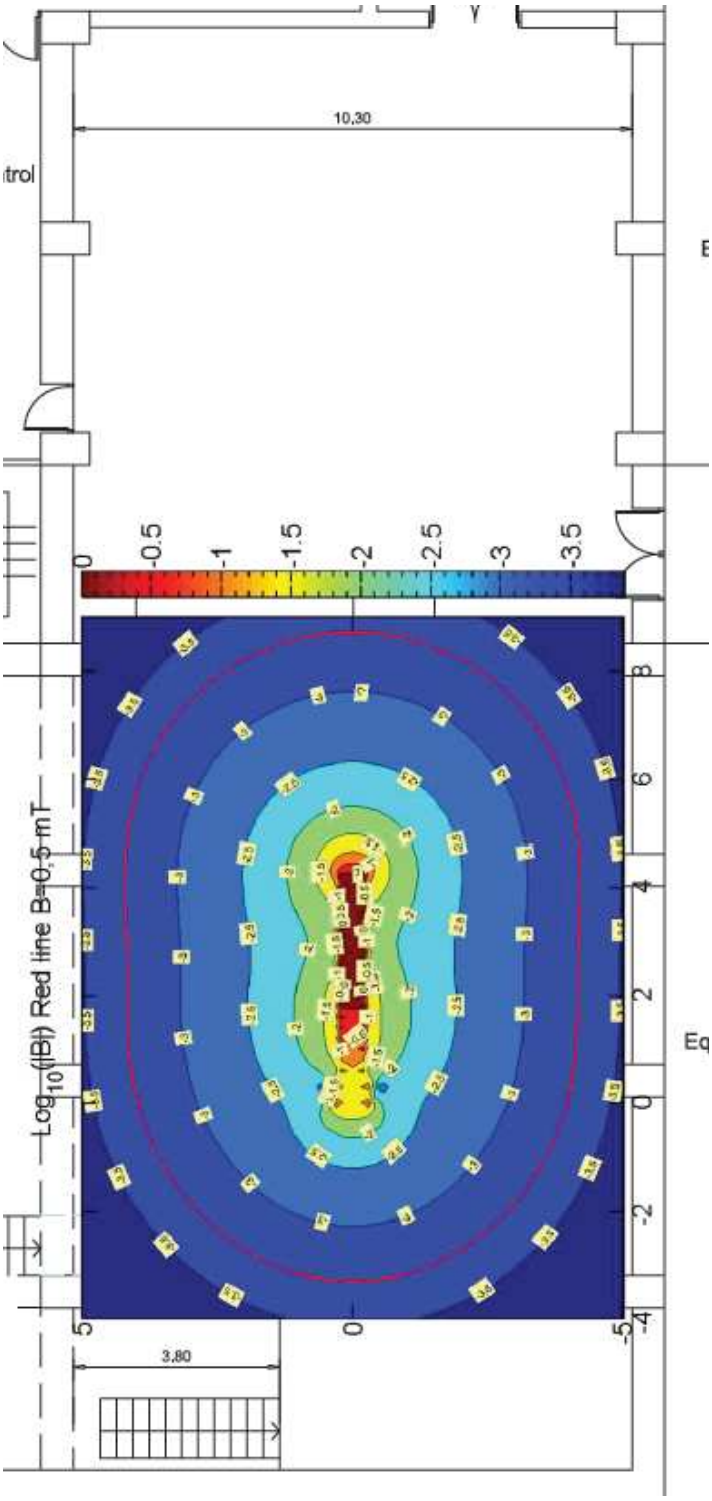

Figure 6.16. Top view of the magnetic field generated by the set-up from Figure 6.15, with its strength on the laboratory ground level. The red line indicates the value of 0.5 mT.

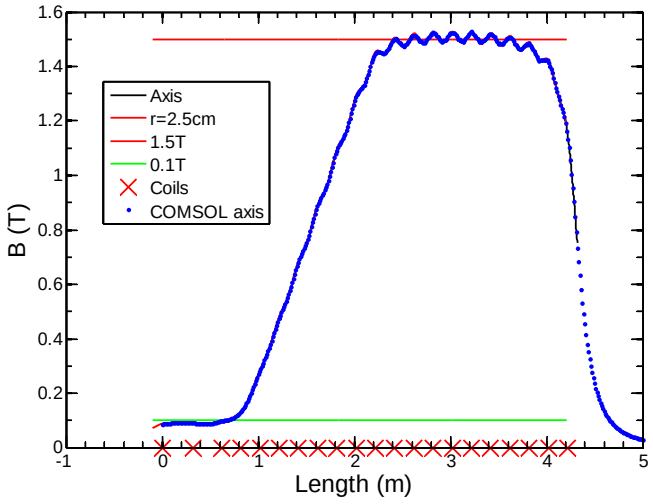

Figure 6.17. Magnetic field amplitude along the machine axis (black line), and along a field line parallel to the axis at r=2.5 cm (red line). Cross simbols indicate the coil positions.

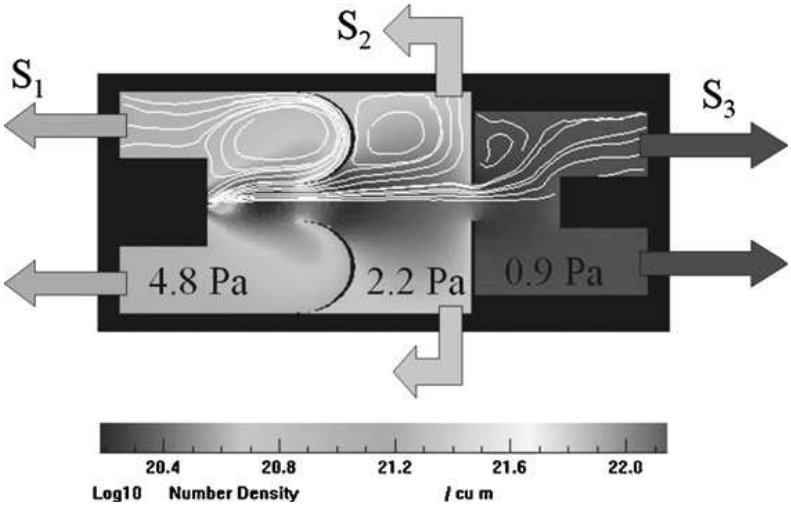

Figure 6.18. Simulation of the vacuum system using the software DS2V, applied to the MAGNUM-PSI facility [72]

Given the spatial restrictions imposed by the coils, the vacuum chamber will be partitioned into sections and designed to maintain a background pressure of the order of a few tenths of Pa. The gas feed will introduce gas at a rate of a few tens of slm (standard litre per

[72] Van Eck H, Koppers W, et al, Fus. Eng. Design 2007;82 1878

minute), so that the most difficult case (the linear plasma device) will require at least three pumping regions with a capacity of several thousands of litres per second. Appropriate pumps (roots, turbo-molecular pumps, etc.) will be chosen to maintain the pressure in each section of the chamber. All vacuum systems will be located underneath the machine, so that the facility will consist of two levels.

All the devices described above are feasible and based on existing technology. Once this proposal is approved, a detailed design of these new devices will be made in order to optimize the solutions for several problems and minimize the differences of the proposed systems with respect to fusion reactor conditions. This process includes: improving the homogeneity of the linear plasma, increasing the impact energy of the ions and electrons in the QSPA, and reducing the plasma density. Moreover, the innovative part of this proposal (operating both plasma devices on the same sample, facilitating plasma-wall interaction studies under reactor-relevant conditions, including both steady state and transient events) requires the integration of two separate plasma production systems. The achievement of this integration will require further detailed studies, but the present report provides a conceptual solution for the problem of irradiating samples by both a steady state plasma and high thermal load pulsed plasmas.

The design of the plasma gun (QSPA) is fixed, but the design of the linear plasma device is open, the next design phase involving the choice of the type of coils. Preferably, the source will be a cascaded arc, although it is also possible to use a modified LaB_6 source, depending on the available budget.

6.5. *Experimental capacity*

The facility proposed in the present report can be used for a wide range of studies, some of which are not even directly related to nuclear fusion technologies. Table 6.5 shows a list of some key experiments that can be performed in the PWI Facility of *TechnoFusión*. Possible applications can be classified according to the adopted approach, as described below.

Table 6.5. Main fields of interest for PWI Facility.

Linear Plasma Device	QSPA	Combination	Irradiated material by ion beams
√ Power deposition experiments √ Chemical erosion √ Tritium retention √ Mixed Material √ Liquid metals in magnetic fields + plasma exposure	√ Transient thermal loads √ Fatigue after repetitive thermal shocks √ The behaviour of liquid layers in magnetic fields after thermal shocks √ Vapour shielding	√ Fatigue Experiments √ Tritium retention under steady state and transient loads √ The alteration of physical properties	√ The alteration of physical properties after irradiation √ Tritium retention after irradiation

6.5.1. Development of plasma diagnostics and training in associated technologies

Linear plasma devices are plasma generators that provide easy access to the plasma (without the geometrical constraints typical of stellerators or tokamaks) and produce long duration plasma beams. These characteristics simplify the development of diagnostics ultimately destined for larger machines, and associated techniques. This simplification constitutes an opportunity both for the optimization of technical aspects and training. Some appropriate diagnostic techniques are: Spectroscopy (active and passive), electric probes (Langmuir, Mach), retarding field analyzers and molecular beam diagnostics.

6.5.2. Research into first-wall materials

The PWI plasma devices described above are specifically designed for studies on first-wall materials for fusion reactors. These studies will focus on the following issues:

1. The long-time effects of irradiation by highly energetic plasma on a test sample. Studies of erosion, fatigue, etc.

2. The effects of high power pulsed loads (higher than the maximum load specifications for the material). This study can be performed using irradiation by a pulsed magnetized plasma (QSPA), and involves the observation of certain known but scarcely studied phenomena, like surface power shielding due to vaporization , the dynamics of melted layers, etc.

3. Studies of liquid materials (e.g. Li) are important because of their attractiveness as a first-wall material for high power handling in a future reactor. An additional difficulty affecting the application of such materials is that they are subject to magneto-hydrodynamic forces. The study of this issue requires interaction with the planned Liquid Metal Facility at the *TechnoFusión* Centre.

4. Analysis of material erosion. The latter may be caused by *ion* impact on the material surface, or by chemical reactions between the material and hydrogen atoms (chemical erosion). This is of special relevance for carbon-based materials.

5. Tritium retention studies (using non-radioactive isotopes). The amount of tritium accumulated in a fusion reactor has to be controlled and kept below safety limits (the amount of tritium permitted in the ITER vessel is 700 g). Studies on the retention of hydrogen isotopes (involving mechanisms such as diffusion, defect trapping, co-deposition with previously eroded material, etc.) can be carried out in linear devices.

6. Mixed materials effects. The fusion reactor environment is highly complex due to the presence of different materials. As a consequence, the first wall materials will be contaminated and mixed with others, changing their physical properties (behaviour under thermal loads, tritium retention, etc.)

7. Studies of irradiated samples at the Material Irradiation Facility, using high power particle fluxes in steady state, as well as high power fluxes combined with pulsed particle fluxes. The possibility of performing such studies make the PWI Facility into a unique facility, capable of managing the three most relevant problems related to the power inside fusion reactors simultaneously: irradiation damage, high energy and particle fluxes in steady state, and high thermal loads produced in transient events.

6.5.3. Plasma-wall interaction studies

The interaction between plasma and the wall produces a great variety of phenomena. For example, atomic physics processes at the first wall determine the plasma edge profiles. These processes include mechanisms such as gas recycling at the surface, impurity transport through the plasma, etc.

6.5.4. Plasma physics research

Low temperature plasmas are suitable for fundamental plasma physics studies involving MHD, turbulence, etc., the results of which can be compared to simulations, which is facilitated by the simple device geometry. These studies can also be of special interest for the training of research staff.

6.5.5. Study of materials under extreme conditions

High power fluxes in an aggressive environment (with the possibility of injecting corrosive gases like oxygen) allow the study of materials under extreme conditions, which is of interest for various fields of research (technology for the aerospace industry, power electronics, etc.[73]).

6.6. Layout, supplies and safety requirements

The availability of a set of measurement techniques and simulation methods related to the fusion reactor environment (high thermal loads, irradiation, etc.) in a single laboratory creates an important added value for the proposed facility, which would be unique in Europe and in the world. However, it also implies that the facility must have a flexible organization, allowing it to execute diverse experiments in different experimental areas. Therefore, special attention must be paid to this issue in the design of the facility.

[73] ExtreMat http://www.extremat.org/

(I) Space and buildings

The spatial needs for the activities of the PWI Facility of *TechnoFusión* are:

- One building (100 m^2 and 7 m height) to house the linear plasma device and the QSPA, as well as their vacuum systems.
- One auxiliary building to house the power supplies for coil operation and the plasma sources of both devices (100 m^2).
- One 40 m^2 room to house the equipment for the analysis and control of the materials irradiated by the plasma, and to assemble the diagnostics that will be installed in the machine.
- One 80 m^2 room to house the control systems.
- One 30 m^2 workshop.
- One 40 m^2 warehouse.

About installation:

(a) Electrical installation:

One high power supply will be required for the plasma sources of the devices. An additional and independent supply is needed for the vacuum systems and cryo-coolers (the latter only if superconductor coils are used).

The laboratory will be equipped with power sockets to supply power to the peripheral equipment (i.e., diagnostics, computers, etc.)

(b) Water distribution network:

A water supply is required for cooling the equipment (copper coils, vacuum systems, etc.). In addition, a closed-circuit cooling system may be needed, depending on the cooling specifications of the equipment.

(c) Compressed air and pressurized gas:

The operation of the machine requires several high-pressure gas feed lines (hydrogen, methane, ammonia, oxygen, etc.). Correspondingly, appropriate gas detectors and alarms must be installed in the building where the devices are housed, which will also have to be properly vented.

A supply line of compressed air is also needed to run pneumatic devices. The same line will be used for routine tasks associated with the installation of diagnostics.

(II) Safety

The hazards in the PWI Facility are mainly of an electrical and chemical nature (inflammable, combustive, and/or toxic gases), or associated with experimental activities (the use of lasers, etc.).

The PWI Facility will need high power electrical supplies and strong magnetic fields for its operation. The high power supplies should be electrically insulated and placed inside Faraday cages, with all the necessary security systems for safe operation (cut-off switches, blockers, etc.), preventing access when the systems are active. All components must be grounded when people access the high power supplies and experimental devices. Moreover, due to the prevailing strong magnetic fields of up to 1 T, access to the experimental area will be restricted when the magnetic field is on. The exposure to strong magnetic fields has no documented permanent effect on health[74], so that it is possible to work in locations with fields of up 2 T. However, the WHO recommends time-weighted averages not exceeding 200 mT during the working day for occupational exposure, with a maximum value of 2 T. Therefore, warning signs will be installed indicating the presence of strong magnetic fields, along with entry prohibition signs for people with pacemakers, ferromagnetic implants, or other electronic devices. All these signs will be placed in areas with fields below 0.5 mT. Finally, stray tools and/or ferromagnetic elements will be prohibited in areas where the field exceeds 3 mT, as these objects can be propelled by the field, damaging equipment and/or harming people.

Different types of gases will be used in the PWI Facility (inflammable, combustive, toxic, etc.). The gas supplies will be located in separated areas, which will be properly vented, in accordance with their hazardous potential, and sheltered from any sources of heat and direct sunlight. The electrical installation in storage areas of inflammable gases, if any, will comply with the corresponding legislation. Empty and full gas cylinders will be stored separately in different areas. The gas feed lines will consist of hermetically sealed lines arranged in a sufficiently flexible manner while complying with security requirements. Finally, gas detectors (for hydrogen, methane, acetylene, and oxygen), fire detectors, and the corresponding fire protection will be installed inside the experimental hall.

The use of cryogenic liquids in the PWI Facility constitutes another possible hazard. The main risks are cold burns and asphyxia.

The handling of irradiated samples from the Facility of Material Irradiation implies further safety considerations. These samples should be stored in controlled areas until their activity decays below the exemption limits[75]. Materials considered candidates for plasma

[74] WHO "Electromagnetic Fields and Public Health".
http://www.who.int/mediacentre/factsheets/fs299/en/index.html
[75] *Consejo de Seguridad Nuclear (Council for Nuclear Safety)*, instruction of February 26, 2003, number IS-05, establishing the exemption limits for nuclides according to Tables A and B of Annex I of the Royal Decree 1836/1999, Published in BOE nº 86, April 10, 2003

facing materials, mainly carbon based materials and tungsten, are most likely to be studied in the Plasma-Wall Interaction Facility. For carbon, the storage time will be several days, since the main radioactive isotope produced by irradiation is N^{13}, with a half-life of ~ 9.9 minutes, so that its activity drops to 3 orders of magnitude below the exemption limit in a few days. In the case of W, mostly rhenium isotopes are produced. Re^{183} has a half-life of ~70 days, so that these samples will need to be stored for months before their activity decays to acceptable values. If possible, the irradiation parameters should be adjusted to minimize storage time.

The purpose of storage is to reduce the activity of the irradiated samples to a level at least two orders of magnitude below the exemption limits. In this way, the activity levels will not exceed the threshold for a supervised area in the current legislation, even if the sample is lost inside the vacuum vessel.

The activity of the samples used by the PWI Facility will be monitored by means of the following proposed measures: a) the activity of the irradiated samples will be measured after the estimated storage time, to confirm that the required activity level has been reached; b) laboratory staff handling the samples will use dosimeters, and masks when performing tasks inside the machine. In addition, the cited staff will be subject to routine medical control; c) the contamination of the inner wall of the vacuum vessel will be tested periodically by performing surface activity measurements, which needs to be kept well below the values corresponding to a supervised area (0.04 Bq/cm^2 for alpha radiation and 0.4 Bq/cm^2 for beta and gamma radiation); d) waste products, such as oil from vacuum pumps, or used samples, will be classified and processed as low activity waste; e) as an additional safety measure, the experimental area may be delimited by screens, with access control and specific safety measures.

Finally, since this is an experimental facility, the risks inside the PWI Facility may vary during its operational lifespan. Therefore, an appropriate reconsideration of the safety measures for equipment and personnel will have to be undertaken regularly.

7. Liquid Metal Technologies

7.1. Introduction

In the energy sector, liquid metals have mainly been applied in the manufacturing process of industrial batteries, in nuclear fission reactors (as coolants), and in thermal solar power plants. For such applications, molten metals such as sodium, lead and eutectic lead-bismuth are chosen for their beneficial properties as coolants or their resistance to high temperatures. New technological applications are being developed for liquid metals such as tin, mercury, lithium or eutectic lead-lithium.

In particular, liquid metals have some thermal and physical properties that make them very appropriate for future fusion-related applications. Their thermo-hydraulic properties make them very suitable for use as coolants, allowing the extraction of a large amount of energy, such as that produced by fusion reactions. Due to their reliability at high temperatures, they are candidates for the base material of the first wall facing the plasma, and for divertors and limiters in fusion containment vessels that need to withstand high radiation fluxes.

Aside from its thermo-hydraulic properties, the neutronic features of lithium (Li, tritium production by neutron capture) convert this material in an ideal candidate for the design of *Test Blanket Modules* (TBM), which are a key element for the sustainability of future fusion devices as DEMO. In some conceptual designs of TBMs, lead (in the form of eutectic lead-lithium) is used as an effective neutron multiplier in the range of neutron energies produced by a fusion reactor, increasing the tritium breading capacity of the system and its overall fuel sustainability.

Liquid metals are used as target materials for high intensity neutron sources. Materials with high atomic numbers, such as lead (Pb) or mercury (Hg), and with a high nuclear neutron/proton ratio, are efficient spallation sources. Light nuclei, such as lithium, are also being used as neutron sources, but function by means of stripping reactions. Lithium is also used in particle accelerators, such as the RIA (*Rare Isotope Accelerator*); and it has been proposed to use a thin lithium layer to enhance the static charge and to improve the accelerator efficiency.

Each of these applications of liquid metals, and many others that have not been mentioned, require specific operational conditions, since the behaviour of the metal is affected by various physical phenomena. These phenomena depend on the liquid metal, but they share some common features, so that many technological developments are based on the same physical principles and hypotheses, mainly referring to their use as coolants.

The development of innovative applications for liquid metals (like the one for fusion) requires improving the mastery of many technological aspects. New scientific and technological infrastructures are needed to advance with respect to the following issues:

- The generation of technological data regarding.
- Material compatibility.

- Thermo-hydrodynamic behaviour.
- Liquid metal magneto-hydro-dynamics.
- Validation of design software.
- The analysis of the configuration of proposed components based on liquid metals, either individually or integrated.
- The development of components and equipment for instrumentation and for the characterization of liquid metal loops.
- The development of auxiliary systems for liquid metal loops, such as purification systems, liquid metal charges and instrumentation.
- The adequate transfer of technology from research centres and universities to regional and national engineering and industrial companies, stimulating the formation of scientists and engineers needed for the start-up of technological projects based on liquid metal applications. This is one of the main objectives of the *TechnoFusión* proposal.

Taking into account the above, and focusing on the research needs regarding fusion technology, a flexible **Liquid Metal Technologies Facility (LMT)** is proposed at *TechnoFusión*`s Centre, mainly devoted to lithium, with sufficient flexibility to allow a large variety of experiments.

7.2. Objectives

The main goal of the LMT Facility is to become a scientific and technical infrastructure of reference, insofar the development of liquid metal technology related to international fusion programmes is concerned. This facility, integrated in *TechnoFusión*, will serve as a knowledge hub to promote the technology transfer to the regional and national industrial sector.

A review of the state of the art of liquid metal research activities in fusion has been performed (mainly related to lithium and eutectic lead-lithium). The goal of this review was to establish design requirements and make an inventory of potential experiments that could be performed at the facility. The results of this review, summarised in the next section, show that eutectic lead-bismuth is generally considered to be one of the top materials for future fusion reactors by the scientific community, at least in the medium term. Most of the current experiments in international facilities are devoted to the study of this eutectic material. Therefore, focusing on this material is unlikely to convert this facility into a facility of reference and to allow it to compete on an equal footing with other well-established facilities.

On the other hand, there is an increasing interest in the study of lithium as a material for fusion-related applications, either in neutron sources for material irradiation experiments, or in fusion reactor components such as blankets, divertors or first-wall layers.

In the framework of *TechnoFusión*`s goals, the main interest lies in the construction of a lithium facility in our liquid metal laboratory, for the reasons outlined below:

- In the medium term, it constitutes a strategic commitment in support of the Spanish candidature for the IFMIF laboratory site for material research, which will be based on a lithium neutron source and, therefore, a fully operational lithium loop. The existing know-how and the mastery of lithium technology will be a fundamental factor in the success of any candidature.

- Only very few lithium facilities exist worldwide, which allows reducing the redundancy of any proposed experiments and stimulating competition, so that the LMT Facility can become a reference installation in the short term.

The proposed liquid metal facility will have the following specific objectives:

- The production of critical technical information related to the use of liquid lithium, such as:

  - Free surface phenomena under conditions relevant for fusion applications.
  - Studies of corrosion/erosion and the compatibility of structural materials.
  - Magneto-hydrodynamic effects.
  - Thermo-hydraulic phenomena and modelling.
  - Chemical properties and the effect of impurities.
  - The development and testing of a purification system.
  - Safety.

- The validation of design tools for liquid lithium, such as thermo-hydraulic modelling and the corresponding codes.

In addition, this experimental facility will have the added value of coupling an electron accelerator to a liquid metal loop. Thus, heat will be deposited in the liquid metal flow, mimicking the power deposition produced by deuterons at the IFMIF facility, and producing phenomena similar to those expected with the latter's neutron source. It is foreseen that the electron accelerator will also be used for other purposes, e.g., to study the behaviour of materials in contact with liquid lithium under irradiation. These multi-effect experiments will allow improving our understanding of physical phenomena due to combined irradiation and liquid-metal interaction, in particular regarding such aspects as: corrosion, gas diffusion, chemical properties, and others, fundamental for the development of fusion technology. It is worth pointing out that at present, no laboratory in the world is able to perform this type of experiments.

7.3. *International status of the proposed technologies*

7.3.1. State of the art of liquid lithium technology

The excellent properties of liquid metals and their associated technologies make them an important key of in the following fusion areas.

a) The liquid lithium target at IFMIF [76]

IFMIF consists of a few deuteron accelerators that irradiate a pure liquid lithium stream (Figure 7.1). Stripping reactions between deuteron and lithium then produce a neutron beam with approximately the same energy as fusion reactions. One of the most challenging issues confronting IFMIF is to keep the free surface of the lithium flow stable, so that neutron generation is stable likewise and the deuteron energy is deposited in the required areas. There are huge uncertainties regarding the behaviour of lithium under the impact produced by the deuteron beam: the energy deposited in the metal flow could cause unknown phenomena that might affect surface stability; and lithium evaporation or liquid metal vapour might deteriorate the vacuum of the accelerator line. Furthermore, the study of the phenomena of erosion and corrosion occurring in the structural components that are in contact with the liquid lithium and exposed to neutron irradiation still is a pending issue, as these might increase instability due to an enhancement of impurities in the flow.

Research into and development of the cited issues is of fundamental importance for fusion technology, and the availability of experimental facilities allowing their study and mutual interaction is quite relevant.

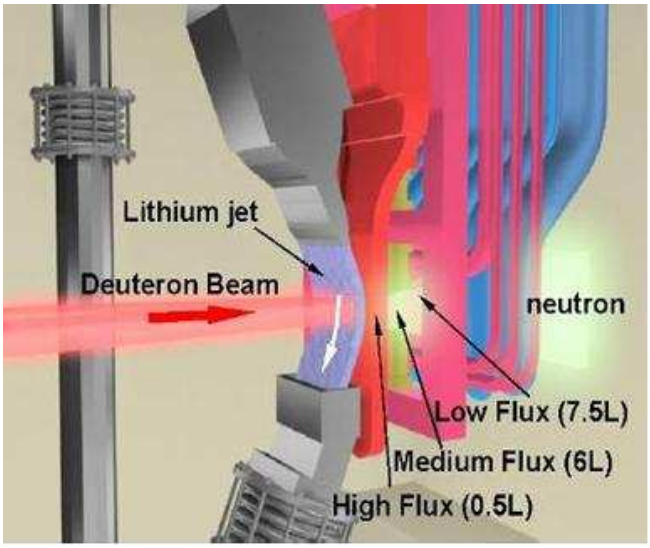

Figure 7.1. IFMIF neutron source.

[76] IFMIF Comprehensive Design Report, January 2004.

b) Plasma first wall, divertors and limiters for novel fusion reactor concepts

Lithium is an attractive material for the first wall facing the plasma, divertors, and limiters for fusion devices (Figure 7.2). Experimental studies have shown the reliability of liquid lithium as a material for the first wall in fusion chambers, either due to its good behaviour in the presence of plasma (low-Z and low plasma recycling), or due to its thermal properties, allowing the distribution of radiated power from the plasma and the handling of very large thermal loads (~10 MW/m^2). Moreover, since this material is liquid, its surface is less affected by the thermal stress produced by transients, due to the protective mechanism based on lithium evaporation (shielding). Solid materials are unable to withstand such high-energy depositions and suffer more radiation damage.

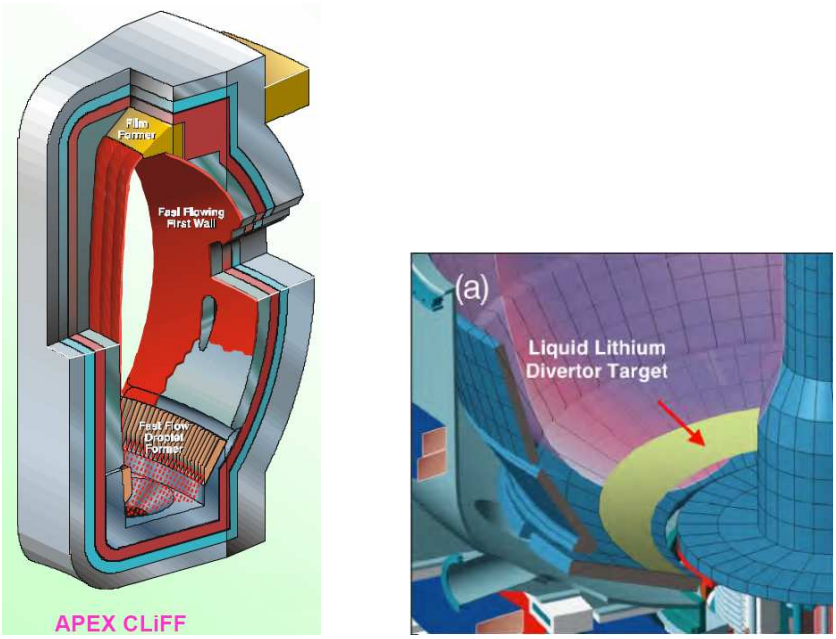

Figure 7.2. Applications of liquid metal technology for the first wall (left) and the divertor structure (right) of a fusion reactor.

Nevertheless, some problems remain, related to free surface instabilities of the liquid metal, due to such unwanted effects as waves, i.e., MHD perturbations produced by mechanical and electromagnetic forces[77]. Moreover, the chemical purity of liquid lithium may be modified by extreme environmental conditions (such as having a free surface in the accelerator vacuum), and possibly the free flow at the surface is different from the mass flow in the bulk, thus affecting the stability of the liquid metal stream.

[77] B.I. Khripunov, "Liquid Lithium surface research and development", Journal of Nuclear Materials ,Volumes 313-316, March 2003

One of the proposed concept designs for Tokamak first wall structures meant to handle free surface instabilities is based on a *Capillary Porous Structure* (CPS), filled with liquid lithium, in which the liquid metal layer is kept stable in high magnetic fields due to its high surface tension in a porous grid.

c) Tritium blanket modules based on liquid metals

Lithium is an important material for fusion technology, whether pure or as an alloy such as the eutectic lithium-lead, or as part of the tritium blanket modules of fusion devices. Some conceptual designs for tritium production plants based on these materials have been proposed for ITER and DEMO (Figure 7.3).

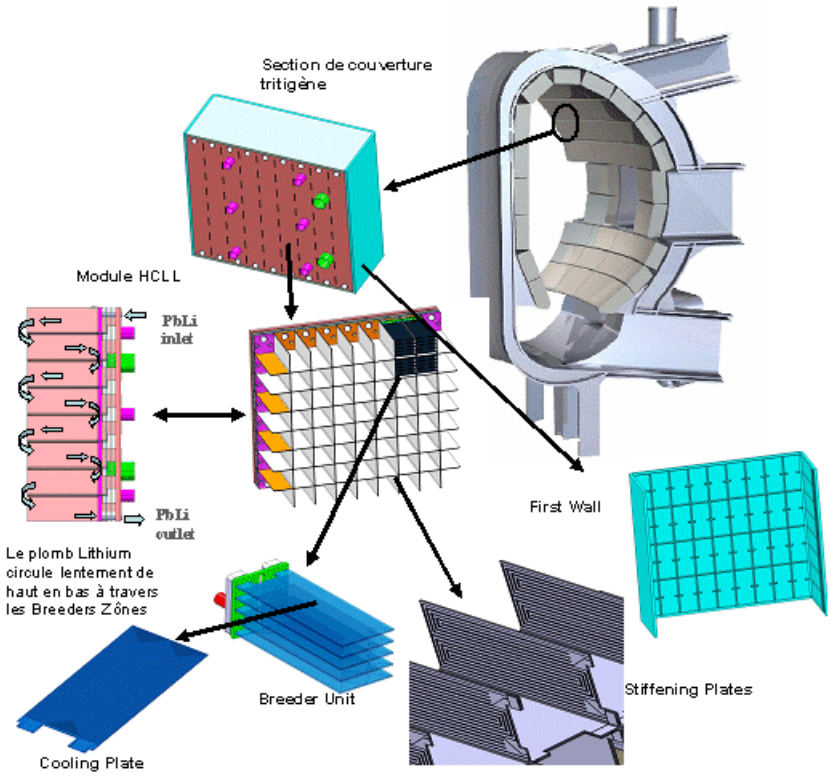

Figure 7.3. Tritium blanket module of the type HCLL (*Helium Cooled Lithium Lead*) for ITER (source: CEA)

The main technological problems associated with these applications are:

- Magneto-hydro-dynamic effects for a wide range of flow velocities of the liquid metal (from mm/s to m/s, depending on the design proposal), leading to pressure

loss, discontinuities in the flow of the liquid metal in different cooling channels, the reduction of heat transfer, etc.

- The corrosion of structural materials that are in contact with the liquid metal.
- Tritium management issues: lithium enrichment techniques, tritium permeation and tritium extraction from the liquid metal flow, etc.
- The safety of liquid metal applications, in particular regarding lithium.

Every one of these technical challenges has spawned a great effort in research and development, in order to validate specific materials designed to reduce permeation, corrosion, or electrostatic problems.

The phenomena described above must also be studied under heavy particle bombardment, which may enhance and increase uncertainties. Moreover, radiation fields can modify important phenomena, such as gas diffusion or the generation of impurities.

Thus, further research and development is needed on lithium applications, and particularly on lithium itself. Many question marks remain regarding the use of liquid lithium, such as the corrosion of structural materials in lithium flows, the compatibility of materials, and purification techniques.

7.3.2. Major international facilities for liquid metal experiments for the development of fusion technology

Worldwide, only a small number of facilities exist whose activities include the study of liquid metal technology for fusion. Table 7.1 shows a list of existing facilities in the world working on Li and eutectic Pb-Li, the main liquid metals for fusion. The lack of lithium technology facilities is evident from this table, particularly in Europe, which is the main area of influence of the facility proposed in this document.

By contrast, Europe has a large amount of experimental installations for Pb-Li. Several loops related to the compatibility of liquid metals with structural materials are available in Italy (LIFUS), Germany (PICOLO) and Latvia (IPUL loop). The former permits the analysis of liquid metal corrosion in combination with magnetic fields. In Europe, the field of MHD is studied mainly at the MEKKA loop in Germany, using eutectic NaK. Other technological issues, such as gas diffusion in Pb-Li, the study of permeation barriers, or tritium extraction, are studied in installations such as TRIEX, VIVALDI or LEDI in Italy, and MELODIE in France. In the latter country one can find another loop, such as PABLITO, built to test different components, such as pumps. The Czech Republic has a Pb-Li loop designed for purification studies.

Table 7.1. List of Li and euctectic Pb-Li facilities in the world.

Lithium	Pb17Li
USA	**ITALY (ENEA)**
University of Illinois ORNL Sandia NL Argonne NL University of California	LIFUS-2 LIFUS-5 TRIEX RELA III LEDI LTF-M SOLE
ITALY (ENEA)	
LIFUS-3	
JAPAN	**FRANCE (CEA)**
NIFS University of Osaka	MELODIE PABLITO DIADEMO
RUSSIA	**GERMANY (FZK)**
IPPE	PICOLO
	RUSSIA
	IPPE
	CZECH REPUBLIC
	IPP
	LATVIA
	IPUL

Research on Pb-Li safety, focusing mainly on its interaction with water, is carried out in Italy at the facilities LIFUS-5 and RELA III. There are at least three dedicated loops for prototype testing of components for fusion blanket modules, such as EBBTF in Italy, DIADEMO in France, which also offers a coupled Helium section.

Regarding pure lithium facilities en Europe, Italy has the LIFUS-3 (Figure 7.4), devoted to research on material compatibility. This loop has a total lithium inventory of 46 litres, providing a flow of 0.5 l/s, with a lithium velocity at the test section of around 12-18 m/s, at a pressure of 2.5 bar and a temperature of 350 ºC.

In the United States, the main choice for fusion coolants and blanket has always been lithium. Therefore, their facilities have been designed for lithium research, mainly focusing on its magneto-hydrodynamic behaviour. Such studies are performed at the LIMITS facility

located at the Sandia National Laboratory (Figure 7.5). This facility has three main test components: a vacuum chamber to study the behaviour of liquid metals, a pumping section, and a transfer tank. In the vacuum chamber, tube sections with different shapes can be tested in a magnetic field. The liquid metal pumps have been custom-made for this loop, due to the lack of commercial providers.

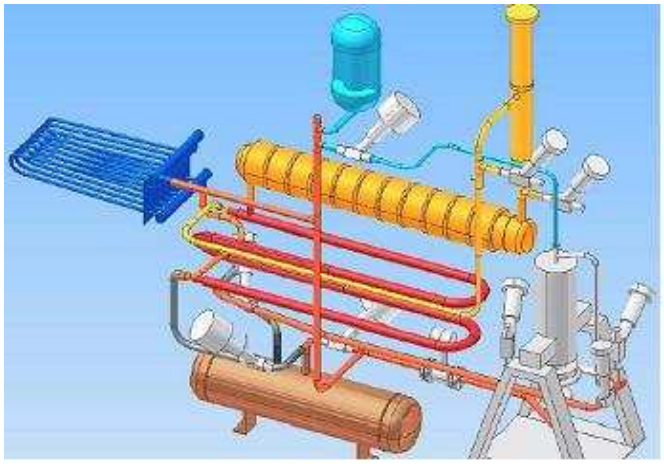

Figure 7.4. LIFUS3 facility (ENEA).

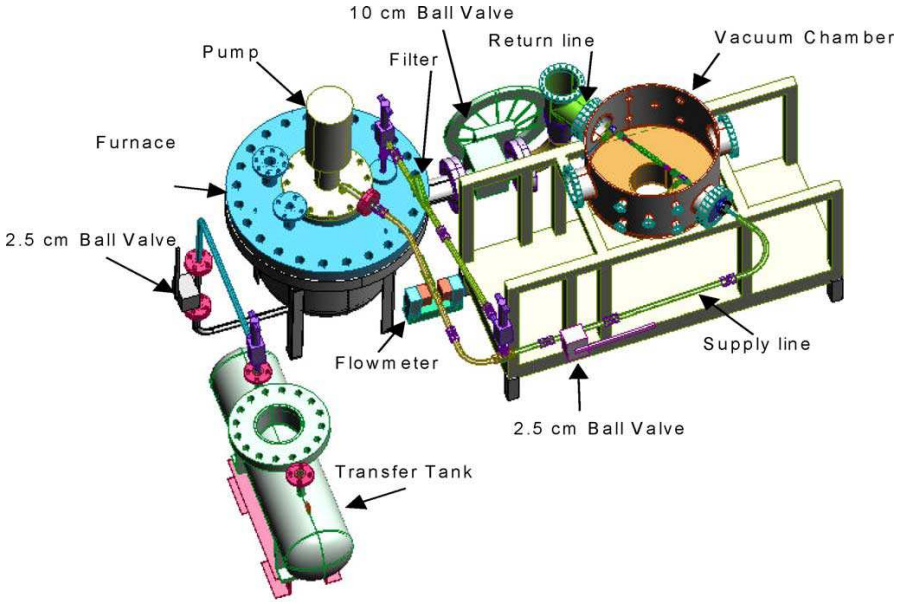

Figure 7.5. LIMITS facility at the Sandia National Laboratory (USA).

In the United States, another loop is installed at the University of Illinois (Figure 7.6), designed for the experimental analysis of deuterium retention in liquid lithium. These phenomena are especially relevant for the application of this liquid metal in the first wall of the plasma chamber of future fusion devices based on magnetic confinement.

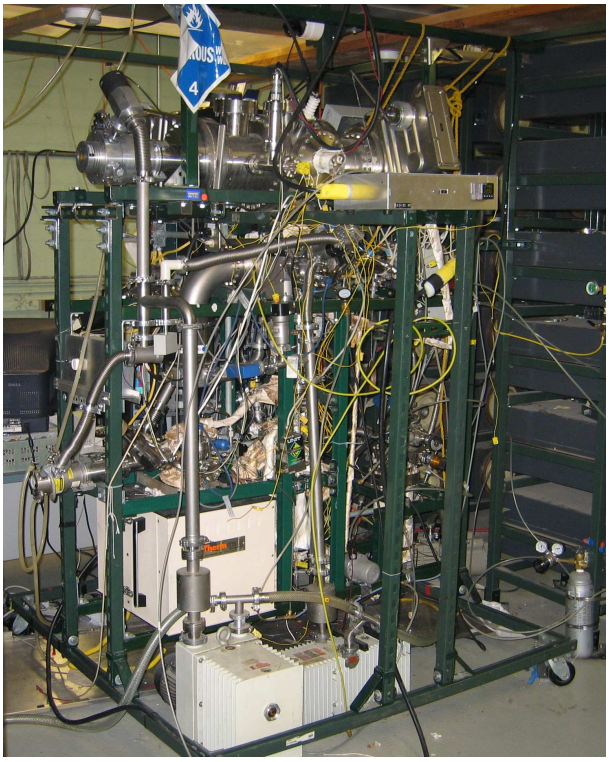

Figure 7.6. Experimental loop at the University of Illinois (USA).

In Japan, the University of Osaka is very active in the field of fusion technology, studying physical phenomena such as the free surface behaviour of lithium at the IFMIF[78] target, and this activity may provide technical support for the Japanese candidature to host the site of this material irradiation facility. The university has a lithium loop (Figure 7.7) with a free surface test section. The loop has a length of 40 m, and consists of 304 stainless steel ducts with a diameter of 53.7 mm. The pressure of the inner loop is of the order of 400 kPa, and it supports lithium flow of 500 l/min at 300 ºC, with a reasonable safety margin to avoid lithium solidification below 180 ºC.

[78] H. Kondo et al. 'Experimental study of Lithium free-surface flow for IFMIF target design'. Fusion Engineering and Design 81 (2006) 687-693.

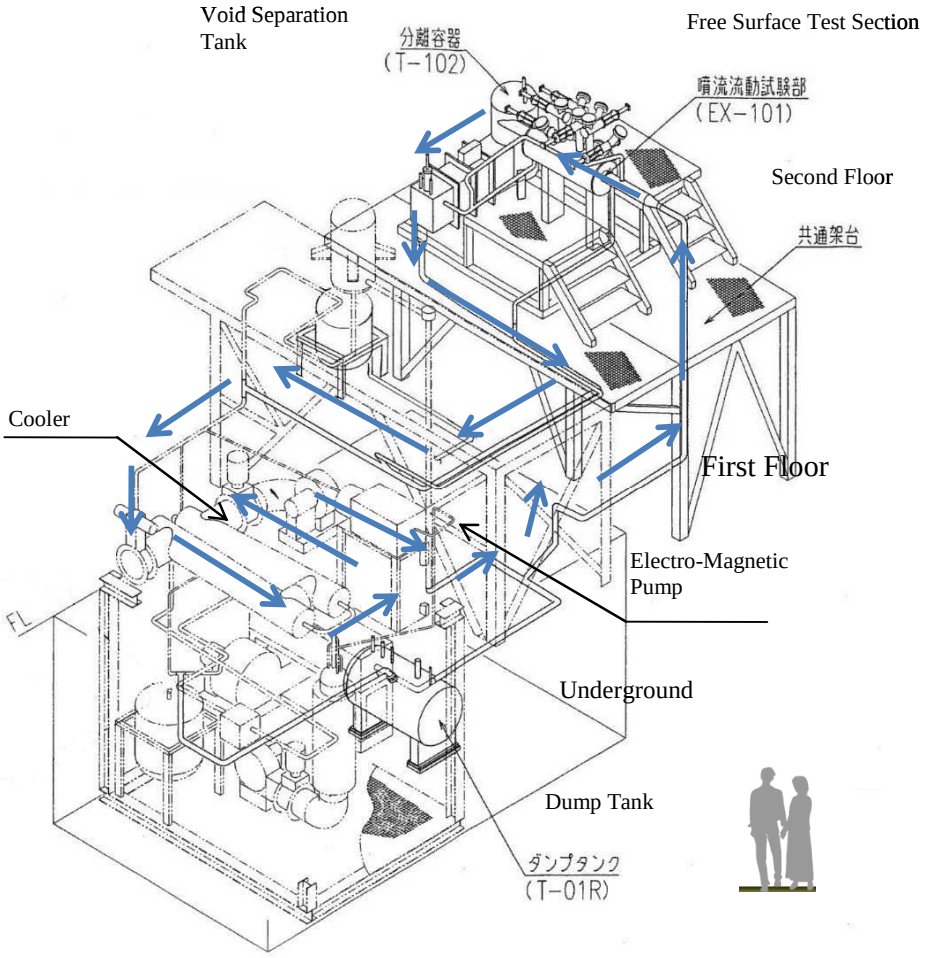

Figure 7.7. Diagram of the lithium loop for IFMIF research at the University of Osaka (Japan).

The free surface test section is shown in Figure 7.8. This is a model at a scale of 1/2.5 of the JAERI design for IFMIF. In contrast with the actual IFMIF design, the model has certain curves to let the centrifugal force help avoid the liquid metal from boiling. The test section at the Osaka loop is plain and horizontal, as with other experiments oriented towards IFMIF. The effect of bends at the target position has been discussed by Itoh[79], and apparently it is negligible in simulations of the behaviour of the free surface.

[79] K. Itoh, H. Nakamura, Y. Kukita, "Free-surface shear layer instabilities on a high-speed liquid jet", Fusion Technol. 37 (2000) 74–88

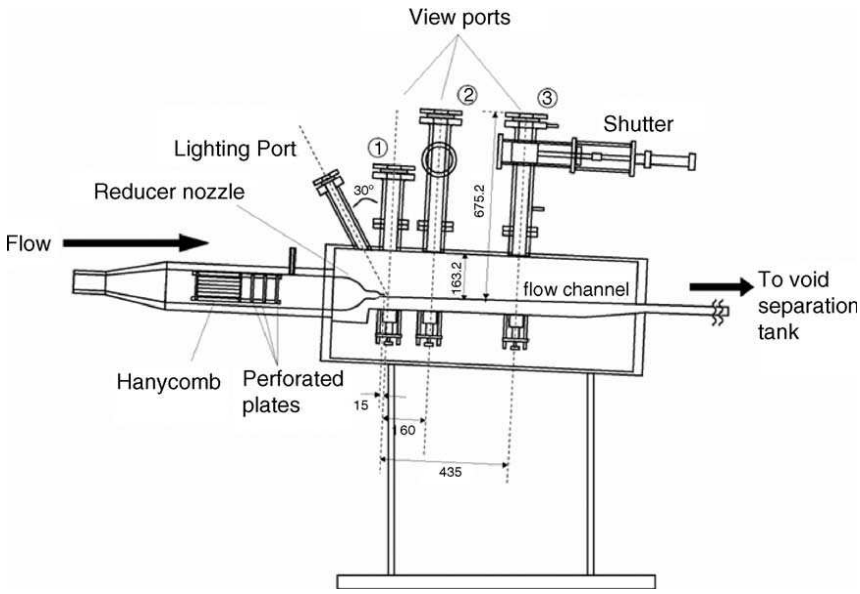

Figure 7.8. Lithium free surface test section at Osaka (Japan).

A limited number of additional facilities are devoted to lithium technology. Among these, it has been highlighted the LTF-M loop (Figure 7.9), developed in Obnisnk (IPPE, Russia) in the framework of an ISTC project. The main goal of this loop is to the study the thermo-hydraulics of water and lithium at the free surface, and it includes auxiliary systems such as lithium impurity monitoring and purification, and control.

Figure 7.9. IPPE loop in Obsnisk (Russia).

In contrast with the American laboratories, mainly devoted to liquid lithium studies for a future fusion reactor, the facilities in Italy, Russia and Japan have made a large effort oriented towards IFMIF. Figure 7.10 presents a comparison between the cross sections of the free surface flow in these international laboratories focused on IFMIF. The geometry of the test liquid flow (thickness, width, bend, straight channel, etc) varies, as well as the fluid, which is either lithium, in the case of Osaka and IPPE, or water, in the case of Italy, where lithium has been used only for material studies.

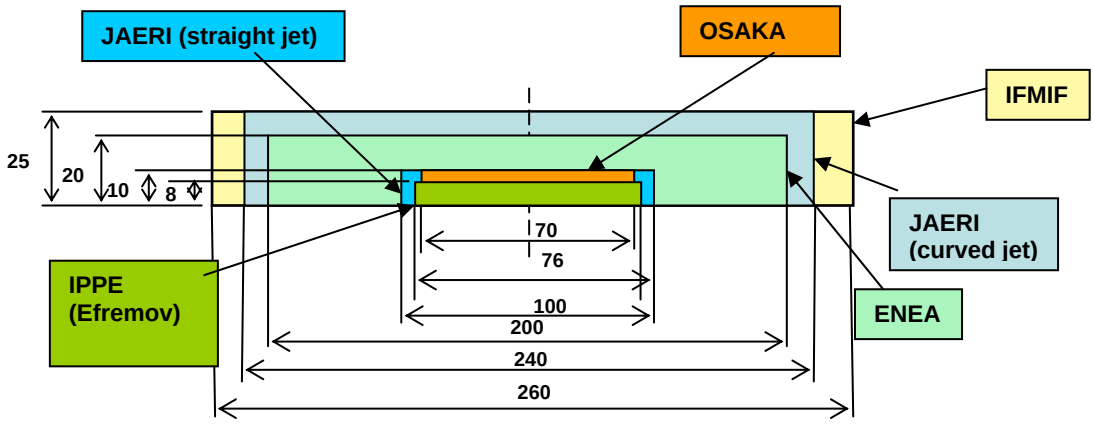

Figure 7.10. Cross section of the lithium flow in some experiments in the world related to IFMIF.

As mentioned above, none of these International laboratories perform experiments that contemplate energy deposition in the lithium flow. Furthermore, the maximum velocity that can be attained in some loops is not always similar to the planned flow velocity at IFMIF, and in some cases the working fluid is not even lithium.

This brief analysis of the experimental facilities available worldwide shows that the amount of installations dedicated to lithium technology is very small, highlighting the need for the construction of new loops, either for carrying out redundant experiments to asses the reproducibility of results, or for increasing the experimental capacity for performing tests needed in view of the cited technological challenges, as is the case of the behaviour of the free surface when heat is deposited into the liquid metal flow, this being of paramount importance for IFMIF. At the present time, no facility in the world is able to test this type of phenomena. Furthermore, most of the tests related to the contact of materials with liquid lithium are performed at low temperatures. This may be appropriate for IFMIF, but is not very useful for the development of a future fusion reactor, where temperatures are expected to reach 1000ºC. There is also a lack of experimental capacity to study coupled effects due to liquid-metal compatibility, electromagnetic fields, and irradiation, which are important for fusion applications.

The goal of the LMT Facility, part of the *TechnoFusión* initiative, will be to raise the temperature data range of studies of materials subject to corrosion by lithium. Moreover, an interface between an electron accelerator and the lithium loop will be made to allow studying the behaviour of the free surface of liquid lithium subject to heat deposition into the internal flow, as well as testing materials under irradiation. With the projected infrastructure, it will be possible to perform relevant tests, either for IFMIF or for any other liquid metal application in the nuclear fusion field, with an approach that combines multiple physics effects.

7.4. Projected devices and equipment

The design of any experimental facility is motivated by a technological objective or is a response to a demand by the national and international scientific community. The technological facilities offered by such a "will then attempt to meet any experimental deficits that have been detected. As mentioned, there is an important shortage of experimental facilities dedicated to the development of lithium technology for fusion applications. Consequently, it is justified the construction of an experimental facility incorporating various liquid metal loops, and in particular a lithium loop, relevant in the framework of fusion. Liquid Pb-Li studies are considered a secondary experimental objective.

The existing international installations of reference were studied to clarify the technical definition of the liquid metal loops proposed here. Also, an initial study was made of the experimental tests that will be carried out (described in detail in the section "Experimental capacity"). The description of these potential experiments has made it clear that the operational requirements of some experiments will be mutually incompatible, in terms of temperature, mass-flow, or time, thus justifying the incorporation of various loops in the proposal, each one for specific experimental objectives.

For instance, a loop devoted to free surface experiments in preparation for IFMIF should be able to handle a certain lithium mass-flow, as the liquid metal velocity is one of the critical factors for the stability of the free surface. Moreover, if an electron accelerator will be used to deposit a certain amount of power in the flow, the beam line should be kept in vacuum, and consequently so should the free surface interface, which then imposes a minimum size requirement on the loop to avoid cavitations. Another factor that affects the design of the loop is the operational temperature. In the mentioned case, temperatures of the order of 250 ºC are required. Another operational constraint that must be taken into account is the time schedule of the experimental campaign. Relate to this, note that a free surface experiment might last a few weeks, depending on other installations.

On the other hand, tests of the compatibility of materials with liquid metals may require much slower liquid metal flows, and more compact loops with less liquid metal. Nevertheless, operational temperatures should be much higher, requiring a powerful heat evacuation system, which in turn may lead to a complex design. Regarding the experimental campaigns, tests are expected to last a few thousands of hours in a continuous, stable mode of operation.

In principle, MHD tests do not require a large amount of flowing liquid metal, but it would be interesting to be able to change operation speeds and temperatures. It would also be interesting to study the influence of magnetic fields in other experiments, such as corrosion

tests or hydrodynamic experiments. One may consider installing some magnets on the track where the hydrodynamic experiments are carried out, as well as on the track for studying material compatibility, provided these facilities are designed with sufficient flexibility.

In the same way, tests can be proposed concerning the diffusion of gases in the liquid metal, or concerning the materials in contact with it, with relevance for the management of tritium in fusion reactors. These tests can be performed on a track that was designed for other trials, provided it has been built with flexibility in mind.

Security tests must probably be carried out at an independent track with a small amount of liquid metal.

Purification tests will be done at several purification systems installed on the various tracks, so these would not require a dedicated track, in principle.

Although it has been mentioned that the study of the Li-Pb eutectic is not the main goal of this experimental Facility, one should not reject this possibility offhand, due to its significance for fusion technology. It has to taken into account the possibility whether a given track, originally designed and dimensioned for working with lithium, can be changed to Li-Pb; or whether experimentation with Li-Pb needs a dedicated track. In any case, as lithium-lead experiments usually require low working speeds (from a few millimetres per second to a few metres per second), it could be also considered installing a basic circuit based on natural convection.

The analysis of the various experiments that could be carried out lead to propose the following basic requirement for the LMT of *TechnoFusión*, namely: two liquid lithium tracks, one mainly dedicated to hydrodynamic studies, and the other dedicated to mechanical tests of materials, corrosion and compatibility. It has not been still rejected the possibility that these two circuits share some components or systems, such as: filling systems, the tank for storage of the inventory, or purification systems.

Both circuits will be designed with enough flexibility to carry out various kinds of tests. The layout of the required floor space in the LMT Facility should allow adding further minor tracks in the future, or enhancing the existing ones. This approach also fits in nicely with the option of a staggered start of the facility.

The Figure 7.11 shows a summary of the objectives that must be met by the Liquid Metal Technologies Facility, including the specific experimental conditions required for each type of test, which have been used for the initial design of the tracks. In the section 7.5 “Experimental capacity”, further detail about the tests is provided.

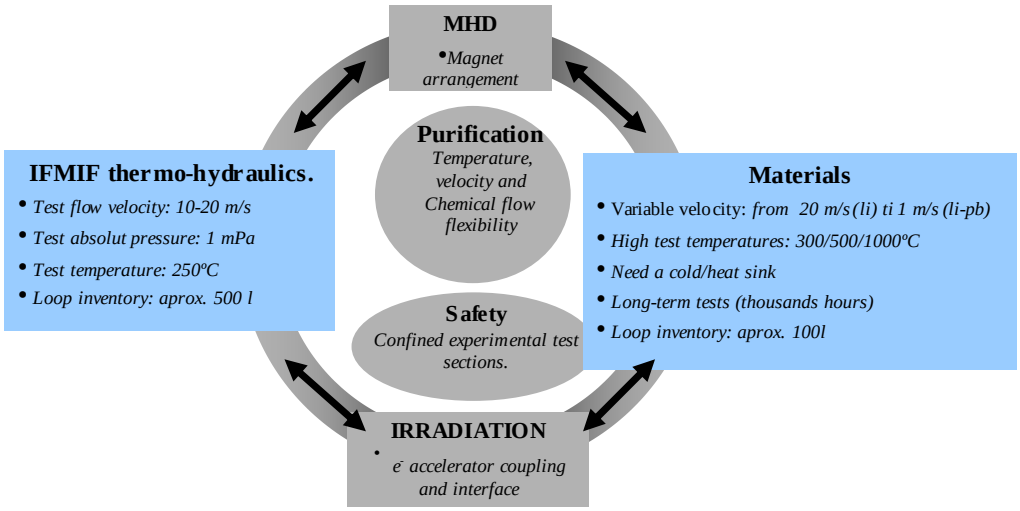

Figure 7.11. Main objetives of the Liquid Metal Technologies Facility of *TechnoFusión.*

7.4.1. Technical definition of the experimental loops

(I) Free surface experimental loop

As mentioned in preceding sections, free surface tests are required for licensing and commissioning the IFMIF target. This experimental loop will be dedicated to experimental work on the free surface. The lithium inventory in this test installation has been estimated at 500 litres. The installation will contain:

1) Basic components:

- Ducts: designed for a liquid lithium velocity in the range 5-20 m/s.
- Pump: able to drive a liquid lithium flow of at most 50 m^3/h, without risk of cavitations.
- Common storage tank: with a capacity of approx. 1000 litres, for storage of all the lithium of the whole facility, including this test section and any other in the LMT Facility.
- Control and diagnostic instrumentation: flow meters, thermometers, pressure gauges, level meters, and so on.

2) Testing zone, that will consist of:

- A free surface zone, basically consisting of an element that forces the flow to become laminar (a "straightener"), an exit tube for the liquid lithium, and a tray where it will circulate with a free surface. The size of these components must be calculated on the basis of their relevance for IFMIF.

- Enough access ports at the test zone to allow installation of the required instrumentation (cameras, speedometers, etc.), to allow entry of the electron accelerator beam, and to provide space for the installation of future diagnostics.

- An intermidium tank ("Quench tank") that will reduce the speed of the liquid metal when it leaves the testing zone, and will absorb the thermal expansion and damp the fluctuations of the fluid before it reaches the pump. It will also be used to separate any gases (mainly argon) that could remain in the liquid metal. This tank should have a capacity of about 200 l.

Other decisive factors for the design of the circuit are:

a) The coupling of the testing zone with the electron accelerator will impose some specific requirements: the vacuum of the testing zone (argon atmosphere 10^{-3} Pa), the viability of the physical connexion between both systems (accelerator-lithium track), shielding, etc.

b) The free surface testing zone will be extractable, in order to install components with different shapes and/or sizes and/or materials.

c) Suitable mechanisms must be implemented in order to change the speed of the liquid metal in the testing zone (up to 20 m/s), for instance by installing flow regulation valves.

d) It should be possible to perform other types of experiments in some stretches of the track. Such experiments are:

    - MHD: There should be enough space to install magnets.
    - Gas diffusion: leaving open this possibility requires the installation of spare access ports on the track, to be linked to additional gas feed lines.
    - Etc.

e) One of the fundamental activities of this facility is the validation of computer tools for the design of components and systems working with liquid metals. Therefore, the loops should be fully diagnosed for a proper computer code validation.

(II) Material testing loop

Structural materials for fusion applications that are in contact with liquid lithium must be able to withstand temperatures above 300 ºC and relatively high velocities, as in the case of

IFMIF (highly turbulent flow), or up to 1000 ºC, as with some TBM designs, although at low velocities (laminar flow). Therefore, the materials testing loop should be designed with sufficient flexibility to be able to perform experiments under these extreme conditions. This materials testing loop will have a lithium inventory of about 200 l, and will consist of the following components:

1) Main components

- As with the free-surface experiments: ducts, valves, pumps, instrumentation, control equipment, diagnostics, etc.
- Some components may be common to all loops in the facility and be shared with the rest of experiments, such as the lithium storage system and the purification system.
- Since high temperature tests will be conducted at this loop, a heat extraction system may be installed, based, e.g., on an intermediate oil loop with an oil-lithium heat exchanger, and a final water heat sink consisting of an oil-water heat exchanger and a cooling system.

2) Testing zone

- The section for corrosion and material compatibility tests should be installed at a duct port where the different material test probes are inserted.
- The design of the mechanical test section should contemplate the coupling to a testing device that produces the mechanical stress.
- The material chosen to construct the loop and the other equipment must withstand high temperatures.

Other issues to be taken into account when designing the loop are:

a) An interface with an electron accelerator should allow performing experiments with gamma irradiation in the loop. This radiation is produced when an electron beam impinges on an appropriate target layer in the vicinity of the material test probe. This interface will impose specific design requirements on the test loop regarding its lay-out, shielding, etc. Radiation detectors should also be contemplated.

b) High temperature tests imply strict requirements for the choice of the structural materials for the loop.

c) Test sections should be designed for easy replacement, and with sufficient flexibility to run experiments with different geometries, sizes and materials.

d) Mechanisms for regulating the flow speed of the liquid metal (from a few mm/s to 20 m/s) in the test sections should be implemented, by means of, e.g., flow regulation valves.

e) The design of the loop should allow different types of experiments, such as:

- MHD: allocating space for the installation of magnets.
- Gas diffusion: installing ports for connecting additional gas lines.

(III) Auxiliary systems

1) All the equipment and components will be heated by means of electric resistors, and will be thermally isolated. Control of the loop temperature will require a suitable amount of thermocouples.

2) One or several vacuum systems, including steam traps, connected to the various tanks and to the free surface testing zone.

3) An Argon supply system, also connected to the various tanks and to the free surface testing zone.

4) A high-pressure air supply system for pneumatic valves and other active components.

5) An electric power supply system to provide power for the pump, the electric heaters, the vacuum systems, and the rest of the active components: a load of about 300kW is expected.

6) A control system (based, for instance, on programmable automatons) to collect and process the instrumentation readings, and to operate the active components of the installation via a user interface.

7) A filling system: lithium is supplied in the form of ingots that will be heated and melted in a dedicated and isolated tank. The liquid lithium will then be transferred to the track via a connecting valve, while injecting argon (cf. the Osaka University loop). In other cases (Obninsk loop) an intermediate step is implemented in the form of another storage tank where impurities are removed. The LMT Facility should have sufficient space to accommodate the mentioned filling tanks.

8) Systems for the purification process and for monitoring the impurities: a further study must be carried out regarding the possibility of installing a common purification system for the free surface tracks and the materials tests; possibly, each track should have its own system. Due to the great importance of these systems, which may be a subject of study on their own, they will be treated separately at the end of this section.

(IV) Comments on the structural material for the proposed facility

Liquid metals cause a relatively intense corrosion process, leading to the progressive wear of the system pipes. Logically, the latter must be designed for safe operation for the lifetime of the installation. The estimated useful lifetime is 20 years.

The speed of corrosion is directly related to the operating temperature of the system. As mentioned before, the free surface studies will be carried out at 250 ºC, while the materials studies will be performed at various temperatures, some of which are quite high. Since the low temperature track could also be used for experiments other than the free surface experiments, and which may require higher temperatures, the pipes will be designed to withstand corrosion rates similar to those of the high temperature loop. A temperature of 500 ºC will be used as reference value. Higher temperatures could be considered, but that would require the use of special materials or steels for the whole loop. Tests that require higher temperatures should be designed so that the track itself is not subjected to temperatures exceeding 500 ºC, by incorporating appropriate systems for local heating/cooling.

Using the information shown in Figure 7.12, and assuming an operating temperature of 500 ºC during 8.760 h/year, the corrosion values listed in Table 7.2 are obtained.

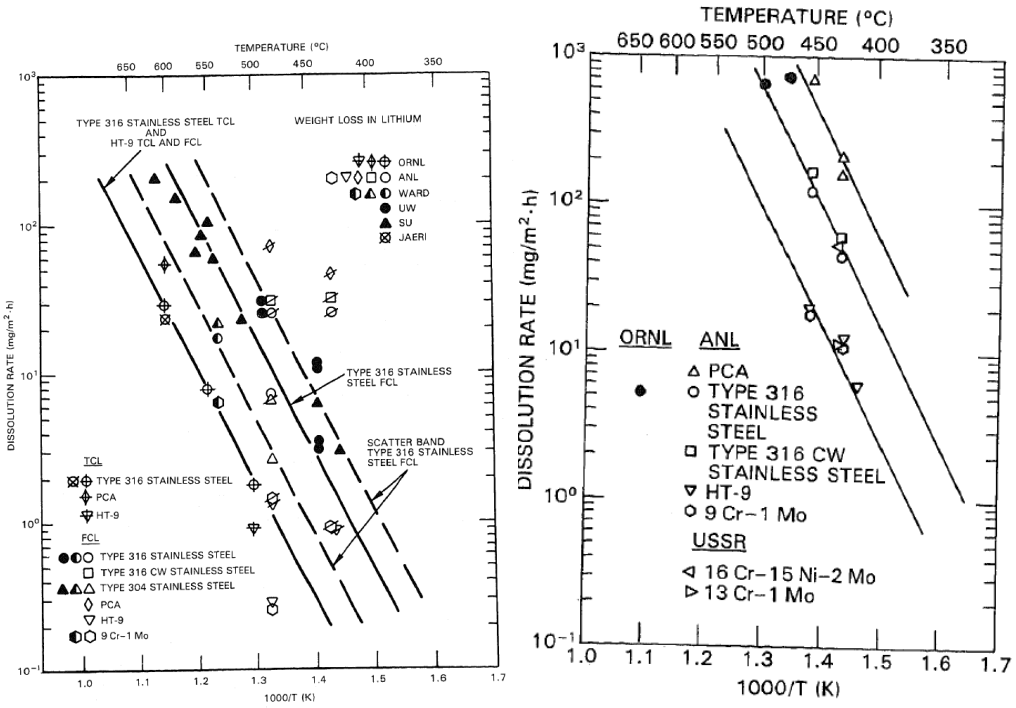

Figure 7.12. (left) Corrosion values for austenitic 304 and 316 stainless steels and ferritic alloys PCA, HT-9, Fe-9Cr-1Mo. Exposure to a lithium flow, speed 1.4 m/s. (right) Corrosion rate for austenitic stainless steels type 316 and ferritic alloys HT-9 and Fe-9Cr-1Mo. Exposure to a lead-lithium flow, speed 1.5 m/s.

Table 7.2. Estimated corrosion rates.

	HT-9 Steel	316 SS Steel
Li (mg /m²-h)	1.43	12.9
PB-Li (mg /m²-h)	66.4	540
Li Density (Kg/m³)	254.75	-
Pb-Li Density (Kg/m³)	10436.99	-
Li Corrosion (µm/year)	49.17	443.58
Pb-Li Corrosion (µm/year)	55.73	453.23
20 years Li Corrosion (µm)	983.44	8871.59
20 years Pb Corrosion (µm)	1114.62	9064.68

Corrosion values are very similar in Li and Pb-Li, so the system of pipes of the *TechnoFusión* loop is probably compatible with both materials, thus permitting the future change of research focus in this sense. Among steels, one can immediately reject austenitic stainless steels, since the corrosion rates multiplied by the lifetime of the facility exceed the pipe thickness by far. To avoid replacing the pipes, HT-9 ferritic base steels or 9Cr-1Mo are considered.

Assuming ferritic base steels are used, the corrosion acting during the 20 years of operation of the installation would imply a reduction of the pipe thickness by 1 mm.

(V) Impurity treatment

One of the most important issues related to the practical operation of the liquid metal, while exposed to the radiation produced by the electron accelerator, is the level of purity of the fluid. The connection of the loop to the accelerator must include an empty tube in order to minimize impurity transport from the last sections to the accelerator. The deposition of energy in the liquid metal, and the high temperatures at which some experiments will be performed, will lead to a release of impurities in gaseous form, which may enter the fluid or affect particle transport.

With experiments not involving the free surface these phenomena are less important, but still they can affect the operation of the liquid metal pumping system. Impurities could act as nucleation kernels for lithium steam, which could have important effects locally.

On the other hand, the motion of lithium along the loop also contributes to the total amount of impurities, as a consequence of corrosion and erosion.

Summarizing, impurities in the Li loop may have different origins, such as:

- Impurities of the lithium provided by the supplier.
- Impurities caused by diffusion in structural materials, originating from the surfaces along which the liquid metal flows.
- Impurities originating from the inert gas that is used in the protection system against lithium corrosion/oxidation.
- Impurities from the corrosion of structural materials.
- Impurities that seep into the loop due to maintenance and from auxiliary systems.
- Impurities from nuclear reactions.

Some elements entering the system by some of the mentioned mechanisms require special attention in the lithium track:

- *Oxygen*: this gas combines with lithium to form the stable lithium oxide, so one may consider that it produces no deleterious effects, or rather that it acts as a protector against corrosion for many materials, such as steels, heat-resistant metals, and some alloys. However, the presence of some impurities, such as beryllium or calcium, may cause its reduction and cause the formation of solid oxides inside the liquid metal flow, in turn causing the erosion of the structural materials. The concentration of oxygen in the lithium flow must not exceed the saturation value (i.e., 30 ppm at 250 ºC).
- *Nitrogen*: this is one of the impurities that dissolve best in lithium. It can form lithium nitrates and complex nitrates when combining with the structural components of steel, even at low temperatures. One may consider that this is the most active impurity from the point of view of corrosion, and in some studies 5 its concentration is therefore limited to 100 ppm at 500 ºC. One of the main impurity systems is the nitrogen purification trap.

In view of the preceding, the liquid metal tracks in the LMT Facility must be fitted with one (or several) purification systems, which have some implications for the experiments, especially regarding purification efficiencies and the kind of impurity to be extracted. The proposed built-in purification system would consist of three sections, namely:

- *An oxygen and hydrogen extraction system*. This extraction is performed using cold traps and diffusion disks up to temperatures of 190 ºC. In the case of oxygen, the saturation concentration at this temperature is about 5.5 ppm. The concentration of hydrogen in lithium does not exceed 50ppm.
- *A nitrogen extraction system*. The nitrogen extraction system consists of an aluminium filter. This process can be operated at moderate temperatures. Using this method, the final concentration will range from 1.6 to 6 ppm. The purification system produces aluminium nitrates that settle down, purifying the

flow in the tank at (200 – 250) ºC, and avoiding their entrance in the main loop by using filters.

- *A system for the separation of solid particles*.

(VI) Impurity monitoring systems

In order to maintain the degree of purity of the liquid metal that is required for satisfactory operation, purification mechanisms such as those described above must be implemented, along with monitoring devices to evaluate the concentration of the main impurities. For this purpose, the design of the experimental installation must include appropriate instrumentation (e.g. Figure 7.13). An analysis system for impurities that can be adapted easily when changing the working fluid is recommended, and additionally this system may perhaps even provide for automatic adjustment of the purification system. In any case, the priority of this facility is lithium operation.

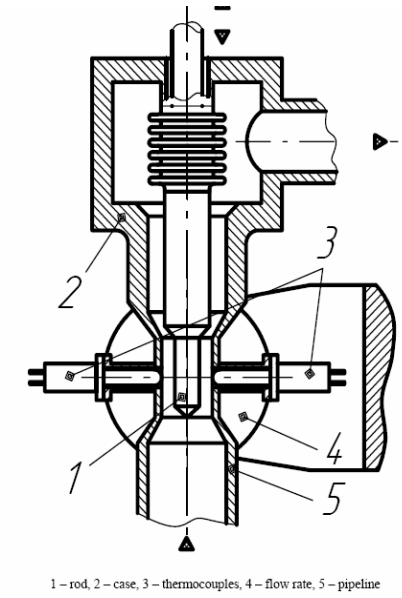

Figure 7.13. Impurity measurement device based on the analysis of the saturation temperature.

Many analysis methods are available, depending on the type of impurity:

1) *Impurity detection system by means of the determination of the saturation temperature,* for non-metallic impurities (nitrogen, hydrogen, oxygen and carbon). This detection process works by continuously cooling the flow through a narrow channel in a controlled way, by means of flowing cold water. The cooling of the liquid metal makes it reach the impurity saturation temperature, causing its decantation

and the reduction of the liquid metal flow due to its blocking action. This approach allows monitoring the impurity level in real time. The temperature at which the flow reduction is detected is the saturation temperature, and equations 7.1 show how the latter relates to the impurity concentrations:

$$\log[H] = 6{,}68 - \frac{2308}{T}$$
$$\log[O] = 6{,}99 - \frac{2896}{T} \qquad \text{eq. 7.1}$$
$$\log[N] = 7{,}57 - \frac{2080}{T}$$

2) *Detection system based on the distillation of liquid metal samples*. Useful for oxygen, and it has been applied in some reactors, such as the BN-600.

3) *Taking samples* to complete the analysis in the Characterization Techniques Facility. This process would involve installing a *by-pass* in the track through which the liquid metal flows until the flow is stabilized. Once stabilized, shut-off valves are closed and the samples are cooled, extracted from the loop, and transported to the laboratory.

7.5. Experimental capacity

Several specific lines of investigation can be followed in an installation of this kind. They can be subdivided into horizontal technological developments, common to any liquid metal installation; and vertical developments, referring to specific issues for specialised purposes, such as the IFMIF neutron source:

(a) Horizontal technological developments:

- Material corrosion and its compatibility with liquid metals (of interest both for fusion reactors and for IFMIF).
- Heat transfer.
- The development of auxiliary systems.
- The development of diagnostics.
- The purification of liquid metals.
- Safety.

(b) Vertical development:

- Studies of the behaviour of liquid metals in a magnetic field, and the development of insulating coatings.
- The diffusion of gases, particularly hydrogen.
- Studies of free surface flow, with and without energy deposition.
- Specific studies of material behaviour at extreme temperatures, and in contact with liquid metal.
- Specific studies of materials bathed in liquid metal, subjected to stress and energy deposition.

Suggested main experiments to be carried out in the LMT Facility are detailed below:

7.5.1. Studies of free surface flow

The studies of free surface flow while coupled to the electron accelerator are, as mentioned above, oriented mainly towards IFMIF and will fill an experimental void, key to the design of the latter's neutron source.

Figures 7.14 and 7.15 show different configurations of the testing zones of some international installations. It has been indicated the possible appearance of the free surface testing zone of *TechnoFusión*`s Installation. The lithium stream will have a medium size cross-section (of about 70mm x 10mm), with a rather high lithium speed (of about 15 or 20 m/s), requiring about 40 m^3/h of fluid flow.

Experiments will include the measurement of the surface ripples (transversal and longitudinal), any change in the flow thickness, the speed and pressure fields, etc. The flexibility of this experimental zone is a basic requirement to study various types of geometry, which is important because the geometry of the pipe and the tray has a direct effect on the generation of surface instabilities in the lithium flow. The dependence of these parameters on the speed of the liquid metal flow will also be studied. Erosion processes in the exit pipe (bursts, material deposits, etc.), distortions, and misalignments of the assembly of the various components, will have an effect on the appearance and development of instabilities, and this will also be studied. These experiments will be carried out at a relatively low temperature of about 250 ºC.

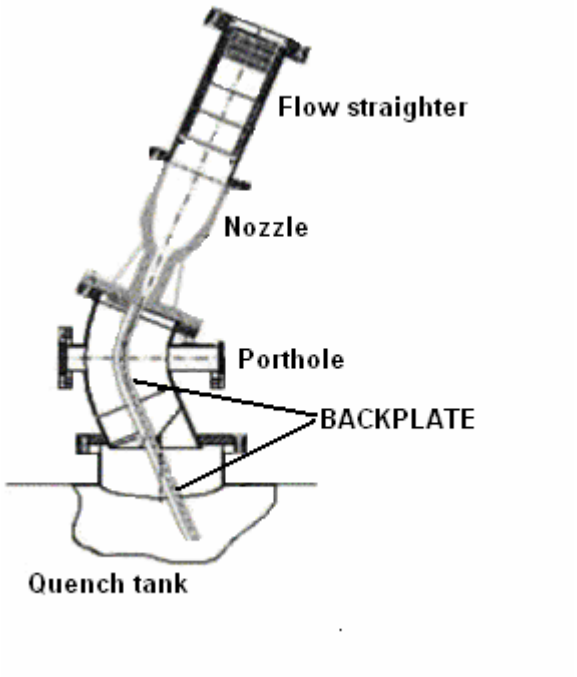

Figure 7.14. Experimental configuration for studies regarding the lithium free surface.

Figure 7.15. Free surface test gate of the ISTC 2036 project for water experiments [80].

[80] Final Report on R&D activities on #2036 project."The thermal-hydraulic and technological investigations for validation of the project of lithium circulation loop and neutron lithium target for IFMIF", Obninsk 2006.

Furthermore, problems associated with heat deposition in the liquid metal will be studied. In the IFMIF liquid lithium target, the deuteron beam that impinges onto the free lithium flow, generating neutrons, leads to a heat deposition with a distribution as indicated in Figure 7.16. At *TechnoFusión*, this heat deposition will be obtained from the accelerator electron beam. Many preliminary calculations have been carried out, using MCNP and hydrodynamic codes like FLUENT and CFX, to show that an electron accelerator with energy of 1MeV, an intensity of 70 mA, and a properly focused beam, can produce local temperature and power density profiles that are similar to those expected at IFMIF. Figure 7.17 shows the heat deposition due to electron beams with different energies.

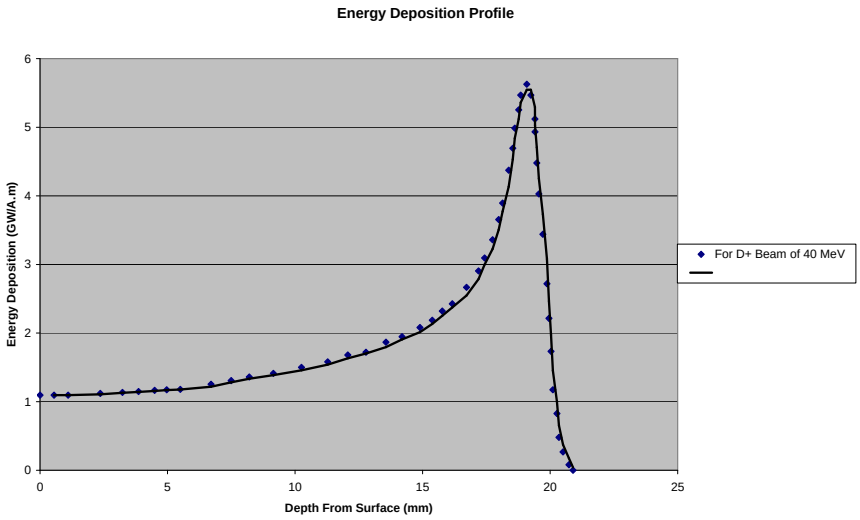

Figure 7.16. Heat deposition in the IFMIF[81] target.

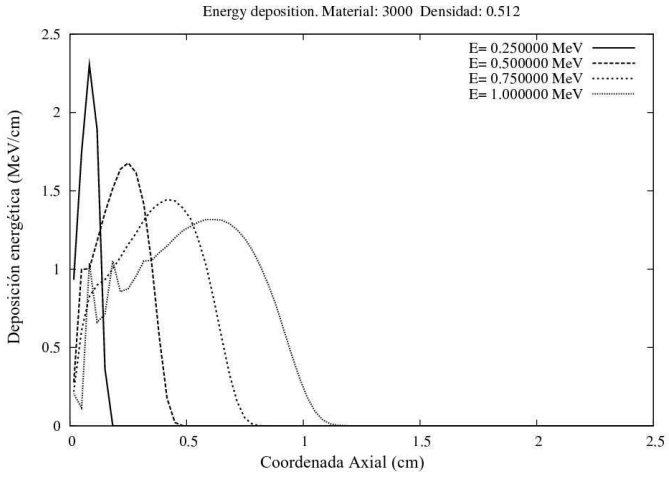

Figure 7.17. Heat deposition produced by electrons in lithium.

[81] M. Ida, Hideo Nakamura, Hiroshi Nakamura, Hiroo Nakamura, K. Ezato, H. Takeuchi, "Thermal-hydraulic characteristics of IFMIF liquid lithium target" Fusion Engineering and Design 63-64, p.333-342, 2002

Other interesting issues are related to the operation under vacuum conditions, which is needed in case of coupling with the accelerator. The experimental operation of a track at the nominal conditions of the IFMIF lithium loop has led to significant technological problems at the international installations that have tried to do so, such as the appearance of cavitations at various points of the loop. The experimental test section by itself constitutes a technological challenge that should be studied in the framework of the thermo-hydraulics of IFMIF and the design of the loop.

The hydrodynamic test loop will also be useful for the study of liquid walls for fusion reactors. For that purpose, the experiments dedicated to IFMIF can be replaced by divertor prototypes (Figure 7.18), first wall, etc. Such work will also involve studies concerning the composition of the free surface, its stability, heat deposition, etc.

Since the components of fusion reactors will be subjected to electromagnetic fields, the test zone will be designed to allow installing a high field magnet. In this framework, new liquid metal concepts can be explored, such as a porous structure filled with liquid lithium (CPS, Figure 7.19), minimizing the problem of liquid metal stability in the presence of the magnetic field by sequestering Li in a porous mesh, making use of its high surface tension.

Each specific experiment will require its own instrumentation, and the latter will also be subject to study and development. This instrumentation includes surface ripple detectors, lasers for obtaining speed profiles, cavitations and vaporization gauges, high speed chambers, etc.

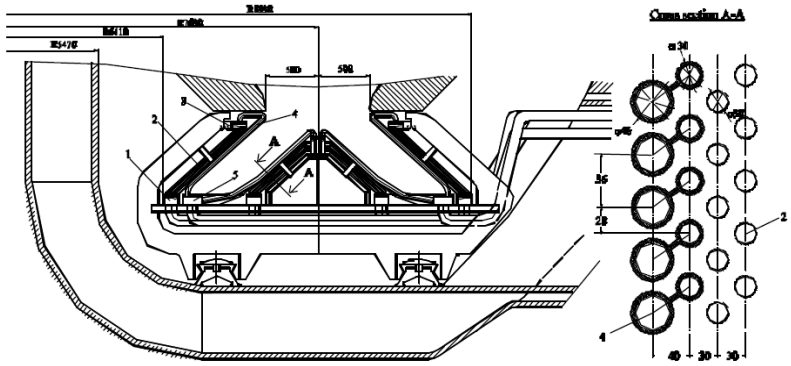

FIG.1. Lithium divertor section design option:
1-input collector, 2-channels of condensation zone, 3-intermediate collector, 4-channels of evaporation zone, 5-output collector.

Figure 7.18. Liquid lithium divertor scheme [82].

[82] H. Kondo et al. 'Experimental study of lithium free-surface flow for IFMIF target design'. Fusion Engineering and Design 81 (2006) 687-693

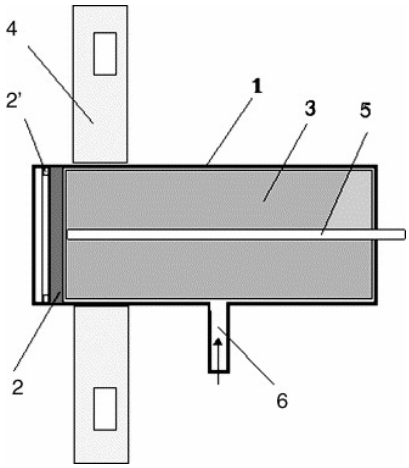

1 – Frame
2 – CPS (d = 40 mm)
2' – Brace
3 – Transport structure
4 – Cooling water flap
5 – Termocouple
6 – Lithium supply

Figure 7.19. Lithium target with CPS technology.

7.5.2. Material tests

In the material testing zone of the LMT Facility, many experiments will be performed, including: material compatibility, corrosion, the diffusion of gas through various materials, the mechanical properties of materials while subjected to fatigue cycles, flowing lithium in contact with the various materials of interest for fusion (ferritic-martensitic steels, EUROFER, ceramic materials, graphite, etc), and all this under extreme environmental conditions, appropriate for fusion applications.

The experimental conditions will depend on the goal of each study. For instance, tests of materials for IFMIF will be carried out at high speeds (up to 20 m/s) and low temperatures (below 300 ºC). Tests related to materials for fusion will require very high temperatures of about 1000 ºC and low speeds (≈ 1 m/s). For the gas diffusion experiments (Figure 7.20), the track will be fitted with the required gas feeds (hydrogen, deuterium, etc.) appropriate for each experiment. For the fatigue tests, machines will be installed to apply loads.

As most aspects of the interaction of lithium with other materials are influenced by a radiation field, the experiments will be carried out with and without radiation. To do so, electrons will impinge on a sheet of a certain material in order to generate the radiation field that will be used to irradiate the testing subject. In Figure 7.21, a sketch of an experiment with radiation is shown. This is the LiSoR experiment (Paul Scherrer Institute of Switzerland), in which the behaviour of materials in contact with the lead bismuth alloy is studied.

Occasionally, the duration of these tests will be quite long (some thousands of hours). Furthermore, key parameters such as the speed, temperature and chemistry of lithium are to be varied.

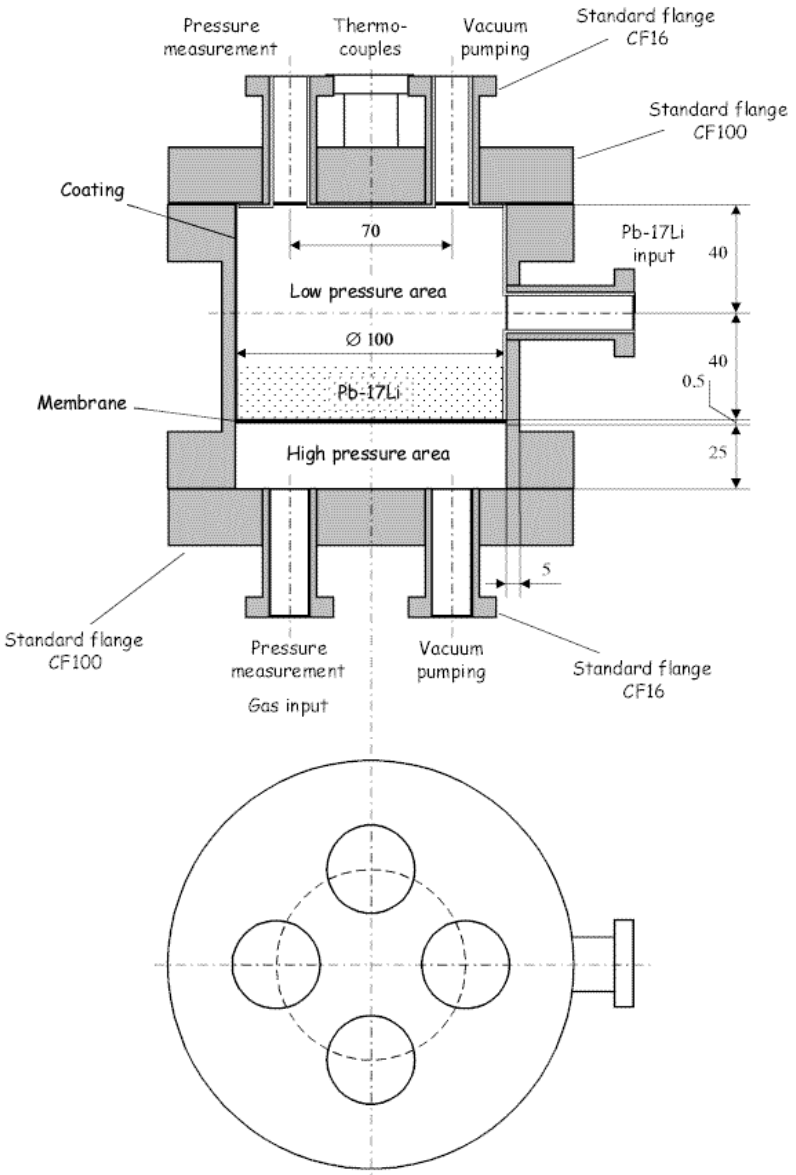

Figure 7.20. Experimental section of the LEDI facility for the study of gas diffusion across membranes in contact with LiPb.

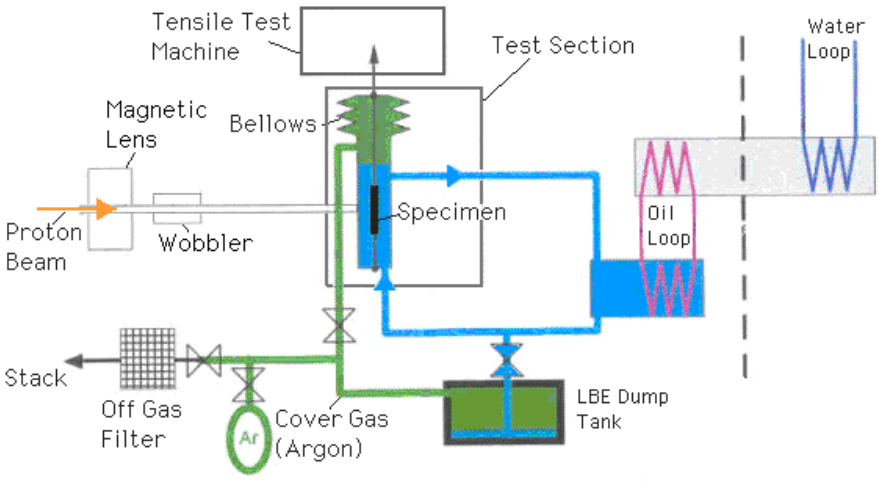

Figure 7.21. LISoR experimental facility of *Paul Scherrer Institut* (Switzerland).

7.5.3. Magneto-hydrodynamic tests

Since environment of a fusion reactor includes electromagnetic fields, the study of corrosion, heat transfer, of the hydrodynamic behaviour of the liquid metal in prototypes should also be carried out in such a field. Thus, the installation of large field magnets is planned at both experimentation zones of *TechnoFusión*.

As mentioned earlier, a magnet can be installed at the free surface experimentation zone in order to study its stability under the influence of an electromagnetic field. At the materials track, studies can also be carried out regarding the influence of an electromagnetic field on, e.g., pressure drops, speed profiles, heat transfer, gas diffusion, impurities, or corrosion. To carry out such experiments, a magnet must be coupled to the materials test loop described above. This track should also be capable of varying the speed and temperature of the lithium to match the range of future liquid lithium blankets.

In the case of, e.g., corrosion tests, samples will be introduced and brought into contact with the liquid metal, while the magnet distorts the flow field. Experimentation times will frequently be of the order of several thousands of hours. For other types of experiment, the required times will be much lower.

Figure 7.22 shows a diagram of the MHD testing facility. To perform heat transfer tests in an electromagnetic field, heating and cooling systems will be required, as well as instrumentation to control the temperature of the track. To measure the pressure drop caused by the electromagnetic fields, the track must be provided with pressure gauges.

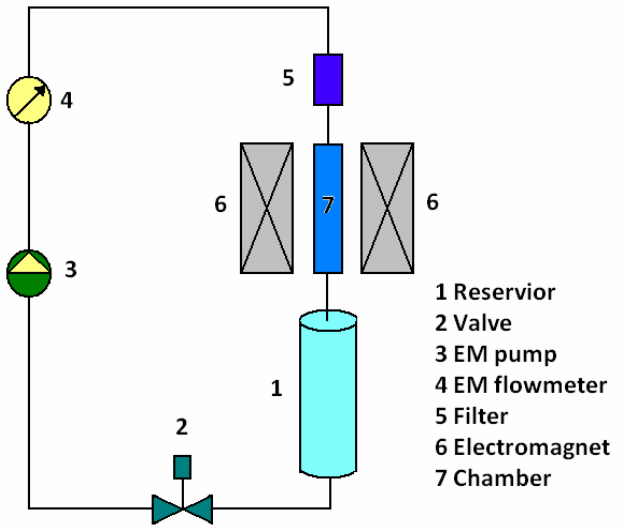

Figure 7.22. Diagram of the MHD[83] experimentation zone.

Summarizing, for this kind of tests, the requirements of the experimentation zone will depend on the type of test. The following points should be taken into account:

1) There must be enough space to install a magnet for generating a high magnetic field, and its auxiliary systems and diagnostics.

2) Since the geometry of the canal is very important for the MHD tests, the materials test loop should have a certain degree of flexibility, permitting the incorporation of different types of track sections, e.g., a circular canal, a square canal, a narrow canal, parallel canals, etc.

7.5.4. Purification and gas treatment tests

When the lithium has passed through the mentioned testing zones, it will be contaminated with corrosion products, solid or gas impurities, etc. In addition, some experiments can require the deliberate addition of impurities to the track. Thus, the lithium loop must be equipped with in installation for purification, so that the lithium enters the track with an optimal degree of purity. Such an installation may be the subject of further development efforts in order to obtain better or innovative components.

In principle, the purification system will consist of a first section to remove any gases dissolved in the lithium (resulting from chemical reactions or purposely added in an experiment), and a second section to remove any corrosion products. An ideal purification

[83] M. Ida, Hideo Nakamura, Hiroshi Nakamura, Hiroo Nakamura, K. Ezato, H. Takeuchi, "Thermal-hydraulic characteristics of IFMIF liquid Lithium target" Fusion Engineering and Design 63-64, p.333-342, 2002

system will include gas trap injectors, cold traps, etc., and lithium purity probes to ensure the cleanliness of the material. In addition, the latter will serve to quantify the effectiveness of the various purification approaches.

The study of the retention, permeability, solubility and diffusivity of tritium, being a particular case of the diffusion of gases in liquid metals, and the associated extraction systems, constitute one of the most interesting issues in the fusion field, with a view to the development of permeation barriers or tritium extraction systems. Although a large amount of information on the subject of LiPb is available, much of it is contradictory, and a similar situation is bound to occur with pure lithium (which has been much less studied). Therefore, this line of investigation will certainly require much international cooperation. The mentioned processes can be investigated in this experimentation zone, for instance by injecting hydrogen or deuterium into a lithium flow. In Figure 7.23, an example is shown of tritium control by means of an Yttrium trap.

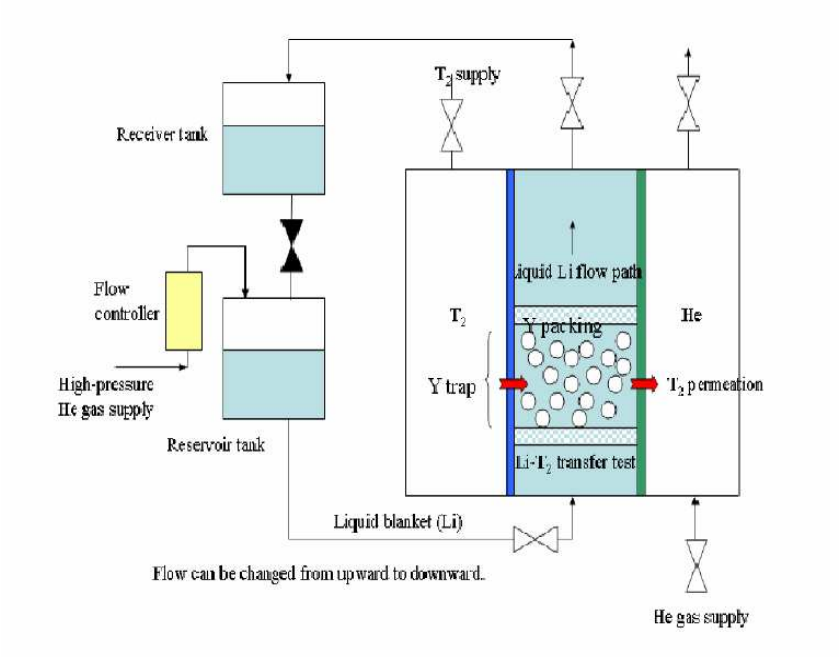

Figure 7.23. Tritium control using an yttrium trap, Kyushu University (Japan).

7.5.5. Safety tests

The handling of pure lithium requires specific safety precautions. Thus, safety will be one of the subjects of study at *TechnoFusión*, and the interaction of Li with water, air, and residues will be analysed, accident analyses will be made, etc.

The main difficulty of using lithium as a working fluid is its reaction with air and water. In order to elaborate an appropriate handling safety protocol, experiments must be performed and calculations must be made. Accordingly, such safety issues have been identified as one of the subjects of study at *TechnoFusión*. These include: the pouring of lithium in the atmosphere and/or in water, the injection of air and/or water, simulations of accidents with a loss of cooling (LOCA) oriented towards future facilities such as IFMIF, fires, etc.

7.5.6. Auxiliary systems and diagnostics

The liquid lithium tracks will be fitted with many diagnostics, such as chambers (Figure 7.24), laser accelerometers, various types of sensors (Figure 7.25), thermocouples, and radiation meters.

The main elements of the loop and the diagnostics will need to be designed specifically due to the lack of commercial technology related to this kind of facilities.

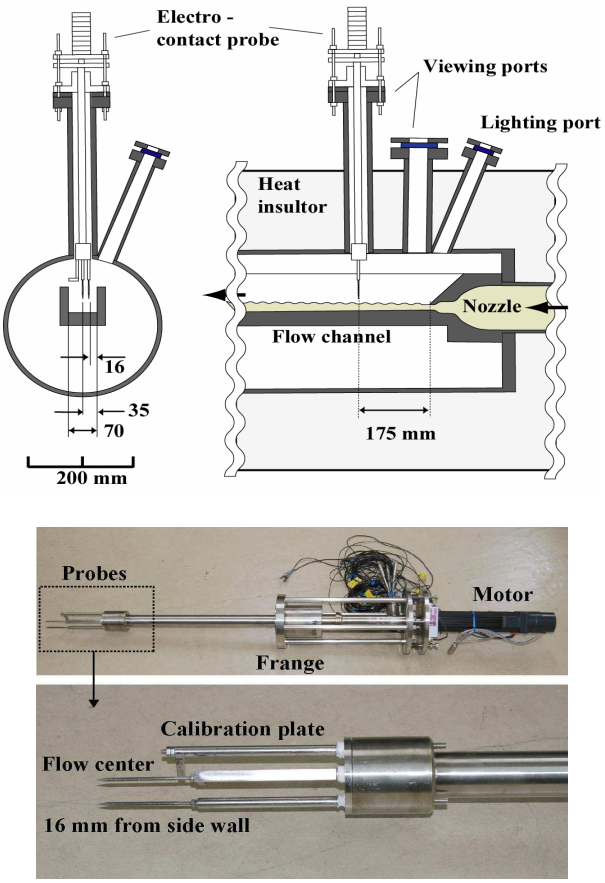

Figure 7.24. Picture and sketch of an electric contact sensor for measuring surface waves.

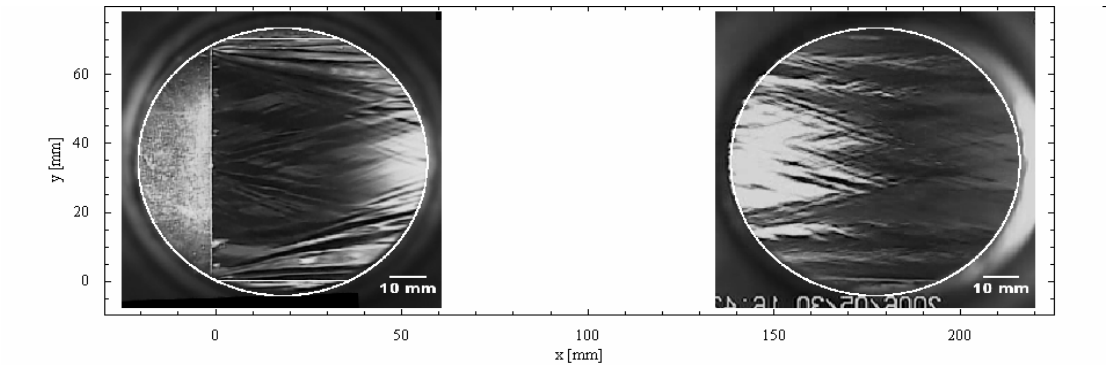

Figure 7.25. Picture taken by the Sensicam QE (PCO AG) camera at the University of Osaka.

7.5.7. Tests with Pb-Li

Due to the great importance of the eutectic lithium-lead in the fusion field, and in spite of the fact that Europe already has a number of facilities dedicated to this material, it is considered appropriate that the possibility of performing experiments with this material at *TechnoFusión* is left open.

Therefore, the tracks should be compatible for operation with LiPb. Since lithium-lead experiments usually require low working speeds, it would be sufficient to have a basic dedicated track based on natural convection. In this way, advantage could be taken of the diagnostics and the experimental zones designed for the lithium track. A sketch of such a loop is shown in Figure 7.26.

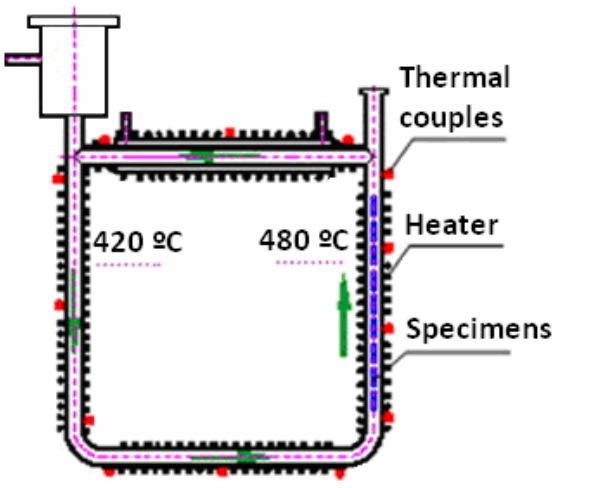

Figure 7.26. Conceptual sketch of a lead-Litium loop for free convection studies.

In addition, this zone might also be subjected to electromagnetic fields and used to test various configurations for future ITER and DEMO blankets.

7.5.8. Validation of computer codes

Computer codes for fusion system engineering and design must be able to manage and simulate the main phenomena related to the behaviour of the materials that will be used. Liquid metals will very likely be one of the main constituents of future fusion devices because of their cooling and neutronic properties.

Therefore, it is important to validate the design tools used to simulate the flow of the liquid metal through the tracks [10]. The design of the cooling channels for ITER and DEMO, as well as the design of the neutron source at IFMIF, is being executed using CFD codes. It has been noted that the full validation of these multipurpose codes is required when liquid metals are used, because of the following:

- The turbulence models that are used in commercial CFD codes are not verified in the full parameter range, i.e., their validity limits in terms of the turbulent Prandtl (Pr) number are not known.

- Models based on commercial CDF codes do not seem suitable for the analysis of liquid metal flow, since they usually assume that the Reynolds analogy holds, in which the thermal and velocity boundary layers are coincident, which is not true in fluids with a low Pr number. The latter is the case of the lithium.

- In CFD codes, the forcing effects due to gravity, and the corresponding multistage models must be improved for fluids with low Pr and Peclet numbers, as is the case of liquid metals.

7.6. Layout, supplies and safety requirements

(I) Layout and equipment

The building for the LMT Facility of *TechnoFusión* will have to comply with a set of requirements, e.g., to provide sufficient space for the physical volume of the planned equipment. It will also need to provide safe experimental conditions in relation to, e.g., the handling of liquid metal, the presence of magnetic fields, high temperatures, etc., and, critically, the utilization of an electron accelerator at the liquid metal loop, considering the relative location of both systems and radiation protection requirements (shielding, access control, etc.)

Regarding the needed space, note that the free surface experiment, including its coupling to the accelerator, should measure about 15 metres. This number arises due to the necessity of having a lithium column large enough to avoid cavitations at the entry of the driving pump. To achieve this height, part of the track could be built underground, placing the

tanks and pumps in a basement, or, preferably, in a ditch (as with the existing installation at the University of Osaka), that could be flooded with argon in case of a lithium leak.

The International installations that have been studied as reference models for the *TechnoFusión* design usually have the experimentation tracks placed in a well-lit building, with cranes to manipulate the equipment. The Obninsk installation is special, as its lithium track is locked inside a metallic box that traverses the various floors of the facility. This design is probably motivated by the reuse of existing installations initially dedicated to other uses. Both solutions are possible, but the first one allows more flexibility when installing the different tracks, and better access to all the parts.

Further research into the track implantation, and the required space for auxiliary systems, will require more specific information about the available space. As a first estimate, the LMT Facility would need an area of approximately 300 m^2.

(II) Safety

The routine handling of alkaline metals in experiments, such as Li, requires establishing specific procedures.

Safety is a key issue in a facility of this kind, as a consequence of the chemical reactions that may occur when the metal comes into contact with components of the air, such as oxygen, nitrogen and water. Lithium reacts violently with water, and can suffer spontaneous combustion when in contact with air at a high temperature.

Lithium reacts with oxygen producing lithium oxide (eqs. 7.2.).

$$2Li + \frac{1}{2}O_2 \longrightarrow Li_2O \quad \left(\Delta H_{25^oC} = -142.65 Kcal/mol\right)$$

eq. 7.2

$$2Li + O_2 \longrightarrow Li_2O_2 \quad \left(\Delta H_{25^oC} = -151.9 Kcal/mol\right)$$

Li_2O is very reactive with water, carbon dioxide and heat-resistant compounds. Its reaction with water produces hydroxide, which causes burns on the skin, eyes and other tissues (eq. 7.3).

$$LiO_2 + H_2O \longrightarrow 2LiOH$$

eq. 7.3

In the presence of nitrogen, lithium reacts according to the reaction (equation 7.4.):

$$3Li + \frac{1}{2}N_2 \longrightarrow Li_3N \quad \left(\Delta H_{25^oC} = -47.5 Kcal/mol\right)$$

eq. 7.4

The generated lithium nitride is highly reactive. In the presence of water, ammonia can be formed. No metal or pottery can resist molten nitride.

Lithium will react with oxygen and any other gas, except the noble gases. The ignition temperature of lithium in air ranges from 180 ºC to 640 ºC. This means that lithium handling must be done in an environment with inert gases.

In the presence of water, lithium reacts violently, forming lithium hydroxide and hydrogen gas. Usually, this reaction is accompanied by an explosion, caused by the secondary reaction of hydrogen with oxygen.

$$2Li + 2H_2O \longrightarrow 2LiOH + H_2 + Q$$
$$2H_2 + O_2 \longrightarrow 2H_2O$$

eq 7.5

The heat generated in the first reaction is enough to drive the second reaction.

The following safety measures must be taken when operating a lithium loop:

- All staff that comes into contact with the installation or that operates it must be qualified.
- There should be emergency plans to stop operation safely.
- Protective emergency gear should be available, such as protective suits, facial masks, and fire extinguishers appropriate for the expected type of fire.
- Protective gear for the operation staff in case of a leak or fissure in the loop.
- Auxiliary lithium tanks for die-casting the track and collecting leakage flows.
- A ventilation system and a filtering system in case lithium oxide or hydroxide fumes are formed.
- Detection systems for lithium leaks and fires, and fire extinction systems.
- Safeguards to prevent the entry of water and other incompatible materials into the lithium loop.
- Protection systems for the equipment in case of anomalous circumstances.
- Appropriate signalling of any rooms containing a certain amount of lithium.

(a) Safety analysis of loop operation

One of the main goals of the LMT Facility of *TechnoFusión* is to serve as an installation of reference for the development of the IFMIF project. In this sense, many of the security issues are identical to the issues that will arise there.

The lithium target of the experimental installation of IFMIF[84, 85, 86] has been subjected to many security tests, and the most important risk factors have been evaluated. The cited studies follow the procedure known as FMEA (*Failure Mode and Effect Analysis).* Failure tree techniques have also been applied to evaluate all possible failures of any component needed for safe loop operation. Testing the safety of a liquid metal loop requires using a thermo-hydraulic simulation code that allows estimating the effects of a given event.

In case of the *TechnoFusión* loop, a particular list of possible events has been identified, based on the studies for the IFMIF installation:

- A loss of lithium flow in the loop.
- A flow loss in the *Cold trap* cooling loop.
- A loss of heat drainage.
- A cooling (LOCA) loss accident in the lithium loop.
- A loss of lithium purification.
- The escape of lithium inside the building.
- A burst in the lithium pipe.
- A loss of vacuum in the free surface zone.
- A loss of argon.

Other events that must be studied further during the design of the track:

- A failure of auxiliary systems (pumps, valves, etc.).
- A failure of the control system.
- A loss of the electric power supply.

[84] L. Burgazzi, "Safety assessment of a lithium target", Nuclear Engineering and Design, 2006
[85] L. Burgazzi, " Probabilistic safety analysis of an accelerator-Lithium target based experimental facility", Nuclear Engineering and Design, 2006
[86] L. Burgazzi, "Hazard evaluation of The International Fusion Materials Irradiation Facility", Fusion Engineering and Design, 2005

- A loss of high-pressure air.
- The entrance of water in the track.
- The entrance of air in the track.
- The entrance of oil in the track.

(b) Safety when filling up or training the system

One of the most hazardous tasks when operating the liquid metal track is filling or draining it. This issue is particularly important when the tracks are used with several liquid metals.

Liquid lithium is a material that requires taking important safety measures, mainly to avoid contact with the atmosphere and water. Most likely, the material will be supplied in a tank fitted with electric heaters, underneath a protective layer consisting of a mixture of oil and paraffin.

(c) Waste Management safety

Spanish legislation regulates the storage of raw materials in any installation where chemical products are handled. The Ministry of Industry issued Royal Decree 379/2001, dated 6th April, concerning the 'Regulations for the storage of chemical products and complementary technical instructions', aiming to establish the safety requirements for the storage, loading, unloading, and transfer of dangerous chemical products. It includes a detailed description of the procedure for requesting the registration of an installation, subject to the approval of a system of periodic controls, as well as administrative controls and sanctions for infringements of the regulation. This regulation also includes Complementary Technical Instructions (ITC) for each product.

In article 2, the scope of the rules is established. Lithium, which is the main constituent of the experimental area of the liquid metal installation, is placed in the group of corrosive solids, provided its inventory is less than 200 kg. Currently, there is no specific regulation for products such as lithium, so there is no requirement to obtain a project license for this kind of installations, although it is foreseen that the installations are subject to the regulations concerning the use and storage of flammable goods.

This means that the LMT Facility only needs to comply with the applicable regulations and principles of the *International Chemical Safety Card* (ICSC), and with the rules described in the Guide for the Response to Emergencies (GRE 2004).

These documents do not have a legal status, but they clearly summarise the essential requirements regarding hygiene and safety for the mentioned chemical substances. The record number for lithium is ICSC 0710, and some of the main instructions are:

- Avoid flames and sparks, and do not smoke.
- Do not expose the product to water.
- In case of fire, do not use water but special quenching agents such as dry sand.
- Keep storage tanks and related installations refrigerated.
- In case of spillage or leakage, remove the spilled substance and collect it in a sealable metallic container, carefully gathering the residue using dry sand or another inert absorbent. Never pour it to the sewer.
- Staff must wear a total protection suit, including respiratory equipment.

8. Characterization Techniques

8.1. Introduction

The structural components of the next fusion reactor, DEMO, will suffer radiation damage of 50 to 150 dpa, and will need to withstand temperatures of up to 1000 ºC, depending on the specifics of its final design. In addition, the structure should be able to accommodate high H and He content, resulting from the transmutation of elements of the material matrix as these interact with high-energy neutrons produced by plasma fusion reactions. The presence of these light elements in the crystalline structure has important consequences for the mechanical properties of the metallic material. In a wide range of operational temperatures, the presence of H and He impedes the recombination of point defects, leading to an increase of the embrittlement of the material. Based on the above, it can be enumerated at least five important effects associated with radiation damage that may lead to the structural degradation of materials in a fusion reactor.

1) An enhancement of structural embrittlement and fragility when the radiation dose and temperature exceed 0.1 dpa and 0.35 MP, respectively (MP being the melting point of the material).

2) Destabilization of the metal matrix structure when the radiation dose and temperature exceed 10 dpa and 0.3 MP, respectively, due to segregation and precipitation of new phases, induced by radiation.

3) Under similar conditions, 3D vacancy aggregates will be formed. The concomitant swelling will induce an unacceptable modification of the size of the structural component.

4) On the other hand, permanent deformations proportional to the dose and the applied stress should be taken into account when the radiation dose and the temperature exceed 10 dpa and 0.45 MP, respectively.

5) Finally, the presence of He at high operational temperatures (above 100 appm and 0.5 MP) will enhance the embrittlement of the grain boundaries, leading to inter-granular fracture, even when the materials are submitted to low stresses. At low temperatures, He generation due to transmutation will also enhance embrittlement and swelling. The high production rate of He by transmutation will modify the precipitation processes induced by radiation in a wide temperature range. In turn, this will diminish the resistance to fracture of the metals due to a lack of cohesion of the grain boundaries.

8.2. Objectives

Understanding the mechanisms by which the material will suffer degradation under fusion conditions will allow predicting the behaviour of devices and components and developing new high resistance alloys, capable of supporting the operational conditions of

future fusion reactors. Therefore, the *TechnoFusión* Facility will require a set of advanced devices and techniques for testing materials and components, in order to clarify the mechanisms of these phenomena. On the one hand, there will be a number of techniques for testing or characterizing materials during irradiation (referred to as *in-beam techniques*) or modification (*in-situ techniques*). On the other hand, there will be techniques that will allow monitoring mechanical, morphological and compositional changes of irradiated materials and making comparisons with the unirradiated samples. In all cases, high-precision techniques are required in order to study very small samples, since the three accelerators proposed in the framework of the *TechnoFusión* facility only allow small irradiation areas.

The following section will list the laboratories and equipments needed for the establishment of the **Characterization Techniques Facility (CT)** of *TechnoFusión*, as follows from the inquiries and studies carried out by the team of experts and consultants. If provided with the described equipment, this facility will be able to make a relevant and competitive contribution to the study of fusion-induced modifications to materials,. The proposed equipment is considered essential in order to be able to undertake such studies, which either have already been proposed, or which will be proposed in the future:

- Irradiation effects in structural materials (low activation steels, tungsten alloys, …)
- Modifications in the mechanical and physical properties, the microstructure of structural and functional materials and technological components, induced by operational conditions
- Synergetic effects of H and He implantation and radiation damage on the mechanical and physical properties and the microstructure of fusion relevant materials.
- The evaluation of the mechanical properties of materials and components under radiation. The study of the mechanisms of the enhancement of embrittlement and fragility of metallic structures (accumulated damage 0.1-10 dpa; testing temperatures between 0.35-0.6 MP (*Melting Point*).
- The determination of the mechanical properties of new alloys.
- Structural modifications induced by radiation damage in fusion relevant materials. The stability of crystalline phases and changes of the microstructure during ion irradiation: the creation of new phases, the segregation of elements, precipitation on grain boundaries, etc
- The chemical characterization (analysis and distribution), on an atomic scale, of fusion relevant materials. The study of physical phenomena related to radiation damage.
- High temperature properties of the interface metal matrix – coating.
- Characterization of the interaction between the plasma and the first wall.
- Plasma facing materials: erosion/redeposition studies.

- H and He analysis of first wall materials and components (the retention of light elements, tritium inventory).
- The corrosion of materials and components under liquid lithium.
- The synergetic effect of dynamic liquid lithium and stress on the degradation of mechanical properties, particularly creep and creep-fatigue.

8.3. International status of the proposed technologies

Due to the large number of techniques and devices considered for this Facility, it was considered more convenient to include a description of the state of the art and the main related research groups at the end of each section corresponding to a technique, rather than provide this information here.

8.4. Projected devices and equipment

In order to address the future demand for fusion technologies, for which a facility such as this should be prepared, the proposed CT Facility will have a broad scope and will be fitted with a highly advanced and ambitious infrastructure for material characterization. In the following chapters, those techniques considered fundamental for the characterization and testing of new materials and components are described in detail. The aim here is to list the techniques required to cover the whole parameter range in order to obtain an optimal characterization of the materials. However, depending on the location of the Facility, in some cases it will be recommended to acquire and install the equipment at *TechnoFusión* building, but in other cases it may be preferable to make use of similar equipment at Facilities and Centres located nearby. Nevertheless, the CT Facility should be considered a service-providing facility, open to future expansion, the regular acquisition of new instrumentation, the upgrading of existing equipment, the modification of testing equipment and techniques, and the on-site development of testing equipment and techniques, which can be manufactured in the workshops of the facility.

8.4.1. Techniques for the analysis of macro-mechanical properties

A large part of the problems associated with fusion technology are related to the selection or modification of the materials required to withstand the extreme conditions inside a fusion reactor.

An important part of the materials that will be developed and analysed in the *TechnoFusión* facility will have structural applications. Their mechanical properties under fusion reactor conditions will determine their future application. In order to guarantee the structural integrity of the proposed materials, their short and long-term durability under

extremely severe conditions must be known. More specifically, the structural materials of a future fusion energy production system will have to operate at temperatures of up to 600 ºC (or even 1200 ºC), while supporting stresses of up to 300 MPa, incorporating high levels of H and He impurities produced by nuclear transmutation, and suffering cumulative radiation damage due to fast neutrons of more than 100 dpa. It is essential that these materials maintain a good balance of their mechanical properties (fracture toughness and creep) during operation, suffering only minimal size changes due to swelling and fluence.

In view of the above, the mechanical properties of the materials should be tested under conditions that are as similar as possible to the actual future environment. Thus, a set of versatile devices will be needed in order to carry out the mechanical tests that allow characterising the materials and the components of the various systems. It is particularly important to determine whether they are affected critically by the environmental conditions during their operational lifetime.

Size is not a determining factor for the testing of new materials, so that the samples for mechanical testing can be standardised. The testing equipment described below has been designed to have maximum versatility.

TechnoFusión will have a facility specifically dedicated to the production and development of materials, which will involve equipment satisfying the standard procedures to new materials testing. In order to characterise the newly developed materials, the facility will dispose of adequate instrumentation to implement standard procedures: universal testing machines, impact testers and creep machines.

8.4.1.1. Universal Testing Machines

These universal characterization machines are designed to perform thermal and mechanical tests, oriented specifically to the issues of high and advanced low cycle fatigue, fatigue crack growth, fracture toughness, component strength and durability.

1) Landmark Servo-hydraulic Test Systems, by MTS

These systems meet a wide spectrum of static and dynamic material test requirements. MTS Landmark Systems integrate the latest in MTS servo-hydraulic innovation, versatile FlexTest controls, proven MTS application software and a complete selection of accessories to provide highly accurate and repeatable static and dynamic testing across the material testing continuum. Available in highly configurable floor-standing and tabletop models, these systems are ideal for testing components ranging from medical devices to shock absorbers, and materials such as plastics, elastomers, aluminium, composites, steel, super alloys and more. These machines are available in a wide range of capacities (5 to 500 kN).

2) The Fast Track 8801 Series, by INSTRON

These servo-hydraulic systems of INSTRON are specially indicated to perform fatigue and static tests of advanced materials and manufactured components that require capacities

from 50 to 100 kN. These flexible materials testing systems feature the widest selection of servo-hydraulic testing frames, controllers, software packages and test accessories available.

8.4.1.2. Electro-mechanical testing machines

This system is able to perform tensile, compression, flex/bend, and advanced tests, such as creep, stress relaxation and multi-cycle fatigue tests. The selection of the model should be based on its versatility in handling different materials, geometries and sizes by means of a simple modification of loading cells, grips, etc. Using commercial or locally manufactured accessories, the testing of small (sub-millimetre) and large specimens will be possible, up to the maximum device capacity.

1) *Model 3380, by INSTRON:*

This floor-standing model is specially suited for performing tension and compression tests with a load capacity of up to 250 kN. Its principal characteristics can be summarized as follows: force ratio 100: 1, 0.5% load accuracy, data acquisition frequency: 100Hz, full software control and automatic transducer recognition. This machine could be completed with a wide range of optional grips and fixtures, and high and low temperature chambers.

2) *Insight® electromechanical testing systems, by MTS*

All MTS Insight models perform both standard and advanced tests reliably. By offering user-defined crosshead speeds and advanced control modes such as load and strain, MTS Insight testing systems can analyze a wide range of materials, including low to high-strength components, structural materials, composites, metals,etc. MTS has a wide variety of models from low (1-5 kN) to high (100-300 kN) force applications, the medium force machine (up to 50kN) being the most appropriate for the static tests to be performed at *TechnoFusión*.

8.4.1.3. Pendulum impact testers

The standard way to establish the resistance of a material to an impact is to prepare specimens with a simplified geometry, and use a pendulum-type machine to break them. The energy absorbed at impact is recorded and divided by the receiving section of the specimen, thus giving the resistance (J/m or kJ/m^2). The traditional technical solution for performing these measurements is to use a swinging pendulum equipped with a device to record the angular position of the hammer. A more sophisticated method is the so-called instrumented test, which involves the direct detection of force during impact, allowing the study of force and deformation, thus providing much more information about the type of failure and the dynamic response of the material.

Non-instrumented tests are based on estimating the absorbed energy (J). The difference between the starting position of the pendulum and its highest position after impact is directly translated to the energy absorbed by the specimen, by considering the available potential energy. Each impact, carried out according to some standard specifications, provides an

estimation of resistance. A series of specimens is tested in order to be able to perform a statistical analysis of the results and obtain a reliable measure of the resistance. This test is a typical quality control test, as it quickly provides a numerical result suitable for control charts and simple comparisons.
However, often instrumented tests are preferred. These tests are based on the direct measurement of the force by means of suitable sensors, such as strain gauges or piezoelectric load cells attached to the hammer or device. These sensors are able to capture the complete force-time curve and provide enough information to calculate the deformation and the rate of change of speed and energy, in addition to the resistance. This method is suitable for advanced quality control or for material processing research and development.

RKP 450, by Zwick:

The Zwick pendulum-type tester RKP 450 (Figure 8.1) is a universal impact tester able to handle up to 450 J for Charpy, Izod, impact tensile and Brugger tests. This machine can be modified to provide semi- or fully automatic specimen temperature control (for both positive and negative testing temperatures), as well as feeding.

Figure 8.1. Impact tester Zwick RKP 450, modified for Charpy and Izod testing.

8.4.1.4. Creep testing systems

The equipment (Figure 8.2) will consist of various identical machines (e.g. INSTRON M3TCS) for performing creep tests of materials. The creep determines the capacity of a material to support a load at a high temperature and for a given period of time. This type of machine can perform the following tests:

- At constant load and temperature, determines the time at which the sample breaks (*stress rupture*).

- At constant load and temperature, measures the gradual deformation of the sample in time up to a maximum test time (*creep*).

The samples may have various calibrated diameters and lengths and are fitted with threaded ends. The sample may be submitted to forces of up to 30 kN and temperatures of up to 1100 ºC. These machines are fitted with devices that provide a continuous measurement of the stretching of the sample using displacement capacitors LVDT (*Linear Variable Differential Transformer*), up to a maximum displacement of 40 mm and with a precision of 0.001 mm. The system is fitted with high precision temperature controllers. The incorporation of a digital system for the acquisition and treatment of data would be desirable.

The maximum operating temperature of fusion power plants will be determined, among others, by the creep properties of the structural materials used. In order to obtain a complete characterization of creep strength in irradiated materials, the facility must have at least ten creep machines. In Figure 8.2, an example of INSTRON's creep test machines is shown. The INSTRON model M3TCS, will allow material testing up to 1100 ºC and 3000 kg.

Figure 8.2. General view of several creep test machines in paralel.

8.4.2. Mechanical tests of irradiated or modified material on micro and nanoscales

As mentioned above, the main objective of the mechanical property testing facility is the measurement and evaluation of the mechanical properties of the irradiated material in a relevant temperature range. The mechanical characterization will involve tensile, fatigue, creep, creep-fatigue and fracture toughness tests.

In particular, the installations at *TechnoFusión* will allow the modification of the tested materials by provoking damages comparable to the expected damage by neutronic radiation.

The possibility of simultaneous irradiation at the triple-beam facility will allow studying the synergic effect of radiation damage and the presence of light impurity ions (H and He) in the structure, in order to obtain a quantification of the properties of materials and device components. Other factors, such as temperature, vacuum conditions, plasma interaction, etc., will be also considered and studied.

From the point of view of mechanical engineering, the test specimens should have the adequate dimensions, i.e., as close as possible to the final material application. The mechanical data obtained from specimens of micrometer or nanometre size are not always fully relevant for macroscopic operational conditions. The size of the tested specimen might affect the material response significantly, and the structure of the material at large scales might dominate over its microscale properties. Currently, the three-beam accelerator facility at *TechnoFusión* is limited to the irradiation of specimens with volumes considered classical in the framework of fracture mechanics. As discussed in chapter 4, the light and heavy ions accelerated in the *TechnoFusión* triple-beam facility will allow producing damage and H and He co-implantation in a single specimen volume. Taking an example from Table 5.4, both implantation processes will penetrate 26.6 µm in steels or 122.4 µm in SiC. The thickness of the affected layer of the sample therefore suggests that the size of the specimen will probably not need to exceed 10 mm. This reasoning leads to the establishment of a suitable compromise regarding test sample sizes, and this compromise lies at the basis of the choices of techniques and equipments considered in the framework of *TechnoFusión*`s Characterization Techniques Facility for the study of the mechanical behaviour of irradiated material and its behaviour during irradiation.

The main structural materials currently under consideration for fusion systems are the following: reduced activation ferritic/martensitic steels (9%CrWVTa), reduced activation ODS-steels, nano-structured ODS ferritic steels and vanadium and tungsten alloys. On the other hand, there is a small group of non-metallic materials that could be applied for certain components instead of structural steels, and that likewise need to comply with certain mechanical requirements. These are ceramic materials with a SiC matrix, specifically those called 2D or 3D SiC_f/SiC. In view of the intrinsic properties of ceramics, these materials have poor fracture toughness but improved high temperature creep properties with respect to steels, since their greater stiffness reduces their susceptibility to catastrophic failure. For historical reasons, the protocols for mechanical performance tests of ceramic materials are less developed than similar tests for steels. As with steels, the geometry and size of test specimens in the *TechnoFusión* facility will be determined by the depth of the irradiation damage.

Therefore, the mechanical test facility for the study of structural materials and device components for fusion reactors should include the equipment described below.

8.4.2.1. Mini machines for mechanical tests

As shown in Figure 8.3, these machines allow performing tests on specimens with a size of a few microns. Due to their reduced size they can be moved easily so that they can be aligned with the ion beams, while their installation and shielding is relatively simple.

Furthermore, they can be coupled to an optical or electron microscope in order to study in-situ deformation mechanisms.

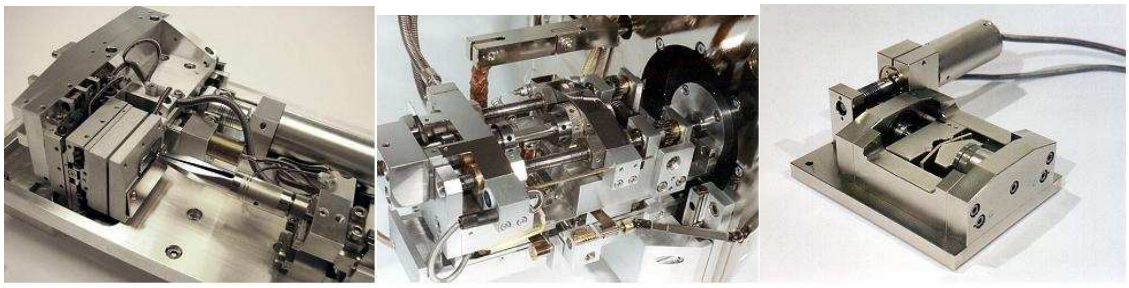

Figure 8.3. Mini-testing machines: (left) experimental module for tensile microtests, (centre) tensile/compression tests, and (right) deformation tests.

8.4.2.2. Environmental chambers for the simulation of operating conditions

These devices allow determining the mechanical properties of structural materials under conditions similar to operational conditions. They allow establishing the environmental temperature in a wide range, from 77 to 1600 K, under different environmental conditions (vacuum, inert atmosphere, controlled humidity, etc.). The following chambers are considered necessary in this respect:

- A cryogenic chamber to evaluate mechanical properties between 77 and 300 K.
- An environmental chamber, specially suited for temperatures ranging from room temperature up to 500 K, and providing controlled humidity.
- High-temperature furnaces. Heating systems designed for testing materials under stress, covering a wide temperature range, up to 1600-1800 K, in an oxidizing atmosphere. The furnaces are suitable for performing tension, compression, bending, and cycling fatigue tests of materials, ranging from metals to composites and ceramics (Figure 8.4). Probably, it will be necessary to acquire two or more furnaces of this kind, in order to accommodate different test types and specimen geometries.
- Furnaces with controlled atmospheres. These are complementary to the above-mentioned equipment, and consist of a chamber for high vacuum with a furnace. They allow studying the effect that atmosphere (vacuum, inert, etc.) has on the mechanical properties at high temperatures (Figure 8.5).

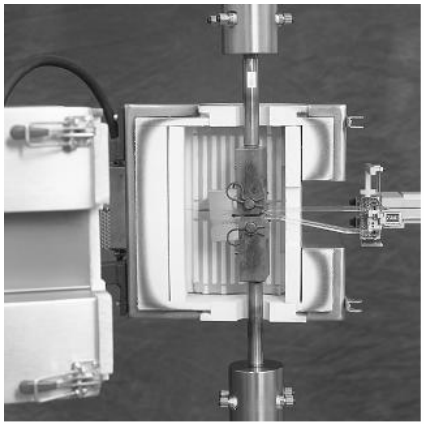

Figure 8.4. Detail of a high-temperature environmental furnace.

Figure 8.5. A high temperature furnace under a controlled atmosphere for mechanical testing.

Additional equipment: the mechanical characterization of samples requires multiple additional accessories, such as grips, compression plates, extensometers, alignment fixtures and calibration systems, force transducers, software, various load cells, etc. Inside the environmental chambers, refrigeration systems and high temperature extensometers should be also installed.

8.4.2.3. Automated ball indentation and stress-strain microprobe system

The *Stress-Strain Microprobe* (SSM) was developed and patented by Advanced Technology Corporation[87] to test small samples and determine key mechanical and fracture properties of metallic structural materials such as ferritic steels, stainless steels, aluminium, electronic solders, etc, including welds and heat-affected zones[88]

The SSM system (Figure 8.6) is based on the *Automated Ball Indentation* technique (ABI)[89], and involves multiple strain-controlled indentations at a single penetration location on a polished metal surface produced by a small spherical indenter (Figure2). The applied indentation loads and the associated penetration depths are measured during the test, and are used to calculate both the incremental stress-strain values from a combination of elastic and plastic analyses[90], and semi-empirical relationships which govern material behaviour under multiaxial indentation loading. By analyzing the flow curve, tensile deformation parameters of the material, such as its yield strength, tensile strength, strength coefficient, and strain hardening exponent, as well as fracture resistance, parameters like K_{JC} and the indentation energy required for fracture can be evaluated.

The correlation between the indentation hardness during indentation tests and the indentation strain associated with a spherical indenter, and the true uniaxial flow stress and flow strain is based on three premises:

I. The monotonic true stress-true plastic strain curves obtained from uniaxial tension and compression tests are reasonably similar.

II. The indentation strain correlates with the true plastic strain in a uniaxial tensile test.

III. The mean ball indentation pressure correlates with true plastic strain in a uniaxial tensile test.

The ABI technique of loading followed by partial unloading during indentation allows the proper evaluation of the indentation depth (h_p) associated with plastic deformation of the material.

For this, a tension-deformation microprobe, with testing bench (SSM-B4000 – 17.80 kN/4000 lb) and a movable system (SSM-M1000 - 4.45 KN / 1000 lb) is proposed, atCT *TechnoFusión* Facility.

---

[87] F.M. Haggag. Field Indentation Microprobe for Structural Integrity Evaluation, US. Patent Nº 4.852.397. 1 August 1989.

[88] K.L. Murty, P.Q. Miraglia, M.D. Mathew, V.N. Shah, F.M. Haggag. Characterization of gradients in mechanical properties of SA-533B steel welds using ball indentation. Int. J. Pressure Vessels Pipping 76 (1999), 361.

[89] F.M. Haggag. *In Situ* Measurements of Mechanical Properties Using Novel Automated Ball Indentation System, Small Specimen Test technique to Nuclear Pressure Vessel Thermal Annealing and Plant Life Extension, eds. W.R. Corwin, F.M. Haggag, W.L. Server. ASTM STP, ASTM, Philadelphia, PA, 1993, 27.

[90] C.H. Mok. The dependence of yield stress on strain rate as determined from ball-indentation tests. Exp. Mechanics 87, 1966, 87.

Figure 8.6. Photograph of an SSM system.

8.4.2.4. Indentation methods: Nanoindentation

(a) Introduction

Recently, mechanical testing methods have been developed to characterize small volumes, interfaces, or individual grains in polycrystalline materials (metal alloys, composites, etc). *TechnoFusión* is interested in the characterization of materials and devices involved in different parts of the fusion reactor. Therefore, the testing techniques must be oriented towards the prediction of the mechanical behaviour of interfaces and thin films (the mechanical response of joints in prototypes, different phases in composites, coating layers, etc), and in particular towards the establishment of the mechanical parameters of the small samples of material irradiated at the Facility.

Nanoindentation techniques are based on materials testing by means of the penetration of an indenter on a very small scale, the displacement being of the order of nanometres. Conventional hardness tests (Brinell, Rockwel, Vickers, etc.) use tens or even thousands of Newton force loads that generate traces with diameters of several millimetres and displacements of tenths of millimetres. In a nanoindentation test, loads used are often of the order of 0.1 N, generating displacements larger than a few hundred nanometers, while the resulting indentation will be only of a few tens of microns in diameter.

Formerly, nanoindentation was called *instrumented indentation* and *monitoring indentation*. In fact, the most characteristic feature of nanoindentation is not the small load and displacement of the material, but the precision required for the control and measurement

of these parameters, which is of the order of tenths of µN and nm, respectively. This technique is considered the only method suitable for the study of mechanical properties at the nanoscale.

The applied load and displacement data are recorded simultaneously and continuously during the experiment. The data obtained in the experiment allow obtaining much more information than merely the hardness at maximum load. Several theoretical models exist, each making different assumptions concerning the behaviour of the material, and offering the possibility to obtain more detailed information, such as the elasticity modulus of multilayer materials, the adhesion between layers, fracture analysis or the onset of creep due to the continuous application of small loads.

The nanoindentation technique is based on solid theoretical principles, and methods for developing numerous applications are available, as well as specialised machinery of great versatility and reliability, and international regulations for the standardisation of procedures to favour the reproducibility of results. However, since this is a technique that operates with small loads, it is sensitive to noise and prone to large errors. Many factors may affect the data, such as the environmental conditions, the thermal drift, the initial penetration depth, the indenter geometry, stacking (pile-up) or sink-in phenomena, and residual stresses.

A classic nanoindentation test involves the application of an increasing load, maintaining the maximum load for a period of time, and the subsequent withdrawal of the indenter, as depicted in Figure 8.7. The recorded variables are the applied load, the indenter displacement and the time.

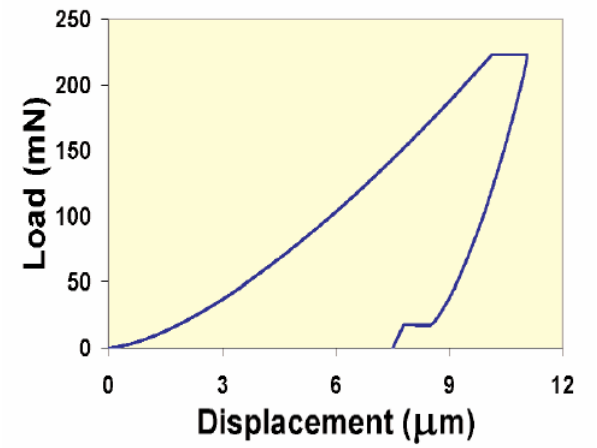

Figure 8.7. Typical load/deformation curve obtained from nanoindentation.

Several models are available to analyze the recorded data during the loading, steady load application, and unloading cycles. Each of these may have its use, depending on the type of material and the various starting hypotheses regarding the behaviour of the material during the test. Most of the existing models can be subdivided into four broad groups:

1) Models that analyse the unloading curve by considering it to be a fully elastic process. These models are among the most used and successful ones, and are especially suited for the study of hard materials, such as steel.

2) Models assuming some degree of plasticity of the material during and after the indentation. These models are more suitable for modelling the phenomena of pile-up and sink-in. Their use is recommended for the study of soft materials.

3) Dynamical models, in which a sinusoidal perturbation is added to the applied load, thus allowing the calculation of the elasticity modulus in "real time". These models allow the study of the variation of this property with depth (which is particularly useful for the analysis of surface layers or composite materials having different layers). They are usually simple variations of static models.

4) Models designed for the implementation of nanoindentation in new fields (the study of friction, the adhesion of coatings, fatigue, creep, etc.).

The first group includes the most widely used model, known as the "Oliver and Pharr" model[91], which will be described in Annex II. Other interesting models are: the Loubet model[92], useful for soft materials and polymers; the Field and Swain model[93], which includes plastic behaviour; the King model[94], suitable for coatings and thin films; and the Mata and Alcalá model[95], specially suited for the calculation of friction coefficients.

(b) Standardization in nanoindentation: UNE-EN ISO 14577

Only recently, protocols have been established to guarantee the reliability and reproducibility of results in this field. The first official standard is the ISO 14577, established in 2002, and published in May 2005 in the Official Gazette of the relevant UNE-EN ISO 14577:2005[96], *Metallic materials. Monitored penetration test to determine the hardness and other material parameters.*

This norm is divided into three parts:

- UNE-EN ISO 14577-1: The testing method
- UNE-EN ISO 14577-2: The verification and calibration of testing machines

[91] OLIVER, W. C; PHARR, G. M. (1992): "An improved technique for determining hardness and elastic modulus using load and displacement sensing indentation measurements". Journal of Materials Research Vol.7, No.6, pp 1564-1583.
[92] LOUBET, J. L; GEORGES, J. M; MEILLE, G. (1986): "Vickers indentation curves of elasto-plastic materials". ASTM STP 889, Microindentation Techniques in Materials Science and Engineering, P. J. Blau and B. R. Lawn, eds., ASTM International, West Conshohoken, PA, pp. 72-89.
[93] BELL, T. J. et al. (1992): "The determination of surface plastic and elastic properties by ultra micro-indentation". Metrología, Vol. 28, No. 6, pp. 463-469.
[94] KING, A. H.; FROST, H. J.; YOO, M. H. (1991). Scripta Metall. Mater., 1991, 25, 1249.
[95] MATA, M; ALCALÁ, J. (2004): "The role of friction on sharp indentation", Journal of the Mechanics and Physics of Solids Vol. 52, Issue 1,
[96] UNE-EN ISO 14577:2005 (Partes 1, 2 y 3), Materiales metálicos. Ensayo de penetración monitorizado para la determinación de la dureza y otros parámetros de los materiales.

- UNE-EN ISO 14577-3: The calibration of reference blocks

UNE-EN ISO 14577-1 defines the limit between micro and nanoindentation for penetration depths less than 0.2 microns. Annex A contains the equations required for the calculation of the hardness and elasticity modulus. Annex F gives the equivalence between nanoindentation (H_{IT}) and the Berkovich and Vickers hardness factors.

UNE-EN ISO 14577-2 emphasizes the necessity of establishing stable test conditions with regard to vibration and temperature. It also defines the types of indenters that are most commonly used, how these should be calibrated, and how often this should be done (more often than once a year when using indirect checking, i.e., when using a material standard and the machine program). It is recommended to perform two indentations on a known standard material every measuring day. Annex B treats the calibration of the tip indenter, and again mentions the possibility of employing the indirect method.

UNE-EN ISO 14577-3 is considered to be of less interest to the end user if he buys calibrated reference blocks (standard materials). Even so, it is interesting to note that this rule recommends performing 15 indentations on the standard material for calibration, and considers such a calibration to be valid for a maximum period of 5 years.

(c) Correlations

The nanoindentation technique is the only technique available to determine the elastic and plastic properties of small volumes of test material. Also, is the appropriate technique when studying the contributions of each of the different phases of a composite material to the mechanical behaviour, or when studying the properties of protective coatings. These three cases are all relevant for the work to be carried out at the *TechnoFusión* facilities.

The extrapolation of results to the macroscopic scale is the main problem of nanoindentation. The amount of defects present in microscopic volumes is insignificant, and therefore the deformation of a small sample will be less than that of a large sample. In general, the data regarding hardness and mechanical strength obtained by nanoindentation will overestimate the realistic values.

Further work is necessary to establish corrections that allow producing reliable data based on this technique. However, published papers on this issue are as yet scarce and restricted to conventional materials[97]. Therefore, the application of this technique requires further work regarding the modelling and simulation of mechanical properties in order to establish the correlations that will allow projecting the results to a realistic scenario.

[97] L. C. Onyebueke. “the impact of modelling, simulation and characterization of the mechanical properties and nanomaterials in the nanotechnology industry” Presented at 2nd US- Korea Nano Forum, LA, USA February 17-19, 2005.

(d) Nanoindentation machines

Nanoindentation machines: Most of nanoindentation equipment can be represented by the diagram of Figure 8.8. Usually, the load is varied, while the indenter displacement (nearly always in the vertical direction) is measured by means of a sensor[98].

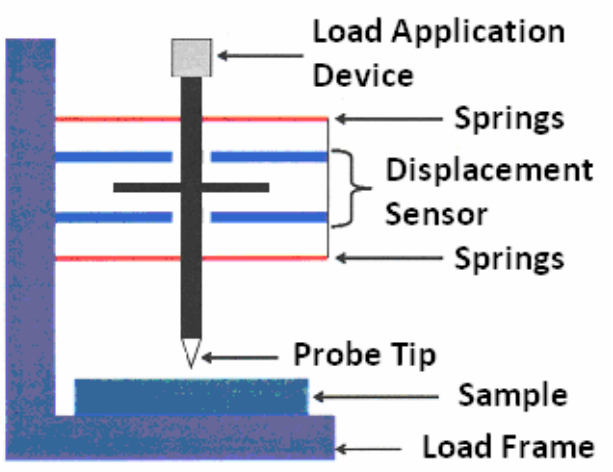

Figure 8.8. Schematic representation of a nanoindentation machine.

To apply the load, one of the following three methods is usually applied:

I. An electromagnetic actuator: A widely used method involves a wire coil inside a permanent magnet. The electrical current is adjusted to control the magnetic field (Figure 8.9). Since system size is rather large, a considerable amount of heat can be generated, leading to thermal drift.

II. An electrostatic actuator: It makes use of a transducer of three plates to generate an electric field between the central plate and one of the others. This system presents no problems regarding size or the generation of heat, but its load and displacement ranges are limited.

III. Actuators through springs: A force is applied indirectly to the indenter via one or more springs (Figure 8.10). The actuator may be one of several types. Designs such as this are used in *Atomic Force Microscopes* (AFMs), which incorporate a piezoelectric displacement actuator attached to a bracket holding the cantilever indenter.

[98] T.L. Anderson. Fracture Mechanics. CRC Press, Boca Raton, FL, USA, (1995),41.

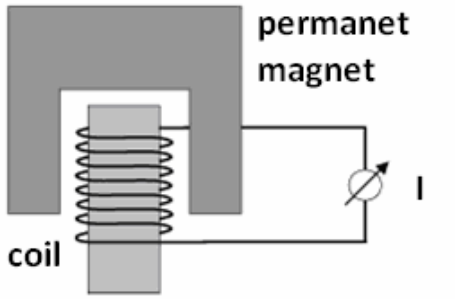

Figure 8.9. Sketch of an electromagnetic actuator.

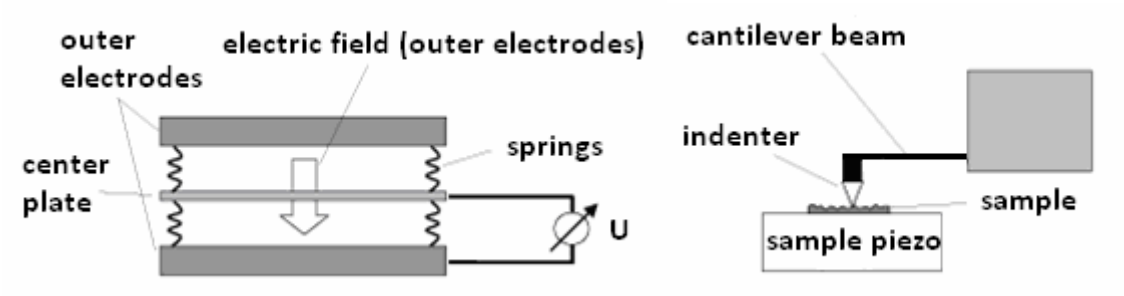

Figure 8.10. Different load actuators: electrostatic (left) and "cantilever beam" (right).

There are also three solutions for measuring the indenter displacement:

I. A capacitive sensor: Basically, it consists of a parallel plate capacitor working at a fixed voltage, so any variations of the current can only be due to a variation of the gap between planar capacitors. These sensors have an excellent resolution (better than 1 Å), and so this solution is adopted almost universally.

II. Laser measurement: This is commonly used in AFMs; here, a laser beam is directed towards the cantilever and the beam deflection is measured by a photodiode. This method also has an excellent resolution.

III. Transducer measurement: If the application of a load is controlled by a voltage operated transducer, then the displacement of the central plate with respect to the other two is measured by means of the capacity difference.

In this respect, two commercial devices are relevant:

1) NANO Indenter®, by TMS

Developed by MTS[99], applies load by means of electromagnetic fields, the indenter being held by springs while the displacement is measured by a capacitive sensor (Figure 8.11).

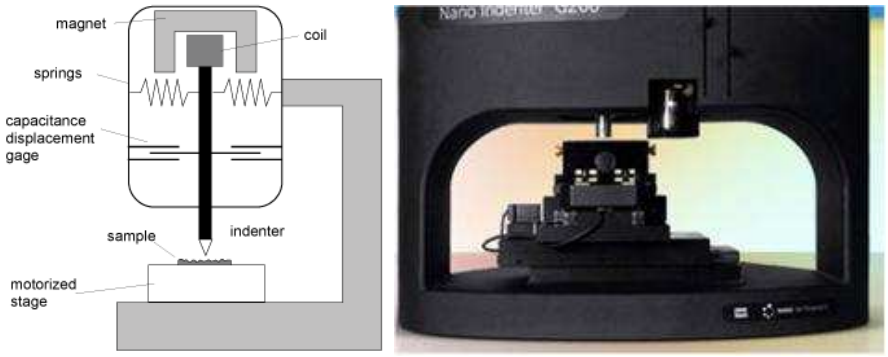

Figure 8.11. Schematic representation (left) and photo (right) of the MTS NANO Indenter®.

2) *TriboScope®, by Hysitron*

The TriboScope® by Hysitron[100], consists of two perpendicularly arranged transducers, one for measuring the lateral force and the other for scratching the surface (Figure 8.12). Transducers are responsible for both the application of the load and the measurement of the displacement.

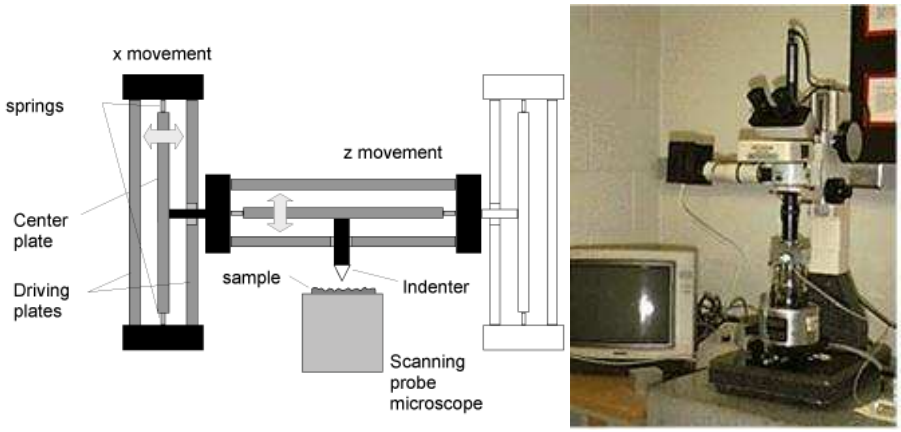

Figure 8.12. Schematic representation (left) and photo (right) of the Hysitron TriboScope®.

[99] www.mtsnano.com
[100] www.hysitron.com

(e) Nanoindenter accessories

- *Lateral Force Measurement (LFM)*: this is an effective tool for characterizing the scratch resistance of bulk materials and coatings, adhesion and mode of failure of thin films. By monitoring the lateral force of the scratch tip along with the normal force, the friction coefficient can be determined.

- *High Load option*: Extends operation of the XP up to 1 kg for vertical loads.

- *Continuous Stiffness option*: Here, a harmonic oscillation is applied on top of the quasi-static motion, allowing the continuous monitoring of stiffness. Force amplitudes range between 60 nN and 300 mN. The frequency range is 0.05 to 200 Hz.

- *TestWorks 4 Explorer Level software*: Controls all components and records and analyzes the data. Operates under the Microsoft NT operating system. Allows full programming of the test protocol. Data output can be exported to Excel files.

- *Nano CDA: The Continuous Dynamic Analysis* (CDA) allows the evaluation of mechanical properties in a wide range of frequencies. The CDA instrumentation subjects the specimen to a constant quasi-static stress. The CDA extension utilizes a technique whereby a nanomechanical actuating transducer (NMAT) applies an oscillatory force that is superimposed on the static force. The amplitude of the oscillation is measured by a capacitive sensor that is an integral part of the NMAT. As a result, the CDA technique can be used to impose oscillatory forces at a higher frequency than what could be achieved by imposing the oscillation via the crosshead. The CDA technique also has the advantage of allowing measurement of the high frequency oscillatory response of the specimen.

- *Nano Vision:* By incorporating the quantitative image analysis provided by the nanovision system, the fracture toughness can be determined accurately in thin films and small material volumes, without the need of using atomic force or microscopic techniques after indentation. It allows control of the indentation head assembly in scanning mode. The experimental procedure specifies the penetration depth, the scan length and the number of indentation-scan cycles to perform. The system operates automatically with the aid of a high precision retrofeeder that allows the exact indenter location to be set time and again.

The experimental procedure is based in a method that allows defining the indentation depth, the length scan as well as the number of indentation-scan cycles that are necessary to carry out. The system makes cycles automatically and the high feedback accuracy allows the exact location of the indentator in order to be well located indentation by indentation.

In order to perform tests fracture toughness and fatigue the most suitable option is the G200 MTS NanoIndenter with the CSM module, the NanoVision system and possibly the module of heavy load.

(f) Special requirements for the TechnoFusión facility

- *Temperature mechanical tests*: Realistic tests of fusion materials require applying high temperatures. This is not easy to do. State-of-the-art nanoindentation is limited to 400º C, and this temperature is too low for materials such as tungsten, whose operating temperature is estimated to be 1200º C. At the moment, the only available system to perform such tests is ONERA, which allows microindentation up to 1000º C, although the company is committed to reach 1200º C in the short term[101, 102].

- *"In-beam" mechanical tests.* The in-beam mechanical testing (real time mechanical behaviour under irradiation) of materials is another interesting possibility. In this case, the configuration of the equipment should be modified, in the sense that the indenter, located close to the radiation incidence region, should be separated from the equipment electronics. Conventional electronic devices are extremely sensitive to radiation and can become useless even at low doses (a few Gy). Therefore, the whole system and the controlling computer must be shielded against the radiation. Currently, no commercial equipment with these properties is available, but it is possible to manufacture it according to a specific design.

8.4.2.5. Research groups and associated bibliography

Below, there is a brief summary of national and international research centres and groups specialized in the study of material mechanical behaviour for nuclear applications. Spanish institutions have been identified as relevant facilities dedicated to the mechanical testing of structural materials. Among the national institutions, only the CIEMAT has a proven trajectory in the field of nuclear materials. Internationally, the review carried out has focused on providing a list of those with experience in the field of development of materials with higher resistance in an aggressive radiation environment. The laboratories listed here have instrumented for testing a wide range of mechanical properties and their experience has been directed through the study of the effect of radiation on mechanical properties:

CIEMAT Madrid, Spain: The Structural Materials Group is characterized by supporting management and life extension of nuclear plants by understanding the behaviour of materials and their aging processes. In the past ten years and in collaboration with the CIEMAT Fusion Material Group there has been an increasing effort in the qualification under irradiation of fusion reactor components and metallurgical characterization of martensitic ferritic low-activation steels. The Facility includes hot cells for the controlled manipulation of irradiated material.

[101] P. Kanoute, F. H. Leroy, B. Passilly « Mechanical Characterization of thermal barrier coatings using a microindentation instrumented technique » Key Engineering Materials Vols. 345-345 (2007) pp 829-832.
[102] B. Passilly, P. Kanoute, F.H. Leroy, R. Mévrel. "high temperature instrumented microindentation: applications to thermal barrier coating constituent Materials" Philosophical Magazine. Vol. 86 Nos. 33-35, 2006 5739-5752.

ETSI de Caminos, Canales y Puertos, Madrid, Spain: research activities of the Materials Science Department aims to characterize the mechanical properties of structural materials and their relationship with the microstructure and with the application of materials in structural elements. The Department has several facilities offering a wide range of experimental techniques to determine the behaviour of materials under various types of loading (monotonic or cyclic, uniaxial or multiaxial) and environmental conditions (temperature, humidity, etc.).That can characterize the mechanic behaviour of all kinds of materials (ceramics, composites, biomaterials, biological samples, concrete, rocks, metals, polymers, etc..) subject to mechanical, thermal and environmental variations.

Mechanical Characterization and Analysis User Centre, ORNL, Tennessee, USA: This Centre is specialized in the mechanical characterization of structural materials, including high temperature materials, analysis and mechanical testing, developing test methods and analytical techniques and conducting additional stress analysis by finite elements. Its experience also includes the prediction of lifetime of monolithic materials, composites and ceramic tiles. These feature installations have a large number of machines for conventional tests (tension, understanding, bending, fatigue, toughness, etc..) and there are in controlled environments and high temperatures.

Forschungszentrum Karlsruhe, Karlsruhe, Germany: Centre founded with the aim of investigate the behaviour of fusion materials. A few years ago, the Institute of Material Research I developed the *in situ* fatigue tests system in the line of junction of two accelerators. The experience is still of great value in the development of a similar system that will allow materials in IFMIF test: the test machine *in situ* of creep-fatigue.

National Institute for Materials Science (NIMS), Tsukuba, Japan: This Institution includes the Cyclotron Materials Irradiation Facility, operating since 1987, that has been fundamental and intensively used to study the effect of radiation on nuclear materials of interest. Of great interest, in this installation, is the ability to perform *in situ* experiments, having a laboratory with the most updated equipment for testing the mechanical behaviour of irradiated material by means of tension, creep and fatigue, and especially for evaluation hardening of metals by inclusions of He[103]: The Materials Reliability group has developed the appropriate instrumentation associated with the cyclotron to perform in-beam creep tests and fatigue under the influence of high energy ions (mainly protons).

8.4.3. Techniques for composition analysis

When studying the impact of radiation damage on materials subjected to a fusion environment, the analysis of the material composition is essential. At the very least, a comparison between the chemical composition before and after material modification is necessary. But from point of view of the future application of the materials, it is essential to obtain an accurate knowledge of the elements constituting the material matrix and the distribution of surface impurities and their depth profile. In this sense, classical analytical techniques are insufficient, since the detection limit of light elements (H, He, Li, C, etc.) is

[103] http://www.nims.go.jp/mrc/index_e.htm.

particularly high. Therefore, use must be made of high mass resolution techniques in order to distinguish between the distribution profiles of hydrogen isotopes (^{1}H/^{2}D, ^{1}H/^{3}T) when characterizing materials for fusion applications. The techniques selected here share the following properties: they are sensitive to low concentration levels of impurities inside high Z material matrices and able to distinguish between isotope masses as a function of depth. Other material characterization techniques mentioned in literature[104] are not considered for application at the *TechnoFusión* Characterization Techniques Facility, because either their efficiency is not adequately demonstrated, or further instrumental development is required. The latter may be considered for a posterior phase of the development of the facility.

8.4.3.1. Secondary ion mass spectrometry

(I) Introduction

The *Secondary Ion Mass Spectrometry* (SIMS)[105] is a powerful technique for material characterization, based on the sputtering of a solid sample surface by primary ion bombardment. Primary ions hitting the sample surface trigger a cascade of atomic collisions. Ejected single atoms and clusters are spontaneously ionized, and separated according to their mass/charge ratio by means of a magnetic field. The detected secondary ions are characteristic of the microscopic composition of the analyzed area. Simultaneously, the distribution of elements and the depth profiles of the material matrix, its dopants, and its impurities can be obtained, as the measurements provide both spatial and quantitative information.

A typical SIMS measurement setup has a number of advantages over other analytical techniques: *sensitivity*, i.e., it can detect all elements and isotopes, many of them at concentration levels as low as a few parts per million, with a signal-to-noise ratio of up to 10^6 (almost no background); a *lateral resolution* of 20-50 nm, together with a typical depth resolution of 1-10 nm; and simple specimen preparation, so that bulk materials can be studied when polished with standard metallographic procedures. The most relevant advantage for fusion applications is the ability to separate isotopes, in particular hydrogen isotopes.

The primary limitation of the SIMS method is associated with the quantification of the secondary ion signal. This is due to the variation of the secondary particle sputtering yield and the ion fraction as a function of the matrix structure and composition, and the emission of neutral species. To obtain quantitative results, it is necessary to compare the results to standard levels of elements in similar matrices. In addition, the detection of light elements using SIMS is affected by the ionization of residual gas contaminants in the sample chamber. To achieve the maximum detection sensitivity, the vacuum in the analysis chamber should be particularly good. The bibliography on SIMS analysis of light elements[106] concludes generally that the background intensity can be reduced by suppressing the signal due to the memory

[104] www.phys.unt.edu/ibmal/

[105] A.Benninghoven, F.G.Rüdenauer and H.W.Werner, Secondary Ion Mass Spectrometry: Basic Concepts, Instrumental Aspects, applications and trends, Wiley, New York, 1987. 1227 pages.

[106] H.Yamazaki, Improved secondary ion mass spectroscopy detection limits of hydrogen, carbon, and oxygen in silicon by suppression of residual gas ions using energy and ejection angle filtering. J. Vac. Sci. Technol. A15 (5), 1997, 2542-2547.

effects (i.e., due to redeposition of the residual gas on the immersion lens in the analyzed area) and by increasing the primary ion current to suppress the signal due to residual gas adsorbed onto the sample surface. Another method to achieve lower detection limits for light elements is to select the energy of the secondary ions. This technique was successfully tested in silicon wafers using a magnetic-sector type instrument[107].

For most trace elements, SIMS detection limits lie between 10^{12} and 10^{16} atoms/cc. Apart from ionization efficiencies (RSF's), two factors can limit sensitivity. The count rate can limit sensitivity when sputtering produces less secondary ion signal than the detector dark current. If the SIMS instrument itself contains the element to be analyzed, then sensitivity to this element is limited. Oxygen, always present as a residual gas in vacuum systems, is an example of an element presenting such background limited sensitivity. Atoms sputtered from mass spectrometer parts back onto the sample by secondary ions constitute another source of background. Mass interferences also cause background-limited sensitivity.

SIMS devices can be fitted with a normal incidence electron gun to study insulating materials. When sputtering the material, the surface emits charged atoms or groups of atoms, so that the surface has a deficit of negative charge. This fact limits the study of non-conductive materials. By providing electrons (with energies between 10 eV and 10 keV), the surface charge of the sample can be compensated easily and effectively, allowing to perform reproducible composition analyses, even of complex multilayer materials.

(II) Operation modes

(a) Static and dynamic modes

Two SIMS modes of operation are possible: static SIMS and dynamic SIMS. The static SIMS spectrum, obtained by sample bombardment under a primary ion dose of 10^{12} ions/cm^2, provides information on the composition in terms of elements, molecules, and isotopes of the first monolayer. It performs a molecular characterization of surfaces, providing imaging down to a depth of 1 µm. Above 10^{12} ions/cm^2, the incident ions start affecting the surface, modifying it physically and chemically: The resulting dynamic SIMS spectrum contains information on the distribution of elements and isotopes to a greater depth than the former method, and provides a greater ease of operation. Dynamic analyses are better performed with magnetic sector analyzers.

The importance of choosing the operating mode of the analyzer and thus under the specific application of *TechnoFusión* deserves an analysis of the kind of equipment separately. This analysis is set out later in the section entitled "Comparative SIMS / ToF-SIMS.

(b) Mass spectroscopy:

Mass spectra are obtained by continuously monitoring the secondary ions while scanning the mass-to-charge (m/z) ratio in a pre-selected range. The mass analyzer can be

[107] C. Poleunis, A. Delcorte and P. Bertrand, Applied Surface Science, 252 (19) 7258-7261, 2006.

either a magnetic sector or a quadrupole. The mass spectrum is due to both atomic and molecular ions. Secondary ions containing more than one atom are called molecular ions with SIMS. Ten mass increments per peak width are sufficient to adequately define the peak shape. Thus, a mass spectrum with a mass range of 100 must contain at least 1000 data channels, with an analysis time of 0.1 s per channel. The Figure 8.13 shows a compressed mass spectrum for a coal fly ash particle. The ion intensities reflect the isotopic abundances of the elements. Here, the silicon isotope intensities at m/z 28, 29, and 30 match the relative natural silicon abundances 92.2 : 4.7 : 3.1.

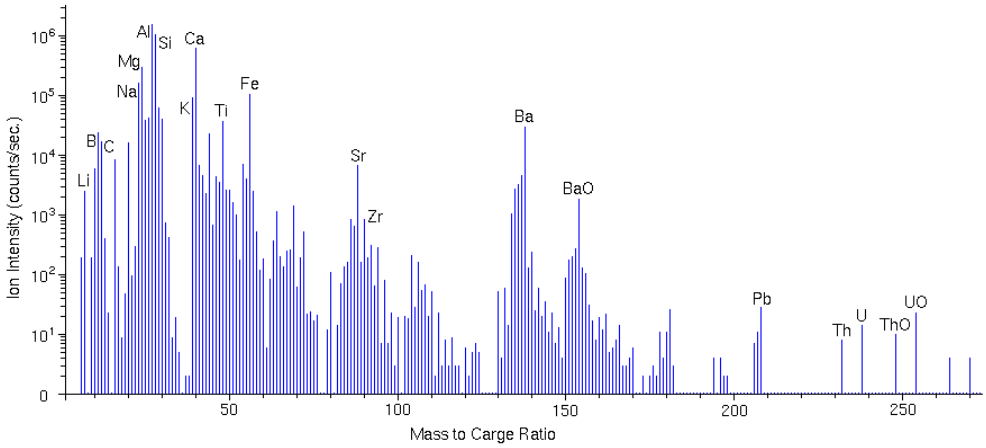

Figure 8.13. SIMS mass spectrum obtained from a carbon combustion ash particle.

(c) Surface analysis. Analysis of elements and molecules

Most of the signal is due to the top 2-3 atomic layers. The depth distribution can be recorded in nanometre steps, down to several tens of microns. Only the static SIMS analysis allows obtaining qualitative molecular information or images from the top monolayer. Analysis of elements from the whole periodic table is possible, from light to very heavy elements, with a typical detection limit of the order of ppm-ppbs.

(d) Bulk analysis

High sputtering rates increase the secondary ion signal for bulk analysis. In this mode of analysis, ion intensity data are displayed as a function of time. The fastest possible sputtering requires intense primary ion beams, sacrificing depth resolution, due to the impossibility to focus the beam on flat bottom (rastered) craters. This technique provides a means for checking that the sample is homogenous. For samples with a homogeneous composition, the bulk analysis offers better detection limits than depth profiling, usually by more than an order of magnitude. In a typical heterogeneous sample, the target elements are concentrated in small inclusions that produce spikes in the data stream.

(e) Quantitative analysis

Quantitative analyses require comparing the results to some pre-established standards. Generally, these are artificial materials with implanted elements with a concentration and a background matrix similar to the sample to be studied. Direct partial quantification is often possible by analyzing the signal due to MCs^+ or MCs_2^+ clusters.

(d) Isotopic studies. Isotopic ratio

Isotope ratio measurements[108] are operationally similar to depth profile measurements, except that the requirements for precision and accuracy are higher. Since all of the isotopes of an element have the same chemical properties, the ionization and detection efficiencies are nearly identical for the different isotopes. A precision of 0.1% is commonplace and accuracies are of the same level. Error analyses indicate that the precision is mainly limited by Poisson counting statistics. To achieve such accuracies, the SIMS instruments must be carefully tuned, and interferences must be eliminated. Peaks in the mass spectrum should have flat tops and steep sides so that a slight instability of the magnet does not affect the ion signal intensity. Figure 8.14 shows the required flat top peaks and the high mass resolution used to eliminate interference of the O_2 signal at m/z = 32. Both were necessary for accurately measuring 34S/32S isotope ratios. The isotope ratios must be corrected for slight variations in the detection efficiency at different masses, and for slight variations that depend on the signal intensity. These corrections are usually larger than the range of expected isotope ratios.

(g) Depth profiling

Monitoring the secondary ion count rate of selected elements as a function of time leads to depth profiles. To convert the time axis into depth, the SIMS analyst uses a profilometre to measure the depth of the sputter crater. A profilometre is a separate instrument that determines depth by dragging a stylus across the crater and recording vertical deflections. The total crater depth divided by the total sputter time provides the average sputter rate. Relative sensitivity factors serve to convert the vertical axis from ion counts to concentrations.

Depth resolution measurements require having flat bottom craters. Modern instruments provide uniform sputtering currents by sweeping a finely focused primary beam in a raster pattern over a square area. The maximum depth resolution of a depth profile is obtained when the secondary ions are emitted from the flat bottom of such a crater without any contributions from the crater edges. In some instruments, aperture limiters are used to select secondary ions from the crater bottoms, but not the edges. Alternatively, the data processing system can be instructed to ignore all secondary ions produced when the primary sputter beam is at the ends of its raster pattern sweeps.

[108] Betti, M., Isotope ratio measurements by secondary ion mass spectrometry (SIMS) and glow discharge mass spectrometry (GDMS International Journal of Mass Spectrometry 242 (2-3), pp. 169-182, 2005.

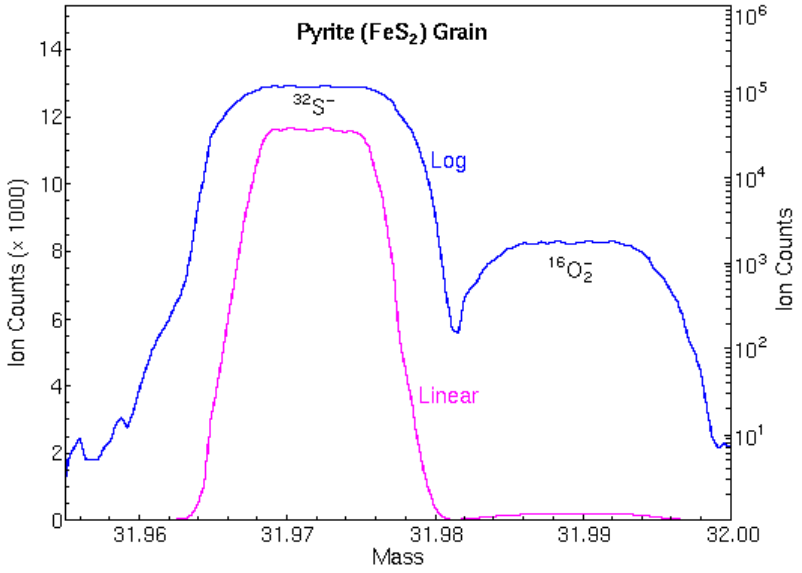

Figure 8.14. Ideal shape of spectral SIMS peaks for the optimum determination and isotope separation

(h) 2D/3D imaging.

Ion images provide a map of the secondary ion intensity on the sample surface. Image dimensions vary from 500 um down to less than 10 um. Ion images can be acquired in two operating modes, referred to as ion microscope or stigmatic imaging, and ion microbeam imaging or raster scanning. Ion microscopy requires a combined ion microscope/mass spectrometer capable of transmitting a selected mass ion beam from the sample to the detector without loss of information on the lateral position. Image detectors indicate the position of the arriving ions. Ion microscope images are usually round because the ion detectors are round. Lateral resolutions of 1 µm are possible. A SIMS analyst can choose to make images with a high lateral resolution at the expense of signal intensity, and with a high mass resolution at the expense of image field diameter. With ion microbeam imaging, a finely focused primary ion beam sweeps the sample in a raster pattern and software stores the secondary ion intensity as a function of beam position. Microbeam imaging uses standard electron multipliers and the image shape reflects the shape of the raster pattern, usually square. The lateral resolution depends on microbeam diameter and can be as small as 20 nm for liquid metal ion guns. Some instruments combine high mass resolution and high lateral resolution. However, the SIMS analyst must establish a trade-off between high sensitivity and high lateral resolution, because focusing the primary beam to smaller diameters also reduces beam intensity.

The example (microbeam) images (Figure 8.15) show a pyrite (FeS_2) grain from a sample of gold ore with gold located at the rims of the pyrite grains. The image on the right is 34S and the one on the left is 197Au. The numerical scales and the associated colours represent different ranges of secondary ion intensities per pixel.

Three-dimensional analyses are possible by acquiring images as a function of sputtering time (to generate image depth profiles). Microscope sputtering rates exceed microbeam rates,

often by several orders of magnitude. Thus microscope imaging produces depth scales that are more compatible with the scale of the lateral images. Microbeam imaging usually provides a better definition of image features, except when faster sputtering is required for three-dimensional analyses or for removing a top layer before image acquisition.

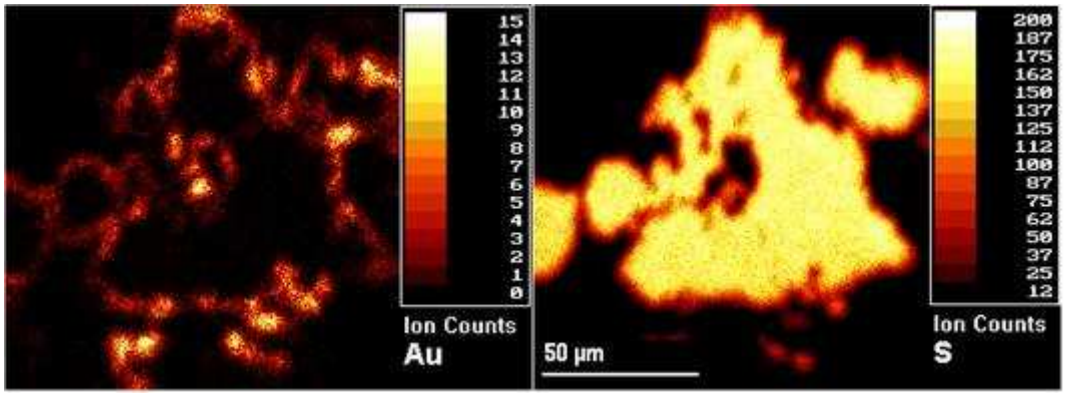

Figure 8.15. Secondary ion images. Left, gold signal obtained from an oxide located at grain boundaries. Right, sulfur data obtained from a pyrite (FeS_2) ore analysis.

(III) SIMS/ToF-SIMS comparison

In the field of surface analysis, it is common to distinguish between *static* SIMS and *dynamic* SIMS. Static SIMS is oriented towards atomic monolayer analysis on the surface, usually with a pulsed ion beam and a time-of-flight mass spectrometer, while dynamic SIMS is oriented towards bulk analysis, making use of the sputtering process and a DC primary ion beam and a magnetic sector or quadrupole mass spectrometer. The ideal dynamic SIMS analyzer needs a reactive primary species (O_2^+ or O^-) to enhance the ionization of electropositive elements (metals, alkalis, etc.) and Cs^+ to enhance the ionization of electronegative elements, and to facilitate their quantification using the MCs^+/MCs_2^+ cluster technique. The energy and angle of incidence of the primary ions is adjusted to optimize the depth resolution by controlling the atom mixing depth and the roughening effect induced by the sputtering process.

Time of Flight (ToF) analysers have a better mass resolution, but they have the disadvantage of a low duty cycle (pulsed mode), leading to a much lower sensitivity. Use of the magnetic sector analyzer is suggested for fusion SIMS applications, since the analysis of light elements and the requirement of accurate isotope separation (H, He, Li, C, etc.) call for a high mass resolution.

An insulating sample submitted to a positive ion bombardment will charge positively. A practical solution to the charge neutralization problem is to saturate the ion impact area with electrons (with energies between 10 eV and 10 keV), in order to restore the surface potential to its original value. SIMS equipment can be fitted with a normal-incidence electron gun for

easy and effective sample charge compensation. Thus, reproducible analyses can be performed in insulators, and even in complex multi-layer samples.

A high mass resolution SIMS device is essential for the *TechnoFusión* facility, due to the importance of distinguishing the profiles of hydrogen isotopes ($^1H/^2D$).

(IV) General description of basic SIMS equipment

(a) Primary Ion Sources

A typical SIMS instrument uses either a duoplasmatron or a surface ionization primary ion source (or both). The duoplasmatron can operate on virtually any gas, although oxygen is most commonly used, because oxygen implantation into the sample surface enhances the ionization efficiency of electropositive elements. The oxygen plasma within the duoplasmatron source contains both O^- and O_2^+, and either can be extracted. The Cesium surface ionization source produces Cs^+ ions and Cs atoms that vaporize through a porous tungsten plug.

(b) Primary Ion Column

Primary ions are extracted from the sources and transmitted to the sample through the primary ion column (Figure 8.16). The column usually contains a primary beam mass filter that only transmits ions with a specified mass-to-charge (m/z) ratio. This mass filter eliminates impurity species in the beam. For example, Cr, Fe, and Ni ions can be sputtered from the stainless steel surfaces within a duoplasmatron. Without a primary beam mass filter, these metal contaminants would deposit onto the sample surface, raising the detection limits for stainless steel constituents. The electronic lenses and apertures control the intensity and width of the primary ion beam. Usually, several aperture diameters are available at each aperture location. Electrostatic deflectors steer the primary beam in a raster pattern across the sample.

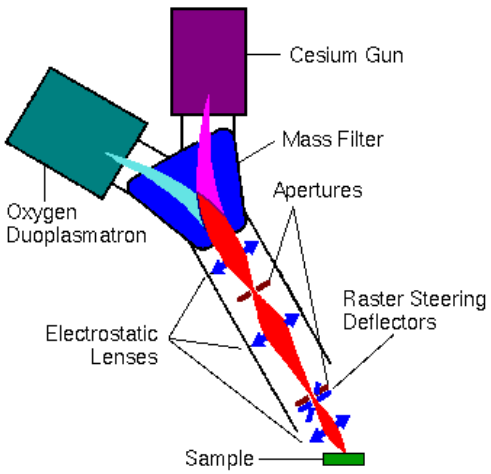

Figure 8.16. Sketch of primary ion column lenses and filters in conventional SIMS equipment.

(c) Secondary ion extraction and transfer

Secondary ions are extracted from the sample as they are produced. If large mass spectrometer components are kept at ground potential, the sample must be kept at a high voltage, the accelerating potential. The secondary ions then accelerate towards the ground plate of a set of electrostatic lenses. This first lens is called the immersion or ion extraction lens. The second (transfer lens) focuses the ion beam onto the mass spectrometer entrance slits or aperture. This double lens system constitutes an ion microscope. The secondary ions can be projected onto an image detector for visualizing the sample surface (Figure 8.17).

(d) Faraday cup

The secondary ion beam is automatically deflected, either towards the electron multiplier for pulse counting or towards the Faraday cup for very high intensity measurements. This combination provides a uniquely large dynamic range. The Faraday cup offers a large flexibility for the selection of a matrix signal, avoiding saturation even for high intensity signals.

Some of the most recommendable instrument accessories are listed below: Electron Gun: an electron injection system, mounted at an inclination on the side of the extraction optics, to dynamically equilibrate the positive charges induced by primary ion bombardment during the analysis of insulators. Eucentric rotating stage, enabling 360º rotation without losing the z position. Metallic samples develop preferential sputtering locations and enhanced roughness. Rotating the sample during the analysis has proven to be a successful technique to mitigate this problem, and it has been extensively used with Auger profiling.

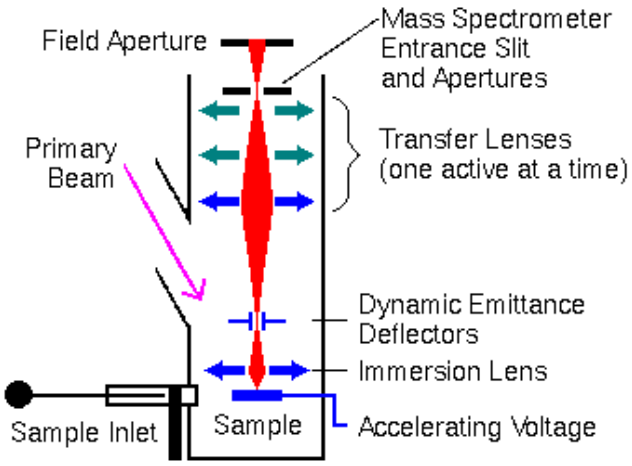

Figure 8.17. Sketch of primary ion column lenses and filters in conventional SIMS equipment.

(V) Commercial equipment options

1) IMS 7f, by Cameca

This analyser is based on a double-focus magnetic sector analyser, offering the enormous advantage of being able to work with secondary ion energies up to 10keV. A strong extraction field allows collecting nearly all the emitted particles and to transmit them through the analyser. Its mass resolution and its transmission efficiency exceed the corresponding characteristics of a quadrupole analyser by at least two orders of magnitude. Compared to other designs, its sensitivity is several orders of magnitude higher than that of a time-of-flight analyser, due to the low-pulse mode of the ToF. This factor increases with analysed depth. Profiles are obtained with a focused primary ion beam of less than 0.2 µm in diameter, able to raster an area of 500 x 500 μm^2 across the sample. Image acquisition requires a few seconds for majority elements and up to a few minutes for trace elements, using the microscope mode. The device includes a third generation electron gun to compensate positive charges generated during SIMS analysis on insulator surfaces. It is mounted at an angle to the side of the extraction optics, with the advantage of allowing normal incidence, making is easy to align ion and electron spots. This equipment is considered a sure choice for a long term investment, as it is sufficiently versatile for future analytical applications: it allows high mass resolution, high sensitivity, easy insulator analysis, high imaging resolution, detection of ultra low energies and a wide range of upgrades.

2) ToF.SIMS 5, by Ion-TOF:

Among the devices that are suitable for a wide range of applications, this equipment[109] is considered one of the best. The device is capable of providing detailed analytical information on elements or molecular constituents of material surfaces, thin films and interfaces. It can also perform 3D analyses. Different versions can handle different sample diameters, the 12" version being the one most appropriate for *TechnoFusión* due to the large sample diameter (up to 300 mm) that the chamber can handle. The basic instrument is equipped with a ToF analyzer that guarantees high secondary ion transmission at high mass resolution. It is also equipped with a 5-dimensional movement, quick admission sample stage (x, y, z translation, rotation and revolution). It includes a charge compensation system for analyses of isolating materials. The following accessories could be of interest for *TechnoFusión* applications: a heating and cooling plate for volatile analyses, a laser for neutral cluster ionization, an in-situ sample preparation chamber with sample transfer systems, etc.

(VI) Research groups and associated bibliography

Although SIMS is not widely used, still a significant number of laboratories in Europe, USA, and Japan are using this and related spectrometry techniques for the microanalysis of materials. Here, there is a list of various Research Centres:

[109] Li, Z. Hirohawa, K., Ga+ primary ion ToF-SIMS fragment pattern of metals and inorganic compounds. Analytical Sciences 19 (9), pp. 1231-1238, 2003.

- *Oxford Materials, Department of Materials at Oxford University*, Oxford OX1 2JD, UK.

- *Central Facility for Electron Microscopy* GFE, Aachen University of Technology, D-52056 Aachen, Germany.

- *Institute for Surface and Thin Film Analysis IFOS,* Kaiserslautern University, Erwin-Schrödinger-Str. Geb. 56, D-67663 Kaiserslautern, Germany.

- *Yurimoto Lab*., Hokkaido University, Sapporo, Japan.

- *Ion Beam Modification and Analysis Laboratory* (IBMAL), University of North Texas, Denton, 76203-1427 Texas, USA.

Relevant SIMS bibliography:

- *High-resolution imaging of complex crack chemistry in reactor steels by NanoSIMS.* Lozano-Perez, S. et al. Journal of Nuclear Materials, 374 (1-2), pp. 61-68, 2008.

- *Isotope ratio measurements by SIMS and glow discharge mass spectrometry (GDMS).* Betti, M. International Journal of Mass Spectrometry, 242 (2-3) 169-182, 2005.

- *SIMS: from research to production control.* Werner, HW. Surface and Interface Analysis, 35 (11) 859-879, 2003.

- *Comparative analysis of a solar control coating on glass by AES, EPMA, SNMS and SIMS*. Pidun, M. et al., Mikrochimica Acta 132 (2-4), pp. 429-434, 2000.

- *The use of Auger spectroscopy and a quadrupole SIMS build on a focused ion beam to examine focused ion beam made cross-sections.* Verkleij, D and Mulders, C. Micron, 30 (3) 227-234, 1999.

- *SIMS methods in reactivity studies on metal-oxides*. Daolio, S et al.. Inorganica Chimica Acta, 235 (1-2) 381-390, 1995.

- *Comparison of basic principles of the surface-specific analytical methods - AES/SAM, ESCA (XPS), SIMS, and ISS with x-ray-microanalysis, and some applications in research and industry*. Hantsche, H. Scanning, 11 (6) 257-280, 1989.

- *Metallurgical applications of secondary ion mass-spectrometry (SIMS)*. Degreve, F. et al. Journal of Materials Science, 23 (12) 4181-4208, 1988.

- *Secondary ion mass-spectrometry (SIMS).* Stuck, R and Siffert, P. Progress In Crystal Growth And Characterization Of Materials, 8 (1-2) 11-57, 1984.

- *Depth profiling by SIMS: depth resolution, dynamic-range and sensitivity*. Magee, CW and honig, RE, Surface And Interface Analysis, 4 (2) 35-41, 1982.

8.4.3.2. Atom Probe Tomography

(I) Introduction

Atom Probe Tomography (APT[110]) is a unique ultra-high resolution micro-analytical technique to detect and identify single atoms, determine their original position in the solid and perform a tri-dimensional reconstruction of the analyzed material. This method can be used to describe both the distribution and composition of small volumes within the material on a sub-nanometre scale[111].

Traditionally, the technique was restricted to the analysis of metals or materials with a high electrical conductivity, but recent developments on the field of both specimen preparation and the APT technique have extended its application to a wide range of materials, including thin films, semiconductors, insulators and, recently, organic materials[112]. Some of these improvements involve the use of Focused-Ion Beam (FIB) technology for sample preparation and laser-pulsed field evaporation in the APT. Most common APT applications are (Figure 8.18): the quantification of individual chemical species, phase determination, the determination of impurity content and distribution, precipitation analyses and segregation studies in selected regions, such as grain boundaries or interfaces. The qualitative and quantitative power provided by this technique facilitates the analysis of a great variety of interesting materials whose characteristics are determined by processes on the nanometre scale.

The fast technological development experienced by the APT technique has allowed wider application across a variety of materials whose behaviour is determined by processes occurring at the nanoscale, due to its analytical capacity, both quantitatively and qualitatively.

APT collects and identifies the species of each atom removed from a needle-shaped specimen (tip radius ~10-70 nm) held in an ultrahigh vacuum environment and cooled to temperatures below 100K (10-70K). Atoms are detected by the combination of a point projection microscope, i.e. a modified *FIeld Ion Microscope* (FIM)[113], and ToF mass spectrometer. Commercially available APT instruments operate by applying either a high voltage pulse or using short laser pulses to remove single atoms from the specimen surface. Advantages and limitations for both operating modes are described below.

[110] APT: Spanish acronym for Tomographic Atom Probe (TAP).
[111] T.K. Kelly y M.K. Miller, "Invited Review Article: Atom probe tomography", Rev. Sci. Instrum. 78, 031101 (2007).
[112] D. Larson y K. Stiller, "Summary of the Atom Probe Tomography Workshop IFES 2006 July 18, 2006 Guilin, China", Ultramicroscopy 107 (2007) 813–818.
[113] The APT allows to make also FIM in the same machine.

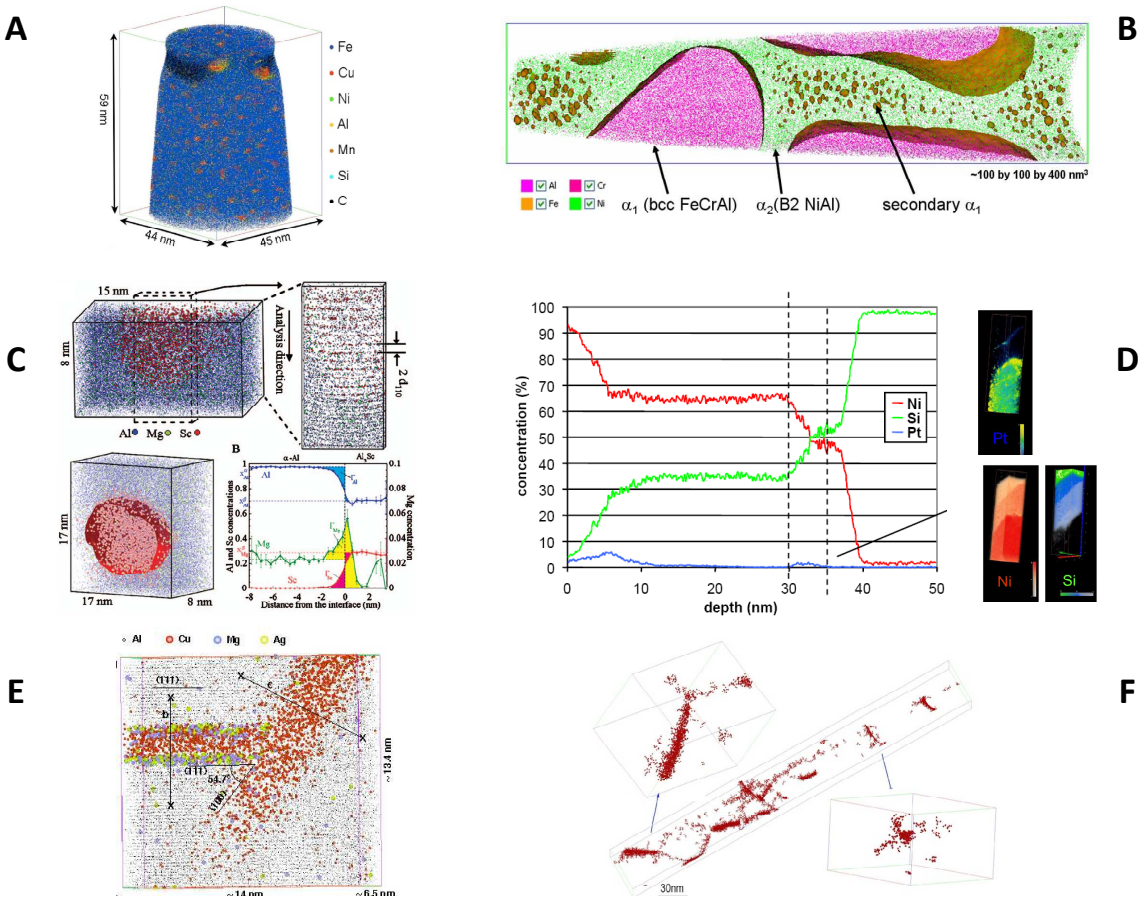

Figure 8.18. APT applications. In each image, one single point represents one single atom. (a) Nanoscale copper-rich precipitates[114] in NU Cu-150 steel. The smallest discernible precipitates are 2 nm in diameter; (b) Heat-resistant ferritic steel microstructure. The high-temperature resistance is due to the presence of coherent (Ni, Fe) Al precipitates in the ferritic matrix; (c) Mg segregation in a Al_3Sc/Al interface. In the bottom image, a 18 % at. Sc iso-concentration surface is drawn in a precipitate. APT concentration profiles are evidence for the segregation of Al, Mg and Sc at the precipitate-matrix interface; (d) Ni (5%Pt contacts in a MOFET nanotransistor. Concentration depth profiles analyzed by APT[115] (e) Atom maps of Ω and θ' phases in an Al-1,9Cu-0,3Mg-0,2Ag alloy aged for 10 h at 180 ºC. The picture was oriented to show the (111) resolved atomic planes[116] and (f) Carbon segregation in steel along dislocation lines[117]

[114] Courtesy of D. Isheim, Northwestern University Centre for Atom-Probe Tomography (NUCAPT) using Imago LEAP 3000.
[115] Courtesy of O. Cojocaru-Mirédin et al. GPM, University of Rouen, Francia.
[116] Courtesy of K. Hono, National Research Institute for Metals, Japan.
[117] Courtesy of E. Pereloma (Monash University, Australia) and M.K. Miller (Oak Ridge National Laboratory) using Imago LEAP 3000.

(II) APT for the study of nuclear materials

The development of materials with a high radiation resistance and an operating temperature window between 550 ºC and 1200 ºC is crucial for both nuclear fission (Generation IV reactors) and nuclear fusion. The required temperatures can be even higher in some critical applications, like the divertor in the future fusion reactor ITER.

In fusion reactors, the particular operating conditions produce interactions and diffusion mechanisms accompanied by changes in the microstructure and the material properties. These effects have been only partly studied and are not fully understood, as a consequence of the extraordinary environmental conditions: interactions between the plasma and the wall, irradiation at high dose rates by highly energetic particles and extreme working temperatures. In the development of reduced activation materials, some studies have been performed that are of special interest: the retention of species that are potentially hazardous from a radiological point of view, i.e. tritium, or the apparition of new atomic species in the materials by transmutation, possibly leading to activation. The study of this issue is the key for the public acceptance of fusion technology as a clean energy source.

Since 1967, when the precursor techniques of APT were launched, this approach has been used to characterize materials for nuclear applications[118], especially steel. Most researches focuses both on determining the micro-structural changes leading to embrittlement of the material and on studying the effect of treatments to recover the mechanical properties of the material after irradiation. APT is suited for the study of the mentioned micro-structural changes due to its high spatial resolution in three dimensions, its resolving power with regard to composition and morphology, even for ultrafine precipitates (~5 nm and below), and the fact that the detection accuracy is the same for all atomic species in the periodic table.

One critical issue with the design of structural materials for nuclear applications, both fission and fusion, is the shift in the DBTT produced by irradiation, especially by neutrons, and embrittlement during service. Using APT, the increase in DBTT and the deterioration of the mechanical properties of various types of steel upon neutron irradiation have been linked to the formation of nanoprecipitates, rich in alloy elements and impurities, whose concentrations have been determined[119] (Figures 8.19a and 8.19b).

The production of ODS alloys is one current line of research devoted to investigating radiation resistant structural materials with a high working temperature. In this research, a great effort has been made to develop RAFM steels, which are Fe-Cr based and improved by the dispersion of oxide nanoparticles, i.e. Y_2O_3. These materials present a complex microstructure that complicates reaching a full understanding of the mechanisms responsible for the reinforcement under tension and creep, or why they have an acceptable ductility and a high operational temperature, but not a good impact resistance. The recent application of APT, in combination with other experimental characterization techniques, has allowed some

[118] E. W. Muller, J. A. Panitz, and S. B. McLane: The atom-probe field ion microscope. Rev. Sci. Instrum.39:83–86 (1968).
[119] M.K. Miller, K.F. Russell, J. Kocik, E. Keilova, Micron 32 (2001) 749-755.

progress in the understanding of the microstructure[120] and its effects on the properties of powder metallurgy ODS-RAFM steels. As a result of this study, changes in the production routes for these ODS alloys have been proposed.

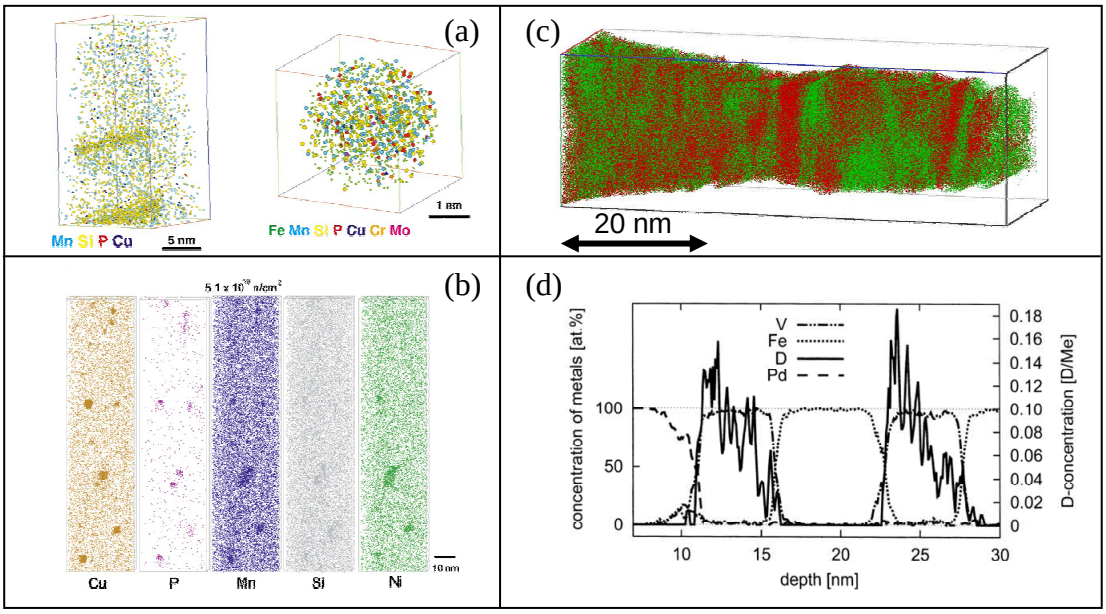

Figure 8.19. (a) Three-dimensional atom probe atom map of a volume of the neutron irradiated weld (having been in a nuclear reactor for 5 years) in 15Kh2MFA Cr-Mo-V steel. Cylindrical and spherical manganese and silicon enriched features can be observed. The core of the spherical feature shows the high resolution achieved by APT. All atoms are shown . (b) Distribution of solutes in pressure vessel steel of an operational commercial nuclear reactor . Micro-structural changes are produced by neutron irradiation during service (5.1×1019 n cm^{-2}). (c) AgCu nanocomposite prepared by high-energy ball milling . Cu (red) and Ag (green). Diffuseness of the interfaces can be observed, having a typical width of 2nm. (d) APT concentration profile for D in a Pd-Fe/V multilayer.

An important line of research deals with the development of nanocrystalline materials for nuclear applications. The reduction of grain size allows reinforcing the material and increasing its radiation resistance. Both effects are due to the fact that the enormously high density of grain boundaries acts as a sink for point defects and light impurities, i.e. helium atoms. In addition, the high fraction of atoms located on the surface of grains or crystalline regions leads to unique material properties, as evidenced by many studies. And yet, the relation between the new properties of the material and its complex microstructure, having a grain size that is always below ~100 nm, is still unknown. The high spatial resolution APT is ideally suited to study these materials, with enough accuracy to resolve nanocrystalline regions and to identify the distribution of the alloy elements and impurities (Figure 8.19c).

[120] V. Castro, T. Leguey, A. Muñoz, M.A. Monge, R. Pareja, E.A. Marquis, S. Lozano-Perez y M.L. Jenkikins, Proceedings del ICFRM-13 (2007). Journal of Nuclear Materials, in press.

Likewise, APT has contributed to the quantitative study of the distribution of light elements, i.e. hydrogen and deuterium (Figure 8.19d). Although the detection limits for light elements are lower in SIMS analysis, APT is the only technique available capable of mapping out the chemistry of a material in three dimensions and with subnanometre spatial resolution, allowing to study the microstructural changes that have been induced in the material. This is an essential issue in the development of candidate materials for the first wall of DEMO, which will be exposed directly to the fusion plasma, yet must comply with very restrictive requirements regarding the maximum amount of tritium retained in the vessel.

Finally, the special geometry and small size required for APT analysis (a sharp needle-shaped specimen) is very suitable for studying the effect of radiation on the material microstructure. Thus, the materials can be irradiated or implanted after being shaped according to APT requirements. The small specimen size will produce homogenous irradiation across its volume, in particular with the particle beams of the accelerators proposed for the *TechnoFusión* facility. So, while this approach allows studying the effects of intense particle fluxes on the microstructure of the whole volume of irradiated materials for future nuclear reactors, the small material volume minimizes the problems associated with the manipulation of activated materials and the corresponding waste.

(III) APT in the high voltage or HV mode

In this mode of operation, a static DC voltage is applied to the needle-shaped specimen. Depending on the sample material, ~10 kV is a typical value for this voltage. The specimen is placed quite close to an electrode, so a high electrostatic field (tenths of MV/mm) will be induced in the tip. This value should not exceed the evaporation field of the material. The surface atoms are ionised and removed after applying HV pulses added to the DC voltage. This process is called field evaporation (Figure 8.20).

This mode of operation is limited to the analysis of materials with a low electrical resistivity (1-10 Ω×cm), i.e. heavily doped semiconductors. Up to date, most results in metallurgy, nuclear materials and materials science were obtained using HV pulsed Atom Probe instruments.

An important feature of this technique is the relative simplicity of sample preparation. The starting material, shaped like a rod (~0.5×0.5×15 mm^3), is subjected to electropolishing to obtain the final specimen shape. Two difficulties are encountered in the analysis: during the measurement, the pulsed HV creates stress and fatigue in the tip, which may produce tip fracture. This problem is enhanced due to the relatively low amount of pulses that produce atom evaporation. The second problem is the small viewing angle of the detector, which limits the reconstructed volumes to ~20×~20×D nm^3, where D is the analysis depth. This analysis depth is limited by system stability and the total measurement time (e.g., the measurement time for a 7×7×24 nm^3 reconstruction volume with a Cu matrix is 1.5 h).

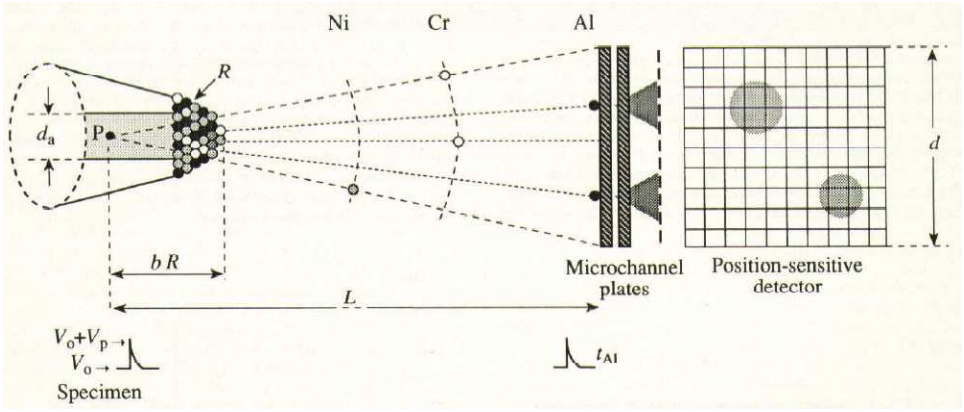

Figure 8.20. Sketch of the tomographic atom probe. A sharp tip is subjected to a constant high positive voltage, V_0. On top of this, high voltage pulses, Vp, are applied to the tip. These cause surface atoms to be evaporated and ionised. Field-evaporated ions originating from the specimen surface are identified by time-of-flight mass spectrometry. Their positions are deduced from the coordinates of ion impacts on the detector[121].

(IV) Laser-assisted APT

The development of femtosecond laser systems allowed the design and subsequent commercialization (in 2006) of laser assisted Atom Probe instruments. The short duration of the impact of the laser pulse on the tip prevents changes in the microstructure due to the redistribution and diffusion of atoms in the material. This technique consists of focusing an ultrashort laser pulse onto the apex of the specimen to induce field evaporation from the specimen at a static voltage. Current instruments can reconstruct the original atom positions with a resolution of ~0.2 nm in depth and ~0.5 nm in the lateral direction.

Benefits of this technique over pulsed voltage APT:

- Semiconductors, thin films, non-conducting materials and some insulators (i.e. Al_2O_3 and SiC) can be characterized.
- It provides high ToF mass resolution, since energy variations in the evaporated ions are minimal.
- Fatigue reduction in the samples: reduction of the amount of tip fracture events during analysis.
- Improvement in detection limits: an increase in the signal to noise ratio of about a factor of 3.
- A large field of view. Currently, analysis volumes of ~100 × 100 × D nm^3 can be handled, with a total number of atoms of several tens of a million, which is not possible in the HV mode.

[121] D. Blavette, A. Bostel, J.M. Sarrau, B. Deconihout, A. Menand, Nature 363 (1993) 432.

The main disadvantage is the high cost of a femtosecond laser, which implies an increased cost per analyzed sample.

(V) Capabilities and limitations of APT in comparison with other characterization techniques

APT's capacity to determine the volumetric microstructure of materials on the subnanometric scale, together with its analytical sensitivity on the atomic scale, makes it a unique technique. The spatial resolution of other imaging techniques (i.e. TEM or AFM) can surpass APT, but the combination of three dimensional spatial resolution and analytical detail convert it into a top technique in its field. Scanning Transmission Electron Microscopy (STEM) can reach a pointwise resolution of ~ 1 nm to 0.2 nm, depending on the operating mode, but it should be remembered that the images are obtained by integrating the signal across the whole thickness of the sample, typically ~10 nm. By contrast, the spatial resolution of APT is always ~0.3 nm in all three spatial directions. *Ultra-High Resolution Transmission Electron Microscopy* (UHRTEM) can reach higher spatial resolutions, but the analysis is limited to one or two spatial dimensions and depends on the atomic chemistry.

Concentration profiles for the atomic distribution in a volume are similar to those obtained by specific characterization techniques like SIMS, but APT profiles have worse statistics and they require special specimen preparation. Nevertheless, the excellent depth resolution reached in APT, ~0.2 nm, and the enhancement of the analysis angle in the more recent instruments enable the observation of interesting features near the interfaces (detection level ~40 appm per atomic layer), undetectable by other techniques. Furthermore, in SIMS analysis it is not possible to obtain concentration profiles in the vicinity of a cluster or precipitate like those presented in Figure 8.19c. In bulk materials, the detection threshold of the device is limited to ~10 appm or better, as a consequence of the signal to noise ratio. However, the detection efficiency of different atomic species in APT does not depend on the element and the detection process does damage the material microstructure, thus simplifying the chemical quantification.

As with any experimental technique, some applications are more suited for APT than others. In the current stage of development of APT, the following limitations apply:

I. *Specimen preparation:* electropolishing methods are straightforward for many metallic materials, but obtaining the required needle-shape in fragile materials, semiconductors, multilayers, interfaces, or insulators is not an easy task. Only recently, the introduction of submicron manipulation methods using *Focus Ion Beam* (FIB) techniques has permitted obtaining suitable specimens for APT of the mentioned materials. Aside from the required skills and the economical cost of FIB, other difficulties are encountered, such as contamination induced by the ion beam in the first atomic layers.

II. *Specimen fracture*: the evaporation process induces mechanical stress in the tip that can lead to tip fracture. This is quite common in APT, sometimes making the analysis of very fragile samples impossible. Stress in the tip increases with the square of the applied voltage. Laser assisted APT may therefore reduce this

problem, as induced stresses decrease by 20% - 40% as compared to the HV mode.

III. *Analyzed volumes:* as of today, the maximum volumes that have been analyzed are of the order of 10^6 nm^3, meaning that APT is only suitable for materials with a microstructure variation fitting completely inside such a volume. Further development of the technology may allow increasing the analysis volume, but depth analyses exceeding one micron are not likely to occur. The maximum number of atoms contained in the current analysis volumes is around 10^8, but this value is expected to increase in the near future.

(VI) Possible companies and instruments

1) LEAP 3.000X Si™ Metrology system, by Imago

Imago Scientific Instruments[122] is the supplier of the LEAP Si™ Metrology System (Figure 8.21), which is a high-performance atom probe microscope providing 3D, atomic resolution, compositional imaging and analysis technology to research and industry. Materials are examined by removing and analyzing individual atoms. Atoms are removed by a combination of a high electrical field and either an ultra-fast voltage pulse or an ultra-fast laser pulse.

The LEAP 3000x Si employs patented innovations that unlock the power of the 3D atom probe to address previously unsolved measurement challenges. One key technical breakthrough behind the LEAP 3000X Si Metrology System is the unique and patented Local Electrode™. Only the LEAP 3000X Si can simultaneously provide wide Field Of View (FOV), high mass resolution, and a high atom-collection rate for a variety of material systems. The Local Electrode also provides the ability to analyze Microtip™ specimens. Microtips are prefabricated tip arrays that facilitate sample preparation. For thin-film studies, the thin film may be deposited directly on the Microtip. For site-specific studies, Microtips are used to mount multiple FIB-extracted samples. The use of Microtips is made possible only by the LEAP Local Electrode. What previously would have been completely impossible can now be accomplished in a matter of hours.

The Laser Pulsing Module expands the universe of applications to low electrical conductivity materials, including semiconductors and ceramics. In laser pulsing mode, the LEAP electrode applies a static field to the specimen, while an ultra-fast laser pulse triggers the removal of an atom. The LEAP 3000X Si Laser Pulsing Module features a high pulse-repetition rate and proprietary real-time, optical-alignment correction, which together enable high mass resolution, a large field of view, and fast time to results.

[122] http://www.imago.com.

Figure 8.21. LEAP 3000X Si™ Metrology (Imago SI).

2) LA-WATAP, by Cameca

The LA-WATAP instrument (Figure 8.22) of Cameca SA[123] is the next generation of Tomographic (or 3D) Atom Probe, providing quantitative 3D atomic scale mapping of elements and chemical heterogeneities in materials. The Laser-assisted evaporation mode allows analyzing metals, semiconductors and thin layers of insulating materials. An excellent data quality is obtained under optimized laser-assisted evaporation conditions that depend on sample composition and shape. Composition accuracy will also depend strongly on the performance of the detector. Key features of the instrument:

- Analysis of semiconductor materials and thin, electrically insulating layers with near-atomic depth resolution is possible using a flexible (IR/ visible/ UV) ultrafast (400 fs) laser setup. The unique hybrid evaporation mode combines reduced heating of the sample with ultra-fast surface polarisation, promoting ion evaporation under a high DC electrical field.

- Very high analyzer transmission (detected ions/evaporated atoms >60%) and a large analysis area (100 nm in diameter), for better statistics with composition measurements.

- Fast acquisition, up to 10^6 atoms per minute, depending on sample strength (flux of at/pulse).

- Top quantitative results using the exclusive *Advanced Delay Line Detector* (ADLD) and its benchmark multi-hit performance.

[123] http://www.cameca.fr/.

- Flexible and fast dedicated FIM detector for metallurgical applications.

Figure 8.22. Cameca LA-WATAP instrument.

(VII) Research groups and associated bibliography

Worldwide, the number of research groups devoted to analysis of materials using APT is very limited. These groups often introduce modifications to commercial instruments with the aim of improving them, e.g., by introducing more effective evaporation sources or more accurate and sensitive detectors. Some relevant research groups applying this technique are:

- *Groupe de Physique des Matériaux* (GPM), Univesité de Rouen, France. Actively collaborating with CAMECA under a technology transfer agreement.
- *Oxford Materials, Department of Materials at Oxford University*, Oxford, UK.
- *National Institute for Materials Science* (NIMS), Sengen, Japan.
- *Northwestern University*, MRSEC, Centre for APT, Illinois, USA.
- *Australian Key Centre for Microscopy & Microanalysis at The University of Sidney, Sidney, Australia.*

8.4.4. Structural and microstructural analysis techniques

8.4.4.1. X-ray diffraction

The versatility of the *X-Ray Diffraction* (XRD) technique allows obtaining detailed information on crystalline systems. In the *TechnoFusión* facility, this technique will be applied particularly to perform structural analyses associated with the design and processing of materials in the MPP Facility. It is also a key technique for determining residual (internal) stresses, of great importance for the study of the mechanical behaviour of crystalline materials. Unfortunately, a single system is not sufficient to cover all experimental needs. For this reason, our proposal contemplates two systems for material characterization, the determination of the main global structural parameters and the identification of the physical state of materials used at *TechnoFusión*.

(I) Introduction

XRD techniques for microstructural characterization are fundamental tools in the design of materials, since they allow the determination of several structural parameters, such as: structural phases present in the materials, crystalline domains size (cells/(sub)grains), texture (micro and macro), lattice deformation (distortion), residual stresses, thin film roughness, etc. In addition, these techniques are non-destructive and require a moderate amount of time for performing measurements, while the cost per sample is low. Although XRD is mostly applied to the study of crystalline structures, it is also useful for the characterization of amorphous materials, such as the determination of the distribution of the interatomic parameter, the atomic coordination number, and the existence of pseudo-ordered zones.

In general, sample preparation for the XRD technique is straightforward, without significant size limitations. The scanned area in a typical XRD measurement does not exceed ~1 cm^2, independent of sample dimensions, but can be as small as ~50 μm^2.

(II) Application in Material Science

The application of XRD to the characterization of crystalline materials mainly produces the following information:

- Crystal type.
- Determination of crystallographic system and parameters of the unit cell.
- Determination of lattice parameters.
- Atom arrangement and distribution in the unit cell.
- Determination of crystalline orientations and texture.

- Determination of crystalline domain size.
- Identification of compounds and phases. Determination of their volume fraction.
- Phase transitions (high quality atmosphere or vacuum controlled furnaces are required).
- Macroscopic and microscopic residual stresses and strain.
- Characterization of thin films.

(a) Characterization of powders and polycrystalline materials (XRPD):

The application of XRD to powdered materials assumes that the orientations of the crystalline domains are distributed randomly (random texture). This may happen in massive polycrystalline materials when most grains (or crystalline domains) are randomly distributed or even adopt a weak texture. However, when grains develop preferred orientations, the intensity of diffracted beams is modified drastically in comparison to the theoretical expectations of random texture.

Powerful and sophisticated software exists for the analysis of crystalline structures on the basis of experimental diffraction spectra. Some are free, such as the Maud and Fullproof[124] software, based on Rietveld's method. This analysis deals with the identification and estimation of the lattice parameters of different phases, taking into account both the peculiarities of the measurement system (resolution, aberrations, X-ray sources, operation mode, specific calibrations) and the microstructural characteristics of the sample (crystalline domain size, residual stresses, texture).

While chemical analysis techniques allow identifying the elements composing the material and even the chemical configuration of a compound, they cannot determine whether the different elements present in the volume material are structured into one or several phases. The XRPD technique overcomes this limitation, allowing both the identification of phases and the determination of their relative volume fraction.

The XRPD technique requires preparing the sample as a powder and either introducing it in a capillary, compacting it, or depositing it on a surface. With metals, the bulk material itself can be analysed directly. In this case, sample preparation often consists simply in creating a polished plane surface. This avoids the difficulties associated with the pulverization of a conducting material and the introduction of new material phases, as well as with the contamination of the material during pulverization.

[124] www.ing.unitn.it/~maud/. FullProf, Rodríguez-Carvajal, J. Recent Developments of the Program FULLPROF, in Commission on Powder Diffraction (IUCr). Newsletter (2001), 26, 12-19. http://www.ill.eu/sites/fullprof/

(b) Thin films:

In order to be able to analyze thin films or thin plates, conventional diffractometers must possess some specific features. The most relevant requirement is the control of the penetration depth of the incident radiation to avoid overshooting the film thickness. Furthermore, a high peak-to-background ratio is required. The latter is achieved by keeping the incident angle below 5º or 10º. For that purpose, the diffractometer must provide independent control of the θ and 2θ angles. Unfortunately, a small angle of incidence leads to a loss of focus in the detector, resulting in the broadening of diffraction peaks as 2θ increases. To solve this problem, the collimation system is modified by incorporating parallel system optics.

XRD can be applied to powdered compact materials, polycrystalline materials, or thin films, simply by changing the system optics. When the same XRD system is used frequently for low angle incidence measurements, the use of a θ - θ geometry instead of a θ - 2θ geometry is suggested.

(c) Study of residual stresses

XRD allows determining macroscopic residual stresses as well as lattice deformation. Also, microscopic residual stresses can be revealed, assuming a linear elastic behaviour of lattice structure. This can be done with all polycrystalline materials having relatively small grains. Again, the technique is non-destructive, and has a high spatial resolution while requiring only simple sample preparation.

It is worth mentioning that XRD is the only non-destructive method allowing a simultaneous analysis of microscopic and macroscopic residual stresses. The main limitation of this technique is that the determination of stress is limited to the material surface[125].

The two main applications of this technique are:

I. *Macroscopic residual stresses*. The determination of macroscopic residual stresses is important for the design of materials and the study of resistance and fracture mechanisms. The term macroscopic residual stress refers to stress at scales larger than the typical grain size. The residual stress is a tensor, so its value depends on the direction of measurement at every point. To make a global measurement of such stresses, measurements must be made in at least three directions. The maximum and minimum of both residual and shear stress, as well as their orientations can be evaluated using Mohr's circle. In many cases, the macroscopic stress fields are uniformly distributed on the material surface, resulting in an angular shift of the diffraction peaks, proportional to the magnitude of the residual stresses.

[125] This only applies to X-ray sources commercial equipment. With synchrotron radiation, studies in volume could be done.

.

II. *Microscopic residual stresses.* The microscopic stresses are scalar magnitudes quantifying the amount of cold work (stored energy) in the material or its hardness. They are associated with short-range lattice strain (distortions) on the scale of the grain size or smaller. This kind of stresses can produce a broadening of the XRD peaks due to the variation of the lattice parameter inside grains.

Macroscopic and microscopic residual stresses are determined from the position of a peak and its width in a diffraction spectrum. The accuracy of the stress measurement depends mainly on the precision of the position of the peak. A slight deviation in the device alignment may lead to systematic errors[126]. Thus, the system must allow aligning the system and the material sample by means of rotation about the main axes of the diffractometer.

(d) Determination of crystallographic texture

Polycrystalline materials are an agglomerate of crystalline domains, called *grains*, separated by thin regions, called *grain boundaries*. The domains are relatively free of defects, with sizes between 1 µm and 1 mm, each with its specific orientation. A typical sample subjected to tensile tests can contain some 10^{10} grains. Its mechanical behaviour and fracture resistance will depend strongly on the grain size, shape, arrangement and orientation. When the grains collectively develop a preferred spatial orientation, the material acquires a crystallographic texture. The determination and analysis of the grain texture is necessary to understand the correlation between material properties and microstructure.

For texture measurements, the samples must be flat and without roughness, and contain enough small grains to ensure the presence of about 5.000 grains in the volume irradiated by the x-rays. If the texture analysis is based on the technique denominated pole figures (PF), no data can be obtained for angles superior to 80º, due to a loss of focus and aberrations. In this case, the use of orientation distribution functions (ODF), calculated from a set of various experimental pole figures, will provide a more complete picture and allow a detailed visualization of the texture. Currently, a range of software is available to facilitate rapid texture analysis. The typical time required for measuring three pole figures is about 150 min.

(III) Suggested companies and equipment

Unfortunately there is no system for implementing the relevant techniques in an unique equipment. The reason is the incompatibility between some requirements. For this reason, this report proposes the acquisition of two techniques that allow obtaining basic parameters for the characterization of materials of interest in *TechnoFusión*.

[126] A misalignment of 25 µm gives a tension error of about ~14 MPa.

1) D8 Advance, by Bruker

This XRPD diffractometer is useful for analysis of powders. It is versatile and has a high resolution (Figure 8.23).

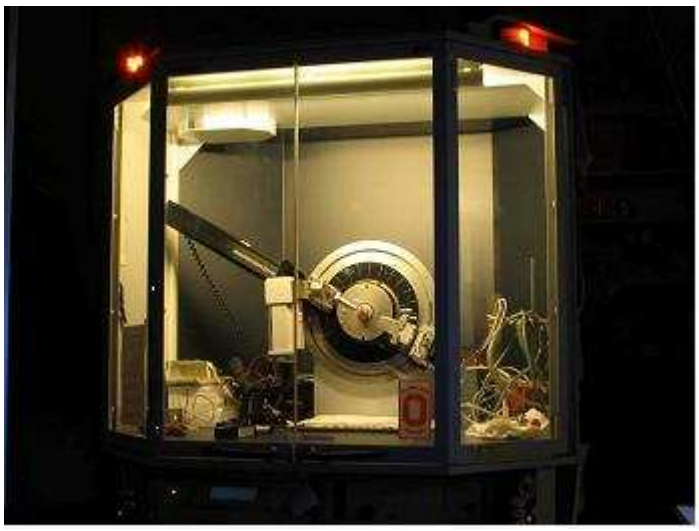

Figure 8.23. X D8 Bruker Advance diffractometer for the study of powders.

The monochromatic signal from a Cu $K_{\alpha 1}$ source can be selected in a tube using a Vario monochromator. The device offers a large selection of sample holders, allowing different sample preparation methods. The Braun position detector allows initiating scans at a diffraction angle of 2θ = 8º in continuous mode. This increases the detection sensitivity in comparison with the conventional sparkle detector, located behind the aperture.

Some of special characteristics of this technique for *TechnoFusión* are:

- Easy user-controlled switching between θ-2θ and θ-θ geometry.
- System alignment optics for changing between Bragg-Brentano and parallel beam geometry at small angle incidence.
- Göbel Mirrors for Cu, Co and Cr radiation.
- Possibility of changing X-ray sources.
- Detector VANTEC-1 for high-speed data acquisition.
- Chamber for in *situ* operations under vacuum and controlled atmosphere
- Furnace for *in situ* tests up to temperatures of 1500 ºC.

- Vacuum system coupled to the measurement equipment.
- Cooling system with closed circuit circulation.

2) D8 Discover, by Bruker

This diffractometer, similar to the previous device, incorporates several accessories for various analyses: textures, residual stresses, and X-ray reflectometry. Fe fluorescence has been eliminated from Cu radiation by adopting the Sol-X detector, which allows selecting the detection energy range. Thus, monochromators are not necessary, avoiding the loss of beam intensity. A vacuum system (Vacuum Check System) is coupled to the device, facilitating the analysis of wafers and thin films, while allowing analyses in a high temperature BTS-SOLID chamber at a temperature of up to 1200 ºC.

Some of special characteristics of this technique for *TechnoFusión* are:

- Assembly of θ-2θ geometry with a rotation radius of 258 mm.
- Focus and alignment systems assisted by LASER.
- Solid state high-speed detector in 2D HI-STAR.
- Adapter arm for residual stress determination.
- Euler's completely motorized Goniometer for ϕ,χ, X, Y, Z.
- Alignment system and central positioning.
- Göbel mirrors for Cu radiation.
- The possibility of changing X-ray sources.
- Cooling system with closed circuit circulation

8.4.4.2. Transmission Electron Microscope

(I) Introduction

The latest advances in material studies rely on their characterization and qualification at the nanometre scale. *Transmission Electron Microscopy*[127] (TEM) is a commonly used technique and a very powerful tool for imaging and analysis. Rather than a mere imaging technique, TEM

[127] D. B. Williams, C. B. Carter, "Transmission Electron Microscopy" Ed. Plenum Press, New York, 1996

allows obtaining structural detail (morphology, crystallography, etc.) and, with suitable accessories, chemical, mechanical, magnetic and electrical information at the nanometre scale for a wide range of materials. The information provided by TEM complements other techniques with the advantage of being direct.

Transmission electron microscopes have sufficient resolution (from some nanometres down to Armstrongs) to allow studying nanostructured materials and materials containing nanoparticles. They have contributed in a very important way to the study of irradiation damage in materials, by revealing the evolution of the microstructure under irradiation exposure.

Complicated processes take place in materials under irradiation. Radiation can induce microstructural and micro-chemical changes. Therefore, the study of microstructures damaged by radiation is a highly complex field. Even in pure materials, defect clusters of different nature, size and type can appear[128]. Depending on irradiation conditions and on the material studied, these clusters can consist of interstitial or vacancy dislocation loops, tetrahedral stacking faults, bubbles, and voids, all below the nanometre scale. In alloys, secondary phases can be induced, enhanced, suppressed or inhibited by radiation. In addition, impurity or solute elements can be segregated to or from sinks such as grain boundaries or dislocations.

TEM has played a very important role in the analysis of these complex microstructures and their interpretation in terms of fundamental radiation damage mechanisms. Other complementary techniques, such as SANS (*Small Angle Neutron Spectroscopy*), PAS (*Positron Annihilation Spectroscopy*), APT (*Atom Probe Tomography*), can also provide information about cluster population and are often essential for a proper characterization of the microstructure. However, they are not generally suited for the characterization of a wide range of samples. By contrast, TEM is able to provide direct routine images with magnifications of up to a million times and a resolution better than 1 nm. This allows the observation of clusters of point defects. In combination with associated analytical techniques, TEM can also provide information about local changes in the microchemistry at a very fine scale.

Like other experimental techniques, TEM has certain limitations that have to be known and understood to obtain reliable information. The examined samples are thin foils, and the processing methods can introduce artefacts that are not related to the phenomenon under study, but rather with their thickness and preparation. Other limitations are associated with the actual process of TEM image formation and its limited resolution: very small defect clusters are not visible, and the corresponding image depends strongly on the experimental conditions.

Several methods have been developed to deal with the specific problems related to the characterization of radiation-induced microstructure, especially small point defect clusters.

[128] M.L. Jenkins, M.A. Kirk “Characterization of radiation damage by transmission electron microscopy” Institute of Physics, Bristol, 2001

(II) Fundamentals

The basic microscope[129] consists of an electron source and several electromagnetic lenses placed in a vertical column, in a vacuum with a pressure below 10^{-7} torr. The electron source produces a coherent electron beam, whose diameter can be varied by means of a double condenser lens system. The sample is mounted on a sample holder between objective poles. Electrons transmitted through the sample are focused on the back focal plane of the objective lens; as all electromagnetic lenses, this lens is convergent and forms a diffraction pattern at the back focal plane. On the first image plane an inverted image is formed, and the next three sets of lenses in the column (diffraction, intermediate, and projector lens) are used to magnify the image or the diffraction pattern. Therefore, when the diffraction lens is focused on the back focal plane of the objective lens, a diffraction pattern is formed, but when the diffraction lens forms an image of the first image plane, a magnified image of the sample is obtained. With a typical modern microscope, the final magnification factor obtained on the fluorescent screen can reach about one million.

The usual method for characterizing defects in crystals is the diffraction contrast technique[130], which involves the insertion of an objective aperture to select the diffracted beam that contributes to the formation of the image. If the selected beam is the transmitted beam, the image formed is called Bright Field, BF, while the image formed after selection of the diffracted beam is called Dark Field, DF.

With the diffraction contrast method, the defect image is reflects the associated elastic deformation field. The crystal is moved to a position with well-known diffraction conditions, and the image is formed using the objective aperture to select the diffracted beam. Since the image characteristics depend on the selected diffraction conditions, it is very important to prepare this condition carefully. This mode is most commonly employed to characterise radiation damage. The elastic deformation field associated with the defects produces local changes in the diffraction conditions, e.g., the diffracting planes are curved locally and produce changes in the diffracted beam amplitude.

(III) Basic characteristics of TEM

The basic characteristics of any TEM device are:

I. A microscope with a field emission electron gun.

II. An acceleration voltage of 300 keV, which can be adjusted to intermediate voltages, e.g., 200 keV, since 300 keV electrons can cause irradiation damage in some materials, which needs to be avoided when characterising the material.

III. A polar device allowing the inclination of the samples, as explained, because the appropriate orientation of the samples is essential when characterising the radiation damage and obtaining information on defects.

[129] J. W. Edington, “Practical electron microscopy in Materials Science” Ed. Macmillan Philips Technical Library
[130] M. H. Loretto “Electron beam analysis of materials” Ed. Chapman and Hall, 1984.

(IV) Specific applications at *TechnoFusión*

(a) TEM coupled to an ion accelerator

The TEM offers the possibility to perform *in-situ* irradiation damage studies by coupling the microscope to one or two ion accelerators. In other words, the dynamic evolution of the microstructure under ion irradiation can be studied. This direct information on the processes occurring under irradiation cannot be obtained by any other characterization technique.

A microscope that can be coupled to an ion accelerator is not a conventional one, but should be designed specifically for this purpose. Therefore, its installation requires careful planning. An important requirement is the definition of the incident ion beam angle with respect to the surface sample. The ion beam and the electron beam should be as parallel as possible, in order to allow the maximum sample area to be observed during ion irradiation. Also, the installation should be protected against vibrations, magnetic fields, etc… to avoid noise.

The interest of such a characterization technique for *in situ* microstructural observations coupled to one or two of the planned accelerators of the *TechnoFusión* Facility is evident, and thus requires a more detailed analysis. The study of the advantages and disadvantages of coupling the microscope to the accelerators, the facility's effective cost, and site requirements are now in progress.

(b) In-situ nanomechanical tests in a TEM

The field of application of TEMs is very broad, and so the equipment is versatile and allows the incorporation of several advanced accessories to perform different types of *in situ* experiments. This is the case of different sample holders developed to study the mechanical behaviour of materials while micro-structural changes are taking place. Micro-structural changes can be followed in real time as the small material sample is submitted to specific mechanical forcing (tension, compression, etc.). Several technological developments attempt to solve the problem of direct visualization of the material microstructure when stress is applied; these are published elsewhere[131, 132, 133].

The main objective of CT Facility is the characterization of the samples irradiated at the various *TechnoFusión* facilities. These samples will be rather small as a consequence of the size of the impact region of the ion radiation, the dynamic liquid lithium, and the geometry of the plasma facilities. Therefore, mechanical characterization of the samples using conventional instruments is not feasible. As a consequence, the existence of TEM sample holders, developed to test samples of millimetre and micrometer sizes mechanically while they are being treated, is essential.

[131] Qian, D. & Dickey, E. C. *In-situ* transmission electron microscopy studies of polymer–carbon nanotube composite deformation. *Journal of Microscopy* 204 (1), 39-45.
[132] Kameda, J y Mao, X. Small-punch and TEM-disk testing techniques and their application to characterization of radiation-damage. *Journal of Materials Science*, 27, 1992, 983-989.
[133] Wang, JJ; Lockwood, AJ; Gay, R; Inkson, BJ, Characterising ambient and vacuum performance of a miniaturised TEM nanoindenter for in-situ material deformation, en Electron Microscopy and Analysis Group Conference 2007, vol. 126, pp. 12095-12095. Edited by Baker, RT; Mobus, G; Brown, PD, IOP Publishing Ltd, 2008.

Nowadays, various TEM sample holders are available commercially that can be used for this goal. By way of example, the deformation mechanisms of dislocation-radiation induced defect interaction are usually studied with an *in situ* straining sample holder at low and high temperatures. A sample holder provided by Gatan (Figure 8.24) makes this possible, allowing strain rates as low as 0.01 µm/s. This particular device provides an analogical output to record the thermal history as well as the applied stress–strain curve.

Hysitron, one of the leading companies in nanoindentation, has developed a system that allows direct observation of materials at the nanometric scale in a TEM and analysing their mechanical response. This firm has patented the picoindenter PI 95 TEM that allows creating sample deformation while simultaneously acquiring quantitative strain-stress data. 3D piezoelectric actuators are coupled to capacitive sensors to follow sample displacements with high accuracy. A small impact tester can also be added to perform nanocompression tests on nanopillars and other nanostructures.

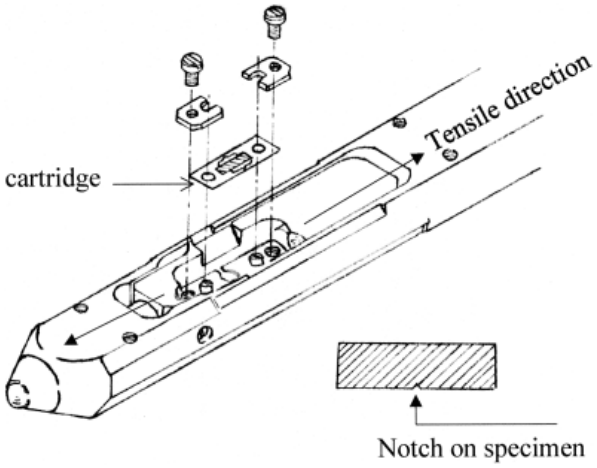

Figure 8.24. Sample holder developed for stress-strain tests inside a transmission electron microscope.

(V) Preparation of metallic samples

TEM samples are commonly prepared as discs with a diameter of 3 mm and a thickness of 100 µm by means of cutting, punching and polishing. The discs are etched electrochemically in order to obtain a thin area transparent to the electrons, required for TEM examination. For ferritic/martensitic steels, the best method involves using an electrolyte solution with 5% perchloric acid in methanol at a temperature of -60 ºC. Figure 8.25 shows an image of a TEM sample fabricated from pure iron with the above methodology. The described methodology is the employed for metals; in the case of ceramics other well-developed methods are used.

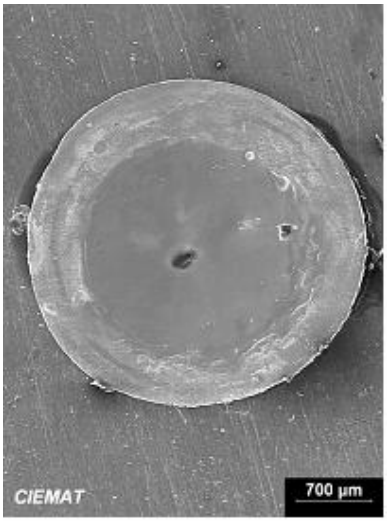

Figure 8.25. Image of a metallic sample thinned for TEM observation.

Nowadays, focussed ion beams (FIB) are commonly used for sample preparation, which is especially useful when specific sample regions must be selected carefully. This situation is common when analysing materials damaged by radiation.

(VI) Equipment

a) Sample holders:

- Double inclination
- *In situ* annealing
- *In situ* straining/heating
- Low Temperature

b) EDX
c) EELS
d) GIF
e) HAAD
f) Photographic and video CCD (*Charge-Coupled Device*) camera.

(VII) Suggested companies and equipment

There are but few specialized companies producing transmission electron microscopes. FEI, JEOL and Hitachi, in particular, have implemented microscopes coupled to ion accelerators at the cited North American, Japanese and French facilities (Figure 8.26).

1) TECNAI F20 FEG TEM-STEM, by FEI

The Tecnai microscope family was designed to offer universal solutions for imaging and analysis in, among others, material science and nanotechnology. In these microscopes, a high definition is combined with a high resolution, which is essential to 2D and 3D imaging and the structural analysis of defects in solids. They can be configured with *Scanning Transmission Electron Microscopy* (STEM) and *Energy Dispersive Spectrometry* (EDS) systems to achieve optimal performance of the microscope. The high coherence and brilliant electron beam of the microscope allows making chemical analyses of regions with a diameter of up to 1 nm. The possibility of obtaining images with atomic resolution, crystallographic information, and chemical composition data for regions down to 1 nm in size, converts this electron transmission microscope into a powerful tool for performing analyses on the nanoscale, which is an essential feature for both research and industry.

The microscope can perform studies with nanodiffraction, *Convergent BEam Diffraction* (CBED), and *Selected Area (electron) Diffraction* (SAD), nanoanalysis (pointwise chemical analysis, profiles of chemical composition, and mappings of the distribution of elements on the nanometre scale).

The Tecnai F20 is a *Field Emission Microscope* (FEG). The acceleration voltage is 200 kV. It is fitted with S-Twin lenses that provide a pointwise resolution of 0.24 nm. It includes an X-ray energy dispersion spectrometer (EDS) with an ultrafine window. The imaging system consists of a TV 626 Gatan camera and a slow-sweep CCD 794 Gatan. The detectors are embedded in the microscope's control unit.

2) JEM-2200FS, by JEOL

This is a versatile device offering the required properties and techniques for its application in research and nanoscience. The column includes an energy filter allowing the capture of energy-filtered images and obtaining electron energy loss spectra. This filter produces distortionless data due to the optimized design of the electron transmission optics. A novel imaging system, consisting of four lenses at the intermediate level and two projection lenses allows obtaining energy-filtered images without rotation limits and diffraction patterns in an ample range of magnifications and focal lengths. The goniometer incorporates a piezo-electrical mechanism that facilitates the smooth operation of the device when selecting the field of view at the atomic level. The main components of the microscope (optics, goniometer, and vacuum system) are fully computer controlled.

3) EFTEM Libra 200 FE, by Carl Zeiss

The Libra series of electron transmission microscopes by Zeiss offer solutions for the present needs and future developments. The device Libra 200FE is the first electron transmission microscope incorporating an energy filter, *Energy-Filtered Transmission Electron Microscopy* (EFTEM) and combines the advantages of Koehler lighting and a field emission electron source.

This is a Schottky type field emission system that combines coherence, high brightness, and reduced energy spreading in order to obtain high resolution images. The acceleration voltage is 200 kV. It features EELS and EFTEM analysis systems, with a high energy resolution

(<0.7 eV to 200 kV). An omega energy filter is included in the column to achieve an optimal resolution with EELS, maximum angles with CBED, and high values of non-isochromaticity in the EFTEM mode. The 300 mm column is designed for optimal mechanical stability and perfect shielding. Complementary analysis of elements is possible with the EDX (*Energy Dispersive X-ray analysis*) detector.

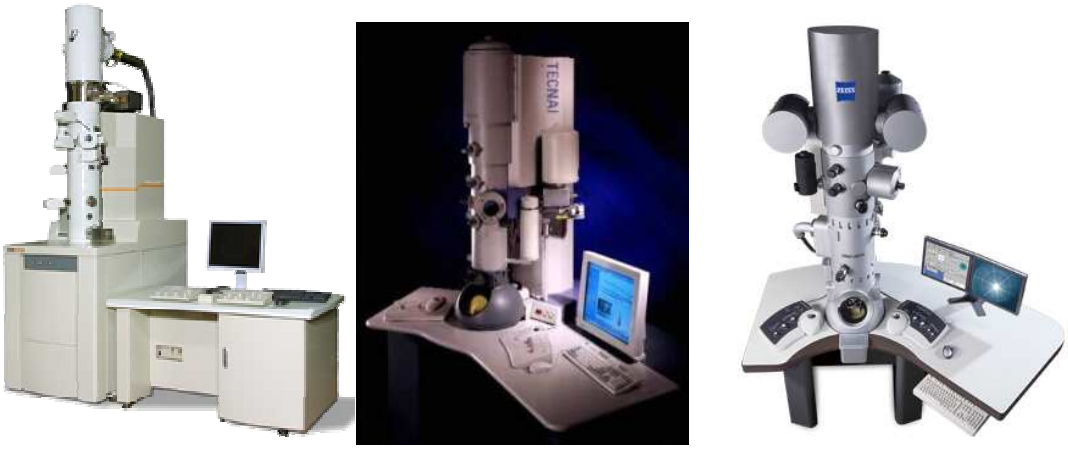

Figure 8.26. Electron transmission microscope images: (left) JEM 2200 FS, (centre) Tecnai F20 by FEI, (right) Libra 200FE by Zeiss.

8.4.5. Material processing techniques

8.4.5.1. Focussed Ion Beam

(I) Introduction

In a scanning electron microscope (SEM), electrons are accelerated and focused onto the sample surface. The beam can be scanned over the sample surface to create an image, or can execute a pattern to expose the sample to the beam locally, as in e-beam lithography. These same basic functionalities are found in a focused ion beam system. Ions are much larger than electrons. Their interaction mainly involves outer shell interactions, resulting in atomic ionization and the breaking of the chemical bonds of the substrate atoms. This is how secondary electrons and changes of chemical state are created. There is no x-ray emission when the sample is irradiated with an ion beam. The ion rapidly loses its energy. The result is that the penetration depth of the ions is much lower than the penetration of electrons at the same energy. When the ion has come to a halt within the material, it is trapped in the matrix of the material. The sample is doped with bombarded ions along roughly the total penetration depth of the beam for a given energy and material. Ions are far heavier than electrons. When the ion hits an atom, its mass is comparable to the mass of the sample atom, and as a consequence it will transfer a large amount of its momentum to it, i.e. the sample atom will move with a speed and energy high enough to remove it from its matrix. The removal of atoms

from their matrix is a phenomenon known as sputtering or milling. The rate will depend on the mass of the target atom, its binding energy to the matrix and the matrix orientation with respect to the incident direction of the beam. Ions are positive, large, heavy and slow whereas electrons are negative, small, light and fast. The most important consequence of the properties listed above is that ion beams can be used to remove material locally in a highly controlled manner, down to the nanometre scale.

A Focused Ion Beam, also known as FIB[134], is a scientific instrument that resembles a scanning electron microscope. However, whereas the SEM uses a focused beam of electrons to image the sample in the chamber, a FIB instead uses a focused beam of gallium atoms. Gallium is chosen because it is easy to build a gallium liquid metal ion source (LMIS). In a Gallium LMIS, gallium metal is placed in contact with a tungsten needle and heated. Gallium wets the tungsten, and a strong electric field (greater than 10^8 volts per centimetre) causes ionization and field emission of the gallium atoms. These ions are accelerated to an energy of 5-50 keV, and then focused onto the sample by electrostatic lenses. A modern FIB can deliver tens of nano-Amperes of current to a sample, or can image the sample with a spot size on the order of a few nanometres.

Unlike an electron microscope, the FIB is destructive to the specimen. When the high-energy gallium ions strike the sample, several phenomena occur: atoms from the surface are sputtered, the accelerated primary atoms are implanted, and the surface becomes amorphous. Because of its sputtering capacity, this technique is used as a precision tool to modify or machine materials at the micro- and nanoscale.

An additional problem occurs when working with completely isolating samples. These non-conducting materials (e.g., glass) will charge positively because of the implanted positive ions and the emitted secondary electrons. This charge can be compensated by an additional, in-chamber low energy electron gun that sprays electrons over the surface.

(II) Features and applications

The various features of the FIB technique make it suitable for diverse applications[135, 136], such as:

(a) Milling

The milling capacity of the FIB is so important that patterning (structure creation) is a standard feature of the system (Figure 8.27). Milling is a continuous process that occurs during beam exposure. The milling rate is proportional to the beam current. Precise control is possible by the use of small spot sizes, corresponding to small currents. Milling can be used to create a

[134] "Introduction To Focused Ion Beams, Instrumentation, Theory, Techniques and Practice". Edited by L.A. Giannuzzi and F.A. Stevie, Springer, 2007.
[135] "High Resolution Focused Ion Beams: FIB and Its Applications". Edited by J. Orloff, M. Utlaut, and L. Swanson, Kluwer Academic/Plenum Publishers, NY, 2003.
[136] "Ion Implantation, Sputtering and Their Applications" Edited by P.D. Townsend, R. Kelly and H. New, Academic Press, pp. 137-42, 1976.

simple structure such as a square or round hole in the material, but also a more complex pattern. The milling rate is directly related to the choice of ion, its energy range and the momentum of the particle (its weight). Using the milling feature, the sample can be manipulated to create any possible shape. The main difference with etching using a sample mask is in the control of the lateral milling position, and in local depth control. The removal rate of atoms can be enhanced by local chemistry, via a gas delivery system (using gases such as I_2 and XeF_2) that substantially speeds up the milling process, while reducing the local re-deposition of released atoms.

Although the majority of atoms emitted from the sample are not used, the emitted ions can be used. In principle, the ions can be analysed and their species and properties can be determined using SIMS.

Figure 8.27. Silicon surface showing both the milling and deposition features, as examples of the creation of local structures. A, B, C and D are micro-depositions, whereas E, F and G are structures milled into the sample.

(b) Manufacturing nanostructures using ions:

In the semiconductor industry, FIB is often used to patch or modify an existing semiconductor device. For example, with an integrated circuit, the gallium beam could be used to cut unwanted electrical connections, or to deposit conductive material in order to make a connection.

The FIB is also commonly used to prepare samples for the transmission electron microscope. The TEM requires very thin samples, typically ~100 nanometres. Other techniques, such as ion milling or electropolishing can be used to prepare such thin samples. However, the nanometre-scale resolution of the FIB allows the exact thin region to be chosen[137, 138]. This is vital, for example, in integrated circuit failure analysis. If a particular

[137] Tartuani M, Takai Y, Shimizu R, Uda K, and TakahashiH, "Development of a Focused IonBeam Apparatus for Preparing Cross-Sectional Electron Microscope Specimens," Tech. Rep. Osaka Univ., Vol. 43 (2143), 1993, 167-73.

transistor out of several million on a chip is bad, the only tool capable of preparing an electron microscope sample of that single transistor is the FIB (Figure 8.28). There are several ways to extract the FIB machined foil from the bulk sample (the so-called *ex-situ* and *in-situ lift-out* techniques (Figure 8.29) or the more conventional *H* and *tripod* procedures).

Figure 8.28. Ultrathinned copper lamella for TEM observations, that have been fabricated completely automatically.

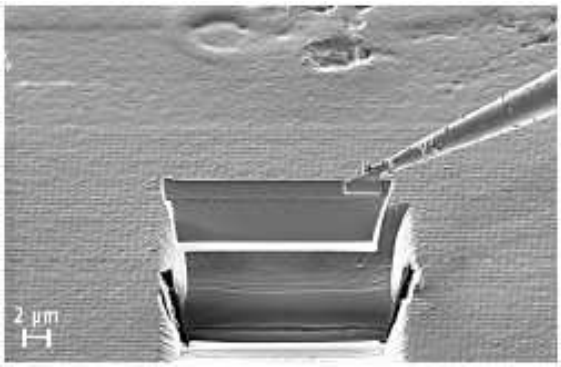

Figure 8.29. In-situ lift-out technique. The sample is cut out and lifted out of the substrate after a rough milling by welding the tool to the lamella using metal deposition. The lamella is transferred to a TEM grid and welded to the grid using GIS metal deposition . After retracting the tip, the sample is thinned for electron microscopy.

The ET detector (*Everhart and Thornley*) of a typical FIB device is located behind the sample and records the secondary electrons that are emitted from the sample reverse side. This signal provides information about the transparency of the lamella being thinned.

[138] J.P. McCaffrey, M.W. Phaneuf and L.D. Madsen, "Surface damage formation during ion-beam thinning of samples for TEM", Ultramicroscopy, 87, 2001, 97-104.

FIB is the ideal instrument to provide micro machining and micro patterning solutions for current and future applications. As a FIB provides accurate control over milling parameters and deposition parameters, it is the ideal tool for the rapid creation of small structures for nanotechnology. It is a maskless technique and highly flexible and fast for serial 3D patterning.

(c) Chemical etching and material deposition

The FIB equipment provides a complete solution for sophisticated gas chemistry. Gas injection systems allow metal and insulator deposition, enhanced etching, device modification, etc. FIB-assisted chemical vapour deposition occurs when a gas, such as tungsten carbonyl ($W(CO)_6$), is introduced into the vacuum chamber and allowed to chemisorb onto the sample. By scanning an area with the beam, the precursor gas will be decomposed into volatile and non-volatile components; the non-volatile component, such as tungsten, remains on the surface as a deposition. Metal and insulator depositions are used for various purposes. Such applications are: the deposition of protective layers to preserve the sample surface in preparation for TEM during the ion milling process, or the deposition of conductive layers.

To avoid the redeposition of sputtered material, and to enhance the milling rate on many materials, gas injection systems are used to insert special precursor gases into the specimen chamber. These volatile products react with the substrate after being activated by the ion beam.

(d) Image

The following particles leave the sample when irradiated with ions: neutral atoms, positive and negative ions, and electrons. Charged particles, whether ions or electrons, can be used as an imaging signal (Figure 8.30). Since the ion beam can be strongly focused and scanned over the area, it can be used to create images at high magnification. Note that the milling process itself continues during imaging, but at a very low rate, because this application uses small spots and low beam currents. Although the top layer is removed continuously with every scan during imaging, in practice this effect is often negligible. Another advantage of this gradual low rate milling is that the sample is “continuously cleaned” during imaging. In crystalline materials such as metals the (secondary) ion signal will produce an excellent additional contrast that reveals the different grains of the material.

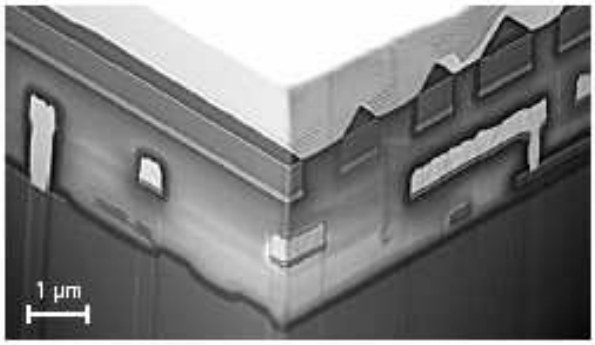

Figure 8.30. 3D ion image of an integrated circuit.

(III) Dual beam technology (FIB and SEM)

This technique combines the ultra high resolution of a scanning electron microscope with the focused ion beam. The system consists of live e-beam imaging during FIB and/or gas injection, satisfying even the most demanding needs. It is a state-of-the-art combination of real-time 3D analysis, nano-scale manipulation and imaging. The double beam tool opens a new dimension in TEM sample preparation. The risk of destroying the ultra-thinned TEM lamella is reduced to a minimum, as the sample can be imaged at high resolution in real time with the aid of the electron gun, while the thinning process is being achieved with the ion beam. A dual beam device combines ultra high resolution imaging with the full analytical capabilities of an EDS detector (energy dispersive spectrometer).

The main dual beam equipment is:

(a) Ion source and gun

The ion optics provides an excellent resolution, high current densities and a large beam voltage, between 3 and 30 kV. The ion beam is generated in a high brightness liquid metal ion source and focused onto the specimen surface by an electrostatic dual lens system. Computer controlled stabilization of the emission current and the selection of different probe currents give the user full control in automatization processes. An integrated Faraday cup allows accurate probe current measurements during operation. In the case of a dual beam device, the final lens of the SEM is designed as a magnetic/electrostatic compound lens in order to avoid magnetic fields interferences with the ion beam. Thanks to this, the SEM can be operated at nm resolution during ion beam milling, allowing full control over the process and excellent end-point detection and cut location. The dual beam tool can operate in three different imaging modes. First, by using only the electron beam as a high resolution SEM. Second, by using only the ion beam, which is especially indicated for grain analyses, voltage contrast imaging and the definition of milling areas. The last imaging mode uses both beams, the SEM being used to acquire the high resolution, real time image, while the ion beam is milling a defined area. This enables the operator to control the milling process visually on a nanometre scale.

(b) Chamber

It has a highly flexible configuration allowing the incorporation of detectors and analytical systems through several admission ports.

(c) Large specimen holder

The large 200x200 mm holder allows positioning bulky samples, i.e., wafers of up to 8", to speed up the transfer process. The optical microscope is equipped with a binocular head with a magnification of 10 times and a high-resolution video system with a colour camera, and a monitor that includes automatic brightness and contrast control.

(d) High precision micromanipulator

The device includes one high-precision 3-axes hanging joystick, of the hydraulic oil micromanipulator type, to transfer the lamella. The rounded hanging joystick configuration

requires a constant driving force, which is achieved with improved springs in the drive unit. Changing over from left to right hand usage is a simple matter of adjusting two setting screws.

(IV) Material Science Applications

The literature mentions a large variety of applications for the FIB technique. The extremely fine ion beam that can be controlled with high precision allows performing a large number of studies, involving a very broad range of materials, which in some cases cannot be handled by other techniques, and with applications in many different fields.

The cutting and the preparation of TEM samples is a standard operation, carried out according to a common and well-studied procedure.

The imaging of sequential cuts using this method is a powerful tool for obtaining a three-dimensional reconstruction of a modified material. Here, it has to be cited the case, absolutely relevant for future studies in *TechnoFusión*, of the analysis and measurement of the distribution of the cracks created around an indentation imprint in a slice of silicon glass[139]. The equipment allows controlling the position and the size of the cuts with a precision better than 100 nm. 3D FIB tomography offers the additional advantage of quantifying the three-dimensional shape and size of the web of cracks and of the cracks individually, at a high spatial resolution.

(V) Suggested equipment

1) Quanta 3D FEG Dual Bea, by FEI

This Dual Beam instrument of FEI company[140] is a double column SEM and FIB device in which the electron beam is positioned to image the surface of a cross section milled by a focused ion beam. It is the most versatile high-resolution, low vacuum SEM/FIB for 2D and 3D material characterization and analysis. Using a field-emission electron source, it delivers clear and sharp electron imaging. An increased electron beam current enhances EDS and EBSP analysis. Featuring three imaging modes (high-vacuum, low vacuum -up to 4000 Pa- and ESEM) it accommodates the widest range of samples of any Dual Beam system. With low and ESEM vacuum it offers charge-free imaging and analysis of non-conductive specimens and/or hydrated specimens. The in-situ study of the dynamic behaviour of materials at different humidity levels (up to 100% relatively humidity) and temperatures (up to 1500 ºC) is also within the possibilities of the Quanta 3D FEG. This unprecedented high-current FIB enables fast material removal. Automated FIB sectioning recipes enable accurate cross-sectioning. On top of the site-specific milling and excellent imaging capabilities of the FIB, a large selection of gases is available to deposit materials or further enhance the FIB milling rate, by avoiding re-deposition or material selectivity. The Dual Beam features SEM imaging while milling.

[139] Elfallagh, F. and Inkson, B.J. "3D analysis of crack morphologies in silicate glass using FIB tomography", J. Europ. Ceram. Soc., 29 (1) 2009, 47 – 52.
[140] www.fei.com

2) NVision 40, by Zeiss

This device[141] is a new and powerful combination of FIB and GEMINI® column. The NVision 40 CrossBeam® workstation combines the imaging and analytical capabilities of the high resolution field emission GEMINI® SEM with the high performance SIINT zeta FIB column. Together with the new SIINT GIS supporting liquid, solid state and gaseous precursors, as well as gas mixing technology and carbon free SiO2 deposition, the NVision 40 represents a powerful tool for 3D high resolution nanoscale imaging, structure determination and analysis. The NVision 40 features a dome type chamber design and a pendulum vibration insulation system for enhanced stability. It offers numerous access ports for various detectors (EDS, EBSD, STEM, 4QBSO), as well as sample manipulation and probing systems that ensure full support for all analytical and micromanipulation needs. These versatile features and flexible upgrade possibilities make the NVision 40 a highly valuable platform for your current and future nanotechnology needs.

(VII) Research groups and associated bibliography

- *Oxford Materials Group*. Oxford University. Parks Road Oxford, OX1 3PH. Prof. A. Cerezo.
- *Imaging damage evolution in a small particle metal matrix composite.* R. D. Evans, M. W. Phaneuf and J. D. Boyd., Journal of Microscopy, 196, 1999, pp. 146–154.
- *Introduction to focused ion beams: instrumentation, theory, techniques and practice. FIB for materials science applications - A review.* pp 143-172. Phaneuf, MW. Ed. SPRINGER, New York, NY 10013, USA 2005.
- *Micromachining by focused ion beam (FIB) for materials characterization.* Jud, PP, Nellen, PM and Sennhauser, U., Adv. Eng. Mater., 7 (5) 2005, 384-388.
- *TEM investigation of FIB induced damages in preparation of metal material TEM specimens by FIB.* Yu, JS, Liu, JL, Zhang, JX and Wu, JS., Mater. Lett., 60 (2) 2006, 206-209.

8.4.6. In-situ characterization techniques

8.4.6.1. In-beam micromechanical measuring systems

As mentioned above, the mechanical properties of structural materials for future fusion applications will degrade due to radiation damage, modifying their characteristics. During

[141] www.smt.zeiss.com/crossbeam.

irradiation, the point defects that are continuously generated will move across the material structure, and its mechanical behaviour may depend on external loads being applied. Among others, the irradiation may produce significant plastic deformation. In order to characterise the mechanical properties under irradiation, the study of creep and creep-fatigue is considered essential (in so-called *in-situ* experiments). It is widely acknowledged that in-situ creep-fatigue experiments provide much more realistic estimates of the lifetime of the structural material than laboratory experiments performed on test samples after irradiation. Therefore, the study of the synergic effect of the application of stress and irradiation on mechanical properties is considered a priority at *TechnoFusión*, for which in-beam measuring techniques are required. Furthermore, the study of mechanical properties while the material is subject to modification was extended to include the analysis of creep and creep-fatigue while the materials are submitted to lithium liquid flow or while they are in contact with fusion plasmas.

In-situ mechanical testing is so exceptional that it was considered convenient to perform a technological study to develop *in-beam* creep and fatigue testing modules and the corresponding tools, particularly to test very small specimens. Only a few papers [142, 143], have been published ¡on mechanical testing during irradiation, due to the fact that this approach is still very novel. Such is the case of the creep-fatigue modules for in-situ testing at the IFMIF test facility, whose operational radiation conditions for validation are only now being established. The conclusions of that effort, referring to experiments with a neutron radiation source, have inspired the initial approach to the design of the creep-fatigue testing modules for the *TechnoFusión* triple ion beam facility. The mechanical testing of materials in contact with dynamic metal liquids will require of non-commercial micromachine adapters.

The results and conclusions of both technological analyses are annexed to this report. Even so, the existing techniques for the detection of deformations without physical contact are summarised below.

Contactless extensometry:

These techniques allow measuring deformations at a distance. They are especially useful when deformation data are required for samples placed inside conditioning chambers or furnaces. Their use is also recommended when the samples are small or when the samples are being irradiated, as contact methods could suffer malfunctions. Laser extensometry is one of these techniques. Many laser-based systems exist (Figure 8.31), that differ with regard to the methods for signal detection and deformation measurement: one technique uses digital image correlation (Figure 8.32), allowing the detection of a deformation field instead of just pointwise deformation measurements; another is based on Speckle interferometry (Figure 8.33), and yet another on video recording (Figure 8.34).

[142] P. Vladimirov, A. Möslang, P. Marmy. Fusion Engineering and Design 83 (2008) 1548–1552.
[143] K. Ueno, J. Nagakawa, Y. Murase, N. Yamamoto. Journal of Nuclear Materials 329–333 (2004) 602–606.

Figure 8.31. Laser extensometry systems.

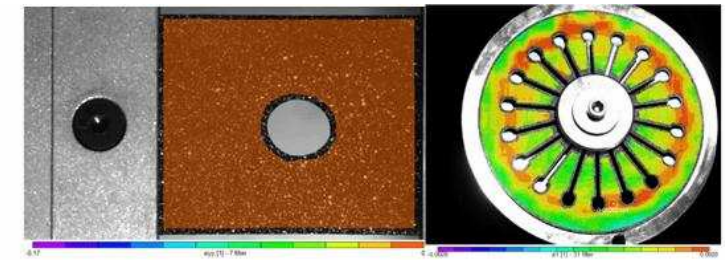

Figure 8.32. A laser extensometry system based on digital image correlation.

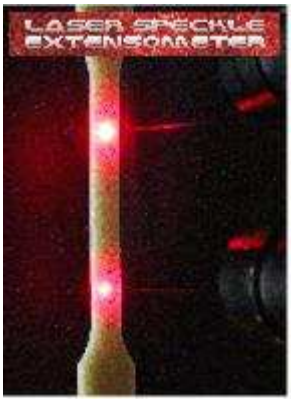

Figure 8.33. A laser extensometry system based on Speckle interferometry.

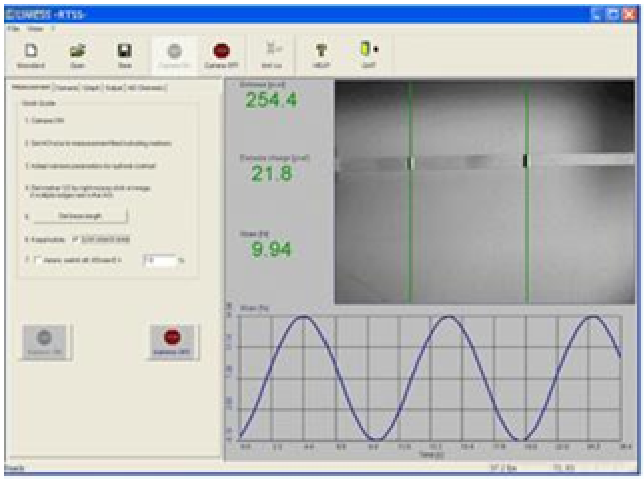

Figure 8.34. Laser extensometry: video system.

8.4.6.2. Ion beam analysis techniques

(I) Introduction

Ion Beam Analysis techniques (IBA) refer to all techniques involving the interaction of an ion beam with matter. The following processes might occur, depending on the type of interaction between the incoming particle and the target, as shown in Figure 8.35.

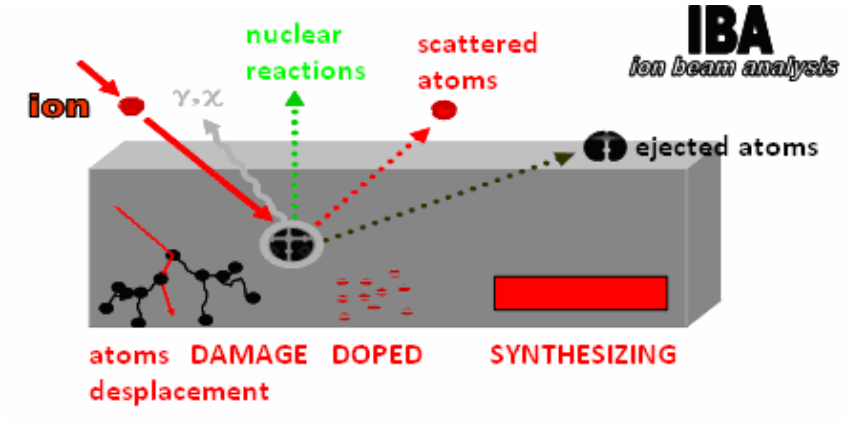

Figure 8.35. Reaction products generated by the interaction ion-solid.

In general, IBA techniques are non-destructive and constitute a powerful tool to characterize the structural composition of materials in the near-surface region (2 nm ~ 1µm, depending on the selected technique), and their breakdown in terms of elements. One of the most interesting properties of these techniques for material analysis is that they allow the detection of most chemical elements with a high accuracy. Moreover, samples do not require any special treatment prior to analysis. It should also be mentioned that some IBA techniques can be used simultaneously, allowing the accurate qualitative and quantitative characterization of the atomic composition, and the determination of the distribution of target elements as a function of depth below the surface.

Among the IBA techniques listed in Table 8.1, the most promising ones for the study of material properties for fusion applications are: Rutherford Backscattering Spectrometry, non-Rutherford Backscattering Spectrometry and Nuclear Reaction Analysis. A brief description of these techniques is given in the following sections.

Table 8.1. Classification of IBA techniques.

Energy	Typical ion	Technique name
1 – 10 MeV	He^{2+}, p	PIXE, PIGE, RBS, Channeling, ERDA
1 – 10 MeV	H^+, D^+, He^+	NRA
10 – 100 MeV	Ag, Cu^{10+}	ERDA

PIXE: *Particle Induced X-ray Emission*. PIGE: *Particle Induced γ-ray Emission*. RBS: *Rutherford Backscattering Spectroscopy*. ERDA: *Elastic Recoil Detection Analysis*. NRA: *Nuclear Reaction Analysis*.

(II) Rutherford Backscattering Spectrometry

Rutherford Backscattering Spectrometry (RBS) [144] is based on the elastic two-particle scattering of energetic ions on sample atoms due to the repulsive Coulomb force acting on positively charged atomic nuclei. It involves measuring the number of ions in the backscattered beam and their energy.

The energy of a backscattered particle at a given angle depends on two processes: the energy loss of the particle along its trajectory through the sample, both before and after the collision (the amount of energy lost depends on the material's stopping power) and the energy lost as the result of the collision itself. The collisional energy loss depends mainly on atomic masses of the projectile and the target. The ratio of the energy of the projectile before and after collision is called the *kinematic factor*. The number of backscattered particles for a given

[144] Tesmer J R, Nastasi M 1995 Handbook of Modern Ion Beam Materials Analysis MRS p. 158.

element in a sample depends on the concentration of that element and on its *scattering cross section*.

Backscattering spectrometry with beams of ions in the MeV range has been extensively used to determine stoichiometry of the target and the distribution of target elements as a function of depth below the surface. For a typical RBS analysis, He beams with energy in the range of 1-2 MeV are commonly used. He is used because He beams are easily obtained, the stopping power for He ions is known for almost all elements of the periodic table, the energy resolution of a standard Si detector is typically around 11-15 keV, and, most importantly, its cross section for elements heavier than Be is close to the Rutherford cross section in this energy range.

A typical backscattering geometry is depicted in Figure 8.36, together with an RBS spectrum corresponding to a thin film coating deposited on a Si substrate. A detailed description of the physical principles of the technique is given below.

The RBS process can be described in terms of a simple model of elastic collisions between the incoming particle and the constituent atoms of the material. The relation between the energy of the backscattered ion, E_1, after colliding with the sample atom, M_2, and the energy of the incoming ion, E_0, is given by the kinematic factor, K, defined by the following expression, 8.1:

$$K = \left[\frac{\left(M_2^2 - M_1^2 sen^2\theta\right)^{1/2} + M_1 \cos\theta}{M_1 + M_2} \right]^2 \qquad \text{eq. 8.1}$$

Where M_1 is the mass of the incoming ion and ϑ is the dispersion angle. Thus, the value of K lies between 0 and 1, such that small values of K correspond to large energy transfers.

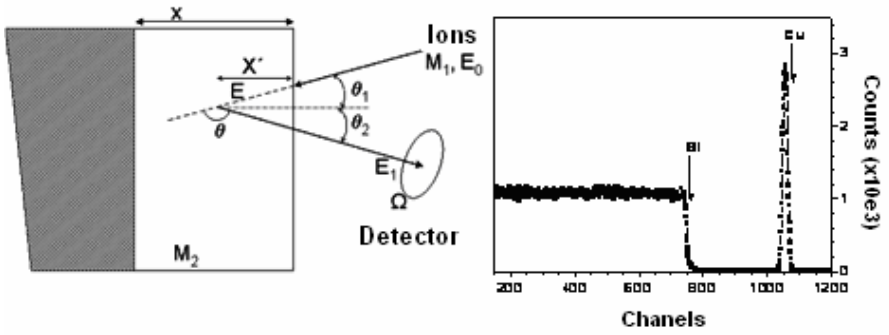

Figure 8.36. Typical backscattering geometry (right). RBS spectrum taken with a 2 MeV He beam on a Cu_3N thin film (left).

The measured energy of a particle that is backscattered at a certain depth *x* depends on the energy loss $\Delta E = E_0 - E$, where E_0 is the initial energy and *E* the final energy in units of eV. The quantity that quantifies the energy loss is the stopping power (*S(E)*), defined as the "loss of particle energy per unit distance", according to equation 8.2:

$$S(E) = \frac{dE}{dx} \qquad \text{eq. 8.2}$$

Usually, the stopping power is expressed in units of keV/nm or eV/(10^{15} at/cm^2).

Figure 8.37 shows a sketch of the energy loss in a material with a thickness of Δx.

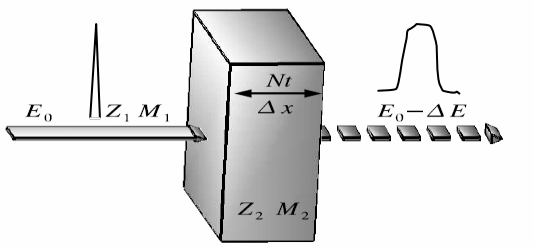

Figure 8.37. Sketch of the energy loss of an ion beam with ions of mass M_1 and atomic number Z_1, impacting with energy E_0 on a slice of material with thickness t and density Nt (N being the atomic density). After traversing the material. the exit energy of the particle is E_0-ΔE, where ΔE is the energy loss

The number of backscattered particles by a given element depends both on the concentration of the latter in the sample and on its elastic dispersion cross section (σ), which is essentially proportional to the square of the elements in the target. If one assumes that the force between the incoming nucleus (M_1, Z_1, *e*, *E*) and the target nucleus (M_2, Z_2, *e*, initially at rest) is the Coulomb force, $F_{12}=(Z_1Z_2e^2/r^2)r$, then the cross section of the interaction, $\sigma i(E,\vartheta)$, can be written as the Rutherford cross section, σ_R, which is given by equation 8.3 in the laboratory system of reference:

$$\sigma_R(E,\theta) = \left(\frac{Z_1 Z_2 e^2}{\alpha E}\right)^2 \times \frac{4\left[\left(M_2^2 - M_1^2 \sin^2\theta\right)^{1/2} + M_2 \cos\theta\right]^2}{M_2 \sin^4\theta \left(M_2^2 - M_1^2 \sin^2\theta\right)^{1/2}} \qquad \text{eq. 8.3}$$

The surface density $(Nt)_i$ expressed in atoms per unit area, can be calculated for the i constituents of the material from the solid angle of the detector (Ω) and the number of counts of the corresponding signal A_i for a given accumulated ion charge (*Q*) and cross section $\sigma i(E,\vartheta)$, using the equation below, where ϑ_1 is the incident angle of the beam with respect to the normal of the sample surface, N_i the atomic density, and *t* the thickness:

$$\sigma_R(Nt)_i = \left(\frac{A_i \cos\theta_1}{QW\sigma_i(E,\theta)} \right) \qquad \text{eq. 8.4}$$

To obtain information on the depth profiles from the backscattering data, it is necessary to relate the energy of the scattered particle to the sample depth where the scattering occurred. To translate the energy to a depth value, the measurement must be calibrated, taking into account the stopping power of the backscattered particles in the material under study. Basically, this calibration consists in establishing a relationship between the channel number at which the surface peaks are observed for two elements with significantly different mass number and backscattered energy. For calibration purposes, the density of the material has to be known.

(II) Non-Rutherford Backscattering Spectrometry

Experimental measurements indicate that cross sections depart from the Rutherford estimate at both high and low energies for all projectile-target pairs. Usually, a significant enhancement of the cross section with respect to the Rutherford value is observed in these particular energy ranges. This enhanced cross section is commonly known as resonant or non-Rutherford, and it constitutes the basis for an analytical technique known as *non-RBS*.

The departure at low energy of the cross sections from the Rutherford value is caused by the partial screening of the nuclear charges by the electron shells surrounding both nuclei. The high-energy departures are caused by the presence of short-range nuclear forces.

Advantages offered by the non-RBS technique are: improved accuracy in the determination of stoichiometric ratios and enhanced sensitivity to the detection of light elements in heavy-element matrices. Moreover, the narrow energy window in which the resonances occur allows characterizing the depth distribution of light elements with a very high resolution (excitation curve)[145], as shown in Figure 8.38.

[145] Andrzejewska E, Gonzalez-Arrabal R, Borsa D, and Boerma D O 2006 Nucl. Instr. Meth. B. 249 838.

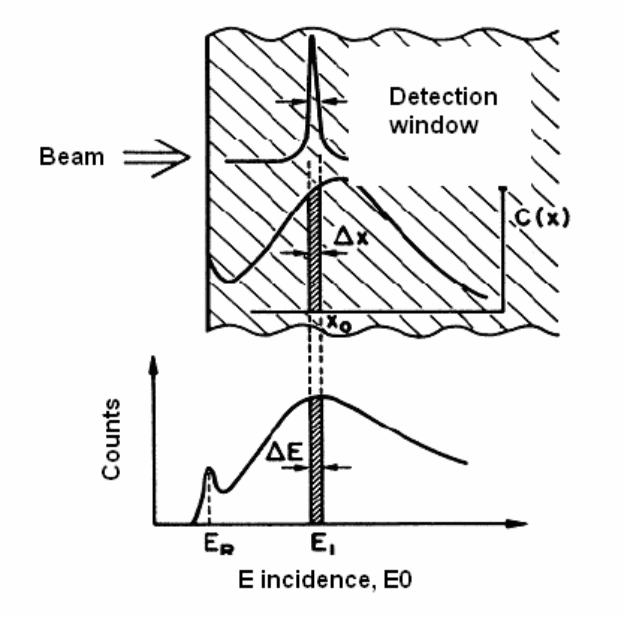

Figure 8.38. Resonant measurements for the determination of the depth distribution of light elements in heavy-element matrices.

(IV) Nuclear reaction analysis

Nuclear Reaction Analysis (NRA) consists of the detection of the reaction products produced by the nuclear reactions that occur when the energy of the incident beam (usually ionized H, D or He) is above a certain threshold.

The main advantage of the NRA technique is that the energy of the reaction products is usually higher than the energy of the incident beam. Therefore, the backscattered particles are well separated from the reaction products in the spectrum, which enhances the sensitivity of this technique to light elements notably. Indeed, it is commonly used to detect small concentrations of light elements (~10^{13} cm^{-2}) in heavy-element matrices.

Nevertheless, NRA also has some disadvantages that are to be taken into account when designing an experiment. Some are listed below:

- Usually, the cross section of the nuclear reactions is much lower than that of RBS. Therefore, it is necessary to perform measurements for a very long time in order to obtain the same statistics.

- More than one nuclear reaction can occur in the sample, resulting in the production of different particles and complicating the interpretation of the spectrum. In order to avoid this problem, absorber foils can be used, so that the products of different nuclear reactions can be distinguished.

- At the beam energies that are typical of NRA analysis, often neutrons are generated (especially with a deuterium beam). Therefore, strict safety rules must be observed.

- In order to determine the concentration of elements, the results must be compared to standards.

(V) Equipment

The study of materials using ion beam techniques requires the following equipment: ion beam sources, particle accelerators, a beam line (all described in section 5.4.), an analysis chamber and an electronic connection to transport the signal to the analysis computer.

(a) Beam line:

This is a metal pipe guiding the beam from the accelerator to the analysis chamber. It is equipped with specialized devices and equipment used for particle beam maintenance, monitoring, and focussing. The beamline includes sophisticated lenses, collimators, deflectors, Faraday cups and beam profile monitors.

(b) Analysis chamber and detectors:

The analysis chamber is normally made of steel and equipped with multiple ports to house fixed detectors and a mobile detector (Si-barrier, Ge- or Li- doped, NaI) to collect the backscattered particles and the nuclear reaction products. The mobile detector is built on a ring with a micrometer screw that allows selecting the scattering angle in the experiment (sample-detector angle). A rotating filter holder, with foils of a different thickness and with different slit apertures to change the solid angle, is generally placed in front of the mobile detector in order to select certain particles. Semiconductor detectors are commonly used, and their polarization requires the application of high voltages. Therefore, high voltage sources are also needed.

(c) Sample holder and goniometer:

The samples are placed in a holder fitted in a goniometer. The goniometer should be specially designed for low activation and high thermal conductivity. The positioning of the sample with respect to the incident beam is typically done by a goniometer with three axes, fitted to an x-y table to allow four-dimensional movement (Figure 8.39).

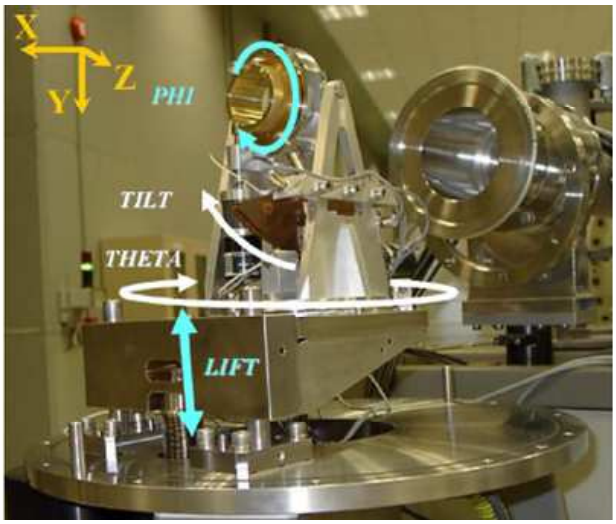

Figure 8.39. Goniometer with three axes used in the standard beam line at the Centro de Microanalisis de Materiales (CMAM/UAM).

During the ion-matter interaction, a certain number of secondary electrons are produced. Therefore, it is common to use electron suppressors to avoid that these secondary electrons affect the measurements of the beam current. An electron suppressor is a metallic ring that is polarized with a negative voltage. It is placed near to the sample holder.

(d) Vacuum components:

Since the ion beam analysis is usually carried out in vacuum conditions, the following equipment is needed: pumps (rotary and turbo-molecular) to achieve a vacuum in the 10^{-6} mbar range, full-range pressure gages (Penning-Pìrani) and a nitrogen gas circuit to vent the analysis chamber when needed.

(e) Electronic circuitry:

The electronic circuitry delivers the detector signal to the multi-channel acquisition system. This circuitry includes preamplifiers, amplifiers, converters and a PC for data storage.

(f) Data acquisition:

This is usually done using commercial programs (High Voltage Engineering), although in some cases custom-designed expert software may be needed.

(VI) Research groups and relevant literature

- Gordillo N, González-Arrabal R, Martín-González M S, Olivares J, Rivera A, Briones F, Agulló-López F, and Boerma D O. J. Crystal Growth. V.310 p. 4362. 2008

- *Handbook of Modern Ion Beam Materials Analysis.* Tesmer J R, Nastasi M MRS. p. 158. 1995

8.4.6.3. *In-beam* measurement of electrical conductivity

Due to the fact that a future fusion reactor is an electromagnetic device, the study of the degradation of electrical insulation properties of candidate insulator materials in the hostile environment (high temperature, irradiation, and particle bombardment) of a fusion reactor is of utmost importance. It is known that the electrical conductivity of insulators is enhanced when they are exposed to a radiation field.

Three types of such degradation are well known:

I. *Radiation Induced Conductivity* (RIC). The radiation field produces electron–hole pairs, and when the insulator is subjected to an electric field this gives rise to an electrical current. This type of enhanced electrical conductivity disappears when the radiation field is turned off.

II. *Radiation Induced Electrical Degradation* (RIED). In this case, the material that has been subjected to a radiation field at an elevated temperature and with an applied electric field is permanently damaged, so even after removing the radiation field the electrical conductivity of the material is enhanced by several orders of magnitude.

III. *Surface Electrical Degradation*. The preceding two types of conductivity enhancement occur in the bulk. When an oxide is subjected to purely electronic excitation or particle bombardment, much oxygen is removed from the surface and as a consequence, an enormous increase in electrical surface conductivity occurs.

These electrical degradation effects must be quantified for all materials to be used in fusion reactors. It is necessary to perform such experiments in accelerators, considering the access and economy offered by such devices.

In order to perform electrical conductivity measurements of the insulating materials, the samples will be placed in a sample holder inside an oven that is connected to earth. The temperature of the sample will be measured with a thermocouple on the surface of the oven, right underneath the sample. The samples will be prepared with electrodes, deposited on both sides, one in the shape of a guard ring while the other will act as a common ground electrode, connected with the oven and therefore grounded. On top of the central and guard electrodes, tungsten wires will be placed to hold the sample in place and to guarantee a proper electrical

contact. Tungsten is chosen in order to avoid mechanical problems due to the heat produced by the oven or the particle beam. In turn, these tungsten wires are connected to electrical feedthroughs with a high degree of insulation. Outside the irradiation chamber, a connection is made to a doubly screened coaxial wire in order to carry the corresponding electrical currents and applied voltages to the test sample. The coaxial wire will be several meters long, according to the distance from the irradiation chamber to the control room. Power supplies will apply voltage to the sample and the resistance of the sample will be evaluated from the voltage drop across the resistors placed in series with the sample. By applying an identical or a different voltage to the central and guard electrodes, the conductivity of the sample can be measured, while separating the surface from the bulk contribution. While the sample is being irradiated, the conductivity of the sample will increase and the experimental system will allow measuring the RIC. Also, it will be possible to heat the sample and to measure the surface and bulk conductivity as a function of temperature.

8.4.6.4. Measurement of in-beam optical properties

The system described here will allow measuring both the optical absorption and the radio-luminescence during irradiation by the beam.

The beam and the optical axis will intersect each at an angle of 90 degrees in the irradiation chamber at the sample position. The irradiation chamber will be fitted with an electrical oven and a beam collimator to perform the measurements at a controlled temperature and flux. The irradiation chamber will have a pair of vacuum silica windows on the optical axis to allow the transmission of UV, VIS and IR light.

The following equipment will be needed outside the irradiation chamber:

1. A high intensity (1000 W) Xe UV lamp, and the corresponding starter system and power supply.

2. A monochromator for optical absorption measurements (Lamp monochromator).

3. A rotating light chopper to separate light from noise due to the radiation background.

4. An optical lens to concentrate light on the sample.

5. A second rotating chopper to separate the radio-luminescent emission from the radiation background.

6. A second monochromator to measure the radio-luminescent emission (RL monochromator).
7. A photomultiplier to convert the light intensity at different wavelengths to an electrical signal.

8. A stepping motor (and the corresponding drivers and power supply) to move the lamp monochromator.

9. A stepping motor (and the corresponding drivers and power supply) to move the radio-luminescence monochromator.
10. A stepping motor to insert or remove the radio-luminescence monochromator into or from the optical axis.

11. A control room computer fitted with a data acquisition and control board will be required to control the experimental system and to acquire the data. A software programme will have to be developed to perform the measurements

Note: All electronic systems placed near the radiation chamber (stepping motor drivers, power supplies, preamplifiers, etc.) will need to be shielded from the radiation environment in order to avoid radiation damage to sensitive electronic components.

The light emitted by the UV lamp will be split by the monochromator, while a stepper motor will rotate the monochromator to measure optical absorption spectra at different wavelengths. The light is chopped and passes through the vacuum silica glass window before it reaches the sample. During irradiation, point defects are produced that absorb light, so it is possible to evaluate the production of such defects by measuring the optical absorption. Also, it will be possible to perform in situ thermal annealing (under vacuum and in the beam).

In order to perform radio-luminescence measurements, the RL monochromator will need to be placed on the optical axis by remote control. The rotating chopper will allow distinguishing the light emitted from the sample from the radiation background. As the sample is irradiated, point defects are produced that emit light (radio-luminescence), so it is possible to evaluate the radiation damage as a function of temperature, dose rate and dose.

8.4.6.5. In-beam diffusion measurements of ionic species

The knowledge of transport phenomena and parameters related to the inventory of hydrogen and its isotopes is a relevant issue for fusion security, reproducibility and fuel generation[146, 147].

In this framework, the study of the diffusion and permeation of tritium in structural materials that are candidate materials for fusion has received a strong impulse. Presently, a number research groups are developing coating materials for structural components in order to reduce tritium transport in a concept design for a Pb-Li cooled breeder blanket[148].

[146] J. Konys, A. Aiello, G. Benamati y L. Giancarli. Status of tritium permeation barrier development in the EU. *Fus. Sci. Tech*., **47**, 2005, 844-850.
[147] G. Benamati, E. Serra y C.H. Wu. Hydrogen and deuterium transport and inventory parameters through W and W-alloys for fusion reactor applications. *J.Nucl.Mater.,* **283-287**, 2000, 1033-1037.
[148] G. Benamati, A. Donato, A. Solina, R. Valentini y S. Lanza. Experimental studies on hydrogen diffusion and trapping in martensitic and austenitic stainless for fusion application. *J. Nucl. Mater.,* **212-215**, 1994, 1401-1405.

Recent studies[149] on ODS steels have shown that the solubility of hydrogen isotopes increases due to their specific microstructure: the dispersion of yttrium oxide particles favours hydrogen trapping and consequently reduces its transport. These results suggest shifting the focus of materials research towards new reinforced alloys with dispersed oxide that will act as tritium barriers.

Considering the proven experience of some Spanish technology groups, and the specialized facilities soon to be available at *TechnoFusión*, the development of an experimental chamber for the study of the transport properties of D and H during irradiation and at high temperatures is proposed here.

A disc-shaped test specimen will be placed inside the experimental chamber and submitted to a differential pressure across the surfaces. After injecting a pressurized gas, the pressure increase on the opposite side, due to the gas permeation, will be registered as a function of time. Leaks are prevented by placing the sample disc between two gold rings and pumping out any leaking gas to a secondary chamber. Figure 8.40 shows a chamber used to perform similar permeation experiments. The need to test materials under fusion-relevant conditions has inspired the further development of the measuring module by adding an electrical oven to heat the specimen to 600-1000 ºC. Additionally, one of the specimen surfaces could be subjected to *in-situ* ion implantation by means of the triple ion beam facility, increasing the interest of the experiment.

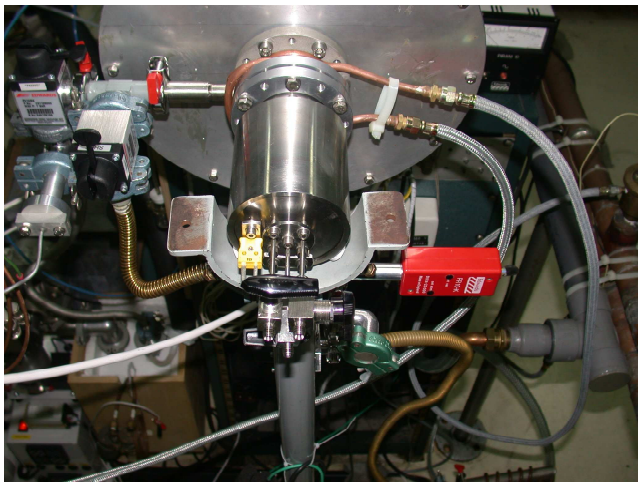

Figure 8.40. Experimental device for H permeation tests of candidate materials for fusion applications during electron irradiation at CIEMAT, Madrid, Spain.

[149] G.A. Esteban, A. Pena, F. Legarda y R. Lindau. Hydrogen transport and trapping in ODS-Eurofer. *Fus. Eng. Des.*, **82**, 2007, 2634-2640.

8.4.7. Non-destructive methods for the characterization of components and joints

8.4.7.1. Photothermal thermography

This method is based on the study of the propagation of thermal waves in reactor components, after applying an external stimulus consisting of IR sinusoidal waves. Specific software is needed to store and process the material response[150, 151]. The calculated delays will depend on the thermal diffusivity of the material along the path followed by the heat wave, which depends on cracks in the material.

8.4.7.2. Ultrasound

As an ultrasound wave propagates through a given material, it is affected by the material characteristics and presence of defects[152,153]. In the particular case of an interface between two different materials, as in the case of a material coated with CFCs, some waves are reflected and others transmitted. Sound that is reflected back towards the transducer produces an echo that is registered on the screen, and can be characterized according to its amplitude and time delay. Defects in the material volume also reflect back the sound. When the defects are located at the joint or the interface, the reflection is intensified. Likewise, attenuation indicates a bad joint or an increase of pores, vacancies and defects at the interface. Efficient wave propagation from transducer to the joint is achieved using water as an acoustic coupling media.

8.4.8. Auxiliary laboratory for sample preparation

The study of the materials through the characterization techniques present in the different Facilities of *TechnoFusión* (Plasma-Wall Interaction, Materials Production and Processing, etc.) will require an auxiliary laboratory for the sample preparation. This laboratory will be of common use for all the experimentation facilities of the Centre and it will have the following equipment:

- *High accuracy cutting tools* (automatic and manual diamond saws).

[150] D. Wu, Th. Zweschper, A. Salerno, G. Busse, Lock-in Thermography for Nondestructive Evaluation of Aerospace Structures, vol. 3, no. 9, NDT.net, 1998.
[151] F. Escourbiac, S. Constans, X. Courtois, A. Durocher. "Application of lock-in thermography non destructive technique to CFC armoured plasma facing components", Journal of Nuclear Materials, 367–370 (2007) 1492–1496).
[152] A. Durocher, J. Schlosser, J.J. Cordier and G. Agarici, "Quality control of plasma facing components for Tore Supra", Fusion Engineering and Design, 66–68 (2003), 305.
[153] M. Merola, M. Akiba, V. Barabash y I. Mazul, "Overview on fabrication and joining of plasma facing and high heat flux materials for ITER", Journal of Nuclear Materials 307–311 (2002) 1524–1532.

- *Polishing equipment*: filler, metallographic polishing machine, for plane-parallelism polisher.

- *Sample preparation equipment for Transmission Electron Microscopy:* ultrasonic disk cutter, disk punch cutter for ductile materials, TEM disk pre-thinning machine, dimple grinder, precision ion beam thinning, electrolytic polishing machine, Focus Ion Beam (FIB) instrument, plasma cleaner, etc.

- *Sample preparation equipment for Atom Probe Topography: FIB*

- *Surface and metrology equipment:* roughmeter, profilemeter.

- *Complementary equipment:* mills and mixers, metallographic optic microscope, metal evaporator or sputter, analytical balances, pycnometers, equipment abrasion blasting, etc.

8.5. Experimental capacity

In the framework of the need for fusion relevant studies, several basic experiments have been identified that can be performed at the CT Facility of the *TechnoFusión* with the described techniques and equipment. These will allow a complete characterization of the induced damage on structural and functional materials, including components and final complex pieces. This will allow an assessment of the viability of the materials under fusion-relevant conditions, including radiation, direct contact with fusion plasmas, or immersion in flowing liquid metals.

With the equipment suggested above, the CT Facility will have the capability to perform the main experiments listed below:

8.5.1. Mechanical tests of modified material

The study of the mechanical behaviour of irradiated materials will be undertaken. Experiments will be performed on miniaturized test samples after storage in hot cells until the required activation level is reached. The following tests will be performed:

- Tensile tests.
- Fatigue tests.
- Creep tests.
- Creep-fatigue tests.

- Bending tests.
- Determination of hardness and fracture toughness at room conditions using impact methods (SSM-ABI, small punch) and nanoindentation.
- High temperature nanoindentation (above 800 ºC).

8.5.2. *In-beam* mechanical tests

These tests refer to the study of mechanical behaviour during irradiation. They will be performed on miniaturized samples placed in the beamline of the ion accelerators. Some planned tests are:

- *In-beam* fatigue tests.
- *In-beam* creep and deformation measurements using non-contact or laser extensometry.
- *In-beam* creep-fatigue tests:
  a) as a function of temperature (up to 850-1000 ºC).
  b) as a function of the atmosphere.

8.5.3. Evaluation of new materials and components

These tests will allow the certification of newly developed alloys and materials. The tests that will be performed are:

- Tensile tests.
- Fatigue tests.
- Creep tests.
- Creep-fatigue tests.
- Bending tests.
- Determination of hardness and fracture toughness.
- Coating adhesion tests.
- Metal/CFC joint resistance, applying heat loads with a laser or an e-beam.

8.5.4. Characterization of composition and structure

Studies of the modification of the microstructure and the composition of materials subjected to conditions similar to those encountered in a fusion reactor (ion irradiation, liquid metals, plasmas, etc.) will be performed. Several characterization techniques will be utilized:

a. *In-situ techniques*

- Determination of the implantation or diffusion profile of light ions, using ion beam analysis techniques (NRA, RBS, PIXE, etc.).
- The measurement of the erosion of, and redeposition on, materials and components interacting with a plasma, using laser interferometry (using the same approach and equipment as that used for non-contact extensometry).

b. *SIMS*

- Qualitative and quantitative determination of the chemical composition of:
  - Metals (pure, alloys, from Li through W).
  - Ceramics (insulating oxides, carbon, etc,).
  - Composite materials (ODS steels, SiCf/SiC).
  - Bulk material and fine layers (coatings of structural materials).
- Depth profiles of implanted ions (including H, D and He).
- H, D, He, Li or O diffusion in matrices of interest using isotopic markers.
- The measurement of isotopic ratios (including H/D).
- 3D imaging of the distribution of the components of an alloy, impurities, implanted ions, etc.
- Material corrosion in a liquid metal loop.

c. *APT*

- Chemical composition at atomic scale.
- Defects due to the separation impurities and their effect on the mechanical behaviour of metal alloys.
- Heterogenities of the chemical composition of irradiated materials.

d. *Electron microscopes (SEM y TEM)*

Applied to irradiated and non-irradiated materials:

- Chemical composition.
- Local or crystalline structure.
- Defect studies (visualization of deposits, clusters, aggregates, radiation induced chemical incompatibility).

In-situ tests as a function of temperature:

- In-situ micromechanical tests.
- The propagation of microcracks.
- Electron Energy Loss Spectra (EELS).

e. *DRX*

- Identification of crystalline phases.
- The study of crystalline evolution as a function of temperature in materials produced at *TechnoFusión*, in coatings and fine layers, under grazing incidence.
- The identification of textures.
- The estimation of tensions and residual deformations.

f. *DUAL-FIB*

- The preparation of thin samples for TEM observation (selection of the area of interest).
- The preparation of specific points for tomographic analysis using the atom probe.
- The creation of microfractures and the study of their propagation.
- In-situ mechanical tests (compression of micropillars, nanotraction, the bending of microbridges, nanoindentation, etc.).

8.5.5. The physical characterization of radiation damage

The studies listed below will be used to characterise the physical properties of the materials. The majority of these studies will require observing the evolution of the properties during irradiation, so that the experiments must be placed in the ion accelerator beamline of the MI Facility. The proposed study objects include metals, ceramics, and compound materials, as well as technological components.

- *In-beam* optical characterization (radio-luminescence, optical absorption).
- *In-beam* measurement of the conductivity at a variable temperature.
- Measurement of the resistivity under irradiation for materials of interest for fusion applications. Measurements are made of the electrical resistivity at a low temperature for samples with a submillimetre thickness.
- Modification of the dielectrical properties of insulating materials under irradiation. Measurement of the permittivity and the loss angle as a function of the temperature and the frequency.
- Study of transport and diffusion (diffusivity, absorption, permeability, solubility) of gases of light elements under irradiation conditions. Measurements will be made, at temperatures close to the operational values, of the absorption, desorption, and permeation induced by radiation in structural and functional materials (SiC, aluminium, etc.).

8.5.6. Non-destructive methods for the characterization of components or joints

This involves photothermal thermography, ultrasound, microtomography and microradiography.

8.6. Layout, supplies and safety requirements

This section, concerning the required volumes and safety of the facility will be covered in future under detailed studies to be done by an engineering company.

9. Remote Handling Technologies

9.1. Introduction

The consolidation of nuclear fusion as an energy source in the coming years will require an extraordinary development of robotic systems for *Remote Handling* (RH) that can be autonomous or remotely manipulated by an operator. The reasons for considering Remote Handling for performing a wide range of operations in nuclear fusion installations are several for instance the large dimensions and weights of parts to be handled and in particular, the presence of harmful radiation in equipment and materials close to the fusion device. Moreover, envisaged future fusion energy plants (e.g. DEMO) will require an intense and complex maintenance which can only be undertaken by means of Remote Handling. Indeed, the ability to perform such tasks will play a critical role in the proliferation and viability of future fusion reactors. Even in current and near future experimental fusion devices, such as ITER and JET, RH is also present and is/will be continuously improved and adjusted.

The requirement for RH is not just limited to the above scenarios as other related facilities may also depend on the intensive use of Remote Handling, e.g. IFMIF. This facility will allow studies to be carried out on the behaviour of materials under neutron radiation; hence both facility component and test material activation will be considerably high. Thus, the use of RH will be therefore compulsory for both maintenance and operation tasks in this facility.

Table 9.1 provides a comparison of the three fusion devices mentioned above. The different needs for each of them, with regards to Remote Handling, are introduced together with their key features and the foreseen challenges. The most important factors in RH include the degree of activation of components in the toroid and in their areas of influence, the increase in contamination inside the device due mainly to tritium, RH availability, the size and weight of components, and the number and complexity of parts to be maintained. As can be observed in Table 9.1, all these factors, except for complexity, increase in magnitude from the simplest device JET to the reactor DEMO.

In nuclear reactors using deuterium-tritium, the resulting high-energy 14 MeV neutrons can create radioactive isotopes by transmutation of the chemical elements in the internal part of the toroid. Moreover, there are areas (see Figure where the activation could be higher due to the geometrical design of the device, for instance the first level of wall, blankets or shields, divertors, gauge and other port plugs as well as experimental ports. In addition, the vacuum chamber, as the components located outside the toroid, could be activated but at lower degree.

Now, the highest levels of activation are found inside fusion reactors, thus access to operators is strictly prohibited (Figure 9.1). For instance, the doses are estimated to be several hundreds of Sieverts/hour (Sv/h) inside the ITER toroid and such values are several orders of magnitude above permissible levels for exposure (1 mSv/h during a very brief period of less than an hour). Moreover, activated internal impurities and the accumulation of toxic gases and materials make human entry impossible.

Table 9.1. Comparison of three fusion devices in relation to remote handling.

Remote Handling in fusion devices					
Device	**Availability**	**Complexity of facility**	**Weight & Size of components**	**In-torus dose (Gy/h)**	**Status**
JET	Important, medium av.	High	$2x10^3$ Kg <2 m	~10^3	Presently operating *
ITER	Important, medium av.	Very high	<50 $x10^3$ Kg <10 m	~10^2	Near future
DEMO, commercial	Decisive, high av.	Medium-High	<10 $x10^3$ Kg <10 m	~10^2	Long term
*JET is equipped with Remote Handling systems that have proven the feasibility of applying robotics to nuclear fusion and has provided valuable knowledge to this field.					

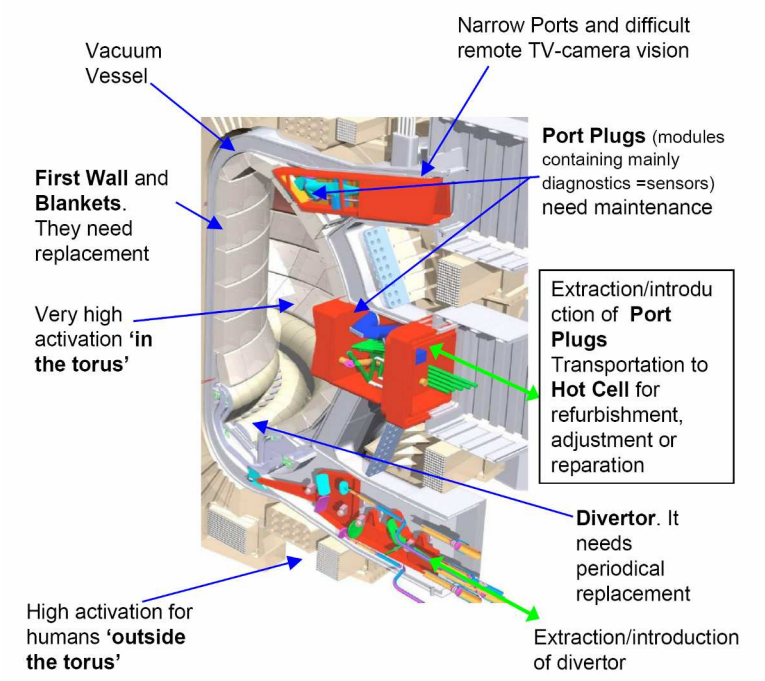

Figure 9.1. Poloidal section view of ITER

Maintenance rooms, where many activated components that require adjustment, refurbishment, or repair after extraction from the toroid are held, are also restricted areas. Thus, a bunker equipped with remote manipulators to perform the above mentioned operations as quickly and efficiently as possible is needed. Such rooms are referred to as *Hot*

Cells and maintenance operations that can be executed in these areas include: movement, extraction, lifting, assembling/disassembling, cutting and re-welding of pipes and containers, bolting or unbolting, connecting or disconnecting flanges and electrical connectors, cleaning, inspection, etc.

As is well known, the performance of the reactor is directly related to the time spent on scheduled or unscheduled maintenance shutdowns. During scheduled maintenance, a series of inspections, adjustments, repairs, and replacements are carried out within the required and planned time. However, unscheduled maintenance can arise during programmed activity and therefore, it requires unplanned shutdowns of the facility, which corresponds to a reduced energy output. The scheme in Figure 9.2 highlights reasons why Remote Handling is essential for future fusion devices.

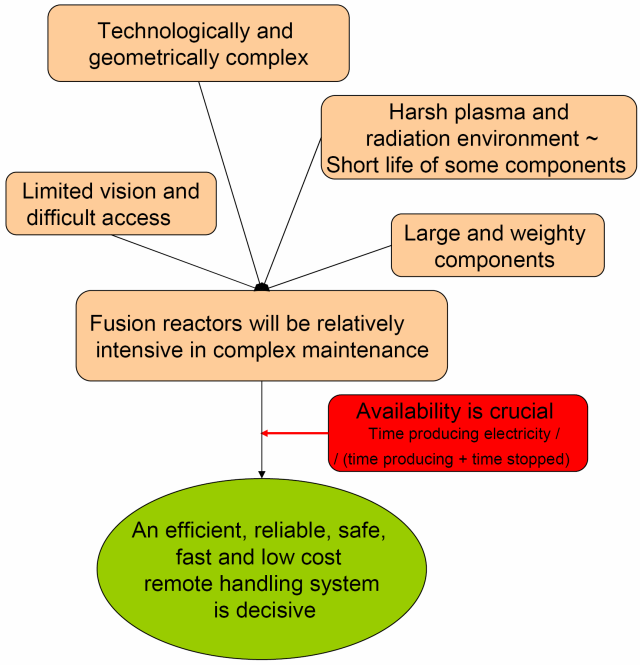

Figure 9.2. Factors that increase the importance of using remote handling in fusion.

In industrial manufacturing, the use of robots and manipulators is widely applied. Robots perform tasks such as the manipulation of components, welding, assembly of parts, as well as numerous other tasks. The design of the components and the operation processes for such systems are undertaken after taking into account available and well tested robotics Technologies. In the case considered here, a remote handling system has to be tested experimentally on every component and part destined for nuclear fusion facility. Thus, such work will not only be used for testing manipulators and possible operation processes, but also for gaining experience in synergies between remote handling and devices by improving their design. Hence, the experience gained from testing remote manipulators with *TechnoFusión* prototypes, models, and equipments will provide valuable and necessary knowledge for

application to future fusion devices. Among others, it will enable improvements to maintenance reliability, time cost, and simplicity to be made.

Thus it can be justified that remote handling is essential for nuclear fusion facilities. Moreover, RH systems should be reliable, secure, fast, and economical and they are essential for the technical and economic viability of fusion reactors and related installations. The **Remote Handling Technologies Facility (RHT)** of *TechnoFusión*, should be conceived as a dynamic force to drive science and technology developments in Madrid, Spain, as a long term global strategy.

9.2. Objectives

The main short term objective of RHT Facility is to create an installation where telerobotic tasks for the maintenance and repair of nuclear fusion installations, in particular ITER, DEMO, and IFMIF, can be developed and tested. Furthermore, the installation has to serve as a platform to promote the development of required technologies and as a base to undertake experiments and activities (dissemination, training, and know-how transfer). It means that, in the first instance, the necessary resources must be invested in technical equipment for remote handling and, in the second instance, the distribution of the knowledge acquired on the technologies involved.

In summary, the objectives of the RHT Facility could be summarized as follows:

1) To develop, test, and certify remote handling devices for nuclear fusion installations.

2) To promote the development of knowledge and technology in the field of remote handling in general and for nuclear installations in particular.

In order to fulfill these objectives, the following aspects will have to be achieved:

- To create an installation for the developing, revising, and testing equipment and procedures for remote handling in nuclear fusion.
- To create a remote handling infrastructure that will permit the testing and certifying of equipment destined for nuclear fusion installations.
- To propose and develop research activities on robotics and remote handling by staff and associated researchers.
- To be an active and dynamic centre for the dissemination of scientific and technological results and studies in the areas of advance robotics, service robots, and remote handling in nuclear fusion.

- To contribute to the development of knowledge and distribution of results from research work carried out in the laboratory by having close collaborations with the industrial sector and start-up companies.

Thus, it can be concluded, that given the provisions of suitable resources and infrastructure, together with highly qualified personnel, will allow *TechnoFusión* to be very innovative in the area of remote handling specially focused on fusion. Next, regarding activities to be performed, the following should be highlighted:

- Testing, certification, and homologation: The planned infrastructure, personnel, methods, and procedures will enable the RHT to perform testing, certification, and homologation of equipment and systems that are destined for use in areas with high radiation levels. In addition, this Facility will collaborate with international entities charged with regularization methods and criteria for testing such systems.

- Research and development of technology for remote handling: Having as an objective to contribute with new solutions, tools, and technology for performing remote handling tasks in nuclear fusion, the laboratory will undertake continuous research and development of relevant technologies. Such independent developments, through patents and technological results, will be applied in future in-house research and development projects.

- Provision of infrastructure and installations: It is intended will to provide state-of-the-art installations. In some aspects, these will be unique and will be adequate to evaluate and test procedures and equipment developed by other companies or institutions before their application. Such companies will provide a complementary means of financing *TechnoFusión*. Additional earnings will come from hiring services, since the singular features of the installation will allow it to adapt to the requirements for specific evaluations, tests, and training.

9.3. International status of the proposed technologies

9.3.1. Major international reference facilities for remote handling technologies

The majorities of current remote handling technologies are international and focus mainly on remote handling tasks for ITER due to the urgency involved and the numerous areas that need to be validated and improved. Some of the activities to be developed are related to the handling and the manipulation of different elements, such as divertor cassettes, experimental connecting doors for diagnostics, protection modules, etc. However, new nuclear fusion projects, such as IFMIF, also require laboratories devoted to remote handling. At present three principal Remote Handling laboratories dedicated to Nuclear Fusion currently exist in the world, two of which are in Europe and one in Japan.

(I) Divertor Test Platform 2, Tampere (Finland)

The *Divertor Test Platform 2* (DTP-2) is an installation for testing systems for the extraction, insertion and movement of divertor cassettes in ITER (see Figure 9.3). The installation was commissioned at *Technical Research Centre of Finland* (VTT) premises in May 2007. VTT stands for *Technical Research Centre* of Finland, and an important applied research organization that contributes with valuable technological solutions and innovations. VTT is a non-profit research organization within the *Finnish Innovation System*. The new VTT experimental warehouse is located in the Technological Campus next to the Technical University of Tampere.

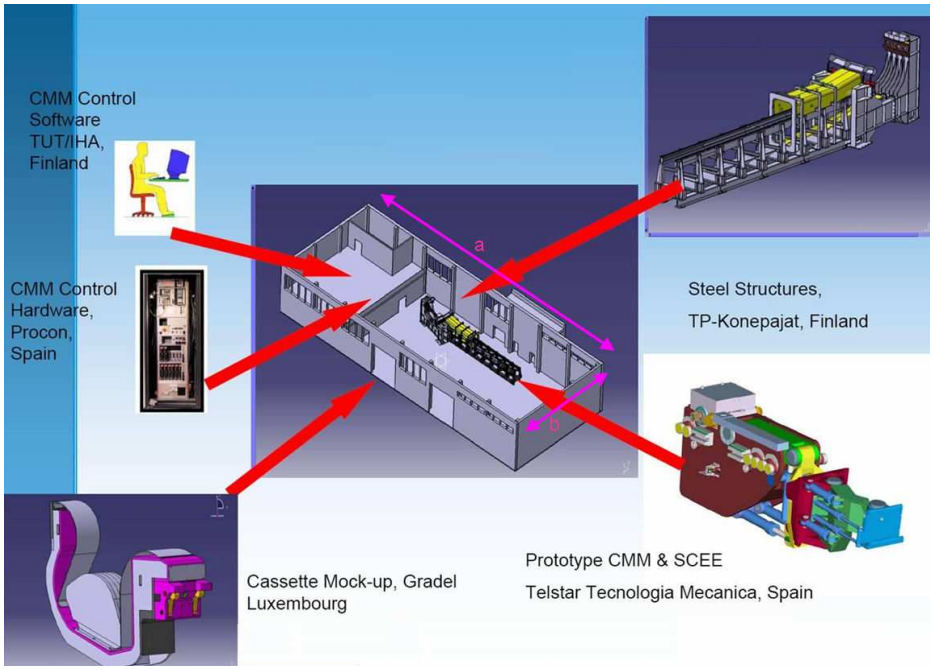

Figure 9.3. Layout and equipment of DTP-2 installation at Tempere,[154]. Dimensions (aprox.): a ≈ 50 m , b ≈ 20 m.

A layout of the installations and its main rooms and equipment is shown in Figure 9.3. The contributions of two Spanish companies are noted in the captions. Figure 9.4 shows a picture of the experimental area.

[154] 'TEKES ITER-projects since1994 = ITER RH interests' ; Jouni Mattila ; Presentation in Tampere meeting ; Tampere, Finland ; December 2007

Figure 9.4. Experimental area in DTP-2[155] with a divertor cassette in the foreground (black and grey).

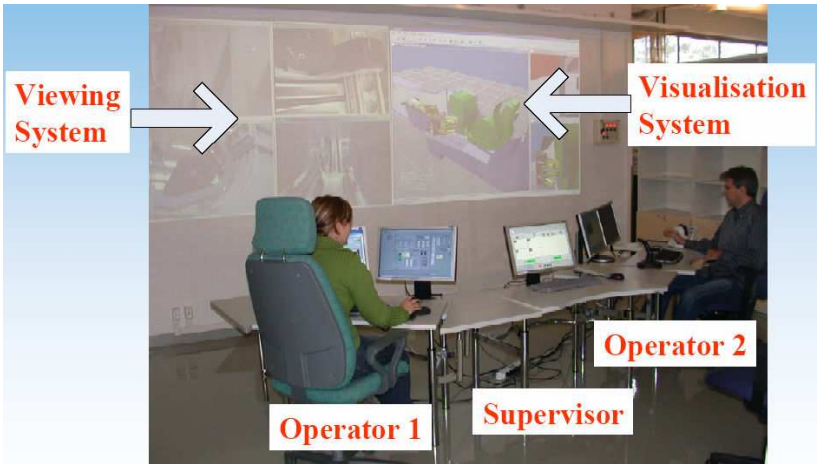

Figure 9.5. DTP-2 control room in 2007. Vision and simulation system.

The test installations at DTP-2 were initially focused on performing radial movements (i.e. from inside the ITER toroid towards the radial exterior) of the divertor cassettes, developed by *Cassette Multi-functional Mover* (CMM) (see Figure 9.3). In a second stage, the installation extended its studies to subjects related to the toroidal movement of the cassettes inside the ITER toroid. Moreover, the installations are equipped with lifting devices, a maintenance robot, a support rail for the divertor, a prolonged metal structure for the

[155] 'RH Activities of the EURATOM/IST Association Portugal' ; Isabel Ribeiro et al. ; Presentation in Tampere meeting ; Tampere , Finland ; December 2007

extraction of divertor cassettes, hardware and software control, plus a control room (see Figures 9.3, 9.4, and 9.5).

(II) Remote Handling Laboratory at the ENEA Brasimone Research Centre (Italy)

This laboratory develops a range of Remote Handling tasks for different fusion devices, thus the project and equipment have been modified since operation began. Three of its installations are descried briefly below.

1) Divertor Refurbishment Platform

The *Divertor Refurbishment Platform* (DRP) is comprised of two stages. In the first stage, refurbishment of the ITER divertor, designed in 1998, was tested, showing correct performance during the test period 1999–2003. Note; a crane was used to perform this test (see Figure 9.6).

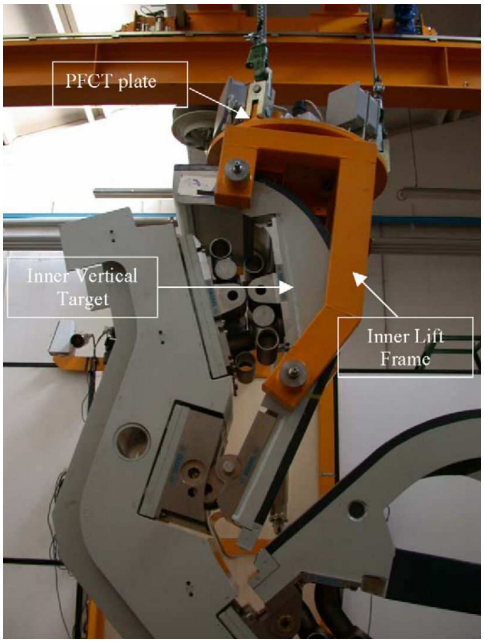

Figure 9.6. Extraction of PFC of ENEA.

However, the current design, called ITER FEAT, is equipped with different divertor cassettes, hence the DRP installation was modified during 2003–2005 in order to adapt it to these new requirements. For this, three lifting devices were designed and installed (Figure 9.7). This experimental machine is called the *Plasma Facing Components Transporter (*PFCT). The principal elements of PFCT are a cart, a set of cables, and a suspended platform (Figure 9.7).

The PFCT is a device capable of elevating, or inclining, loads up to 5 tons. It has six degrees of freedom on a suspended platform, it moves at very low speed when performing remote operations of maximum precision, it can rotate at 1 degree/second and it can perform precise positioning up to 0.25 mm.

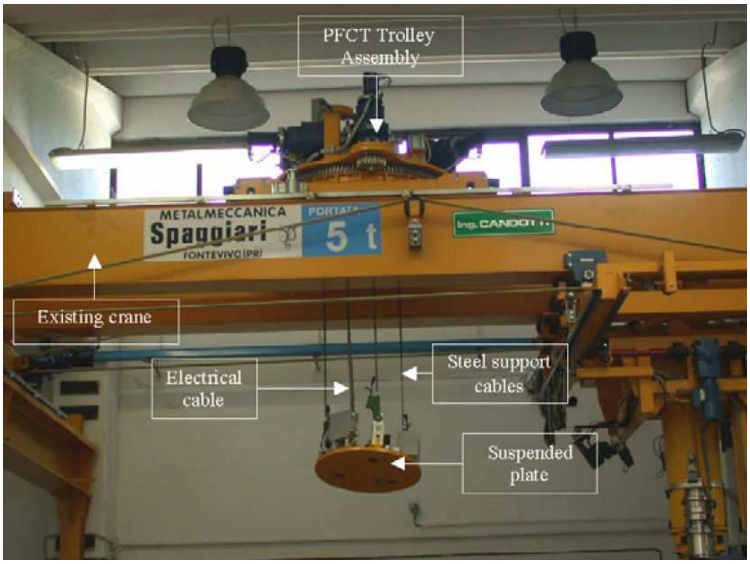

Figure 9.7. General view[156] of the Plasma Facing Components Transporter (PFCT). Assembly cart, cables, and suspended platform.

Furthermore, several tests with PFCT features have been carried out. Some tests of operations and components have also been performed. For instance, some basic features in Remote Handling have been improved, such as elevation, evaluation of position reproducibility, blocking and unblocking of the suspended platform (Figure 9.6), axis testing of the suspended platform (rotation, inclination, elevation of the PFC), as well as tests of hardware and software control execution and other operations.

2) Divertor Test Platform (DTP)

The DTP installation (Figure 9.8), also called DTP1, was the first installation for Remote Handling testing of complete divertors by means of a scale model. The installation was used until 1998 and the initial design of the divertor cassette (ITER 1998) was successfully tested. The current and definitive design of ITER-FEAT will be tested and checked in DTP-2, in Finland.

[156] 'The plasma-facing components transporter (PFCT): A prototype system for PFC replacement on the new ITER 2001 casete mock-up' ; G. Miccichè et al. , ENEA ; Fusion Engineering and Design ; January 2007.

Figure 9.8. General view of the DTP[157] of ENEA.

The DTP, which can be seen in Figure 9.9, consists of the following elements:

- Sector ‘72" of the lower region of ITER,
- A Cassette Divertor Prototype with blocking system, gripping points, and refrigeration connections,
- A prototype for simulating the inner vessel environment that includes toroidal rails, divertor ports, and other devices,
- A displacement prototype (a device similar to CMM).
- Prototypes of auxiliary Remote Handling equipment, and
- Control and localized data acquisition systems in the control room.

[157] ‘What we do in The Vessel in-Vessel Field’ ; Michael A. Pick ; EFDA activities 2006

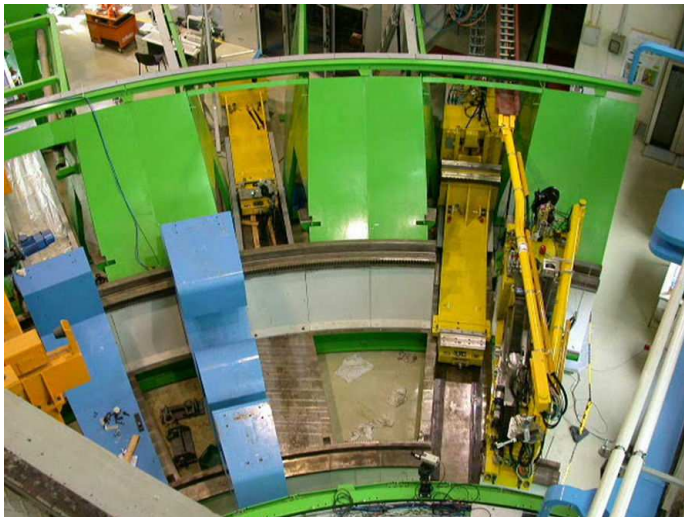

Figure 9.9. Area of the DTP installation showing the cassette Mover inside the vessel (yellow), the divertor model (blue) and Sector '72" of the lower region of ITER and its rails70 (green).

3) IFMIF Test

With the development of IFMIF, new needs have arisen requiring different tests of RH to be carried out. Thus an area is needed to test IFMIF components. The structure and dimensions of such a laboratory can indicated in Figures 9.7 and 9.10.

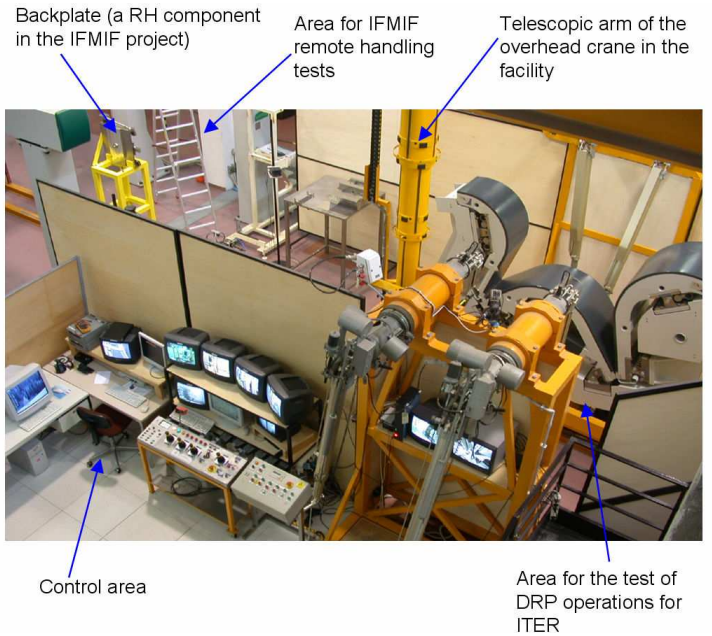

Figure 9.10. A general View of the Remote Handling laboratory at ENEA, Brasimone.

(III) Installations of the Internal Vessel Transporter (Japan)

Figure 9.11 shows a general view of the *Internal Vessel Transporter* (IVT) installations which are a complex for the certification and development of manipulators for interchanging ITER *blanket modules* (a module located on the inside of the ITER toroid to protect the metallic vacuum chamber from plasma induced. It suffers neutron radiation damage and extracts the heat it receives). The *blankets* need to be renewed periodically by substitution because of the damage and deterioration due to being exposed to the plasma and in particular, the neutron irradiation. It may also be necessary to interchange *blankets* in order to make improvements to the device or in case of a failure.

Figures 9.12 and 9.13 show the details of the vacuum chamber transporter inside the IVT. This transporter is the manipulator that permits docking, undocking, and displacing the *blanket* inside the toroid. The three installations were assigned experimental development and certification tasks in accordance to factors such as excellence of the installation, scientific and technical features, experience in past developments, as well as research and development of projects.

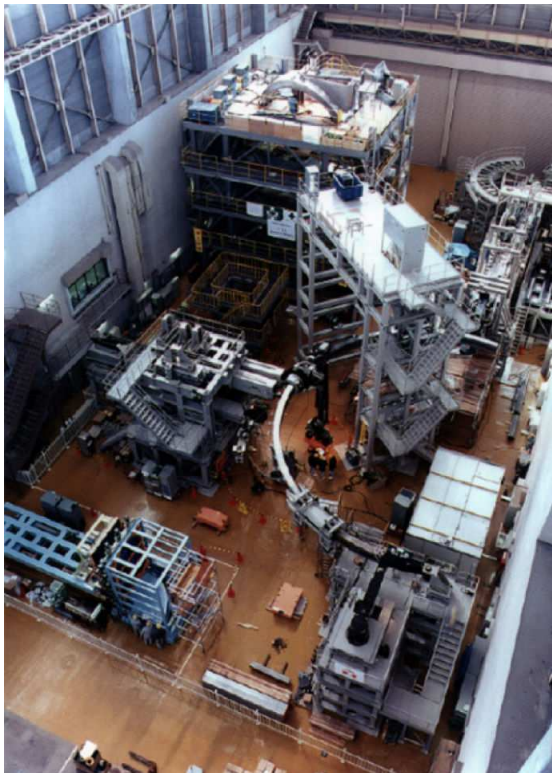

Figure 9.11. A general view of the Japanese IVT installation. The building is 30 m long and 10 m high. The semi-circle in the photograph is the 12 m diameter IVT rail [158].

[158] 'Overview of ITER Remote Handling' ; ESC04-001 / ITA 23-28 Task Motivation , ITER IDM, Remote Handling and Assembly Engineering Support (277VHR_v1_0), Appendix 1-1 - Overview of ITER RH.pdf ; Dr. J. D. Palmer ; 2007

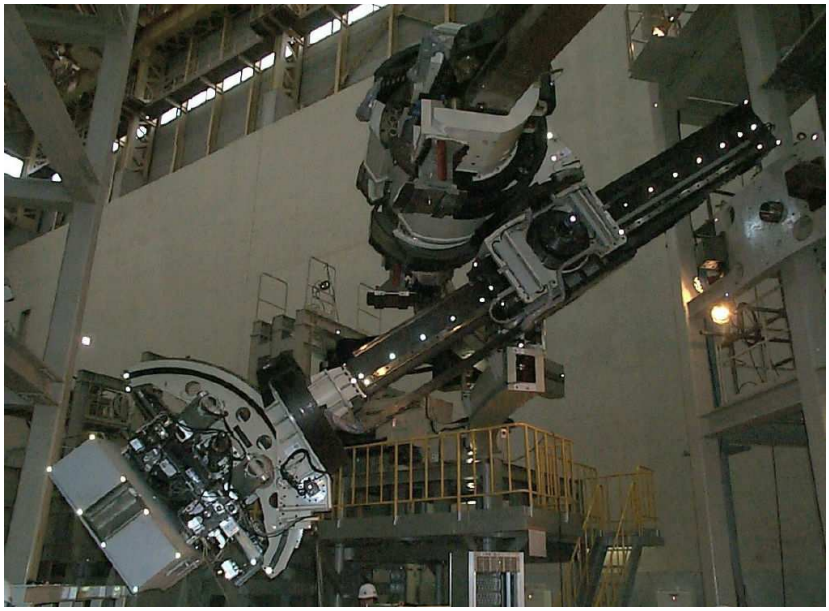

Figure 9.12. The vacuum vessel transporter.[158]

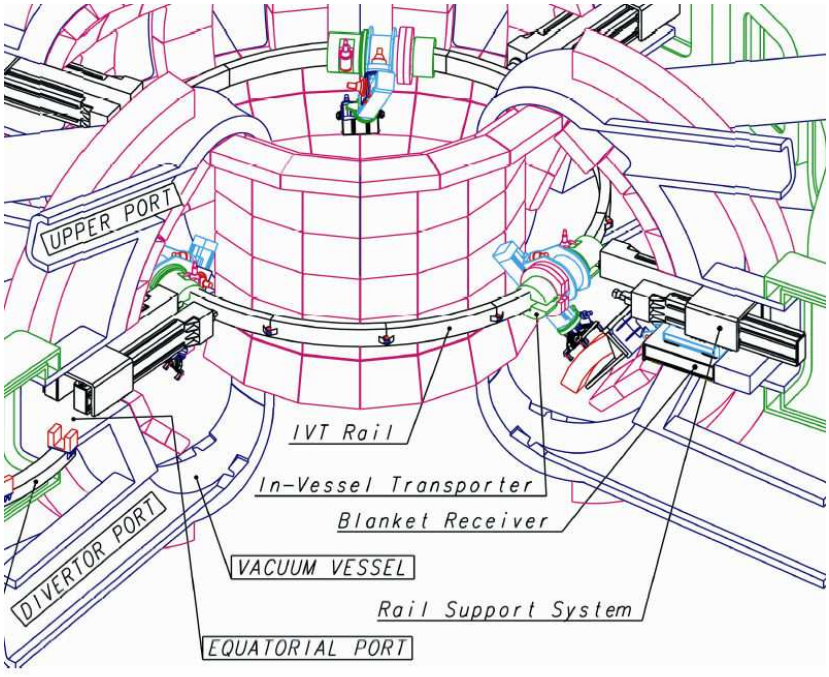

Figure 9.13. A schematic representation of the internal vacuum vessel in the interior of the ITER toroid. [158]

9.4. Projected facilities

The equipment requirements for the RHT Facility are defined by the needs of different projects to be developed. In order to determine the basic equipment that will be needed for the laboratory, a variety of relevant activities related to nuclear fusion have been considered. Moreover, in order make it unique the contemplated activities are not currently performed in other installations. The activities are:

(a) Remote Handling operations:

A cold installation is needed to manipulate prototypes for the:

- Diagnostic Port Plugs (DPP) of ITER.
- TBM of ITER.
- IFMIF Irradiation Modules.

Considering the large number of activities related to the above tasks, as well as additional tasks that can arise within a laboratory framework, a bridge crane has been considered in order to control the movement of required elements from the warehouse to the *Laboratory for Experimentation with Large Prototypes (LELP)*:. For this, it is considered that the DPP weights can range from approximately 20 tons (Upper Port Plugs - UPP) up to 45 tons (Equatorial Port Plugs - EPP) (see Figure 9.14).

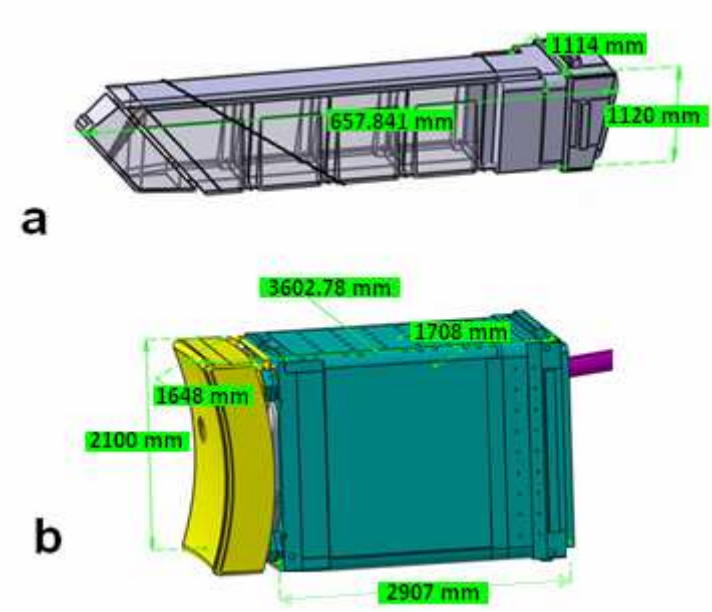

Figure 9.14. Dimensions of UPP (a) and EPP (b) Port Plugs.

In addition, the RHT Facility will need robot manipulators for general use, as well as sensorial and control systems. The warehouse area will also require similar systems. Furthermore, having a crane for transporting large elements (DPP, TBM), the Facility will also require robots and auxiliary systems capable of transporting and storing parts having different sizes and weights.

(b) *Homologation of RH equipment under irradiation*

The RHT Facility will also require an irradiated room in order to carry out validation, certification, and characterization of equipment destined for Remote Handling applications under gamma radiation. Such irradiation procedures will be carried out in an *Irradiation Room* through coupling with an accelerator.

Next, these activities will be explained in detail in the following subsections.

9.4.1. Remote handling operations

9.4.1.1. Remote handling of ITER Diagnostic Port Plugs

DPP for ITER contain diagnostic equipment for controlling, optimising, and evaluating ITER plasmas. Among the 18 ITER UPP, 12 have diagnostic equipment, while 10 of the 18 *Equatorial Port Plugs* (EPP)[159] have such equipment.

The most important features of the UPP's are (see details in Figure 9.15):

- Weight: 20 T
- Dimensions: (6.1 x 1.1 x 1.1) m
- In many cases, they have a central tube to locate diagnostic elements. These tubes are installed in the UPP's by rail guides.

In general, the preferred means for extracting a diagnostic module is to open the upper part of the UPP. However, alternative opening possibilities exist such as opening its lower part. According to the most recent conceptual ideas, it should be rotated with respect to its horizontal axis and vertically accedes from the top to the bottom of the UPP.

[159] "Preliminary data for ITER *Hot Room* RH facilities in *TechnoFusión*"; CI-TF-RHSF-002 ; V. Queral ; March 2008.

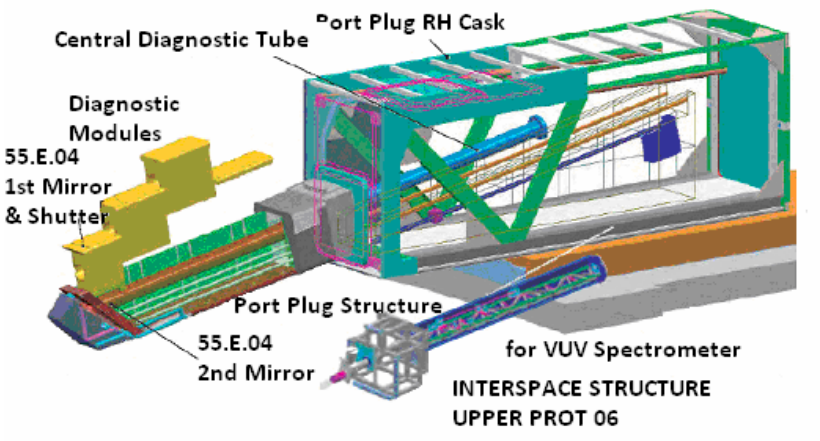

Figure 9.15. Details of an UPP of ITER.

The general characteristics of an EPP are (see details in Figure 7.16):

- Weight: up to 45 T
- Dimensions: (3.6 x 1.7 x 2.1) m
- There exist modules in the EPP that permit replacement of some parts of diagnostic components (mirrors, wave guides, detectors, etc.).
- Diagnostic modules are usually taken out from the top.

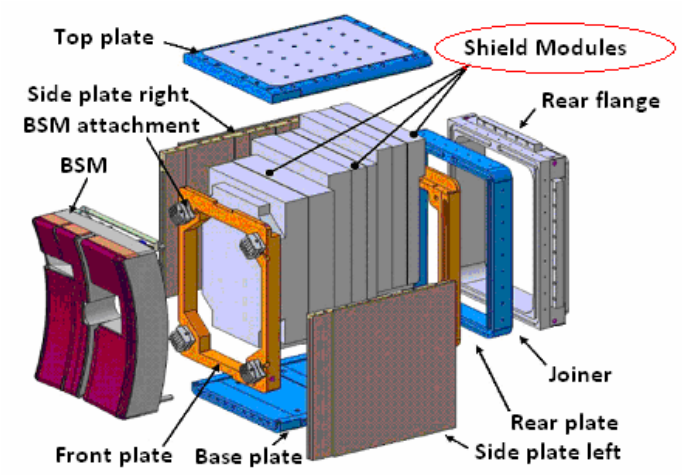

Figure 9.16. EPP details of ITER.

Some diagnostic modules inside an EPP are accessible by removing the BSM (*Blanket Shield Module).* The Blanket Shield Modules are EPP parts situated at the plasma facing end and have perforations to allow the emission or reception of signals. Their approximate weight is 13 tons and their dimensions are 2.1 m x 1.65 m x 0.5 m. Blanket Shield Modules are anchored to the EPP by a system of rivets or by a similar system.

In many cases, the maintenance work on a DPP consists of replacing components or subcomponents. Generally, subcomponents are pre-checked, pre-aligned modular assembled structures which are replaced by extraction and insertion rather than being repaired in-situ. Examples of such subcomponents include telescopes, mirrors, mechanical actuators, etc.

The typical tasks to be carried out for during these procedures are:

- Extraction of *Port Plugs* (PP) from the vacuum vessel (with associated operations).
- Transport of the container to the *Hot Room.*
- Performance of maintenance tasks in the *Hot Room.*
- Transport of the container back to the vacuum vessel.
- Insertion of the PP into the vacuum vessel.

Hence the foreseeable Remote Handling operations for DPP are:

- Elevation and movement of *Port Plugs*, modules, sub-modules, BSMs, and other elements that need replacement.
- Screwing and Unscrewing.
- Cutting of pipes and other elements.
- Soldering of pipes.
- Displacement and adjustment of diagnostic elements.
- Replacement of modules, sub-modules, and other damaged elements.

Taking into account the Remote Handlling of DPP, it is necessary to consider tasks related to the extraction of the DPP from the vacuum vessel, its mounting onto *In-Cask Handling Equipment,* the inverse action of separation from *In-Cask Handling Equipment,* and the reinsertion of the DPP into the vacuum vessel.

In-Cask Handling Equipment is primarily formed by a tractor type system for elevating and placing tasks, or for removing a load from a C*ask* (see Figure 7.16). It also consists of one or two manipulators that perform tasks such as extraction, sealing, removal and cutting of refrigeration pipes, reconnection of pipes by soldering, as well as inspection of soldering work.

The diverse designs of the DPP's that have been presented to date, make it difficult to firmly establish equipment needs. However, it is envisaged that such systems must be equipped with tools for screwing, cutting and soldering. They could also be equipped with pressurized clams and specialized tools adaptable to a particular task.

The DPP Remote Handling tasks to be undertaken in the *Hot Room* require at least a manipulator capable of opening and extracting the *Port Plug* lids. Such a system could be the same as the system used for manipulating TBM's in the *Hot Room*. Considering the dimensions of elements to be manipulated (an Upper DPP is over 6 m in length), it would be convenient to extend the working area of the manipulator by means of a rail. A teleoperated auxiliary system for clamping lids during opening and sealing operations will also be required. In addition, the movement of lids from the storage room while manipulating subcomponents and diagnostic equipment of DPP's will require specific features.

Diagnostic modules inside a DPP can be extracted from the PP at the top. A robotic system with a load capability up to 10 tons (the weight of the EPP[160] screening module) will be required for this. Since the separation distance is 5 mm precise movement capabilities will be necessary even though module position guides are present. Moreover, in order to extract and move a BSM from an EPP, a system capable of transporting approximately 13 tons will be required. Thus, considering both of the above requirements, a robotic system capable of translating 13 tons of load with high precision has to be considered. Finally, a manipulator system will aid in screwing, unscrewing, cutting, or soldering tasks.

In summary, all tasks related to mounting or dismounting of diagnostic equipment located inside a DPP, as well as maintenance tasks to be done in-situ, will require the design, development and construction of specific robotic systems.

Next, RH tasks of complex equipment within a DPP, which require a number of operations with high precision (e.g. alignment of mirrors, cameras, optical devices, etc.), will require systems capable of uploading visual information and haptic devices for the teleoperation of a light manipulator arm that carries out such tasks.

Another foreseen task is the inspection of a PP after RH operations. It will be carried out in a measuring station in order to measure and verify the positioning of some critical PP components. In such a measuring station, a complete visual inspection of all DPP critical areas needs to be performed. Measuring stations and visual inspections will have to done with automated vision equipment and/or a telemetric laser, which is fixed or teleoperated. Some could be placed in pre-set fixed positions. It is also necessary to consider mobile equipment displaced by a robotic arm. In particular, Measuring and Inspection tasks will be designed for performing such operations in ITER. However, some basic equipment for inspection and metrology should be also integrated into the permanent parts of the RH *TechnoFusión* Facility.

[160] "Technical Specification for the Diagnostic Equatorial Port Plug" ; C.I.Walker ; ITER_D_22FNKA Draft 11 Nov 2005

9.4.1.2. Remote handling of ITER Test Blanket Modules

TBMs (Figure 9.17) are ITER components for testing Breeding Blankets (these are modules for producing tritium) for DEMO and other fusion reactors. In total, there will be 6 TBMs in ITER to be checked.

The main characteristics of the TBMs are:

- Approximate weight: 2 tons
- Approximate dimensions: 1.7 m x 0.54 m

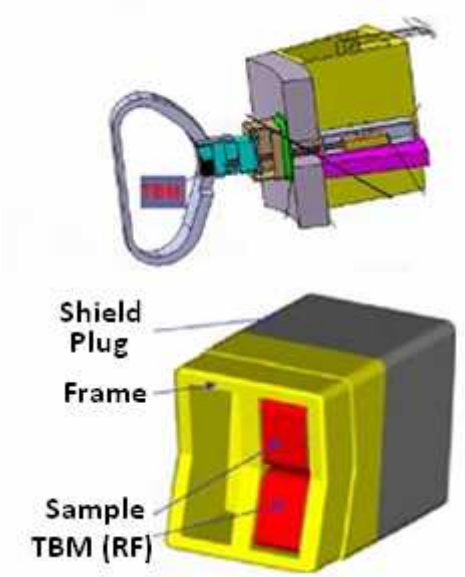

Figure 9.17. TBM structure for ITER.

For the majority of cases, it will be necessary to transfer the TBMs to the *Hot Cell* in order to perform operations related with their replacement.

The tasks to be carried out are:

- For Remote Handling of a TBM in the *Hot Cell*:
  - Arrival of the vessel.
  - Cutting and disconnecting of TBM pipes and electrical connectors.
  - TBM extraction.

- Displacement to the work area.
- Extraction of the TBM from the EPP.
- Displacement to the blanket detritiation area.
- Placement of a new TBM.
- Soldering and connecting of TBM pipes and electrical connectors.
- EPP water-tightness.

- Remote Handling operations to be carried out with the TBM:
  - Elevation and movement of the TBM that is to be replaced.
  - Disassembly, replacement, and mounting of parts that form the component.

The TBM has to be disconnected from the *Port Plug* clamping and to be extracted and replaced by a new TBM.

Regarding the robot for connecting and disconnecting (soldering and cutting), there will be a need for a robotic manipulation system capable of handling 2 tons.

Moreover, the extraction system should be equipped with a manipulator for loading and unloading TBMs. The manipulator can also be used for moving the device from the transport module to the extraction system.

9.4.1.3. Remote handling IFIMIF irradiation modules

Some tests will be performed at the IFMIF on materials destined for the construction of a nuclear fusion plant. The objective is to study the behaviour of materials under nuclear fusion and generate a materials database for the design of the DEMO reactor. Figure 9.18 shows a scheme of IFMIF irradiated zone.

Due to the radiation, the maintenance or inspection of materials and IFMIF components and the handling of samples for testing irradiation need to be done remotely. Considering all possible Remote Handling tasks in IFMIF to be carried out in the RHT Facility the most demanding one is the handling of irradiated modules, due to the weight and size of the parts. Therefore, it is important to determine tasks to carry out in order to adapt the dimensions of the installations.

Figure 9.18 shows: a) two VTA's (*Vertical Test Assembly*) to locate samples of high irradiation and medium flow, b) a VIT (*Vertical Irradiation Tube*), which is a set of tubes used

for inserting test capsules in the region of low flow and test cell covers that support the VTAs and have to be removed in order to accede to the entire cell.

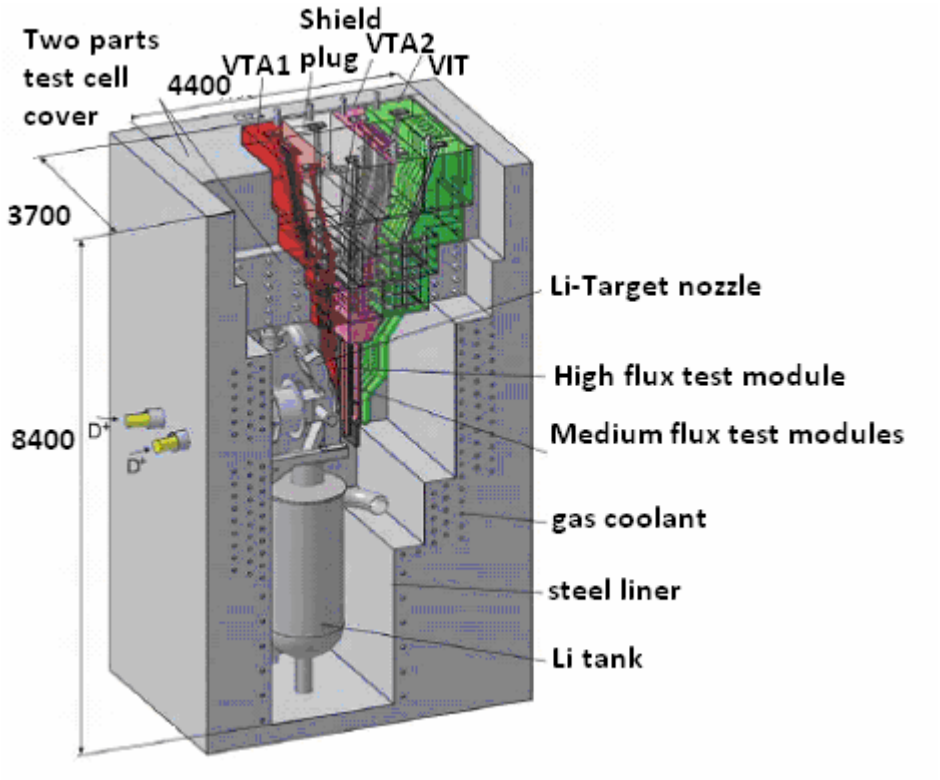

Figure 9.18.. Scheme of IFMIF irradiated zone.

In general, the tasks to be carried out in IFMIF[161] are:

- Extraction of the Test Cell irradiation module,
- Dismounting and treatment of samples therein, and
- Insertion of the Test Cell irradiation module.

The following Remote Handling tasks have been established for remote maintenance of irradiated modules in the IFMIF:

- Disconnection of connectors and bridles in the upper part of the VTAs.
- Hoisting of irradiated modules.

[161] "Preliminary data for IFMIF remote handling facilities in *TechnoFusión*" ; CI-TF-RHSF-001; V. Queral ; November 2007

- Extraction of the Back Plate (the part that supports high neutron radiation) of the Test Cell (if required).
- Insertion of the Back Plate in the Test Cell.
- Insertion of irradiated modules.

In order to carry out these remote handling operations, at least one teleoperated robot manipulator with an interchangeable end-effector will need to be implemented. The robot can perform every operation with the corresponding tool. If the elements to be manipulated have very different properties (weight, size, or shape), different robots could be required for each case. Such robots could be used for elevation, extraction, and posterior insertion of the VTA and VIT. A crane type high-precision robotic system, with the possibility of inclining and rotating parts with respect to three spatial axes, is considered most suitable for this application.

9.4.1.4. Summary of adequate manipulation systems for the majority of remote operations

The RHT Facility must be equipped with a basic system for general manipulation in order to perform validation tasks for research and development, independently from the specific areas previously assigned in the laboratory. Furthermore, it should be recalled that such a basic system has to compete internationally with other laboratories that already possess robotic Installations for testing and validating of fusion components.

The difficulty of predicting and evaluating needs with activities that are still largely unknown is complex. Based on the three examples that have been previously analysed in depth, and also based on budget constraints, an estimate of the minimum installation required to accomplish the basic objectives, while being capable of competing internationally for ITER projects, is defined as follows:

a) A crane bridge referred to as the “Main Crane” with an adequate weight capability (required load between 20 and 40 tons to be decided in future studies) and high precision for part positioning. It must be equipped with a system for the rotation of a part with respect to the vertical axis and with respect to two horizontal axes. Moreover, it has to be equipped with sensors for absolute precise positioning, these being adequate for tasks that require very high precision (to within millimetres or less, obtained by telemetric lasers or similar for absolute reference), a weighing scale, and a weight balance. The type of tow or crane should be the most common and significant of the ITER and IFMIF facilities in order to include the vast part of the experiments without the need of buying specific components.

b) A system for transporting and positioning robotic manipulators about different areas and heights in the *LELP Laboratory:* by means of rails, an articulated arm, crane hoists, and/or vertical or horizontal telescopic systems.

c) Robot Manipulators with two different load capabilities, i.e. 100-500 kg for maximum load capability and 10-50 kg for reduced load capability. Two kinds of robotic manipulators have to be considered: one a commercial type (high reliability and recognition from international groups) and various non-commercial robotic manipulators mainly developed by universities and research centres based around *TechnoFusión* (GIAs[162] and related companies). Non-commercial robots have to be equipped with open and flexible software, have open and modifiable mechanical performance, and moreover, systems that are adequate to research and development around *TechnoFusión*. The minimum number of robots required is: a commercial robot equipped with two arms and minimum load capability of 10 kg (50 kg is the minimum desirable load) and two non-commercial robots equipped with at least one high quality arm.

d) A remote camera vision system, a fixed telemanipulation and control system, and another teleoperated system at the door of the installation for performing minor operations plus a real-time interaction system and a virtual human model.

e) Powerful Graphic Computers for virtual reality and specific software.

9.4.2. Irradiation Room

The RHT Facility of *TechnoFusión* will require an irradiation room to undertake validation, certification, and characterization of equipment designed for performing Remote Handling operations under radiation conditions. The irradiation of such equipment will be carried out in a room called *Irradiation Room*, where such components can be irradiated by gamma radiation via an access port to the electron accelerator (see Chapter 5 on Material Irradiation Facility for more details). Remote handling equipment to be irradiated include servo-manipulators, cranes, stackers, manipulated arms, telescopic posts, articulated arms, in addition to other RH equipment developed for use in ITER, IFMIF, or DEMO, as well as commercial fusion reactors.

The goal of this section is to irradiate manipulator equipment. In the case where irradiation cannot be performed due to space restrictions, the testing will be restricted to the most significant parts of the robot under evaluation. Its capacity to irradiate entire manipulator parts makes this installation unique within its sector.

Gamma radiation is generated by the irradiation of a tungsten plate with electrons accelerated by a *Rhodotron®* (see Chapter 5 for more information). Appendix II describes the results of the simulations to evaluate the dimensions of this W plate and the characteristics of the electron beam.

Table 9.2 shows a brief summary of the simulations. The optimized parameters are shown in order to maximize the final volume with doses between 100 and 500 Sv/h.

[162] The GIAs are the *TechnoFusión* Associated Investigation Centres for technological support..

Table 9.2. Conditions recommended (on the basis of simulation results) for the *Irradiation Room* of Remote Handling Facility.

Irradiated material	W
Density	19.25 g/cm^3
Cosine of the angle of incidence	0.6
Beam footprint	Square area: 1.5 x 1.5 m^2
Plate thickness	0.6 cm
Beam radius	0.5 cm
Total volume	74.80 m^3
Irradiation Room size	100 m^3

9.4.2.1. Estimation of Space and Radiation Dose

In order to estimate the minimum space required for the equipment of *Irradiation Room* as well as a reasonable irradiation dose it is necessary to first necessary to take the following criteria into account. First, it should be recalled that the electron accelerator will be used by different experiments groups within *TechnoFusión*. Remote Handling is just one such area and, as a consequence, the size requirements of the *Irradiation Room* and the irradiation dose will be defined as a function of the performance and limitations imposed by the electron accelerator design specifications.

The size and dose of irradiation in the *Irradiation Room* will depend on:

a) The world market regarding testing and certification of manipulators for fusion and the participation of the *TechnoFusión Irradiation Room* in the world market. In the following sections, some preliminary estimates are made within the limits imposed by the uncertainty of future markets.

b) The size of robots for Remote Handling (including manipulators, cranes, articulated arms, etc.)

c) The irradiation rates for robotic manipulators (in units of robots per unit of time, e.g., four robots irradiated in one year)

d) The dose received by manipulators will depend on the size of the room and accelerator power.

e) Robots in the first line of irradiation will receive higher radiation doses than those located in the second line. For these latter robots, the absorption of radiation depends on the size, shape, and materials of the robots that act as a screen in the first line.

9.4.2.2. Market for the Irradiation of Robotic Manipulators

In ITER, it is estimated that the number of robots working in high-radiation areas of ITER will be between 50 and 100. These estimates include servo-manipulators, the crane bridge, other bridges, stackers, telescopic posts and articulated arms, Plasma Facing Component Transporters (PFCT) in the ITER *Hot Room*, IVT that work inside the vacuum chamber, robots for performing inspections inside the vacuum chamber, as well as CMM and *Second Cassette End Effectors* (SCEE) in ITER ports for replacing divertors.

In IFMIF, the total number of robotic manipulators in the entire installation, including cranes, manipulators, and articulated arms, is estimated to be between 7 and 10 units.

In DEMO and future reactors, it is predicted that the number of robotic manipulators that will have to be validated and certified will be immense. However, due to the large number of existing unknowns, the installations that will be required for such tasks will be considered in future expansions of the *Irradiation Room* as this will need very long term planning.

Other activities that require robotic manipulators as nuclear plants need validated and reliable manipulators. Even though *TechnoFusión* will focus on research and development, some marginal activities related to other fields can be performed. Around 30% of total *TechnoFusión Irradiation Room* activities could be considered in this sector.

Elements not included in the list of robots mentioned above are:

- Components and replacement parts for robots.
- Mechanisms and manipulators found inside the ITER Cask.
- Other robots that work under conditions of reduced radiation (0.1-1 Sv/h) have not been included since validation tests can be performed quickly or can be even avoided.
- Tools for Remote Handling have not been included since their sizes are very small. However, the number of tools will be relatively high, around 200 to 1000 tools.

Estimate and hypothesis of work:

An estimated number of robots has been considered for their use in the *Irradiation Room* under some hypothesis of work:

- There are two types of robots in the installation. Only one type will need certification, this being about 80 robots. The total number of robots is 160 (ITER + IFMIF + other non-fusion units).
- Replacement parts will not need certification or testing.
- The majority of robotic manipulators considered above will be developed and validated during the ITER construction phase, (which means from the present to around 2020), this period being about 10 years.

- A 50% share of the total world market for irradiation services is considered for the *TechnoFusión Irradiation Room*. The number of robots considered for *TechnoFusión* is around 40 robots in 10 years.

In conclusion, it is considered than on average about 4 robotic manipulators per year should be tested and certified in the *Irradiation Room* in order to significantly contribute to near-future world needs.

9.4.2.3. Average robots sizes

The term Robotic Manipulator includes a broad range of Remote Handling equipment such as those as mentioned previously: servo-manipulators, cranes, stackers, telescopic post, articulated arms, etc. The size of such equipment will vary considerably, but here, the largest robotic manipulator is considered to be the most relevant for this study. For this, the robot surroundings, including space to allow partial movement of the robotic manipulator, are considered. The surroundings for some large manipulators (e.g. 4 m x 4 m x 3 m) will be used for stacking machines, partly for ITV as well as for PFCT. The surroundings for large ITER servo-manipulators will be 1.5 m x 1.5 m x 1.5 m, approximately.

9.4.2.4. Estimated gamma radiation dose alter stopping for different areas in ITER and IFMIF

(I) ITER [163]:

- Inside the vacuum chamber: about 7,500 Gy/h, for 2.8 hours after shut off. Manipulators cannot work inside the chamber under such conditions.
- Outside the ITER Cask: 10 Gy/h during 11.6 days after shut off.
- Typically <0.5 mGy/h in the most unfavourable volumes between the bioshield and the vacuum chamber. Manipulators intended for such areas are not considered for radiation testing in this document.
- The radiation dose outside the bioshield is expected to be of the order of several µSv/h except near conductors.
- ITER *Hot Room*: 155 Gy/h per 1 m^2 of a Blanket surface[163]. A value of than 10 Gy/h can be considered for the majority of the areas.

(II) IFMIF:

- The dose inside the most activated volume, which is the Test Cell, will be between 20 and 1000 Gy/h immediately after shut off. The dose will vary

[163] "DESIGN DESCRIPTION DOCUMENT: Remote Handling Equipment (DDD 23) Chapter 1, General", N 23 DDD 66 R0.3 ; ITER IDM ; 2004

significantly with distance from the test modules, since the radiation source is relatively concentrated.

9.4.2.5. Reasonable gamma doses for electron accelerators and robots

Various studies show that a dose rate between 100 and 500 Gy/h could be reasonable attained in a volume of a few cubic meters exposed to radiation from a 10 MeV accelerator with a maximum current of several mA. The objective is to test robotic manipulators at a radiation rate of Gy/h which is 10 times higher than the dose received in a real installation. It is thereby convenient to reduce irradiation periods to practical values. Therefore, a dose rate of 500 Gy/h for the first row of robots in the *Irradiation Room* can be considered as the first step in the design.

Two robot categories are considered due to the different operative conditions both in ITER and IFMIF:

1) Critical robotic manipulators: only manipulators working inside the ITER vacuum chamber will receive doses as high as 500 Gy/h for long periods of time. Inside the vacuum chamber, only an IVT requires long periods of time, about half a year of continuous performance. The integrated dose received by these critical robot manipulators is around 2 MGy so such robots will be placed in the first row inside the *Irradiation Room*.
2) Other robotics manipulators: the majority of the other robots that will occupy a volume of about 10 m^3 in the *Irradiation Room* will receive an integrated dose of 1 to 100 Gy/h. Such robots will require certification for 0.1 MGy to 1 MGy of integrated dose. The client needs are unknown, but 10 years of operation at 10 Gy/h and a 10% workload would be a reasonable starting point. The irradiation dose in the second row of the *Irradiation Room* can be around 100 Gy/h and the total volume occupied by 4 robots will be around 40 m^3. Under such conditions, the average time for 4 such robots to receive 0.1 MGy/h will be about 40 days.

Considering that the electron accelerator will be shared with other laboratories, the *Irradiation Room* availability will become reduced, since various robots with different requirements can be irradiated simultaneously. Therefore, an average of 10 robots could be simultaneously irradiated in the second row for one year to achieve 0.1 MGy of integrated dose. A longer period will be required to irradiate robots in the second line if 1 MGy of integrated dose is required for all robots in the *Irradiation Room*. The values presented here are reasonable with respect to the world market for irradiating entire robots as well as for the electron accelerators considered for *TechnoFusión*.

9.4.2.6. Conclusions: *Irradiation Room* requirements

- The minimum effective volume required is 4 x 4 x 3 m^3. An effective volume of 5 x 5 x 4 m^3 would result in higher performance and greater possibilities for irradiation but it has double the irradiated volume. Note: the effective volume is that volume that can be occupied by robots for testing.
- The gamma dose in the first row will be at least 500 Gy/h. The dose in the second row will at minimum be 100 Gy/h.
- Beam sweeping should be concentrated on a relatively reduced area (about 4m^2 or less) from the wall of the gamma ray generator in order to obtain as high as 2000 or 3000 Gy/h in a small volume inside the *Irradiation Room*. Such characterization may be needed occasionally for special certification cases.

Other requirements that need to be considered include:

- Wall, floor, ceiling, and shelve elements that are used to support the irradiated robotic manipulators.
- Cranes and stacking machines used to position small robots and robotic manipulator tools on structures such as shelves.
- Robot power supply. They must have an adequate power supply as some robot parts will be validated under conditions where these are moving. In other words, the robots are performing the required displacements while being irradiated for their validation and certification. Thus each robot will require an electrical or hydraulic supply as well as conductors for signal cables.
- Standard wireless communication systems will need to be installed. These should be flexible systems in order to have dedicated wireless systems for each client.
- The cell will have to be prepared to permit the future installation of heating systems that could result in room temperatures up to 70 ºC.
- Safety requirements and construction norms related to gamma radiation chambers and rooms will have to be complied.

9.5. Experimental capacity

The RHT Facility will develop its tasks around two main work areas: the development of specific robotic systems plus teleoperation and robot control. These areas could be detailed out as:

- Teleoperation of tasks, such as communications, interface, man-machine and bilateral control.
- High performance robots (dimensions and effort) with both parallel and modular structures.

- Perception around semi-structures with 3D vision and force sensors.
- Virtual Reality for the representation of realistic virtual environments and simulation of maintenance operations.
- Mobility and transport (inside and towards the exterior) of robots and mobile manipulators, humanoids, and other locomotion alternatives.
- Radiation hard robot components.

9.5.1. *TechnoFusión* teleoperation tasks

The RHT Facility will have to ensure the efficient performance of teleoperated manipulation tasks, such as component testing for ITER diagnostics or testing of IFMIF module prototypes. A Remote Handling installation consists of two central components, the operator control post and the manipulation remote. Figure 9.19 illustrates the relationships between both posts.

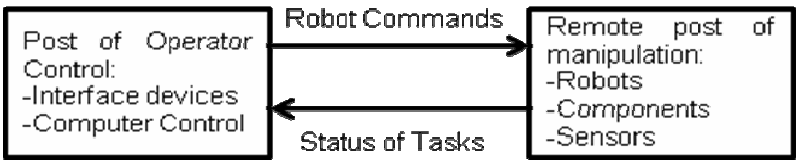

Figure 9.19. Scheme showing how a teleoperated system works.

The operator control post has two objectives: the first, the transmission of orders generated by the operator to remote robots and, the second, to inform the operator about the status of the work in progress. In order to carry out this operation, an advance teleoperation interface is required. The main installations needed for this are:

- Master with force reflection. These devices follow the movement of the operator's hands. This movement is used to generating the corresponding trajectories of movement of the remote robot (also called slave). The forces that are generated when the remote robot interacts with its environment are reflected on the master in a manner that the operator perceives the generated forces. Various types of telemanipulation systems exist on the market, such as those shown in Figure 9.20, which correspond to a master-slave architecture. Moreover, it is important to point out that a haptic interface that complies with the functionality of the master solely would be connected to the remote robot. A clear requirement of tasks relevant to the RHT Facility at *TechnoFusión* is the

need to perform bimanual tasks. It will require the use of two masters with force reflection. These are tasks that do not use both masters simultaneously for manipulation. One master usually serves as support for the other. However, using both masters offers a clear advantage and a simplification of the procedure is obtained.

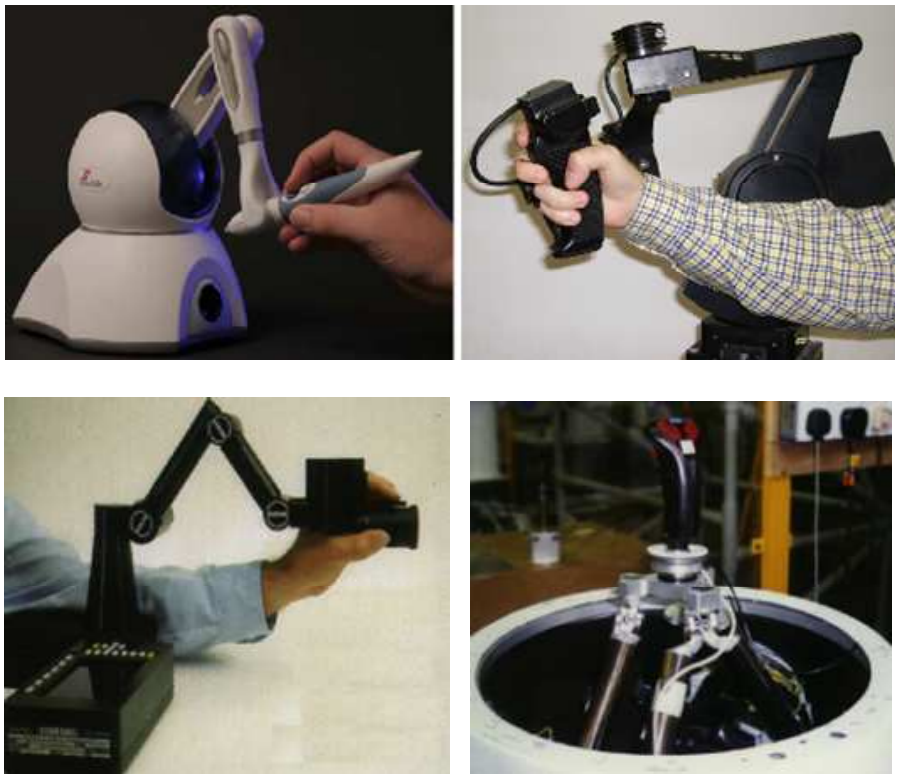

Figure 9.20. Different haptic devices used as masters for controlling remote robots Telemanipulation tasks.

- Visualization of stereoscopic and panoramic images. The visualization of a manipulation procedure being undertaken in a remote environment is done using only two monitors. One monitor shows a panoramic and general images of the environment. The other one is used for visualizing stereoscopic images of the objects to be manipulated. The visualization of panoramic images allows the operator to determine the relative position of objects inside the remote environment and consequently, increases the operator's perception. The stereoscopic images allow the operator to know the size of and distance to the object to be manipulated with precision. Although the use of several monitors is common in Remote Handling laboratories, it is of little use since the operator will have difficulty visualizing several monitors at the same time. Figure 9.21 shows devices of stereoscopic vision.

Figure 9.21. Stereoscopic Visualization System. Robot with binocular camera (left), operator with glasses for correct visualization of a stereoscopic image (centre), image of object as seen on the screen (right).

A teleoperation interface also relies on other devices that permit the efficient performance of tasks. These devices, such as switches, handles, etc., will be specific to the task to be carried out. Other devices that are commonly used include voice monitoring systems that allow the operator to generate voice commands or to record technical comments about the work being undertaken or about situations encountered.

9.5.2. High performance robots

Conventional structures are inefficient, since they require actuators with large torque features that are difficult to apply for the manipulation of very large or very heavy objects. As an alternative, parallel structures can be used. Such structures allow actuating on the object to be manipulated at several points in a synchronized manner. Another structure is a modular type formed by simple properly connected elements, which can lead to more complex structures.

Parallel robots are robots whose mechanical structure is formed by a closed-chain mechanism whose end-effector is connected to the base by at least two independent kinematic chains. Figure 9.22 shows three examples of parallel robots in which the advantages of their use in relation to their required performance can be clearly observed.

By careful observation and study of these structures, some of the problems for their development could be figured out: kinematics study, control, and dynamics. All will need some requirements for precision of position and control of force.

Modular structures (Figure 9.23) have demonstrated great flexibility in performing robotic tasks relevant to *TechnoFusión*. These systems have the advantage of adapting to the task by adopting different configurations.

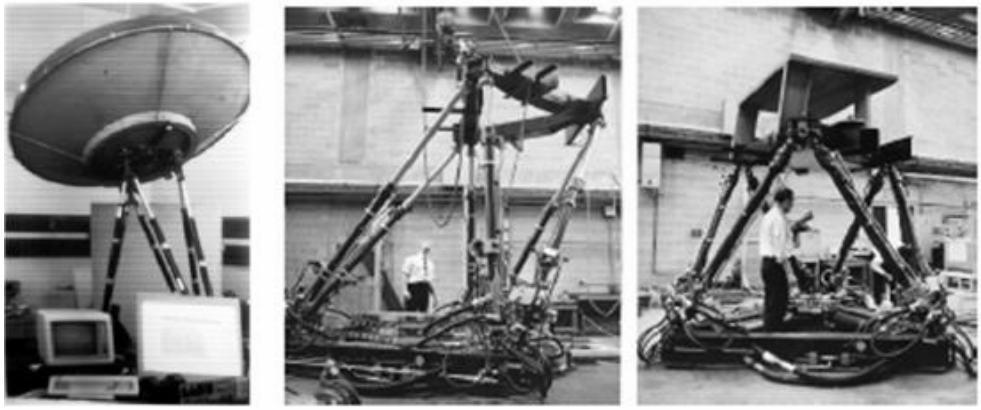

Figure 9.22. Example of parallel robots.

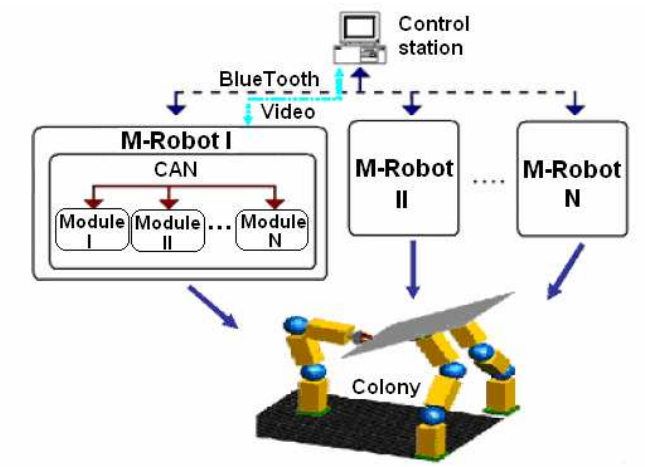

Figure 9.23. Modular system cooperating to perform tasks.

9.5.3. Perception of semi-structured environments

The reconstruction of the work environment is a key point for the semi-automation of teleoperated tasks. It is usually based on using computer visual systems that allow the reconstruction of the work environment from images captured by the cameras. These systems are of great interest, due to the fact that they allow the semi-automation of tasks when the position of certain objects is known. Processing commands of high level relative to the task being carried out can then be performed. Also, 3D laser telemetry can also be considered as a useful tool for environment reconstruction. The direct information of distance to objects that the laser telemetry gives also allows the semi-automation of tasks with great precision.

Figure 9.24 shows a system for environment reconstruction for teleoperation, which allows the monitoring of the work process. Efficient performance of a teleoperated task requires a previous definition of the procedure to perform. It allows a control shared between the operator and the system computers, where computers carry out the task and the operator only intervenes when the operation becomes complex.

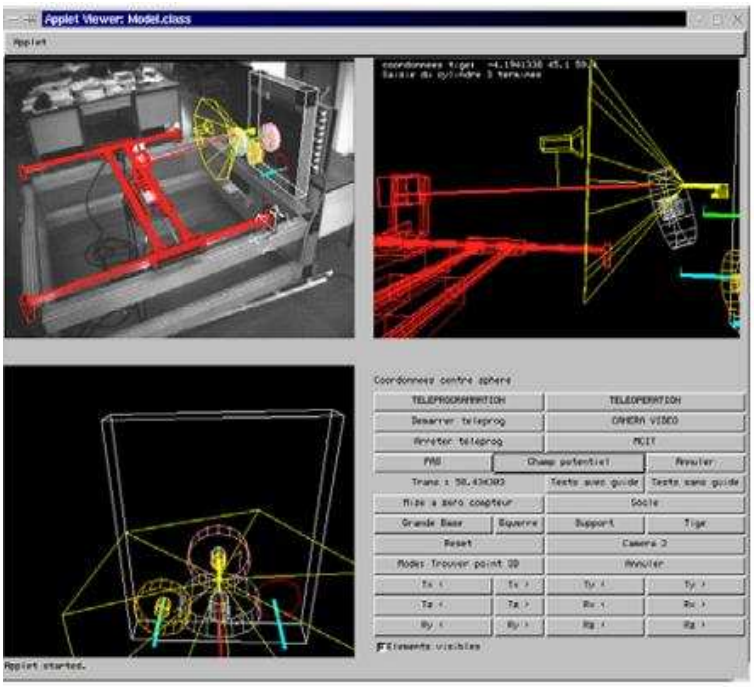

Figure 9.24. System for the reconstruction of the environment for telemanipulation.

9.5.4. Virtual reality

One of the most promising technologies is the incorporation of Remote Handling tasks into Virtual Reality for recreating artificial environments through techniques of realistic virtual representation of objects and properties. These techniques, which are applied to games and also to industrial equipment such as simulators, are considered here for testing manipulator designs and for verifying solution adopted for the operation, especially in situations that require Remote Handling.

Virtual reality is starting to be applied in multiple fields, such as promoting tourism, real estate, and construction projects. The RHT Facility will play an important role in training operators of complex equipments.

Virtual representation is fundamentally important, since the work areas of the manipulators are inaccessible. Regarding operators, the perception is as if they were being governed directly. That is why this area has to be perfectly integrated in the points expressed in 9.5.1 "Teleoperation of tasks for *TechnoFusión*" and 9.5.3 "Perception of semi-structured environments", taking advantage of the sensorial information that these areas give.

9.5.5. Mobility and transport (inside and towards the exterior)

Considering the different operations to be performed, especially in the context of equipment maintenance in fusion installations, the transportation of components of different systems by the same robot is required in order to perform manipulation tasks.

One of the very important transport systems in this type of installation is the Crane Bridge (Figures 9.25, 9.26, and 9.27). In order to define the most suitable type of Crane Bridge to be applied, the specific transport needs of a certain task need to be studied. However, in general terms, cranes with various independent cables can be proposed for the type of installations[164, 165] under consideration.

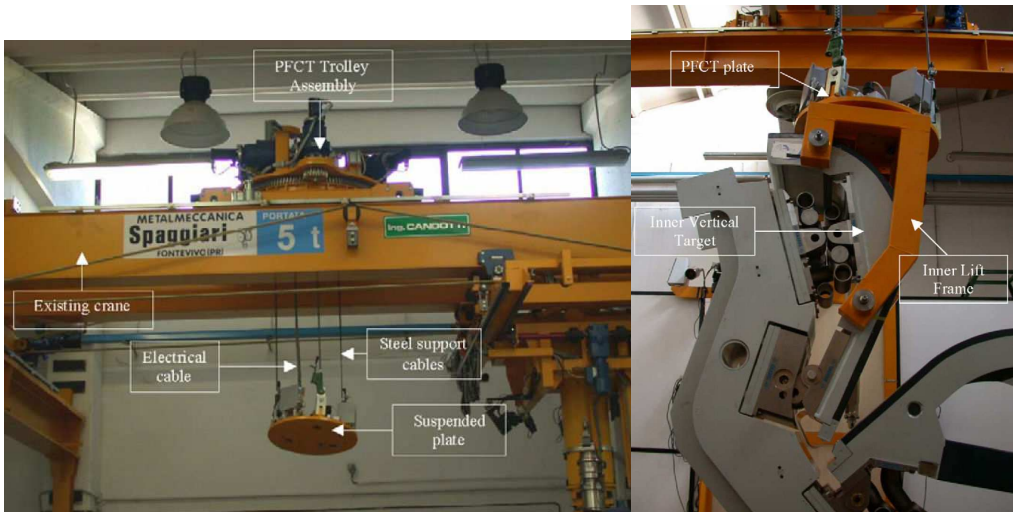

Figure 9.25. A general view of the component transporter from the first wall (PFCT). The principal elements of the PFCT are the trolley assembly, cables, and suspended disc (left). Part of the vertical corner of PFC (right).[164].

[168]'The plasma-facing components transporter (PFCT): A prototype system for PFC replacement on the new ITER 2001 casete mock-up'; G. Miccichè et al., ENEA; Fusion Engineering and Design; January 2007.

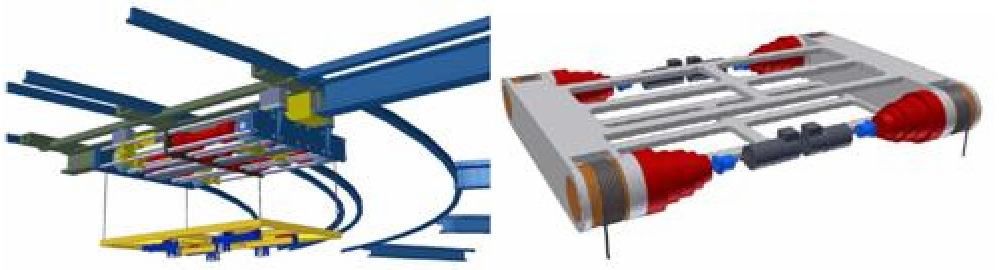

Figure 9.26. Conceptual design of two cranes proposed for IBERTEF for ITER NBI RH [165].

Figure 9.27. Robotic Crane, University Carlos III of Madrid [166].

In this particular case, the crane has to be incorporated with anti-balancing systems and techniques for precise positioning. Such systems have been developed for cranes with heavy loads[167,168] as commercial systems with such characteristics are not available in the markets, so

[165] "ITER neutral beam remote maintenance system design, crane design report" ; EFDA Task: TW6-TVR-NBRH ; Gonzalo Taubmann (SENER). With permission to reproduce the two figures in this document.

[166] S.Garrido; M.Abderrahim; A.Giménez; R.Díez; C.Balaguer. Anti-swinging Input Shaping Control of an Automatic Construction Crane . IEEE Transactions on Automation Science & Engineering. Vol. 5. No. 3. pp.549-557. 2008.

[166]"A Feedback Control System for Suppressing Crane Oscillations with On-Off Motors". Keith A. Hekman and William E. Singhose. International Journal of Control, Automation, and Systems, vol. 5, no. 3, pp. 223-233, June 2007.

it will require building this type in accordance with *TechnoFusión* specifications. In relation to such needs, it is important to take into account the experience of the research team at the *RobotisLab* of University Carlos III of Madrid in anti-balancing systems for controlling cranes.

9.5.6. Radiation-hard robot components

One area for further study is the Robotic Systems resistance to radiation. Systems developed in *TechnoFusión*, as well as other robotic manipulators, could be studied in detail. The resistance of the main components, such as actuators and sensors, has traditionally been covered, which led to developments of others specific components with guarantees of working under irradiated conditions for a given time. The aspect to be studied by *TechnoFusión* is mainly the effect of radiation on complete manipulator equipment: robots, tools, cranes, etc.

Installations for validation, testing, and certification of robots such as the ROVVER 4 (Figure 9.28), used for nuclear energy generation applications in Palo Verde Nuclear Plant, are practically nonexistent, especially for robots larger than certain dimensions. In this field, the RHT Facility could contribute and work on making large scale robots given its large installation and extensive capabilities.

Figures 9.29 and 9.30 show a preliminary concept and results for the planned installations for testing manipulators, based on calculations done for the *Irradiation Room*, and its gamma irradiation distribution carried out by Y. Herreras[169].

Figure 9.28. Camera and ROVVER 4 robot for PVNGS maintenance and inspection.

[167] "A controller enabling precise positioning and sway reduction in bridge and gantry cranes"; Khalid L. Sorensen, William Singhose_, Stephen Dickerson; Control Engineering Practice 15 (2007) 825–837.

[169] Internal Report "Cálculo para la optimización del diseño del Laboratorio de Manipulación Remota". Y. Herreras. Instituto de Fusión Nuclear."

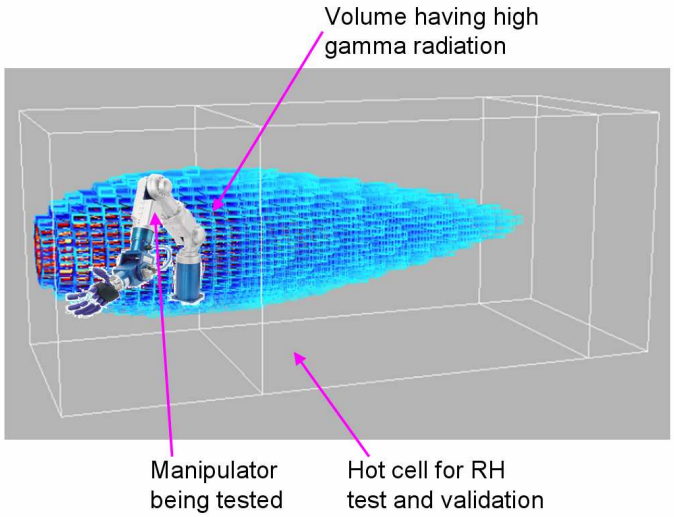

Figure 9.29. Preliminary concept for testing and certifying of manipulators inside the *Irradiation Room* of the RHT Facility.

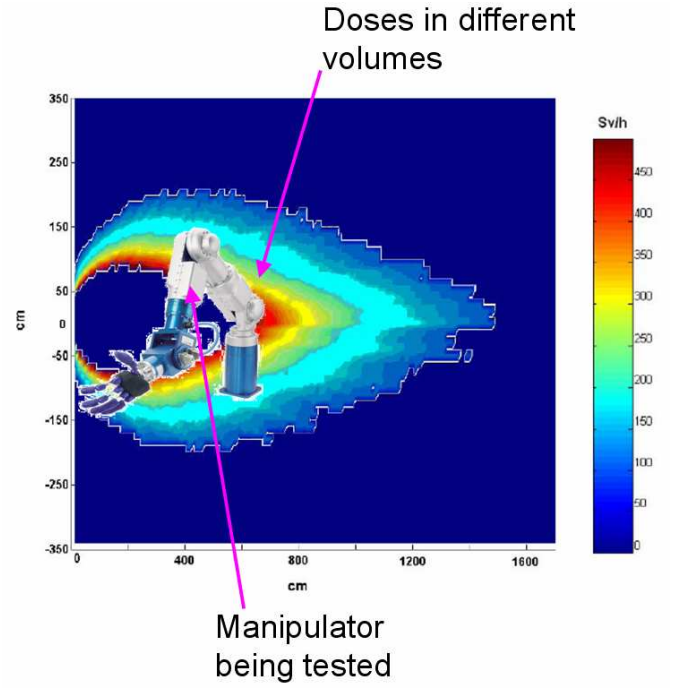

Figure 9.30. Preliminary calculation of the dose for the certification of manipulators and tools for the robotic manipulator.

9.6. Layout, supplies and safety requirements

(I) Required physical space and installations

In order to develop the research activities, the RHT Facility requires the use of the following rooms:

Laboratory for Experimentation with Large Prototypes: a laboratory where part models of fusion reactor installations can be assembled. It will also be used to test the performance of teleoporated robots. This room will accommodate different validation experiments for IFMIF, ITER, and DEMO, although not simultaneously. It is estimated that the minimum space required to carry out such work will be (30 x 13 x 15) m (see Table 9.3).

Irradiation Room: this will be where the performance of entire robotic manipulators as well as robot parts will be validated under low irradiation levels. Manipulators will be placed in this room for irradiation during the required period of time with the possibility to carry out repetitive manipulation tasks while being irradiated.It is estimated that the minimum dimensions (see Table 9.3) is of the order (4 x 4 x 3) m. An area of (5 x 5 x 4) m would be more appropriate in order to achieve more flexibility when certifying large manipulators such as those destined for fusion installations, e.g. DEMO. It should be noted that these estimates may change as they depend on the final engineering and architectural design.

- *Research Laboratory:* 400 m^2
- *Robotic System Design Department:* 100 m^2
- *General storage room:* 500 m^2

The two specific experimental installations must permit both evaluation of the performance of operation tasks of robotic systems and their development and set-up. Taking into account the proximity of the buildings, it would be advisable to consider rails or tunnels that could facilitate the transportation of irradiated equipment as well the sharing of installations such as storage or decontamination rooms. In addition, it there must be a set-up area for teleoperating the robot that should simulate parts of a real teleoperation room in a nuclear fusion plant or any other fusion installation. Moreover, although the occupied space is small, a portable in-situ control panel will be required to facilitate test operations and system performance.

Additionally, a minimum space for general services, such as toilets and washrooms, has to be included. Finally, Table 9.3 shows the space requirements for the *LELP Laboratory*, the warehouse, and *Irradiation Room*.

A detailed description of the two main laboratories of the *TechnoFusión*'s Remote Handling Technologies Facility are explained below:

(a) Laboratory for Experimentation with Large Prototypes

The term "simulation space" implies a minimum space of 30 (l) x 13 (w) x 15 (h) m^3. Some of the criteria to be taken into account for this are:

- The *LELP Laboratory* walls need to support the weight of the main Crane. It would be advisable to consider rails and to have the walls prepared for a second Crane with reduced capabilities that can cover the whole experimental installation or only parts of it. This second crane will emulate the crane of the ITER *Hot Room*. The validation of operations in the testing room cannot be performed correctly "in-service" with the Main Crane so some kind of specific crane may be required.

- An area of the *LELP Laboratory* walls will support the load of a future hoisting crane for manipulating loads in the ITER *Hot Room*.

- Access to the main Crane from the upper part of the *LELP Laboratory* has to be possible. Access times, although quite long, have to be acceptable in order to change the Crane Bridge Cart every 3 to 10 years. Such changes will be necessary in order to adapt the cart to future experimental requirements. Similar changes have already been undertaken, to a certain degree, for example in the ENEA-Brasimone test installation.

- The *Storage Room* has to have easy access through the crane bridge located in the experimental installations. The movement of oversized parts (several metres in length and/or several tons in weight) has to be done in a safe, easy and fast manner. At first, the most convenient manner would be to connect the storage room to the experimental installations in a longitudinal manner so as to use the Crane Bridge both in the storage room and the experimental installations. For small parts, the distribution inside the plant is not needed, as any location could be considered as being adequate.

Table 9.3. Space requirements for the installations of the *TechnoFusión* Remote Handling Technologies Facility.

Remote Handling Operation	Simulation space L x W x H (m^3)	Storage space L x W x H (m^3)	Observations
Extraction and insertion of DPP and TBM	30 x 6.5 x 7	10 x 6.5 x 7 3 units	A module of interchangeable parts is considered
Cask Displacement	20 x 13 x 4.5	8.7 x 2.6 x 3.7 2 units	While one *Cask* is being worked on and the other is in storage
Remote Handling in *Irradiation Room*	5 x 5 x 4*	25 m^2	Small equipment that could have variable shapes for its storage.
Extraction and insertion of irradiated modules	4.4 x 3.7 x 15	4.4 x 3.7 x 2	Determines height of the building. can not be displaced.

(b) Irradiation Room

An isolated and independent room has to be considered for the *Irradiation Room*. Its exact size is difficult to determine, as this will require some knowledge of the size of the robotic manipulator, the cranes to be validated under irradiation, and the number of robots to be irradiated at the same dose level (TANDRA). However, it is clear that the greater the number of robots to be irradiated simultaneously, the larger the investment needed for the accelerator and the installations. An investment balance based on the following has to be reached:

- For example, the cost of an *Irradiation Room* to validate real sized cranes for ITER. It would be excessive to only consider some parts of the crane to validate and certify. For example, the crane cart equipped with all components and some minimum tracks.

- Robots and structures for the manipulation of large sizes can be relatively big. However, in some exceptional cases, oversized structures can be split into two or three parts (the division into more parts is not possible since it affect the aims a test). The largest envisaged IFMIF robotic manipulator can be placed inside a space of 2 (l) x 2 (w) x 1 (h) m^3. Some manipulators, such as Movers, used for extracting ITER Port Plugs, fit in a space of 3 (l) x 3 (w) x 3 (h) m^3. The main robotic manipulator for maintenance of the UPP ITER Port Plugs could be placed in a volume of approximately 1.5 (l) x 1.5 (w) x 1.5 (h) m^3.

- The potential worldwide market for robot certifications for existing activated environments, which considers more than one hundred different large robots, hundreds of tools over the next 10 years, as well as hundreds of robots.

- The value of gamma radiation ITER, IFMIF and other worksites where more robots perform their tasks and in places of maximum radiation. Values of radiation dose received by robots are very diverse, from 500 Gy/h inside the vacuum chamber during 12 days after shut off the installation to 1 Gy/h or less outside the vacuum chamber. The *Irradiation Room* has to reach a point of equilibrium in order to irradiate the maximum number of robots for the maximum number of potential clients.

- The optimum gamma radiation value in the major irradiation zone inside the *Irradiation Room* and the value for the second row of robots. The minimum value of dose required in the first row of robots (see Appendix II) is of the order of 500 Gy/h, while in the second row it will be of 100 Sv/h. A small area of 1 m^3 exposed to a radiation of around 2000 Gy/s will also be very desirable.

- The number of medium-sized robots that fit in the *Irradiation Room*. The absolute minimum size of this room will be 4 (l) x 4 (w) x 3 (h) m^3 although a larger dimension of 5 (l) x 5 (w) x 4 (h) m^3 would be needed in order to make it relevant in the market for irradiating entire robots for fusion.

- The criteria for determining the required volume of the *Irradiation Room* in the RHT Facility is discussed in section 9.4.2 and in Appendix II, specifying the minimum

needed volume to cover the demands that may arise for both fusion and industrial devices. A study has been done regarding the average sizes of robots that can be used in ITER, DEMO, and IFMIF and the required gamma radiation doses in order to certify in equivalent and relevant conditions.

(II) Safety

The RHT Facility will be in compliance with the Labour Risk Law published in BOE nº 269, 10/11/1995 (R.D. 31/1995). Some of the specific risks to be taken into account in the Remote Handling Laboratory will be explained further. These specific risks and the required safety measures associated with this laboratory and *TechnoFusión* have to be developed more exhaustively for the external engineering studies.

As specific safety measures for the RHT Facility, norms related to the safety of robots inherent in the industrial installations have to be complied. The mentioned norms are based on ISO 12100, written by the Technical Committee ISO/TC 184 (Industry and Integration of Automated Systems) and the Sub-committee SC2 (Robots for Industrial Purposes), and have to be applied to both the *LEPL Laboratory* and *Irradiation Room*. The main points to consider from these norms are relative to the areas of safety that have to be taken into account in the installation and systems for stopping the robots. The space of safety is understood by all areas of work covered by the robots and the rest of the equipments that intervene in manipulations. This area has to be clearly delimited and access to it prohibited while performing tasks with robots. Shut off can be done as a response to an emergency that normally is activated by a corresponding operator action, or as a protection measure due to an unforeseen entry to the robot safety area. The ISO 10218-1 normative gives a more detailed description about the requirements and recommendations that have to be considered in the design of these installations.

The installations have to be equipped with safety and health signs in the work area as outlined in BOE nº 97 23/1997 (R.D. 485/1997).

Safety measures that have to be taken into account in the *Irradiation Room* of the RHT Facility are subjected to protocols and norms for health protection against ionizing radiation (R.D. 783/2001), since the devices are exposed to the effects of ionizing radiation. The gamma radiation present in the installation, with a dose rate of 100 to 700 Sv/h, obliges the *Irradiation Room* to be equipped with shielding, as mentioned in the norms. It is important note in particular the required shielding for doors from the exterior. The door has to be equipped for easy access while also being large enough to allow manipulators under irradiation to enter. In cases where workers are exposed during operation, there exists the Specific Health Vigilance protocol for workers exposed (category A and B) to ionizing radiation risks, undergoing periodic health examinations by Radiological Prevention Service personnel.

It has to be taken into account that gamma radiation could result in the activation of some of the irradiated components and, in such cases, the undertaking of decontamination and storage of slightly activated material and equipment in the *Irradiation Room*.

10. Computer Simulation

10.1. Introduction

The interaction between theory, including both speculations and logical demonstrations, and direct experimental observation lies at the basis of modern science. Theory, developed to a high degree of complexity with the help of ever more powerful mathematics, has allowed explaining many features of nature, and has often produced predictions that have only later been confirmed by experiment. The maximum attainable level of knowledge is obtained when models reproducibly predict events, given the same initial conditions.

The translation of theoretical models into computational models has made it possible to perform detailed simulations of physical phenomena with ever increasing accuracy. Today, the importance of computer simulation as a complement to experimentation is generally accepted. Simulation is used in research to generate new knowledge, and in engineering to facilitate the design of new technological facilities based on existing knowledge.

There is a wide international (and, of course, European) consensus that the design of components for facilities like ITER, IFMIF, DEMO, etc., requires computer simulations of both physics and engineering issues, alongside the appropriate experimental validation of the theories on which these simulations are based. In some cases, these computational models cover disparate spatial and temporal scales, so that Multiscale Models are required. Such models call for advanced programming knowledge, and require extensive computing resources and special visualisation tools. These resources are generally not available to every research group, making it difficult for a researcher without previous experience in this field to take full advantage of the undisputed potential of this technology. The **Computer Simulation Facility (CS)** of *TechnoFusión* aims to offer to research groups and companies expert support (including both personnel and the necessary tools), so that a complex Multiscale Simulation task can be undertaken in a relatively short period of time, in the framework of a multidisciplinary collaboration between the Facility and the external user. The proposal does not contemplate the possibility of installing a large computer on the premises of the centre; instead, use will be made of existing national and international computer facilities.

The main field of application of the CS Facility can be subdivided in two broad categories: i) problems related with engineering calculations needed for the detailed design of complex facilities (sometimes consisting of millions of components), and ii) those associated with physical phenomena taking place in a fusion reactor.

In Spain, ample experience in this field is available. However, this knowledge is dispersed among many universities (UPM, UA, UNED, UAM, UAB, UV, etc.) and research centres (CSIC, CIEMAT, etc.), so that the creation of a consolidated and integrated working group is desirable in order to centralise the various tools and make them available to potential users interested in their application to different aspects of fusion technology.

10.2. Objectives

Three major objectives are considered. An immediate objective of the Laboratory will be to undertake the computer simulation of all the components of the *TechnoFusión* (TF) facilities. This task will tackle outstanding challenges in the field of simulation. The second objective is of fundamental importance in medium and long term and involves creating and maintaining a team capable of carrying out computer simulation work as needed in the design of the installations of ITER, DEMO, the Commercial Fusion Reactor, and the supporting IFMIF irradiation facility. The third objective of the laboratory is to provide the required data handling capacity (data acquisition, storage, visualization/interpretation) as data are produced by the experiments performed at the *TechnoFusión* facilities; as well as the software needed to control the operation of the mentioned facilities.

In order to achieve the abovementioned objectives, the following activities must be undertaken:

I) To obtain and/or develop and/or adapt the required (adequately validated) computational methodology needed to assure that the design of the *TechnoFusión* facilities (accelerators, the lithium loop, etc) matches to the requirements for the operation of such facilities.

II) To obtain and/or develop and/or adapt the required (adequately validated) computational methodology needed to assure that the design of the *TechnoFusión* facilities (accelerators, the lithium loop, etc) matches to the requirements concerning radiological protection and safety.

III) To obtain and/or develop and/or adapt the required (adequately validated) computational methodology needed to manage the data (obtained from the experiments), including control systems for the *TechnoFusión* facilities.

IV) Establish sufficient simulation capacity to be able to handle the technologies to be incorporated in irradiation facilities such as IFMIF, based on high intensity accelerators.

V) Establish sufficient simulation capacity to be able to handle the technologies to be incorporated in the design of ITER, DEMO, and a Commercial Reactor.

In many areas of fusion technology, computer simulation can play a significant role. Some of the foremost issues are:

- The identification of particles and radiation emitted from the plasma, and their interaction with matter.
- The effect of radiation on materials.
- The interaction of neutrons with the blanket, requiring a description of energy deposition and the process of tritium generation.

- Knowledge of the fluid dynamics of the coolants (needed for energy extraction), and their effect on system components (corrosion, diffusion, the generation of impurities, etc.)

- The identification of the pathways for the release of tritium and other activated elements.

- Radiation transport, activation and dose calculations (prompt and residual), with implications for safety and the environment (the classification of plant materials, the definition of management, calculations of shielding, etc.)

- The interaction of the plasma with the first wall and its effects on the plasma and the properties of the material.

- Thermo mechanical calculations in complex components for design validation.

The establishment of the CS Facility is essential for the *TechnoFusión* facility itself, and in addition it is considered important to have an expert team at our disposal capable of executing and distributing the required computational work (including theoretical developments, when needed) regarding the various aspects associated with both ITER and future commercial reactors. Additionally, the CS Facility should have the capacity of dealing with the processing (and visualisation) needs that will arise once the experimental data start flowing in, both regarding equipment and personnel.

In the framework of the research and development needed for a future fusion reactor power plant, some well-defined areas exist which will be described next. Once the fusion reaction is initiated, energy is liberated in the form of neutrons, charged particles and electromagnetic radiation. Each of these particles interacts with the environment, thus allowing both the generation of enthalpy, to be extracted by means of a circulating coolant, and of tritium, required for the fuel cycle. But the liberated particles and energy are also responsible for problems associated with very large temperature gradients and damage caused to the crystalline or amorphous structures of the materials employed, affecting their operational lifespan, and causing the activation of the material. Given the fusion power source and a particular reactor design, the study of the following issues is therefore needed (to be modified iteratively):

- Radiation flux and fluency as a function of space (3D) and time:
  - Atomic and nuclear data.
  - Particle transport and interaction mechanisms (neutrons, charged particles and radiation).
- Heat deposition and its consequences, and heat extraction from the reactor:
  - Energy deposition methods.
  - Computational fluid dynamics with high spatial and temporal resolution.

- Thermo mechanical models.

- The effect of neutron irradiation on materials:
  - Multiscale simulation of the irradiation of materials.

- The consequences of tritium management:
  - Diffusion in material models.
  - Paths for tritium release from the system.
  - The evaluation of atmospheric dispersion and its consequences.

- The effect of radiation and activation induced by neutrons and other types of radiation as a function of radioprotection measures:
  - Highly detailed inventory models capable of simulating operational scenarios characterized by different types of radiation and energy spectra, with time dependence.
  - Computational methods for the prediction of the prompt and residual dose rate.
  - The generation, assessment and classification of radioactive waste.

- The implications of a given Plant design:
  - Plant engineering models capable of simulating the energy conversion system, critical points, and the operational situations and accidents that could occur in the Plant (safety issues).

In this preliminary stage, the aim is to identify the models already available for each of these proposed areas, or at least easy to obtain, and their suitability for solving the problems raised in the study of fusion facilities (ITER, IFMIF, etc.), as well as their computational requirements. This pioneering integral approach to knowledge is crucial for the conception of this facility of *TechnoFusión*.

The experimental facilities of *TechnoFusión* will require a suitable system for the acquisition, control, visualization and analysis of data:

- The Area for Visualization and Analysis will provide:
  - Support for data acquisition.
  - Support for data storage and backup.
  - Support for data access.

- Many experiments will require real-time complex control systems (cf. the experience at TJ-II)
- Centralization to simplify quality control.
- Both experiment and simulation require new analysis techniques due to:
  - The data volume (increasing with time).
  - The complexity of the systems analyzed.

- The Area for Visualization and Analysis will allow:
  - Extracting the maximum amount of information possible.
  - Presenting this information in a useful and attractive manner

In addition, the Computer Simulation Facility of *TechnoFusión* should include computational support, in order to provide the following services:

- Acquisition
- Maintenance
- Support
- Training
- Networking

10.3. Resources

The CS Facility will require ample resources (both personnel and infrastructure) in order to tackle the full computer simulation of the components of the facilities and their dynamical behaviour in a future fusion reactor. Therefore, the proposed CS Facility will cover:

- Simulation Models to determination particle fluxes (neutrons, charged particles and radiation) towards the system components. For this purpose, 3D MonteCarlo and Discrete Ordinates codes will be used, such as recent versions of MCNP or ATILA (SN). Also, tools will be developed to translate the graphical description of the plant (usually supplied in CATIA format, as is the case with ITER, for example) to the required input files for these codes.

- Simulation Models for the interaction of charged particles with matter, including phenomena like sputtering and wall erosion, based on basic codes like TRIM and

SRIM, as well as more detailed codes, involving Binary Collisions or Molecular Dynamics, and appropriately coupled to codes for the simulation of the plasma from an electromagnetic point of view. This particular aspect is crucial for the technological description of First Wall phenomena.

- Liquid metal fluid dynamics codes, including codes like FLUENT, STAR-CD or CFX, which can be used for the design of the blanket and the evaluation of its reliability for DEMO, within the framework of ITER.

- Structural simulation models based on programs like CATIA or ANSYS.

- Simulation models for the irradiation damage of materials: metals, ceramics and insulators. With this aim, Multiscale Simulation schemes will be implemented, including:

    - Ab initio quantum-mechanical calculations, to be developed alongside codes like SIESTA (UAM) and VASP.

    - Molecular Dynamics codes, including MDCASK and more flexible codes incorporating fundamental interatomic potentials, some of which are still under development (even for metals), and which ideally should be capable of describing displacement cascades and the basic mechanisms associated with irradiation damage.

    - Defect diffusion, based on Kinetic MonteCarlo or Rate Theory techniques, incorporating recent developments with respect to parallelization (as with BIGMAC), and providing a reliable description of long-term irradiation effects.

    - Dislocation Dynamics (DD), including the development of models suitable for materials with a variety of structures (fcc, bcc and others) on the basis of codes like DD·D or PARADIS, and the incorporation of dislocation and defect interactions.

    - Finite element models that allow calculating the macroscopic properties on the basis of parameters that have been obtained from the simulation of underlying processes.

- Simulation models for dose rate calculations (radioprotection)

    - Prompt dose: Computed on the basis of the most recent transport codes and databases; or by selection and integration of the appropriate computational elements. For many applications, it will be necessary to develop a proper methodology. A key aspect of this process is that the methodology must be validated for all the proposed *TechnoFusión* applications.
    - Residual dose: The ACAB activation code will be one of the main computational tools. ACAB incorporates the quantification of material activation by neutrons, radiation, and charged particles for any energy spectrum and irradiation-cooling scenario. Quantities related to activation are

predicted along with an estimation of the uncertainty due to the error in the cross sections used. Responses provided by the code allow radioprotection-safety assessments and the classification of irradiated materials from the perspective of their post-irradiation management (hands-on management or recycling, surface burial, declassification, etc.).

Below, it is discussed some of the salient features of *TechnoFusión* in more detail, due to their importance for the development of fusion facilities and the interpretation and analysis of results.

10.3.1. Safety area

The numerical evaluation of the consequences of safety hazards, by means of computer simulations, is considered fundamental for the design of a fusion facility and for the determination of its operational parameters. The main requirement would be to avoid the need for evacuation in the worst-case accident scenario. The aim of the safety analysis is to predict the impact on public health of an accident. For this purpose, three basic tasks are contemplated:

- A calculation of the radioactive inventory.
- The determination of the source term of accidental emissions.
- The evaluation of effects or final responses.

Possible tools for carrying out these tasks are:

i) **The calculation of the radioactive inventory:** the ACAB, FISPACT and ORIGEN codes. ACAB allows calculating the evolution of the isotopic inventory after material activation by neutrons, charged particles, or photons. Quite general irradiation/cooling regimes can be modelled as well.

ii) **The determination of the source term**, indicative of the radioactivity released into the environment: one must characterize accident scenarios in a sufficiently detailed manner, and perform the analysis thereof using thermohydraulic and heat transfer codes. Relevant key tools are the heat transfer code CHEMCON and the thermohydraulics code MELCOR. CHEMCON is used to simulate the evolution of the temperature due to decay heat and oxidation reactions. The calculated record of temperature vs. time then allows identifying the source term. The latter is input to the MELCOR code, which simulates the associated thermohydraulic phenomena, including the physics and dispersion of aerosols and the release of radioactive products. Tritium migration, in turn, can be simulated using the TMAP code (*Tritium Migration Analysis Program*)

iii) **Evaluation of consequences:** a method is needed to generate the DCF (Dose conversion factor, expressed in Sievert per released Bequerelium, Sv/Bq) for the released radionuclides, which, in turn, allows estimating the doses and health effects of the emission. These DCF libraries are obtained through codes like MACCS and their associated data libraries.

10.3.2. Waste management area

A widely accepted requirement for waste management in fusion facilities is to avoid deep geological storage of radioactive waste. ACAB and FISPACT allow estimating the generated radioactive inventory and evaluating its classification in the framework of given waste management criteria/strategies: surface burial, recycling by nuclear industry and declassification.

10.3.3. Uncertainties

The evaluation of a nuclear system depends on the ability to understand the physics underlying the whole process, from the fundamental physics of the nuclear reactions to neutronic, thermomechanic and thermohydraulic responses, material science, etc. Energy production, irradiation damage, radioactivity, decay heat and other related magnitudes are the result of the interaction between particles and nuclei. Therefore, in order to improve the description of the macroscopic effects of these mechanisms, an accurate knowledge of these quantities is required.

Therefore, in the state of the art of the nuclear system simulations, the uncertainties of nuclear data play an important role. The ultimate goal is to estimate the uncertainties propagation across all calculation steps, from the generation of nuclear data and its processing to the prediction of the radioactive inventory, particle transport, thermal and thermohydraulic analyses, etc. Through the implementation of, for example, first order perturbation and MonteCarlo techniques, it is possible to perform a complete sensitivity/uncertainty analysis at every stage.

10.3.4. Radiological protection area

In this area, the basic analysis tools are transport codes (and cross sections and/or models used to describe nuclear interactions), able to deal with different types of radiation and to determine the spatial distribution of the source terms and fluxes. Once the particle fluency has been determined, it is possible to obtain a radiological classification by means of the fluency to dose conversion factors, which are dependent on the energy and type of particle.

Transport codes of reference are:

- **MCNPX**: A MonteCarlo method transport code. It allows modelling the transport of neutrons, photons and charged particles. Version 2.5 computes the transport of light particles only (electrons, protons, deuterons, tritons, alpha particles). Version 2.6, still under development and not yet officially released, incorporates improved nuclear models for the determination of the reaction cross sections. It will also allow modelling the transport of heavy ions.

- **PHITS**: A MonteCarlo method transport code. It allows modelling the transport of neutrons, photons and light and heavy charged particles. Cross sections for nuclear reactions are calculated from nuclear models incorporated in the code.

- **FLUKA**: This is a general purpose MonteCarlo simulation tool for the calculation of particle transport and interactions with matter. It can simulate the interaction and propagation of about 60 different particles in matter with high accuracy. The top priority for the design and development of FLUKA has always been the implementation and improvement of sound and modern physical models.

In the case of ion transport, it will be crucial to estimate the corresponding material implantation and diffusion levels. Some selected codes are:

- **SRIM**: A MonteCarlo ion transport code. This code simulates the transport of charged particles, taking account of the dispersion processes only, due to either the electrostatic stopping power or nuclear interactions. It does not consider any nuclear reactions that could take place during particle transport. Its main use is the determination of implantation and energy deposition profiles in matter.

- **TMAP**: A deterministic diffusion code. This is a 1D code that allows establishing the evolution of concentration profiles for implanted ions. Its main purpose is the determination of the number of ions that have entered and left the material. The code is suited for the calculation of tritium diffusion in a material and its eventual release from it, and for estimating the total accumulation of ions inside the material, leading to D-D nuclear reactions as a consequence of high-energy deuterons originating from the accelerator.

Since some of the *TechnoFusión* laboratories will be radioactive installations, their design and the preparation of licensing documents will require prior studies on radiation protection and safety. Therefore, this will be a major task during the first phase of the computational laboratory. Currently, no reliable computational methodology exists to predict prompt and residual dose rates corresponding to the accelerators and associated irradiation modules of *TechnoFusión* (and other irradiation facilities driven by accelerators, such as IFIMF-EVEDA). Thus, one of the key objectives is to develop and implement a computational methodology capable of addressing the needs of *TechnoFusión* regarding radiation protection, and to carry out the evaluation and validation of all its computational elements. A secondary objective will be to apply this methodology to the design and operation of accelerators and irradiation modules, in order to show that an adequate solution has been achieved for all potential radioprotection issues.

10.3.5. Nuclear data analysis: the identification of potential requirements

(I) Nuclear data libraries

- *Neutron, proton and deuteron transport libraries.* Until recently, the FENDL-2.1 library has been adequate for calculations related to fusion facilities (ITER). However, the design of novel neutron sources such as IFMIF will require particle transport data for energies above 20 MeV (IFMIF will even require data up to 60 MeV). The range of data with potential fusion applications extends to even higher energies, namely up to 150 MeV. In order to develop such data libraries, codes will be needed in order to predict the effects of this type of nuclear reactions, in combination with experimental data contained in the EXFOR library. Thus, it is considered essential to develop tools to update existing libraries and extend their range to higher energies. In addition, the libraries must be completed with information on the covariance, derived from theoretical models or experimental results. And finally, programs or procedures need to be developed that are suitable for generating specific libraries through the use of NOY.

- *Neutron, proton and deuteron activation libraries.* The most complete activation library to date is EAF2007, including sub-libraries for neutrons, protons, deuterons and disintegration processes. Proper tools should be developed in order to transform these libraries into the ENDF format, and include the uncertainties or covariance values of the activation reactions for a broad range of energies.

- *Experimental activities.* Studying and evaluating existing experimental data, and identifying the need for additional experimental data.

(II) Codes for cross section generation

In order to estimate the probability of any nuclear reaction, transport codes like MCNPX or PHITS either use cross section libraries or built-in nuclear models. In the latter case, it has been noted that results can vary significantly from one code to the next, due to the specific estimations of cross sections included in each model.

Thus, one can conclude that it is essential to benchmark the cross sections used in the codes against experimental or simulated values.

- *Talys 1.0, EMPIRE-II 2.18.* These codes calculate nuclear reaction cross sections using several nuclear models, such as the optic model, direct reactions, the compound nucleus model, the pre-equilibrium model, etc. These codes produce cross sections for a particular reaction or for the production of a given particle (neutron, proton, etc.), and determine the differential cross section. These cross sections should be benchmarked against the experimental or simulated data contained in libraries like EXFOR.

10.3.6. Thermo mechanical simulation codes

Generally, these codes are finite element codes. Simulation codes designed in the past five years tend to unify the mechanical and thermohydraulic calculations, so that the cooling properties of a body and its mechanical stress distribution can be analyzed simultaneously. Prominent examples of this type of code are those developed by companies like START-CD and ANSYS.

- *The ANSYS code* is a widely used calculation platform that unifies modules originating from several independent codes. Each of these modules allows solving a clearly defined branch of physical problems. Below, a brief description of the various computational modules and their potential application is given:
  - *Ansys Fatigue Module:* starting from an ANSYS standard geometry, this module allows performing fatigue calculations in the following conditions: constant amplitude and linear and non-linear loads.
  - *Ansys Mechanical Module:* this is the module upon which the rest of the code rests. It allows simulating a solid using finite element analysis. It is possible to solve the following physical processes in a coupled way: acoustic, piezoelectric, thermomechanical and thermoelectric analysis, electromagnetic fields in the high and low frequency range, and the mechanical analysis of an elastic solid.
  - *AutoRegas:* is a DCF module developed to solve gas explosion problems in pipes and confinement chambers with complex geometries.
  - *CFX*: is a DCF module that is completely coupled to the generic meshing of ANSYS. By using these meshes it can interact with the mechanical module without interpolating on the solid surfaces. It also allows performing the following simulations: turbulence, chemical reactions, heat and radiation transfer, and multiphase problems.
  - *Fluent:* is a DCF code developed independently from all other ANSYS modules. The company owning the code has recently been acquired by ANSYS, so one can assume that this code will be fully integrated in the near future. Presently, Fluent is a separate program, which can read the ANSYS mesh and export its calculations in generic ANSYS format. It is able to solve the following problems: turbulence, acoustics, chemical reactions, heat and radiation transfer, multiphase problems, and magnetohydrodynamics.
  - *Polyflow:* is an ANSYS module to simulate viscoelastic materials. It allows simulating extrusion, blow moulding and similar shaping processes.
  - *Tgrid y Gambit:* are two generic mesh generators supplied with the ANSYS package. In principle, both are able to import specialized CAD geometries and generate a mesh of hexahedrons and tetrahedrons.

- *The STARCT-CD code* is a general-purpose finite element program, capable of simulating both solids (thermomechanics and heat transfer) and fluids on the same mesh. It allows solving the following problems: thermal analysis, mechanical analysis, chemical reactions, free surface problems, multiphase problems and turbulence.

- *The Open Foam code* is an open source, generic finite element code. It disposes of a number of pre-programmed modules, capable of solving generic problems, such as thermal analysis, turbulence, multiphase, and free surface problems, mechanical analysis, magnetohydrodynamics and electromagnetism, and combustion reactions. In contrast with the codes mentioned above, it is still in a relatively early development stage, and has a poor graphic interface, so that users need to have a thorough background in C++ programming. If this is the case, the addition of new models is quite straightforward, so the code can be applied to almost any subject. The only limitation of the code is that it can only handle a single control volume having the same equations on every node, so that it is not possible to simulate solids and liquids simultaneously.

- *The Flow3D code* is a FDC code with features similar those of CFX, Fluent or Start-CD. Outstanding features include the modelling of turbulence, heat and radiation transfer, acoustics, phase transitions, multiphase problems, free surface problems, mechanical stresses in solids, electro-osmosis, dielectrics, joule heating and viscoelastic solids.

10.3.7. Transitory thermal analysis

Transitory thermal analysis codes (like Relap) are an essential tool for the analysis of the behaviour of complex facilities during thermal transients. Even if the objectives of *TechnoFusión* do not include detailed full plant studies, these tools could nevertheless be very useful for the analysis of experimental facilities like the liquid lithium loop of *TechnoFusión*.

- *Relap5* is the latest branch of a family of codes for analyzing transients in nuclear plants, developed by the government of the UE over the past 30 years. In the last few years, it has been applied to the study of a design basis accident in the AP600 reactor series. Some salient features are: thermohydraulic models, 1D for loops, 2D for complex structures, heat transfer, models for complex systems (vessel, steam generators...), 1D and 2D heat conduction in complex structures, models for generic components like pumps, valves, electric elements and potential implementations of control systems in the module. A drawback is that the models for fluids other than water are unsatisfactory, making it impossible to analyze liquid metal loops.

- *Melcor* is a program developed by *Sandia National Laboratories* and financed by U.S.N.R.C for the study of severe nuclear plant accidents. Some salient features are: thermohydraulic models, heat transfer, in-fuel chemical reactions, hydrogen generation both inside and outside the vessel, and the generation and diffusion of radioactive aerosols.

10.3.8. Evaluation of the environmental impact of an atmospheric release

When a future fusion reactor suffers an accident, gases are released into the atmosphere, including tritium, and these will be dispersed in the atmosphere. The evolution of this dispersion depends on the atmospheric conditions in the area surrounding the discharge. The empirical model used to evaluate the resulting environmental impact is based on the Gaussian equation and a straight plume trajectory from the time of release onward. It is a diffusion model in an ideal atmosphere, yielding a normal distribution in all directions around the central axis of the radioactive plume. To improve the realism of this model, more information on the behaviour of tritium in the environment of a nuclear fusion facility should be added.

Tritium will primarily be released in the form of gas, i.e., elemental tritium (HT), or as tritium water vapour (HTO). All possible migration paths, from the tritium leak to the atmosphere up to its assimilation by the exposed population or maintenance personnel, are calculated for both forms. Based on the data regarding source terms for atmospheric release obtained in ITER studies, the dispersion of elemental tritium (HT) is much higher (by one order of magnitude in some cases) than that of tritium water vapour (HTO). The analysis and assessment of the chronic dose is essential

The scenario models to be considered are: standard operational conditions, unusual events, and cases with accidental tritium release. In all cases, the concentration of HT or HTO (or both) is monitored. In the case of standard operation, NORMTRI was used. This code is based in the ISOLA V dispersion model for events with a long duration, having constant emission rates for the duration of the observation. It evaluates each dispersion process, given a certain climatologic scenario, while taking the probability for that scenario to occur into account. For the accident scenarios, the UFOTRI code, based on the MUSEMET dispersion model, will be used in order to evaluate all the atmospheric parameters, based on experimental databases, on an hourly basis.

For a complete study of the diffusion, the removal and the absorption of tritium by people, two phases are considered, simultaneously in some cases:

- Primary phase: This phase starts at the time of the atmospheric release, and concludes when the tritium is deposited in the environment (soil surface, animals or plants). Some boundary conditions have to be defined for this phase. The statistical assessment considers 4 parameters: wind speed and direction, precipitation, and stability. In turn, these 4 parameters are subdivided into several classes (for example, the wind direction is classified in terms of 10% sectors and 30% amplitude intervals over 36 or 12 sectors). Taking into account the 6 stability classes, 7 wind speed ranges are defined, as well as 4 groups of precipitation intervals, considering all the boundary conditions. The geometry is defined so that the coordinate origin is the point of release. Then, the dispersion of the cloud is analyzed, given the described parameters, and the effects of the height of the tritium release point, the ground roughness and the duration of the emission are calculated. In order to understand the importance of these factors, every event is analyzed deterministically and compared with actual probabilistic data, measured hourly, and combined with

meteorological data to provide a global study that simulates the complete dynamics of the transport and diffusion of tritium into the environment.

- Secondary phase: When the plume drops to the ground, the secondary phase is initiated. This phase starts immediately after the start of the primary phase or, in some cases, in parallel. The tritium flux into each sector of the mesh depends on the air-soil exchange rate. To estimate the tritium concentration on each point of the mesh, one must again consider all the actual meteorological parameters (solar irradiation intensity, humidity, ground roughness, etc.), as previously established in the early and subsequent phase of the release.

Tritium deposited on the surface, the vegetation, or in water can return to the atmosphere by transpiration or evaporation. Such tritium mobilization mechanisms are called re-emission processes. These phenomena affect both chemical forms of tritium, although the mechanism is different: HT from the primary plume returns to the atmosphere as tritiated water, whereas HTO may evaporate or transpire directly, without any type of conversion. The total amount of re-emission depends strongly on HT oxidation due to bacterial action in the first 5 cm of the subsoil. The re-emission increases the tritium level in the air. Thus, the re-emission must be added to the inhalation and skin absorption doses that originate directly from the primary plume. HT levels will be reduced in favour of an HTO rise. Nevertheless, the origin of this tritium increase is not caused by the primary tritium, but by the conversion of HT into HTO. The concentration loss of the initially deposited tritium is represented by an impoverishment rate that translates into a transfer rate of the surface tritium into other subsoil levels or to other elements such as roots or tubers, which will be analyzed later. These processes are strongly dependent on the environment of the deposition site, the floor and/or the vegetation, including parameters such as: floor type, porosity, Darcy laws, photosynthetic activity, humidity and solar intensity. Tritium does not remain on the surface, but it evaporates or penetrates into deeper zones, ending up in the groundwater layer. Once the tritium is deposited on the surface, tritium oxide competes with free surface water to interchange hydrogen. The tritium concentration count is made in layers of 15 cm, down to the usual depth of plant roots. Normal and tritiated water may rise due to capillary forces and due to matrix potential differences, but the speed of ascent is smaller as the potential differences decrease. Roots can absorb water until a limit is reached (the shrivelling point). At this point, water absorption by the root stops. The mentioned transport of water is strongly dependent on the structure of the floor, and in particular its porosity.

Once the tritium has penetrated and has been incorporated, the internal irradiation source is continuous, and the local dose rates increase until the tritium is eliminated from the body by sweating, excretion, or exhalation. Any remaining activity due to tritium in the body is difficult to quantify, because all process involved, the incorporation of tritium in the body, its retention and its cellular incorporation, are very complex. All the soft tissues of the human body are sensible to the radiation from tritium disintegration. In the framework of radiological protection studies, tritium dosimetry is considered to provide an all body dose, because the soft tissues make up 90% of the body weight. Furthermore, one has to consider the chemical properties of tritium, which allow it to substitute internal hydrogen easily in a large number of molecules, not only in somatic cells, but also in the genetic material. Both chemical forms of tritium, HT and HTO, can be incorporated into the respiratory tract, either by direct inhalation from the plume or by absorption through the skin. The conversion of tritium into OBT (*Organically Bound Tritium*) establishes the dosimetry of the ingestion dose calculations. These

calculations start when the early phase, involving deposition, oxidation and re-emission, is past. Because of this, the oxidised form of tritium is used for the internal dose count, whether the emission is HT or HTO.

10.3.9. Radiation damage

Material radiation damage could be studied in two ways:

- Experimentally, by analyzing the results of experiments that provide information about radiation damage of the microstructure and the mechanical material properties, or
- Theoretically, in terms of a computer simulation.

Computer simulation studies are ever more important in all fields of science due to the ever-increasing computing power available. And materials science is not an exception.

Currently, simulation methods that have a large impact on the materials are those based on an atomistic point of view. Here, the idea is obtain knowledge about the macroscopic material properties from data obtained at the atomic level. This is also the methodology currently used to develop models for the study of materials under fusion conditions. This methodology is called Multiscale Simulation.

Multiscale Simulations cover everything from 'ab initio' calculations, based on Quantum Mechanical models, through molecular dynamics, defect diffusion and dislocation dynamics, to finite element models that allow the calculation of macroscopic material properties.

10.3.9.1. The physics involved

The starting point of Multiscale Simulations is quantum mechanical calculations based on *Density Functional Theory* (DFT). Input parameters for the method on the next space-time scale level are generated from the results obtained at this level. The precision of the results at the macroscopic level depends strongly on the precision of the parameters on all lower levels, and ultimately on correct quantum mechanical data. Basically, electrons are responsible for the bonding between the atoms forming the molecules, of which the materials are composed. The nature of the electronic states determines the properties and the response of the material in extreme conditions. Nevertheless, this type of calculations is very expensive, and can at present only be performed for small molecules (consisting of a few hundreds of atoms). Results from this methodology are used to estimate interatomic potentials. The interatomic potentials are required at the next space-time scale level, Molecular Dynamics.

The DFT calculations provide fundamental properties such as the total energy. Knowing the energy exchange at the atomic positions, one can obtain information about the equilibrium geometry, the activation energy of atomic diffusivity, and the stability of the

various types of defects or dislocation structures. The forces and stress tensors can also be obtained, thus facilitating Molecular Dynamics Simulations.

A commonly used code for performing such calculations is SIESTA (*Spanish Initiative for Electronic Simulations with Thousands of Atoms*).

SIESTA is both a method and an implementation in terms of a computer program, oriented towards electronic structure calculations and *ab initio* molecular dynamics simulations of molecules and solids. Its main characteristics are as follows:

- It uses the standard Kohn-Sham self-consistent density functional method, in the *Local Density Approximation* (LDA-LSD) or *Generalized Gradient Approximation* (GGA).
- It uses atomic orbitals as a basis set, allowing unlimited multiple-zeta and angular momenta, polarization and off-site orbitals.
- It projects the electron wave function and density onto a real-space grid in order to calculate the Hartree and Exchange-correlation potentials and their matrix elements.
- It allows using localized linear combinations of the occupied orbitals, so that the computer time and memory requirements scale linearly with the number of atoms.
- It is written in Fortran 90 and memory is allocated dynamically.
- It may be compiled for serial or parallel execution.

This program provides:

- Total and partial energies.
- Atomic forces.
- Stress tensors.
- Electric dipole momenta.
- Atomic, orbital and bond populations (*Mulliken*).
- Electron densities.
- Relaxed geometry, fixed or variable cell.
- Spin polarized calculations.
- Band structure.

- K-sampling of the *Brillouin zone*.

Computational needs: the goal is to make ab initio calculations for thousands of atoms, instead of the hundreds that are typical of present-day calculations, in order to study the defects by irradiation on a scale similar to the experimental samples.

With this type of methods, typical calculations require between 10.000 and 100.000 computer hours on a normal processor.

Regarding communication, scaling behaviour with the number of processors, memory requirements, and total computing time, a typical calculation with the SIESTA code shows the following:

i) Molecular Dynamics

Molecular Dynamics (MD) is a simulation technique used in the field of Physics and Chemistry of the Solid State. In this technique, atoms and molecules can interact for a period of time. In general, molecular systems are complex and are made up of a large number of particles. This makes it impossible to write their properties in an analytical form. To circumvent this problem, MD uses numerical methods. The technique forms is at a crossroads between experiment and theory, and it may be viewed as a computer experiment.

Molecular Dynamics is an interdisciplinary field. The laws and the theory derive from Mathematics, Physics and Chemistry. It makes use of algorithms from Computational Science and Information Theory. Molecules and materials are not described as rigid entities, but rather, as evolving bodies. Its original application was in the field of theoretical physics, but currently it is used mostly in biophysics and material science. Its fields of application vary from catalytic surfaces to biological systems.

This technique shows that a link exists between computational cost and the reliability of the results, as it uses Newton's equations, which are less expensive than quantum mechanical equations. For this reason, some properties cannot be studied with this methodology, such as the breaking and formation of bonds, since excited states or reactivity cannot be handled.

Hybrid methods exist, called QM/MM *(Quantum Mechanics/Molecular Mechanics)* models. These models treat reaction centre using quantum mechanics, and the remainder using classical theory. With these methods, the challenge lies in defining the precise interaction between the two descriptions.

Microcanonical Ensemble (NVE). The simplest model of molecular dynamics is obtained using the microcanonical ensemble description. In such an ensemble, the system is considered isolated: the volume (V) does not change and it does not exchange mass (M) or energy (E) with the environment. In a system consisting of N particles with coordinates X and velocities V, one derives first order differential equations. The potential energy function U(X) describes the attraction and repulsion between the atoms due to the chemical bonds, electrostatic interactions, Van der Waals forces, etc. U(X) is also known as the force field and it is a function of the particle coordinates X. Usually it is derived from quantum chemical calculations and/or spectroscopic experiments. Nevertheless, the force field has a functional form that is typical of

classical mechanics. The particle trajectory is discrete in the time co-ordinate. Usually, a small time step (e.g., 1 fs) is chosen in order to avoid numerical errors due to the discretization. The position X and the velocity V are integrated using a simplistic integration method, such as the Verlet method, for each time step size. Given the initial positions (e.g. the X ray structure of a protein) and the initial velocities (e.g. random and Gaussian) one may calculate all the positions and velocities in the future.

Other ensembles (NVT, NPT). Other methods exist, with different characteristics for similar systems, such as systems with a constant temperature or a constant pressure. These methods greatly enhance the utility of MD for the systems under study.

The Software codes that are most commonly used for computational Molecular Dynamics calculations are the following:

- *LAMMPS (Large-scale Atomic/Molecular Massively Parallel Simulator) and MDCASK* are the most commonly used computational codes in material science. LAMMPS was developed at Sandia National Laboratories, a US Department of Energy laboratory, and MDCASK was developed at Lawrence Livermore National Laboratory, also a US National Energy Supercomputer Centre. Both are parallel codes, and capable of using multiple processors during a calculation, thus increasing the size and timescale of the systems that can be studied. The scalability, i.e., the efficiency of the parallelization, is almost linear. Therefore, by increasing the number of processors, calculations can be performed for a larger number of particles interacting for more time, thus increasing ergodicity and statistics.

- *Kinetic Monte Carlo.* Kinetic Monte Carlo (KMC) is a Monte Carlo method intended to simulate the time evolution of some specific naturally occurring processes. Typically, these are processes that occur at a given known rate. It is important to understand that these rates are inputs to the KMC algorithm, and the method itself cannot predict them.

  The KMC method is essentially the same as the dynamic Monte Carlo method and the Gillespie algorithm. The main difference appears to be in the terminology and the applications: KMC is used mainly in physics, while the 'dynamic' method is mostly used in chemistry.

  By way of example, the KMC algorithm for simulating the time evolution of a system in which some processes occur at known rates r can be written as follows:

  i. Set the time t = 0.
  ii. Form a list of all possible rates in the system r_i
  iii. Calculate the cumulative function for i = 1, etc. N where N is the total number of transitions.
  iv. Obtain a uniform random number u' [0, 1]
  v. Determine which events will occur by finding the i for which $R_{i-1} < u'R \leq R_i$.
  vi. Carry out the event i.

vii. Recalculate all rates r_i which may have changed due to the transition. If appropriate, remove or add new transitions i. Update N and the list of events accordingly.

viii. Obtain a new uniform random number *u* [0, 1].

ix. Update the time with t = t + Δ*t* where Δ*t=-log u/R*.

x. Return to step 2.

In different sources, this algorithm is known variously as the residence-time algorithm, the n-fold way, the Bortz-Kalos-Liebowitz (BKL) algorithm, or just the kinetic Monte Carlo (KMC) algorithm.

KMC has been used in simulations of, e.g., the following physical systems: surface diffusion, surface growth, vacancy diffusion in alloys (this was its original use in (Young 1966)), defect mobility and clustering in solids irradiated by ions or neutrons.

To give an idea what these 'objects' and 'events' may be in practice, here is one concrete and simple example, corresponding to example 2 above.

Consider a system in which individual atoms are deposited on a surface, one at a time (typical of physical vapour deposition), and which can also migrate across the surface with some known jump rate w. In this case, the 'objects' of the KMC algorithm are simply the individual atoms.

If two migrating atoms arrive at adjacent locations, they become immobile. The flux of incoming atoms determines a rate $r_{deposit}$, and the system can be simulated with KMC by considering all deposited mobile atoms which have not (yet) met a neighbour and become immobile. Thus, the following events are possible at each KMC time step:

- A new atom arrives with a rate given by $r_{deposit}$
- An atom that has already been deposited makes a jump with rate w.

When an event has been selected and the KMC algorithm has evaluated it, one needs to check whether the new or migrated atoms have become immediately adjacent to some other atom. If this is the case, the adjacent atom(s) need to be removed from the list of mobile atoms, and their jump events removed from the list of possible events.

Naturally, when applying KMC to problems in physics and chemistry, one has to consider first whether the real system matches the assumptions underlying KMC to a sufficient degree. Real processes do not necessarily have well-defined rates, the transition processes may be correlated, the jumps of atoms or particles may not occur in random directions, and so on. Also, when simulating widely disparate time scales, one needs to consider whether different processes may occur on longer time scales. If any of these considerations apply, the time scales and the system evolution predicted by KMC may be biased, or even completely wrong.

KMC methods can be subdivided according to the type of motion or the nature of the reactions. The following, incomplete, classification is often used:

- Lattice KMC (LKMC) methods refer to KMC on an atomic lattice. Often, this variety is also called atomistic KMC, (AKMC). A typical example is the simulation of vacancy diffusion in alloys, in which a vacancy is allowed to jump around the lattice with rates that depend on the local elemental composition. A code of this type that is commonly used is LAKIMOCA, developed by EDF in France.
- Object KMC (OKMC) methods refer to KMC applied to defects or impurities, jumping in either random or lattice-specific directions. Only the positions of the jumping objects are included in the simulation, not those of the 'background' lattice atoms. The basic KMC step is one object jump. A code using this method is BIGMAC, developed at LLNL, USA.
- Event KMC (EKMC) or First-passage KMC (FPKMC) refers to a variety of OKMC in which the next reaction between objects (e.g., the clustering of two impurities, or vacancy-interstitial annihilation) is chosen by the KMC algorithm, taking into account the positions of the objects, and this event is then immediately carried out (Dalla Torre 2005, Oppelstrup 2006). The code most commonly used is JERK, developed at CEA, France.
- Parallel KMC (PKMC) is a modification of the OKMC algorithm that allows a parallel implementation. Due to this, the study of larger systems, during a longer period of time, becomes possible. The algorithm and its implementation have been developed recently by the UPM (Spain) in collaboration with LLNL, USA.

However, in practice, Monte Carlo simulations are limited to small volumes (cubes of up to 1 µm, depending on the conditions) and become computationally expensive when the irradiation dose is high and/or when time scales of the order of nuclear reactor lifetime are explored.

This limitation can be overcome by using rate theory (RT) as an alternative. In this approach, based on the mean-field approximation, the diffusion of defects is modelled by means of a set of diffusion-reaction rate equations, while the nucleation and/or the growth of clusters is described by the master equation. In this model, the evolution of the medium concentration of an impurity or the evolution of a cluster of a given size is governed by a continuity equation. The system is represented by a set of connected partial differential equations (from hundreds to thousands of equations). Rates, such as the diffusion coefficients or the dissociation frequencies, are calculated from the KMC input data, so these two methods are based on the same parameters.

The RT approach is attractive due to its reduced computational requirements, thus allowing the exploration of defect evolution over large time scales and distances, close to the experimental values. However, one of the basic assumptions in the mean-field approximation is that defect production is uniform in time and space, and set at some appropriate value. In other words, rate theory does not consider the position of each of the defects but it calculates the medium concentration of each type of defect. When complex mechanisms are considered, results obtained by RT

models can deviate from those obtained by KMC. For example, RT cannot deal with the recombination of correlated I-V defects generated by irradiation.

KMC and RT are complementary methods and can be used in a multiscale simulation strategy.

The RT code PROMIS 1.5 has been developed by S. Selberherr and P. Pichler at the Technological University of Vienna. It allows solving general diffusion equations in 1D or 2D under general environmental conditions. Generation-recombination terms, boundary conditions and a diffusion flux that is directed or induced by an electric field can be easily implemented if necessary. Input parameters are the same as those in KMC.

With KMC, the position of each defect is stored. Therefore, the computational requirements increase linearly with the number of defects (for example, in the case of a high irradiation dose). A typical problem might require a few days of computation, or several thousands of hours. Therefore, KMC calculations require a significant computational effort.

RT imposes very little computational requirements. A typical experiment involving He desorption, involving thousands of partial differential equations, would require only a few minutes of calculation on a typical Pentium processor. On the other hand, obtaining free parameters from experimental data may require hundreds or thousands of simulations. In any case, RT may require only a moderate computational effort, in given cases.

ii) Dislocation Dynamics

In distorted materials, crystal plasticity is determined by the collective behaviour of major dislocations. Although laws could be written down for the continuum that describe the macroscopic behaviour of the material under a variety of loading conditions, based on efficient density dislocations, the movement of dislocations and their mutual interactions are heterogeneous phenomena that show an intrinsic dependence on the underlying microstructure. The details of these interactions are usually quite important but are not captured by continuum models that are based on the mean dislocation density. Therefore, atomic methods are commonly used to study the interaction mechanisms of isolated dislocations. However, these methods only describe a limited range of space-time scales, and therefore incorrect results are obtained when one attempts to apply it to the dislocation stress field in the long range, or to describe the statistical nature of the crystal plasticity.

An alternative method is provided by Dislocation Dynamics (DD), which is a direct approach that tries to simulate the collective behaviour of major dislocations on the mesoscale. It does this by breaking down the random curvature dislocation lines in rectilinear segments[170]. However, the number of segments, N, could be large for meaningful simulations, and the long range force calculation requires an effort $O \sim N^2$. Because of this, the problem can be computationally expensive for large systems. For a comprehensive revision of this topic and

[170] Kubin et al., 1992; Devincre y Kubin, 1997; Kubin et al., 1998; Zbib et al., 1998; Schwarz, 1999; Ghoniem y Sol, 1999; Zbib et al., 2000; Bulatov et al., 2001; Cai et al., 2004.

DD in general, please refer to Zbib and Diaz de la Rubia (2002) and the bibliography cited in that reference.

The use of DD for modelling some aspects of crystal plasticity in 3D in fcc metals was established at the end of the 80's in the pioneering work of Kubin et al.[171] and Ghoniem et al. [172]. Nevertheless, studies involving complex geometries and large dislocation densities have not been attempted until just a few years ago [173].

Dislocations are described as a set of nodes, connected to each other by rectilinear segments. The node positions and their connections are called the fundamental degrees of freedom. If a node is connected with n other nodes, it is called a node with a connectivity n. In general, the computational cycle is as follows:

i. Calculate the driving forces ~ fi for each of the nodes.
ii. Calculate the velocity ~vi of each node based on ~ fi and the local dislocation nature.
iii. Set the time step _t.
iv. Evolve all the dislocation nodes in time to t + _t, handling topological changes during [t, t + _t].
v. t: = t + _t. Return to a i.

The two codes that are primarily used by material scientists are ParaDis and Micro3D. Both codes are massively parallel. This increases the maximum number of dislocation segments that can be studied considerably.

In summary, the main experimental features of the Computer Simulation Facility of *TechnoFusión* are:

- **Simulation**
  - Basic research
  - The area is essential in a prestigious centre
  - National experts of known prestige are present, and more can be incorporated
  - The collaboration with other university groups is guaranteed
  - Computational platforms are available (Europe and Spain)
  - Proper platforms (for development, independence)
  - Additional value (a proper centre and external users)

- **Acquisition and Control**
  - An experimental centre requires a centralized computing service for the acquisition and control of data
  - Access, coherence, scalability, security, etc.
  - The possibility of proper developments (I+D+i, R&D)
  - Collaborations with other groups and industries
  - Solve users' problems and facilitate the operation of the Centre.

[171] Lepinoux y Kubin, 1987; Kubin et al., 1992
[172] Ghoniem y Amodeo, 1988; Amodeo y Ghoniem, 1991.
[173] Verdier et al., 1998; Shenoy et al., 2000; Espinilla et al., 2001; Dupuy y Fivel, 2002; Madec et al., 2002; Kubin et al., 2003; Depres et al., 2003; Shehadeh et al., 2005; Devincre et al., 2006.

- **Analysis and Visualization**
  - A new scientific paradigm
  - Data acquisition and generation on a scale not seen before
  - Analysis processes less developed
  - Extraction of all the available information
  - Development of proper techniques
  - Collaboration with other groups (biomedicine, …)
  - Feedback to the national industry

- **Media**
  - Openings for network and office personnel
  - The acquisition, management and support of computer supplies (hardware and software)
  - Consistent centralised management
  - Controlled private networks, acquisition and storage
  - Networks for the connection to other centres and Internet
  - Security

- **Human Resources**
  - Scientists in the field of materials science, plasma physics, nuclear physics, fluid dynamics; robotics and electronic engineers (simulations, …), and computational science scientists (algorithms, …)
  - Technicians
  - Programmers, analysts, operators
  - Personnel for design, essays and production (laboratories, …)
  - Administrative personnel (management, purchases, training, …)
  - Contacts and collaborations are essential

- **Computer Resources**
  - Generics
  - Internal and external (secure) networks
  - Administrative office positions
  - Specifics
  - Storage (secure and massive)
  - Processing (access, analysis and visualization)
  - Computing (development and production)
  - New developments (control, acquisition, real time, …)

Table 10.1 shows the status of art in the different simulation models described above, as well as the experience, development, validation and final use carried out by the people of the CS Facility of *TechnoFusión*.

Table 10.1. State of the art in model simulation by thematic areas and simulation models (E) Experience, (D) Development, (V) Validation, (U) final Use.

Area / Code	Level of knowledge	Area / Code	Level of knowledge
Nuclear data		**TH System**	
Activation Library EAF2003/05/07	E	RELAP INEL-NRC.USA	E, D, V, U
Transport Libraries JEFF31 ENDF/B-VII JENDL-HE FENDL HENDL	E	**Sensitivity and uncertainties**	
		SUSD3D Uncertainty code package. NEA/Kodeli I.	E, D, V, U
Nuclear Data Processing Codes		**Containment**	
NJOY LANL.USA/JEFF.NEA Libraries of ENDF/JEFF	E, D, V, U	CONTAIN Sandia/NRC.USA. Termohidráulic of containment	E, D, V, U
PREPRO2000 LLNL/D.E. Cullen	E, D, V, U	**Severe Accidents**	
Nuclear Physics Codes		MELCOR Sandia/NRC.USA. integral code of serious accidents	E, D, V, U
TALYS Simulation of nuclear reactions NRG/A. Koning	E, D, V, U	MAAP/SCDAP NRC.USA. Severe Accident Phenomena and Plant Evaluations – FAI	E, D, V, U
EMPIRE-II Nuclear Reaction Model Code IAEA	E, D , V, U	**Radiation Damage**	
Transport Code: Monte Carlo		PERFECT/GETMAT EU-FP6/FP7	E, D, V, U
TRIPOLI EU-NURESIM (CEA.fr)	E, D, V, U	MDCASK (Classic Molecular Dynamic)	E, D, V, U
MCNP LANL.USA	E, D, V, U	BIGMAC (Deffects Diffusion – MonteCarlo)	E, D, V, U
PHITS Particle & Heavy-Ion Transport (KEK.jp)	E, D, V, U	SIESTA ("ab-initio")	E, D, V, U
		LAMMPS (Classic Molecular Dynamic)	E, D, V, U
FLUKA/GEANT CERN	E, D, V, U	DD3D (Dislocation Dynamic)	E, D, V, U
		TBSiC (DM Tight Binding for SiC)	E, D, V, U
PENELOPE NEA/Univ. Barcelona.es	E, D, V, U	**Evaluation, location, ambient dose, tritium**	
Transport Code: SN		GASPAR/LADTAP/XOQDOQ NRC.USA (Fluents Dose)	E, D, V, U
TORT-DORT neutron & gamma SN Transport ORNL	E, D, V, U	MACCS2 RSICC.USA radiological and economic consequences of accidents	E, D, V, U
ATILA neutron & gamma			
TWODANT/THREEDANT			
Geometric Interface		PC-CREAM Metodology of European Comission Dose of Efluents	E, D, V, U
MCAM	E, D, V, U		
McCAD			
GEOMIT		COSYMA FZK y NRPB, European Comission. Radiologic and economic consequences of the accidents	E, D, V, U
DAGMC			
SNAM			
Graphic Interface		**Analysis of statistical probability**	
VisualBUS		SHAPHYRE 6.0 INEL for the NRC, USA	E, D, V, U
MORITZ	E, D, V, U		
SABRINA			
Isotopic and Activation Inventory			
ORIGEN/SCALE ORNL+LANL.USA	E, D, V, U		
ACAB UNED.es	E, D, V, U		
FISPACT UKAEA	E, D, V, U		
MONTEBURNS MCNP+ORIGEN/CINDER LANL.USA	E, D, V, U		
TH CFD			
ANSYS-CFX Commercial (ANSYS.USA)	E, D, V, U		
FLUENT *Commercial (ANSYS.USA)*	*E, D, V, U*		

10.4. Layout, supplies and safety requirements

(I) Physical spaces and facilities

Since it is envisioned that use will be made of large national computer facilities, the CS Facility does not need to have an extensive infrastructure; specifically, the following physical space would be needed:

- One 30 m^2 room to accommodate the analysis equipment and acquisitions.
- One 30 m^2 room for the instruments and auxiliary machines.
- One 20 m^2 warehouse.
- 100 m^2 for personnel offices and services.

(II) Safety

The CS Facility should comply with the Law of Professional Risks (BOE nº 269, 10/11/1995 (R.D. 31/1995)).

Nowadays, computer simulations may require long periods of time for processing and operation, so that power cuts or power surges in the local electrical network should be avoided as much as possible. Therefore, *Uninterruptible Power Supply* (UPS) systems are needed. These systems can provide current during a power interruption for at least some hours. In this way, the acquisition and processing systems and the general data storage servers can be protected.

11. Organizational structure of the Centre

11.1. Functional chart and legal form of the Centre

The planned legal form of the Centre is that of a consortium of partners (MICINN, CM), constituting a legal identity separate from the partners. This entity will dispose of its own resources and personnel and will have sufficient autonomy to achieve its goals. It will be closely associated with the Asociación EURATOM-CIEMAT para fusión (the EURATOM-CIEMAT Association for Fusion) in order to guarantee the coherency of the project with the European Fusion Programme and to have access to the financial resources the Asociación receives from the European Commission. The legal aspects of this association will be subject to a separate study.

Figure 11.1 is a functional chart of the proposed organisational structure of *TechnoFusión*. It is drawn attention to the following items:

i) The **Supervisory Council** consists of representatives of all the partners of the Consortium, and establishes the operational strategies of the Centre and oversees their implementation.

ii) The **General Director** is responsible for the scientific, technical, and administrative management of the Centre, and will guarantee that the objectives of the Centre are met.

iii) The **Advisory Scientific Council** consists of prestigious Spanish and international scientists and technological specialists, and its main task is to advise the Supervisory Council and the General Director concerning the long term scientific and technical objectives of the Centre.

iv) The **Time Allotment Committees** are in charge of the evaluation of the requests for user time by the various teams and experimental groups, in order to allot the available experimental time.

v) The **Technical Director** is in charge of the management and the joint coordination of operations in the various experimental facilities and the corresponding technical support.

vi) The **Coordinators of the Research Areas** are responsible for the development and the installation of all equipment and experimental devices of the different *TechnoFusión* Facilities.

vii) The **Scientific and Technical Support Unit** consists of personnel for the installation, operation, maintenance, and repair of equipment, providing general technical assistance to the various Research Facilities of the Centre.

viii) The **General Services** is a set of common infrastructures of the various Facilities (general workshops, a maintenance unit, a security unit, an emergency unit, an administrative department of human resources, a financial department, etc.)

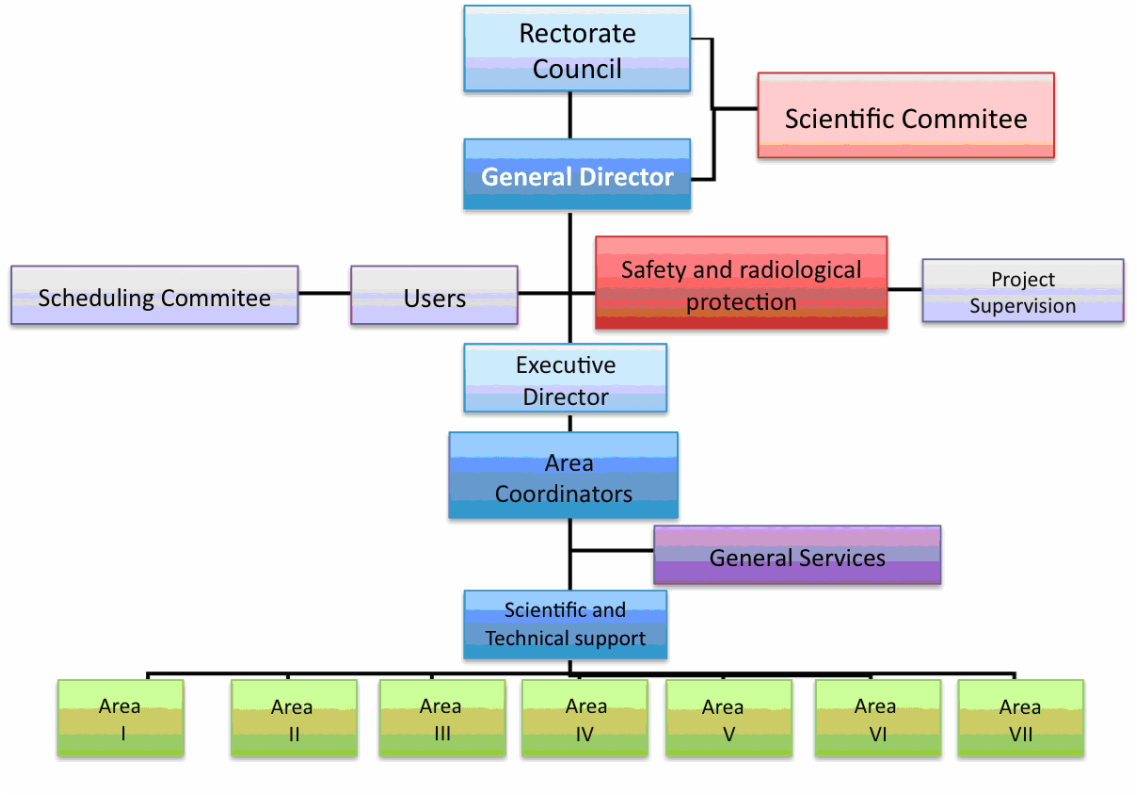

Figure 11.1. Proposed functional chart for ICTS *TechnoFusión.*

11.2. Required personnel

In Table 11.1, the total number of personnel needed for the proper operation of *TechnoFusión* is presented.

The posts will be occupied by personnel with appropriate qualifications. Some personnel will be *University Graduates* (UG), such as Technical Engineers, Engineers, Masters and PhDs of Science, to work as coordinators, supervisors, operators of equipment and installations, technicians of general services, etc. It will also be necessary to hire *Auxiliary Personnel* (AP) with varying levels of studies (Superior and Medium Level Vocational Training, etc.) to work as laboratory technicians, operators, technicians of general services, etc.

The number of workers listed in Table 11.1 has been estimated on the basis of the minimum amount of personnel required for the optimal operation of the Centre. It is emphasised that the numbers are mere estimations and are subject to the revision and approval by each Facility's manager and/or the relevant entity of the organisational structure.

Table 11.1. Total amount of personnel required for the operation of ICTS *TechnoFusión*

Facility	Personnel	
	UG	AP
Production and Material Processing	3	3
Material Irradiation	7	6
Plasma Wall Interaction	4	5
Liquid Metal Technologies	3	3
Characterization Techniques	9	7
Remote Handling Technologies	2	2
Computer Simulation	5	-
General Services	7	12
Total = 78	**40**	**38**

The specific personnel requirements of each of the Facilities of *TechnoFusión* are shown in more detail in Tables 11.2 and 11.3.

The contractual conditions of the personnel of the Centre, whether graduate or not, require special attention. An effective system of incentives should be defined, along with a career path, in order to guarantee adequate motivation of the personnel.

Furthermore, the Centre will consider the possibility of issuing a number of doctorate or post-doctorate grants each year. The scope and number of these grants will depend on the Centre's needs at any moment in time. These will serve to make the activities of *TechnoFusión* known among Spanish research groups, and to stimulate research projects that do not depend on external users, which will guarantee the international competitiveness of the installations of the Centre.

Table 11.2. Specific personnel requirements of the Material Production and Processing, Material Irradiation, and Plasma Wall Interaction Facilities of ICTS *TechnoFusión*.

Facility	Function	Qualification	Tasks	Nº
Material Production and Processing	Coordinator	UG	- Facility Coordinator. - Technical management, organisation and management of the Facility.	1
	Supervisor and Technical operator	UG	- Facility Supervisor. - Operation and maintenance of equipment. - Management of personnel training.	2
	Technical operator	AP	- Operation and maintenance of equipment.	3
	Total personnel			**6**
Material Irradiation	Coordinator and Accelerator Operator (I)	UG	- Facility Coordinator. - Technical management, organisation and management of the Facility. - Operation of the accelerators and irradiation rooms. -Supervisor of the radioactive installations. - Radiological safety.	1
	Operation and assembly technician	2 UG 3 AP	- The operation and assembly of vacuum systems (mainly UHV) - Assembly of accelerators. - Operation and maintenance of the installation.	5
	Accelerator operator (I)	UG	- Operation of the accelerators and irradiation rooms. - Supervisor of the radioactive installations. - Radiological safety.	1
	Accelerator operator (II)	3 AP	- Operation of the accelerators and irradiation rooms.	3
	Operator of experimental stations	UG	- Management of the experimental stations, measuring equipment, etc.	3
	Total personnel			**13**
Plasma-Wall Interaction	Coordinator and Operator	UG	- Facility Coordinator. - Technical management, organisation and management. - Operation and maintenance of the linear plasma.	1
	Researcher	UG	- R+D on the plasma source (computer simulation)	1
	Technician for diagnostics	UG	- Operation of the diagnostics.	2
	Technician for cryogenics and UHV	AP	- Assembly, supervision, maintenance and repair of cryogenic and UHV equipment.	3
	Technician for high voltage equipment	AP	- Assembly, supervision, maintenance and repair of high voltage equipment.	2
	Total personnel			**9**

Table 11.3. Specific personnel requirements of the Liquid Metal Technologies, Characterization Techniques, Remote Handling Technologies, and Computer Simulation Facilities, as well as the Area of General Services of ICTS *TechnoFusión*.

Facility	Function	Qualification	Tasks	Nº
Liquid Metal Technologies	Coordinator	UG	- Facility Coordinator. - Technical management, organisation and management of the Facility.	1
	Supervisor and Technician for operation/maintenance	UG	- Supervisor of the installation. - Operation and maintenance of the liquid metal loops. - R+D	2
	Technician for operation/maintenance	AP	- Operation and maintenance of the liquid metal loops.	2
	Total personnel			**6**
Characterization Techniques	Technician for mechanical testing techniques	1 UG 2 AP	-Operation and maintenance of the mechanical testing equipment (fluency machines, Charpy pendulum, ABI, Nano-indenter, etc.)	3
	Technician for composition analysis techniques	2 UG 1 AP	- Operation and maintenance of the compositional analysis equipment (SIMS, APT)	3
	Technician for micro-structural analysis techniques	3 UG 1 AP	- Operation and maintenance of the structural and micro-structural analysis equipment (DRX, EF-STEM, SEM)	4
	Technician for processing techniques	2 UG 1 AP	- Operation and maintenance of the processing techniques (FIB, etc.)	3
	Technician for *in beam* analysis techniques	1 UG 2 AP	- Operation and maintenance of the *in-beam* analysis techniques (ERDA, RBS, NRA, fluency, etc.)	3
	Total personnel			**16**
Remote Handling Technologies	Coordinator	UG	- Facility Coordinator. - Technical management, organisation and management.	1
	Supervisor and Technical operator	UG	- Supervisor of radioactive installations (Irradiation Experiments Hall). - Technician for robot operation.	1
	Technical operator	AP	- Technician for robot operation.	2
	Total personnel			**4**
Computer Simulation	Coordinator	UG	- Facility Coordinator. - Organization and management.	1
	Technician for simulation	UG	- R+D computer simulation.	4
	Total personnel			**5**
General Services	Coordinator	UG	- Facility Coordinator. - Supervision of maintenance and external services.	1
	Administrative personnel and laboratory technicians (I)	UG	-Support for the Facilities of the Centre. -External user support.	6
	Administrative personnel and laboratory technicians (II)	AP	-Support for the Facilities of the Centre. -External user support.	12
	Total personnel			**19**

11.3. Time schedule

The current schedule assumes achieving full operability in 2015. Table 11.4 presents a diagram detailing the main activities until that time. The time planning can be subdivided into two clearly defined phases. The first and most immediate phase (i.e., the start-up of the Centre) will last two years, and includes such tasks as defining the technical specifications of the equipment, making final designs, studying the issues of licensing and permits, etc., some of which are already quite advanced. The second phase will be developed in the medium and long term (Phases I and II of Table 11.4), and will depend on the technical complexity of the devices, the availability of funds, and the experimental needs of every Facility and working group.

Table 11.4. Planned timeline for ICTS *TechnoFusión* (starting June 2009).

S1 = 1st semester of the year S2 = 2nd semester of the year	2009		2010		2011		2012		2013		2014		2015	
	S1	S2	S1	S2	S1	S2	S1	S2	S1	S2	S1	S2	S1	S2
Start-up of the Centre														
Planning of buildings														
Licensing and administrative formalities														
Functional specifications: light ion accelerators and Rhodotron														
Functional specifications and conceptual design of the cyclotron														
Functional specifications and design of the QSPA and the linear plasma device														
Functional specifications and design of the liquid metal loops														
Design of the Experimental Irradiation and Remote Handling Hall														
Phase I														
Construction of buildings														
Acquisition and installation of the SIMS and APT equipment														
Acquisition and installation of the light ion accelerators														
Acquisition and installation of the Rhodotron														
Acquisition and installation of the VIM and HIP equipment														
Construction of the linear plasma device														
Construction of the QSPA														
Phase II														
Acquisition and installation of the Cyclotron														
Construction of the common chamber of the plasma gun														
Assembly of the plasma gun (linear device + QSPA + chamber)														
Installation of the lithium loops for corrosion and free surface studies														
Assembly of the *in-beam* experiments														
Installation fully operative														

As mentioned, in order to be able to meet this timeline, a number of actions need to be performed in the short and medium term, for each Facility of the Centre. Below, the main actions are described in more detail:

(I) Short-term actions

a) Materials Production and Processing Facility:

- Elaboration of the detailed specifications of the building and the installations of the Facility.
- Detailed design of the building and the installations.
- Contacting laboratories interested in the production of fusion materials on a semi-industrial scale. The purpose of this action is to keep the information regarding the manufacture and processing of such materials, as well as their manufacturing techniques, up to date.
- Start training specialist personnel for the main production and processing techniques.
- Participating in the activities concerning the manufacture and processing of materials in the framework of the European programme on fusion materials.

b) Material Irradiation Facility:

- Elaboration of the functional specifications of the light ion accelerators, the Cyclotron and the *Rhodotron*.
- The conceptual design of the Cyclotron and the *Rhodotron*. Start of the design of the first irradiation zones.
- Visits to Installations and Centres of reference for the *ion* and electronic material irradiation.
- Detailed design of the installation of the Facility.

c) Plasma Wall Interaction Facility:

- Detailed design of the magnetic configuration of the linear device, optimizing the simultaneous irradiation of the *target* by both machines, and evaluation of the costs of the chosen configuration.

- Preliminary design of the vacuum chamber and the associated pumping systems, once the magnetic configuration has been defined.

- Signature of the collaboration agreement with the *National Science Centre, Kharkov Institute of Physics and Technology* of Ukraine, concerning the QSAP design.

d) Liquid Metal Technologies Facility:

- Elaboration of the functional specification of the liquid metal loops.

- Design and detailed specifications of the building and the installations of the Facility.

- Visits to Installations and Centres of reference in the field of liquid metal technology.

e) *Characterization Techniques Facility:*

- Elaboration of the detailed specifications of the building and the installations of the Facility.

- Viability study of the experiments regarding mechanical, electrical, dielectric, and optical properties in the ion beam and the liquid lithium flow. Design of fixtures and devices on the basis of miniature test devices.

- Construction of a prototype device for mechanical tests in the ion beam and for corrosion tests in the liquid lithium flow.

- Visits to Installations and Centres of reference in the field of characterization techniques, especially regarding *in-beam* techniques.

f) Remote Handling Technologies Facility:

- Definition of the specifications of the building and the installations of the Facility.

- Elaboration of the detailed specifications of the equipment, and of new developments needed.

- Establishment of the ARC (Associated Research Centres of *TechnoFusión*, GIA in Spanish).

- Detailed design of the building and the installations.
- Visits to Installations and Centres of reference in the field of remote handling.

g) Computer Simulation Facility:

- Final definition of the simulation areas that must be covered by the Centre (in meetings with Spanish research groups that are potential users of the Facility).
- The establishment of contacts with major Supercomputing Centres, and the installation of computer codes needed for some of the identified areas.
- Design of the data acquisition system.

(II) Medium and long-term actions

After the short-term actions have been completed, the strategy of the Centre is clarified, and all studies, specifications, designs, licenses, etc., related to the installation are available, a new phase will start involving the construction of buildings and the acquisition of equipment. The latter will involve actions on the medium and long term, requiring four years for completion on average, depending on their complexity, with the objective of achieving the full operability of the Centre and its scientific and technical Facilities. These actions are listed below, ordered according to Facility and in chronological order:

a) Materials Production and Processing Facility:

- Construction of the first phase of the building. Acquisition of the VIM oven and the basic equipment of the Auxiliary Laboratory for Sample Preparation (cutting machines, polishing machines, etc.).
- Acquisition of the HIP oven and the auxiliary equipment for mechanical alloys and metal pulverisation techniques.
- Construction of the second phase of the building. Acquisition of the SPS system. Installation of the *swaging* and lamination equipment.
- Possibly, the acquisition of a VPS device.

b) Material Irradiation Facility:

- Acquisition of the light ion accelerators

- Installation of the light ion accelerators and the first irradiation zones.
- Acquisition of the *Rhodotron*.
- Acquisition of the Cyclotron.
- Installation of the additional irradiation zones of the Cyclotron and the *Rhodotron*.
- Acquisition and installation of the high-field magnet.

c) Plasma Wall Interaction Facility:

- Construction of the first phase of the building. Final design of the common chamber for simultaneous irradiation. Detailed design of the linear plasma gun QSAP and the linear plasma device.
- Construction of the common chamber for simultaneous irradiation.
- Study of the assembly of the QPSA and the linear device at the common chamber. Start of the construction of the plasma gun and the linear device.
- Start of the construction of the common irradiation zone. Completion of the construction of the plasma gun and the linear device, and commissioning.

d) Liquid Metal Technologies Facility:

- Acquisition of the basic infrastructure and auxiliary equipment of the lithium loop (tanks, resistors, pumps, conduits, auxiliary systems, etc.).
- Start of the construction of the common areas of the liquid metal loops. Installation of the purification system.
- Installation of the required infrastructure for operation. Start of the installation of the corrosion and free surface sections.
- Establishment of the connection between the various loops and the purification system. Connection of the liquid metal loops with the *Rhodotron*.

e) Characterization Techniques Facility:

- Acquisition of the SIMS device.

- Acquisition of the EF-STEM and FIB devices.
- Acquisition of the APT device and the mechanical testing equipment.
- Acquisition of the SEM, DRX, and nano-indentation devices.
- Construction and assembly of all *in-beam* experiments.

f) Remote Handling Technologies Facility:

- Construction of the first phase of the building. Acquisition of the first devices.
- Installation of the first remote handling devices. Acquisition and installation of the required infrastructure for starting operations in the Experimental Hall for Large Prototypes: bridge cranes, handling machines, etc. Design of the gamma radiation homogenizing system. Start of the certification procedure for the devices inside the cited Hall.
- Start of the construction of the second phase of the building (including the Experimental Irradiation Hall). Installation of the required infrastructure for the operation of the cited Hall. Connection with the Hall containing the *Rhodotron*. Acquisition of the gamma radiation homogenizing system inside the Hall.
- Completion of the construction of the second phase of the building. Acquisition and installation of the rest of the remote handling equipment. Installation of the gamma radiation homogenizing system.

g) Computer Simulation Facility:

- Acquisition of software licences and UPS systems.
- Installation of computer codes for the rest of the identified areas.
- Start of detailed and specific simulations, as needed by each experimental Facility.
- Development of the data acquisition system.

APPENDICES

Appendix I: Reports related to simulations of the *TechnoFusión* Material Irradiation Facility

I.A. Report on the TechnoFusión Multi-ion-irradiation Facility and its relevance for fusion applications

Authors: *TechnoFusión Material Irradiation Group*

(I) INTRODUCTION

The effect of neutrons on materials involves two physical phenomena: i) the displacement of ions from their lattice sites creating point defects, and ii) the generation of nuclear transmutation reactions that will contribute to increasing impurities inside the materials, He and H being the most important. Therefore, for many years, the scientific community has being using accelerators to simulate both effects. At present it is well known that neutron effects can be well represented by irradiating simultaneously with He, H (in similar amounts as expected by transmutation) and heavy ions capable of creating point defects [1, 2, 3].

The *TechnoFusión* Centre is envisaged to contribute to such neutron damage studies by means of the multi-irradiation ion facilities that form part of the Material Irradiation Facility (MI) [4]. An in-depth study has been done to demonstrate and optimize the use of ion accelerators to reproduce a damage evolution that mimics that expected in fusion devices (target damage plus helium and hydrogen production). The MI Facility scheme consists of three different ion beams to irradiate samples with medium to high energies.

The aim of the Material Irradiation Facility of *TechnoFusión* is to become a relevant user-facility for the selection of functional materials. MI Facility will incorporate three ion accelerators: two for implantation of light ions (H and He), and one for heavy ions that produce lattice displacements (Fe, Si, C, others). The ion energies chosen for the different ion accelerators are shown on Table I.A1. The effect of neutron radiation on candidate materials for ITER and DEMO will then be simulated by simultaneous triple ion beam irradiation.

(II) OBJETIVES

The main goal of MI Facility is to test and develop materials for fusion reactors [5]. Due to the lack of facilities to study material damage, multi-ion beam facilities are necessary to investigate ion-induced damage mechanisms, the synergistic effects of a dual/triple beam irradiation, and ion-beam modification of materials [1]. One of the requirements of the initial R&D in the material field is to show that a combination of heavy and light ions (in terms of microstructure and impurities) can produce similar damage to that expected in a fusion reactor (damage induced by neutrons). During the design phase this equivalence will be

evaluated and the most suitable accelerators will be selected. The next objective of MI Facility will be to irradiate samples homogeneously over a large volume and to produce damage uniformly in the material. To achieve this, two approaches are proposed, depending on the damage-production process and the generation of H and He:

I) Irradiation of a material with ions of the same species (e.g., irradiation of Fe with Fe ions), together with a simultaneous double implantation with light ions (H and He). This triple irradiation solution is expected to produce the same level of defects and the same quantity of light ions (via H and He implantation) that are expected to be reached under neutron irradiation in the fusion facilities. Furthermore, choosing the correct energies for each ion, one can produce the 3 effects in the same region of the material. For example, SRIM and Marlowe codes [6, 10] have been used to calculate the implantation profile of He and H and the damage produced by Fe ions in an iron sample. Results as a function of depth are shown in Figure I.A1. This figure illustrates the methodology used to select energies for each ion in different materials. The triple irradiation procedure must look for a coincidence between the depth for damage produced by heavy ions and the penetration ranges of H, and He implantations.

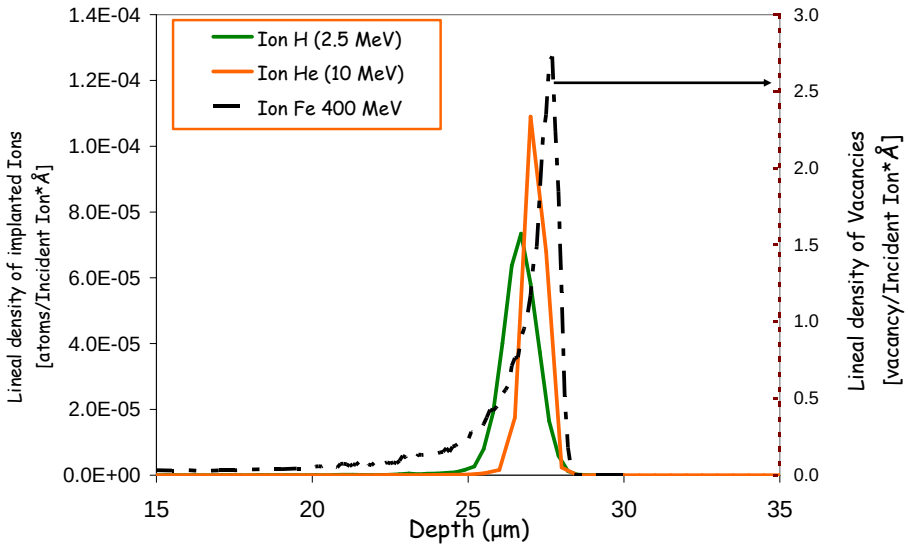

Figure I.A1. Depicts the in-depth coincidence of damage generated by Fe ions and implantation of light ions (H and He) of several energies in an Fe sample.

II) The second method is to irradiate with protons up to 70 MeV in order to produce directly damage and generate light elements in a similar way to that generated by neutrons in fusion reactors. Protons and neutrons have a similar mass and thus could generate a similar amount of displacement. On the other hand, protons can also produce H and He in a material by nuclear transmutations, similarly to neutrons. The displacements produced by different proton energies were

estimated by means of SRIM code [6]. In addition, this method presents the important advantage of easily achieving, implantation over large thicknesses (in the millimeter range), much larger than those accessible with ion implantation. A drawback is that during operation radiation and sample activation are produced.

The next section is devoted to calculating the energies and intensities of the ion beams and protons needed to generate the same level of damage in materials as produced by the neutrons expected in nuclear fusion facilities. The main factors taken into account are the following:

i) The minimum beam energy needed for the required penetration in the material.

ii) The homogeneity of beam damage along the whole penetration range.

iii) To maintain an accurate ratio between the concentration of light ions over the damage, as generated in a fusion facility.

iv) The reproduction of an accurate spectrum of the Primary Knock-on Atoms (PKA).

(III) METHODOLOGY AND RESULTS

a) Triple Ion beam

The first technique consists on the irradiation of a target with ions of the same chemical species with the goal of avoiding implantation of other impurities. The typical system is iron ions on an iron target. In order to emulate the damage created by neutron irradiation, the calculations must bear in mind that damage should be homogeneous along the penetration depth. Table I.A1 shows the maximum energies expected for heavy ions in a typical k=110 cyclotron and the penetration ranges of these ions considered for irradiation, as a function of target species. The last four columns show the maximum light ion energies needed to implant these species (hydrogen and helium) along the same penetration ranges established by the penetration of the heavy ions. All these calculations were performed using the SRIM code [6].

One particular condition is that the He energy is limited to a maximum value of 18 MeV. This is due to the fact that, for tandem accelerator, the maximum terminal voltage has been fixed at 6 MV. As the charge states of He can be -1 and +2 in both accelerating sections respectively, this gives the 18 MeV limit. We see that this condition is the limiting one in some cases, but the correction in the respective heavy ion energy is not too high.

After obtaining energy values, and therefore depth profiles, we need to estimate the magnitude of beam currents. For this purpose, the irradiation conditions of fusion materials in an environment as close as possible to the one expected in DEMO have been emulated. The first step has been to calculate the amount of damage as well as H and He generation expected at different positions for the main candidate materials. This combination of materials and positions give rise to a wide range of dpa's and H/He generation amounts that are shown in Table I.A2. These are consequently the values that must be simulated using the *TechnoFusión*

accelerators. As can be observed, the range is quite broad. Obviously a selection of conditions must be made, taking into account the main applications of each material. For example, Fe, FeCr alloys and steels will be located in positions going from the first wall to the back, so the most severe conditions must be, in principle, applied. However, at present, SiC is envisaged only for channel insertions in the Breeding Zone and finally many of the insulators included in the table are for diagnostics, therefore located in the Breeding Zone (BZ) Back. Exceptions include some systems located quite close to the first wall (as ICRH antenna) and insulators used as coatings of SiC channels. Therefore a compromise would be to use the BZ Middle conditions as a first study to obtain typical operation conditions. In any case, these values will be defined when specific work-plans will be approved.

Table I.A1. Ion energies that will be used in the MI Facility assuming a He energy inferior or equal to 18 MeV (tandem at 6MV terminal voltage and charge states of -1 and +2).

		Heavy ion accelerator Cyclotron k = 110		Light ion accelerator 4 MV		Light ion accelerator 6 MV	
Irradiated material	**Range (µm)**	**Ion**	**Energy (MeV)**	**Ion**	**Energy (Mev)**	**Ion**	**Energy (MeV)**
Fe (7.8 g/cm^3)	26.6	Fe	385	H	2.5	He	10
W (19.3 g/cm^3)	10.1	W	373	H	1.6	He	6
C (2.3 g/cm^3)	148.0	C	96	H	4.5	He	18
SiO_2 (2.2 g/cm^3)	175.0	Si	337	H	4.6	He	18
SiC (3.2 g/cm^3)	122.4	Si	337	H	4.6	He	18
SiC (3.2 g/cm^3)	122.4	Si	337	D	6.0	He	18

With the energies shown in Table I.A1, plus the vacancy/implantation profiles calculated for each ion, together with the required values of dpa's, He and H in Table I.A2 determine the three different intensities (heavy ions and light ions) needed to generate the damage equivalent to that produced by neutrons. For each combination of material and position, the intensity of heavy ions (see Table I.A2) can be calculated to obtain a damage rate. In Table I.A3, these values have been calculated for the case of 1 dpa per week, which is similar to the damage estimated [7] in a nuclear fusion environment. These are therefore minimum values or "normalized" values. Higher irradiation rates will be required to accelerate the total damage and to obtain convenient irradiation times. For example if it is required to have the total lifetime damage estimated for DEMO (around 300 dpa) in only a week, the current values are directly multiplied by this factor. This very high dose rate would provide the maximum currents needed for each ion at the exit of the cyclotron.

In a similar way, the intensities for each of the light ions (H and He) to obtain the transmutations expected in Table I.A2, are in the range of 50-100 pnA. The defining factor for the light ion intensities is the ratio between implantation (in appm) and damage (in dpa)

estimated for fusion facilities [7, 8]. Again, accelerated rates will require proportionally higher currents.

The important fact is that with the values of Table I.A2, while fixing the total irradiation time in *TechnoFusión*, the values of currents needed for each material/position and each accelerator (heavy ions from cyclotron, H and He from tandems) can be directly obtained. Together with the irradiation thickness requirements, that fix the energy, the above quantities define the main accelerator parameters (energies and currents). Another correction must be done to take into account the fact that the beam will pass through a beam degrader and therefore, for strong energy losses, a fraction of the beam will be lost.

Possible future changes in DEMO design can be accommodated thanks to the independent tuning of dpa's, H and He generation available using 3 independent accelerators. Initial accelerators design must be flexible enough to reach the above initial figures plus some margins.

Table I.A2. Calculated values of damage (in terms of dpa) and gas generation (H and He) for several candidate materials in a DEMO scenario. These values are calculated at different typical positions including First Wall (FW)) and Breeding Zone (BZ).

dpa/fpy appm/fpy		*DEMO HCLL (4000MW)*			
		FW (front)	**FW (back)**	**BZ (middle)**	**BZ (back)**
Fe-56	*dpa*	30	29	8	2
	H	982	870	53	4
	He	270	241	16	1
SiC	*dpa*	20	20	8	3
	H	1053	939	62	5
	He	2596	2304	144	11
SiO2	*dpa*	*48*	*49*	*21*	8
	H	929	827	53	4
	He	1477	1319	87	7
Al2O3	*dpa*	19	20	9	3
	H	1114	987	60	4
	He	1290	1150	75	6
Si2N4	*dpa*	*17*	*17*	*7*	*3*
	H	2511	2339	398	117
	He	1287	1207	150	17
CaO	*dpa*	17	17	7	3
	H	2975	2698	215	18
	He	1475	1335	103	8
AlN	*dpa*	*21*	*21*	*9*	*3*
	H	2545	2350	363	104
	He	1076	1011	127	14
W	*dpa*	*12*	*11*	*3*	*1*
	H	12	10	0.5	0.04
	He	3	3	0.2	0.01

Table I.A3. Target intensities for each ion species from the cyclotron planned for the TechnoFusión MI Facility to obtain a **nominal 1 dpa/week** damage level. Intensities data appear as particle nanoAmps for each single charged ion.

	Ion Currents (pnA)
C	500 – 1 μA
Si	200
O	200
Fe	25
W	3

As a special case to illustrate this point, Figure I.A2 shows the ratio of He produced (in appm of He) versus damage (in dpa) in the process of irradiating a Fe target with Fe ions for a week in two different kinds of facilities: a) existing facilities —nuclear fission reactors and particle accelerators—, and b) future facilities under development for nuclear fusion such as IFMIF, ITER and DEMO. In the later case, the figures are computational estimations. The highlighted area on the graph corresponds to the range where the *TechnoFusión* facility is expected to operate (yellow square), and this region covers the values of generated He vs. damage expected from the new nuclear fusion facilities.

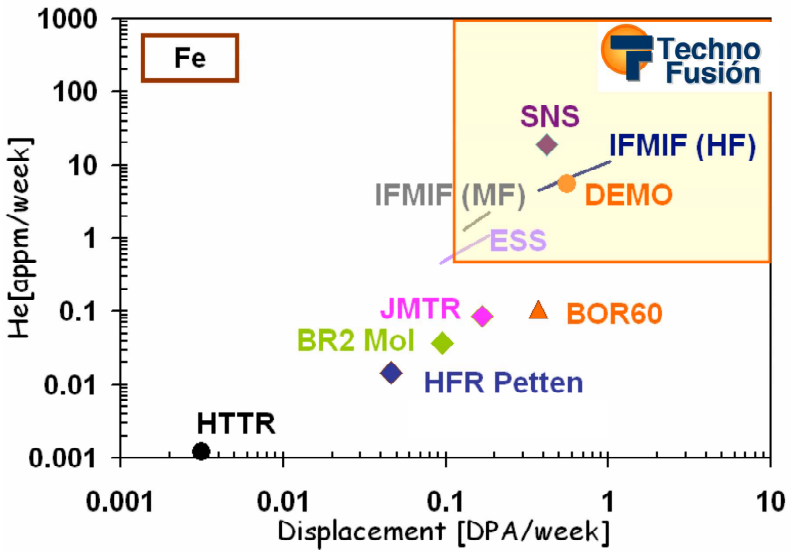

Figure I.A2. Comparison of results from different facilities (particle accelerators, fission facilities and future fusion facilities). He appm/week versus displacement in dpa/week during homogeneous irradiation of Fe and He ions beam with a maximum energy of 300 and 10 MeV respectively, on Fe samples using different intensities.

An additional factor to be taken into consideration to ensure the accuracy of the simulation of neutron damage by other means is the Primary Knock-on Atom (PKA) energy spectrum; up to now, the only parameter considered was the total damage. The PKA spectrum describes how the damage is produced. The damage function W(T) [9] connects the PKA spectrum with the total damage in the material. It is well known that different primary recoil energy spectra can produce completely different damage morphologies, and therefore W(T) indicates the cumulative damage production by all PKAs up to the energy T:

$$W(T) = \frac{1}{D/t}\int^{T} \sigma_{PKA}(T')N_d(T')dT' , \qquad \text{(I.A1)}$$

where $\sigma_{PKA}(T)$ is the PKA spectrum, $N_d(T)$ is the number of Frenkel pairs produced by PKA of energy T, and D/t is the rate of damage created by the atomic displacement.

The PKA spectrum was calculated with the SRIM code. On the contrary, the Marlowe code [10] was used to evaluate the function of Frenkel pairs generated by PKA with energy T because it resolves the cumulative damage better. Therefore, $\sigma_{PKA}(T)N_d(T)$ is integrated to obtain the damage function on eq. I.A1.

The damage functions generated in iron by Fe ions of 500, 300 and 50 MeV are shown on Figure I.A3, and are compared with those expected in DEMO HCLL (first wall and breeder zone). This graph shows that ions with higher energy become closer to the present calculations for DEMO HCLL damage area.

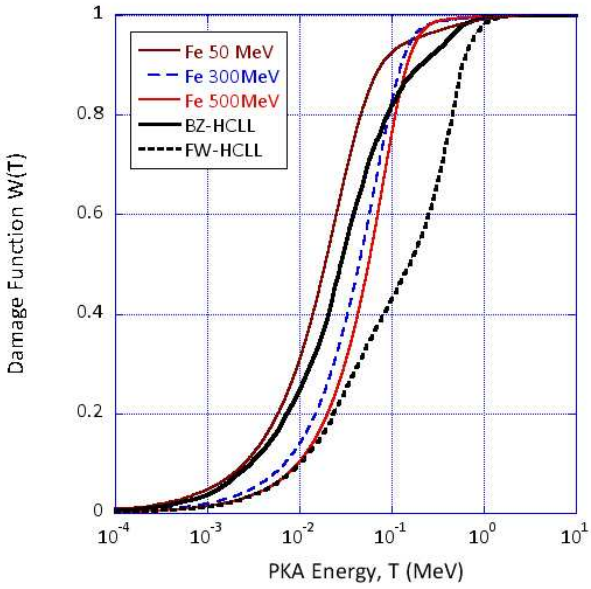

Figure I.A3. Damage function generated in Fe material by Fe ions of 50, 300 and 500 MeV. Comparison with results from DEMO HCLL (first wall [FW] and breeder zone [BZ]), calculated with NJOY code.

b) Proton Irradiation

The second irradiation approach to study the neutron damage is based on the irradiation of high energy protons. SRIM and Marlowe codes were also used to calculate the damage function generated by protons with energies up to 70 MeV. On Figure I.A4 we represent the damage functions obtained for the high energy range (40 and 70 MeV) protons in a 1 mm thick iron sample. It can be seen that the results are also very close to those calculated for DEMO HCLL.

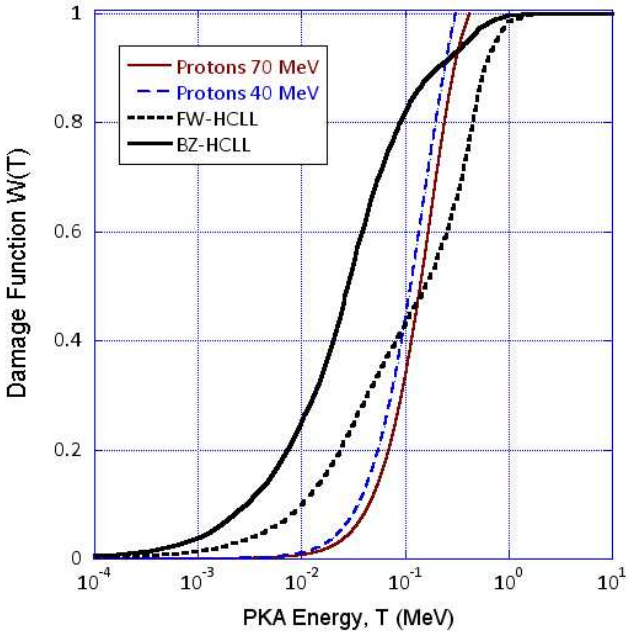

Figure I.A4. Damage function generated in Fe material by protons of 40 y 70 MeV. Comparison with the results from DEMO HCLL (first wall [FW] and breeder zone [BZ]), calculated with NJOY code.

An important factor is the He/dpa ratio. Table I.A4 shows the rough ratios of appm He/dpa calculated for iron targets using cross sections for the generation of He by transmutation [11] and displacements by SRIM code. Sample thickness is chosen in each case in such a way that the protons can pass through the sample and energy deposition is quite constant. This value of thickness is also shown in Table I.A4. In this method, choosing the proton E, we can adjust the He/dpa ratio to values close to the one expected in DEMO. On the other hand, the damage functions are still close to DEMO.

With these initial calculations 40 MeV-protons seems to be a good option for simulating the neutron damage in terms of damage function, while 20 MeV protons can be the best candidate given the good dpa/He ratio and the reduced nuclear activation. Anyway more accurate calculations must involve the use of the MCNPX code to obtain a better PKA distribution and the study must be extended to other materials and positions in DEMO that obviously change the target value of He/dpa.

Other important differences between both methods (triple beam or only protons) are a) the radiation level produced during irradiation with proton beams at these energies and b) the amount of activation present in the irradiated samples. This has strong implications in the radioprotection requirements of the installation. This is the subject of the next section.

Table I.A4. He/dpa relations obtained from simulations in iron irradiated with protons of 10, 20, 40 and 70 MeV compared to the corresponding value near first wall in fusion facilities.

	Sample thickness (mm)	He/dpa
Fusion	---	11
10 MeV	0.2	~1.5
20 MeV	0.5	~11
40 MeV	1	~33
70 MeV	2	~70

(IV) SUMMARY

Triple beam irradiation and proton irradiation are good candidates to simulate the damage on materials by neutrons in a nuclear fusion facility. Each method presenting some advantages and disadvantages.

*TechnoFusión´*s Material Irradiation Facility aims at exploiting this property by creating a laboratory where materials could be irradiated simultaneously with up to three different ion beams. This facility will test the performance of materials to be used in future fusion reactors, such as ITER, DEMO and IFMIF.

(V) REFERENCES

[1] Y. Serruys, P. Trocellier, S. Miro, E. Bordas, M.O. Ruault, O. Kaïtasov, S. Henry, O. Leseigneur, Th. Bonnaillie, S. Pellegrino, S. Vaubaillon and D. Uriot, "JANNUS: A multi-irradiation platform for experimental validation at the scale of the atomistic modelling", J. Nucl. Mater 386-388 (2009) 967-970

[2] R.S. Averback et al., "Correlations between ion and neutron irradiations; Defect production and stage I recovery", J. Nucl Mater. 75 (1978) 162-166.

[3] H. Ullmaier et al., "The simulation of neutron-induced mechanical property changes by light ion bombardment", Ann. Chim Fr. Sci. Mat. 9 (1984) p.263-274.

[4] J. Sánchez, A. Ibarra, J. M. Perlado, A. Abánades, R. Aracil, N. Casal, J. Ferreira, A. García, I. García-Cortés, M. González, D. Jiménez-Rey, A. Muñoz, F. Mota, R. Pareja, V. Queral, R. Román,

J. Sanz, F. Sordo, F. L. Tabarés, and R. Vila, "*TechnoFusión*: A new centre for the development of fusion technologies and fusion reactor devices", proceeding of the 14th International Conference on Emerging Nuclear Energy Systems (ICENES), Ericeira Portugal.

[5] R&D Needs and Required Facilities for the Development of Fusion as an Energy Source, Report of the Fusion Facilities Review Panel, October 2008.

[6] J.F. Ziegler, J.P. Biersack y M.D. Ziegler, "SRIM: The Stopping and Range of Ions in Matter", http://www.srim.org (2008).

[7] P. Vladimirov, and S. Bouffard "Displament damage and transmutations in metals under neutron and proton irradiation" C.R. Physique 9 (2008) p.303- 322.

[8] P. Vladimirov, A. Möslang, U. Fischer and S. Simakov "Material irradiation conditions for the IFMIF medium flux test module" Journal of Nuclear Materials Volumes 367-370, Part 2, 1 August 2007, Pages 1574-1579.

[9] H.Wiedersich, "Effects of the primary recoils spectrum on microstructural evolution", Journal of Nuclear Material. 179-181 (1991) 70-75.

[10] M. T. Robinson, Phys. Rev. B 40, (1989).10717.

[11] C.H.M. Broeders, A. Y. Konobeyev, "Helium Production in Solid target and metallic windows materials irradiated with intermediate and high energy protons" Journal of Nuclear Science and Technology, Vol. 42, No. 10 (2005) p. 897-902.

I.B. First radioprotection studies for the preliminary design of the TechnoFusión facilities

A. Mayoral, J. Sanz, D. López, P. Sauvan, F. Ogando, M. García, J.P Catalán, P. Antón
Departamento de Ingeniería Energética, UNED, Madrid, Spain, jsanz@ind.uned.es
Instituto de Fusión Nuclear, UPM, Madrid, Spain

(I) INTRODUCTION

In the *TechnoFusión* Centre, three particle accelerators are expected to be focused in the simulation of the radiation damage in fusion reactor materials: two linear accelerators for H, D and alpha ions and a cyclotron for heavy ions and high energy protons [*TechnoFusión*, 2009]. These three accelerators will be located in the same building. The beams from these accelerators are inter-connected, that is, two or three beams can be focused on the same target at once and the functions of the accelerator systems are inter-related. In this way, single, double or triple beams can be utilized in the target irradiations.

This report is focused on assessing radioprotection issues associated only to the irradiation of different targets. Issues associated to irradiations with low energy H, D, and alpha as well as with high energy protons are analyzed. The issues associated to irradiation with heavy ions are not considered here.

The results of this task will be used in other radioprotection studies, with regard to the necessary bio-shielding of the vault and the required precautions to handle the irradiated targets to assure that the levels of doses reached are acceptable for workers and public.

Although the methodology to compute the prompt dose due to the neutron production from nuclear interactions of the proton beam with the target is available for many materials, there are not reasonable solutions to compute the prompt dose from alpha and deuteron beams.

This difficulty is due to the fact that the built-in nuclear models included in MCNPX [Pelowitz, 2008] do not allow an accurate assessment of the prompt dose at low energy and there are not available libraries for these particles in the MCNPX code [Sanz, 2008; Joyer, 2009; Mayoral, 2009].

A new methodology has been developed to solve these difficulties in the radioprotection studies for *TechnoFusión* facilities. The details with regard to the computational tools (scenario, the XS libraries and the codes) are described and discussed in the methodology section. The results of the simulations and the main conclusions of this work will be presented in a separate section.

(I) METHODOLOGY: IRRADIATION SCENARIO AND COMPUTATIONAL TOOLS

Regarding the simulation scenario, the target geometry is the same for all the materials analyzed (Fe, SiO_2, SiC, C and W): a solid cylinder of 2 cm diameter and 1 mm of thickness.

All the particle beams have the same shape: circular section of 1cm^2, uniform current density and axis lined-up with the axis of the target. There is a vacuum cylinder between the beam source and the target. The vault is filled with air. The current intensity for the beams (proton, alpha, deuteron, high energy proton) is the characteristic for each target material. At the moment of writing this report, the data related to the current intensity for SiC, C and W targets as well as the highest energy proton beam value for all the targets are not known. Provisional values of 50 pA for double beams and 1 μA for the highest energy beam will be used for the simulations. True values for the prompt dose can be calculated using the correction factor (the prompt dose is lineal with the current).

The information achieved from the simulations is: i) for the beam on phase, the production rate and dose rate field for emerging neutrons and photons. ii) for beam-off phase, the isotopic inventory and the residual dose rates due to the activation of the target material.

The dose rate due to the radiation is presented through the magnitude named ambient dose equivalent [ICRP-103, 2007]. The values of the conversion factors from fluency to dose rates come from ICRP74 [ICRP-74, 1996].

The ACAB code [Sanz, 2009] with EAF2007 libraries [Forrest, 2007] has been used for activation calculations.

We propose to use a new tool named MCUNED [Sauvan, 2009] for the beam-on phase simulations. The MCUNED code is an extension to the MCNPX code that allows a computational solution much better than the poor accuracy results provided by the MCNPX simulations for alpha and deuteron beam at low energy. This extended MCNPX code is able to handle ACE files format, so MCUNED can use the data from TENDL transport library [Koning, 2008]. This procedure solves the difficulties in those cases where TENDL library is available. This code has been successfully used in our former work to compute the neutron and tritium production rates for EVEDA-IFMIF facility, where low energy deuteron beam interacts with copper material [Mayoral, 2009].

The advantage to apply this procedure to the simulations for *TechnoFusión* facilities is illustrated in Table I.B1. This table shows results of the dose rates and neutron production rate from the simulations made with MCNPX and MCUNED for 10 and for 15 MeV alpha energy beams over iron target.

Table I.B1. MCNPX vs MCUNED code: simulation of alpha beam over Iron target

Fe (α, nx)	MCNPX				MCUNED TENDL08	
	ISABEL		INCL4			
	10 MeV	15 MeV	10 MeV	15 MeV	10 MeV	15 MeV
MAXIMUM DOSE (μSv/h)	0	0	0	0	1.21	14.3
NEUTRON SOURCE	0	0	0	0	8.98E-06	9.84E-05

There is a significant discrepancy between the results obtained with MCUNED and MCNPX simulations. Therefore it was necessary to discuss which one of these results is the more accurate solution. The following figures and comments are the base to recommend the MCUNED option.

- The threshold energy of the reactions are lower than 10 MeV for all the iron isotopes; therefore it is possible the neutron production proposed by MCUNED option. (Table I.B2, National Nuclear Data Center [NNDC]).

Table I.B2. Features of different alpha induced reactions on Iron (From National Nuclear Data Center)

Remote Handling Operation	Q value (keV)		Threshold (keV)	
^{54}Fe(4He, n)^{57} Ni	-5816.89	1.87	6248.53	2.010
^{55}Fe(4He, n)^{58}Ni	-2898.08	0.55	3109.22	0.590
^{56}Fe(4He, n)^{59}Ni	-5096.10	0.54	5460.761	0.579
^{57}Fe(4He, n)^{60}Ni	-1354.45	0.54	1449.667	0.578
^{58}Fe(4He, n)^{61}Ni	-3578.93	0.56	3826.191	0.599

- The reasoning will be focus on Fe^{56}, the main contributor to the neutron production (Figure I.B1).

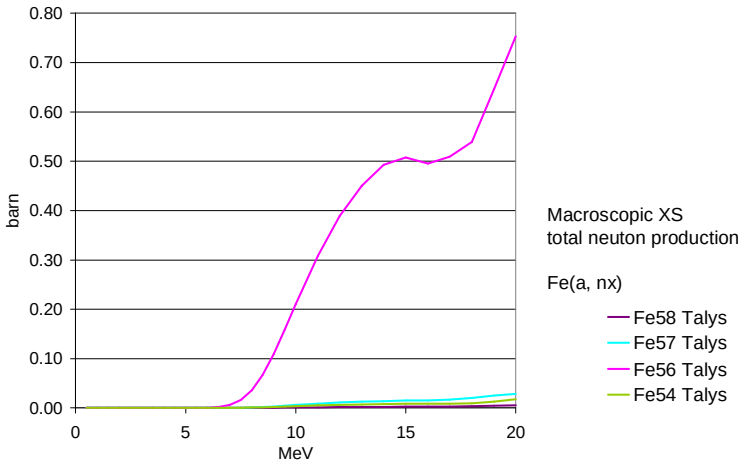

Figure I.B1. Macroscopic XS for Fe(α, nx).

- The Figure I.B2 presents the aim of this discussion: the macroscopic cross section for the total neutron production for Fe^{56} from Talys and from MCNPX Models (Isabel, Bertini and Incl4).

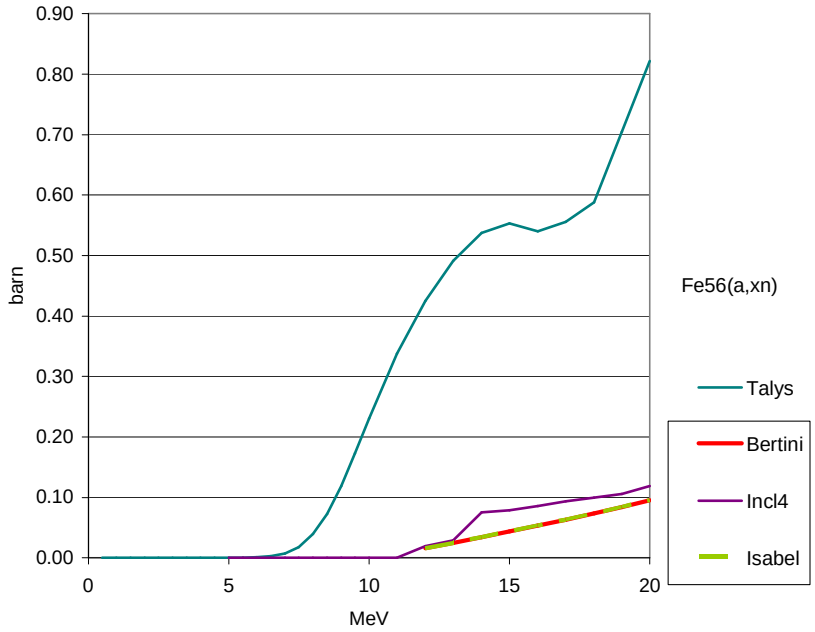

Figure I.B2. XS for total neutron production from Talys & from MCNPX Models.

- Only for Fe^{56} (α, np) there are available XS from experimental data (Figure I.B3). The figure includes the XS from Talys for this reaction. The neutron production at 19.6 MeV for Fe^{56} (α, np) from Tanaka experience [EXFOR 2009] is more than twice of the value for total neutron production predicted by MCNPX models. This fact confirms that the MCNPX models are not able to compute the neutron production for alpha nuclear interactions on Fe up 20 MeV. However there is a good agreement between the values predicted by Talys and the experimental data for the XS of Fe^{56} (α, np) reaction.

- With regard to the dose obtained by using the Talys code, the energy spectrum of the emerging neutrons, rules out the error due to high energy tail (Figure I.B4, Table I.B2).

Additionally, MCUNED code is able to reduce the computation time in a factor of 5.000 (depending on the simulation) due to the incorporation of a technique of variance reduction which allows decreases the number of histories necessary to achieve a good statistics for secondary particles [Sauvan, 2009].

The details with regard to the composition of the targets (Fe, C, W, SiO_2 and SiC) and to the availability of XS libraries for the simulation of the nuclear interaction with the particle of the beam (H, D, α) are related in Table I.B3.

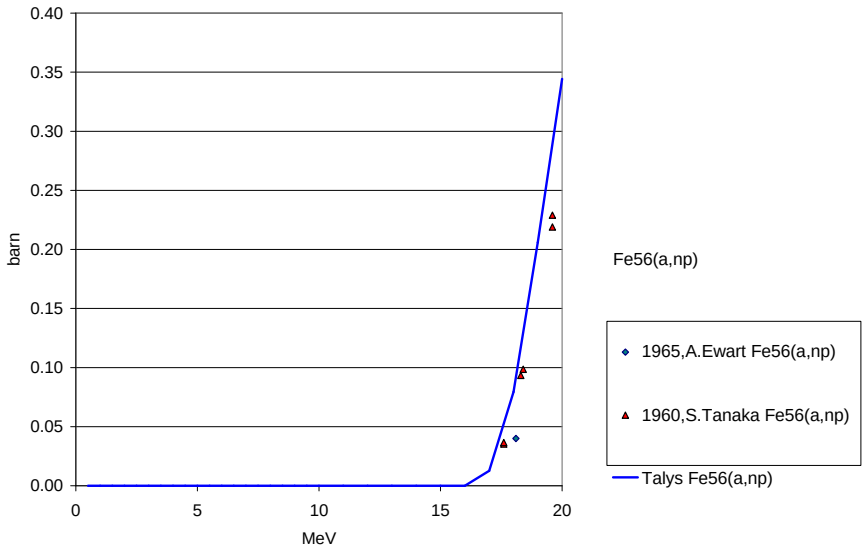

Figure I.B3. Fe^{56}(α,np) experimental & Talys.

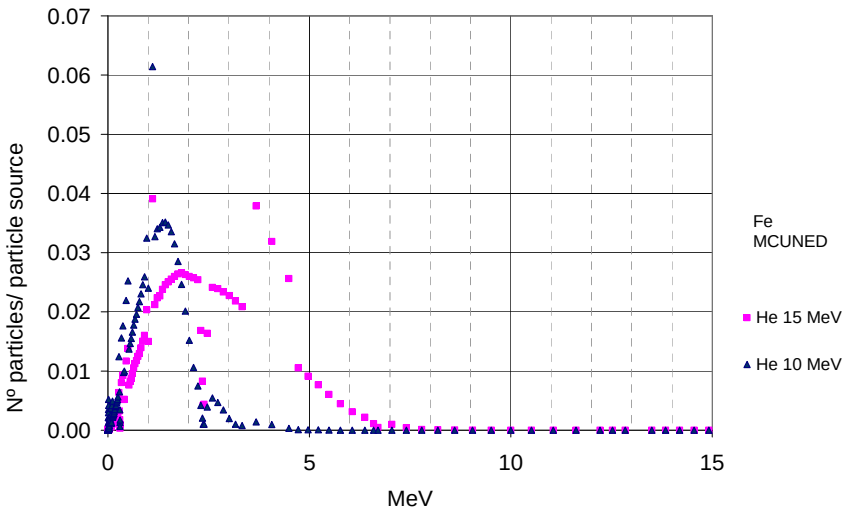

Figure I.B4. Normalize energy spectrum for emerging neutron from Fe (α,nx) 10 and 15 MeV.

Table I.B3. Libraries and built-in MCNPX model used for transport simulations. The isotopes marked with (*) have not been taken into account since there is no XS library available and its contribution to the prompt dose is negligible.

TARGET			XS LIBRARY / MODEL			
MATERIAL DENSITY (g/cm^3)	Isotope		N	p	PARTICLE H	PARTICLE α
Fe 7.8	26054	0.058	ENDF/b vi6	mcplib02	la150	TENDL08
	26056	0.917				
	26057	0.022				
	26058	0.003	* not taken into account			
SiO_2 2.2	14028	0.307	ENDF/b vi6	mcplib02	la150	TENDL08
	14029	0.016				
	14030	0.010				
	8016	0.665				TENDL09
	8018	0.001	* not taken into account			
SiC 3.2	14028	0.461	ENDF/b vi6	mcplib02	la150	TENDL08
	14029	0.023				
	14030	0.016				
	6012	0.494	ENDF	cplib04	la150	Isabel
	6013	0.006	* not taken into account			

			D
14028	0.461		TENDL08
14029	0.023		
14030	0.016		
6012	0.494		TENDL09
6013	0.006	* not taken into account	

C 2.3	6012	0.9889	ENDEF	mcplib04	la150	Isabel
	6013	0.0111	Isabel	cplib04	Incl4 E<5MeV Isabel E<20Mev	Isabel
W 19.3	74180	0.0012	* not taken into account			TENDL08
	74182	0.2650	ENDF/b vi6	cplib02	la150	
	74183	0.1431				
	74184	0.3064				

Those cases in which there are not available libraries for MCUNED code, the different XS options from built-in MCNPX models have been checked. The reference data to evaluate the

best estimation are from: i) experimental data [EXFOR, 2009], ii) Talys code [Koning, 2007], iii) JENDL library [JENDL, 2002]. The details related to the problematic cases, alpha and proton interaction over carbon, are presented below.

The dose rates presented in this report for 18 MeV alpha beam over SiC target could be a very poor estimation. The contribution of C^{12} to the total neutron production is very significant (C^{12} and Si^{28} are the main contributors, Figure I.B5a). Only for C^{12} (α,n) reaction experimental data is available. The results by Talys code show that C^{12} (α,n) reaction is the main contributor to the total neutron production, although the values from the simulation have poor fitting with the experimental data. The same conclusion is obtained for simulations using TENDL09 but with a better agreement with the experimental data. We have selected the Isabel model trying to get the more conservative result (Figure I.B5b).

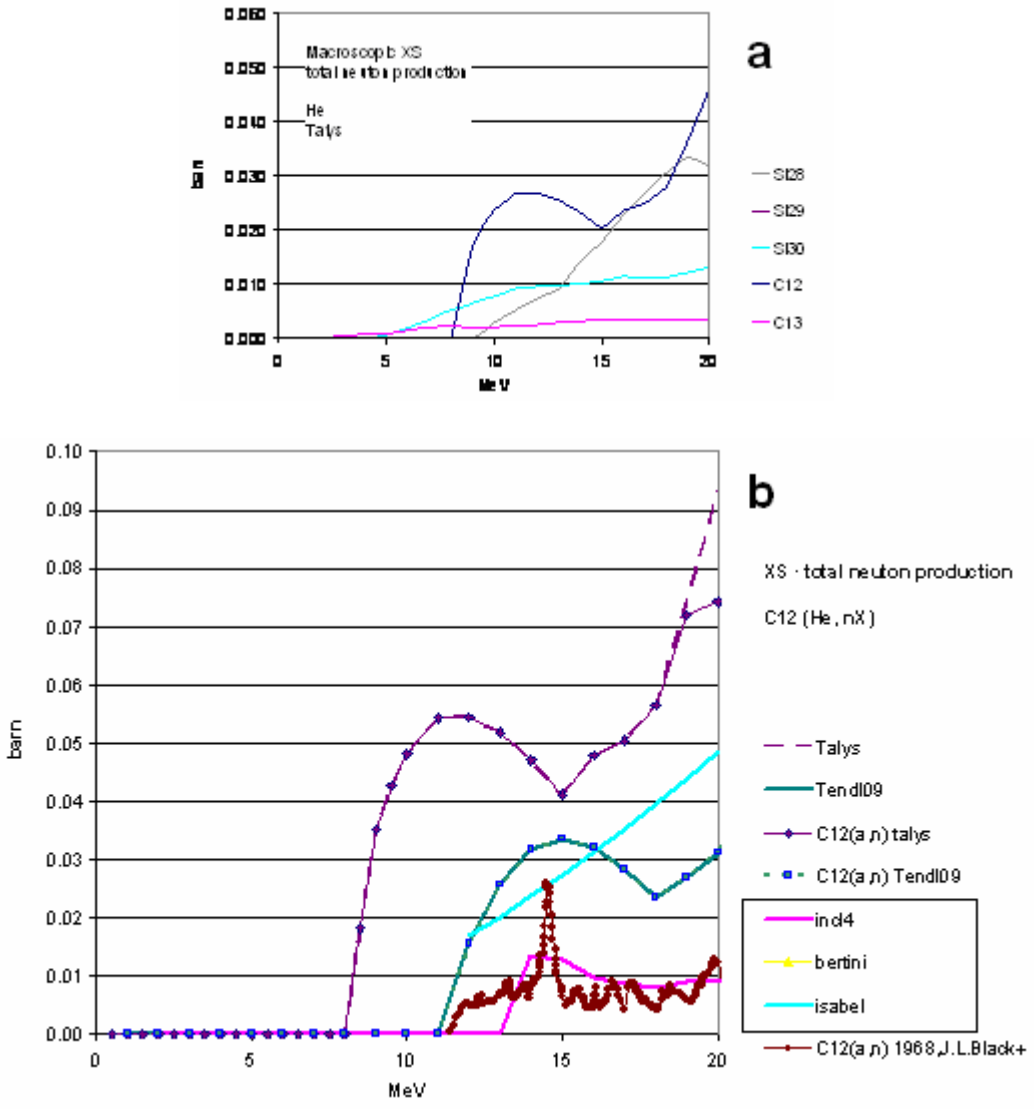

Figure I.B5. SiC (α,nx): (a) Macroscopic XS from ACSLAM. (b) Built-in MCNPX vs Talys & ACSLAM.

The simulation of the neutron production for 18 MeV alpha beam over carbon target could be a very poor estimation. The C^{12} is the main contributor to the total neutron production (Figure I.B6). For the same reason presented above related to the SiC target, the Isabel model was used for C^{12} (Figure I.B5b).

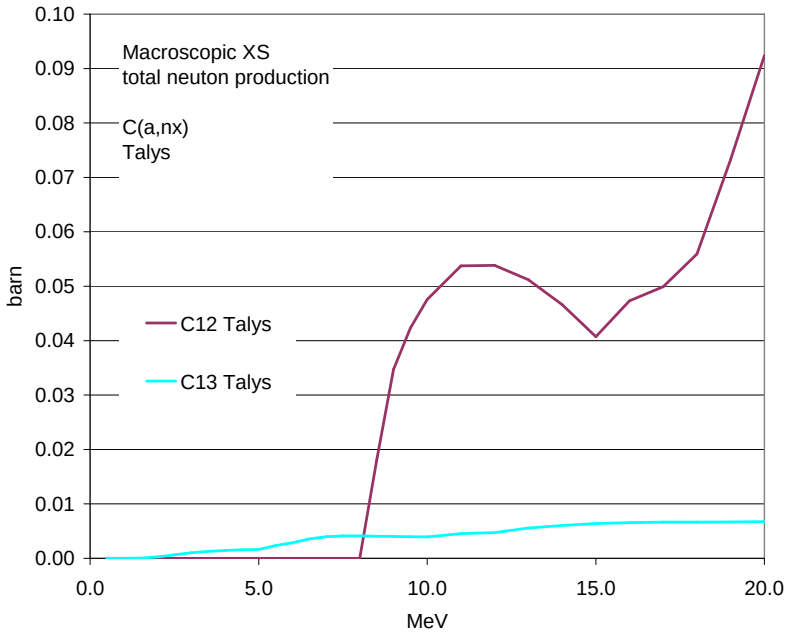

Figure I.B6. Macroscopic XS C(α,nx) from Talys.

The dose value presented in this report for a 4.6 MeV proton beam on Carbon target could be a very poor estimation. The C^{13} is the main contributor to the total neutron production (Figure I.B7). There are not experimental reference data for the test, since we have taken the JENDL library as reference. Therefore we have selected the Incl4 model for proton energy up to 5 MeV and Isabel up to 20 MeV.

With regard to the neutron energy spectrum from the cases simulated with built-in MCNPX models, there are not agreement with the physic of the system but the relevance of the error due to the unphysical high energy tail is expected to be not significant.

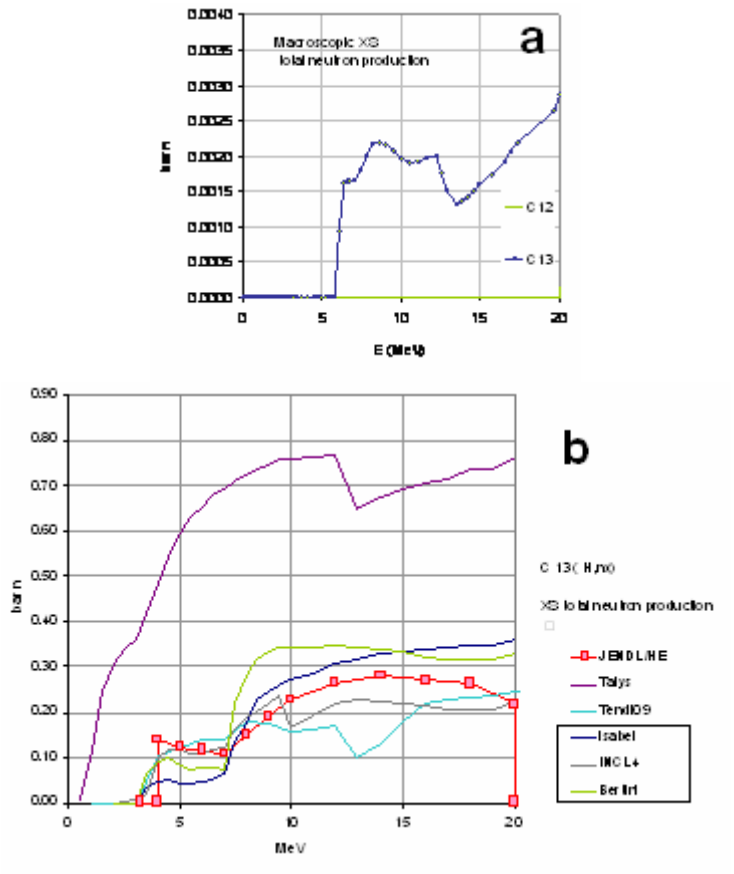

Table I.B2. C^{13} (H,nx): (a) Macroscopic XS from JENDL. (b) Built-in MCNPX vs TENDL & Talys & JENDL.

(III) RESULTS

The results of the simulations presented in this section are provisional. This fact is due to the ignorance of the current beam values for all the cases at the moment of writing this report.

The results for beam-on phase are presented in Table I.B4: neutron and photon production rate and the maximum value of the ambient dose equivalent.

The results on beam-off phase due to the activation for one week irradiation time, are presented only for iron target. The information presented includes the time evolution after shutdown for residual dose, photon production rate and the isotopic inventory.

Table I.B4. Results for double beams and for high energy proton beam (* values for a provisional current of 50 pA) (⊥ the values can be a poor estimation).

Fe	**H** 2.5 Mev 15 nA	**α** 10 MeV 4 nA	**Total**	**H** 20 MeV 1μA
MAXIMUM DOSE (μSv/h)	450	97	547	7.66.E+06
NEUTRON SOURCE (n/particle source)	1.59E-08	8.98E-06		2.56E-03
PHOTON SOURCE (p/particle source)	2.90E-07	6.10E-06		1.34E-02

SiO_2	**H** 4.6 Mev 0.2 nA	**α** 18 MeV 0.3 nA	**Total**	**H** 20 MeV 1μA
MAXIMUM DOSE (μSv/h)	0	42	42	0.36E+06
NEUTRON SOURCE (n/particle source)	0.0	3.056E-05		1.20E-04
PHOTON SOURCE (p/particle source)	3.54E-05	5.79E-05		8.34E-03

SiC	**H** 4.6 MeV 3.5 nA	**$\alpha^{\perp}$** 18 MeV 8.5 nA	**Total**	**H** 20 MeV 1μA
MAXIMUM DOSE (μSv/h)	0	826	826	0.56E+06
NEUTRON SOURCE (n/particle source)	0	4.74E-05		1.72E-04
PHOTON SOURCE (p/particle source)	0	1.94E-04		1.01E-02

W	**H** 1.6 MeV	**α** 6 MeV	**Total**	**H** 20 MeV 1μA
MAXIMUM DOSE (μSv/h)	0	0	0	9.0E+06
NEUTRON SOURCE (n/particle source)	0	0		4.13E-03
PHOTON SOURCE (p/particle source)	0	0		6.89E-03

C	**$H^{\perp}$** 4.6 MeV	**$\alpha^{\perp}$** 18 MeV	**Total**	**$H^{\perp}$** 20 MeV 1μA
MAXIMUM DOSE (μSv/h)	0	6.11 *	6.11*	0.21E+06
NEUTRON SOURCE (n/particle source)	0	2.62E-05		9.87E-05
PHOTON SOURCE (p/particle source)	0	3.82E-05		5.01E-03

SiC	**D** 6 MeV	**α** 18 MeV	**Total**
MAXIMUM DOSE (μSv/h)	7.57 *	4.86 *	12.43*
NEUTRON SOURCE (n/particle source)	6.74E-05	4.74E-05	
PHOTON SOURCE		1.94E-04	

III.1. Beam-on phase

The worst condition for radioprotection issues happens during beam-on phase and for the high energy proton beam (the values presented were calculated for a provisional current of 1μA). The contribution of the emerging photons to the total prompt dose was negligible for all the beam and materials (it is more than eight orders of magnitude lower than the dose due to the emerging neutron). With regard to the material target, the tungsten presents the worst behaviour and the dose arising from the iron target is slightly lower.

The dose rate fields arising from the nuclear interaction of 20 MeV proton beam (1μA) over tungsten target and over iron target are showed in Figure I.B8. The maximum value of the dose (located in the target) is higher than 7 Sv/h. These dose levels represent an important risk for health. Therefore it will be necessary to include a shielding to assure that the levels of doses reached are finally acceptable for workers and public.

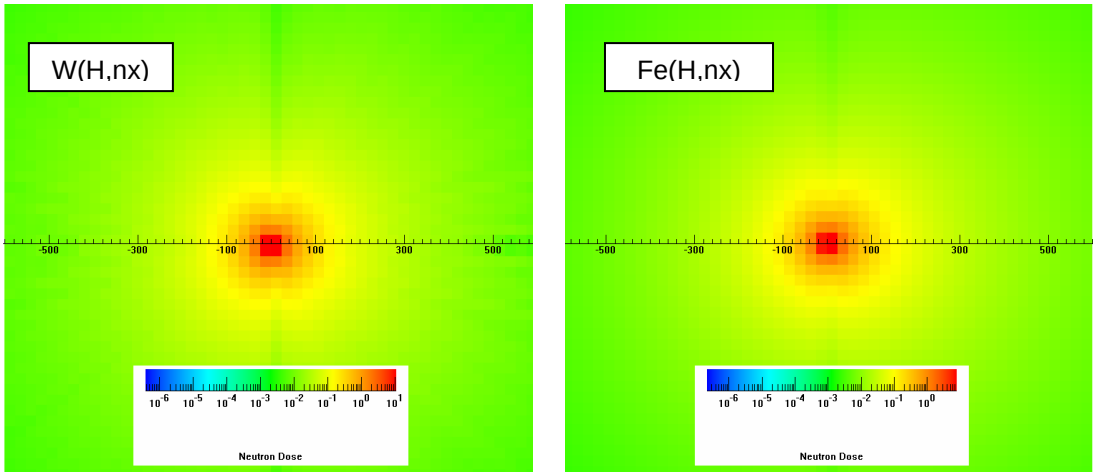

Figure I.B8. Dose field (Sv/h) for a 20 MeV H beam of 50 pA. (left) W(H,nx), (right) Fe(H,nx).

At the date of writing this report, the worst operation conditions for double-beam-on-phase cannot be identified. It is due to the fact that the current beam for some target is not known. The worst material from the point of view of the radioprotection implications is SiC and the safety zone (the distance necessary to reduce the dose to 10 μSv/h) is higher than 3 m from the target in the beam direction (Figure I.B9).

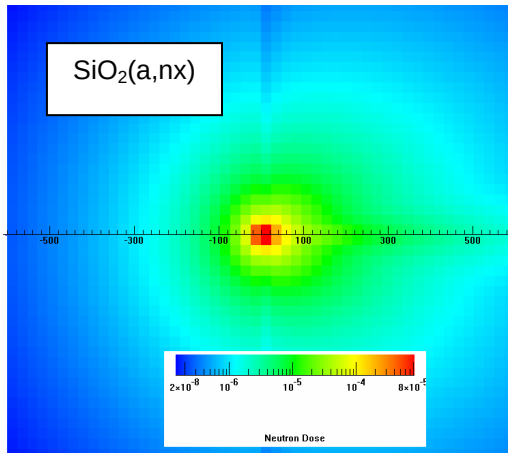

Table I.B9. Dose field (Sv/h): 18MeV - 8.5 nA.

III.2 Beam-off phase

The following figures show the results on beam-off phase for the iron target. This preliminary study is a conservative assessment and it was done taking into account the activation due to uniform proton flux of energy equal to the energy beam in the whole volume. The volume of the material activated is 1cm^2 of area and a thickness equal to the maximum penetration of the proton for the energy of the beam. The irradiation time is 1 week.

The maximum dose rate value using the MCUNED tool after 1ms and 1 month of cooling time with the proton beam (15 nA of 2.5 MeV) is showed in Figure I.B10. The arising photon source obtained with the ACAB code is included in this figure. The maximum value of the residual dose (located in the target) is lower than 3E-4 µSv/h. One hour after shutdown, the isotopic contributions to the total dose are: 76% Co^{55} (T1/2 = 17 hours), 15% Co^{58} (T1/2 = 79 days), 8% Co^{57} (T1/2 = 270 d). In any case, dose rate is negligible.

The maximum dose value using MCUNED for 1ms, 1day and 1 month of cooling time (10 µA and 20 MeV proton beam) is showed in Figure I.B10. The arising photon source obtained by ACAB are also included. The maximum value of the residual dose (located in the target) at 1 msec after shutdown is higher than 45 µSv/h. For one week of cooling time, the maximum value of the residual dose is lower than 10 µSv/h. The main contributor to the total dose, after 1 week after the shutdown, is Co^{56} (98%, half life 77 days).

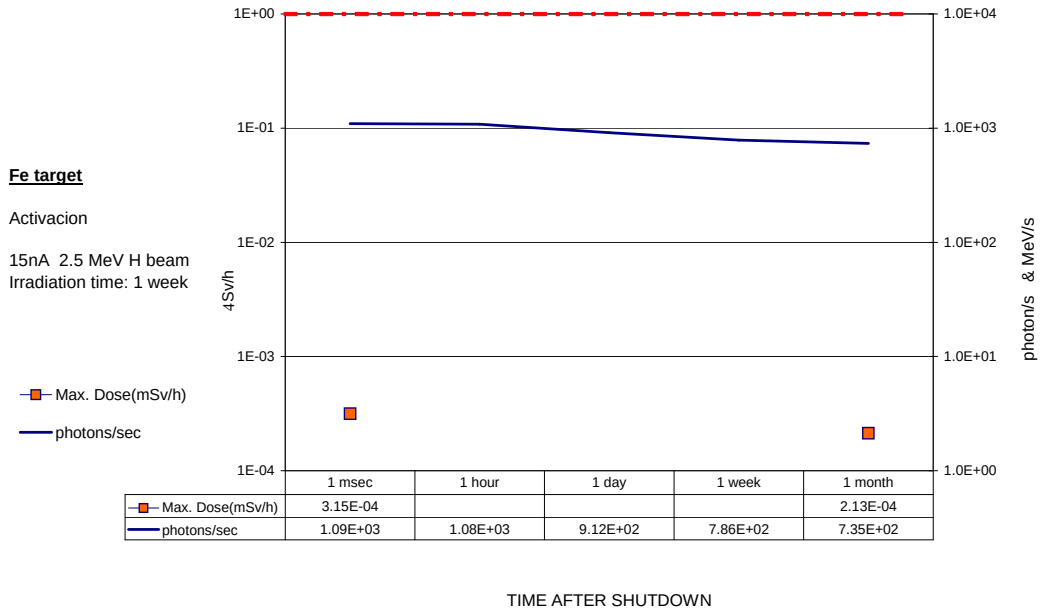

Figure I.B10. Activation results for 15nA proton beam at 2.5 MeV on iron target.

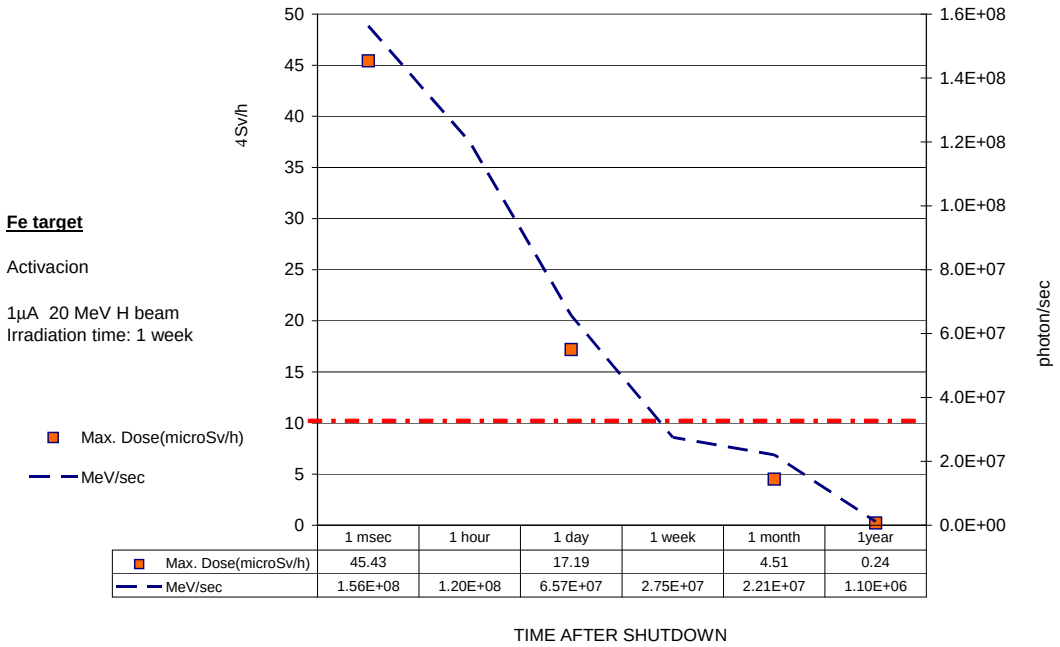

Figure I.B11. Activation results for 1μA proton beam at 20 MeV on iron target.

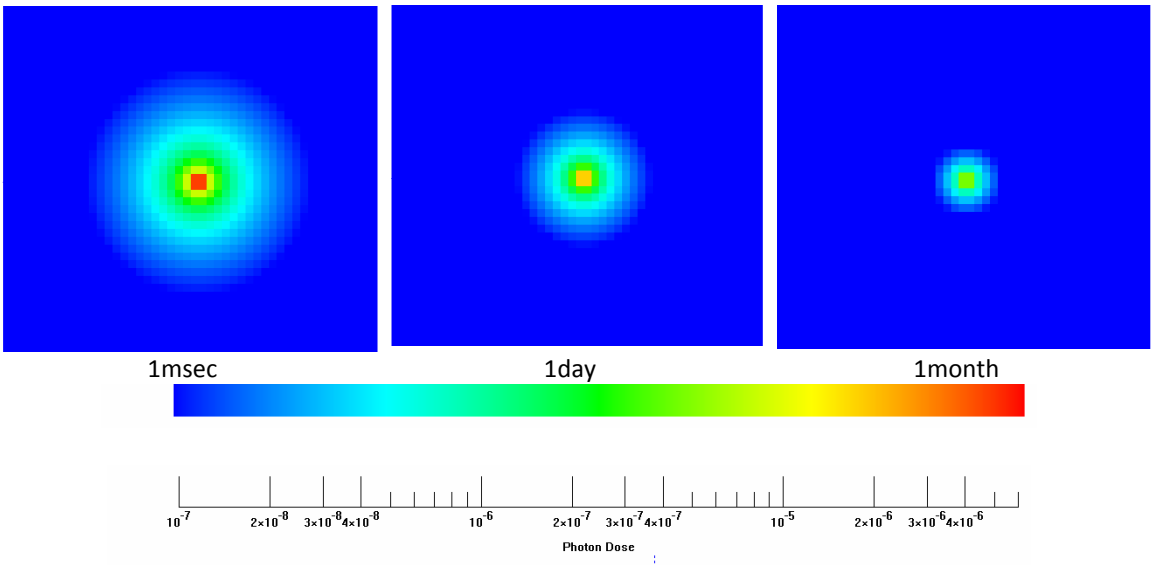

Figure I.B12. Dose field after 1ms, 1day and 1 month after the shutdown. The target is in the center of a vault, full air, of 6 meters of length in all the directions.

(IV) CONCLUSIONS

The MCNPX transport code is not reliable enough tool to predict prompt dose rates in *TechnoFusión* applications based on the use of alpha and deuteron beams.

The use of a new computational tool, an extension of the MCNPX code named MCUNED, allows a more accurate evaluation of the neutron production, and therefore, a more reliable prompt dose rate assessment for those cases where evaluated light-ion cross section libraries are available.

In cases where evaluated libraries are not available, experimental data, and some recent nuclear data compilations from the literature are used to determine the best built-in MCNPX model and to estimate the uncertainties in the calculations. If no evaluated data can be used for the very low energy proton, deuteron and alpha beam irradiations, there is no use in performing any MCNPX calculations.

One the main milestones of this report has been to propose a new methodology, MCUNED plus external evaluated data libraries generated by the Talys code, which is capable to provide better accuracy in the results of the radioprotection simulations for *TechnoFusión* accelerators. The MCUNED code has been recently verified and is now available to make future safety studies.

Regarding to dose rate results from irradiated samples, the values presented in this report are provisional since the values of the beam current are not known for all the cases. Therefore, final conclusions cannot yet be reached about several cases. At the state of this

study, the worst condition concerning to radioprotection is obtained during beam-on phase. In the case of the 20 MeV proton irradiations, maximum values are higher than 9 Sv/h when irradiating tungsten and higher than 7 Sv/h for iron using provisional operation conditions of 1μA current. Dose rates during double-beam irradiations are found to be around one order of magnitude lower than those for 20 MeV proton irradiations. Maximum values are 826 μSv/h and 547 μSv/h for SiC and iron samples respectively.

Therefore, due to the significant values of the prompt dose rate around the irradiated targets, the preventive measures during beam-on phase, such as shielding definition, is an issue to be adressed.

Regarding to the dose rates around the irradiated target during beam-off phase, the study has been done only for iron target. The residual dose in the worst case, that is 20 MeV protons at shutdown and inside the target, is around 45 μSv/h. At shutdown and for a distance from the target around 50 cm the value decreases to less than10 μSv/h. For a cooling time of a week the residual dose rate in the target is also something less that 10 μSv/h.

The ongoing work is focused on the recalculation of dose rates for the problematic cases and on the improvement of the methodology limitations.

Current effort to increase the reliability of cross section libraries for *TechnoFusión* applications is based on benchmarking of Tendl libraries against differential and integral experiments and on the fitting of the libraries to the experimental data.

(V) REFERENCES

[EXFOR 2009] EXFOR Systems Manual, IAEA-NDS-207 (BNLNCS-63330-00/04-Rev.)

[ICRP-103, 2007] The 2007 Recommendations of the International Commission on Radiological Protection, Ann. ICRP 37(2-4), 2007.

[ICRP-74, 1996] Conversion Coefficients for Use in Radiological Protection, Ann. ICRP 26(3-4), 1996.

[JENDL, 2002] Japanese Evaluated Nuclear Data Library. http://wwwndc.jaea.go.jp/jendl/jendl.html

[Koning, 2007] A.J. Koning, S. Hilaire and M.C. Duijvestijn, “Talys-1.0”, Proc. of the Int. Conference on Nuclear Data for Science and Technology - ND2007, April 22-27 2007 Nice France editors O. Bersillon, F. Gunsing, E. Bauge, R. Jacqmin, and S. Leray, EDP Sciences pp 211-214 (2008).

[Koning, 2008] A.J. Koning, D. Rochman. Consistent Talys-based Evaluated Nuclear. Data Library including covariance data (TENDL2008 http://www.Talys.eu/TENDL-2008/).

[Koning, 2009] A.J. Koning, D. Rochman. TENDL-2009beta: "TALYS-based Evaluated Nuclear Data Library http://www.talys.eu/TENDL-2009beta/).

[Mayoral, 2009] A. Mayoral, J. Sanz, P. Sauvan, D. López, M. García, F. Ogando. Relevance of d-D interactions on neutron and tritium productions in IFMIF- EVEDA prototype. ICFRM.14 Sapporo Japan 2009.

[NNDC] National Nuclear Data Center. Brookhaven National Laboratory. http://www.nndc.bnl.gov/

[Pelowitz, 2008] D.B. Pelowitz. Ed. MCNPX User's manual, Version 2.5.0, LA-CP-05-0369 (2005). User's Manual, Version 2.6.0, LA-CP-07-1473. J.S. Hendricks et al.: MCNPX 2.6.0 extensions, LA-UR-08-2216 http://mcnpx.lanl.gov (2008).

[Sanz, 2008] J. Sanz, M. García, F. Ogando, A. Mayoral, D. López, P. Sauvan, B.Brañas. First IFMIF/EVEDA radioprotection studies for the preliminary design of the accelerator beam dump. Fusion Science and Technology In press 2009

[Sanz, 2009] J. Sanz et al., ACAB: Inventory code for nuclear applications, User's manual v2008, NEA-1839 (2009)

[Sauvan, 2009] P. Sauvan, J. Sanz, F. Ogando, M. García, D. López, A. Mayoral, "MCUNED: an improved MCNPX code for deuteron transport. Internal Report, Departamento de Ingeniería Energética, UNED (2009)

[TechnoFusión, 2009] *TechnoFusión*. Informe Científico - Técnico del Centro Nacional de Tecnologías para la Fusión. (*TechnoFusión*). CIEMAT

[Tanaka, 1994] S. Tanaka, N. Yamano K. Hata, K., et al.: (Sumitomo Atomic Energy). ACSELAM library. http://wwwndc.jaea.go.jp/ftpnd/sae/acl.html

[Forrest, 2007] R.A. Forrest, J. Kopecky, J.-CH. Sublet, 'The European Activation File: EAF-2007 deuteron and proton-induced cross section libraries", UKAEA FUS 536 (March 2007)

[Forrest, 2007] R.A. Forrest, J. Kopecky, J.-CH. Sublet, 'The European Activation File: EAF-2007 neutron-induced cross section libraries", UKAEA FUS 535 (March 2007)

Appendix II: Simulations to optimize the plate thickness and the maximum irradiation volume at Irradiation Room of Remote Handling Facility of *TechnoFusión*

The main goal is to estimate the maximum volume under irradiation on the Remote Handling Facility of *TechnoFusión* (at *Irradiation Room*). This requires the design a sheet of metal (in this case tungsten) emitting gamma radiation under the impact of an electron beam with 10 MeV of energy.

(I) Optimization of the plate thickness

In order to calculate the optimum thickness of the W plate by maximizing the gamma radiation in the *Irradiation Room* (see section 9.4.2), a series of simulations with a beam without divergence of 0.5 cm radius have been carried out. Figure II.1 shows the variation of the irradiation volume as a function of the plate thickness. The maximum value is around the 0.3 cm. However, using this small thickness there is a significant proportion of electrons passing through the plate. To mitigate this effect, a thickness of 0.6 cm will be used. This value is decided upon taking into account the absorption of photons produced by increasing the thickness of the plate.

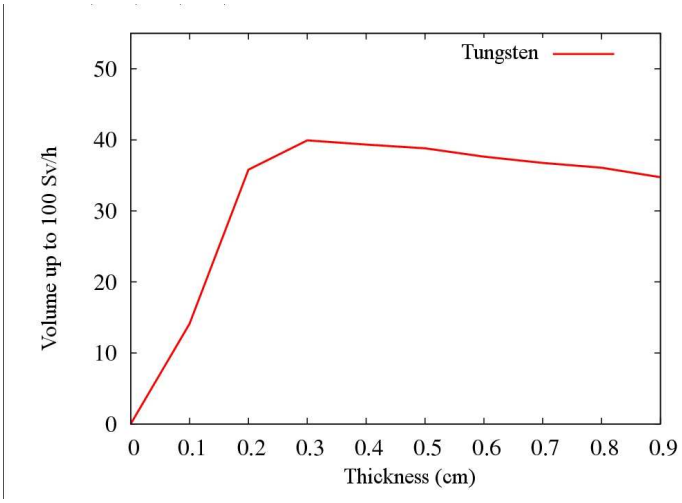

Figure II.1. Evolution of the irradiation volume with the plate thickness.

(III) Beam to generate a square scan

Figure II.2 shows the geometry used in Fluka model (code use for the simulations). The model considers an infinite circular plate with variable thickness on which the electron beam hits. The divergence point is located at 2 m from the plate, and the beam generates a square footprint on it. This shape allows the use of two electronic fields for the sweeping, without increasing the installation complexity. Later sections explore other beam configurations.

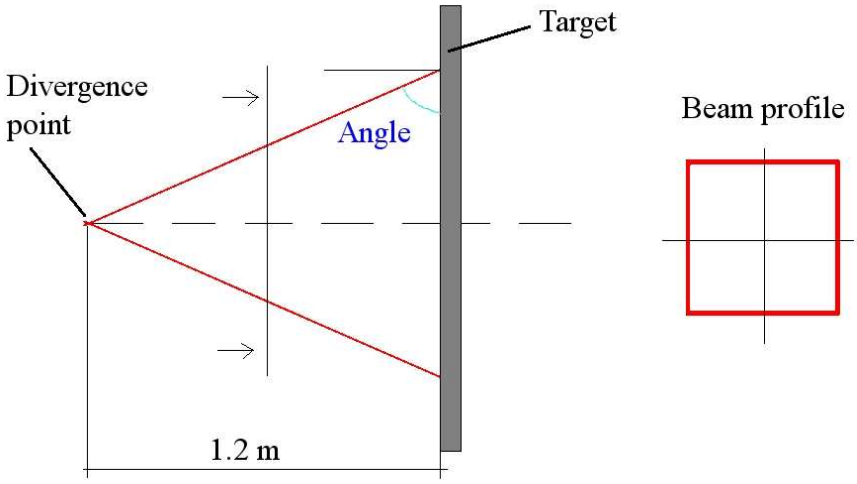

Figure II.2. Simulation model with the geometry introduced for the plate thickness calculation.

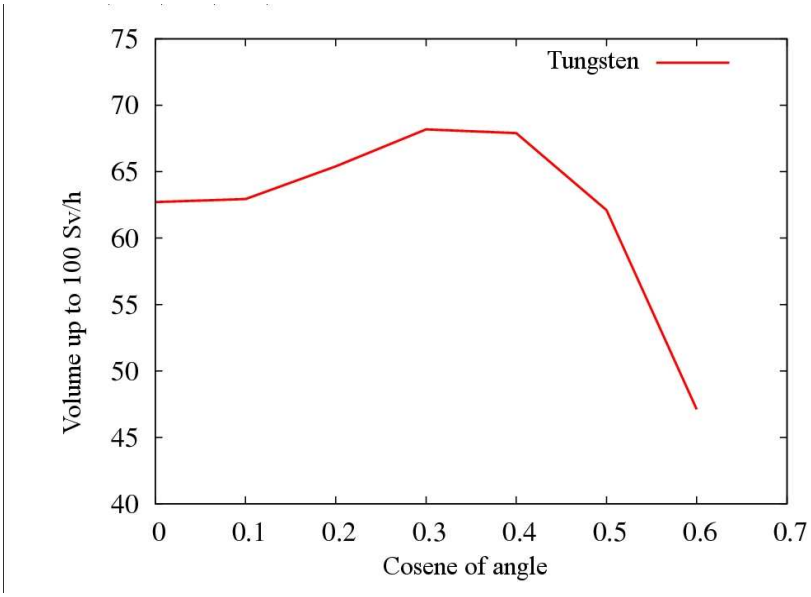

Figure II.3. Irradition volume with dose rates of 100-500 Sv/h for a beam scanning a square area.

Figure II.3 shows the evolution of the room volume with a dose rate between 100 and 500 Sv/h as a function of the cosine of the angle of incidence of the electrons. As shown in the figure, for values between 0 and 0.4, the change in the irradiation volume is very small, reaching its maximum for 0.3. This value will be considered as optimal for a homogeneous radiation.

Figures II.4 and figure II.5 show the distribution of the radiation within the room. The results are obtained by varying the angle of incidence of the neutrons. It can be seen that with a slightly increase of the angle (cos 0.3 and cos 0.4) a substantial homogenization of the dose rate in the room is achieved.

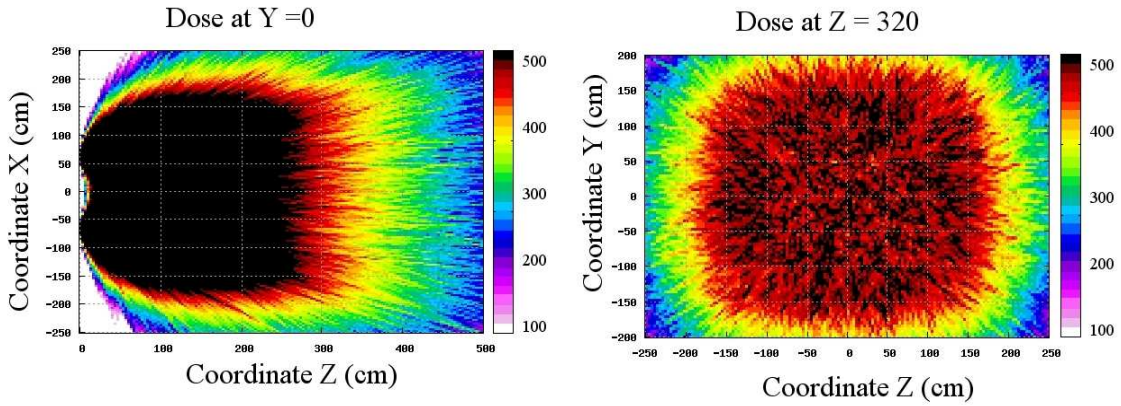

Figure II.4. Dose rate produced by electrons of 10 MeV impacting in a W sheet. The cosine of the incidence angle is 0.3.

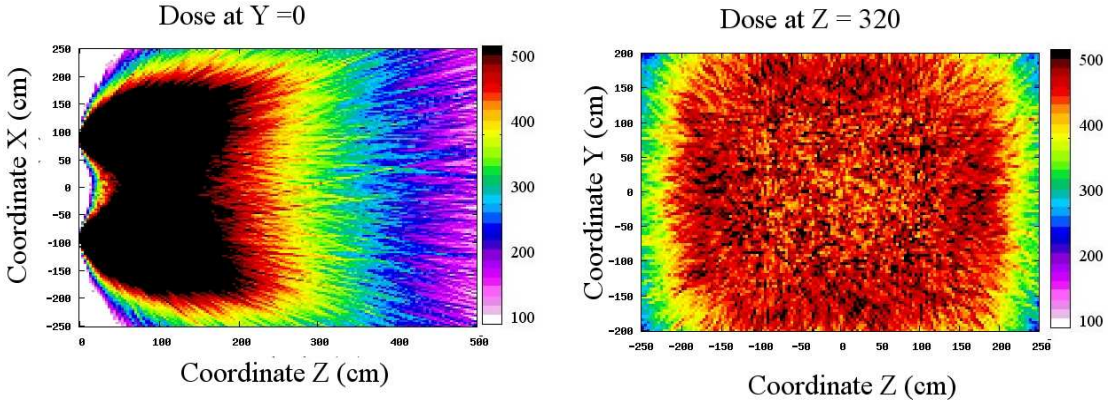

Figure II.5. Dose rate produced by electrons of 10 MeV impacting in a W sheet. The cosine of the incidence angle is 0.4.

(III) Beam scanning a square area

In this section, an evaluation of the irradiation volume obtained by using a beam able to sweep the whole square surface described in figure II.2, is shown.

Figure II.6 shows the evolution of the total irradiation volume as a function of the angle of incidence of electrons. It can be seen as the optimal value is obtained for a cosine value of 0.6.

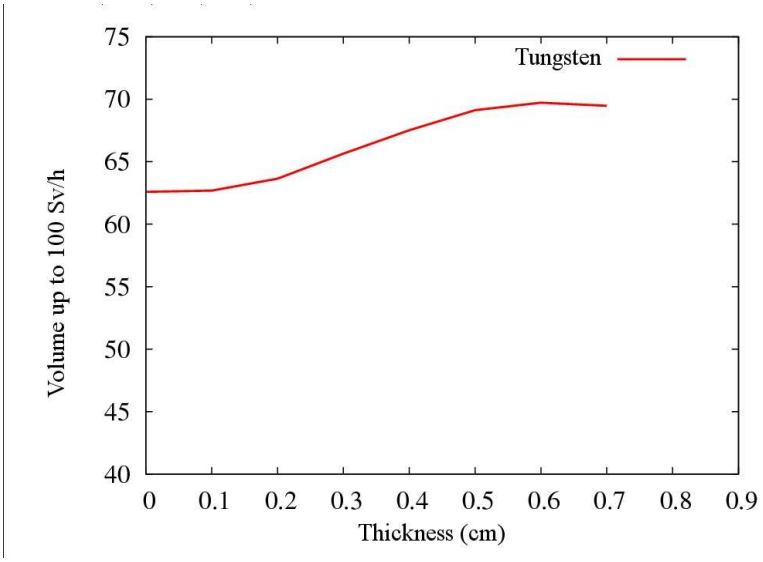

Figure II.6. Irradiated volume with dose rate between 100 and 500 Sv/h for a beam that sweeps the square area.

Figures II.7 and figure II.8 show the dose distribution for an angle of incidence of electrons with a cosine of 0.6. Under these conditions the distribution is very homogeneous. However, the irradiated volumes are lower than those shown in Figure II.5.

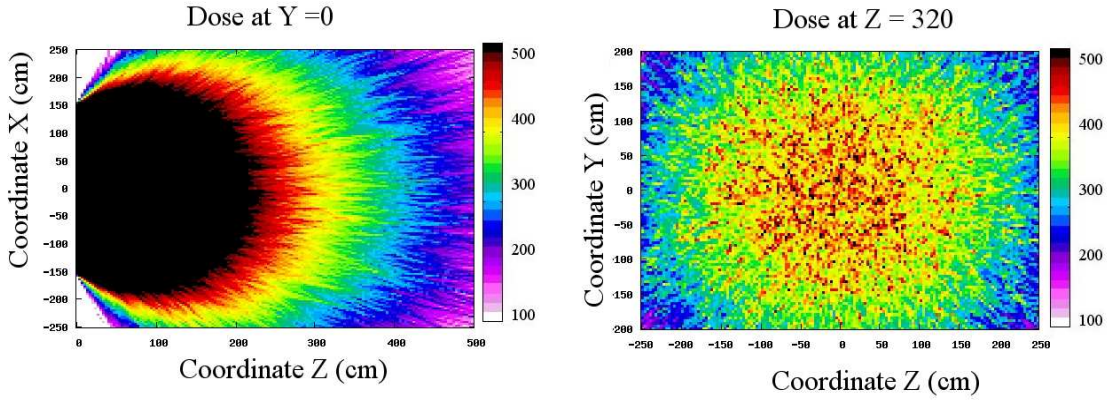

Figure II.7. Dose rate produced by electrons of 10 MeV impacting in a W sheet. The cosine of the angle is 0.6.

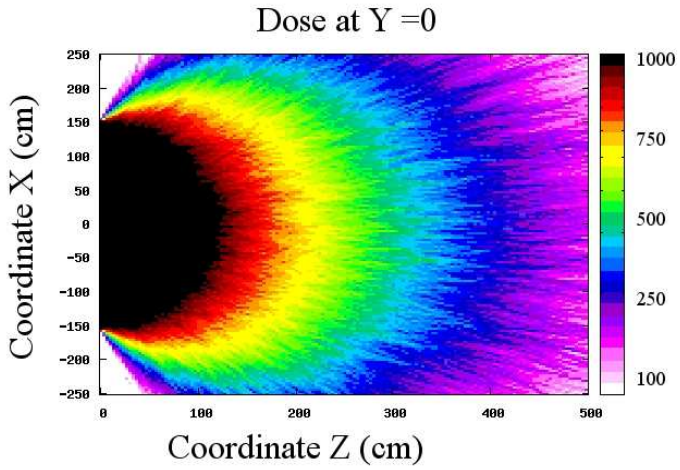

Figure II.8. Dose rate in the range of 100 and 1000 Sv/h produced by electrons of 10 MeV impacting in a W sheet. The cosine of the angle is 0.6.

(IV) Conditions recommended on the basis of simulation results

Table II.1 shows a brief summary of the simulations. The optimized parameters are shown in order to maximize the final volume with doses between 100 and 500 Sv/h.

Table II.1. Simulation summary.

Irradiated material	W
Density	19.25 g/cm^3
Cosine of the angle of incidence	0.6
Beam footprint	Square area: 1.5 x 1.5 m^2
Plate thickness	0.6 cm
Beam radius	0.5 cm
Total volume	74.80 m^3
Irradiation Room size	100 m^3

Appendix III: R&D for the Quasi-Stationary Plasma Accelerator (QSPA) for *TechnoFusión* Facilities

NATIONAL SCIENCE CENTRE "KHARKOV INSTITUTE OF PHYSICS AND TECHNOLOGY"

INSTITUTE OF PLASMA PHYSICS

R&D for the Quasi-stationary plasma accelerator (QSPA) for *TechnoFusión* Facilities

Part 1: Basic specifications for the QSPA device

I.E. Garkusha[1], V.V. Chebotarev[1], N.V. Kulik[1], V.V. Staltsov[1],

D.G. Solyakov[1], V.A. Makhlaj[1], A.V. Medvedev[1], P.B. Shevchuk[1],

B.A. Shevchuk[1], V.I. Tereshin[1], F. Tabares[2]

[1] INSTITUTE OF PLASMA PHYSICS OF THE NSC KIPT, 61108, Kharkov, Ukraine

[2] CENTRO DE INVESTIGACIONES ENERGETICAS, MEDIOAMBIENTALES Y TECNOLOGICAS (CIEMAT), Madrid, Spain

May 2009

Abstract

This report analyzes the definition of the basic design specifications of the Quasi-stationary plasma accelerator (QSPA) for the *TechnoFusión* Facility in Madrid. The final goal of this effort is the deployment of a new combined plasma device for studying the material damage caused by a fusion-grade plasma and the role played by ELMs. In this facility, such situation is simulated by means of a pulsed linear plasma. The facility will provide a better understanding of material behaviour under irradiation by a fusion-grade plasma, and allow quantifying the effects. The proposed new device is an appropriate combination of a QSPA and a steady-state linear PSI device. Below, it will be referred to this newly designed QSPA plasma source as QSPA-SLIDE – where the latter stands for Spanish LInear DEvice.

A general design is made of the *TechnoFusión* QSPA-SLIDE plasma source . The electrodes are assumed to be of the profiled rod type. The main dimensions of the plasma source elements are established.

Plasma flow is calculated for the chosen accelerator geometry on the basis of an MHD model, using 2 different approximations.

Various gas feed schemes are considered for the plasma accelerator. A combination of gas supply at the end and gas injection from the cathode region is chosen.

The effects of applying a small external magnetic field in the discharge region (by means of Helmholtz coils surrounding the plasma accelerator) are analyzed. It is concluded that a longitudinal magnetic field of $0.1.B_{int}$ enhances the streaming stability of the plasma and facilitates the entry of the plasma into the external B-field of the L-shaped vacuum chamber of the *TechnoFusión* facility.

The basic specifications of QSPA-SLIDE device are established. Key parameters of the various QSPA systems are determined.

The electronic characteristics of the power supply systems for the various elements of the QSPA-SLIDE device are calculated.

1. Introduction

The goal of this report is to establish the basic design specifications of the Quasi-stationary plasma accelerator (QSPA) for *TechnoFusión*. The global objective of this effort is the deployment of a new combined plasma device for studying material damage caused by a fusion-grade plasma and the role played by ELMs [1,2]. These effects are simulated by means of plasma streams, in order to obtain a better understanding of material behaviour under irradiation by a fusion-grade plasma, and allow quantifying the effects. The proposed new device is an appropriate combination of a QSPA and a steady-state linear device (we will refer to this newly designed QSPA plasma source as QSPA-SLIDE – where the latter stands for Spanish LInear DEvice).

The first stage of this activity involves a computational and experimental study, as well as a general analysis, oriented towards the design of the advanced quasi-stationary plasma accelerator (QSPA-SLIDE), including the configuration of the electrodes, the geometry of the nozzle, insulators, gas valves and various basic components, necessary for the adequate operation of the QSPA-SLIDE device. Also, studies are made of MHD plasma flows in the QSPA channel, for different geometries of the nozzle, subject to their compatibility with the external magnetic field.

The next stage of this activity will be executed after approval of the present report in the framework of part 2 below, focused on establishing the detailed specifications of the design of the QSPA facility and executing the corresponding studies, drawings and calculations, documented in the QSPA-SLIDE technical reports.

This report consists of two main parts. The first part describes the general considerations and the physical ideas and principles that underlie various design features and dimensions of the proposed QSPA-SLIDE device. The focus will be on the most relevant issues in order to provide clarity for physicists who were not involved in any preliminary QSPA studies, and will avoid unnecessary complications, omitting some details that are less important at this stage and that can be taken into account during the posterior detailed design of the components.

The second part of the report concerns key elements of QSPA-SLIDE, general design features of the plasma source, and component descriptions. Some cost estimations and characteristics of various components are also presented.

2. Main principles of QSPA

The general scheme of a typical QSPA acceleration channel is presented in Fig. III.1. A quasi-steady-state plasma flow is obtained in a profiled acceleration channel between two electrodes. Neutral gas is injected through the entrance of accelerator by means of electronically operated gas valves. The resulting discharge current in the acceleration channel produces an azimuthal magnetic field (Fig. III.1). The interaction between the discharge current and the azimuthal magnetic field results in an Ampere force $F = \frac{1}{c} j \times H$ that accelerates plasma.

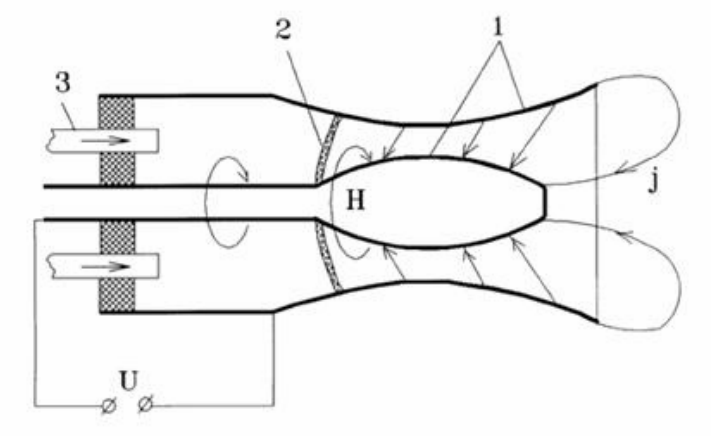

Figure III.1. Scheme of a QSPA acceleration channel: 1 – electrodes; 2 – ionization front; 3 – gas injection.

The acceleration by the Ampere force can also be considered as being due to the difference of magnetic pressure $P_m = \frac{H^2}{8\pi}$ along the acceleration channel. From this point of view, all the equations describing the plasma flow in the acceleration channel under the influence of the Ampere force look like the equations for gas flow in the magneto-hydro-dynamic analogue of the Laval nozzle, where magnetic pressure is applied instead of hydrodynamic pressure. Thus, one may estimate the maximum value of the plasma stream velocity achieved at the exit of the acceleration channel by: $\upsilon \propto \sqrt{P_{m,0}/\rho_0} \propto H_0/\sqrt{4\pi\rho_0} \propto C_{A0}$ where $P_{m,0}$ is the magnetic pressure in the entrance cross-section of the acceleration channel, ρ_0 is the plasma density and C_{A0} is the Alfvén velocity at the entrance cross-section of the acceleration channel.

However, this simple consideration is not capable of handling both stationary and pulsed operation. In this respect, both types of accelerators have to operate similarly. Pulsed plasma accelerators (plasma guns) have been designed and studied for many years in many different laboratories, and their efficiency limit has been established [3,4]. For maximum efficiency, it is necessary to establish the energy transfer time from the capacitor bank to the gun and the time needed for plasma motion along the acceleration channel. Increasing the energy content of the power supply systems, usually capacitor banks, is not a problem, but with increasing energy the energy transfer time also grows. Therefore, it is desirable to increase the time needed for plasma motion along the acceleration channel, and thus to increase the length of the plasma gun. An increased length of the plasma gun and of the time needed for plasma motion along the channel also increases the duration of the interaction of the plasma stream with the gun electrodes and, as a consequence, impurities are emitted from the electrodes into the plasma stream, so that the plasma stream parameters degrade. So, on the one hand, one would like to increase value of L/r to achieve maximum efficiency, where *L* is the length of the acceleration channel and *r* is the radial dimension of the acceleration channel, in order to provide an increased time for plasma motion along the channel. But on

another hand, one needs a small value of L/r to decrease the level of impurities emitted from the gun electrodes into the plasma stream. Thus, the requirements for L/r are conflicting.

The most promising device, from the point of view of achieving the required highly energetic plasma stream and a maximum efficiency of the plasma source, is a steady-state or quasi-steady-state plasma accelerator. In such a device, the requirements regarding the energy transfer from the power supply system to the acceleration channel are not very strict.

The first quasi-steady-state plasma accelerators, or magneto-plasma compressors, based on this simple theory, were designed and manufactured at the Kurchatov Institute, Moscow, Russia. However, the first experiments carried out with such a device were not successful. In particular, the plasma stream velocity was much less than what was predicted from elementary theory. Very large potential jumps were observed in regions close to the electrodes. The electrical current flowing from anode to cathode slid along the electrode surface, and as a consequence plasma flow was halted and impurities were emitted from the electrodes into the plasma stream [3, 4]. All these phenomena resulted in the annulment of the gradient of the magnetic pressure $P_m = \frac{H^2}{8\pi}$ along the acceleration channel in steady state mode.

Some key theoretical ideas for resolving these problems of steady-state (or quasi-steady-state) plasma acceleration were proposed by Prof. A.I. Morozov (Kurchatov Institute, Moscow, Russia). He suggested a two-stage acceleration scheme; the formation of a discharge in which the current is mainly carried by ions; the protection of the electrodes by magnetic screening; etc. [5]. A theory for steady-state flows in profiled channels was developed (which it has been used in the next chapter to model plasma flow in the proposed QSPA-SLIDE device).

Experimentally, an ion current in the discharge channel was obtained for the first time at Kharkov, and steady-state acceleration was achieved at the Kharkov and Minsk QSPA devices, where experiment showed ways to influence the potential jumps near the electrode and to keep the discharge current radial for a sufficiently long time to maintain the required gradient of the magnetic pressure [6-12].

3. Plasma flow modelling in the acceleration channel of the *TechnoFusión* QSPA

Calculations of plasma flow and the main plasma parameters were performed in acceleration channels with various different geometries, in order to find an adequate solution for the design of the QSPA-SLIDE plasma source (size, geometry, conceptual components, output plasma characteristics etc.). In doing so, several models for plasma motion in the discharge nozzle were used.

A system of two-fluid magneto-hydrodynamic equations can be written down for a steady-state plasma flow under the reasonable assumption that the electron mass is much smaller than the ion mass:

$$div(nv_i) = 0 \qquad Mn(v_i grad)v_i = grad(p_i) + en(-grad\Phi + \frac{1}{c}[v_i, H])$$

$$div(nv)_e = 0 \qquad 0 = grad(p_e) + en(-grad\Phi + \frac{1}{c}[v_e, H]) \qquad (1)$$

$$p_i = p_i(n) \qquad p_e = p_e(n) \qquad rotH = \frac{4\pi e}{c} n(v_i - v_e)$$

If the plasma flow has axial symmetry (and here it shall be only considered this case), the magnetic field has only one component – namely, azimuthal: $H = H_\Theta$. In this case, one can obtain the ion and electron flux functions from

$$rnv_r^{i,e} = -\frac{\partial \Psi_{i,e}}{\partial z}, \qquad rnv_z^{i,e} = -\frac{\partial \Psi_{i,e}}{\partial r} \tag{2}$$

Thus, the system of two-fluid magneto-hydrodynamic equations can be written in the following form:

$$\begin{gathered}
\frac{Mv_i^2}{2} + w_i(n) + e\Phi = U_i(\Psi_i) \\
\frac{1}{nr}\frac{\partial}{\partial r}\frac{1}{nr}\frac{\partial \Psi_i}{\partial r} + \frac{1}{nr}\frac{\partial}{\partial z}\frac{1}{nr}\frac{\partial \Psi_i}{\partial z} = \frac{1}{M}\left[\frac{\partial U_i}{\partial \Psi_i} - \frac{e}{c}\frac{H}{rn}\right] \\
w_e - e\Phi = U_e(\Psi_e), \quad \frac{H}{nr} = -\frac{c}{e}\frac{dU_e}{d\Psi_e}, \quad rH = \frac{4\pi e}{c}(\Psi_i - \Psi_e), \quad w = \int \frac{dp(n)}{n}
\end{gathered} \tag{3}$$

where $U_{i,e}(\Psi_{i,e})$ is the full energy (kinetic + thermal + potential) of a small "drop" of ions or electrons. In general, $U_{i,e}$ depends on the flux function and can be represented by an arbitrary function $\Psi_{i,e}$ that remains unchanged along the ion or electron trajectory. In reality, the value of $U_{i,e}(\Psi_{i,e})$ is determined by the boundary conditions at the input cross section of the acceleration channel. Provided the electron and ion pressures ($nkT_{e,i}$) may be neglected with respect to the other terms, the energy equations can be written as follows:

$$\frac{Mv_i^2}{2} + e\Phi = U_i(\Psi_i) \qquad -e\Phi = U_e(\Psi_e) \tag{4}$$

These equations are similar to the equations for particle motion. The second equation shows that the electrons are moving along equipotential lines. Another important consequence of this equation is that with metal (equipotential) electrodes, the electrons will not cross these surfaces. Which implies that it is impossible to achieve a regular plasma flow without potential jumps near the electrodes in the acceleration channel. In the case of metal electrodes (equipotential surfaces), the electrical current should be carried by the ions in plasma. The electron drop energy depends on the flux function $U_e(\Psi_e)$ in the following way:

$$U_e(\Psi_e) = U_0 - \kappa(e/c)\Psi_e, \qquad \kappa = const \tag{5}$$

In this case, the following holds in the whole flowing plasma volume:

$$\frac{H}{rn} = \kappa = const \tag{6}$$

This type of plasma flow is known as isomagnetic flow.

The same energy equation can also be written for the ion component

$$U_i(\Psi_i) = U_0 - \kappa(e/c)\Psi_i \tag{7}$$

This type of plasma flow is known as isobernoulli flow. From equation (3) it can be retrieved the Bernoulli integral, i.e., the energy conservation law for ion (or electron) drops:

$$\frac{v^2}{2} + i(\rho) + \frac{H^2}{4\pi\rho} = U = const \text{, where } i(\rho) = \frac{1}{M}(w_i + w_e),\ \rho = nM \tag{8}$$

The system of equations (3) can be solved analytically for two different models corresponding to two different approximations. The first model assumes thin flux tubes, in which the plasma parameters do not change across a flow tube. The second model assumes the channel changes only slowly, so that the acceleration channel is strongly stretched along the axis, and one neglects the proportional part of the equation $\left(v_r/v_z\right)^2 << 1$.

In the thin flux tube model, and taking into account that plasma flow is isomagnetic, the system of equations (3) can be transformed to a system of three algebraic equations for five independent variables (9):

$$\begin{aligned} rf\rho v &\equiv \frac{\dot{m}}{2\pi} = const, \\ \frac{H}{r\rho} &\equiv \kappa = const, \\ \frac{v^2}{2} + i(\rho) + \frac{H^2}{4\pi\rho} &\equiv U = const \end{aligned} \tag{9}$$

In this system of equations, $f(z)$ is the flux tube width, $r(z)$ the average radius of the flux tube and $\dot{m}$ the mass flow rate. Taking $v_0^2/(2C_{A0}^2) << 1$ and $i(\rho)/C_{A0}^2 << 1$ at the entrance of the flux tube, the constant in the third equation of (9) will be equal to the Alfvén velocity at the entrance of the flux tube, $U = C_{A0}^2$. With this assumption, one can obtain two asymptotic solutions,.corresponding to two different modes of QSPA operation. The first asymptote corresponds to the pure accelerating mode of operation in which all stored energy is converted into kinetic energy, $\frac{H^2}{4\pi\rho} \to v^2/2$, and the plasma enthalpy at the QSPA exit converges to zero. The second asymptote corresponds to the ideal compression mode of operation, in which all magnetic energy is converted to thermal energy, $\frac{H^2}{4\pi\rho} \to i(\rho)$, and the plasma stream velocity tends to zero.

If one assumes, for the pure accelerating mode of QSPA operation, that the average radius of the flux tube is constant along the axis ($r = r_0 = const$), one can eliminate the magnetic field from (9) and obtain the following system of equations:

$$f\rho v = const \quad \left(v^2/2\right) + i(\rho) = const \quad \text{and} \quad i(\rho) = i(\rho) + \left(\kappa^2/4\pi\right) r_0^2 \rho$$

This system of equations is fully analogous to the system of equations that describes gas flow in a Laval nozzle, except for of the appearance of the signal velocity (in hydrodynamics: sonic velocity). In the dynamic plasma equations, the signal velocity is defined as $c_s^2 = c_T^2 + c_A^2$ where c_T is the thermal velocity and c_A the Alfvén velocity. Thus, the accelerating channel should be profiled. The channel width should decrease from the entry to the critical cross section, where channel width has its minimum, and after the critical cross section the channel width should increase again. At the critical cross section, the local plasma stream velocity will be equal to the local magnetosonic velocity $v_c = c_{sc}$.

The second model deals with a slowly changing plasma flow (the slowly changing acceleration channel model). In this model, terms in the equations like $\partial^2/\partial r^2$ and $(\partial/\partial r)^2$ can be neglected. Thus, with the assumption $(v_r/v_z)^2 << 1$, one can transform the system of equations (3) into a set of equations including only the derivative along r. For isobernoulli plasma flow, the ion flux function can be written as:

$$\Psi_i = \frac{r_0^2 v(z)}{2} n_0 \left(1 - \frac{v^2(z)}{v_m^2}\right) \ln \frac{r}{b(z)}$$

$$n = n_0 \left(\frac{r_0}{r}\right)^2 \left(1 - \frac{v^2(z)}{v_m^2}\right), \qquad \frac{H}{nr} = \frac{H_0}{n_0 r_0} \tag{10}$$

where r_0 is the radius at the entrance of the acceleration channel and b(z) is the radius of central electrode (cathode).

One of the important properties of isobernoulli plasma flow is that the plasma stream velocity does not depend on the radius

$$v_z = \frac{1}{nr}\frac{\partial \Psi_i}{\partial r} = v(z) \tag{11}$$

If the mass flow rate $\dot{m}$ and the discharge current I_d are known, it is possible to calculate the plasma flow velocity in terms of the discharge current:

$$v_m = \Theta\left(\frac{I_d}{c}\right)\frac{1}{\dot{m}}, \quad \Theta = \frac{4}{3\sqrt{3}} \ln \frac{a_*}{b_*} \tag{12}$$

Where a_* and b_* are radius of cathode and anode at the critical cross section, respectively.

Thus, this model allows computing the geometry and the profiles of the electrodes that form the discharge channel. Also, the main plasma parameters, such as the plasma density and the ion and electron velocities can be calculated locally in any region of the acceleration channel. These calculations lead to the proposed geometry and key dimensions of the QSPA-SLIDE source, as will be described below.

4. Basic Specifications for the QSPA device

4.1. General Remarks regarding the QSPA design

In many previous experiments, carried out using small quasi-stationary plasma accelerators and magnetic plasma compressors having discharge currents of up to 200 kA, it was shown that with solid (monolithic) electrodes it is impossible to achieve plasma flow in the acceleration channel without large electric field jumps near the electrodes. The measured plasma stream velocity was much less than predicted by theory.

As can be deduced from the theory of plasma flow in the framework of two-fluid magneto-hydrodynamic models, in profiled acceleration channels the electron component moves along equipotential lines, while the ions cross the equipotential lines. In this case, there are two different ways to organize the plasma flow in the discharge gap.

First – if the discharge current is carried by the electrons, these will need to cross the electrode surface, and to close the electric circuit of the power supply system, so that one has to design non-equipotential electrodes (for example, sectioned electrodes). However, such a design is very complicated technically.

Second – if the discharge current in the plasma flow is carried mainly by the ions (the accelerator operation mode), it can bed use equipotential electrodes but in this mode of operation one needs to convert the current from electron-carried in the power supply system to ion-carried in the plasma flow. In the discharge gap, the ions will move from the anode surface into the plasma flow and thus one must inject ions into the anode region during the discharge in order to maintain the discharge current and so one must protect the cathode surface from this high energy ion bombardment.

Fig. III.2 shows a sketch of the acceleration channel in the operational mode in which the discharge current is carried by ions in the discharge gap.

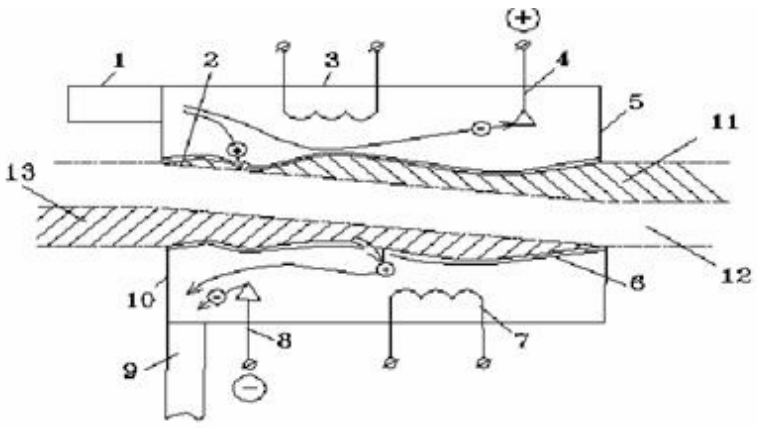

Figure III.2. Scheme of acceleration channel. 1 – ion source in anode volume; 2 – ion emitting surface; 3 – anode magnetic field system; 4 – electron collectors; 5 – anode cover; 6 – cathode collecting surface; 7 – cathode magnetic field system; 8 – electron source in cathode volume; 9 – plasma pump; 10 – cathode cover, it shapes the channel; 11 – near anode flow; 12 – main plasma stream; 13 – near cathode flow.

As can be seen in Fig. III.2, there are three different fluxes in the acceleration channel. The near-anode flux is the ion flux from the anode surface to the acceleration channel, needed to support the discharge current. The core plasma stream is accelerated in the central region. The near-cathode flux is the ion flux from the accelerated plasma stream boundary to the cathode surface, needed to close the electrical current circuit.

Thus there are three key areas involved in achieving long-pulse QSPA operation, avoiding electrode erosion and plasma contamination, and achieving the required plasma parameters (velocity and density). These areas are also important for the transport of plasma in an external B field:

- The input zone, which is the ionization zone;
- The anode zone, that supports the electrical current between electrodes, carried by ions;
- The cathode zone, to protect cathode elements from bombardment by high energy ions;

The conceptual design of the QSPA-SLIDE plasma source, including these 3 zones, is presented in Fig III.3.

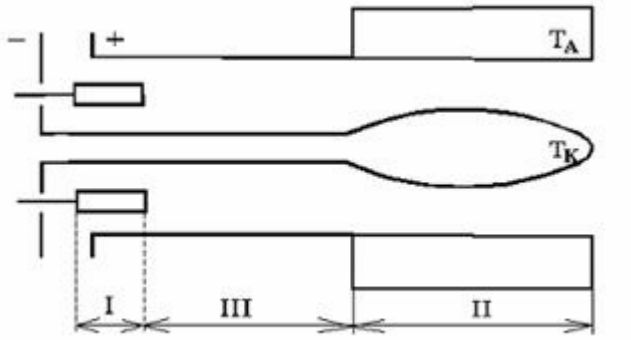

Figure III.3. Conceptual design of the QSPA-SLIDE plasma source: I – input part, II – drift channel, III – main acceleration channel, T_A – anode transformer (anode), T_K – cathode transformer (cathode).

4.2. Design of the main QSPA parts

(a) Entrance section

As mentioned above, the working gas is injected and/or ionized in the entrance section. In previous experiments with MPC and QSPA it was found that the ionization region of the working gas is strongly unstable.

An initial solution to this problem, associated with the ionization zone, is to separate the injection of the working gas, its ionization and its acceleration spatially. In this case, what

enters the acceleration channel is not a neutral gas, but a plasma that has been produced previously in several small ionization chambers, operating with a small discharge current.

Another problem that should be taken into account in view of the long-pulse operation of the QSPA device is that the plasma produced by the ionization of gas during later stages of the discharge should move across the magnetic field produced by the discharge current in the main acceleration channel. It is difficult to transport this new plasma across the magnetic field without an additional external force. A theoretical study of isomagnetic plasma flow in the acceleration channel shows that the radial distribution of the plasma density in the entrance section of the QSPA should be proportional to $1/r^2$. As confirmed by many experiments, the necessary $1/r^2$ distribution in the drift channel can be obtained in several ways.

The ionization zone can also be stabilized by, e.g., supersonic gas flows. In this case, the design of the gas tubes should be similar to Laval nozzles. In any case, it is still needed to solve the problem of transporting the plasma from the ionization zone to the acceleration channel, and of creating a radial distribution of plasma density proportional to $1/r^2$.

The simplest way to solve this problem in the QSPA-SLIDE device is to create an additional electromagnetic force in the drift channel, to drive plasma transport towards the main acceleration channel and to shape the radial distribution of the plasma density proportional to $1/r^2$. The proposed scheme is shown in Fig.III.4.

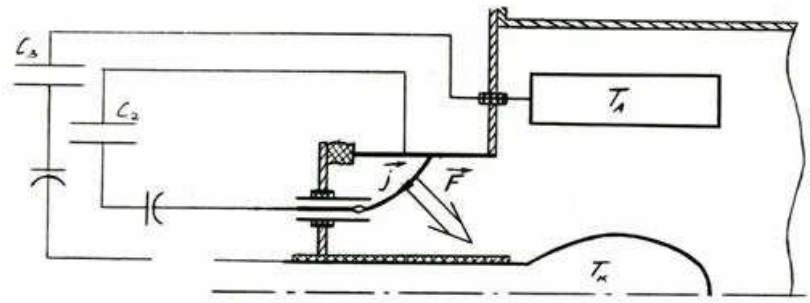

Figure III.4. Scheme of creation of an additional force to drive plasma transport towards the acceleration channel for long-pulse operation of the QSPA-SLIDE device

In this case, an additional current $\vec{j}$ is supplied by an independent power supply system (a capacitor bank), which, together with the existing azimuthal magnetic field, produced by the main discharge current, create an electromagnetic force $\vec{F}$ that transports the plasma towards the acceleration channel and simultaneously focuses the plasma towards the axis.

All three methods described above can be applied to the design of the input section of QSPA-SLIDE. It is possible to apply these methods separately or in combination. For this reason, the design of QSPA-SLIDE contemplates 4 gas tubes (see below) and an additional gas

valve in the cathode area. Details of the design are described below in the corresponding chapters.

(b) Anode section

As mentioned above, in the anode the particles carrying the electrical current must be switched from electrons (in the power supply system and cables) to ions (in the plasma), since ions emitted from the anode will carry the discharge current in the acceleration channel.

The simplest design for such an anode transformer is a multi-rod electrode – a anode consisting of rods with an additional outer screen. The volume between the rods and the outer screen is filled by a neutral gas, injected via the entrance section. Our previous experiments show that part of discharge current is distributed in the area exterior to the acceleration channel, by forming a short current path on the outer side of the anode rods. This part of the discharge current sustains the ionization of the neutral gas in the region between the anode rods and outer screen. Thus, a continuous influx of ions to the acceleration channel is provided, the discharge current can be sustained, and electrons will flow to the anode rod surfaces to close the electrical current circuit.

(c) Cathode section

In the operation mode in which the discharge current in the acceleration channel is carried by ions, the plasma ions cross the equipotential lines and move (shift) from the anode surface to the cathode surface. Thus, part of the ions of the accelerated plasma stream should reach the cathode surface and close the current circuit. This implies that energetic ions will reach the cathode surface. Therefore, the electrons in the cathode section of QSPA should neutralize the ion charge and the metal cathode surface should be protected from ion bombardment. As shown in previous experiments with MPC and QSPA in which a monolithic solid cathode was used, the discharge current between the electrodes slides along the surface of the solid cathode, and a high level of cathode erosion accompanied by a significant jump of the electric potential in front of the cathode surface was observed.

Here again the simplest (and effective) design for the cathode section is a multi-rod structure for the profiled area of the cathode. In this way, the neutral gas or cold plasma that is stored inside the cathode volume (under the cathode rods or lamellas) will flow to the discharge area and will produce electrons to close the current circuit. A small part of discharge current, about 20-30 %, will flow to the cathode rods (lamellas), and this part of the discharge current will produce a magnetic field that protects the solid cathode elements from excessive bombardment by high energy ions (by magnetic screening).

The cathode shape, which defines the profile of the acceleration channel, can be computed on the basis of the ideal one-fluid magnetohydrodynamic model, under the assumption that the particle velocity at the entrance of the acceleration channel is close to zero. This assumption is quite reasonable since the neutral gas will arrive at the entrance of the acceleration channel with the thermal velocity, which is much less than the drift velocity or the Alfvén velocity. The profile of the channel width can be written as follows: $h(z) = \frac{2}{3\sqrt{3}} \frac{h^*}{\sqrt{\frac{z}{L}\left(1-\frac{z}{L}\right)}}$, where h^* is the minimum channel width at the critical cross

section, and L is the channel length. In this ideal model, the channel width goes to infinity at the entrance and exit sections. But it allows computing the profile of the middle part of the acceleration channel. Assuming the anode diameter is 25 cm (based on: the required plasma parameters, the plasma entrance to the external B-field structure, and the plasma stream diameter due to plasma transport in a strong magnetic field of up to 1 T), the cathode profile was calculated. The results of the 2 types of calculation are presented in Fig. III.5.

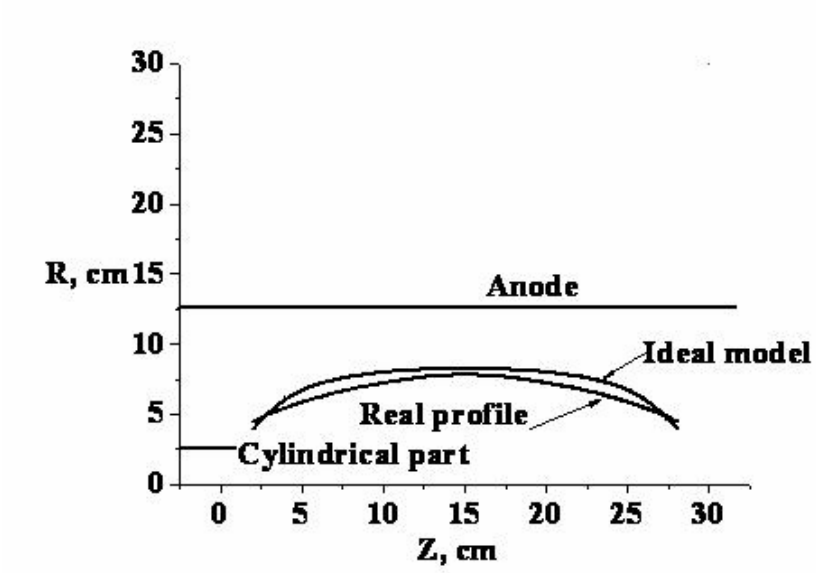

Figure III.5. Results of calculations and the proposed profile of the QSPA-SLIDE acceleration channel.

From this, it has been concluded that the agreement between the calculated cathode profiles on the basis of the ideal model and the real cathode profile proposed for the QSPA-SLIDE device is rather good.

Next, there will be an estimation of some quantities using realistic plasma parameters for the QSPA-SLIDE device, with the proposed profile of the acceleration channel. For example: taking a discharge current of 600-650 kA and an average channel radius of 10 cm; a plasma density at the entrance of the acceleration channel of 10^{15} cm^{-3}, and hydrogen as the working gas, the maximum velocity of the plasma stream at the accelerator output is $v_{\max} = \sqrt{2}C_{A0}$, i.e., approximately (1.1 – 1.3)x10^8 cm/s.

More detailed estimations and results from calculations concerning the dynamics of the plasma stream in the QSPA SLIDE device are provided in Annex 1 of this report.

4.3. General specification of the QSPA device

Figure III.6 shows a block diagram of the QSPA-SLIDE plasma source.

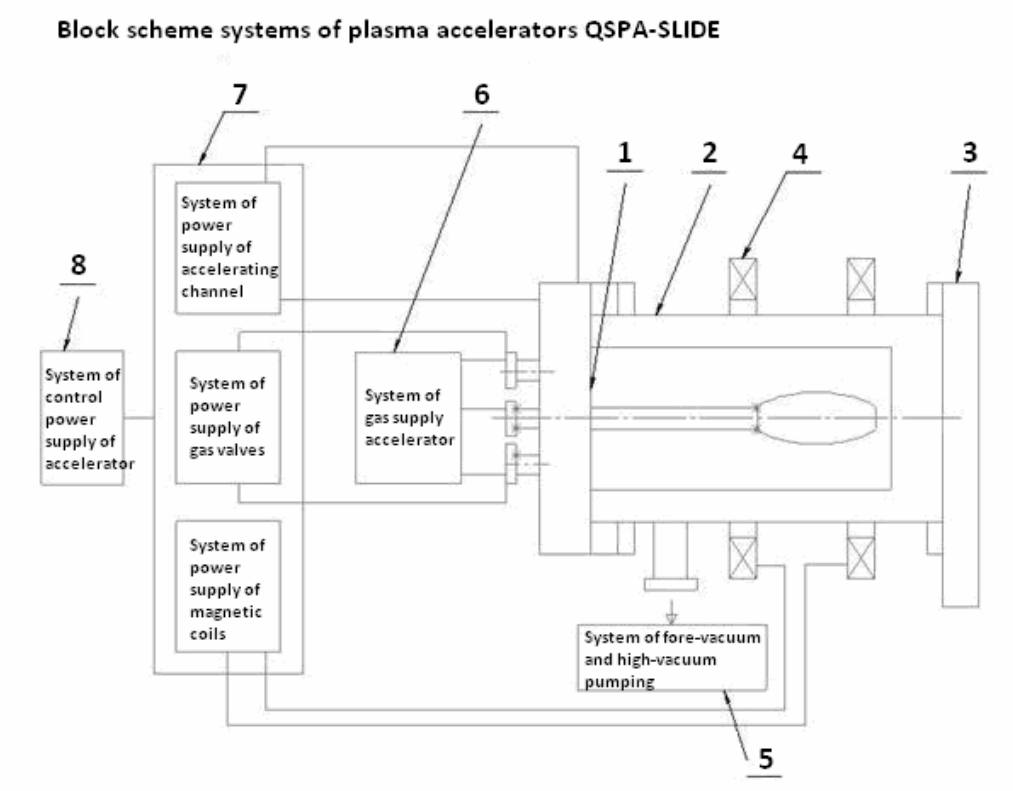

Figure III.6. Block diagram of the QSPA-SLIDE plasma source.
1- plasma accelerator, 2-QSPA vacuum chamber, 3-vacuum gate between QSPA plasma source and L-type vacuum chamber of the combined device, 4- Helmholtz coils for an external magnetic field in the acceleration channel, 5- vacuum pump system of the QSPA chamber, 6- gas supply to electronic valves, 7- power supply of the plasma source and gas valves, coils for the external magnetic field and the main discharge in the accelerator, 8- control system of the power supply.

4.4. Description of QSPA components

The planned experiments to simulate the effect of transient events like ELMs or disruptions on the divertor surfaces of ITER require the generation of plasma streams with parameters similar to that of the SOL plasma flows produced by instabilities [1, 2].

To meet this objective, the recently designed QSPA-SLIDE plasma source will generate plasma streams having the following parameters at the exit of the acceleration channel: electron density 10^{15}-10^{16}cm^{-3}, electron temperature ~ 3÷5 eV, ion impact energy up to 1 keV, plasma stream energy density >2 MJ/m^2, and pulse length ~0.5 ms. After injection of the plasma into the longitudinal magnetic field with axial symmetry and increasing along the path of the plasma stream, the plasma will be magnetized, and transverse compression may elevate the electron temperature to 60 ÷100eV, as has already been achieved in pulsed devices. The energy density of the plasma stream can be varied in a wide range.

The proposed QSPA-SLIDE complex includes the following systems:

- A coaxial plasma accelerator with four electronic valves on the end flange and one valve inside the cathode, and some integrated diagnostics embedded into the structure;
- The QSPA vacuum chamber, with its own pumping system;

- The gas system, gas balloons, pipes etc.
- Two Helmholtz coils for field correction, producing a relatively small external magnetic field of up to 0.1T in the discharge area;
- The power supply system for the QSPA discharge;
- Power supply systems for the electronic valve coils - 5 units in total;
- The power supply of the Helmholtz coil system;
- A synchronization unit;
- A control panel;

(a) Coaxial plasma accelerator

A diagram of the QSPA-SLIDE plasma source is shown in Fig. III.7. Detailed drawings for different parts of the source are still being made. However, the general conceptual design is completed.

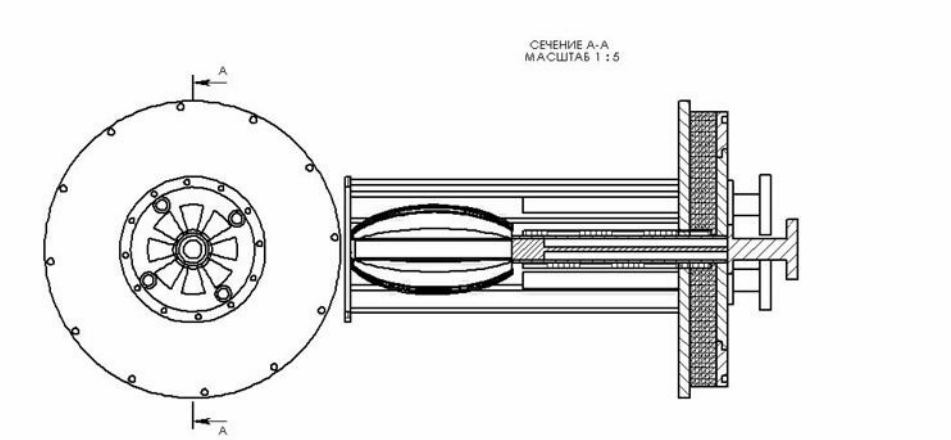

Figure III.7. Drawing of the QSPA-SLIDE plasma source (front and lateral sections)

A front view of the proposed QSPA-SLIDE plasma source is shown in Fig. III.8.

The proposed plasma accelerator consists of two coaxially arranged electrodes: the proposed outer cylindrical rod electrode (anode) (number 2 in Fig. III.8.) consists of a set of rods, forming a “squirrel cage” with an inner diameter of 260 mm and a length of ~700 mm. One side of the rod electrode structure is attached to the ring (4), while the other side is fixed to the end flange (3).

The inner electrode (cathode number 1 in Fig. III.8.) consists of a cylindrical tube with a diameter of 50mm and a length of 300mm, and has a lamellar rod structure at the end. This lamellar structure forms the ellipsoid having a maximum diameter of 160 mm at the critical

cross-section. The length of the ellipsoid is 300 mm. The other end of the cylindrical tube is welded to the electrode-cathode disk. 5 electro-dynamic valves are mounted on this disk. The anode and cathode flanges are meant function as cable collectors. All electrode components of the plasma accelerator are produced from oxygen-free copper. The total weight of electrode system is about 100 kg.

The anode and cathode electrodes are separated by a plastic isolator disk, to which 5 vacuum-sealed ceramic tubes are attached. One ceramic tube (5), having an inner diameter of 55 mm and a length of 270 mm, is placed in the centre of the isolator disk to maintain the discharge only in the profiled part of the acceleration channel, and to provide a separation of the cathode and anode compatible with the high voltage. Four other tubes (6) with a diameter of 20 mm each and having the same length of 270 mm are situated at 100 mm from the system axis. These tubular isolators protect the cathode and the electronic valves of the gas supply from secondary electrical breakdown during the discharge. This is especially important for the long-pulse operation of the proposed plasma source.

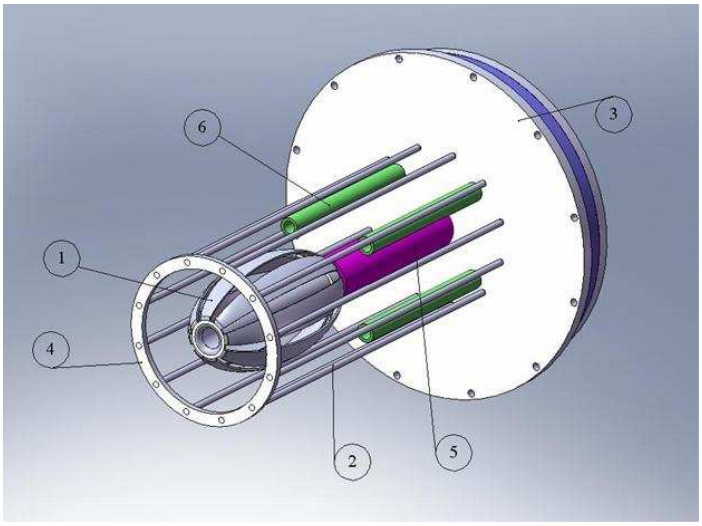

Figure III.8. Front view of the QSPA –SLIDE plasma source. 1-Profiled part of the cathode, 2-anode rods, 3-anode flange, 4-cathode ring, 5-ceramic tube of the cathode, 6- insulator tubes of the gas supply system (the gas valves are inside the tubes).

The electronic valves can inject up to 500 cm^3 of working gas into the discharge gap. Four valves for axial gas supply are located inside the tubes (6). A fifth valve is located inside the cathode tube to provide additional radial injection of gas, directly from the cathode into the discharge zone. The simultaneous operation of several compact gas valves can be useful to achieve more flexibility with regard to the plasma parameters and to decrease electrode erosion with long pulse operation. This flexibility can also be important if it is decided to use other gases than H_2, such as D_2, He or others (or mixtures).

A rear view of the proposed plasma source is shown in Fig. III.9. The gas valves are triggered by pulsed coils (number 8 in Fig. III.9.), mounted on the end flange of the internal electrode (9).

The power supply connections are fed through the flange (3) of the external electrode and flange (9). To prevent high-voltage breakdown between flanges (3) and (9), a face plate isolator (10) will be installed.

A rear view of the QSPA –SLIDE plasma source with an axial cut is presented in Fig. III.10, showing the additional gas valve in the cathode region.

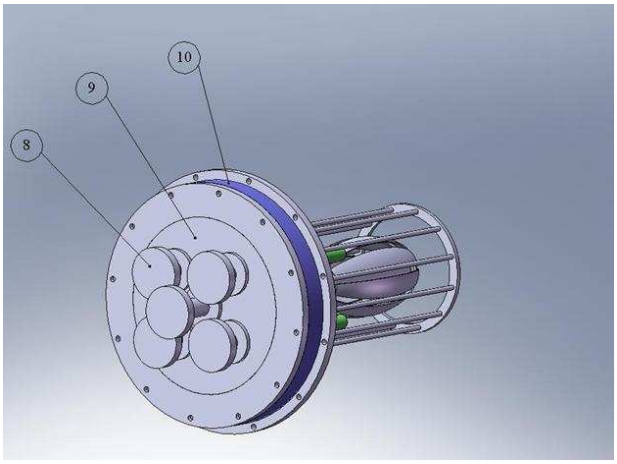

Figure III.9. Rear view drawing of the QSPA –SLIDE plasma source. 8- electro-magnetic coils of the gas valves, 9- the cathode flange, 10- the face plate insulator.

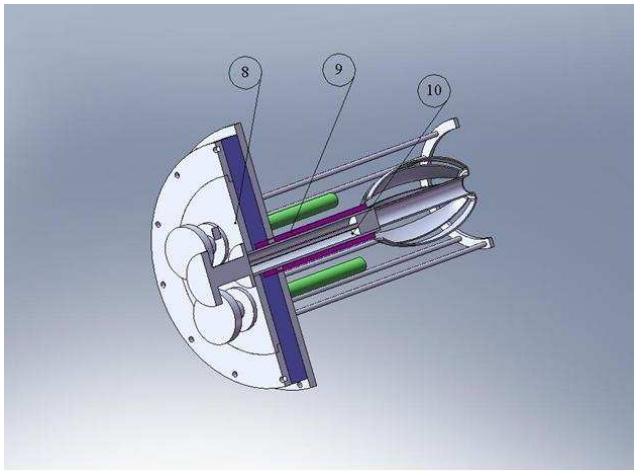

Figure III.10. Rear view with an axial cut of the QSPA –SLIDE plasma source, showing the cathode gas valve. 8- cathode flange, 9- ceramic tube of the cathode, 10- gas valve plate.

(b) QSPA vacuum chamber with pumping system

The cylindrical QSPA vacuum chamber has a length of 800 mm and a diameter of 350 mm. It is made of non-magnetic steel. The plasma accelerator is mounted on one end of the vacuum chamber. The other end is connected to the vacuum vessel of the combined device by means of a sliding shutter with an opening diameter of 350÷360 mm. Four branch tubes with a diameter of 50÷60mm are placed in diametrical opposition on the lateral surface of the vacuum chamber, and provide windows for diagnostic purposes.

The QSPA chamber is pumped through the 180÷200mm diameter branch tube, installed on the lateral surface of the vacuum chamber, with an attached sliding shutter (gate valve). A turbo-molecular pump with an effective pumping speed of up to 600 l/s and a fore-vacuum pump with an effective pumping speed > 5 l/s will create a background pressure in the QSPA chamber of 10^{-6} torr. The crude pumping of the vacuum chamber is performed by a rotary pump with a pumping speed > 5 l/s via the bypass line and the gate valve with an opening diameter of 50÷60 mm, connected to the system pumping branch tube. The estimated cost of the elements of the pumping system is as follows:

- Vacuum installation consisting of a turbo- pump and a fore-pump: - up to 20 TE
- Rotary pump for preliminary pumping : - 4 TE
- Sliding shutter with an opening diameter of 350÷360mm: - up to 1 TE
- Gate valve for rotary pump: up to 0.5 TE

The QSPA vacuum chamber must be attached to one of the ends of the L-type main chamber of the combined *TechoFusión* device. The size and openings of its end flange should be compatible with a sliding shutter, separating the QSPA from the L-type main chamber of the combined *TechoFusión* device

Diagnostics of the QSPA plasma stream, such as calorimeters, electric and magnetic probes, piezo-detectors, spectroscopy, interferometry, etc., should also be provided in order to monitor the operation of the device and the plasma parameters.

(c) Gas supply system

The gas supply system of the QSPA will consist of five bottles with a volume of 5 litters and an operating pressure of up to 15 atmospheres each. Each bottle is connected to one of the five electronic valves by means of a T connector and metal tubes. A high-pressure bottle fitted with a pressure regulator valve allows filling up each of the 5 litter bottles periodically to operational pressure. The gas supply system corresponding to each electronic valve is galvanically isolated from the other gas systems and the ground circuit, so that it will be at high voltage during operation.

(d) Helmholtz coils

The proposed design contemplates Helmholtz coils inside the vacuum chamber to stabilize the discharge in the acceleration channel. Additionally, these Helmholtz coils allow correcting the geometry of the axial magnetic field at the exit of the plasma accelerator. Each magnetic coil has a diameter of 600 mm and a width of 60 mm, and has a low inductance. The magnitude of the magnetic field created by the Helmholtz coils must be about 0.1 of the internal (proper) magnetic field produced by the accelerator discharge current. The pulse shape should match the waveform of the discharge current and have the same duration.

The plasma flow in the presence of both a weak longitudinal B-field, below 0.1 T, and the proper azimuthal B-field of about 1 T is calculated using a simplified model. Any rotation of the plasma column will add stability at the point where the plasma stream enters the transportation chamber.

(e) QSPA Plasma Transportation in an External B-field

The QSPA will be placed in a region with a field of 0.1T (Helmholtz coils), so it is convenient that the B-field increases slowly from 0.1 T to 1T along the plasma path for further transportation of the plasma stream.

The B-field should only reach 1 T at the last 2 coils. At the first coils (close to the QSPA) the field should be lower, i.e. (0.1-0.5) T, to avoid large plasma losses at the entrance to the magnetic system. The QSPA discharge will be perturbed by external fields of 1T in the discharge area.

Even a calculation of a single iteration yields a strong B-field ripple in the combined *TechoFusión* device. Thus, near the QSPA output the coils should be close to each other (either using wider coils or adding additional coils) to provide a more favorable scenario for plasma compression and to decrease the diameter of the plasma stream.

The entry of the QSPA plasma into the magnetic field system of the combined *TechoFusión* device can be controlled by varying the electric current in both the Helmholtz coils and the entrance coils of the L-shaped chamber. Also, modifications to the coil positions, their size, and the distance between the Helmholtz coils and the entrance coils of the L-shaped chamber are considered. Corresponding numerical simulations have been performed. As an example of such calculations, the result of varying currents and coil displacements is shown in Fig. III.11 for a maximal field of 2 T and a diameter of the chamber coils of 25 cm. Final calculations will be performed after the detailed design of the L-shaped chamber has been established.

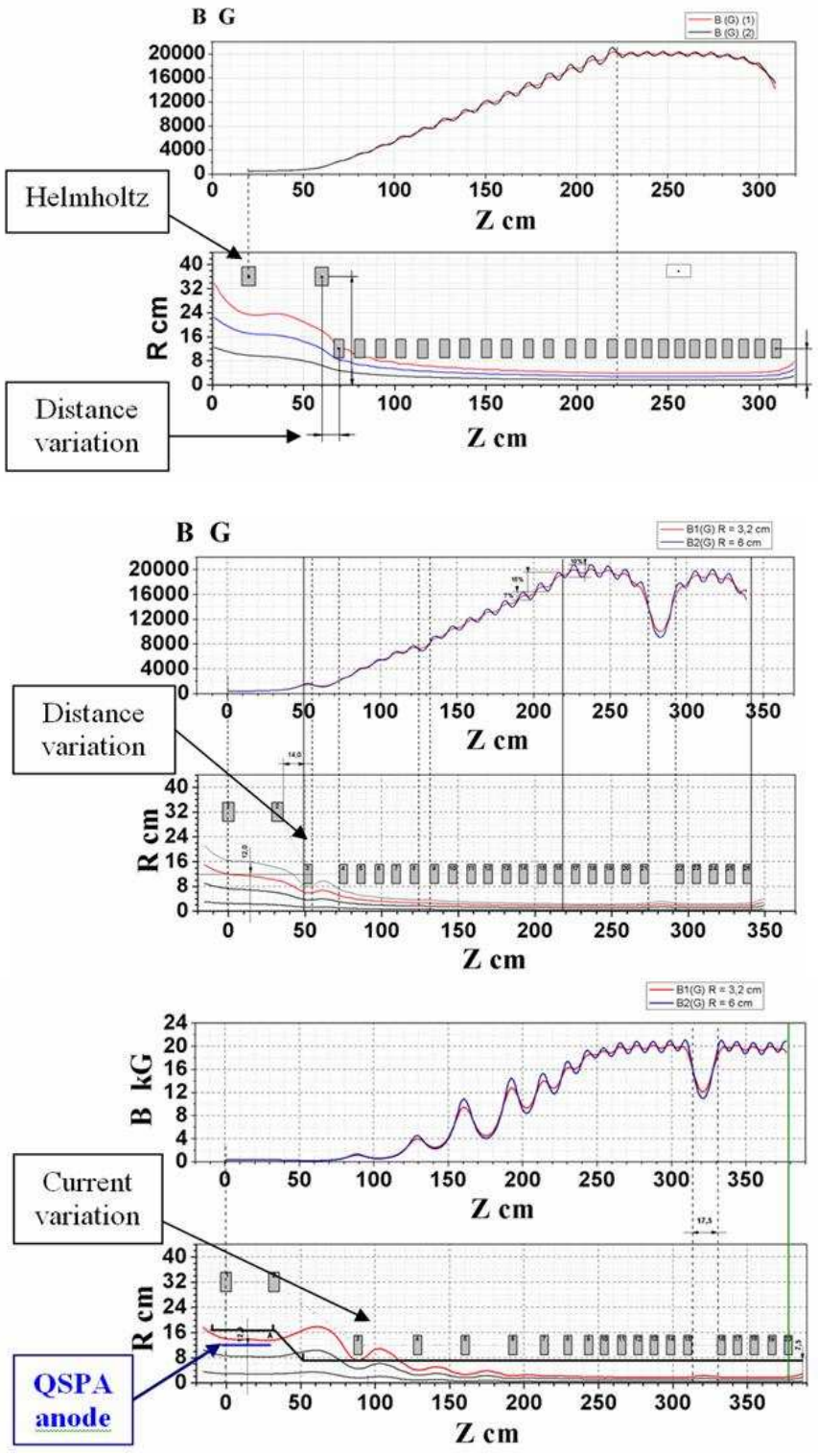

Figure III.11. Example showing the effect of varying currents and coil displacements.

(f) Power supply system of the QSPA discharge

The power supply system of the accelerator consists of a high-voltage device to charge the capacitor banks to the operating voltage, a capacitor bank for energy storage with a total capacity of 0.01F, and a set of switch tubes (switchers) to connect the energy storage capacitor bank to the plasma accelerator. A block diagram of the power supply for the QSPA-SLIDE plasma accelerator is shown in Fig III.12.

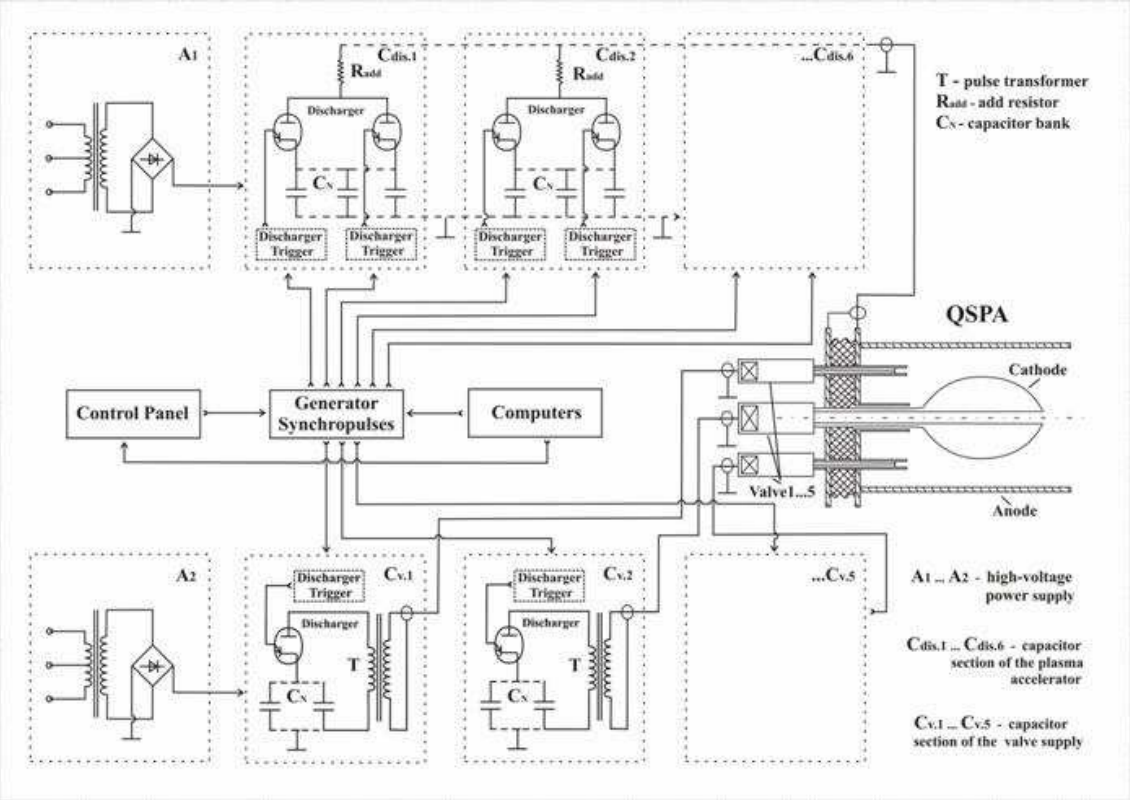

Fig.III.12. Block diagram of the QSPA-SLIDE power supply

The high voltage power supply for charging the capacitors must be capable of regulating the operating voltage up to 20 kV and provide a charging rate of 10 kJ/s, with either positive or negative output polarity, for 3÷3.5 min. “General Atomics Energy Products” designs and manufactures Standard and Custom high voltage, high power AC/DC switching power supplies; for example: the CCS10025P1C module with the following parameters:

- output voltage: 0-25 kV;
- output current: 0.8A;
- power rating: 10 kJ/s;
- size: 222 mm height x 482 mm width x 508mm depth;
- weight: 29 kg.

Such a power supply satisfies our requirements and can be used for the QSPA-SLIDE device.

Custom designed or home-made power supply systems can also be considered.

The capacitor battery should consist of six sections, each with a different capacity.

The calculations that have been performed suggest the following solution for the QSPA-SLIDE power supply system: the first section of the capacitor battery must have a capacity of 0.0034 F, the second 0.0022 F, the third and fourth 0.00167 F each, the fifth and sixth 0.00042 F. Each section is composed of e.g. Maxwell energy storage high voltage capacitors with a capacity of 206 μF, and an operating voltage of 22kV (for instance, series C part number 32349). The casing of each capacitor has a size of 305×407×696 mm and a weight of 145.2 kg. The total area occupied by the capacitor battery will then amount to 6.5 m^2. The cost of a capacitor is about 2,200$. The overall cost of the capacitor bank is estimated to be below 103.5 thousand $.

The operation of the capacitor bank will be non-periodic. The sections should be switched on in series with a preset time delay, allowing the shaping of the current waveform in the plasma accelerator, with a maximum current of 700kA at the capacitor bank voltage of 20kV and pulse duration of 0.5ms.

Based on the electro-technical characteristics and the parameters of the discharge circuit, numerical calculations were performed to study different scenarios for the discharge of capacitor sections, with the aim of controlling the pulse shape of the discharge current and the voltage. An example of such calculations for the current waveform and voltage is shown in Fig. III.13. The effect of switching the various sections on the discharge current can be observed. After selecting an appropriate scenario, the discharge current can be kept rather constant during 0.5 ms.

Alternative solutions exist for the parameters of the capacitor battery, depending on the available capacitors.

Note also that the capacitor battery can be designed with several segments, which allows varying the discharge duration (for example, either 0.5 ms or 0.25 ms by switching on or off a segment).

The planned setup contemplates switch tubes (switchers) in the discharge circuit of the plasma accelerator in order to control the connection of the capacitor bank energy to the plasma accelerator. Each capacitor section has one or a few switch tubes, allowing it to be switched on independently from the other sections. The choice of switch tube depends on the voltage, the commutated current, the charge and the pulse duration. The T-150 Spark Gap Switch and TG-1292 Trigger Generator produced by **“L-3 Communications Pulse Sciences”** are suitable for this purpose. Nevertheless, other solutions can be considered.

The T-150 Spark Gap Switch has the following parameters: operating voltage: 20-40 kV; peak current: 300 kA; charge transfer: 120 coulomb per pulse; gas flow rate > 30 scf/hr. In view of the technical characteristics of the T-150 Spark Gap Switch, it is convenient to use twelve T-150 Spark Gap Switches to commutate the capacitor bank. They will be mounted between the sections in following sequence: in threes for the first and second sections, in twos for the third and fourth sections, and in ones for the fifth and sixth sections. The cost of a T-150 unit is approximately 14.5 thousand USD.

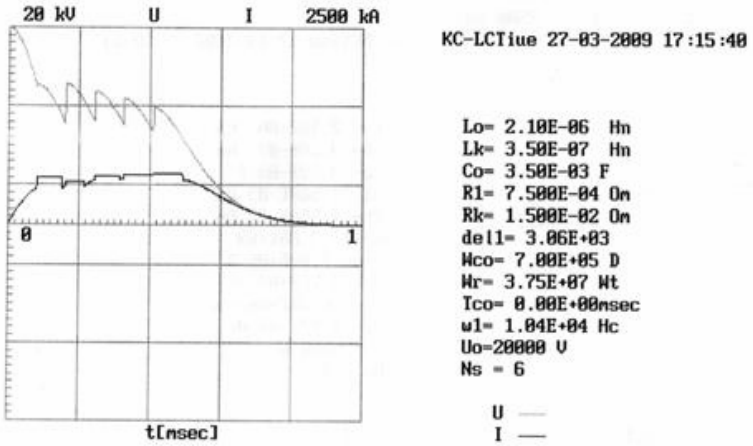

KC-LCTiue 27-03-2009 17:15:40

Lo= 2.10E-06 Hn
Lk= 3.50E-07 Hn
Co= 3.50E-03 F
R1= 7.500E-04 Om
Rk= 1.500E-02 Om
del1= 3.06E+03
Wco= 7.00E+05 D
Wr= 3.75E+07 Wt
Tco= 0.00E+00msec
w1= 1.04E+04 Hc
Uo=20000 V
Ns = 6

U —
I —

n	Ln mkH	Cn mF	Rn mOm	dTn ms	Tn ms
1	2.4500	3.582	0.7500	0.0820	0.0820
2	1.4000	5.974	0.3750	0.0820	0.1640
3	1.0500	7.622	0.2500	0.0820	0.2460
4	0.8750	9.270	0.1875	0.0820	0.3280
5	0.7700	9.682	0.1500	0.0820	0.4100
6	0.7000	10.094	0.1250	0.0820	0.4920

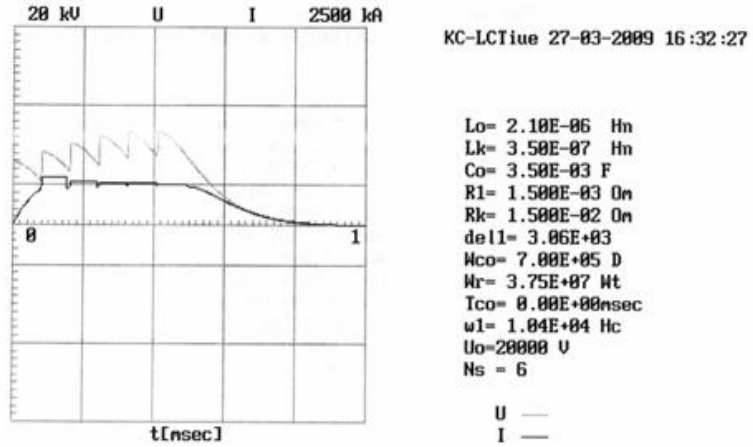

KC-LCTiue 27-03-2009 16:32:27

Lo= 2.10E-06 Hn
Lk= 3.50E-07 Hn
Co= 3.50E-03 F
R1= 1.500E-03 Om
Rk= 1.500E-02 Om
del1= 3.06E+03
Wco= 7.00E+05 D
Wr= 3.75E+07 Wt
Tco= 0.00E+00msec
w1= 1.04E+04 Hc
Uo=20000 V
Ns = 6

U —
I —

n	Ln mkH	Cn mF	Rn mOm	dTn ms	Tn ms
1	2.4500	3.582	1.5000	0.0820	0.0820
2	1.4000	5.974	0.7500	0.0820	0.1640
3	1.0500	7.622	0.5000	0.0820	0.2460
4	0.8750	9.270	0.3750	0.0820	0.3280
5	0.7700	9.682	0.3000	0.0820	0.4100
6	0.7000	10.094	0.2500	0.0820	0.4920

Figure III.13. Example of calculation results using different pulse shapes for the discharge current and the discharge voltage in QSPA-SLIDE.

(g) Power supply systems for the coils of the electronic valves

The design of the QSPA contemplates five electronic valves to control the injection of working gas (e.g. hydrogen, helium, deuterium, or various mixtures, including Xenon) into the discharge region of the plasma accelerator. Due to the interaction between the magnetic fields produced by an inductive current in the valve disk and the magnetic coil of the valve, the **electronic** valve opens and injects gas. The power for the magnetic coil of the valve is supplied by a capacitor bank with a capacity of 500 µF and an operating voltage of up to 5 kV each. The capacitor bank consists of 5 capacitors with a capacity of 100 µF and a nominal voltage of 5 kV (for example type IK41-I7).

An ignitron switcher (IRT-6) is used to commutate the discharge current in the valve circuit. The discharge is periodic. All electrical circuits of the electronic valves are galvanically isolated from each other and from the accelerator electrodes. A high voltage capacitor power supply is used to charge each capacitor bank and must be able to regulate the voltage from 0.5 kV to 5 kV and provide a charge time of about 3 min at a voltage of 5kV (the nominal power is about 35J/s).

(h) Power supply of the Helmholtz coils

The power of the Helmholtz coils is also supplied by a capacitor bank. The required magnetic field in the Helmholtz coils is produced by 67 kiloampere-turns. For coils with 32 turns, the capacity of the battery is 1600 µF at a voltage of 3 kV. The proposed high voltage power supply for the capacitor must be able to regulate the voltage from 0.1 kV to 3 kV and have a nominal power rating of 40 J/s.

(i) Synchronization unit

A synchronization unit (pulse generator) is needed to provide synchronised triggers to switch the capacitor banks of the Helmholtz coils, the gas valves and the main discharge of the plasma accelerator with appropriate time delays. Each channel of the synchronization unit triggers one discharge with an adjustable time delay. In addition, a few triggering channels are needed for the oscilloscopes and the computer ADCs. The pulse height and duration will be determined in the detailed design phase.

It should be noted that industrial solutions are available for the synchronization unit.

(j) Control panel

The control panel includes the following control blocks:

- A control block for the activation and deactivation of the elements of the vacuum system;
- A control block for the power supply for charging the discharge capacitor bank. It controls the activation and deactivation of the power supply, it regulates the charge level of the capacitor bank, and it generates a signal indicating the readiness of the capacitor bank for operation.
- A control block for the coil valves, and the power supply for charging its capacitor banks. It fulfils similar functions;
- An interface board for connection to a computer;

- Voltmeters for visual inspection of the charge (voltage) of the capacitor banks;
- A start signal that is sent to the input of the synchronization block after receiving acknowledgement of readiness from the capacitor banks;
- An interlock system controlling the electromagnetic contactor, short-circuiting the capacitor banks and the high-speed electric protection;
- In addition to conventional tasks, the control system should be able to monitor and disconnect any part of the power supply while keeping the rest of the device operational. The control panel should offer both a manual and a programmed mode of operation. The elements of the control panel are not very costly and will be defined in detail as the engineering design of the circuits progresses.

5. Conclusions

A general design has been made for the QSPA-SLIDE plasma source for the *TechoFusión* facility in Madrid. Profiled electrode rods were chosen for its basic design. The external electrode of the plasma source will have a diameter of 260 mm and a length of ~700 mm. The profiled part of the internal electrode will have an ellipsoidal shape with a maximum diameter of 160 mm at the critical cross-section. The length of the ellipsoid is 300 mm.

The plasma flow was calculated for the chosen accelerator geometry on the basis of an MHD model in 2 different approximations.

Several methods were considered for the gas feed. A combination of gas supply at the end and gas injection in the cathode region was chosen. Electronic valves are able to feed up to 500cm^3 of working gas into the discharge gap. The design contemplates four valves for axial gas supply. A fifth valve is located inside the cathode tube to provide additional radial gas injection from the cathode directly into the discharge zone.

The application of small external magnetic fields in the discharge area (Helmholtz coils) was considered. It was concluded that a longitudinal magnetic field of $0.1.B_{int}$ improves the stability of the plasma stream and the transport of plasma into the external B-field of the L-shaped vacuum chamber of the *TechoFusión* facility.

A basic specification of the QSPA-SLIDE device was made. The key parameters of various QSPA systems were determined.

Estimates were made of the electro-technical specifications of the power supply systems for the different elements of the QSPA-SLIDE device

Globally, the QSPA-SLIDE device designed here is smaller and simpler (but more effective and powerful) than the existing QSPA Kh-50 device. Compared to QSPA-T, the designed facility is somewhat more complicated, but qualitatively enhanced in several respects, which will provide some important advantages: the possibility to transport plasma into a strong B-field, a much lower level of impurities, higher particle energies, etc.

References

[1] A. Loarte et al., *Plasma Phys. Control. Fusion* **45**, 1549 (2003).

[2] G. Federici et al., *Plasma Phys. Control. Fusion* **45**, 1523 (2003).

[3] A.I. Morozov. Plasma dynamics, in Encyclopedia of Low Temperature Plasma, V3. ed. V.Fortov(in Russian);

[4] A.I. Morozov. Introduction to Plasmadynamics. Moscow. FIZMATLIT. 2006, 576 p (in Russian).

[5]. A.I. Morozov. Sov. J. Plas. Phys 1990, v.16, N2.

[6] Tereshin V.I. Quasi-stationary Plasma Accelerators (QSPA) and their Applications // Plasma Physics and Controlled Fusion.-1995.- Vol. 37.- P. A177-A190.,

[7] V. I.Tereshin et al., *Brazilian Journal of Physics* 32, № 1, 165-171 (2002).

[8] Ya. F. Volkov et al, Sov. J. Plas. Phys. 1992, V.18, N. 9, p. 1138.

[9] Ya. F. Volkov, A.Yu Voloshko, I.E. Garkusha et al. Sov. J. Plas. Phys. 1992, V. 18, N. 4, p.456

[10] Ya. F. Volkov, I.E. Garkusha et al. Sov. J. Plas. Phys. 1994. V.20, N.1, P.77

[11] A.I. Morozov, O. A. Shchurov, O.S. Pavlichenko et. al. QSPA Kh-50 full-sale high-power quasistationary plasma accelerator // Plasma devices and operations. - 1992. - Vol.2, № 2. - P. 155-165.;

[12] V. I. Tereshin et al., Plasma Phys. Control. Fusion 49 (2007) A231

ANNEX TO APPENDIX III

Analysis of plasma flow in the SCC model for the QSPA-SLIDE geometry

Some properties of plasma flow in the acceleration channel were analyzed with the Slowly Changing Channel (SCC) model. The main assumption in this model is that the acceleration channel varies slowly along the axis, so that $\left(v_r/v_z\right)^2 << 1$. This model is appropriate for the description of the main central part of the acceleration channel, but not for the entry section, where large gradients in plasma stream velocity exist, or the exit section, where dissipative processes play a large role. Here, it is assumed that the thermal energy of the particles is much less than the kinetic energy $W << \mathrm{E}_i$, and that the exchange parameter $\xi = \frac{I_d}{I_{\dot{m}}} << 1$, where I_d is the discharge current and $I_{\dot{m}}$ the mass flow rate in electric current units. The latter assumption means that the electron and ion trajectories are rather similar to one another. It has been stressed that in this model, the discharge current between the electrodes flows in the radial direction only, and the plasma stream velocity does not depend on the radius.

Considering the above, the ion flux function can be written:

$$\Psi_i(r,z) = \sqrt{2}a_*^2 n_{0*} C_{A0} \alpha(z) \sqrt{(1-\alpha(z))} \ln\left(\frac{r}{b(z)}\right)$$

Where $\Psi_i(r,z)$ is the ion flux function; a_* the average radius at the entry section of the acceleration channel; n_{0*} the plasma density at this point; C_{A0} the Alfvén velocity at this point; $\alpha(z)$ the dependence of the discharge current on the channel axis; $b(z)$ the cathode radius (assuming that the anode is a cylinder) and r the radius.

Thus, the ion flux function (i.e., a function such that $\Psi_i = const$ corresponds to ion trajectories) depends on the distribution of the discharge current along the channel axis $\alpha(z)$ and on the channel profile, namely the cathode profile $b(z)$, since the anode is cylindrical. Two different types of dependency of the discharge current on z were considered in these calculations. The first is linear dependence. This case is simple, but produces a value of the discharge current at the accelerator exit that is close to zero. In recent experiments, a part of the discharge current, typically about 25-30%, flows in the plasma stream outside the acceleration channel. Thus, another dependence was used to estimate the ion flux function, taking into account that about 25% of the total discharge current flows outside the acceleration channel.

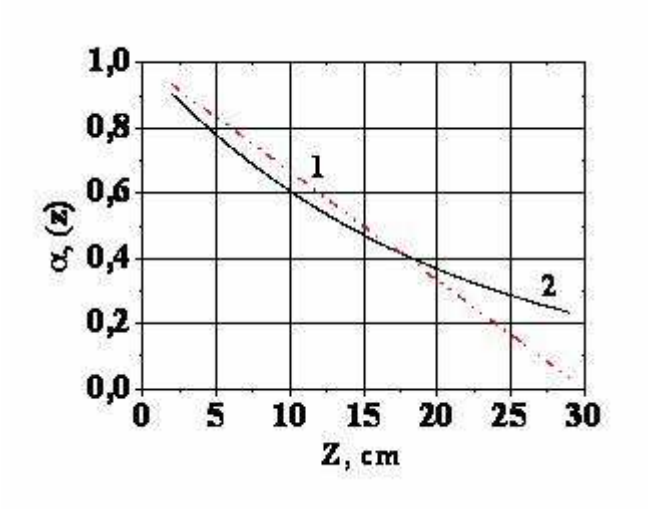

Two dependencies of $\alpha(z)$.

Ion flux functions were calculated for two different discharge current distributions along the axis and for two acceleration channel profiles. The results of these calculations are presented in the figure below.

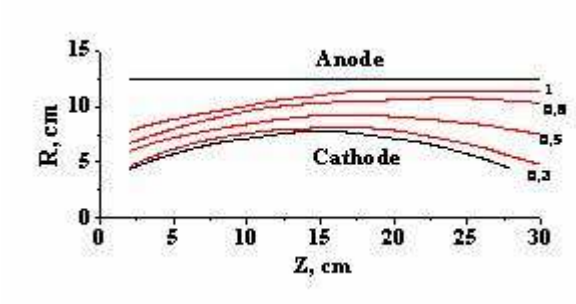

Ion flux function for dependence $\alpha(z)$ - 1.

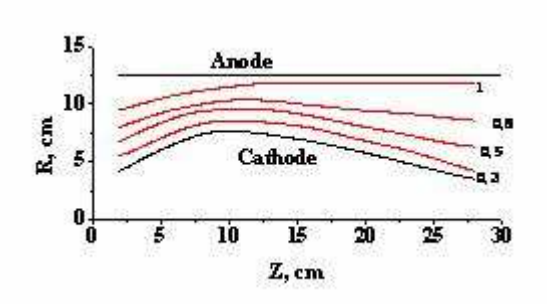

Ion flux function for dependence $\alpha(z)$ - 1.

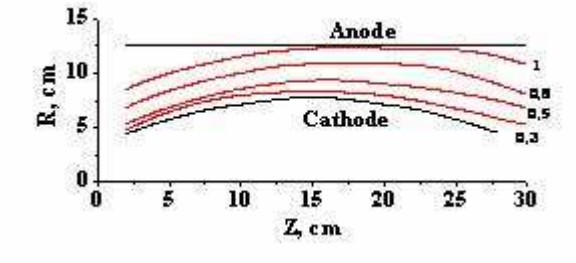

Ion flux function for dependence $\alpha(z)$ - 2.

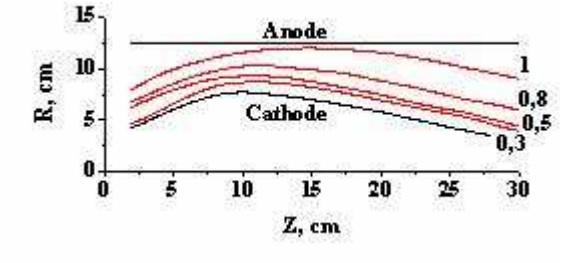

Ion flux function for dependence $\alpha(z)$ - 2.

These figures show that about (70-80)% of total plasma stream flows outside the acceleration channel, inside a cylinder with diameter of 16-17 cm.

Based on the ideal SCC model, the ratios of the ion velocity v_i to the local signal velocity $v_s = \sqrt{v_A^2 + v_{Ti}^2}$ were calculated. Taking into account that the thermal energy of the particles is much less than their kinetic energy, the local signal velocity is equal to the local Alfvén velocity: $v_s \approx v_A$. Calculated ratios, i.e., lines of equal levels of v_i / v_A, are shown in the figure below for two different channel profiles and a linear dependence of the discharge current along the axis.

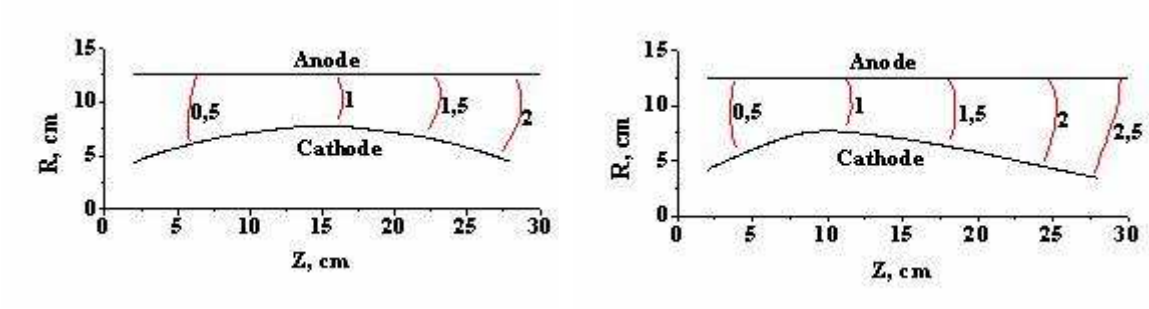

Lines of equal values of v_i / v_A.

These figures show that the plasma stream is accelerated along the channel, while the achieved velocity is about (2-2.5) times the local Alfvén velocity at the channel exit.

Based on the SCC model, the value of the plasma density at the entrance of the acceleration channel and its radial distribution was estimated. It is seen that the total mass flow rate equals $\dot{N} = 2\pi\Psi_i^{\max}$. It has been expected to reach a maximum discharge current in the acceleration channel of about 600 kA, and an exchange rate of $\xi = 0.1$. In this case, the total mass flow rate should be $I_{\dot{m}} \approx 3.6\times10^{25} s^{-1}$ and $\Psi_i^{\max} = 6\times10^{24} s^{-1}$. The average radius at the entrance of the acceleration channel is $r = 10cm$. Thus, the plasma density at $r = 10cm$ should be $n \approx 5\times10^{15} cm^{-3}$, and its radial distribution should look like what is shown in the figure.

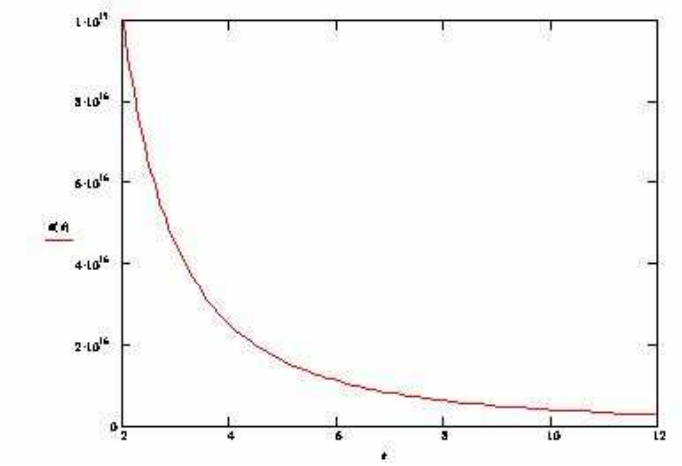

Radial distribution of the plasma stream density et the entrance of the acceleration channel of QSPA SLIDE.

Two different methods exist to obtain such a radial distribution of plasma density. The first is to inject some neutral gas from the cathode into the acceleration channel at the entrance of the channel. The second is to create an electromagnetic force at the entrance of acceleration channel that pushes the plasma towards the cathode. Both methods can be applied in the QSPA facility.

The maximum exit velocity can be calculated based on the calculations above. For a discharge current of $I_d = 600kA$ and plasma stream densities at the entrance cross-section of $n = 5\times10^{15} cm^{-3}$, the maximum velocity should be $v_{\max} = 1.1\times10^{8}\, cm/s$. It has been emphasized that this value of the plasma stream velocity requires that the discharge current between the electrodes flows only in the radial direction.

Appendix A: list of acronyms

A

ABI – Automated Ball Indentation.

ACAB – ACtivation ABacus Code. Computer code for radioprotection calculations.

ADLD – Advanced Delay Line Detector.

AFM – Atomic Force Microscopy.

AKMC – Atomistic Kinetic Monte Carlo.

ANSYS – Computer Fluid Dynamics code.

AP – Auxiliary Personnel.

appm - atomic part per million.

APS – Atmospheric Plasma Spray.

APT – Atom Probe Tomography.

ATILA – Computer simulation code for simulation model generation to determination particle fluxes.

AVF – Azimutally Varying Field.

B

BA – Broader Approach agreement.

BF – Bright Field.

BIGMAC – Kinetic MonteCarlo computer code.

BN-600 – Fission Reactor.

BOE – Boletín Oficial del Estado.

Breeding blanket – set of modules covering the interior of the fusion reactor vessel, capable of supporting a high heat load and an intense flux.

BSM – Blankets Shield Modules.

C

CAN – Centro Nacional de Aceleradores de Sevilla (Spain).

CATIA – Software of graphic design.

CBED – Convergent Beam Electron Diffraction.

CCD – Charge-Coupled Device.

CDA – Continuous Dynamic Analysis.

CEA – Commissariat á l´Energie Atomique.

CFC – Carbon Fiber Composites.

CFD – Computational Fluid Dynamics

CFX – Computer Fluid Dynamics code.

CHEMCON – Heat transfer computer code.

CIEMAT – Centro de Investigaciones Energéticas, Medioambientales y Tecnológicas (Madrid-Spain)

CIP – Cold Isostatic Press.

CMAM – Centro de Microanálisis de Materiales (Universidad Autónoma de Madrid-Spain)

CMM – Cassette Multi-functional Mover.

CPS – Capillary Porous Structure.

CS – Computer Simulation Facility.

CSIC – Consejo Superior de Investigaciones Científicas (Spain).

CSN – Consejo de Seguridad Nuclear (Spain).

CSNSM – Centre de Spectrométrie de Masse et de Spectrométrie Nucléaire of Saclay (France).

CT – Characterization Techniques Facility.

CTF – Compact Tokamak Facility, a plasma-based massive neutron source for testing the radiation response of large-scale components

D

DBTT – Ductile-Brittle Transition Temperature.

DC – Direct Current.

DCF – Dose Conversion Factor.

DD – Dislocation Dynamic.

DD.D – Dislocation Dynamics computer code.

DD3D – Computer simulation code.

DEMO – DEMOstration Fusion Power Reactor.

DF – Dark Field.

DFT – Density Functional Theory.

DIADEMO – Liquid metal loop of Pb-Li for prototype testing of components for fusion blanket modules, located in France.

dpa – Displacement per Atom.

DPP – Diagnostics Port Plugs.

DRP - Divertor Refurbishment Platform.

DTP – Divertor Test Platform.

DTP-2 – Divertor Test Platform 2.a platform to test divertor maintenance.

E

EAF2007 – European Activation File 2007. Activation library which contains data for 66864 reactions.

EBBTF – Liquid metal loop of Pb-Li for prototype testing of components for fusion blanket modules, located in Italy.

EBSP – Electron Backscatter Pattern.

ECAP – Equal Channel Angular Pressing.

EDS – Energy Dispersive Spectrometry.

EDX – Energy Dispersive X-ray analysis.

EELS – Electron Energy Loss Spectroscopy.

EFDA – European Fusion Development Agreement.

EFTEM – Energy-Filtered Transmission Electron Microscopy.

EKMC – Event Kinetic Monte Carlo.

ELMs – Edge Localized Modes.

EMPIRE-II – Computer simulation code of radiological protection and analysis of nuclear data.

ENDF – Evaluated Nuclear Data Formats.

ENEA – Ente per le Nuove Tecnologie, l'Energia e l'Ambiente (Italy).

EPP – Equatorial Port Plug.

ERDA – Elastic Recoil Detection Analysis.

ET – Everhart-Thorney.

ETSII – Escuela Técnica Superior de Ingenieros Industriales (Madrid-Spain).

EU – European Union.

EURATOM – EURopean ATOMic Energy Community.

EUROFER – Ferritic-martensitic low-activation steel that will constitute the main structural material of DEMO.

EXFOR – Library of experimental nuclear reaction data.

F

FEG – Field Emission Gun.

FENDL-2.1. – Fusion Evaluated Nuclear Data Library. Collection of high-quality nuclear data for fusion applications.

FIB – Focused Ion Beam.

FIB/SEM – Focused Ion Beam/Scanning Electron Microscopy.

FIM – Field Ion Microscopy.

FISPACT – Computer code for calculation of the radioactive inventory.

Flow3D – FDC code flow modelling software.

FLUENT – Computer Fluid Dynamics code.

FLUKA – Monte Carlo simulation tool. FLUKA is the acronym of the German for "Fluctuating Cascade".

FMEA – Failure Mode and Effect Analysis.

FOV – Field Of View.

FPKMC – First-Passage Kinetic Monte Carlo.

G

GGA – Generalized Gradient Approximation.

GPM – Groupe de Physique des Matériaux.

GRE – Guide for the Response to Emergencies.

H

HCLL – Helium Cooled Lithium Lead.

HIP – Hot Isostatic Pressing technique.

HRTEM – High Resolution Transmission Electron Microscopy.

I

IAI – Instituto de Automática Industrial (CSIC-Spain).

IBA – Ion Beam Analysis techniques.

IBA – Ion Beam Applications company, Belgium.

ICSC – International Chemical Safety Card.

IEA – International Energy Agency.

IEEE – The Institute of Electrical and Electronics Engineers.

IFMIF – International Fusion Materials Irradiation Facility. An installation for testing the materials that will be used in a fusion reactor.

IPPE – Institute of Physics and Power Engineering. (Russia).

IPUL – Liquid metal loop of Pb-Li located at Latvia.

IR – Infra-Red.

ISOLA V – Mathematic dispersion model for events with a long duration.

ITC – Complementary Technical Instructions.

ITER – International Thermonuclear Experimental Reactor.

IVT - In-Vessel Transporter (Japan).

J

JAERI – Japan Atomic Energy Research Institute (Osaka-Japan).

JANNUS – Joint Accelerators for Nanosciences and NUclear Simulation (Saclay-France).

JET – Joint European Torus (Abingdon, United Kingdom)

JT-60 – Superconducting tokamak that will allow experimenting with alternative concepts for the operation of ITER.

K

KMC – Kinetic Monte Carlo.

L

LAKIMOCA - The OKMC code developed at EDF (France).

LAMMPS – Large-scale Atomic/Molecular Massively Parallel Simulator.

LDA-LSD – Local Density Approximation-Local-Spin-Density.

LEDI – Liquid metal loop of Pb-Li located in Italy.

LENTA – Linear plasma device of Kurchatov Institute, Moscow (Russia).

LFM – Lateral Force Measurement.

LIFUS –Liquid metal loop of Pb-Li located in Italy.

LIMITS – Liquid lithium facility located at the Sandia National Laboratory (USA),

LKMC – Lattice Kinetic Monte Carlo.

LMIS – Liquid Metal Ion Source,

LMT – Liquid Metal Technologies Facility.

LPPS – Low Pressure Plasma Spray.

LVDT – Linear Variable Differential Transformer.

M

MA – Mechanical Alloying.

MACCS – MELCOR Accident Consequence Code.

MCNP – Monte Carlo N-Particle Transport computer simulation code.

MCNPX – MonteCarlo method transport computer code.

MDCASK – Molecular Dynamics. Molecular dynamics computer code for radiation damage.

MEKKA – Liquid loop of eutectic NaK located in Germany.

MELCOR – Thermohydraulics computer code.

MELODIE – Device for liquid metal studies of France.

MHD – Magneto-Hydrodynamic

MI – Material Irradiation Facility.

MICINN – Ministerio de Ciencia e Innovación (Spain).

MIT – Massachusetts Institute of Technology (USA).

MK-200 (UG y CUSP) – QSPA accelerator located at Troitsk Institute for Innovation & Fusion Research (Russia).

MP – Meeting Point.

MPP – Material Production and Processing Facility.

MUSEMET – Mathematic dispersion model.

N

NAGDIS-II – Linear plasma device located at Nagoya University (Japan).

NIMS – National Institute for Materials Science. (Tsukuba-Japan).

NMAT – NanoMechanical Actuating Transducer.

NORMTRI – Computer simulation code to evaluate the environmental impact.

NPT – Model ensemble of molecular dynamics.

NRA – Nuclear Reaction Analysis.

NVE – Microcanonical Ensemble.

NVT – Model ensemble of molecular dynamics.

O

OBT – Organically Bound Tritium.

ODF – Orientation Distribution Functions.

ODS – Oxide Dispersion Strengthened steel.

OFD – Orientation Distribution Function.

OKMC – Object Kinetic Monte Carlo code.

OpenFoam – Open Field Operation And Manipulation. Open source computational fluid dynamics toolbox.

ORIGEN – Computer code for calculation of the radioactive inventory.

ORLN – Oak Ridge National Laboratory.

P

PABLITO – Liquid metal loop built to test materials for fusion (CEA – France).

PARADIS – PARAllel DIslocation Simulator computer code.

PAS – Positron Annihilation Spectroscopy.

PFCT – Plasma Facing Components Transporter.

PFM – Plasma Face Materials. Materials for fabricating blanket modules and divertor system parts.

PHITS – Particle and Heavy Ion Transport code. MonteCarlo method transport computer code.

PICOLO – Liquid metal loop available in Germany.

Pilot-PSI – Linear plasma device of Holland.

PISCES-B – Linear plasma device of California University (San Diego).

PIXE – Particle Induced X-Ray Emission.

PKA – Primary Knock-on atom. The PKA is the recoil atom being displaced by the direct collision – atomic or nuclear – of the incident particle.

PKMC – Parallel Kinetic Monte Carlo.

PPCS –Power Plant Conceptual Study.

PROMIS 1.5 – RT code developed by S. Selberherr and P. Pichler.

PSI-2 – Linear plasma generator of Humboldt University (Berlin-Germany)

PWI – Plasma Wall Interaction Facility.

Q

QHPA P-50M – Quasi-stationary High-current Plasma Accelerator.

QM/MM – Quantum Mechanics/Molecular Mechanics.

QSPA – QuasiStationary Plasma Accelerator.

R

R&D – Research and Development.

RAFM – Reduced Activation Ferritic-Martensitic steels.

RBS – Rutherford Backscattering Spectroscopy.

RELA III – Device for liquid metal studies (Italy).

Relap5 – Transitory thermal analysis code.

RH – Remote Handling.

Rhodotron – Commercial electron accelerator working at fixed energy.

RHT – Remote Handling Technologies Facility.

RIA – Rare Isotope Accelerator.

RIC – Radiation Induced Conductivity.

RIED – Radiation Induced Electrical Degradation.

RL – Radio Luminescence.

ROVVER 4 – Installation for validation, testing and certification of robots.

RT – Rate Theory

RTA – Reverse Transferred Arc.

S

SAD – Selected Area (electron) Diffraction.

SANS – Small Angle Neutron Spectroscopy.

SCEE - Second Cassette End Effectors

SEM – Scanning Electron Microscopy.

SIESTA – Spanish Initiative for Electronic Simulations with Thousands of Atoms. Ab initio quantum-mechanical computer code.

SIMS - Secondary Ion Mass Spectrometry.

SPD – Severe Plastic Deformation techniques

SPS – Spark Plasma Sintering technique

SRIM – The Stopping and Range Ions in Matter. Monte Carlo computer simulation code.

SSM – Stress Strain Microprobe.

STAR-CD – Computer Fluid Dynamics code.

STEM – Scanning Transmission Electron Microscopy.

T

Talys 1.0 – Computer code to calculate nuclear reaction cross sections.

TBM – Test Blanket Modules.

TechnoFusión – National Centre for Fusion Technologies.

TEM – Transmission Electron Microscopy.

TFTR – Tokamak Fusion Test Reactor.

TIARA – Takasaki Ion Accelerators for Advanced Radiation Application (Japan).

TJ-II – Torus JEN-II. (Ciemat-Madrid)

TMAP – Tritium Migration Analysis Program.

ToF – Time of Flight.

TPE – Tritium Plasma Experiment, Idaho (USA)

TRIEX – TRItium EXtraction System from PbLi of ENEA-Brasimore (Italy).

TRIM – TRansport of Ion in the Matter. Monte Carlo computer simulation code.

TUM – *Technische Universität München* (Munich-Germany).

U

UA – Universidad de Alicante (Comunidad Valenciana-Spain).

UAB – Universidad Autónoma de Barcelona (Cataluña-Spain).

UAH –Universidad de Alcalá de Henares (Madrid-Spain).

UAM – Universidad Autónoma de Madrid (Madrid-Spain).

UC3M – Universidad Carlos III de Madrid (Madrid-Spain).

UFOTRI – Computer simulation code for the evaluation of the environmental impact.

UG – University Graduates.

UHRTEM – Ultra-High Resolution Transmission Electron Microscopy.

UHV – Ultra High Vacuum.

UNED – Universidad Nacional de Educación a Distancia (Spain).

UPM – Universidad Politécnica de Madrid (Madrid-Spain).

UPP – Upper Port Plugs.

UPS – Uninterruptible Power Supply.

URJC – Universidad Rey Juan Carlos de Madrid (Madrid-Spain).

UV – Ultra-Violet.

UV – Universidad de Valencia (Comunidad Valenciana-Spain).

V

VASP – Vienna Ab initio Simulation Package. Ab initio plane-wave all-electron computer code.

VIM – Vacuum Induction Melting technique.

VIT – Vertical Irradiation Tube.

VIVALDI – Device for liquid metal studies of ENEA (Brasimore-Italy).

VPS – Vacuum Plasma Spraying.

VTA – Vertical Test Assembly.

VTT – Technical Research Centre of Finland.

WHO – World Health Organization.

X

XRD – X-Ray Diffraction.

XRPD – X Ray Powder Diffraction.

Appendix B: list of units

Symbol	Name	Derivation	Base unit	Quantity
A	ampere	--	A	electric current
Å	angstrom	meter	10^{-10}m	length
A	mass number	total number of protons and neutrons in the nucleus of an atom		
appm	atomic part per million	--	--	concentration
Bar	bar	--	10^{5} Pa	pressure
Bq	becquerel	l/s	s^{-1}	activity
C	coulomb	A s	A s	charge
cm	centimetre	meter	10^{-3} m	length
dpa	displacement per Atom	number of ion displacements per atom		
eV	electronvolt	--	1.6 10^{-19}J	voltage
F	farad	A s/V	kg^{-1} m^{-2} s^{4} A^{2}	capacitance
Gy	gray	J/kg	m^{2} s^{-2}	absorbed dose
H	henry	V s/A	kg m^{2} s^{-2} A^{-2}	inductance
Hz	hertz	l/s	s^{-1}	frequency
J	joule	N m	kg m^{2} s^{-2}	energy
K	kelvin	--	K	temperature
kg	kilogram	--	kg	mass
kW	kilowatt	W = J/s	kg m^{2} s^{-3}	power
lb	libra	--	1 lb = 0.4536 kg	mass
m	meter	--	m	length
m/z	mass-to-charge ratio	--	kg/C	--
mol	mole	--	mol	concentration
N	newton	Kg m/s^{2}	Kg m s^{-2}	force
$n/m^{2}s$	neutron flux	--	$n/m^{2}s$	flux
Pa	pascal	M/m^{2}	kg $m^{-1}s^{-2}$	pressure
ppb	part per billion	--	1 ppb = 1 µg/l	concentration
ppm	part per million	--	1 ppm = 1 mg/l	concentration
rad	radian	--	rad	plane angle
s	second	--	s	time
S	siemens	1/Ω	Kg^{-1} m^{-2} s^{3} A^{2}	electric conductance
slm	standard litres per minute	--	--	flux
Sv	sievert	J/kg	m^{2} s^{-2}	dose equivalent
T	tesla	Wb/m^{2}	kg s^{-2} A^{-1}	magnetic flux density
Torr	torr	133.322368 Pa	1 mm Hg	pressure
V	volt	W/A	Kg m^{2} s^{-3} A^{-1}	voltage
W	watt	J/s	Kg m^{2} s^{-3}	power
wt%	Weight percent	--	--	concentration
Z	Atomic number	number of protons found in the nucleus of an atom		
θ	Theta	--	--	angle
µm	Micron	--	10^{-3} m	length
Ω	ohm	V/A	Kg m^{2} s^{-3} A^{-2}	resistance

Appendix C: list of symbols

Symbol	Name	Description
Al_2O_3	aluminum oxide	ceramic material
Ar	argon	periodic table element
Au	gold	periodic table element
Be	berylium	periodic table element
C	carbon	periodic table element
^{60}Co	cobalt 60	cobalt isotope
Cs^+	cesium cation	cesium ion
D	deuterium	hydrogen isotope
Fe	iron	periodic table element
FeS_2	iron disulfide	chemical compound
H	hydrogen	periodic table element
He	helium	periodic table element
HT	tritium gas	--
HTO	water gas	--
K	cyclotron constant	--
LaB_6	lanthanum hexa- boride	chemical compound
Li	lithium	periodic table element
MCs^+, MCs_2^+	cesium metallic cation	--
N	nitrogen	periodic table element
Na	sodium	periodic table element
Ni	nickel	periodic table element
O^-, O_2^+	oxygen ions	--
P	phosphorus	periodic table element
Pb-Li	lead-lithium	lead-lithium eutectic
S	sulfur	periodic table element
Si	silicon	periodic table element
U	uranium	periodic table element
W	tungsten	periodic table element